Growth factor modulation of TGF-beta (TGF-β)-induced epithelial-to-mesenchymal transition (EMT) in the eye lens

Mary Flokis

A thesis submitted to fulfil requirements

for the degree of Doctor of Philosophy

Lens Research Laboratory
Molecular and Cellular Biomedicine
School of Medical Sciences
Faculty of Medicine and Health
The University of Sydney, Australia

February 2024

To little Mary,
we did it.

"Begin at the beginning … and go on till you come to the end: then stop."
— Lewis Carroll, *Alice's Adventures in Wonderland (1865)*

DECLARATION

This declaration certifies that to the best of my knowledge, the content of this thesis is my own work. This thesis has not been submitted for any degree or other purposes.

I certify that the intellectual content of this thesis is the product of my own work and that all the assistance received in preparing this dissertation and sources have been acknowledged.

Chapter 5 of this thesis is published as the following:

Flokis, M., Lovicu, F.J., 2023. FGF-2 Differentially Regulates Lens Epithelial Cell Behaviour during TGF-β-Induced EMT. *Cells* 12, 827. https://doi.org/10.3390/cells12060827.

I co-designed the study with the co-author, analysed and extracted the data, and wrote the drafts of the MS.

Mary Flokis

18th December 2023

DECLARATION BY SUPERVISOR

As corresponding author for '*FGF-2 Differentially Regulates Lens Epithelial Cell Behaviour during TGF-β-Induced EMT*' included in this thesis as Chapter 5 (Flokis and Lovicu, 2023), I certify that the candidate, Mary Flokis, has made the following contributions:

- Designed and executed experiments as described
- Analysed and interpreted the data
- Writing and assembling the manuscript

As supervisor for the candidature upon which this thesis is based, I can confirm that the authorship attribution statements, as well as any relevant contribution statements indicated in the following chapters, are correct.

Professor Frank J. Lovicu
18th December 2023

ACKNOWLEDGEMENTS

This dissertation would not be possible without the guidance and mentorship from my supervisor, Professor Frank J. Lovicu. I would like to acknowledge all the support (both mental and physical) that you have provided throughout my candidature. My time with the lens laboratory has been very memorable and I thank you, Frank, for giving this underdog a chance all the way back in 2016 when I first volunteered for the laboratory.

I would like to thank my mum for all the sacrifices she has made throughout my tertiary education. You have been my rock through thick and thin, my shoulder to cry on, and my voice of reason when I thought I would not be able to make it to the end of this dissertation. I adore you, Katrin. Thank you for everything. Thank you for helping me "see the light." To George, my brother and Uber driver, thank you for keeping me upbeat and helping me de-stress when I had a writer's block. You and mum have truly been such a supportive and encouraging team for me.

To my MFB Room 152 Crew; Julianne, Winston, Kevin, Zoe, Arta, and Furkan, thanks for keeping me sane throughout this process. I will always cherish our coffee runs, mini dance breaks, troubleshooting western blot workshops, and especially our lunchtime crossword puzzle breaks (*thanks for that, Furkan*). I am so happy that I got to spend this time with you all and have watched each and every one of you transition into amazing scientists. A big shoutout to the lovely staff at Grounded 2050 for supplying my caffeine fix to get me through long experimental days. I would also like to thank my co-supervisor Dr. Zaklina Kovacevic, and Dr. Katie Dixon, for mentoring me and providing additional support throughout my candidature.

Throughout my years I have gotten to know various lens lab members that have helped, guided, and shaped me into the scientist that I am today. A huge thank you to Markus, Shahan, Antonia, James, Kevin, Brooke, Daisy, Shannon, Magda, Tayler, and Fatima. I will never forget our fun times back in Anderson Stuart, our lab Christmas parties and lunch outings, as well as the strong community you all brought and embodied in the lab.

To the talented students that I have had the privilege of collaborating with throughout my PhD; Ellen Wu and Zi Lin Wang, thank you for being great mentees. Your technical support and contributions towards the greater p38 MAPK story, some of which have been included in this dissertation, are greatly appreciated and I could not have asked for better students.

I would like to acknowledge Professor's Peter Gunning and Edna Hardeman, as well as Dr. Jeff Cook from the University of New South Wales, Australia, for supplying, transporting, and granting usage of their wild type and generated tropomyosin knockout mice lines (Tp7 and Tp16). In addition, thank you for donating the various tropomyosin antibodies and anti-tropomyosin compounds, as well as providing technical assistance, for usage in our lens epithelial cell explant model. A majority of this dissertation would not be possible without the efficient collaborative work between our two laboratories.

Surprisingly, I would like to thank the COVID-19 pandemic for commencing at the beginning of my PhD. Although I missed out on a few opportunities to network with the wider Lens research community, I am glad that the various lockdowns taught me resilience and perseverance that I channelled back into my PhD. On the topic, to my PhD Covid crew, Tiffani and Aleen, we did it, girls! To think that we all started our PhD's at the beginning of a pandemic is mind blowing. I cannot thank you both enough for supporting me through regular check-ins that I found so rewarding and worthwhile, given that we were all in the same boat.

I would like to extend a heartfelt thank you to my dad, my extended friends and family, as well as my best friends Maree and Fatima. Thank you for the emotional support and holding me together throughout this process.

To the people who are no longer with us, particularly my Pappoú Kon, thank you for being my life guides. I know you have helped me in some way or form to get me to where I am today. Pappoú, you were always my biggest cheerleader and I hope that I have made you proud.

I would like to give a special thanks to Dr. Elizabeth Guy. Thank you so much for being my role model. Without you, I would have never thought of aspiring to commence a PhD (*given that you were the first person, and woman, I had ever met with a PhD*). I had the privilege of working with you throughout the end of my High School education. Your strong work ethic and tenacity reconfirmed for me that women can accomplish anything, especially in Academia.

Finally, I would like to acknowledge all the rodents that were sacrificed throughout this study in the name of science. Your sacrifice for the purpose of scientific advancement, that will hopefully lead to improving human visual impairments, is greatly appreciated.

ABSTRACT

The eye lens is a transparent organ that is dependent on growth factors within the surrounding ocular media, such as fibroblast growth factor (FGF), to regulate its normal development and functionality. During stress and/or inflammation, activation of the pro-inflammatory cytokine transforming growth factor-beta (TGF-β) can disrupt normal lens cellular processes, as well as the epithelial cell phenotype, resulting from epithelial reorganisation of cytoskeletal proteins, such as tropomyosin (Tpm). As a result, TGF-β promotes an epithelial-to-mesenchymal transition (EMT) leading to the development of lens fibrotic opacification (cataracts), namely, anterior subcapsular cataract (ASC) or secondary cataracts such as posterior capsular opacification (PCO). Cataract is one of the leading visual impairment pathologies worldwide and its only current treatment involves surgical intervention. *In situ*, ASC and PCO both present differential cell types that are either myofibroblastic or fibre-like, that are induced and maintained by ocular growth factors. With this, it is important to investigate the mechanisms resulting in lens fibrosis and better understand how growth factors are responsible for the regulation or modulation of lens EMT. This thesis will examine the interactions between FGF-2 and TGF-β2 during rodent lens EMT, and will target specific molecules involved in TGF-β canonical and non-canonical downstream signalling that regulate lens cell behaviour during fibrosis. We initially investigate the role of different Tpms in cataractogenesis using *in vivo* postnatal lens sections from wild type and an established overexpressing TGF-β1 transgenic mouse line that develops ASC postnatally. We follow this by establishing a potential model for ASC and PCO *in vitro* given cotreated FGF-2 and TGF-β2-treated rat LEC explants led to a heterogenous cell population of lens fibre-like cells and myofibroblasts, that were differentially regulated in a dose-dependent manner. We identified several Tpm isoforms, including Tpm1.6/1.7, Tpm2.1, Tpm3.1/3.2, and Tpm4.2, as potential markers for lens fibre-differentiation and/or TGF-β-induced EMT, in lens epithelial cells, fibre-like cells, and myofibroblasts. We then go on to characterise Tpm3.1/3.2 and Tpm4.2 deficient mouse models to determine the ability of lens cells to undergo EMT, and use pharmacological compounds targeting Tpm3.1/3.2, to further elucidate their role during TGF-β2-induced lens EMT. We report that Tpm3.1/3.2 and/or Tpm4.2 are not required for TGF-β2-induced EMT in rodent lens, and confirmed Tpm1.6/1.7 and Tpm2.1 as markers for lens EMT. We extend our studies by examining TGF-β-activated downstream non-canonical signalling protein, p38α MAPK, and revisit its role during lens EMT. We showed that pharmacological inhibition of p38α impacted TGF-β2-induced rat lens EMT, particularly the morphological and cytoskeletal changes. The findings of the present study demonstrate the importance of understanding how the lens is dysregulated during lens pathology. In doing so, targeting specific growth factor signalling molecules and cytoskeletal remodelling mechanisms in rodent lenses may lead to a better understanding of lens fibrosis *in situ* and may help find new alternative non-invasive treatments for fibrotic cataract.

ABBREVIATIONS AND ACRONYMS

Akt	Protein kinase B (PKB)
ANOVA	Analysis of variance
ASC	Anterior subcapsular cataract
α-SMA	Alpha-smooth muscle actin
ATMs	Anti-tropomyosin compounds
ATM-3507	Tpm3.1/3.2 targeted inhibitor
BCA	Bicinchoninic acid
β-merc	2-Mercaptoethanol
BMP	Bone morphogenetic protein
BSA	Bovine serum albumin
CLECs	Central lens epithelial cells
Co-Smad	Common Smad
DMSO	Dimethyl sulfoxide
ECLE	Extra capsular lens extraction
ECM	Extracellular matrix
EGF	Epidermal growth factor
EGFR	Epidermal growth factor receptor
EMT	Epithelial-to-mesenchymal transition
ERK	Extracellular signal-regulated kinase
FBS	Foetal bovine serum
FGF	Fibroblast growth factor
FGFR	Fibroblast growth factor receptor
GAPDH	Glyceraldehyde 3-phosphate dehydrogenase
HMW	High molecular weight
Hoechst	bisbenzimide H 33342 trihydrochloride dye
HRP	Horseradish peroxidase
HSPGs	Heparan sulfate proteoglycans
H_2O_2	Hydrogen peroxide
IGF	Insulin-like growth factor
IOL	Intraocular lens
imLECs	Immortalised lens epithelial cells
JNK	c-Jun N-terminal kinase
kDa	Kilodalton
KO	Knockout
LECs	Lens epithelial cells
LFCs	Lens fibre cells
LMW	Low molecular weight
MAPK	Mitogen-activated protein kinase
M199	Medium 199
NBF	Neutral buffered formalin
Nd:YAG	Neodymium-doped yttrium aluminum garnet
NGS	Normal goat serum
NT	Non-treated
OVE918/853	TGF-β1 mutant mice lines
PBS	Phosphate-buffered saline
PCO	Posterior capsule opacification
PCS	Post cataract surgery

PI3K	Phosphoinositide 3-kinases
PLECs	Peripheral lens epithelial cells
PVDF	Polyvinylidene difluoride
p38 MAPK	p38 mitogen-activated protein kinase
RTK	Receptor tyrosine kinase
SD	Standard deviation
SDS-PAGE	Sodium dodecyl-sulfate polyacrylamide gel electrophoresis
SEM	Standard error of the mean
SiRNA	Small interfering or silencing RNA
Skep	Skepinone-L
Smad	Small mothers against decapentaplegic
TBS	Tris-buffered saline
TBST	Tris-buffered saline with Tween-20
TG	Transgenic
TGF-β	Transforming growth factor-beta
TGF-βR	Transforming growth factor-beta receptor
Tm	Tropomyosin (old nomenclature)
Tpm	Tropomyosin (new nomenclature)
Tp7	Tpm3.1/3.2-deficient mice
Tp16	Tpm4.2-deficient mice
TR100	Tpm3.1/3.2 targeted inhibitor
WT	Wild type

LIST OF PUBLICATIONS

INCLUDED AS PART OF THIS THESIS

1. **Flokis, M.,** Lovicu, F.J., 2023. FGF-2 Differentially Regulates Lens Epithelial Cell Behaviour during TGF-β-Induced EMT. *Cells* 12, 827. https://doi.org/10.3390/cells12060827

NOT INCLUDED AS PART OF THIS THESIS

1. Lovicu FJ, Wishart TFL, Mao BP, **Flokis M,** Wazin F, Shu DY. The ocular lens epithelium: modelling growth factor signalling in physiological and pathological conditions. Advances in Medicine and Biology Volume 146 2019; 1-66.
2. Lovicu, F.J., **Flokis, M.**, Wojciechowski, M., Mao, B., Shu, D., 2020. Understanding Fibrotic Cataract: Regulation of TGFβ-Mediated Pathways Leading to Lens Epithelial to Mesenchymal Transition (EMT). The Journal of The Japanese Society for Cataract Research 32, 23–32. https://doi.org/10.14938/cataract.12-004.
3. Shu, D.Y., Ng, K., Wishart, T.F.L., Chui, J., Lundmark, M., **Flokis, M.**, Lovicu, F.J., 2021. Contrasting roles for BMP-4 and ventromorphins (BMP agonists) in TGFβ-induced lens EMT. Experimental Eye Research 206, 108546. https://doi.org/10.1016/j.exer.2021.108546.
4. Wishart, T.F.L., **Flokis, M.**, Shu, D.Y., Das, S.J., Lovicu, F.J., 2021. Hallmarks of lens aging and cataractogenesis. Experimental Eye Research 108709. https://doi.org/10.1016/j.exer.2021.108709.

PAPER AND POSTER PRESENTATIONS

INTERNATIONAL

Flokis M., Lovicu F.J. Fibroblast growth factor (FGF) potentiates transforming growth factor-beta (TGF-β)-induced EMT of lens epithelial cells in a spatially dependent manner. [Paper Presentation]. Association for Research in Vision and Ophthalmology (ARVO) 2021 Annual Meeting: Revolutionary Eye and Vision Research, May 2021 (Virtual: San Francisco, California, United States of America)

Flokis M., Lovicu F.J. FGF differentially regulates lens epithelial cell behaviour during TGF-β-induced EMT. [Paper Presentation]. International Conference on the Lens hosted by the National Foundation for Eye Research (NFER), December 2022 (Kona, Hawaii, United States of America)

Flokis M., Hook J., Hardeman E.C., Gunning P.W., Lovicu F.J. Characterisation of Tropomyosin activity in TGF-β-induced lens EMT. [Paper Presentation]. XXV Biennial Meeting of the International Society of Eye Research (ISER), February 2023 (Gold Coast, Queensland, Australia)

Wu Y., **Flokis M.,** Lovicu F.J. p38 MAPK in TGF-β-induced lens Epithelial Mesenchymal Transition. [Abstract for Poster Presentation]. Association for Research in Vision and Ophthalmology (ARVO) 2024 Annual Meeting: Revolutionary Eye and Vision Research, May 2024 (Seattle, Washington, United States of America)

LOCAL

Flokis M., Lovicu F.J. A role for Gremlin in TGF-β-induced epithelial-to-mesenchymal transition (EMT): A necessary antagonist? 19th Annual Bosch Young Investigators Symposium, November 2019 (Charles Perkins Centre, The University of Sydney)

Flokis M. Three-minute thesis (3MT): I see the light! Faculty of Medicine and Health Virtual Semi-Final Heats, July 2020 (The University of Sydney)

Flokis M, Lovicu F.J. A role for Gremlin in TGF-β-induced epithelial-to-mesenchymal transition (EMT): A necessary antagonist? [Twitter Presentation]. Australian Society for Medical Research (ASMR) NSW Annual Scientific Meeting, November 2020 (Virtual: New South Wales, Australia)

Flokis M. Three-minute thesis (3MT): Finding the light: The role of growth factors in cataract. Faculty of Medicine and Health Virtual Semi-Final Heats, July 2021 (The University of Sydney)

Flokis M. FGF differentially regulates TGF-β-induced lens EMT in a spatially dependent manner. [Paper Presentation]. 6th Annual Higher Degree Research (HDR) Save Sight Institute Symposium: Vision Science and Ophthalmology, November 2021 (The University of Sydney)

Flokis M. FGF differentially regulates lens epithelial cell behaviour during TGF-β-induced EMT. [Paper Presentation]. 7th Annual Higher Degree Research (HDR) Save Sight Institute Symposium: Vision Science and Ophthalmology, 3rd November 2022 (The University of Sydney)

AWARDS/GRANTS

INTERNATIONAL

2021: Association for Research in Vision and Ophthalmology (ARVO) International Lens and Cataract Virtual Travel Grant, USD$200

2022: Biennial National Foundation for Eye Research (NFER) International Conference on the Lens (ICL; Kailua-Kona, HI, USA) Young Investigator Travel Award, USD$2400

LOCAL

2019: Head of Discipline Prize for Best research presentation, University of Sydney, AUD$250

2019: 3rd Place, Oral Presentation at the 19th Annual Bosch Young Investigators Symposium, AUD$25

2019–2023: Research Training Program (RTP) Stipend Scholarship, AUD$27,596 pa

2020–2023: University of Sydney RTP Supplementary Scholarship, AUD$5,000 pa

2022: University of Sydney Postgraduate Research Support Scheme (PRSS), AUD$527.24

2022: University of Sydney Postgraduate Research Support Scheme (PRSS), AUD$512.50

2022: 2nd Place, Oral Presentation at the 7th Annual Higher Degree Research (HDR) Save Sight Institute Symposium, AUD$100

2023: University of Sydney Postgraduate Research Support Scheme (PRSS), AUD$1,060

TABLE OF CONTENTS

DECLARATION ..... **IV**
DECLARATION BY SUPERVISOR ..... **V**
ACKNOWLEDGEMENTS ..... **VI**
ABSTRACT ..... **VIII**
ABBREVIATIONS AND ACRONYMS ..... **IX**
LIST OF PUBLICATIONS ..... **XI**
PAPER AND POSTER PRESENTATIONS ..... **XII**
AWARDS/GRANTS ..... **XIII**

CHAPTER 1: GENERAL INTRODUCTION **1**
1.1 THE VISUAL SYSTEM **1**
1.2 THE OCULAR LENS **1**
1.2.1 Lens morphogenesis and development 3
1.3 REGULATION OF LENS HOMEOSTASIS **3**
1.3.1 Fibroblast growth factor (FGF) 5
1.3.2 Transforming growth factor-beta (TGF-β) 6
1.4 DYSREGULATION OF THE LENS **7**
1.4.1 Epithelial-to-mesenchymal transition (EMT) 7
1.4.2 Classification of EMT 10
1.5 CATARACT DEVELOPMENT **11**
1.6 PATHOGENESIS OF FIBROTIC CATARACT **12**
1.6.1 Anterior subcapsular cataract (ASC) 13
1.6.2 Posterior capsule opacification (PCO) 14
1.7 CATARACT TREATMENT AND PREVENTION METHODS **15**
1.8 GROWTH FACTOR INDUCED EMT **17**
1.8.1 The TGF-β paradox 17
1.9 GROWTH FACTOR DOWNSTREAM SIGNALLING **18**
1.9.1 FGF signalling pathways 18
1.9.1.1 FGF-induced MAPK/ERK1/2 signalling 19
1.9.2 TGF-β signalling 20
1.9.2.1 TGF-β-induced Smad-dependent signalling transduction 21
1.9.2.2 TGF-β-induced Smad-independent signalling during EMT 22
1.9.3 TGF-β-induced EMT in the lens 23
1.10 MODULATION OF LENS EMT: IMPLICATIONS FOR CATARACT PREVENTION **24**
1.11 p38 MAPK **25**
1.11.1 p38 MAPK family 25
1.11.2 Targeting TGF-β during EMT: A role for p38? 26
1.11.3 Targeted inhibition of p38 MAPK 27
1.12 TROPOMYOSIN **28**

1.12.1 Nomenclature, structure, and function 28
1.12.2 Tropomyosin in the lens 31
1.12.3 A role for Tropomyosin in fibrosis 33
1.12.4 Tropomyosin in lens fibrosis 34
1.12.4.1 Tpm1 lens-specific conditional knockout 35
1.12.4.2 Tpm2 CRISPR-Cas9 heterozygous knockout 35
1.12.4.3 Pharmacologically targeting or knocking Tpm3 36
1.13 RESEARCH AIMS AND OBJECTIVES 38
1.13.1 Hypothesis 1: Tropomyosin isoforms are differentially expressed and localised in the postnatal rodent lens 38
1.13.2 Hypothesis 2: Tpm3.1/3.2 and Tpm4.2 are required for TGF-β-induced lens EMT 38
1.13.3 Hypothesis 3: FGF-2 differentially regulates lens epithelia behaviour during TGF-β-induced EMT 39
1.13.4 Hypothesis 4: p38α MAPK activation is required during TGF-β-induced lens EMT 39

CHAPTER 2: GENERAL METHODOLOGY 40
2.1 ANIMALS AND TISSUE ACQUISITION 40
2.2 RODENT (RAT AND/OR MOUSE) LENS EPITHELIA EXPLANT SYSTEM 40
..... 41
2.3 TISSUE CULTURE 41
2.4 PREPARATION OF GROWTH FACTORS 41
2.4.1 Fibroblast Growth Factor-2 (FGF-2) 41
2.4.2 Transforming Growth Factor-beta 2 (TGF-β2) 41
2.5 GROWTH FACTOR TREATMENT 42
2.6 TPM3.1-SPECIFIC AND P38 MAPK INHIBITOR COMPOUNDS 42
2.7 ASSESSMENT OF CHANGES IN LENS EPITHELIA MORPHOLOGY 42
2.8 TGF-β1 TRANSGENIC MOUSE MODEL 42
2.9 OCULAR TISSUE PREPARATION FOR HISTOLOGY 43
2.10 IMMUNOFLUORESCENT LABELLING 43
2.10.1 Lens epithelia explants 43
2.10.2 Whole eye sections 44
2.11 PROTEIN QUANTIFICATION AND WESTERN BLOTTING ANALYSIS 44
2.11.1 Collection of lens epithelia protein from wholemount explants 44
2.11.2 Lysing of lens epithelia samples 45
2.11.3 Measuring total protein 45
2.11.4 SDS-PAGE and electrophoresis 45
2.12 STATISTICAL ANALYSIS 46
2.13 REAGENTS AND CONSTITUENTS 48

CHAPTER 3: EXPRESSION OF TROPOMYOSIN IN THE POSTNATAL RODENT LENS .. 51
3.1 INTRODUCTION 51
3.2 MATERIALS AND METHODS 52
3.2.1 Wistar rat tissue acquisition and cell culture 52

3.2.2 Growth Factor treatment 52
3.2.3 Immunofluorescence for rat LEC explants 52
3.2.4 Transgenic mice overexpressing TGF-β1 53
3.2.5 Immunofluorescence of WT and TG mice lens sections 53
3.2.6 Western blotting analysis 54
3.2.6.1 Collection of rat and mouse lens epithelia 54
3.2.6.2 Protein extraction and measurement of total protein 54
3.2.6.3 SDS-PAGE 54
3.2.7 Statistical analysis 55
3.3 RESULTS 56
3.3.1 Postnatal expression of Tropomyosin in the rat LEC explant system 56
3.3.2 In vitro fixative-dependent expression and localisation of Tpm in TGF-β2-induced rat lens EMT 59
3.3.2.1 Tropomyosin 1 60
3.3.2.2 Tropomyosin 2 62
3.3.2.3 Tropomyosin 3 63
3.3.2.4 Tropomyosin 4 65
3.3.3 Tropomyosin is elevated during rat lens TGF-β2-induced EMT in an isoform-specific manner 66
3.3.4 Tropomyosin expression in overexpressed TGF-β1-transgenic mice in vivo 70
3.3.4.1 Tropomyosin 1 70
3.3.4.2 Tropomyosin 2 73
3.3.4.3 Tropomyosin 3 74
3.3.4.4 Tropomyosin 4 76
3.3.5 Total Tpm protein expression of WT vs. 918 mice 78
3.3.6 Tropomyosin is a potential marker for fibre differentiation in rat LEC explants 80
3.4 DISCUSSION 83
3.4.1 Identification of Tpm isoforms during TGF-β2-induced lens EMT 83
3.4.1.1 High molecular weight Tpms: Tpm1 and Tpm2 84
3.4.1.2 Low molecular weight Tpms: Tpm3 and Tpm4 86
3.4.2 Identification of Tpm isoforms during FGF-2-induced fibre differentiation 87
3.4.3 Overexpression of TGF-β1 promotes Tpm isoform-specific reactivity in ASC 89
3.5 CONCLUSION 92

CHAPTER 4: CHARACTERISATION OF TROPOMYOSIN ACTIVITY IN TGF-β INDUCED LENS EMT 93
4.1 PREFACE 93
4.2 INTRODUCTION 94
4.3 MATERIALS AND METHODS 95
4.3.1 Wild type and Tropomyosin-deficient mice 95
4.3.2 Wistar rat LEC explants and Assessment of Cell Morphology 95
4.3.3 Preparation of Anti-Tropomyosin Compounds 95

4.3.4 Treatment of LECs with TGF-β2 and ATMs 95
4.3.5 Immunofluorescence of LEC explants 96
4.3.6 SDS-Page and Western blotting 96
4.3.6.1 Non-lens tissue collection and sample preparation 96
4.3.6.2 Lens tissue collection and sample preparation 96
4.3.6.3 SDS-PAGE electrophoresis 97
4.3.7 Statistical analysis 97
4.4 RESULTS 99
4.4.1 Tpm3.1/3.2 and/or Tpm4.2 are not required for TGF-β2 induced EMT 99
4.4.1.1 Phase contrast microscopy 99
4.4.1.2 Immunofluorescence 101
4.4.1.3 Western blotting 103
4.4.2 Confirmation of Tpm protein deficiency in Tpm KO mice 105
4.4.2.1 Wild type and Tpm-deficient whole organ tissue 105
4.4.2.2 Wild type and Tpm-deficient lens tissue 105
4.4.3 Tpm3.1/3.2 and Tpm4.2 are confirmed KO in lens epithelial cell explants using immunofluorescence 107
4.4.4 Elimination of Tpm3.1/3.2 and/or Tpm4.2 does not cause Tpm1 isoform compensation in Tpm KO mice 109
4.4.5 Inhibition of Tpm3.1/3.2 does not prevent TGF-β2-induced EMT in wildtype or Tpm4.2-deficient mice 113
4.4.5.1 Pharmacological inhibition of Tpm3.1/3.2 in WT mice 113
4.4.5.2 Pharmacological inhibition of Tpm3.1/3.2 in Tp16 mice lens epithelial explants 115
4.4.5.3 Inhibition of Tpm3.1/3.2 does not reduce EMT protein levels in WT or Tpm4.2-deficient TGF-β2-stimulated mice lens epithelial explants 117
4.4.5.4 Inhibition of Tpm3.1/3.2 does not lead to Tpm1 isoform compensation in lens epithelial cell explants 118
4.4.6 Inhibition of Tpm3.1/3.2 partially inhibits TGF-β2-induced EMT in the rat LEC explant model 120
4.4.6.1 ATM-5307 and/or TR100 impact on TGF-β2-induced rat lens EMT 120
4.5 DISCUSSION 124
4.5.1 Tpm3.1/3.2 is expressed in WT and Tpm4.2 deficient mice lens tissue 124
4.5.2 The absence of Tpm3.1/3.2 and/or Tpm4.2 does not impair TGF-β2-induced lens EMT .. 125
4.5.3 Loss of Tpm3.1/3.2 or Tpm4.2 does not lead to Tpm1 isoform compensation 127
4.5.4 Pharmacological inhibition of Tpm3.1/3.2 in lens epithelial explants differentially mediates TGF-β2-induced lens EMT 129
4.5.5 Tpm1.6/1.7 and Tpm2.1: Potential markers for TGF-β induced lens EMT 131
4.6 CONCLUSION 134

CHAPTER 5: FGF-2 DIFFERENTIALLY REGULATES LENS EPITHELIAL CELL BEHAVIOUR DURING TGF-β-INDUCED EMT 135
5.1 PREFACE 135
5.2 ABSTRACT 136

5.3 INTRODUCTION **137**
5.4 MATERIALS AND METHODS **139**
5.4.1 Animals and Tissue Culture 139
5.4.2 Lens Epithelial Explants 140
5.4.3 Assessment of Cell Morphology and Immunofluorescence 140
5.4.4 SDS-Page and Western Blotting 141
5.4.5 Statistical Analysis 142
5.5 RESULTS **144**
5.5.1 Induction and rate of progression of TGF-β2-induced lens EMT is dose dependent 144
5.5.2 FGF-2 promotes dose-dependent modulation of TGF-β2-induced EMT 146
5.5.3 FGF-2 promotes a spatially dependent TGF-β2-induced EMT response in lens epithelial explants 148
5.5.4 FGF-2 promotes spatial differences in labelling for EMT and fibre differentiation markers in TGF-β2-treated LECs 151
5.5.4.1 Immunofluorescent Labelling 151
5.5.5 A high dose of FGF-2 exacerbates EMT and fibre differentiation markers in TGF-β2-treated LEC explants 154
5.5.6 Protein expression in CLEC vs. PLEC lysates 155
5.5.7 Protein changes in wholemount LEC lysates 158
5.5.8 Impact of FGF-2 on TGF-β2-Mediated Intracellular Signalling 160
5.5.8.1 Nuclear Translocation of Smad2/3 160
5.5.8.2 Smad2/3-Signalling 162
5.5.8.3 MAPK/ERK1/2-Signalling 163
5.6 DISCUSSION **166**
5.7 CONCLUSION **172**

CHAPTER 6: THE ROLE OF p38α MAPK IN TGF-β INDUCED LENS EMT **173**
6.1 PREFACE **173**
6.2 INTRODUCTION **174**
6.3 MATERIALS AND METHODS **176**
6.3.1 Rodent tissue collection and primary cell culture 176
6.3.2 Preparation of p38α MAPK inhibitor compound 176
6.3.3 Treatment with TGF-β2 and Skepinone-L 176
6.3.4 Phase contrast microscopy 177
6.3.5 Immunofluorescence with LEC explants 178
6.3.6 Western blotting analysis 178
6.3.7 Statistical Analysis 179
6.4 RESULTS **180**
6.4.1 Skepinone-L inhibits TGF-β-induced EMT in rat LEC explants 180
6.4.1.1 Cell Morphology 180
6.4.1.2 EMT marker immunolocalisation in TGF-β2-induced LECs 182
6.4.1.3 Skepinone-L regulates Tpm1 and Tpm2 derived isoforms in TGF-β2-induced LECs 188

6.4.2 Pre-treatment with Skepinone-L does not impact TGF-β canonical Smad signalling 192
6.4.3 Cotreatment with Skepinone-L prevents TGF-β2-induced lens EMT 193
6.4.4 Skepinone-L inhibits p38 activation in TGF-β2-treated LECs 195
6.4.5 Post-treatment with Skepinone-L does not prevent TGF-β2-induced lens EMT 197
6.5 DISCUSSION 200
6.5.1 Tropomyosin and p38 MAPK 200
6.5.2 p38 MAPK is required for cell phenotypic changes during TGF-β-induced lens EMT 202
6.5.3 Early onset of Smad2/3 and p38 MAPK signalling during TGF-β-induced EMT 204
6.5.4 p38 MAPK signalling mechanisms in the eye lens 205
6.5.5 Transient immunolocalisation of p38 206
6.6 CONCLUSION 207
6.7 SUPPLEMENTARY FIGURES 209

CHAPTER 7: GENERAL DISCUSSION 212
7.1 TROPOMYOSIN: MARKERS FOR LENS FIBROSIS 213
7.2 THE INTERPLAY BETWEEN FGF-2 AND TGF-β2 DURING LENS FIBROSIS 218
7.3 p38 MAPK: AN EARLY MEDIATOR OF TGF-β-INDUCED EMT? 221
7.4 CLINICAL SIGNIFICANCE 223
7.5 CONCLUDING REMARKS 224

REFERENCES 225

APPENDIX 267
PEER-REVIEWED JOURNAL ARTICLE 267

CHAPTER 1: GENERAL INTRODUCTION

1.1 THE VISUAL SYSTEM

The eye is one of the most vital sensory organs of the mammalian body. As a highly active and specialised organ, the eye provides us with the ability to see and perceive the world around us. It is through the collaborative action of a variety of ocular structures that highlights the significance of the mammalian eye for vision and sensory perception.

1.2 THE OCULAR LENS

Within the eye, the lens is a transparent organ facilitating light refraction onto the retina. Structurally, the ellipsoidal/biconvex shape of the lens allows the eye to focus on close and far images, with the assistance and constant contractions of the ciliary musculature (Lovicu and McAvoy, 2005; Michael and Bron, 2011).

In situ, the avascular lens is located within the anterior compartment of the eye, suspended, and surrounded by the aqueous and vitreous humours (the ocular media) (Lovicu and McAvoy, 2005) (Figure 1.1 A). The intact ocular lens has an external thick basement membrane known as the lens capsule, that encases its cells (Gordon-Thomson et al., 1998). The distinct robust cellular architecture of the lens is specialized, since its cell types are not orientated towards external structures or microenvironments, and do not line a lumen (Martinez and de Iongh, 2010; Wang et al., 2010). Within the lens, two main cell types can be found: lens epithelial cells (LECs) and elongated lens fibre cells (LFCs).

Lens epithelial cells are characterised as a simple cuboidal monolayer situated in the anterior compartment of the lens, firmly anchored to the lens capsule (Figure 1.1B) (Gordon-Thomson et al., 1998; Wang et al., 2010). Unlike epithelia found in other systems, lens epithelia interact solely with the apical poles of LFCs. The apical-basal orientation of lens cells determines the characteristic polarity of the lens (Lovicu and McAvoy, 2005; Martinez and de Iongh, 2010). LFCs are located within the lens nucleus (core), as well as its lateral, anterior, and posterior sides (Lovicu and McAvoy, 2005). Throughout life, the maturing lens experiences a constant cycling of cells undergoing secondary fibre differentiation, to form the new populous of lens cells, consequently adding to the fibre mass around the lens nucleus, originating from the embryonic primary fibre cells (Kirby, 1927; Lovicu and McAvoy, 2005). The compartments in which these cell types reside can be spatially delineated anatomically by the lens equator; the zone of the lens fulcrum following the lens germinative and transitional zones (McAvoy, 1978).

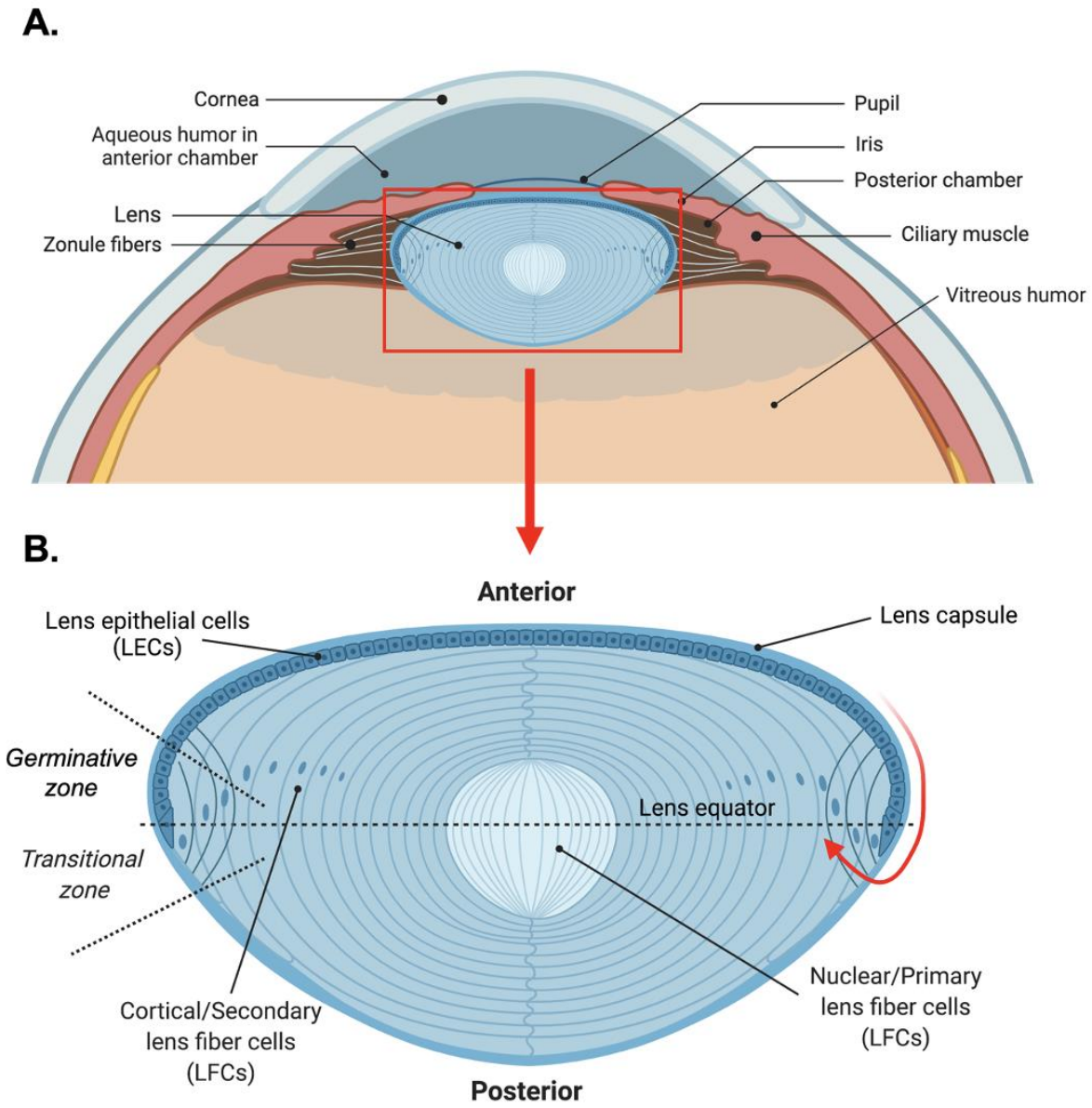

Figure 1.1. Anatomy of the Eye. A schematic sagittal section of the anterior compartment of the eye (A). The lens (B) is a transparent structure situated within this compartment and is surrounded by ocular media (aqueous and vitreous humor). There are two lens cell types that comprise the lens: a monolayer of cuboidal epithelial cells (LECs) and an internal mass of primary/nuclear and secondary/cortical fibre cells (LFCs). Throughout lens growth, LECs proliferate between the germinative and transitional zones of the lens to form secondary lens fibre cells. These secondary fibre cells elongate within the bow region (red arrow) and differentiate to form a dense mass within the lens nucleus. All lens cell types are encased within the lens capsule. Diagram created using *Biorender.com*.

1.2.1 Lens morphogenesis and development

Embryogenesis of the mammalian lens is marked by several key stages throughout its development. Many components of the mature ocular eye are derived from the embryonic ectodermal germ layer (Lovicu et al., 2011). During gestation, the head ectoderm is apposition to a pouch-like out-pocketing of the developing brain, the optic vesicle, the precursor of the neural retina (Li and Ding, 2016). The close contact between these two structures consequently results in a thickening of the surface ectoderm to form the lens placode (Robinson, 2006; Li and Ding, 2016). The placode invaginates, along with the optic vesicle, to create a lens pit, in conjunction with the formation of the optic cup (Robinson, 2006; Fuhrmann, 2008). As the lens pit increasingly deepens into the optic cup, it pinches off from the surface ectoderm, fusing at its anterior pole to form the lens vesicle, with the remaining surface ectoderm differentiating to develop the cornea (Lovicu and McAvoy, 2005). Between E12.5–E13.5, in the mouse, the lens vesicle separates and establishes two distinct cell types, according to their polar region; anterior lens vesicle cells will differentiate to form the lens epithelium and cells at the posterior pole of the lens vesicle will elongate anteriorly to form the primary lens fibre cells, losing the vesicle lumen in the process (Lovicu and McAvoy, 2005; Robinson, 2006).

Following lens formation, the maturation and maintenance of its growth and development relies on a constant cycle of epithelial cell proliferation and their subsequent differentiation into secondary fibre cells (Lovicu et al., 2011). Epithelial cell proliferation occurs largely at the germinative zone of the lens with the resultant migrating or being displaced through the transitional zone to differentiate into secondary lens fibres (de Iongh et al., 1996; Lovicu et al., 2011). A delineated bow region (demarcated by fibre cell nuclei) specifies secondary lens fibre cells elongating and moving from more cortical to nuclear regions to make up the lens fibre mass (de Iongh et al., 1996; McAvoy et al., 1999). This growth cycle continues throughout postnatal maturation to consistently form a larger, denser mass of lens fibres (Lovicu and McAvoy, 2005).

1.3 REGULATION OF LENS HOMEOSTASIS

Within the anterior compartment of the eye, the aqueous ocular media not only provides further refractive properties to assist with vision, but also promotes the regulation of normal lens biology. The complete immersion of the lens between these compartments, bathed by aqueous humour anteriorly and vitreous humour posteriorly, provides a molecular environment largely

responsible for the normal growth and development of the lens (Lovicu et al., 1995; Lovicu and McAvoy, 2005; Iyengar et al., 2009; Wang et al., 2010).

Over the years, the lens and its associated ocular tissues have been studied extensively elucidating the mechanisms by which its two lens cell types are formed, regulated, and maintained (Lovicu and McAvoy, 2005; Iyengar et al., 2009; Wang et al., 2010; Lovicu et al., 2011). In 1927, the first embryonic chick model was established, and it was concluded that LECs could be cultured *in vitro* under specified biological conditions (Kirby, 1927; Wang et al., 2017). Following studies have continued to adapt and investigate this model to provide insight into the nature of the ocular media and its influence on lens cell maintenance and growth (Philpott and Coulombre, 1965; Okada et al., 1971). As a result, it was proposed that factors within the ocular media were important in encouraging lens cell growth, and maintaining its distinct lens polarity, through a constant cell cycle of proliferation and differentiation (Philpott and Coulombre, 1965; Okada et al., 1971; Lovicu and McAvoy, 2005).

It is currently understood that the ocular microenvironment contains multiple growth factors and cytokines that promotes lens morphogenesis and maintains its normal homeostasis through regulating cellular processes such as proliferation and differentiation (McAvoy and Chamberlain, 1990; Arnold et al., 1993; Burren et al., 1996). Previous studies have identified and confirmed the importance of key growth factors and their associated families in regulation of lens and ocular tissue growth (McAvoy and Chamberlain, 1990; Lovicu et al., 2011). Growth factor families that have been shown to be influential in ocular cell growth and development include transforming growth factor-beta (TGF-β), bone morphogenetic protein (BMP), epidermal growth factor (EGF), hepatocyte growth factor (HGF), heparin-binding epidermal growth factor–like growth factor (HBEGF), platelet-derived growth factor (PDGF), vascular endothelial growth factor (VEGF), fibroblast growth factor (FGF), and insulin-like growth factor (IGF) (McAvoy and Chamberlain, 1990; Arnold et al., 1993; Wang et al., 2010; Shu et al., 2019b; Shu and Lovicu, 2019). An array of other growth factors, such as Wnts (Stump et al., 2003; Dawes et al., 2013), granulocyte-macrophage colony stimulating factor (GM-CSF), lens epithelium-derived growth factor (LEDGF), and nerve growth factor (NGF), have also been shown to be either present within the lens, ocular media, or influence the growth and development of other ocular tissues (McAvoy and Chamberlain, 1990; Fujimura, 2016).

Various rodent and human *in vitro* models have been adopted to study the regulation of lens cell proliferation and fibre differentiation via the activity of different growth factor families (Arnold et al., 1993; Ibaraki et al., 1995; Iyengar et al., 2009; Wang et al., 2010). Activation of

signalling mechanisms and pathways by growth factors identified in the aqueous and vitreous humour are responsible for LEC and LFC growth, and lens development (Ibaraki et al., 1995; Lovicu and McAvoy, 2005; Iyengar et al., 2009; Wang et al., 2010; Lovicu et al., 2011). Regulatory growth factors, such as TGF-β family members, EGF, FGF, and IGF, have shown to interact in an orchestrated fashion to influence normal lens polarity, cell maintenance, and growth (Lovicu and McAvoy, 2005; Iyengar et al., 2009; Martinez and de Iongh, 2010).

1.3.1 Fibroblast growth factor (FGF)

Fibroblast growth factor (FGF) is a potent growth factor regulating cell proliferation and normal tissue development in multiple systems (Le and Musil, 2001; Makrides et al., 2022). The FGF family consists of over 22 polypeptide members with similar structural components, found in both vertebrates and invertebrates, and each member has been previously reviewed (Yun et al., 2010; Teven et al., 2014; Farooq et al., 2021; Bollenbecker et al., 2023). All FGF family members have differential affinities for binding to tyrosine kinase FGF receptors (FGFRs); FGFR1–5, to enact downstream intracellular signalling cascades (Ornitz et al., 1996; Sarabipour and Hristova, 2016; Farooq et al., 2021).

Within the ocular media, FGF-1 (acidic) and FGF-2 (basic) isoforms are most potent and have been studied due to their inducive roles in cell processes, including proliferation, differentiation, migration, survival, and regeneration (Schulz et al., 1993, 1997; Chamberlain and McAvoy, 1997; Rio-Tsonis et al., 1997; Lovicu and McAvoy, 2001; Wormstone et al., 2001; Garcia et al., 2005; Iyengar et al., 2007). Due to high concentrations of both FGF isoforms within the aqueous and vitreous humours, there is a dose-dependent responsibility of FGF to potentiate these regulatory cell processes within the lens (McAvoy and Chamberlain, 1989; Schulz et al., 1993; Lovicu and McAvoy, 2001). Interestingly, *in vitro* FGF can induce both proliferation and differentiation in lens epithelial cells models (Lovicu and McAvoy, 1992, 2001; Iyengar et al., 2007, 2009; Wang et al., 2010; Dawes et al., 2014; Flokis and Lovicu, 2023) that mimics the fibre-specific responses and characteristics observed in lens fibre cells.

Lens cell proliferation and differentiation are associated with low to high concentrations of FGF, respectively (Schulz et al., 1993; Chamberlain and McAvoy, 1997; Lovicu and McAvoy, 2001; Iyengar et al., 2007; Flokis and Lovicu, 2023). Lens cell behaviour is reliant on an antero-posterior gradient of FGF that exists within ocular media, with a gradual increase in FGF activity from the aqueous to vitreous humour (Figure 1.2) (Schulz et al., 1993; Chamberlain and McAvoy, 1997). Evidently, FGF bioavailability is heightened below the equatorial region

of the lens (de Iongh et al., 1997; Robinson, 2006), supporting areas undergoing secondary fibre cell differentiation throughout lens development and postnatal growth (McAvoy et al., 1992).

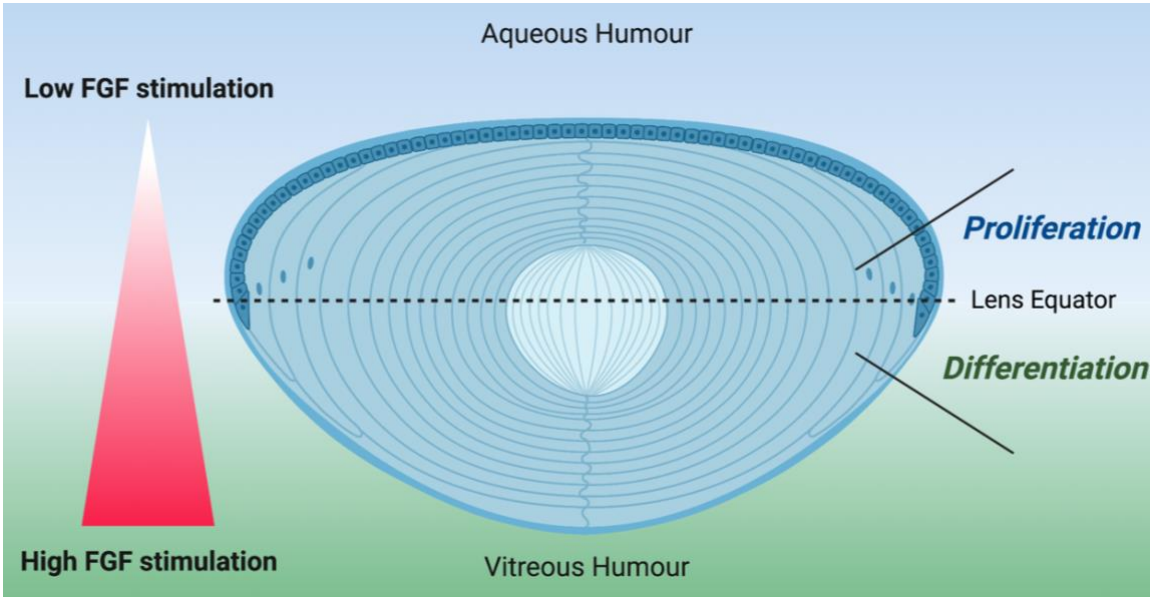

Figure 1.2. FGF concentration gradient in the ocular media. Diagram illustrating anterosuperior gradient of FGF concentrations in the aqueous and vitreous humour dictating postnatal lens cell behaviour. Anterior lens epithelial cells exposed to the aqueous humour (blue background) are stimulated with low concentrations of FGF to induce cell proliferation. Proliferating cells approaching the lens equator (dotted line) in the germinative zone will undergo a shift and migrate from epithelial to fibre cells in the transitional zone. This region below the lens equator, containing newly forming elongated fibre cells, has an increase in FGF stimulation due to high concentrations in the vitreous humour (green background). Pink triangle intensity indicates increased FGF stimulation *in vivo*. Diagram adapted from *(McAvoy and Chamberlain, 1989; Lovicu and McAvoy, 2005)* and created using *Biorender.com*.

1.3.2 Transforming growth factor-beta (TGF-β)

The transforming growth factor-beta (TGF-β) superfamily contains different growth factor sub-family members, that are all vital for regulatory cell behaviour. The TGF-β superfamily is made up of a variety of polypeptide family members such as TGF-β (originally termed Type β transforming growth factor), activin/inhibin, BMP, nodal, growth differentiating factor (GDF), as well as other members sharing homogenous structural properties (Massagué et al., 1987; Kingsley, 1994; Zhang, 2009). Each associated member contains a conserved cysteine knot and structural motif, formed by three disulfide bridges, archetypical of TGF-β superfamily (Miller et al., 1990; Derynck and Zhang, 2003). First discovered in the early 1980s, these secreted polypeptides were titled “transforming growth factors” due to their ability to promote cell

growth while facilitating morphological transformations (Sporn and Todaro, 1980; Sporn and Newton, 1981; Massagué, 1990).

In mammalian tissue types, the TGF-β protein has three main isoforms: TGF-β1, TGF-β2, and TGF-β3 (Massagué, 1990; Meng et al., 2016). All TGF-β isoforms are composed of homodimers and are required to be in their bioactive dimer form to bind to transmembrane serine/threonine kinase receptors, receptor type 1 (TGF-βRI or TGF-βR1) and type 2 (TGF-βRII or TGF-βR2) (Massagué, 1990, 2000). TGF-β ligand isoform binding to high affinity TGF-βR2 results in TGF-βR1 recruitment to activate downstream receptor signalling (Meng et al., 2016). In the aqueous and vitreous humours surrounding the lens, TGF-β isoforms and associated transmembrane receptors have been identified, with TGF-β1 and -β2 specifically expressed in the lens (Cousins et al., 1991; Gordon-Thomson et al., 1998; de Iongh et al., 2001a). Activation of TGF-β in homeostatic conditions requires tight regulation, in combination with other regulatory growth factors, for normal lens cell growth and maintenance.

1.4 DYSREGULATION OF THE LENS

Throughout maturation, the lens, like many other biological structures, undergoes fluctuations in normal cell maintenance and homeostasis in response to internal and external factors. Factors such as stress and inflammation have proven to cause an imbalance in the normal function of regulatory molecular mechanisms in the lens (Wormstone et al., 2008; Li and Ding, 2016). By unbalancing these regulatory scales in the lens and its associated microenvironment, cell dysregulation ensues leading to abnormal cellular behaviour and lens pathology. In fibrotic cataracts, a highly common cell response that occurs in the lens is the morphological shift of the normal LEC phenotype undergoing an epithelial-to-mesenchymal transition (EMT).

1.4.1 Epithelial-to-mesenchymal transition (EMT)

Epithelial-to-mesenchymal transition (EMT) is an occurrence marked by disrupting and altering the regulation of normal epithelial cell phenotypes and can be influenced by a variety of factors. This change occurs in response to an array of intracellular and extracellular conditions, such as oxidative stress or hypoxia, trauma, inflammation, elevated glucose levels, as well as increased upregulation of numerous regulatory growth factors (Zeisberg and Neilson, 2009; Das et al., 2016; Shu et al., 2017; Shu and Lovicu, 2017; Z. Han et al., 2018; Cui et al., 2020). First established by Trelstad and Hay in embryonic chick development (Trelstad et al., 1967; Hay, 1968), the originally termed epithelial-to-mesenchymal

transformation/transdifferentiation defines a biological modification of normal cell morphology as a direct response to biochemical and physiological propagators, encouraging a new mesenchymal-like cell type (Kalluri and Weinberg, 2009; Zeisberg and Neilson, 2009; Yang et al., 2020).

The EMT process is characterised by biochemical influences on apico-basal-polarised epithelia, that are adherent to their homeostatic extracellular matrix (ECM)-containing basement membrane (Kalluri and Weinberg, 2009; Tzanakakis et al., 2017). Firstly, the switching on of the mesenchymal phenotype causes tightly regulated and simple epithelia (cuboidal, columnar and/or squamous) to undertake a new identity by losing normal cell organisation and polarity, and undergo a morphological transformation through the removal of intercellular adhesion junctions (cell-to-cell dissociation) (Boyer et al., 2000; Kalluri and Neilson, 2003; Kalluri and Weinberg, 2009; Tzanakakis et al., 2017; Kopantzev et al., 2019). Epithelial cell remodelling and reorganisation of the ECM and cytoskeleton causes the formation of stress fibre actin filaments and cell protrusions, such as filopodia and lamellipodia, that survey the surrounding microenvironment to enact cell movement and migration (Kalluri and Neilson, 2003; Mattila and Lappalainen, 2008; Zhang, 2009; Kopantzev et al., 2019; Datta et al., 2021; Leggett et al., 2021). Enhanced cell migratory properties with the removal of epithelia anchorage to the basement membrane and ECM causes cells in transition to experience gradual morphological elongation and transdifferentiation into a myofibroblastic phenotype (Figure 1.3) (Shu and Lovicu, 2017; Tzanakakis et al., 2017). The concluding result is signalled

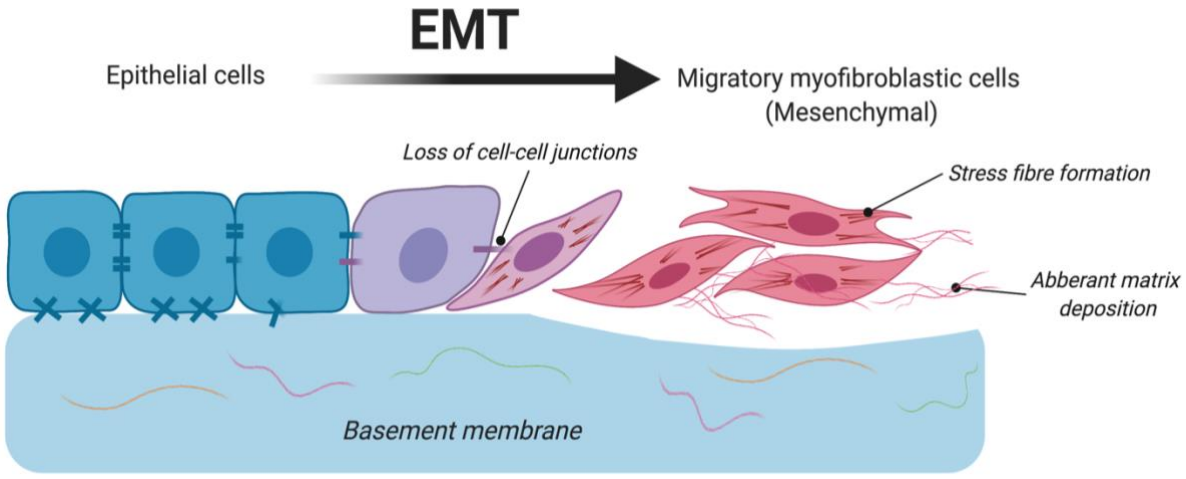

Figure 1.3. Epithelial-to-mesenchymal transition (EMT). Epithelial cells undergo morphological changes in response to external influences, thereby losing their cell-cell junction complexes and adherence to the basement membrane. Transitioning cells begin to change cell types from cuboidal to mesenchymal through acquiring migratory and contractile properties. As a result, newly transitioned and reprogrammed cells migrate from the basement membrane and produce aberrant ECM deposition. Schematic created using *Biorender.com*.

by newly formed, spindle-shaped mesenchymal cells that are highly invasive and migratory due to the removal of their basement membrane anchorage (Kalluri and Neilson, 2003; Tzanakakis et al., 2017; Yang et al., 2020). The final stage of the EMT process is signified by the degradation of the basement membrane that, in turn, induces an aberrant accumulation in ECM deposition (Figure 1.3) (Kalluri and Weinberg, 2009; Lamouille et al., 2014).

Although the EMT process is distinguished by clear endpoint morphological alterations of epithelial to mesenchymal cells, recent research has studied a hybrid/partial EMT phenotype in developmental, fibrotic, and morphogenetic processes (Jolly et al., 2015; Nieto et al., 2016; Tzanakakis et al., 2017; Yang et al., 2020). The epithelial/mesenchymal (E/M) hybrid phenotype encompasses cells in-between the transitional process, that have an acquired loss in epithelial properties, such as weak intercellular adhesion, while attaining cell migration properties characteristic of the mesenchymal phenotype (Jolly et al., 2015; Nieto et al., 2016). The plasticity of intermediate hybrid E/M cells denotes this phenotype as metastable, due to their ability to independently induce or invert EMT morphological changes (Jolly et al., 2015; Nieto et al., 2016; Tzanakakis et al., 2017; Yang et al., 2020).

During EMT, epithelial and glycoprotein markers associated with assisting intracellular adhesion and junctional complexes, such as β-catenin, E-cadherin, and zonula occludens-1 (ZO-1), are lost or downregulated due to aberrant cell migration and motility (Boyer et al., 2000; Kalluri and Neilson, 2003; Shu et al., 2017; Cui et al., 2020). Despite the loss of known epithelial markers, a key feature of the EMT process is the concurrent acquisition of myofibroblastic and specialised ECM transdifferentiation markers, particularly alpha-smooth muscle actin (α-SMA), collagen 1, fibronectin, N-cadherin, vimentin, as well as cytoskeletal marker Tropomyosin (Tpm) (Boyer et al., 2000; Bakin et al., 2004; Lamouille et al., 2014; Shu and Lovicu, 2017; Shu et al., 2017; Kopantzev et al., 2019). In addition, molecular and neural crest developmental studies using chick embryonic models investigated known regulatory transcription factors (EMT-TFs), such as *SNAI1* (*Snail1*), *SNAI2* (*Slug*), *TWIST1*, and zinc finger E-box-binding homeobox 1 (*ZEB1*) and *ZEB2* (or *SIP1*), that have demonstrated the ability to promote upstream EMT events (Nieto et al., 1994, 2016; Batlle et al., 2000; Bolós et al., 2002; Jolly et al., 2015; Cui et al., 2020; Yang et al., 2020). These factors are often called EMT transcription inhibitors since they are capable of direct/indirect suppression of gene transcription of known epithelial cell molecular markers, particularly E-cadherin (Shirakihara et al., 2011; Jolly et al., 2015; Cui et al., 2020; Yang et al., 2020).

1.4.2 Classification of EMT

To delineate the distinct characteristics of EMT in various systems, a model was proposed that classified three main subtypes of EMT (Kalluri and Weinberg, 2009; Zeisberg and Neilson, 2009). This model provides a guide to distinguish between physiological contexts and EMT responses that are naturally occurring or primitive, and those induced or involved in the development of pathological conditions (Kalluri and Weinberg, 2009; Lamouille et al., 2014). Although this model has proven advantageous in the classification of EMT, it has also raised discrepancies due to the various EMT phenotypic events that occur across various tissues, as well as differences in associated marker expression based on contextual tissue microenvironments (Yang et al., 2020).

The first class of EMT (Type 1) is associated with developmental processes due to epithelial transitioning and acquiring primary mesenchyme cells, and the associated phenotype, through neural crest migration, embryonic gastrulation, and organ development (Nieto et al., 1994; Boyer et al., 2000; Kalluri and Weinberg, 2009; Zeisberg and Neilson, 2009; Tzanakakis et al., 2017; Yang et al., 2020). Type 1 EMT is a non-invasive EMT event that does not require DNA sequence altering, which, as a result, often leads to the formation of secondary epithelia through inducing the reversal process of mesenchymal-to-epithelial transition (MET) (Kalluri and Weinberg, 2009; Yang et al., 2020). This is due to the advanced plasticity of preliminary epithelial cells during developmental events such as mesoderm formation and gastrulation, that can experience several morphogenic cycles of shifting between EMT to MET (Cui et al., 2020; Yang et al., 2020).

Type 2 EMT characterises fibroblastic cell types that are involved with pathological conditions such as wound healing, scarring, and organ fibrosis (Kalluri and Weinberg, 2009; Shu and Lovicu, 2017; Tzanakakis et al., 2017; Cui et al., 2020). This EMT type is elicited in response to inflammation and is responsible for recruiting cells for tissue regeneration/repair following injury or trauma (Kalluri and Weinberg, 2009; Zeisberg and Neilson, 2009). In the context of persistent inflammation during organ fibrosis, Type 2 EMTs can lead to organ degradation due to their inability to seize or mediate the origin of inflammatory insult (Kalluri and Weinberg, 2009; Zeisberg and Neilson, 2009).

Similar to the extreme Type 2 EMT circumstances, Type 3 EMT is attenuated by an inability to modulate inflammatory insult, thereby causing further organ injury. As a result, Type 3 EMT cells become metastatic due to their increased and persistent invasiveness, often leading to carcinoma manifestation (Kalluri and Weinberg, 2009; Tzanakakis et al., 2017). This primary

tumour and carcinoma progression process occurs due to increased cell motility and migration, where epithelial phenotypes are lost and an amass of mesenchymal cells is acquired (Kalluri and Weinberg, 2009; Shu and Lovicu, 2017; Cui et al., 2020). Another characteristic of Type 3 EMT is evidently the increased stimulation and overproduction of ECM proteins, such as collagen types I, III, and XVIII, and fibronectin, that have proven to increase cancer progression (Shu and Lovicu, 2017; Tzanakakis et al., 2017).

Overall, EMT is considered a paradigm due to its beneficial role in embryonic development, and wound healing, yet can be detrimental to cells in the wrong microenvironment, often leading to fibrosis and other pathologies (Yang et al., 2020).

1.5 CATARACT DEVELOPMENT

Cataract as a pathological condition of the lens is considered to be the leading cause of blindness worldwide, particularly in third world countries that have minimal, if any, access to suitable healthcare and treatment (Kleiman, 2012; Khairallah et al., 2015; Liu et al., 2017). This ocular pathology is marked by opacification of the once transparent lens due to densely packed lens fibres and/or aberrant ECM deposition, preventing its refractile function of focusing light onto the retina (West-Mays et al., 2009; Michael and Bron, 2011).

There are numerous types of cataracts that are dictated based on their location within the lens and/or age-related circumstances (see Table 1.1). The most prevalent cataractogenesis (cataract formation) cases arise from an array of causes, such as inflammation, oxidative stress, diet, ultraviolet (UV) radiation, and eye trauma (West-Mays et al., 2009; Michael and Bron, 2011; Kleiman, 2012; Das et al., 2016; Liu et al., 2017; Wishart et al., 2021). Circumstantial and age-related cataract are caused as a result of inherited or congenital factors and maturation (Michael and Bron, 2011; Khairallah et al., 2015).

Table 1.1. Classification of Cataract

Age-related and congenital cataracts		
Type	**Occurrence**	**Characterisation**
Juvenile	Congenital (before birth) Acquired (developed after birth) Genetic abnormality/disorder	Visual axis opacification (VAO) following cataract surgery (Khokhar et al., 2017)
Senile	Age-related (>50 years of age)	Development of Cortical or Nuclear cataract (Chylack and Cheng, 1978; Garner and Spector, 1980; Segev et al., 2005)
Secondary	Ocular injury Ocular disease Unhealthy lifestyle choices (e.g. smoking, diet, UV exposure) Prolonged radiation exposure (low-dose and high-dose) Post-surgery complications	Small vacuoles and opaque sheen along posterior capsule (Kleiman, 2012) PCO developed post cataract surgery
Cataract types based on location		
Type	**Cell types affected**	**Characterisation**
Cortical	Lateral cortical LFCs	'Shades' phenomena; radial or circular opaque shapes. Minute spherical dots (Michael and Bron, 2011)
Nuclear (sclerotic)	Nuclear LFCs	Onset development: yellow-brown opaque appearance Advanced development: blackened opaque appearance (Michael and Bron, 2011)
Subcapsular	LECs	Opacification of anterior monolayer sheet and posterior capsule

LECs: Lens epithelial cells, LFCs: Lens fibre cells, PCO: Posterior capsule opacification

1.6 PATHOGENESIS OF FIBROTIC CATARACT

Despite the various delineations of cataract subtypes, the prevalent causation of cataract is through the development of fibrosis in response to ocular inflammation or stress, as well as an array of cytokines (Kalluri and Neilson, 2003; Jiang et al., 2018). In the lens, the primary form of fibrotic cataract is commonly known as anterior subcapsular cataract (ASC) (Figure 1.4).

1.6.1 Anterior subcapsular cataract (ASC)

Anterior subcapsular cataract (ASC) impacts the epithelial monolayer situated within the anterior lens capsule, preventing its physiological function of light refraction. ASC is characterised by dysregulated LECs that have altered morphologically and results in the acquisition a fibre-like cell phenotype (Shu et al., 2017). These built-up masses of multi-layered, myofibroblastic cells encourages an aberrant accumulation of ECM deposition (de Iongh et al., 2005; Lovicu et al., 2015; Shu et al., 2017).

In moderate and/or severe cases of primary fibrotic cataract, surgical intervention is an option offered to patients to remove, minimise, or potentially mediate further cataract development. Phacoemulsification is the most common cataract surgical procedure involving the insertion of a biconvex intraocular lens implant (IOL) following lens content removal (Vasavada and Praveen, 2014; Liu et al., 2017; Jiang et al., 2018). Initially, a small corneal incision is made to access the underlying lens, that is then opened at the anterior capsule through continued curvilinear capsulorhexis (CCC) (Liu et al., 2017). Developed by Howard Gimbel, this anterior capsulotomy technique involves continual stretching and a circular opening of the capsule to prevent unwanted tears (Gimbel and Neuhann, 1991). By leaving an intact capsular bag, a barrier is created to prevent unsolicited vitreous leakage, as well as acting as a supportive vessel for IOL implantation (Gimbel and Neuhann, 1991; Liu et al., 2017). Following the removal of the ASC plaque using capsulohexis, a balanced salt solution is injected into the lens (hydrodissection) to facilitate further plaque dislodging from the leftover capsular bag (Liu et al., 2017; Jiang et al., 2018). Following this, an emulsifying device is inserted to irrigate and break up the remaining lens contents for aspiration removal (Liu et al., 2017). The extraction of cataractous lens material allows for a monofocal, foldable silicone or acrylic IOL to be implanted into the remaining lens capsular bag (Vasavada and Praveen, 2014; Liu et al., 2017). The use of foldable IOLs is both convenient and beneficial, due to the sensitive nature of cataract surgery, as these materials superseded previously used non-foldable polymethylmethacrylate (PMMA) lens implants, thereby reducing the likelihood for post-surgical complications (Vasavada and Praveen, 2014; Liu et al., 2017). For structural support and suspension, IOLs have protruding haptic hooks to situate the IOL within the lens capsular bag (Gimbel and Neuhann, 1991; Liu et al., 2017). Overall, this cost-effective surgical procedure has proven beneficial for increasing the quality of life for patients, through enhancing visual acuity as well as correcting existent refractive errors, and minimising astigmatism (Liu et al., 2017; Shihan et al., 2019).

Despite the advantageous benefits and success rates of undergoing cataract surgery, the attempt to remove all residual LECs from the compromised lens often proves futile, due to their strong anchorage to the lens capsule (Shu and Lovicu, 2017). As a result, any residual LECs can transdifferentiate into new myofibroblasts and migrate posteriorly over the lens capsule (Figure 1.4) (Shu and Lovicu, 2017). In most cases, this migration of transdifferentiated cells promotes the formation of a secondary fibrotic cataract known as posterior capsule opacification (PCO) (Batur et al., 2016; Shu et al., 2017).

1.6.2 Posterior capsule opacification (PCO)

Posterior capsule opacification (PCO) is one of the most common post cataract surgery (PCS) complications that occurs in patients worldwide. In most instances, PCO onset is often delayed in patients, as it commonly occurs within 2–5 years PCS (Mansfield et al., 2004; Wormstone et al., 2008; Karahan et al., 2014). Residual LECs following cataract surgery can cause two types of PCO, regenerative/pearl-like and fibrotic, that occur in different posterior compartment regions of the lens (Kalluri and Weinberg, 2009; Shihan et al., 2019). Pearl-like PCO is derived from residual LECs that can result in cell regeneration of aberrant fibre cells, leading to a pearl-like clouding or cataract at the equatorial region of the lens, causing two visual impairment phenomena, Elschnig's pearls and Soemmerring's ring (Buehl et al., 2004; Mansfield et al., 2004; Wormstone et al., 2008, 2020; Boswell et al., 2017; Shihan et al., 2019; Konopińska et al., 2021). The inability to remove residual ASC-affected LECs, due to peripheral attachment to IOL implants, as well as intraoperative inflammation, re-ignites and intensifies aberrant LEC transdifferentiation (Kleiman, 2012; Liu et al., 2017; Shu and Lovicu, 2017; Jiang et al., 2018). As a result, fibrotic PCO or posterior capsular plaque formation (scar tissue) is created by the migration of morphologically altered LECs, characterised as a form of Type 2 fibrotic EMT, to the posterior region of the lens (Kalluri and Weinberg, 2009; Nieto et al., 2016; Liu et al., 2017; Yang et al., 2020). Once migrated, these differentiated cell types begin to contract and create capsular folds or wrinkling, thus causing light scattering, decreased visual acuity, and impairing overall vision (Mansfield et al., 2004; Martinez and de Iongh, 2010; Vasavada and Praveen, 2014; Shu et al., 2017; Jiang et al., 2018).

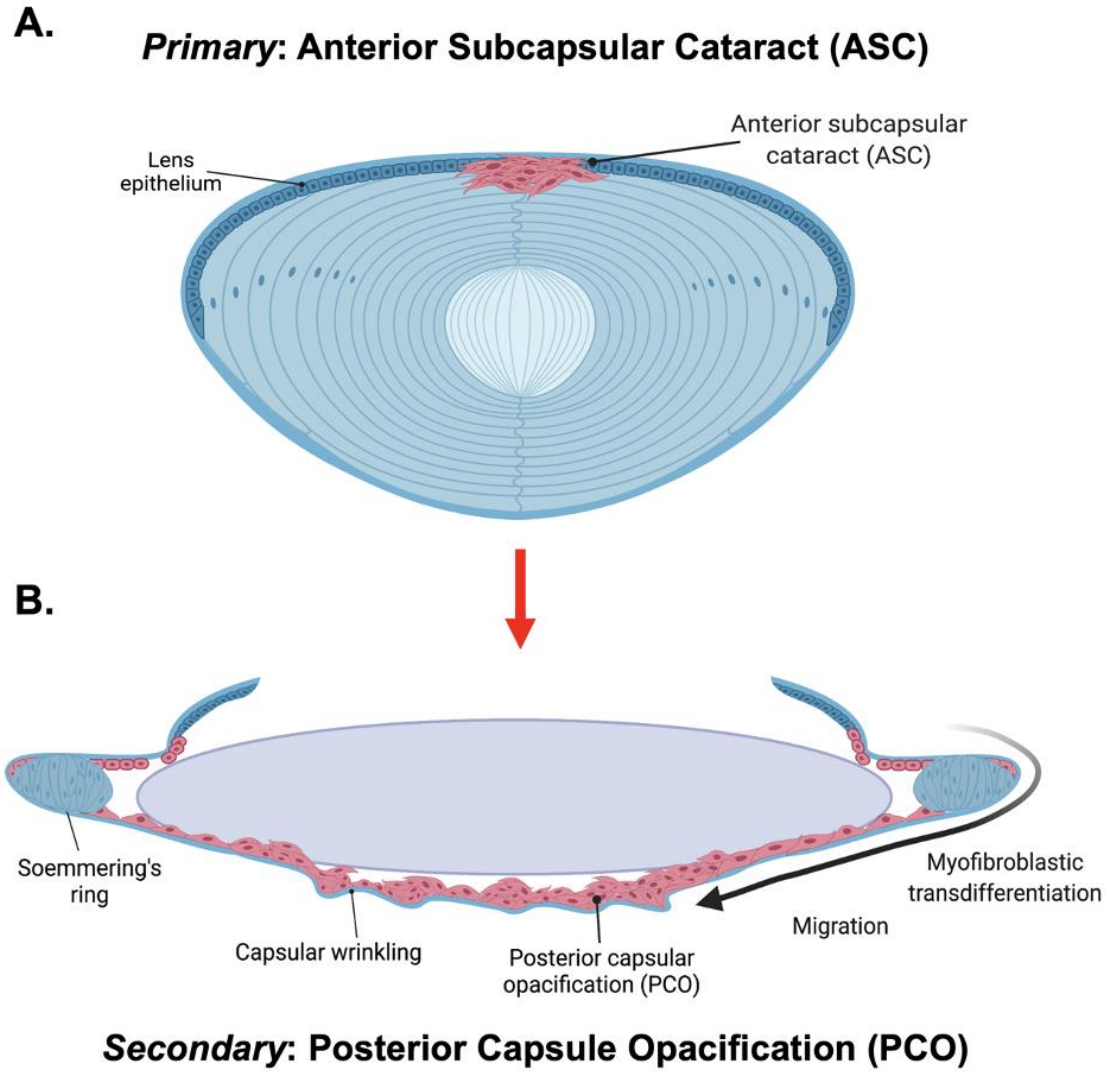

Figure 1.4. Fibrotic Cataract. A) The formation of a fibrotic plaque in the anterior compartment of the lens, impacting the lens epithelium, is known as an anterior subcapsular cataract (ASC). B) Treatment of ASC through surgical intervention whereby the plaque and epithelium are removed and replaced with an intraocular lens implant (IOL, purple circle). Post cataract surgery, in some cases, residual cells activated by TGF-β (pink cells) will begin to migrate to undergo an epithelial-myofibroblastic transdifferentiation. These newly contractile cells will accumulate at the posterior capsule bag, causing capsular wrinkling, and a plaque known as fibrotic posterior capsule opacification (PCO). A second type of PCO, pearl-like or regenerative (light blue cells), occurs at the equatorial region of the lens due to a deposit of aberrant fibre cells. Schematic created using *Biorender.com*.

1.7 CATARACT TREATMENT AND PREVENTION METHODS

Despite the onset of PCS side effects and secondary fibrotic cataract, previous and current studies are testing a variety of preventative methods and treatments to manage or limit the effects of this complication. Most commonly, Neodymium-doped yttrium aluminum garnet (Nd:YAG) treatment using a non-invasive laser can remove the PCO (Karahan et al., 2014; Vasavada and Praveen, 2014). During treatment, the YAG infrared laser is directed towards the

posterior capsule for tissue photo-disruption, that frees a sector around the visual or optical axis of the eye (Vasavada and Praveen, 2014). Although costly, this treatment has proven to be beneficial for patients suffering decreased visual acuity as a result of PCO (Karahan et al., 2014; Liu et al., 2017; Shihan et al., 2019). Nd:YAG has not been implemented as routinely for the majority of paediatric and juvenile patients, due to the fear of potential long-lasting damage (Karahan et al., 2014; Shihan et al., 2019). Among the common side effects of the Nd:YAG laser are uncontrolled inflammation and irritation, retinal detachment, IOL damage or its dislodgement, and oedema (Karahan et al., 2014; Batur et al., 2016; Liegner et al., 2017; Shihan et al., 2019).

There has been an increase in experimentation to prevent PCO, from introducing novel IOL designs, alternative materials to develop IOLs, and surgical procedures required for cataract treatment. For example, studies have investigated the potential use of a sharp-edged silicone (Buehl et al., 2004) or polymethyl methacrylate (PMMA) (Joshi and Rasal, 2023) IOLs to minimise PCO onset in adults, due to the sharp-edged design obstructing and reducing lens epithelial cell migration to the posterior lens capsule (Findl et al., 2010; Vasavada and Praveen, 2014; Shihan et al., 2019). However, this IOL design led to the development of pseudophakic dysphotopsia in numerous patients: a combination of positive (e.g. halos or flashes of light, glare phenomenon) and negative (e.g. peripheral shadows) unwanted visual symptoms (Ellis, 2001; Buehl et al., 2004; Findl et al., 2010; Liu et al., 2017; Hu et al., 2018; Shihan et al., 2019; Pusnik et al., 2022). Another treatment example is the use of a post-operative, dropless cataract procedure whereby a solution containing combined antibiotics and corticosteroids are injected intravitreally following IOL implantation (Liegner et al., 2017; Liu et al., 2017). This treatment, compared to the routine self-administration of anti-inflammatory (NSAID) drops following surgery, has proven to reduce the amount of PCS inflammation (Vasavada and Praveen, 2014; Liegner et al., 2017; Liu et al., 2017). Despite a lowered acute inflammation following administration, to date, none of these drug-administering therapies are successful in modulating the induction of other ocular pathologies, such as glaucoma, as well as the eventual regeneration of fibrotic cataract and PCO (Khairallah et al., 2015; Liu et al., 2017; Shihan et al., 2019).

Overall, the past decade has seen a rapid increase in the rate of cataract surgeries undertaken globally in response to ageing populations (Khairallah et al., 2015). Despite various attempts to minimise the onset of primary cataract and secondary fibrotic onset, further testing and experimentation is required to develop more efficient, cost-effective, and less-harmful therapeutic agents.

1.8 GROWTH FACTOR INDUCED EMT

In numerous systems, stress and inflammation have proven to be key catalysts for upregulating growth factors that are known to induce or propagate an EMT response. Mediation of EMT has been accredited to the potentiation of various mechanisms and growth factors, particularly TGF-β (Xu et al., 2009; Boswell et al., 2017; Z. Han et al., 2018; Lovicu et al., 2020), FGF (Cerra et al., 2003; Kubo et al., 2017, 2018), HGF (Choi et al., 2004), IGF (Cevenini et al., 2018), and EGF/EGFR (Konturek et al., 1995; Shu and Lovicu, 2019), acting through different downstream signalling mechanisms involving Smad2/3 (Valcourt et al., 2005; Dawes et al., 2009; Li et al., 2011; Walton et al., 2017), MAPK (ERK1/2, p38 MAPK, JNK) (Boswell et al., 2017; Wojciechowski et al., 2017, 2018; Hou et al., 2021), PI3K/Akt (Nakanishi et al., 2014), and Wnt and Notch (Chong et al., 2009; Bao et al., 2012; Jiang et al., 2023). These growth factors can upregulate downstream EMT-TFs, such as *Snail* and *Zeb*, to suppress epithelial transcription factor marker expression and thereby promote an EMT (Jolly et al., 2015; Cui et al., 2020). While research into different growth factors and their respective signalling pathways has solidified their role in EMT induction, it is the TGF-β superfamily member, TGF-β, that is most widely researched for its primary influence in driving EMT (Cevenini et al., 2018).

1.8.1 The TGF-β paradox

The mechanisms of TGF-β signalling have been aptly termed the TGF-β paradox due to its multifaceted functions in both normal cell regulation, as well as promoting carcinoma and tumourigenesis (Morrison et al., 2013; Zhang et al., 2014). During the mid 1990s, Miettinen et al. (1994) investigated the role of TGF-β in the transdifferentiation of normal epithelia to mesenchyme cells, concluding that TGF-β is essential for the induction and propagation of all EMT types (Miettinen et al., 1994; Cui et al., 2020). Since the discovery of this TGF-β-induced EMT phenomenon, studies have tried to understand the actions of TGF-β. The presence of TGF-β in different developmental microenvironments, such as the lung (Li et al., 2008; Saito et al., 2018) or embryo (Roelen et al., 1994; Olivey et al., 2003), is essential for regulating non-invasive Type 1 EMT and organogenesis. Despite this, aberrant or overexpression of TGF-β, particularly TGF-β2, often leads to EMT in numerous fibrotic and late-stage carcinoma models where it promotes cell migration, invasiveness, and metastasis (Inatani et al., 2001; de Iongh et al., 2005; Cui et al., 2020). In short, TGF-β can switch between positive and negative cell regulation, depending on its bioavailability, signalling activation, and tissue microenvironment contexts.

1.9 GROWTH FACTOR DOWNSTREAM SIGNALLING

1.9.1 FGF signalling pathways

FGF is largely dependent on MAPKs for signalling activation, particularly MEK, extracellular signal-regulated kinase 1 and 2 (ERK1/2), p38 MAPK, and c-Jun N-terminal kinase (JNK) family members (Tan et al., 1996; Powers et al., 2000; Sørensen et al., 2008; Teven et al., 2014; Farooq et al., 2021). Aside from the Ras-Raf-MAPK signalling pathway, FGF can also activate downstream signalling through PLCγ and PI3K/Akt pathways, as previously reviewed (Teven et al., 2014; Ornitz and Itoh, 2015; Farooq et al., 2021). MAPK/ERK1/2 signalling activation is of most interest given its influential role during FGF-induced normal lens cell proliferation, differentiation, and survival (Le and Musil, 2001; Lovicu and McAvoy, 2001; Robinson, 2006; Iyengar et al., 2007, 2009; Wang et al., 2008). ERK1/2 has been shown to mediate different lens cell responses that are highly dependent on the levels and/or duration of its activation (phosphorylation) (Iyengar et al., 2007). Although both MAPK/ERK1/2 and PI3K/Akt signalling are required during FGF-induced LEC proliferation and regulatory mechanisms (Lovicu and McAvoy, 2001; Weber and Menko, 2006; Wang et al., 2008; Iyengar et al., 2009), we will focus on the cascade downstream mechanisms surrounding only MAPK/ERK1/2 signalling (Figure 1.5).

1.9.1.1 FGF-induced MAPK/ERK1/2 signalling

FGF signal transduction requires ligand binding to high affinity RTKs that dimerise, and in certain conditions, involve the ECM, or cell surface heparin sulfate proteoglycans (HSPGs), to trigger a series of downstream signalling pathways (de Iongh et al., 1997; Schulz et al., 1997; Robinson, 2006). Besides FGFRs, HSPGs are often referred to as co-receptors for FGF, assisting ligand recruitment to high affinity receptor domains and, in some instances, mediating FGF signalling independent of its FGFRs (Zhang et al., 2003, 2009; Chua et al., 2004; Forsten-Williams et al., 2008). Each FGFR is comprised of several delineated regions, including the extracellular (immunoglobulin-like ligand binding domain, I–III), transmembrane, and

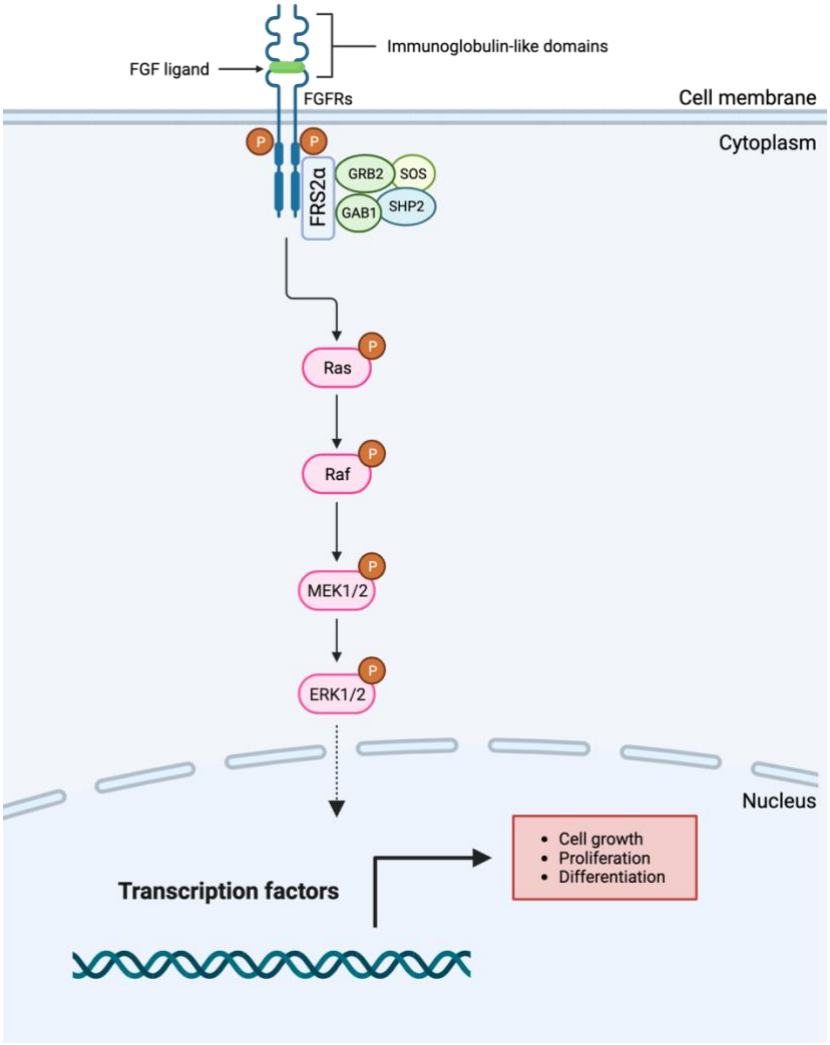

Figure 1.5. A simplified diagram of FGF-induced MAPK signalling. Fibroblast growth factor (FGF) ligands bind to immunoglobulin-like domains along two FGF receptor tyrosine kinases (FGFRs). An FRS2 complex forms at the intracellular domain, consisting of FRS2α, GRB2, GAB1, SHP2, and SOS. Once activated or phosphorylated (orange "P"), the FRS2 complex activates Ras-Raf-MAPK (pink) downstream signalling. Phosphorylated ERK1/2 translocates into the nucleus and activates transcription factors responsible for cell proliferation and differentiation. Diagram created using *Biorender.com*.

intracellular (tyrosine kinase) domains (Powers et al., 2000; Farooq et al., 2021). Following FGFR dimerisation, FGFRs undergo auto- or transphosphorylation at tyrosine kinase (TK) domains, where a docking protein, fibroblast growth factor receptor substrate 2 alpha (FRS2α) activates and recruits downstream molecules to transduce various pathways (Powers et al., 2000; Lax et al., 2002; Teven et al., 2014). Following the complex of FRS2 with GRB2, GAB1, SHP2, or SOS at the TK domains, MAPK signalling is initiated (Dailey et al., 2005; Teven et al., 2014). GRB2 and SOS are recruited to FRS2 that leads to the activation (phosphorylation) of the Ras substrate (Ornitz et al., 1996; Ornitz and Itoh, 2015). Ras experiences a cycling switch between active (GTP) to inactive (GDP) forms before the activation of Raf at its N-terminal domain (Schlessinger, 2000; Tsang and Dawid, 2004; Wang et al., 2008). Following this, a cascade of phosphorylation occurs, initiating at MAPK-kinase 1 and 2 (MAPKK, MEK1/2) to ERK1/2 (Turner and Grose, 2010; Ornitz and Itoh, 2015; Xie et al., 2020). Translocation of active ERK1/2 into the nucleus switches on genes required for cell proliferation and differentiation (Lovicu and McAvoy, 2001; Ochi et al., 2003; Iyengar et al., 2006).

1.9.2 TGF-β signalling

TGF-β signal activation is a vital mechanism for the regulation and mediation of EMT. To enact TGF-β influenced cell responses, both Smad-dependent (canonical) and Smad-independent (non-canonical) signalling pathways can be activated (Figure 1.6) (Moustakas and Heldin, 2005; Zhang, 2009; Shu et al., 2017; Cui et al., 2020). TGF-β signalling is tightly regulated by pre- and post-transcriptional factors to influence cell processes and fates (Nalluri et al., 2015). To commence, the homodimer TGF-β ligands affiliate and bind to the extracellular cysteine-rich domain of two transmembrane receptors that form the TGF-β receptor complex: type 1 (TGF-βRI) and type 2 (TGF-βRII) (Massagué, 1990, 2000; Cui et al., 2020). TGF-β receptors are serine/threonine kinases known for their promiscuity and specificity in facilitating ligand/receptor interactions (Moustakas and Heldin, 2005; Aykul and Martinez-Hackert, 2016). This is due to the unique nature of TGF-β ligands that have varying affinities for various receptors. Following ligand/receptor binding, TGF-βRII autophosphorylates to facilitate subsequent recruitment and transactivation of TGF-βRI, to form a phosphorylated and active heterodimerised receptor complex (Massagué, 1990; Bierie and Moses, 2009).

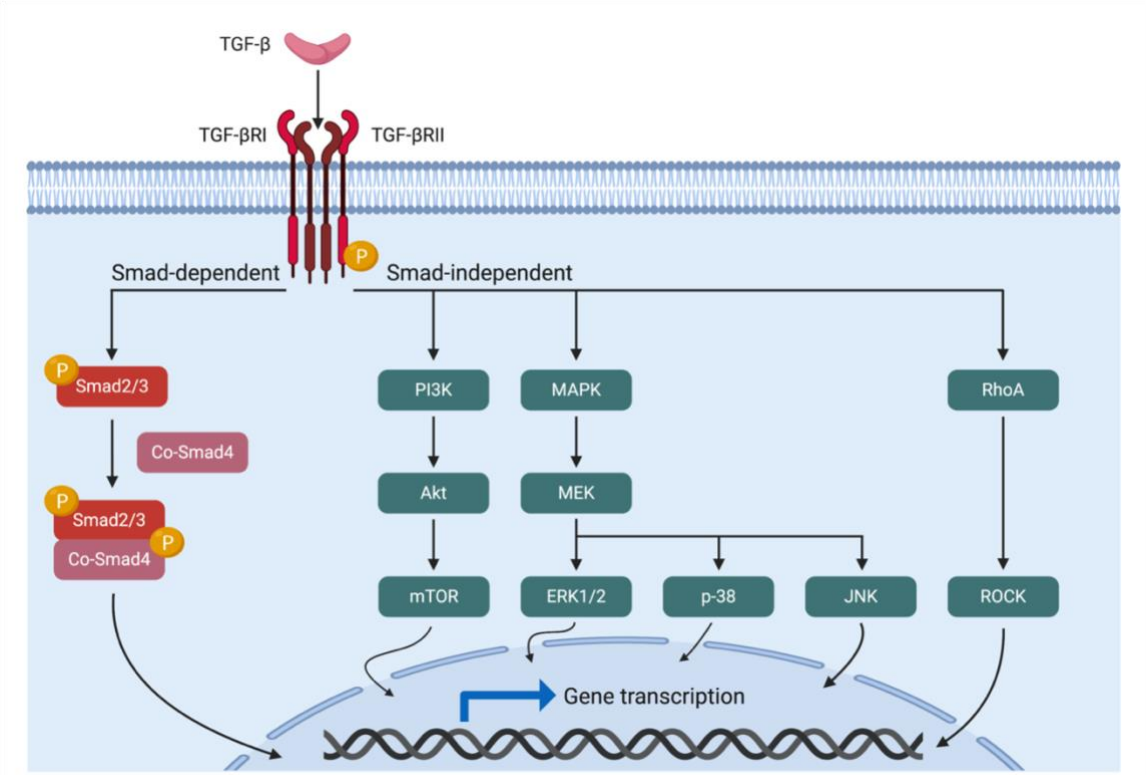

Figure 1.6. TGF-β signalling. Following TGF-β ligand binding to transmembrane receptors (TGF-βRI and TGF-βRII), the receptor heterodimerised complex is phosphorylated (orange "P") and activates either canonical (Smad dependent, red) or non-canonical (Smad independent, green) downstream signalling. Schematic created using *Biorender.com*.

1.9.2.1 TGF-β-induced Smad-dependent signalling transduction

For Smad-dependent pathways, following the phosphorylation of the TGF-β receptor complex, intracellular effector proteins known as regulatory, or receptor activated Smads (r-Smad), particularly Smad2 and Smad3 (Smad2/3), relay signals for downstream mechanism activation (Massagué, 2000; Zi et al., 2012). Smad2/3 complexing with a common mediator Smad (Co-Smad4) facilitates nuclear translocation (Figure 1.6) (Massagué, 2000; Derynck and Zhang, 2003). As a result, the MH1 domain on phosphorylated Smad2/3/4 complex binds to a respective DNA site, as well as other co-factors, to switch on target genes (Massagué, 2000; Massagué et al., 2005; Zhang, 2009; Cui et al., 2020). Smad activation regulates transcription factors from the Snail, ZEB, and bHLH families, for the purpose of encoding proteins responsible for initiating or inhibiting cell processes, such as cell survival, proliferation, differentiation, and EMT, as has previously been reviewed (Massagué, 2000; Derynck and Zhang, 2003; Massagué et al., 2005; Zi et al., 2012; Cevenini et al., 2018; Kamato et al., 2020). In addition, the linker region of Smad2 and Smad3, and their associated phosphorylation site,

has been the subject of numerous studies investigating the direct/indirect signalling modulation of TGF-β activity (Matsuzaki, 2012; Ooshima et al., 2019; Kamato et al., 2020).

1.9.2.2 TGF-β-induced Smad-independent signalling during EMT

Due to the diverse nature of TGF-β, Smad-independent signalling cascades are also initiated to mediate TGF-β-induced cellular activity and associated responses, particularly proliferation, migration, EMT, and apoptosis, as previously reviewed (Moustakas and Heldin, 2005; Zhang, 2009; Heldin and Moustakas, 2016). Following the autophosphorylation of TGF-βRs, TGF-β has been shown to activate several MAPK family members, such as ERK1/2, p38, and JNK (Yu et al., 2002; Xie et al., 2004; Chen et al., 2014; Wojciechowski et al., 2017, 2018; Xu et al., 2018; Shu et al., 2019b), as well as PI3K/Akt-signalling (Cho et al., 2006; Chen et al., 2012; Guo et al., 2016), that has been linked to the induction of EMT. In mouse LEC lines (α-TN4), TGF-β stimulation in truncated Smad3ΔC-expressing or antisense Snail-expressing α-TN4 cells prevented Akt phosphorylation (Cho et al., 2006). This study concluded that TGF-β-induced Smad2/3/4 signalling as well as Snail expression, a transcription factor normally upregulated by TGF-β, was required for PI3K/Akt activation during EMT (Cho et al., 2006).

The Rho/ROCK signalling mechanism acts through Rho GTPases (e.g., Rho, RhoA, and Rac1), that are activated by TGF-β, independent of Smads, and can influence cell cytoskeletal reorganisation, and therefore cell motility and migration properties (Maddala et al., 2003; Masszi et al., 2003). Targeting the Rho/ROCK pathway in TGF-β-induced rat LECs using a ROCK inhibitor (Y-27632) prevents EMT stress fibre formation, with a significant reduction in α-SMA expression, while maintaining cell membrane localisation of epithelial markers E-cadherin and β-catenin (Korol et al., 2016). Our laboratory has also shown that Sprouty (Spry) and Spreds, RTK antagonists of MAPKs, can negatively regulate non-canonical signalling associated with TGF-β in the lens (Lovicu et al., 2015; Shin et al., 2015) and, like Rho/ROCK inhibition, can suppress the acquisition of EMT-associated phenotypic changes and marker expression (Zhao et al., 2022). Overall, TGF-β-induced EMT can occur independently of Smads through various signalling cascades, and therefore it is important to further explore alternative downstream molecules that may lead to a deeper understanding of the fibrotic process.

1.9.3 TGF-β-induced EMT in the lens

Numerous studies have shown a correlation between TGF-β activation and the induction of EMT leading to fibrotic cataract development (de Iongh et al., 2005; Das et al., 2016; Shu et al., 2017; Z. Han et al., 2018; Jiang et al., 2018). TGF-β has proven to be a major driving force of ASC and PCO development both *in vitro* and *in vivo* (Mansfield et al., 2004; Robertson et al., 2007; Jiang et al., 2018; Shu and Lovicu, 2019; Wang et al., 2019; Lovicu et al., 2020). This is due to the readily available level of potent TGF-β in the eye, that can be activated in response to varying stimuli including stress and inflammation (Gordon-Thomson et al., 1998; de Iongh et al., 2001b; Mansfield et al., 2004; Wormstone et al., 2006).

Lens cell and capsular bag models derived from chick (Walker et al., 2007, 2015, 2018; Boswell et al., 2017), rodent (Lovicu et al., 2002, 2005, 2015; de Iongh et al., 2005; Kubo et al., 2013), or human (Wormstone et al., 2002, 2006; Raghavan et al., 2016; S. Shibata et al., 2021) ocular tissues, have been used to study and imitate the development of lens fibrosis as seen *in situ*. For example, a study by Basta et al. (2021) used an *ex vivo* post cataract surgery model in the embryonic chick lens that exhibited regenerative and fibrotic injury repair mechanisms, modelling the two types of PCO, in a spatially dependent manner. Furthermore, our laboratory has adopted the use of transgenic mice that overexpress, under the control of a crystallin promoter, an active form of TGF-β1 in the lens (Srinivasan et al., 1998), resulting in ASC plaque formation postnatally (Figure 1.7 B) (Srinivasan et al., 1998; Lovicu et al., 2002, 2004, 2005). Compared to lenses of wild type mice (Figure 1.7 A, C), these ASC plaques contain a heterogenous multilayered population of aberrant fibre-like cells and myofibroblastic cells, as well as abundant ECM deposition (Figure 1.7 D) (Lovicu et al., 2002, 2004). It is expected that other ocular factors *in situ* are contributing to this ASC, given studies implementing an *ex vivo* lens epithelium explant model, treated with TGF-β, only produce myofibroblastic cells (Liu et al., 1994; Hales et al., 1995; Boswell et al., 2017; Shu et al., 2017; Wojciechowski et al., 2017; Shu and Lovicu, 2019). When compared to *in situ* PCO models, post primary cataract surgery, reports have commented on a differential population of cells, similar to that of ASCs, that are either, i) migrated and transitioned myofibroblastic cells (fibrotic), and/or ii) a deposition of differentiated fibre cells causing Elschnig's pearls and Soemmerring's ring (pearl-like) (Mansfield et al., 2004; Wormstone et al., 2008, 2020; Boswell et al., 2017).

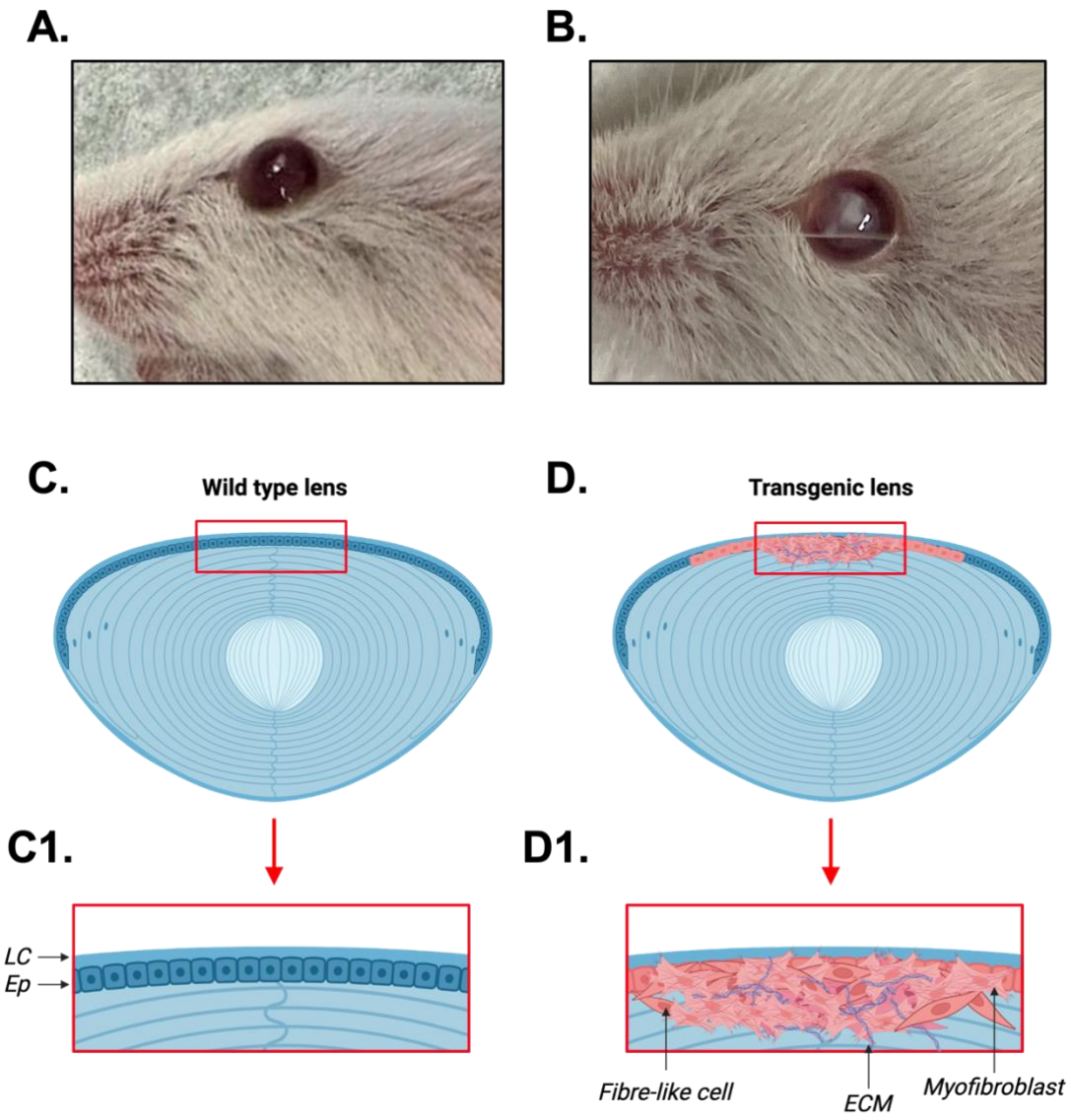

Figure 1.7. Wild type vs. transgenic ASC mice. (A) A wild type mouse (FVB/N) and (B) a transgenic (OVE918) overexpressed TGF-β1 (ASC and corneal opacity) mouse at 20 days old. In wild type lenses (C, C1), the lens epithelium is a unified monolayer of cuboidal epithelial cells (Ep, dark blue) attached to the anterior lens capsule (LC) or basement membrane. Throughout early postnatal development in transgenic mice lenses overexpressing TGF-β1, the lens epithelium becomes multilayered in the central region and loses uniformity (D). In the boxed area in (D1), these transformed cells form either myofibroblasts or fibre-like cells, with excessive deposition of extracellular matrix (ECM). Schematic diagram created using *Biorender.com.*

1.10 MODULATION OF LENS EMT: IMPLICATIONS FOR CATARACT PREVENTION

The detrimental effects of fibrotic pathologies and diseases has resulted in an ever-growing interest into finding potential mechanisms or agents that could potentially inhibit/prevent EMT. In most cases, the inhibition of EMT has somewhat been achieved by antagonising and/or

negatively regulating TGF-β-induced signal activation, both canonical and non-canonical pathways. Growth factors found within the ocular media, including FGF (Liu et al., 1994; Mansfield et al., 2004; Kubo et al., 2017; Flokis and Lovicu, 2023) and BMP (Xu et al., 2009; Shu et al., 2017, 2021), associated receptor signalling molecules such as EGFR (Shu et al., 2019b; Shu and Lovicu, 2019), as well as downstream signalling antagonists Sprouty (Lovicu et al., 2015) and Spred (Zhao et al., 2022), have proven to modulate EMT development in lens exposed to TGF-β in a dose-dependent manner. Additionally, targeting or selectively inhibiting specific downstream signalling molecules induced by TGF-β, including Smad3 (Meng et al., 2018; Shu and Lovicu, 2019; Taiyab et al., 2019), JNK (Santibañez, 2006; Ranganathan et al., 2007; Liu et al., 2008; Hou et al., 2021), MEK1/2 or ERK1/2 (Bakin et al., 2004; Meyer-ter-Vehn et al., 2006; Hou et al., 2018; Shu and Lovicu, 2019), and p38 MAPK (Zhou and Menko, 2004; Meyer-ter-Vehn et al., 2006; Boswell et al., 2017), has also shown promise in reducing cytoskeletal reorganisation, as well as stress fibre formation associated with EMT.

1.11 p38 MAPK

1.11.1 p38 MAPK family

p38 MAPK are downstream signalling molecules commonly known as stress-induced proteins, due to responding and exhibiting a high affinity to extracellular (e.g., environmental, cytokines, inflammation) and/or intracellular (e.g., oxidative stress, DNA damage) stress stimuli (New and Han, 1998; Risco and Cuenda, 2012). Despite being characterised as a stress-induced protein, p38 MAPK is also recognised for its role in cell differentiation, proliferation, morphogenesis, survival, and regulating immune responses, as previously reviewed (Nebreda and Porras, 2000; Cuadrado and Nebreda, 2010; Canovas and Nebreda, 2021). The p38 MAPKs belong to the MAPK family and are comprised of four isoforms: p38α (MAPK14), p38β (MAPK11, SAPK2b), p38γ (MAPK12, ERK6, or SAPK3), and p38δ (MAPK13, SAPK4) (Cuadrado and Nebreda, 2010; Han et al., 2020). The primary isoform, p38α, is commonly referred to as p38 within wider literature due to being first studied in 1994 as a protein kinase activated/tyrosine phosphorylated, during an endotoxin stress response in mammalian cells (Han et al., 1994; Lee et al., 1994; New and Han, 1998; Risco and Cuenda, 2012). These p38 MAPK isoforms can be further delineated into two subgroups based on structural similarities: p38α and p38β (75% similarity), and p38γ and p38δ (70% similarity) (Cuadrado and Nebreda, 2010; Canovas and Nebreda, 2021; Pua et al., 2022). p38α/β are universal isoforms expressed throughout most cell and tissue types, whereas p38γ/δ only possesses approximately 60% similarity with p38α and

expression is often tissue-specific (Cuadrado and Nebreda, 2010; Risco and Cuenda, 2012; Canovas and Nebreda, 2021; Pua et al., 2022), as p38γ is abundant in skeletal muscle (Lechner et al., 1996; Tortorella et al., 2003) and p38δ is expressed in tissues derived from the endocrine system (Wang et al., 1997; Sumara et al., 2009).

1.11.2 Targeting TGF-β during EMT: A role for p38?

Smad-dependent and Smad-independent TGF-β signalling collaborate to promote EMT and ECM deposition in various models, including human fibroblasts (Leivonen et al., 2013), renal tubulointerstitial fibrosis (Sebe et al., 2008), and lens fibrosis (Saika et al., 2004; de Iongh et al., 2005; Dawes et al., 2009; Boswell et al., 2010, 2017; Chen et al., 2014). Wound healing, cytoskeletal remodelling, cell migration, apoptosis, and proliferative responses have shown to be driven by TGF-β-mediated p38 MAPK activation during EMT (Bakin et al., 2002; Yu et al., 2002).

Studies have shown that by targeting TGF-β and/or its TGF-βRs, an EMT response can be inhibited (Doi et al., 2011; Yu et al., 2014; Ghorbaninejad et al., 2023), with the suppression of EMT-associated markers (e.g., α-SMA, vimentin, and collagen I and IV) and/or the mesenchymal/myofibroblastic phenotype. In our laboratory, we have shown that this is also the case when EGF/EGFR is targeted in an *in vitro* LEC explant model (Shu et al., 2019b). Despite this, when MAPKs such as ERK1/2 are blocked in TGF-β-induced conditions, only some aspects of the EMT process are impacted, given Smad2/3-signalling is still intact (Xie et al., 2004; Sisto et al., 2020). Our laboratory has also shown that targeting p-ERK1/2 partially prevents an EMT in TGF-β2-treated rat LECs as lens cell death, but not cell morphology changes, is reduced (Wojciechowski et al., 2017). This suggests that ERK1/2 is not the only MAPK involved in lens EMT induction and, as such, alternative downstream MAPKs, such as p38 or JNK, may be required during this process.

A role for p38 MAPK during lens EMT has previously been reported, along with its activation in other systems associated with stress (internal or external) and cytokine activity, as reviewed previously (Han et al., 2020; Canovas and Nebreda, 2021). For example, in human LE cells exposed to H_2O_2, p38 activation was linked to cell apoptosis (Bai et al., 2015), which is a common feature of an EMT response. Another lens study showed myofibroblastic formation in DCDMLs was dependent on TGF-β-induced p38 and/or ERK1/2 activity, and the inhibition of p38 reduced apoptosis in these cells (Boswell et al., 2017). Since there are reported low levels of TGF-β activity in neonatal ocular tissue (de Iongh et al., 2001a), it is possible that p38 may

not be active in normal lenses. A study by Dawes et al. (2009) showed that p-p38, as well as p-ERK1/2, was elevated in the presence of TGF-β2 (10 ng/mL) in a human lens cell line (FHL 124), further emphasising that p38 activation is reliant on cytokine growth factors like TGF-β, during pro-inflammatory and apoptotic cell responses, as seen in cancer and other fibrotic models (Hanafusa et al., 1999; Bakin et al., 2002; Laping et al., 2002; Xiao et al., 2002; Ranganathan et al., 2007; Sebe et al., 2008; Bai et al., 2015; Boswell et al., 2017; Hou et al., 2021). From these studies, targeting p38 to better identify its role in this process may promote our understanding of the intracellular mechanisms responsible for TGF-β-induced lens EMT.

1.11.3 Targeted inhibition of p38 MAPK

Various models have been established to chemically inhibit the catalytic activity and activation of p38 MAPK during TGF-β-induced EMT (Hanafusa et al., 1999; Bakin et al., 2002; Yu et al., 2002; Meyer-ter-Vehn et al., 2006; Ranganathan et al., 2007; Ling et al., 2016; Boswell et al., 2017). A variety of inhibitor compounds have been trialled that have targeted one or several p38 isoforms, mainly p38α or p38β, using SB202190 (Bakin et al., 2002; Düzgün et al., 2017), SB220025 and SB239068 (Meyer-ter-Vehn et al., 2006), Skepinone-L (Koeberle et al., 2012), VX-745 (Duffy et al., 2011), and the most commonly used p38 inhibitor, SB203580 (Birkenkamp et al., 2000; Lali et al., 2000; Zhou and Menko, 2004; Wang et al., 2009; Kumphune et al., 2010; LaJevic et al., 2011; Shi et al., 2015; Ling et al., 2016; Sreekanth et al., 2016; Boswell et al., 2017; X. Han et al., 2018; Hao et al., 2021). For example, SB203580 at low concentrations, can target p38α/β, and MAPKAP K2 which is a p38 MAPK substrate (Kumar et al., 1999). Given that p38 MAPK is implicated during EMT, models that target its activity found that it may be responsible for morphological changes during TGF-β-induced EMT. A study by Bakin et al. (2002) showed that the p38 inhibitor SB202190 prevented cytoskeletal reorganisation, with no phenotype changes in TGF-β stimulated NMuMG cells. Another study demonstrated short-term inhibition of p38 was not enough to prevent long-term or complete myofibroblastic phenotype transition in TGF-β-treated DCDMLs (Boswell et al., 2017). Based on these studies, p38 MAPK appears to be required for regulating the cell cytoskeleton in stress-induced conditions, particularly when stimulated by proinflammatory cytokines like TGF-β (Hedges et al., 1999; Bakin et al., 2002, 2004; Meyer-ter-Vehn et al., 2006).

1.12 TROPOMYOSIN

1.12.1 Nomenclature, structure, and function

Actin (F-actin) filaments are one of three intricate cytoskeletal networks found in muscle and non-muscle cells (other components include microtubules and intermediate filaments), responsible for cell force, contractility, and intercellular transport (Gunning et al., 2005; Brayford et al., 2015; C. Cheng et al., 2017). These filaments are formed through G-actin monomers, or globular actin, that are then polymerised to form F-actin filamentous chains (Figure 1.8) (Ecken et al., 2015; Hohmann and Dehghani, 2019). Tropomyosin (Tpm, or previously abbreviated as Tm) is a family of ubiquitous regulatory actin filamentous proteins found throughout all eukaryotic cells (Marston and Gautel, 2013; Geeves et al., 2015; Janco et al., 2016). In non-muscle cells, among its overarching role in cell-cell filament stabilisation, regulation, embryogenesis, and cell morphology, Tpm is commonly associated with facilitating assembly of various actin-binding proteins into the cytoskeletal system (Schevzov et al., 2011; Geeves et al., 2015; Janco et al., 2016; Robaszkiewicz et al., 2016).

First discovered in the 1940s in striated muscle (Bailey, 1946), the Tpm family in vertebrates is comprised of four main genes (*TPM1–4*; *Tpm1–4* for rodent tropomyosin) with a corresponding nomenclature of isoforms: α-tropomyosin (α-Tm), β-tropomyosin (β-Tm), γ-tropomyosin (γ-Tm), and δ-tropomyosin (δ-Tm) (Gunning et al., 2005; Marston and Gautel, 2013; Geeves et al., 2015). Recent studies by Geeves et al. (2015) and Marston (2015) have redefined each Tpm isoform by generating a systemic classification that accounts for Tpm gene alternate splicing of exons/RNA processing, or novel splice variants, across various research fields (Pittenger et al., 1994; Schevzov et al., 2011; Marston and Gautel, 2013; Marston et al., 2013). The variance of Tpm genes has often proved futile in nomenclature cohesion due to the generation of tissue-specific protein isoforms, that, in turn, have specialised roles in different tissues and systems (Schevzov et al., 2011; Geeves et al., 2015). Due to the diverse nature of alternate internal splicing of exons, there are currently over 40 mammalian Tpm isoforms expressed, and each have respective structural differences (Gunning et al., 2005; Schevzov et al., 2011). Given the large amount of splice variants, the current body of work will discuss specific Tpm splice isoforms derived from all 4 *Tpm* genes and found in rodents, based on the new nomenclature classification and isoform molecular weights (see Table 1.2).

Tpm are rod-like dimeric, coiled-coil proteins and are comprised of two polypeptide chains (Pittenger et al., 1994; Robaszkiewicz et al., 2016). These two chains are incorporated into lateral surfaces of α-helical indentations along F-actin filaments to modulate and gatekeep

actin-binding protein connections with the actin cytoskeleton, as well as stabilise inter-connections with other end-to-end Tpm molecules (Figure 1.8) (Gunning et al., 1998; Schevzov et al., 2011; Geeves et al., 2015; Robaszkiewicz et al., 2016; Gateva et al., 2017). Originally termed the "backbone" of actin filaments (Huxley, 1960), Tpm interacts with three troponin proteins that comprise the troponin complex (TnT, TnI, and TnC) to regulate muscle contractility (Bicer and Reiser, 2013; Marston et al., 2013; Janco et al., 2016).

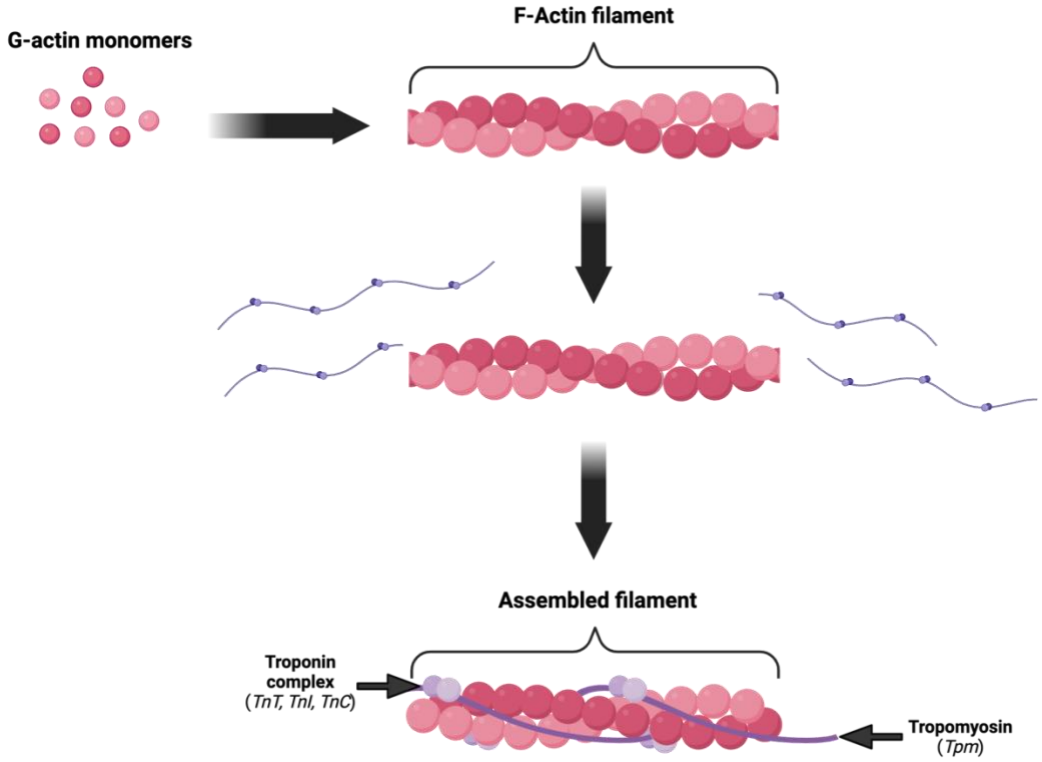

Figure 1.8. F-actin filament assembly. G-actin monomers (pink globes) are polymerized to form helical filamentous chains (F-actin). F-actin recruits rod-like chains known as tropomyosin (Tpm, purple rod) containing the troponin complex: troponin T (TnT), troponin I (TnI), and troponin C (TnC). The troponin complex binds to Tpm to modulate calcium during muscle contraction. The actin filament is assembled with the embedding of Tpm/troponin complex into the grooves of actin filament chains. Schematic adapted from (Meiring et al., 2018) using Biorender.com.

Based on their biomechanical properties during muscle contraction, Tpm isoforms can be classified as enabling slow or rapid dynamic activity (Gateva et al., 2017; Pathan-Chhatbar et al., 2018). Tpm isoforms are often divided into separate categories; low molecular weight (LMW; 245–251 residues, ~28–33 kDa) and high molecular weight (HMW; 281–284 residues, >34 kDa) (see Table 1.2) (Perry, 2001; Gunning et al., 2005; Janco et al., 2016; Humayun-Zakaria et al., 2019). The *Tpm2* gene only generates HMW Tpm isoforms, whereas *Tpm1*, *Tpm3*, and *Tpm4* genes encode both LMW and HMW Tpm isoforms (Gunning et al., 2005;

Savill et al., 2012; Janco et al., 2016; Humayun-Zakaria et al., 2019). The overarching role of Tpm is to promote and modulate actin filament versatility and dynamic activity (Robaszkiewicz et al., 2016). Since the discovery of tissue-specific Tpm isoforms, numerous studies have begun to establish the function of different isoforms, as well as the significance of their specialised roles in both muscle and non-muscle tissue (Pittenger et al., 1994; Schevzov et al., 2005; Vrhovski et al., 2005; Hook et al., 2011; Peng et al., 2013; Stefen et al., 2018; Hardeman et al., 2019).

Table 1.2. Classification of Tpm isoforms and genes based on molecular weight

Gene	Tropomyosin isoform nomenclature		Molecular weight on SDS PAGE gels (kDa)	Sizing Classification	
	Old	Current		LMW	HMW
Tpm1	Tm6	Tpm1.4	40		✓
	Tm2	Tpm1.6	36		✓
	Tm3	Tpm1.7	34		✓
	Tm5a	Tpm1.8	30	✓	
	Tm5b	Tpm1.9	30	✓	
Tpm2	Tm1	Tpm2.1	38		✓
Tpm3	Tm5NM1	Tpm3.1	30	✓	
	Tm5NM2	Tpm3.2	30	✓	
	Tm5NM3	Tpm3.3	30	✓	
	Tm5NM5	Tpm3.5	30	✓	
	Tm5NM8	Tpm3.8	30	✓	
	Tm5NM9	Tpm3.9	30	✓	
Tpm4	Tm4	Tpm4.2	30	✓	

Tpm isoforms classified as low (~28–33 kDa) or high molecular weight (>34 kDa) based on molecular weight on SDS PAGE gels. HMW: high molecular weight, LMW: low molecular weight, Tpm: Tropomyosin. Table adapted from Schevzov et al. (2011), Geeves et al. (2015), and Humayun-Zakaria et al. (2019).

1.12.2 Tropomyosin in the lens

The eye lens has been used extensively as a model to study cell biomechanics and structural changes of lens epithelial and fibre cells (C. Cheng et al., 2017), and how their dysregulation can cause the onset of cataract. As mentioned in Section 1.5, lens epithelial cells *in situ* that experience dysregulation of normal cell morphology and actin cytoskeletal biomechanics results in the development of a fibrotic plaque. Differential regulation of Tpm in the lens has proven to modulate cell actin dynamics and consequently induce phenotypic changes in lens cells (Kubo et al., 2013). In most cases, aberrant activation of cytokine TGF-β, particularly isoforms TGF-β1 and -β2, have been reported to interrupt normal Tpm regulation in the lens (Kubo et al., 2013). Broader research of Tpm in wound healing and ECM reorganisation in models like skin (Lees et al., 2013) and lung (Bradbury et al., 2021) suggests a role for Tpm in other fibrotic systems involving stress and inflammation. These conditions result in the recruitment of fibroblastic cells to sites of injury, as seen in lens EMT during ASC and PCO formation (Bakin et al., 2004; Kubo et al., 2017; Shu and Lovicu, 2019), and the importance of an active actin cytoskeleton to facilitate cell contractility, as previously reviewed (Eldred et al., 2011; Taiyab and West-Mays, 2022).

Recently, Parreno et al. (2020) identified differential expression of eight Tpm isoforms in native lens cells of 8–10 weeks old mice (Figure 1.9). Expression of each isoform was compared in both LECs and LFCs using RT-PCR, with all eight isoforms present in LECs, whereas only three isoforms (Tpm1.13, Tpm3.5, Tpm4.2) were expressed in fibre cells (Parreno et al., 2020). When compared to immortalised lens epithelial cells (imLECs) previously established from 10-day-old mice, the same Tpm isoforms were expressed in these imLECs as seen in native lens epithelia, except for Tpm2.1 that was unique to imLECs (Parreno et al., 2020).

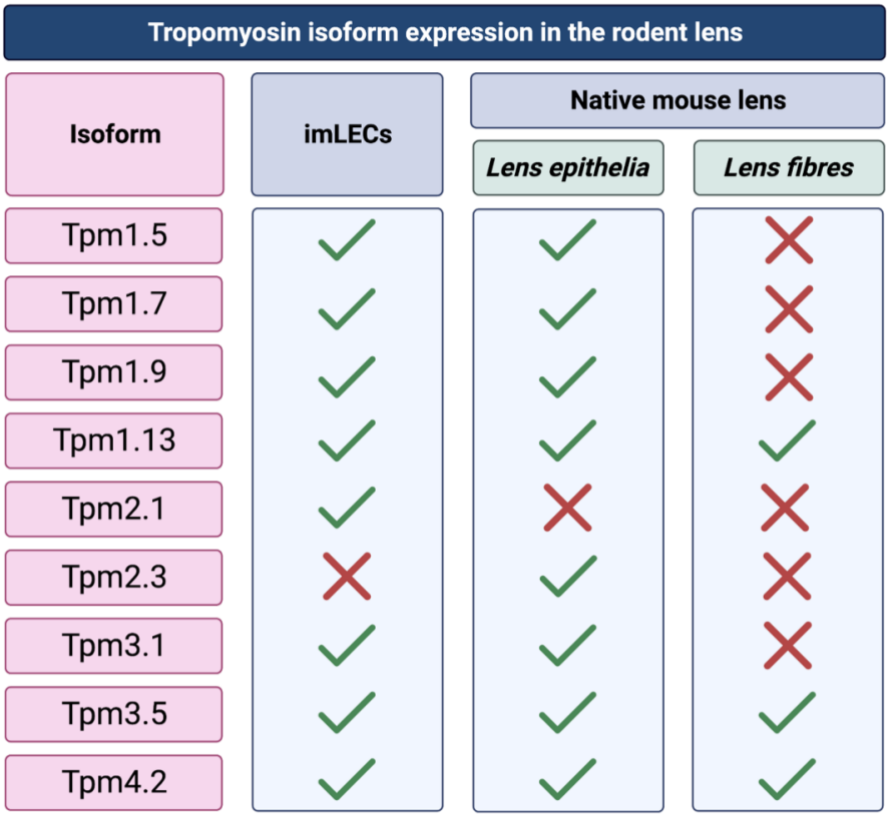

Figure 1.9. Tropomyosin expression in the rodent lens. Semi-quantitative RT-PCR tabled results of RNA expression of Tpm isoforms, Tpm1.5, 1.7, 1.9, 1.13, 2.1, 2.3, 3.1, 3.5, and 4.2, isolated from anterior lens capsule sheet (lens epithelia) and lens fibre cells of native mouse lenses. Presence (green tick) or absence (red cross) of Tpm isoforms. Immortalised lens epithelial cells (imLECs) express the same isoforms as seen in native lens epithelia, apart from Tpm2.1 that is expressed solely in imLECs. Tpm2.3 is only characteristic to native lens epithelia. Data originally represented and adapted from Parreno et al. (2020).

1.12.3 A role for Tropomyosin in fibrosis

Disruption of Tpm association with dynamic actin filaments can be detrimental to normal cell stability, stiffness, and behaviour, and, as a result, often leads to the development of numerous pathologies and fibrotic disorders. There has been a growing interest in the role of the cell cytoskeleton, and its associated proteins, during the transformation of epithelial cells into mesenchymal-like/myofibroblastic cells (EMT), as well as the importance of actin remodelling during cytokinesis, morphogenesis, differentiation, and regulation of cell apoptosis in response to oxidative stress (Mahadev et al., 2002; Gunning et al., 2008, 2015; Desouza et al., 2012; Janco et al., 2016; Izdebska et al., 2018). For example, during cancer metastasis, Type 3 EMT involves polarised recruitment of cytoskeletal components that, in turn, affect cell biomechanics, encouraging the formation of cell protrusions and causing these cells to become invasive (Morris and Machesky, 2015; Izdebska et al., 2018).

The upregulation of Tpm in fibrotic and tumour microenvironments has been investigated when cells are stimulated by growth factors and cytokines, particularly TGF-β (Bakin et al., 2004; Kubo et al., 2018; Bradbury et al., 2021). Interestingly, of all the identified mammalian Tpm isoforms, six key isoforms; Tpm1.6, Tpm1.7, Tpm2.1, Tpm3.1, Tpm3.2, and Tpm4.2, have been correlated with stress fibre formation and interaction in systems such as human osteosarcoma cells (Tojkander et al., 2011; Gateva et al., 2017), rodent lens cells (Kubo et al., 2017, 2018; Cheng et al., 2018; Shibata et al., 2018; Parreno et al., 2020; T. Shibata et al., 2021), lung fibroblasts (Bradbury et al., 2021), lung carcinoma cell lines (Tada et al., 2000), urothelial carcinoma (Liu et al., 2018; Humayun-Zakaria et al., 2019), and breast cancer cell lines (Bhattacharya et al., 1990; Jeong et al., 2014). These isoforms have been shown to express and differentially localise to stress fibres that suggests potential Tpm isoform-specific bundles, with different functionality, in regions of actin stress fibres (Tojkander et al., 2011; Prunotto et al., 2015; Gateva et al., 2017; Jansen and Goode, 2019).

Numerous studies have silenced or selectively targeted Tpm isoforms to demonstrate their importance and role for the actin cytoskeleton during wound healing and repair, as well as stabilising ECM components (Kubo et al., 2013; Lees et al., 2013; Cheng et al., 2018; Bradbury et al., 2021). In particular, silencing RNA (siRNA) transfection models showed that targeting specific Tpm isoforms, such as Tpm1 (Prunotto et al., 2015; Takenawa et al., 2023), Tpm2.1 (Jalilian et al., 2015; Shin et al., 2017), Tpm3.1 (Bach et al., 2009; Creed et al., 2011; Jalilian et al., 2015), and Tpm4.1/Tpm4.2 (Jeong et al., 2014), effect cell migration, proliferation, wound healing, invasiveness, and tumour progression.

1.12.4 Tropomyosin in lens fibrosis

A study by Fatma et al. (2005) on lens, characterised a genetically modified mouse deficient for Peroxiredoxin 6 ($Prdx6^{-/-}$); a gene involved in antioxidant defense through regulating reactive oxygen species (ROS) levels during oxidative cell stress (Fatma et al., 2005; Kubo et al., 2013). This study found that a loss of Prdx6 in lens enhanced overactivation and expression of TGF-β1, elevating levels of ECM and EMT-associated proteins, such as α-SMA (Fatma et al., 2005), suggesting that Prdx6 is required for maintaining homeostatic levels of TGF-β1 to prevent cataractogenesis. Subsequently, Kubo et al. (2010) confirmed that TGF-β1 and/or H_2O_2 stimulation of LECs from WT mice induced oxidative stress, EMT-specific transdifferentiation, and cytoskeletal modulation through the expression of other ECM and cytoskeletal proteins, including Tpm1α (Tpm1.6) and Tpm2β (Tpm2.1). The study demonstrated that the absence of Prdx6 in mice LECs ($Prdx6^{-/-}$) increased stress fibre activity, with elevated Tpm1α/2β, while the inverse occurred with the addition of exogenous Prdx6, with cells decreasing Tpm2β levels (Kubo et al., 2010, 2013). It was concluded that since TGF-β1 can induce EMT in LECs with or without Prdx6, cytoskeletal biomechanics and consequent stress fibre formation are directly correlated to elevated Tpm in these cells (Fatma et al., 2005; Kubo et al., 2010, 2013, 2018).

Additional studies from the Kubo laboratory implemented rodent PCO and human cataractous models to determine whether Tpm elevation and requirement during cataractogenesis is translated across species (Kubo et al., 2013). These studies established a model for PCO following extracapsular lens extraction (ECLE) in 13-week-old rats to observe LEC migration during secondary cataract formation, as well as the role of the cell cytoskeleton during this transdifferentiation process (Kubo et al., 2013). Across a 2-week observation period, it was noted that α-SMA was elevated in migrating and elongating fibroblastic cells (Kubo et al., 2013). This increase in α-SMA correlated with a significant increase in Tpm1.6/1.7 and Tpm2.1 protein and mRNA levels, particularly Tpm2.1, in this rat PCO model, as well as in Shumiya cataract rat (SCR) lenses, and a human PCO model (Kubo et al., 2013). These studies showed the colocalisation of Tpm1.6/1.7 and Tpm2.1 with filensin, a lens fibre-specific intermediate filament protein, in human LECs that migrated posteriorly in the lens capsular bag following IOL implantation (Kubo et al., 2013). The increase levels of Tpm1.6/1.7 and Tpm2.1 in both rodent and human cataractous models suggests that isoforms derived from *Tpm1* and *Tpm2* genes are potentially required for lens fibrosis (Kubo et al., 2010, 2013).

1.12.4.1 Tpm1 lens-specific conditional knockout

In the lens, the mechanisms of Tpm operating during EMT-induced cell contractility has been explored by eliminating or knocking out specific Tpm genes, such as *Tpm1* (T. Shibata et al., 2021), *Tpm2* (Shibata et al., 2018), and exon 9d from *Tpm3* (Tpm3.1/3.2) (Cheng et al., 2018; Parreno et al., 2020). The study by T. Shibata et al. (2021) established a conditional knockout mice line with a loss of *Tpm1* isoforms specifically in the lens (Tpm1-CKO). The study showed that deletion of *Tpm1* impacted the development and size of mouse lenses, compared to WT (*Tpm1*$^{+/+}$) lenses, across embryonic day 14 (ED14) to postnatal stages (1, 11, 48-weeks-old) (T. Shibata et al., 2021). In *Tpm1*-CKO mice, lens fibre cell morphology and polarity throughout development was disrupted, with the presence of large cavities within the anterior compartment of the lens where apical fibre cell tips are normally in contact with the lens epithelium (T. Shibata et al., 2021). *Tpm1* plays a role in cytoskeletal stability and organisation in lens cells, given that a deficiency of *Tpm1* led to a reduction of F-actin in ED14 and 11-day-old *Tpm1*-CKO lenses compared to WT mice (T. Shibata et al., 2021). F-actin is essential for the maintenance and stabilisation of lens cell shape and cytoskeletal arrangements in lens fibre cells (C. Cheng et al., 2017). Therefore, the reduction of F-actin suggests the destabilisation of F-actin filament assembly in *Tpm1*-CKO lenses is impacting normal lens development, as lens fibres cannot elongate or form normally during lens fibre differentiation (T. Shibata et al., 2021).

1.12.4.2 Tpm2 CRISPR-Cas9 heterozygous knockout

Studies from the Kubo laboratory also established a Tpm2$^{+/-}$ KO mouse line using CRISPR/Cas9 to target Tpm2 during lens injury, and ageing, leading to cataractogenesis (Shibata et al., 2018). From this study, an increase in *Tpm2* and α-SMA mRNA expression was observed in lens epithelia 1-week post extracapsular lens extraction surgery in 7-week-old wild type (WT, Tpm2$^{+/+}$) mice (Shibata et al., 2018); similar to a result previously demonstrated in a rat PCO model (Kubo et al., 2013). Stimulation of an injury in these Tpm2$^{+/-}$ mice lenses prolonged wound healing responses across a 10-day period, compared to the instant and acute response observed in injury-induced WT mice lenses (Shibata et al., 2018). This prolonged EMT response was supported by a reduction in α-SMA and Tpm1/2 immunolabelling in injury-induced Tpm2$^{+/-}$ mice lenses, specifically in lens cells surrounding the site of injury, compared to WT mice (Shibata et al., 2018). Overall, this study suggested a potential role for Tpm2 in the

regulation of the lens during mouse fibrotic PCO, EMT development, and wound healing responses.

1.12.4.3 Pharmacologically targeting or knocking Tpm3

An earlier study by Cheng et al. (2018) acquired cDNA and protein from 6-week-old Tpm3.1 deficient (Tpm3/Δexon9d$^{-/-}$) and WT (Tpm3/Δexon9d$^{+/+}$) mice lenses, and showed using RT-PCR and immunolabelling that no transcripts or protein for Tpm3.1 was present in these lenses. However, a later study by this same group using a different antibody were now able to detect Tpm3.1 in lens cells (see Figure 1.9) (Parreno et al., 2020). This study also showed Tpm isoforms can be induced in mouse imLECs under the influence of TGF-β2 (5 ng/mL), along with other stress fibre associated Tpm isoforms, particularly Tpm1.7, Tpm2.1, Tpm3.1, and Tpm4.2 (see Figures 1.9–1.10) (Parreno et al., 2020). To further evaluate the role of Tpm3.1 in stress fibre formation, the study used an anti-cancer pharmacological compound, TR100 (1–2 μM), that targets a binding site of Tpm3.1 (at exon 9d), preventing Tpm from F-actin filament

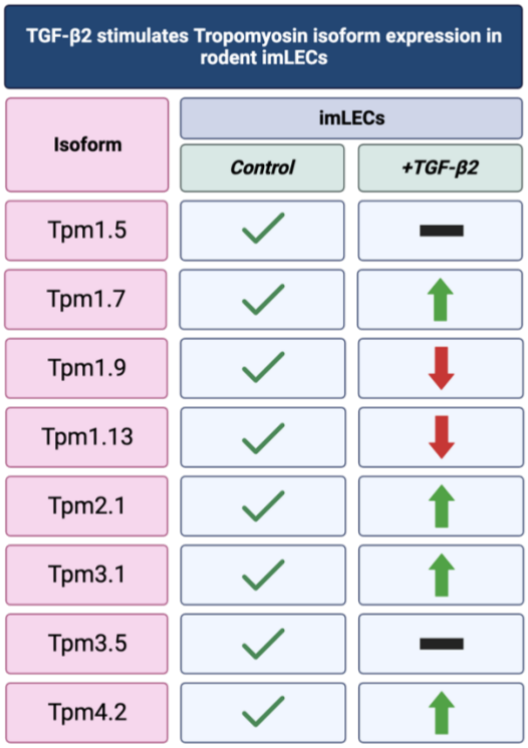

Figure 1.10. Tropomyosin expression in the rodent lens. Semi-quantitative RT-PCR tabled results of mRNA expression of Tpm isoforms, Tpm1.5, 1.7, 1.9, 1.13, 2.1, 3.1, 3.5, and 4.2, from immortalised lens epithelial cells (imLECs). Presence (green tick) of Tpm isoforms in control (unstimulated) imLECs. TGF-β2 stimulated (green arrow) stress fibre isoforms Tpm1.7, Tpm2.1, Tpm3.1, and Tpm4.2 in imLECs, while downregulating Tpm1.9 and Tpm1.13 (red arrows). Expression of Tpm1.5 and Tpm3.5 remained unchanged in TGF-β2 (5 ng/mL) treated with imLECs, compared to control imLECs. Data originally represented and adapted from Parreno et al. (2020).

incorporation (Stehn et al., 2013; Bonello et al., 2016; Parreno et al., 2020). This study showed that in the presence of TGF-β2, TR100 reduced Tpm3.1 F-actin incorporation in imLECs that evidently compromised TGF-β2-induced stress fibre formation (Parreno et al., 2020). Since stress fibre formation is a crucial element in the development of myofibroblasts during EMT, mRNA and protein levels of α-SMA were examined, and inhibition of Tpm3.1 in TGF-β2-treated imLECs suppressed α-SMA stress fibre localisation (Parreno et al., 2020). This same study also examined the Tpm3/Δexon9d$^{-/-}$ (Tpm3.1 deficient) mice model and exposed these lenses to TGF-β2 (Parreno et al., 2020). They showed that TGF-β2 treatment of Tpm3.1 deficient lenses reduced F-actin stress fibre formation in the basal region of LECs, the region adjoining the anterior lens capsule, when compared to WT mice lenses (Parreno et al., 2020). In this model, TGF-β2 treatment transformed F-actin filaments into stress fibres at basal LEC regions, leading to capsular modulation (wrinkling) in WT mouse LECs, that was prevented in TGF-β2-treated LECs of Tpm3.1 KO mice (Parreno et al., 2020). From this result, it was hypothesised that Tpm3.1 and F-actin assembly is required particularly in the basal region of LECs to form cytoskeletal stress fibre arrangements in contractile lens cells during TGF-β2-induced EMT (Parreno et al., 2020). In addition, as reported in imLECs treated with TR100, intact lenses of Tpm3.1 deficient mice treated with TGF-β2 had reduced α-SMA protein levels, suggesting that without Tpm3.1 in LECs, stress fibre formation in response to TGF-β2 stimulation is impaired (Parreno et al., 2020). Given the similarities and/or differences in Tpm expression in both murine and human cataract models (Kubo et al., 2010, 2013; Parreno et al., 2020), further research into the involvement of Tpm in the aetiology of lens fibrosis, leading to cataractogenesis, could provide promising avenues to the development of specific therapeutics.

1.13 RESEARCH AIMS AND OBJECTIVES

The overarching aim of this dissertation is to expand our understanding of how different growth factors within the ocular media and their respective signalling contribute to the modulation of fibrotic cataract development. Specifically, we plan to further investigate the mechanisms of key growth factors, particularly FGF and TGF-β, as well as their downstream signalling cascades, and the role of the cell cytoskeleton during lens EMT.

1.13.1 Hypothesis 1: Tropomyosin isoforms are differentially expressed and localised in the postnatal rodent lens

We aimed to first identify and characterise the expression and localisation of various Tpm isoforms in the rodent lens. As previously mentioned, the ASC plaques of our TG mice contain a heterogenous population of cells that are comprised of either myofibroblastic and/or fibre-like cells (Lovicu et al., 2002, 2004). Using different mice models we will examine the expression of Tpm during cataractogenesis at different postnatal stages to identify which Tpm is associated with myofibroblastic and/or fibre-like cells in ASC plaques. We will validate this *in vitro* using lens explants treated with TGF-β2 and/or FGF-2, to induce different cell phenotypes, and examine changes to Tpm isoforms. We hypothesise that Tpm has a differential role in lens EMT and cataractogenesis when compared to normal lens epithelial cells in wild type mice and/or control (non-treated) LEC explants.

1.13.2 Hypothesis 2: Tpm3.1/3.2 and Tpm4.2 are required for TGF-β-induced lens EMT

Tropomyosin has shown to be present in the lens and is required for TGF-β-induced lens EMT in an isoform-specific manner, particularly stress fibre associated isoforms Tpm1.6/1.7, Tpm2.1, Tpm3.1/3.2 and Tpm4.2. We aimed to further characterise five stress-fibre associated cytoskeletal isoforms, Tpm1.6/1.7, Tpm3.1/3.2, and Tpm4.2, and their expression in lens cells and, in doing so, determining which of these specific Tpm isoforms contribute to lens EMT. By selectively targeting Tpm3.1/3.2 using anti-tropomyosin compounds (ATMs), as well as examining Tpm3.1/3.2 and Tpm4.2 deficient mice, we aim to determine whether the loss of Tpm3.1/3.2 and Tpm4.2 is indeed required for TGF-β-induced EMT. To do this, we will treat lens explants from these mutant mice with TGF-β and, to validate our findings, cross the mutant lines to the TG lines of mice overexpressing TGF-β to show that a loss of Tpm3.1/3.2 and/or Tpm4.2 is required for ASC formation *in situ*.

1.13.3 Hypothesis 3: FGF-2 differentially regulates lens epithelia behaviour during TGF-β-induced EMT

FGF and TGF-β contribute to the regulation of lens cell processes and behaviour, such as cell proliferation, differentiation, and EMT leading to fibrotic cataract. *In situ*, elevated TGF-β levels in the eye leading to ASC development, may impact the normal activity of FGF in the anterior compartment of the eye (Boswell et al., 2010). In contrast, FGF-2 has previously also been shown to antagonise and/or propagate TGF-β-induced EMT in the lens (Cerra et al., 2003; Mansfield et al., 2004; Kubo et al., 2017); however, there has been no consensus as to what specific conditions FGF can modulate TGF-β, and vice-versa, to modulate lens EMT. Here we will use different doses of FGF and TGF-β to determine and further characterise their combined activity in lens epithelial cell explants, and to what extent they can differentially regulate each other leading to EMT. By understanding the differential regulation of FGF-2 in TGF-β2-induced conditions, this may be more reflective of the heterogenous population of cells (both aberrant fibre cells and myofibroblastic cells) evident *in vivo* with ASC and PCO.

1.13.4 Hypothesis 4: p38α MAPK activation is required during TGF-β-induced lens EMT

p38α is a downstream signalling protein activated by TGF-β in stress-induced and wound healing microenvironments. We examined p38α *in vitro* using rat LEC explants to identify its role during lens EMT using a selective inhibitor. To determine whether p38 is required for cytoskeletal regulation and remodelling during TGF-β-induced lens EMT, we examined the expression of Tpm1.6/1.7 and Tpm2.1 when p38α is inhibited. We aim to further understand how p38 acts independently of Smad2/3-signalling during TGF-β2-induced lens EMT. Overall, we wished to understand the mechanisms of p38 activity and determine how this protein is involved in TGF-β-induced lens EMT.

CHAPTER 2: GENERAL METHODOLOGY

2.1 ANIMALS AND TISSUE ACQUISITION

All procedures conducted using animals abided by the Australian Code for animal care and usage for scientific purposes, as well as the Association for Research in Vision and Ophthalmology (ARVO) Statement for the Use of Animals for Ophthalmic and Vision biomedical research (USA). Experiments conducted in this study were approved by the Animal Ethics Committee of The University of Sydney (NSW, Australia, AEC #2021/1913 and #2021/1930). Prior to tissue collection, all animals were humanely euthanised with CO_2 followed by cervical dislocation. A breeding colony of Wistar rats (*rattus norvegicus*) were housed and maintained in the Medical Foundation Building (K25) Animal Holding Facility at The University of Sydney, Australia.

A breeding colony of transgenic (TG) mice were previously generated in the laboratory of Prof Paul Overbeek; OVE853 (853) and OVE918 (918) on an FVB/N background using a modified crystallin promoter, to overexpress an active form of TGF-β1 in the lens, leading to fibrosis in the form of an anterior subcapsular cataract (Srinivasan et al., 1998). These inbred lines were housed and maintained at the Australian BioResources (ABR) animal breeding facility (NSW, Australia), along with wild type (WT) mice that exhibited normal lens growth and morphology. Ocular tissues were collected from postnatal 10-day-old (P10) and 21-day-old (P21) Wistar rats (± 1 day), as well as 21-day-old WT and TG mice (± 2 days) for lens epithelial cell (LEC) explants.

2.2 RODENT (RAT AND/OR MOUSE) LENS EPITHELIA EXPLANT SYSTEM

The lens epithelial cell (LEC) explant system is a well-established model isolating the primary anterior lens epithelial sheet that remains attached to its native lens capsule. We acquired this using previously described methods (West-Mays et al., 2009), whereby postnatal eyes were extracted and placed under a dissecting microscope (Lieca M125 Spot Illuminating, Leica Microsystems) to remove the lens. The lens was orientated so that the posterior pole was facing superiorly, identified by its more convex surface, while the anterior pole faced the inferior surface of the culture dish (Figure 2.1). With fine watchmaker's forceps (#5), the posterior capsule was gently torn in quadrants to the lens equator, while the internal mass of fibre cells

was rolled off and discarded. The newly exposed anterior capsule sheet of epithelia was then pinned down to the base of the dish (Figure 2.1).

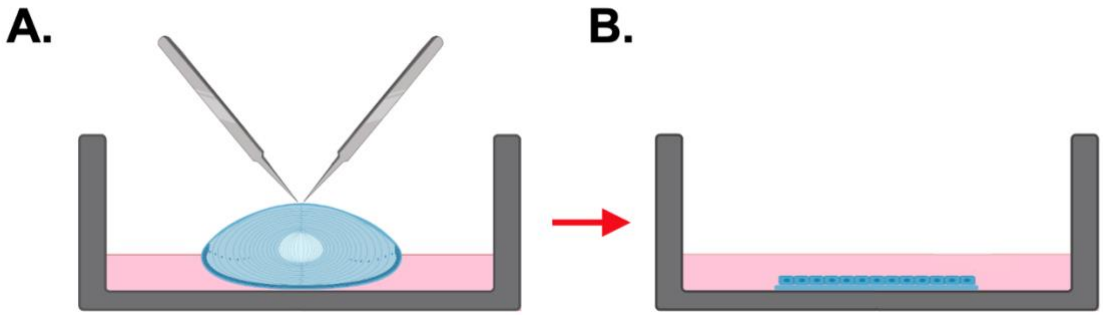

Figure 2.1. Preparation of lens epithelial cell (LEC) explants. Rodent lens orientated with posterior capsule facing superiorly (A). Anterior lens capsule explants were acquired, and the internal mass of fibres were discarded. Isolation of the LEC explant by pinning the anterior sheet to the base of the culture dish (B). Diagram created using *Biorender.com*.

2.3 TISSUE CULTURE

LEC explants were cultured in Medium 199 (M199) with Earle's Salts (10X) in 35mm Nunc™ tissue culture dishes. To make 1X M199, 100 mL of M199 was diluted in 900 mL sterile Milli-Q H_2O and pH to 7.2 (± 0.01). M199 was then filtered into sterile 100 mL sterile schott bottles and stored short-term at 4°C. When needed, 1X 100 mL was warmed to 37°C in a EuroClone CO_2 Incubator (SafeGrow 188 pro Model), and media was supplemented with 2.5 µg/mL Amphotericin/Amphostat B, 0.1% bovine serum albumin (BSA), 0.1 µg/mL L-glutamine, and penicillin (100 IU/mL)/streptomycin (100 µg/mL) (see Table 2.1). Lens epithelia explants were contained in a humidified incubator (37°C, 5% CO_2) for the duration of the culture period.

2.4 PREPARATION OF GROWTH FACTORS

2.4.1 Fibroblast Growth Factor-2 (FGF-2)

Recombinant human fibroblast growth factor 2 (FGF-2) was reconstituted in 5mM Tris (pH 7.6) containing 0.1% BSA (*w/v*) diluent and stored long-term at -80°C. Working aliquots of different FGF-2 concentrations were made for later use at a low dose (100 ng/10 µl) or higher dose (1000 ng/10 µl) (Table 2.2).

2.4.2 Transforming Growth Factor-beta 2 (TGF-β2)

Recombinant human transforming growth factor-beta 2 (TGF-β2) was reconstituted in 4mM HCl/0.1% BSA (*v/v*) and aliquoted into 2 µg/mL stock tubes. Working aliquots of TGF-β2 (5 ng/25 µL) were prepared and stored at -80°C.

2.5 GROWTH FACTOR TREATMENT

Growth factor working aliquots were removed from -80°C and thawed by vortex then prepared in freshly supplemented M199. Growth factors were added to respective culture dishes in a laminar flow hood. Homogeneity of growth factors throughout the M199 was ensured by rotating treated dishes several times (clockwise/anti-clockwise) before placing into the incubator. Table 2.2 provides detail regarding the growth factors and dosages used in this thesis.

2.6 TPM3.1-SPECIFIC AND P38 MAPK INHIBITOR COMPOUNDS

This thesis adopted the use of several pharmacological inhibitor compounds, targeting downstream signalling proteins, including p38 MAPK, and cytoskeletal tropomyosin protein Tpm3.1. Table 2.3 provides a brief outline of inhibitor compounds, their specific targets, and doses used in the current thesis.

2.7 ASSESSMENT OF CHANGES IN LENS EPITHELIA MORPHOLOGY

Following 0 to 7-day culture periods, LEC explants were monitored and screened daily using phase contrast microscopy (CK2, Olympus microscope) to monitor alterations in normal and/or aberrant lens epithelia morphology. Explants were photographed using Leica FireCam imaging software (Version 1.5, Leica) at varying several stages of culture: day 0, day 1, day 3, day 5, and day 7, prior to collection for immunolabelling assays. Phase contrast images were observed and captured with a 10X objective unless otherwise stated.

2.8 TGF-β1 TRANSGENIC MOUSE MODEL

In comparison to the LEC rodent explant model, an *in vivo* model was established to produce and monitor the development of fibrotic plaques *in situ* (Srinivasan et al., 1998; Lovicu et al., 2004). These TG OVE853 (853) and OVE918 (918) mice lines on an FVB/N background have been described previously (see Section 2.1). At several postnatal ages (± 2 days; P7, P14, P21), WT and TG mice were obtained, and euthanised in accordance with methods stated (see Section

2.1) so that collected ocular tissue was fixed and processed for subsequent histology and immunolabelling.

2.9 OCULAR TISSUE PREPARATION FOR HISTOLOGY

WT and TG mice eyes were removed and placed immediately into clear 5 mL tubes containing 10% neutral buffered formalin (10% NBF) fixative. Tissue was then placed on an inverting rocker overnight. Following 24 hours, tissues were removed from the 10% NBF, rinsed and stored in 70% Ethanol in histology embedding cassettes. The cassettes were placed in a tissue processor (Excelsior ES, Thermo Fisher Scientific) programmed to first dehydrate the tissues in a progressive ascending concentration of Ethanol (70%–100%) over 7 hours at 40°C, and then cleared through a series of rinses in Xylene (2 x 1 hour at 40°C). Cassettes were then exposed to 3 x 1-hour molten paraffin wax changes at 60°C. Ocular tissue were then embedded in paraffin wax using a Tissue Embedding Station (Sakura Tissue-Tek, TEC 5 Embedding System). Following embedding, eye tissue was sectioned into ribbons of 7 µm thickness, using microtomy and collected onto positive-charged glass histology slides (J1800AMNZ, Thermo Scientific™). Following sectioning, slides were placed into a drying chamber overnight (37°C) prior to usage for histology or immunofluorescent labelling. Approximately 3–4 eyes at each stage of postnatal development were collected and processed.

2.10 IMMUNOFLUORESCENT LABELLING

2.10.1 Lens epithelia explants

Following tissue culture treatment, rat and mice LEC explants were fixed at specific timepoints throughout culture in 10% NBF for 10 minutes or cold 100% methanol for 45 seconds. For immunolabelling, at room temperature, explants were rehydrated several times (3 x 5 min) in phosphate-buffered saline (PBS) supplemented with BSA (0.1%, *v/w*; PBS/BSA), and permeabilised (3 x 5 min) with PBS/BSA supplemented with 0.05% Tween-20 (*v/v*) (9005-64-5, Sigma-Aldrich). Subsequent rinses in PBS/BSA (2 x 5 min) were conducted and explants were then incubated at room temperature (30 min) with 3% normal goat serum (NGS; PCN5000, Invitrogen) diluted in PBS/BSA, to reduce non-specific binding of the secondary antibody. NGS was removed and primary antibodies targeting epithelial (β-catenin), EMT (α-SMA), fibre differentiation (β-crystallin), Smad-dependent (t-Smad2/3), Smad-independent (p38 MAPK) (see Table 2.4), and cytoskeletal (Tpm) (see Table 2.5) proteins were diluted in blocking buffer (NGS) and applied to respective dishes. Following an overnight incubation,

explants were brought to room temperature and rinsed in PBS/BSA (3 x 5 min). Respective Alexa-Fluor® tagged anti-mouse and/or anti-rabbit secondary antibodies were applied for a 2-hour incubation in the dark (see Table 2.6). All secondary antibodies were diluted 1:1000 with PBS/BSA. Explants were briefly rinsed in PBS/BSA (2 x 5 min) and exposed to 3 µg/ml bisbenzimide H 33342 trihydrochloride (Hoechst® dye; B2261, Sigma-Aldrich) for 5 minutes. Following consecutive PBS/BSA rinses (3 x 5 min), explants were mounted with 22 mm Menzel circle coverslips (CS22100, Grale HDS, Trajan) coated in 10% glycerol (BIOGB0232, Astral Scientific) in PBS/BSA (*v/v*), followed by image capture using epifluorescence microscopy (DMLB 100S, Leica Microsystems) and software (Version 4.8, Leica Microsystems).

2.10.2 Whole eye sections

Paraffin-embedded ocular tissue sections on slides were dewaxed in Xylene (3 x 5 min) and rehydrated in a fume hood using a descending series of alcohol washes [100% Ethanol (2 x 2 min), 90% Ethanol (1 x 2 min), 70 % Ethanol (1 x 2 min), and 50% Ethanol (1 x 2 min)]. Slides were then washed in PBS/BSA (3 x 5 min). Excess PBS/BSA was removed from the sections and slides were placed flat in a humidified chamber. Whole eye sections were blocked for 30 minutes at room temperature using 3% NGS in PBS/BSA. Excess blocking agent was removed, and the appropriate primary antibody was added to each respective slide (see Table 2.5). Sections were incubated with the primary antibody at 4°C overnight. Following overnight incubation, sections were brought to room temperature (30 min) and rinsed in PBS/BSA. Sections were probed with specific Alexa Fluor conjugated secondary antibodies (Table 2.6) and left to incubate in the dark for 2 hours. Slides were rinsed of excess secondary antibody in PBS/BSA (2 x 5 min) and nuclear stained with Hoechst dye for 5 minutes. Consecutive rinses in PBS/BSA (3 x 5 min) were conducted to remove excess Hoechst dye. Sections were prepared for coverslip mounting by wiping off excess PBS/BSA. Mountant (10% glycerol/PBS/BSA) was added to a 24 x 50 mm rectangle coverslip (HDS Scientific Supplies Pty Ltd) that was then placed facedown onto the whole eye sections.

2.11 PROTEIN QUANTIFICATION AND WESTERN BLOTTING ANALYSIS

2.11.1 Collection of lens epithelia protein from wholemount explants

At different timepoints, M199 was discarded from each dish and replaced with cold PBS on ice. Consecutive rinses in PBS were conducted until M199 was removed and explants appeared

transparent. Explants in respective treatment groups were harvested with forceps and pooled into allocated Eppendorf tubes. Sample tubes were spun down to pool the tissue.

2.11.2 Lysing of lens epithelia samples

Following collection, cold RIPA lysis buffer (25 µL) was added to each allocated sample tube. RIPA lysis buffer contained the following reagents: 150 mM NaCl (0241, Amresco), 0.5% $C_{24}H_{39}NaO_4$ (D6750, Sigma-Aldrich), 0.1% SDS (BIOSB0485, Astral Scientific), 1 mM Na_3VO_4 (56508, Sigma-Aldrich), 1 mM NaF (S-7920, Sigma-Aldrich), 50 mM Tris-HCl pH 7.5 (T2319, Sigma-Aldrich), 0.1% Triton X-100 (93443, Sigma-Aldrich, as well as phosphatase (04906837001, Roche Applied Science) and protease (05892970001, Roche Applied Science) inhibitor tablets. Each tube was homogenised to accelerate lysis. Sample tubes were placed in a rotor centrifuge for 20 minutes at 4°C (13,200 x g, Eppendorf™ Centrifuge 5424 R), to facilitate separation of supernatant (lysate) and cell debris (pellet). Lysed sample tubes were stored at -80°C until ready for use.

2.11.3 Measuring total protein

Quantification of total lens protein of each supernatant sample was conducted using the Pierce™ Micro bicinchoninic acid (BCA) protein assay reagent kit (23235, Thermo Fisher Scientific). In a 96-well microplate (82.1581, Sarstedt AG & Co.), standard samples for low concentrations of protein (0.5–25 µg/mL^{-1}) were prepared using the manufacturers BSA stock dissolved in MQ-H2O diluent. Protein supernatant samples were prepared and diluted in MQ-H2 (1:200). Following sample preparation, a BCA working reagent was added to each allocated well, initially turning samples light green. The microplate was then covered and incubated at 60°C for 1 hour. Activity of the BCA working reagent was confirmed by observing a purple colour gradient reaction emitted from the standard sample wells. A fluorescent CLARIOstar*Plus* microplate reader (software version 5.40 R2, BMG Labtech) measured total protein absorbance and raw data was exported to MARS analysis software (version 3.31). BSA standards were quantified and mapped against known concentrations on a standard curve using Microsoft Excel (version 16.73). Supernatant sample concentrations were calculated by implementing a line of best fit along the mapped standard curve using slope-intercept form ($y = mx + b$).

2.11.4 SDS-PAGE and electrophoresis

Following calculations of all unknown sample concentrations, LEC protein sample lysates were prepared appropriately using MQH_2O as a diluent and a sample buffer; 5% 2-mercaptoethanol (β-merc; M6250, Sigma-Aldrich) incorporated in 2 x Laemmli buffer (1610737, Bio-Rad Laboratories). LEC protein lysates were placed on a heat block (100°C) for 8 minutes to ensure denaturing of samples. Samples were then cooled on ice and an equal loading of 10 µg of protein was placed onto 10-well (1.0 mm thickness) 12% Acrylamide (1610156, Bio-Rad Laboratories) sodium dodecyl-sulfate polyacrylamide gel electrophoresis (SDS-PAGE) gels. 1.5 µl of a dual colour protein standard ladder (1610374, Bio-Rad Laboratories) was also loaded to separate at a range from 10–250 kDa.

Samples were initially run at 30 minutes (70 V) to facilitate appropriate protein stacking and separation, followed by 2 hours at 110 V. Loaded protein was transferred from the SDS-PAGE gel onto an immobilon®-PSQ polyvinylidene fluoride (PVDF), 0.22 µm thick membrane (ISEQ00010, Merk Millipore), for 1 hour (100 V) at 4°C. PVDF membranes were incubated in 2.5% BSA blocking buffer diluted in tris-buffered saline with 0.1% Tween-20 (TBST, *w/v*) and incubated for 1 hour with agitation at room temperature. Primary antibodies probing for epithelial, EMT, fibre differentiation, cytoskeleton, TGF-β canonical and non-canonical signalling markers (Table 2.7), were added to membranes and incubated overnight (at 4°C) with agitation.

Membranes were then rinsed in TBST (3 x 5 min washes), and a secondary horseradish peroxidase (HRP)-conjugated antibody was applied, and membranes remained at room temperature for a 2-hour incubation period. Goat anti-rabbit IgG (7074, Cell Signaling Technology), horse anti-mouse IgG (7076, Cell Signaling Technology), and goat anti-mouse IgG+IgM (ab47827, abcam) secondary antibodies were prepared in TBST (1:5000). Following incubation, membranes were rinsed in TBST (3 x 10 min) and an immobilon chemiluminescent HRP substrate (WBKLS0500, Merck Millipore) was applied for chemiluminescent visualisation. Protein chemiluminescent signals and densitometry were imaged and analysed using Bio-Rad ChemiDoc^{TM} MP imaging (Universal Hood III) and ImageLab software (version 6.1.0 build 7, Bio-Rad Laboratories Inc.).

2.12 STATISTICAL ANALYSIS

For each morphological and immunofluorescent experimental series, a minimum of three individual experimental replicates (n=3) were conducted unless stated otherwise. For western

blot analysis using rat lens tissues, a minimum of 6 x LEC explants were collected per sample, for each treatment group. An average of 12 x LEC explants derived from mice (WT and mutant) were collected per sample for western blot analysis, for each treatment group, across 3 independent experiments. All data acquired was graphed appropriately using GraphPad Prism 10 software. For western blots examining differences in epithelial, EMT, and fibre differentiation marker labelling, all raw intensity values of probed proteins were relatively compared to a loading control protein (GAPDH). Respective data was analysed using one-way analysis of variance (ANOVA) as we assumed equal standard deviation (SD) and residuals demonstrated normal distribution. A multiple comparisons test, post-hoc Tukey, was conducted that compared the mean of one column (treatment) with the mean of every other column (other treatment groups). Phosphorylated protein levels were calculated relative to the density of the total protein to determine differences in TGF-β activity for downstream signalling proteins, including canonical (Smad2/3) and non-canonical (MAPK/ERK1/2, p38 MAPK) pathways. GAPDH was also implemented in these experiments as a loading control.

For western blots examining changes in Tpm marker expression in the presence/absence of TGF-β2, as well as ATM and/or p38α MAPK specific inhibitor compounds, proteins of interest were compared relative to β-actin as a protein loading control. Respective data was analysed using an unpaired, parametric two-tailed t-test. All graphed data was presented as the standard error of the mean (± SEM) and probability values (p) < 0.05 were considered statistically significant.

2.13 REAGENTS AND CONSTITUENTS

Table 2.1. Reagents and Consumables used for Primary Tissue Culture

Reagent/Consumable	Catalogue number and Commercial Source
Amphotericin B	15290-018 Gibco™, Life Technologies, Thermo Fisher Scientific
Bovine serum albumin (BSA)	9048-46-8, Sigma-Aldrich
EuroClone CO2 Incubator (S@feGrow 188 pro Model)	CO20010, LAF Technologies Pty Ltd.
L-glutamine	25030081, Gibco™, Life Technologies, Thermo Fisher
Medium 199 with Earle's salts (M199; 10x)	M0650-100ML, Sigma-Aldrich
Nunc™ EasYDish™ (35 x 10 mm Dishes)	NUN150460, Thermo Fisher Scientific
Penicillin-Streptomycin	15140-122, Thermo Fisher Scientific
Sodium Hydrogen Carbonate	144-55-8, Merck Millipore

Table 2.2. Growth factor and their dosages for functional studies

Dose Classification	Concentration	Diluent	Cell response	Catalogue number and Commercial Source
Recombinant human Fibroblast Growth Factor-2 (FGF-2)				
Low dose	5 ng/mL	M199	Proliferation	233-FB R&D systems
High dose	200 ng/mL	M199	Fibre Differentiation	
Recombinant human Transforming Growth Factor-beta 2 (TGF-β2)				
Low dose	50 pg/mL	M199	EMT	302-B2-002 R&D Systems
High dose	200 pg/mL	M199	EMT	

Table 2.3. Inhibitors and their dosages for functional studies

Inhibitor	Target(s)	Concentrations	Catalogue number and Commercial Source
ATM-3507	Tpm3.1	0.5–2 μM	Provided by Prof. Peter Gunning and Prof. Edna Hardeman from UNSW, Australia
Skepinone-L	p38 MAPK XIX	0.5–5 μM	506174, Merck Millipore
TR100	Tpm3.1	1–2 μM	Provided by Prof. Peter Gunning and Prof. Edna Hardeman from UNSW, Australia

Table 2.4. Primary antibodies for immunofluorescence assays

Antibody	Biological Source and Antibody Type	Dilution	Marker	Catalogue number and Commercial Source
Anti-Actin α-Smooth Muscle antibody (α-SMA)	Mouse monoclonal	1:200	Actin filament stress fibres (during EMT)	A2547 Sigma-Aldrich
β-catenin	Rabbit Polyclonal	1:150	Epithelial/ Cadherins	ab6302 abcam
β-crystallin	Rabbit Polyclonal	1:200	Fibre differentiation	Homemade
Smad2/3 (D7G7) XP® (t-Smad2/3)	Rabbit monoclonal	1:150	TGF-β canonical signalling	8685 Cell Signaling Technology
p38 MAPK (D13E1) XP®	Rabbit monoclonal	1:150	TGF-β non-canonical signalling	8690 Cell Signaling Technology

Table 2.5. Tpm-specific Primary antibodies for immunofluorescence

Gene name	Antibody	Specificity	Cross reactivity	Biological Source and Antibody Isotype	Dilution
Tpm1	α9d (15D12.2)	Tpm1.4, 1.6–1.9, 2.1	Sometimes with Tpm3.1	Mouse mAb IgG	1:150
	CGβ6	Tpm1.6–1.9	n/a	Mouse mAb IgM Hybridoma supernatant	1:100
	α2a	Tpm1.4	n/a	Mouse mAb Hybridoma supernatant	1:100
Tpm2	CG1	Tpm2.1	Sometimes with Tpm4.2	Mouse mAb IgG_1 purified ascites	1:100
Tpm3	γ9d (2G10.2)	Tpm3.1–3.2	Sometimes with Tpm1.6– 1.9, 2.1	Mouse mAb IgG purified ascites	1:150
	γ9a	Tpm3.3, 3.5, 3.8, 3.9	n/a	Mouse mAb	1:150
Tpm4	δ9d	Tpm4.2	n/a	Rabbit pAb Affinity purified	1:150

Table 2.6. Secondary fluorescent conjugated antibodies

Antibody	Target Species and Antibody Type	Dilution	Alexa Fluor Conjugate	Catalogue number and Commercial Source
Goat Anti-Mouse IgG (H&L)	Mouse polyclonal	1:1000	594	ab150116, Abcam
Goat Anti-Mouse IgM mu chain	Mouse polyclonal	1:1000	568	ab175702, Abcam
Goat Anti-Rabbit IgG (H&L)	Rabbit polyclonal	1:1000	594	ab150080, Abcam
Goat Anti-Rabbit IgG (H&L)	Rabbit polyclonal	1:1000	594	A11037, Invitrogen
Goat Anti-Rabbit IgG (H&L)	Rabbit polyclonal	1:1000	488	ab150077, Abcam

Table 2.7. Primary Antibodies and Protein Standards for Western blot analysis

Antibody	Antibody or Protein standard type	Dilution	Molecular Weight (kDa)	Catalogue number and Commercial Source
α-SMA	Mouse mAb	1:1200	42	A2547, Sigma-Aldrich
α2a	Mouse mAb IgM Hybridoma supernatant	1:1000	40	Prof. Peter Gunning, UNSW
α9d	Mouse mAb IgG	1:1000	34-36, 38	
β-actin	Rabbit mAb IgG	1:5000	45	4970, Cell Signaling
β-actin	Mouse mAb	1:5000	42	A2228, Sigma-Aldrich
β-catenin	Rabbit pAb	1:1000	95	ab6302, Abcam
β-crystallin	Rabbit pAb	1:1000	20–25	In House
CGβ6	Mouse mAb IgM Hybridoma supernatant	1:1000	30	Prof. Peter Gunning, UNSW
CG1	Mouse mAb IgG_1 purified ascites	1:1000	38	
δ9d	Rabbit pAb Affinity purified	1:1000	30	
GAPDH	Mouse mAb	1:2000	37	G8795, Sigma-Aldrich
γ9a	Mouse mAb	1:1000	30	Prof. Peter Gunning, UNSW
γ9d	Mouse mAb IgG purified ascites	1:1000	30	
Pre-stained Standards	12x Recombinant proteins	2.5µl/run	2–250	1610377, Bio-Rad Laboratories
p-Smad2/3	Rabbit, mAb	1:1000	52, 60	8828, Cell Signaling
t-Smad2/3	Rabbit mAb	1:1000	52, 60	8685, Cell Signaling
p-p44/42 MAPK	Rabbit mAb	1:1000	42, 44	4370, Cell Signaling
t-p44/42 MAPK	Rabbit pAb	1:1000	42, 44	9102, Cell Signaling
p38	Rabbit mAb	1:1000	40	8690, Cell Signaling
p-p38	Rabbit mAb	1:1000	43	4511, Cell Signaling

CHAPTER 3: EXPRESSION OF TROPOMYOSIN IN THE POSTNATAL RODENT LENS

3.1 INTRODUCTION

The actin cytoskeleton, and its associated F-actin networks, are vital for the maintenance and regulation of cell integrity and stability in both non-muscle and muscle tissue. In the eye lens, the biomechanics of lens development and growth is due to a continuous cycle of epithelial cell proliferation to fibre cell differentiation at the lens equator (Lovicu and McAvoy, 2005; C. Cheng et al., 2017). Actin cytoskeletal proteins, such as tropomyosin (Tpm), are integral regulators of lens cell biomechanics and stability, facilitating lens function to refract light (Fischer et al., 2000; Cheng et al., 2018). The role of Tpm in the behaviour and cytoskeletal function of lens epithelial cells (LECs) and lens fibre cells (LFCs) has previously been reviewed (C. Cheng et al., 2017). Despite the regulatory functions of Tpm, these cytoskeletal proteins play an isoform- and tissue-specific role in stress-fibre formation, particularly in cells transforming during fibrosis or in cancer (Franzén et al., 1996; Bakin et al., 2004; Gateva et al., 2017) as well as in cataract formation (Kubo et al., 2013, 2017; Shibata et al., 2018; T. Shibata et al., 2021). Much research has already established expression and regulatory function of several Tpm isoforms in the eye lens (Kubo et al., 2010, 2013, 2017, 2018; Cheng et al., 2018; Shibata et al., 2018; Shu and Lovicu, 2019; Parreno et al., 2020; T. Shibata et al., 2021; Flokis and Lovicu, 2023); however, the exact role for each of the Tpm splice variants in lens is still unclear.

In this study, we will examine the putative role for different Tpm isoforms during lens cellular processes, including lens epithelial cell maintenance, fibre-like differentiation, and EMT, in lens epithelial cells, fibre cells, and myofibroblasts. We characterised both normal and dysregulated expression and localisation of various Tpm isoforms (coding for all *TPM* genes, see Table 3.1) *in vitro* using rat LEC explants, as well as *in vivo* using lenses from wild type (WT) and transgenic (TG) mice overexpressing TGF-β1 at different postnatal stages.

3.2 MATERIALS AND METHODS

3.2.1 Wistar rat tissue acquisition and cell culture

10-day-old (P10) and 21-day-old (P21) Wistar rats were used to prepare lens epithelial explants. Rats were euthanised, lens tissue acquired, and cultured in conditions previously described (see Chapter 2: Sections 2.1–2.3).

3.2.2 Growth Factor treatment

Preparation of growth factors, fibroblast growth factor 2 (FGF-2) and transforming growth factor-beta 2 (TGF-β2), were described in the previous chapter (see Chapter 2: Section 2.4–2.5). Rat LEC explants were exposed to either FGF-2 (200 ng/mL), to induce a fibre-like differentiation response, or TGF-β2 (200 pg/mL) to induce an EMT response (see Chapter 2: Table 2.2). Explants not treated with either growth factor were considered controls (non-treated). All explants were assessed and photographed across a 5-day culture period using phase contrast microscopy (see Chapter 2: Section 2.7).

3.2.3 Immunofluorescence for rat LEC explants

A detailed methodology for 10% NBF fixation, rehydration, permeabilisation, and blocking of LEC explants in 3% NGS blocking buffer has been described (see Chapter 2: Section 2.10). For subsequent experiments, examining the fixative-dependent localisation and expression of Tpm, explants were fixed in cold 100% methanol for 45 seconds. Explants were then rinsed in PBS/BSA (2 x 5 min). NGS blocking buffer was then applied to explants and incubated as previously described (Chapter 2: Section 2.10). Tpm-specific isoforms were immunolabelled using the following primary antibodies: α9d, CGβ6, α2a, CG1, γ9d, γ9a, and δ9d (see Chapter 2: Table 2.5 and Chapter 3: Table 3.1). All primary Tpm antibodies were provided by Professor's Peter Gunning and Edna Hardeman from The University of New South Wales, Sydney, Australia. Dishes containing explants were stored in a humidified container and incubated at 4°C overnight. Explants were rinsed (PBS/BSA) and goat anti-mouse 594 (IgG), anti-mouse 568 (IgM), and/or anti-rabbit 594 (IgG) were all secondary antibodies used and diluted in PBS/BSA (1:1000). Following a 2-hour darkroom incubation, secondary antibodies were removed, and a nuclear stain (Hoechst) was applied to explants for 5 minutes, followed by several rinses in PBS/BSA, and mounted to coverslips with PBS/glycerol, as previously described (see Chapter 2: Section 2.10).

Table 3.1. Tropomyosin antibodies

Antibody	Isoform Specificity	Cross Reactivity
α9d (15D12.2)	Tpm1.4, 1.6–1.9, 2.1	Sometimes with Tpm3.1
γ9d (2G10.2)	Tpm3.1–3.2	Sometimes with Tpm1.6–1.9, 2.1
CG1 (ascites)	Tpm2.1	Sometimes with Tpm4.2
CGβ6	Tpm1.6–1.9	-
δ9d	Tpm4.2	-
α2a	Tpm1.4	-
γ9a	Tpm3.3, 3.5, 3.8, 3.9	-

A list of Tpm-specific antibodies provided by Prof. Peter Gunning and Prof. Edna Hardeman from the University of New South Wales, Sydney, Australia.

3.2.4 Transgenic mice overexpressing TGF-β1

This chapter will utilise transgenic (TG) mice as previously described (see Chapter 2: Section 2.1), that overexpress an active form of TGF-β1 specifically in the lens (originally generated in the laboratory of Professor Paul Overbeek, at the Baylor College of Medicine, Houston, TX, USA) (Srinivasan et al., 1998). TG lines referred to here as OVE853 (853) or OVE918 (918), both on an FVB/N background (see Chapter 2: Section 2.8). These TG mice develop signs of ASC within the first week of birth that progresses to a mature fibrotic plaque within weeks. Control wild type (WT) mice on the same background demonstrate a normal lens phenotype. For this chapter, WT and TG ocular tissue was collected from several postnatal ages; P7, P14, and P21 (± 2 days). Methods regarding fixation of ocular tissue, tissue processing, and microtomy have previously been described (see Chapter 2: Sections 2.8–2.9).

3.2.5 Immunofluorescence of WT and TG mice lens sections

For experiments investigating changes in postnatal expression and localisation of Tpm in WT and TG mice lenses, slides containing paraffin-embedded sections of eyes from each respective line were dewaxed in Xylene and rehydrated following serial washes in descending concentrations of ethanol (see Chapter 2: Section 2.10.2). Slides were then rinsed several times in PBS/BSA (3 x 5 min) and were carefully wiped around the sections to remove excess PBS/BSA leaving enough of a film covering the tissue to prevent drying out. A 3% NGS blocking buffer (NGS/PBS/BSA, *w/v*) was applied to each section for 30 minutes at room temperature in a humidified chamber. Primary mouse and rabbit antibodies targeting Tpm-specific isoforms (see Chapter 2: Table 2.5 and Table 3.1) were diluted appropriately in blocking buffer and were applied to eye sections overnight at 4°C. Primary antibodies were

then removed by rinsing in PBS/BSA (3 x 5 min) and the appropriate goat anti-mouse (ab150116) and anti-rabbit (ab150080) secondary Alexa Fluor conjugated antibodies (see Chapter 2: Table 2.6) were added to respective slides, where they remained for 2 hours in a dark humidified chamber. Unbound secondary antibody was removed by rinsing in PBS/BSA, and nuclei of cells were stained using Hoechst dye diluted in PBS/BSA for 5 minutes. Slides were then rinsed to remove excess Hoechst stain and mounted using 10% glycerol/PBS with coverslips (24 x 50 mm), in preparation for immunofluorescence microscopy.

3.2.6 Western blotting analysis

3.2.6.1 Collection of rat and mouse lens epithelia

Following treatment, rat LEC explants were washed on ice in cold PBS until media was rinsed from explants. Explants were then harvested and pooled into respective treatment group allocated tubes on ice. For one experimental replicate, each sample had approximately 6–8 explants. For a detailed description on rat LEC explant harvesting, see Chapter 2: Section 2.11.1. For experiments examining normal and aberrant protein expression of Tpm in mice lens epithelia, tissue was collected from P20–30-day-old weanling WT and 918 TG mouse lines. To determine the initial protein levels of Tpm in both WT and TG tissue, epithelia was collected fresh from mixed sexes. For one experimental replicate, approximately 12–14 mouse lens epithelial explants were collected per sample.

3.2.6.2 Protein extraction and measurement of total protein

Each sample tube containing rat LEC or mouse lens explants was lysed in 25–30 µl of cold RIPA lysis buffer and homogenised using previously described methods (Chapter 2: Section 2.11.2). Methodology regarding measuring and standardisation of total protein concentrations from each sample lysate were all previously described (see Chapter 2: Sections 2.12.1–2.12.4).

3.2.6.3 SDS-PAGE

Rat LEC explant lysates, as well as WT and TG mice lens epithelia lysates, were prepared in 5% β-merc (2-mercaptoethanol) in 2x Laemmli sample buffer (1:1) on ice. Denaturing of protein was conducted through heating the samples for 5–8 minutes at 100ºC. All prepared lysates were then briefly cooled and centrifuged before loading onto a 12% SDS-PAGE gel. Samples were run at 70 V for 30 minutes, followed by 1.5 hours at 120 V to ensure even separation of proteins. Loaded protein was then transferred onto a PVDF membrane for 1 hour

at 100 V (4ºC). Membranes were then blocked in BSA (2.5% *w/v*) in TBS with 0.1% Tween-20 (TBST, *w/v*) for 1 hour at room temperature on a rocker for gentle agitation. Membranes containing samples from either rat and/or WT and TG mice were incubated overnight (4ºC) with the appropriate Tpm primary antibodies. Tpm antibodies; including α9d (mouse), CG1 (mouse), CGβ6 (mouse), α2a (mouse), γ9a (mouse), γ9d (mouse), and δ9d (rabbit), were all diluted 1:1000 in BSA/TBST. Primary antibodies were removed, and membranes were washed in TBST (3 x 5 min) followed by the addition of appropriate secondary antibodies. Anti-mouse IgG (#7076, Cell Signaling), anti-mouse IgM (#ab47827, abcam), and anti-rabbit IgG (#7074, Cell Signaling) HRP-conjugated secondary antibodies were applied (1:5000 in TBST) to respective membranes and incubated for 2 hours at room temperature. Membranes were then washed in TBST (3 x 10 min) and briefly dried using Kimtech wipes before applying a chemiluminescent substrate (1:1 ratio, WBKLS0500, Merck Millipore) for 2 minutes to facilitate protein visualisation using a ChemiDoc Imaging system. Excess chemiluminescent substrate was then rinsed off (3 x 5 min) with TBST. Tpm proteins were then compared relative to loading control β-actin (rabbit, #4970, Cell Signaling). β-actin was applied to membranes and remained on for 1 hour at room temperature (1:5000 in TBT). The loading control was then removed with several washes in TBST and probed using an anti-rabbit secondary (1 hour incubation). Membranes were rinsed before the application of the chemiluminescent substrate for further imaging. Protein chemiluminescent signals were acquired using ImageLab software (version 6.1.0, Bio-Rad Laboratories Inc.) and analysed through densitometry.

3.2.7 Statistical analysis

Each experiment series contained a minimum of three independent replicates (n=3), unless stated otherwise. For rat LEC samples collected from control (non-treated), FGF-2, or TGF-β2-treated rat explants, approximately 8 explants were collected per sample for three independent experimental replicates. All respective densitometry data was analysed using an unpaired, parametric two-tailed t-test (GraphPad Prism Version 10.0.2). All graphed data represented as the standard error of the mean (± SEM) and probability values ($p < 0.05$) was considered statistically significant.

3.3 RESULTS

3.3.1 Postnatal expression of Tropomyosin in the rat LEC explant system

Using a publicly available gene transcript database, *iSyTE* (Lachke et al., 2012; Kakrana et al., 2018), we processed data from a microarray dataset (Illumina MouseWG-6 v2.0) to observe any changes in *Tpm* expression throughout the postnatal 4–60 days old in WT ICR mice. Differential regulation was noted for all 4 Tpm genes across postnatal stages, particularly with *Tpm4* raw expression increasing with age (Figure 3.1). Expression of *Tpm1* and *Tpm3* were lower than *Tpm4*, with minimal *Tpm2* expression throughout postnatal stages.

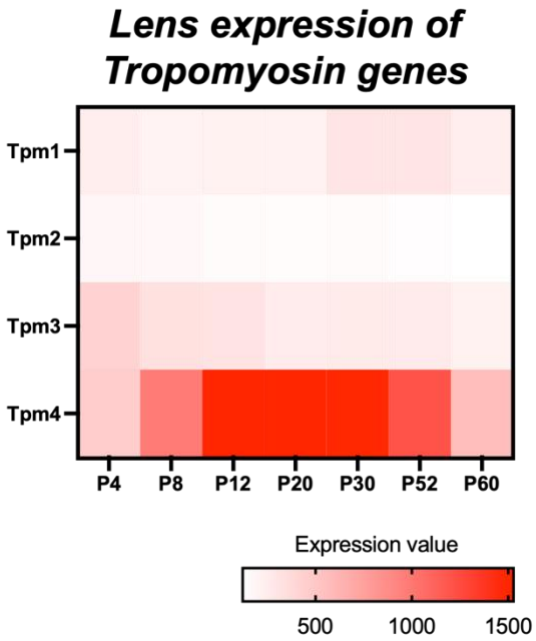

Figure 3.1. Transcript lens expression profile of Tropomyosin across postnatal mouse development. Transcript expression profile of genes encoding for tropomyosin 1 (Tpm1), tropomyosin 2 (Tpm2), tropomyosin 3 (Tpm3), and tropomyosin 4 (Tpm4), from postnatal wildtype mouse lens at stages P4, P8, P12, P20, P30, P52, and P60. Normalised expression using postnatal development dataset processed from Illumina MouseWG-6 v2.0 microarray platform. Low to high intensity (red) of the heat map reflects an increase in Tpm gene expression. Lens gene expression data sourced from open access database iSyTE 2.0 (integrated Systems Tool for Eye gene discovery) *(Lachke et al., 2012; Kakrana et al., 2018)*.

Based on this dataset, all 4 *Tpm* genes are normally present within the mouse lens. We looked at whether Tpm protein expression levels were similar in the current study's rat LEC explant system. We first conducted isotype controls on all provided Tpm isoforms in control 10-day-old (P10) LEC explants 24 hours after explant acquisition (Figure 3.2 A–C, G–I, M). Tpm1 was

immunolabelled using α9d, CGβ6, and α2a, that are specific for various Tpm1 isoforms. Of all Tpm1-specific antibodies, α9d demonstrated the strongest label, with cytoplasmic actin filament localisation indicative of Tpm1.4, Tpm1.6–1.9, and Tpm2.1 bundles in these cells (Figure 3.2 D). Compared to α9d, CGβ6 (Tpm1.6–1.9, Figure 3.2 E) and α2a (Tpm1.4-specific, Figure 3.2 F) immunolabelled explants demonstrated low immunoreactivity, with speckled background α2a labelling and little to no clear region of Tpm isoform localisation in these LECs. Immunolabelling for Tpm2.1 using CG1 was weak, and localisation was mostly diffuse background in LECs (Figure 3.2 J). Tpm3.1/3.2 was probed using γ9d (Figure 3.2 K) and localisation of Tpm3.1/3.2 remained cytoplasmic. Minimal immunoreactivity was observed in γ9a labelled LEC explants (Figure 3.2 L). Cytoplasmic localisation of Tpm4.2 using δ9d was similar to that seen in γ9d probed explants, with moderate levels of δ9d intensity (Figure 3.2 N).

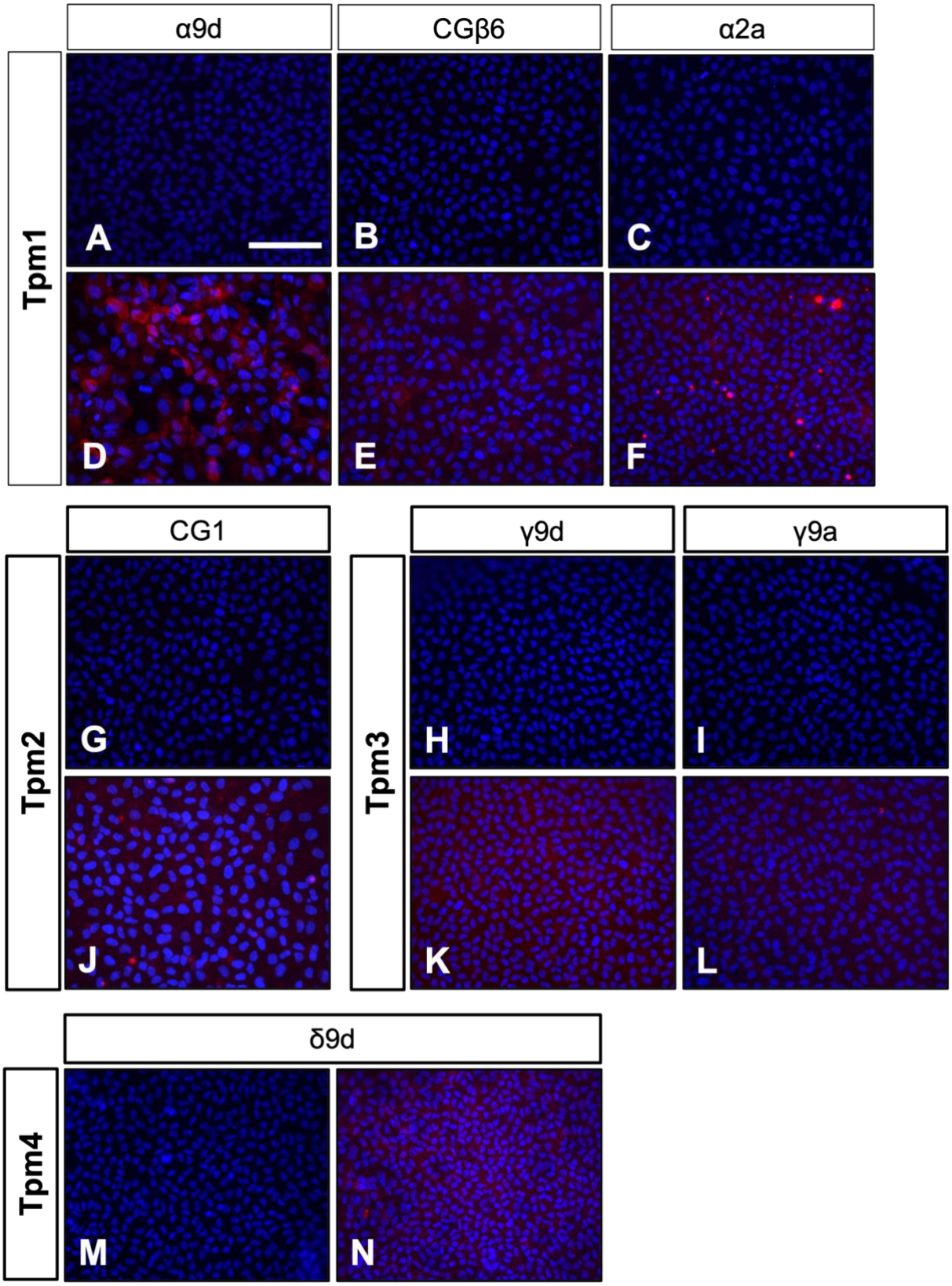

Figure 3.2. Tropomyosin expression in P10 rat lens epithelial cell explants. Control (non-treated) P10 rat LECs fixed in 10% NBF 24 hours after explant acquisition. Merged representative images of Tpm (red) and nuclear visualisation using Hoechst dye (blue). Isotype controls for all Tpm antibodies (A–C, G–I, M). Explants immunolabelled for Tpm1 with α9d (A, D), CGβ6 (B, E), and α2a (C, F); Tpm2 with CG1 (G, J); Tpm3 with γ9d (H, K) and γ9a (I, L); and Tpm4 with δ9d (M, N). Scale bar: 100 μm.

3.3.2 In vitro fixative-dependent expression and localisation of Tpm in TGF-β2-induced rat lens EMT

We compared control and TGF-β2-induced P21 explants with P10 explants from the same treatment groups at 3 days of culture (Figure 3.3); a stage at which the most significant phenotypical changes tend to occur in the current model. P10 explants in the absence (Figure 3.3 A) or presence of TGF-β2 (Figure 3.3 C) maintained the epithelial phenotype and LECs were sustained at day 3 of culture. Treatment with TGF-β2 evidently did not induce an EMT response in P10 explants (Figure 3.3 C). In control P21 explants, no phenotypical changes occurred to the cobblestone-like appearance of these lens epithelial cells (Figure 3.3 B). Unlike TGF-β2-treated P10 explants, P21 explants exposed to TGF-β2 underwent a transdifferentiation response, whereby epithelial cells transitioned into myofibroblastic cell types (Figure 3.3 D). This new cell phenotype is characterised by the modulation of the underlying lens capsule, with heightened capsular wrinkling as a direct result of myofibroblastic cells acquiring contractile properties.

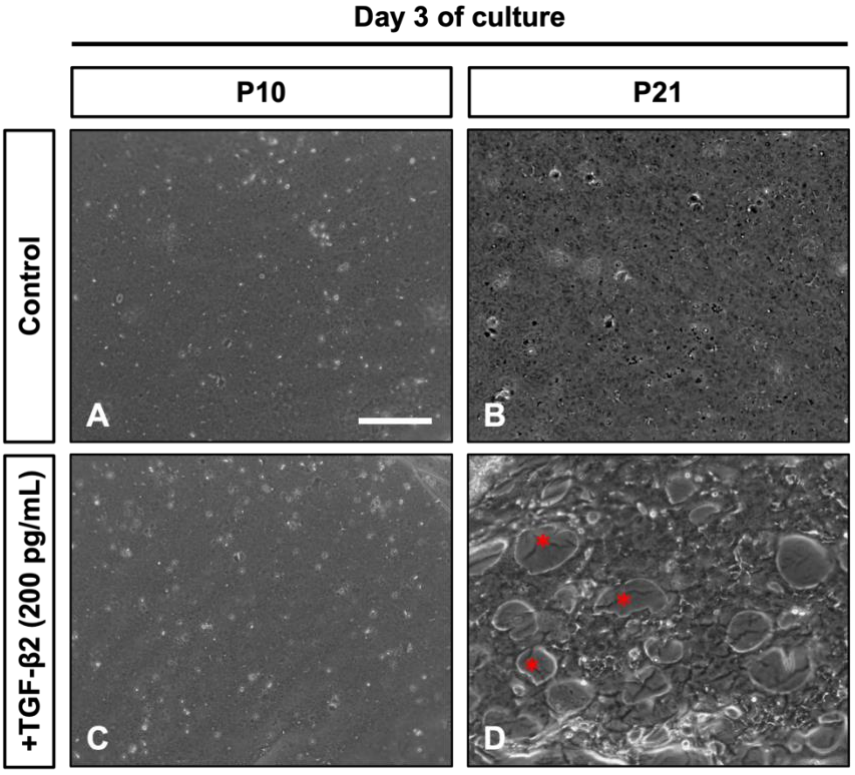

Figure 3.3. TGF-β-induced rat lens EMT is age-specific. Representative phase contrast images of lens epithelial cell explants of postnatal 10-day-old (P10) and 21-day-old (P21) Wistar rats at 3 days of culture. Control explants in both P10 (A) and P21 (B) explants maintained the archetypical cuboidal epithelia phenotype. Treatment with TGF-β2 (200 pg/mL) did not alter the LEC phenotype in P10 explants (C). Transdifferentiation from epithelial to mesenchymal/myofibroblastic cells evident in P21 explants treated with TGF-β2 (D). Capsular wrinkling (red asterisks) and exposed regions of the anterior lens capsule caused by newly contractile cells. Scale bar: 200 µm.

To investigate the specificity of Tpm isoforms in the lens, particularly during TGF-β2-induced EMT, immunolabelling was conducted in control and TGF-β2-treated P21 rat LEC explants after 72 hours of culture: a previously established timepoint indicative of α-SMA upregulation and associated stress fibre assembly in TGF-β-induced conditions (Wojciechowski et al., 2017; Shu et al., 2021; Flokis and Lovicu, 2023). Since LECs did not respond to TGF-β2 at stages earlier than P21, we only conducted further characterisation of Tpm using LECs from P21 rats.

3.3.2.1 Tropomyosin 1

In control explants, immunolabelling for Tpm1 using methanol fixation did not show immunoreactivity for α9d (Figure 3.4 A) or CGβ6 (Figure 3.4 B). Despite this, methanol-fixed control explants immunolabelled strongly for α2a, particularly in the cytoplasmic actin filaments of LECs (Figure 3.4 C). The addition of TGF-β2 did not induce α9d (Figure 3.4 D) or CGβ6 (Figure 3.4 E) reactivity in these explants, although there was high background in α9d-labelled explants. Reactivity for α2a remained strong and cytoskeletal localisation of Tpm1.4 did not alter regardless of TGF-β2 exposure (Figure 3.4 F). LEC explants fixed with 10% NBF displayed differences in Tpm1 expression and localisation in comparison to methanol-fixed explants. Control LEC explants (Figure 3.4 G) expressed relatively strong basal levels of α9d localised in bundles or patches in stress fibres of LECs. Unlike methanol fixation, 10% NBF-fixed explants treated with TGF-β2 had increased immunoreactivity for α9d with clear actin filament localisation in cells undergoing morphological alteration during TGF-β2-induced EMT (Figure 3.4 J). Minimal reactivity for CGβ6 was observed in both control and TGF-β2-treated explants (Figure 3.4 H, K). Immunolabelling for Tpm1.4 (α2a) was lower than α9d in control 10% NBF-fixed explants (Figure 3.4 I), with localisation appearing cytoplasmic in grouped patches. In comparison, TGF-β2-treated explants promoted α2a actin filament/stress fibre localisation and slightly increased levels (Figure 3.4 L) when compared to control explants (Figure 3.4 I). Based on differences between expression and localisation of Tpm1 in α9d, CGβ6, and α2a immunolabelled explants, localisation of Tpm1 in non-treated and TGF-β2-treated LECs may be isoform-specific.

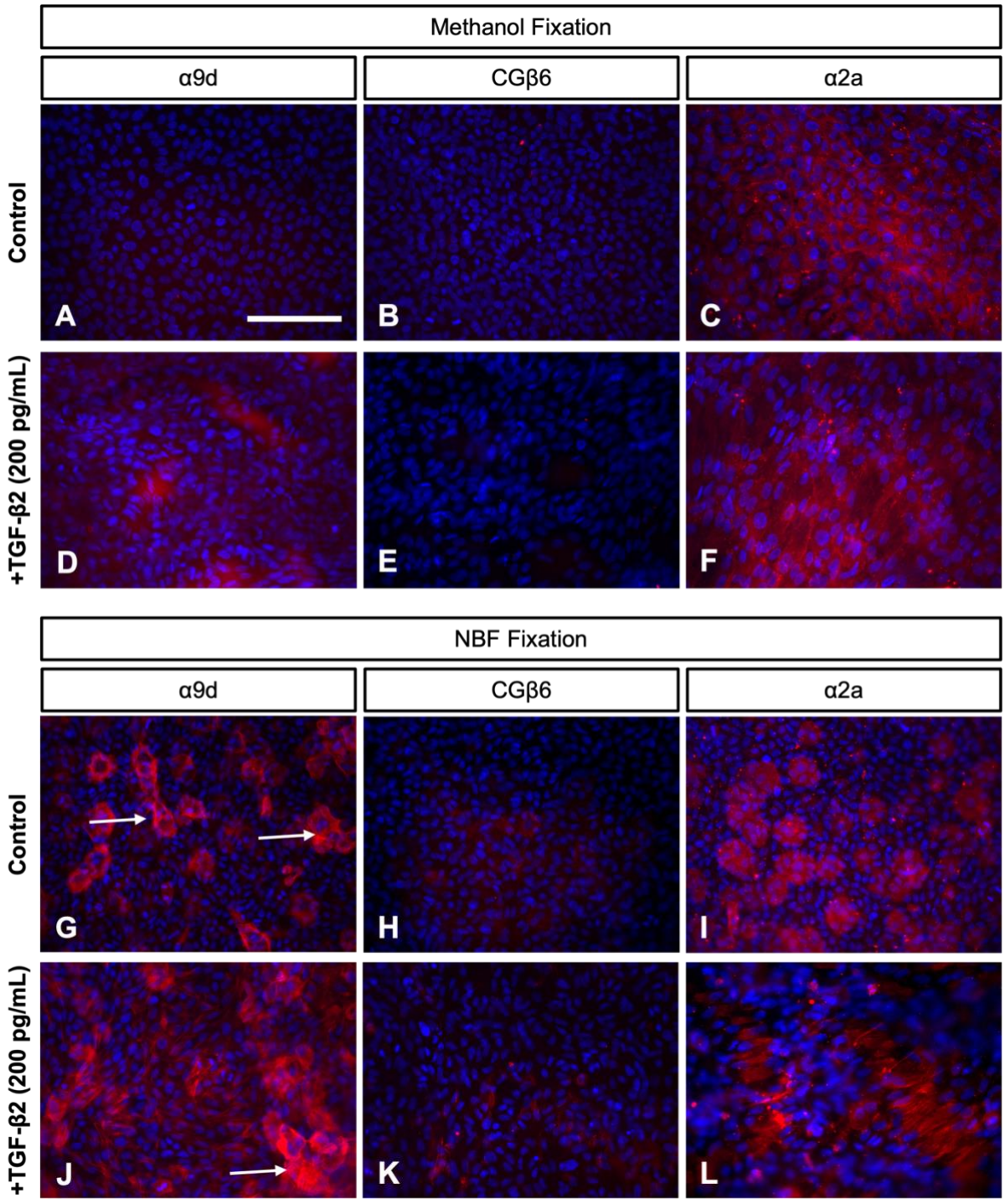

Figure 3.4. Fixative-dependent immunolabelling of Tropomyosin 1 during TGF-β2-induced lens EMT. Control (A–C, G–I) and TGF-β2 (200 pg/mL)-treated (D–F, J–L) P21 LECs after 72 hours of culture, fixed in 100% methanol (A–F) and 10% neutral buffered formalin (NBF, G–L). Merged representative images of Tpm (red) and nuclear visualisation with Hoechst (blue). Explants were immunolabelled for Tpm1 using isoform-specific antibodies: α9d (A, D, G, J), CGβ6 (B, E, H, K), and α2a (C, F, I, L). Tpm isoform bundles in actin filaments (white arrows). Scale bar: 100 μm.

3.3.2.2 Tropomyosin 2

Tpm2.1-specific CG1 antibody revealed minimal reactivity for Tpm2.1 in control LEC explants fixed with methanol (Figure 3.5 A) and/or 10% NBF (Figure 3.5 B). The localisation of Tpm2.1 appeared speckled in regions surrounding LEC nuclei. Speckled actin localisation of CG1 was increased in TGF-β2-treated explants fixed with methanol (Figure 3.5 C); however, NBF fixation promoted no specific CG1 reactivity with regions of background labelling (Figure 3.5 D).

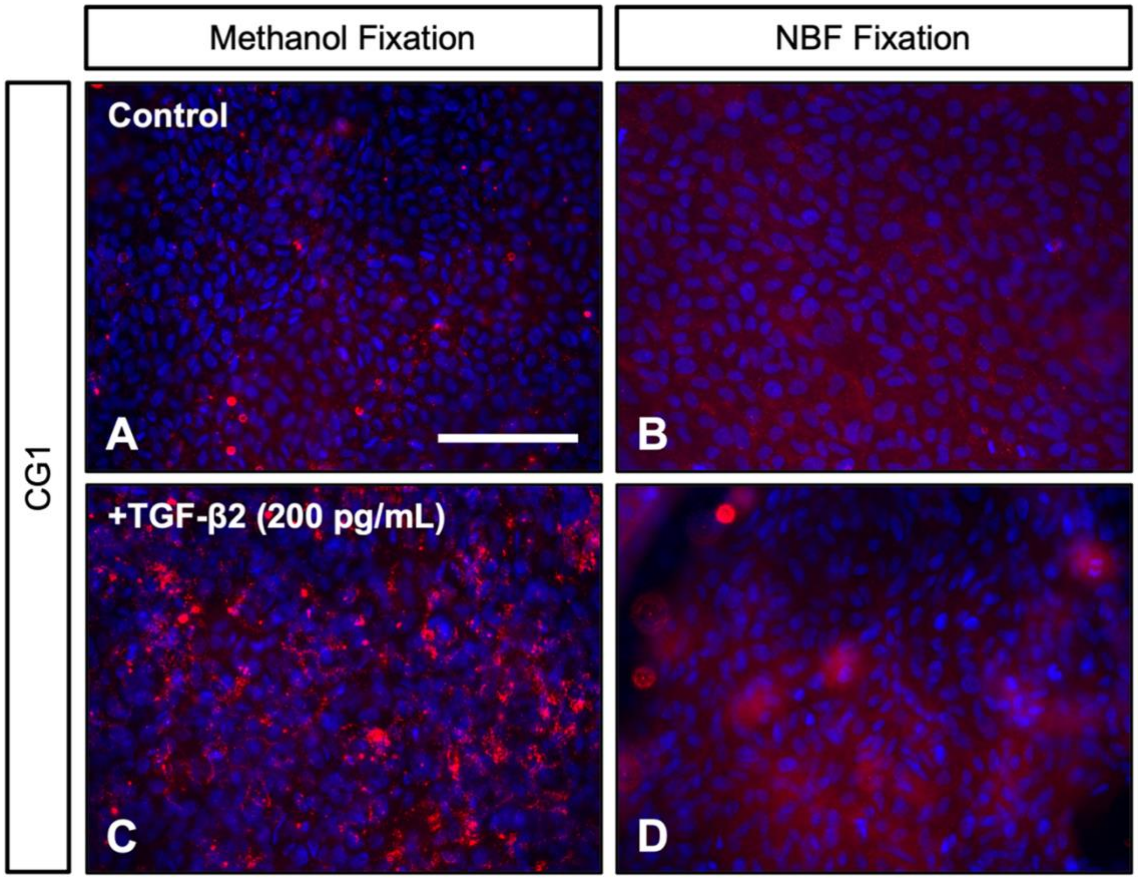

Figure 3.5. Fixative-dependent immunolabelling of Tropomyosin 2 during TGF-β2-induced lens EMT. Control (A, B) and TGF-β2 (200 pg/mL)-treated (C, D) P21 LECs after 72 hours of culture, fixed in 100% methanol (A, C) and 10% neutral buffered formalin (NBF, B, D). Merged representative images of Tpm2.1, using a Tpm2.1-specific antibody (CG1, red) and nuclear visualisation with Hoechst (blue). Scale bar: 100 μm.

3.3.2.3 Tropomyosin 3

Control lens explants immunolabelled with γ9d exhibited strong but diffuse cytoplasmic localisation of Tpm3.1/3.2 when fixed with methanol (Figure 3.6 A). The speckled immunolocalisation of γ9d mirrored that observed in methanol-fixed explants treated with TGF-β2 and immunolabelled for CG1 (Figure 3.5 C). Methanol fixation did not alter the immunolocalisation of γ9d when cells were exposed to TGF-β2 (Figure 3.6 C), and similar expression levels and speckled localisation in the cell cytoplasm of myofibroblastic cells, seen in control explants, was observed. High reactivity and actin filament localisation of Tpm3.1/3.2 was evident in control explants fixed with NBF (Figure 3.6 E). In addition, this high reactivity for γ9d was seen in TGF-β2-treated NBF-fixed LECs, with clear stress fibre localisation in elongating myofibroblastic cells (Figure 3.6 G). γ9a immunolabelled control lens epithelial explants fixed with methanol (Figure 3.6 B) displayed a reduced intensity of Tpm3 compared to γ9d control explants (Figure 3.6 A); however, the localisation of Tpm3.3, Tpm3.5, and Tpm3.8/3.9 was similar, with widespread speckled/punctate localisation in the cell cytoplasm. TGF-β2-treated LECs immunolabelled for γ9a had slightly increased intensity in newly transdifferentiating cells, evident by elongating nuclei, when fixed with methanol (Figure 3.6 D). The localisation of γ9a was relocated to the actin fibres of these cells. Control NBF-fixed explants had moderate immunoreactivity for γ9a, with circular patches of Tpm3.3, Tpm3.5, Tpm3.8/3.9 bundles located within the cell cytoplasm of these cells (Figure 3.6 F), as seen in NBF-fixed control LECs probed for α2a (Figure 3.4 I). γ9a immunoreactivity and actin filament stress fibre localisation increased in TGF-β2-induced myofibroblastic cells, compared to control LECs, when lens explants were fixed with either fixative (Figure 3.6 D, H).

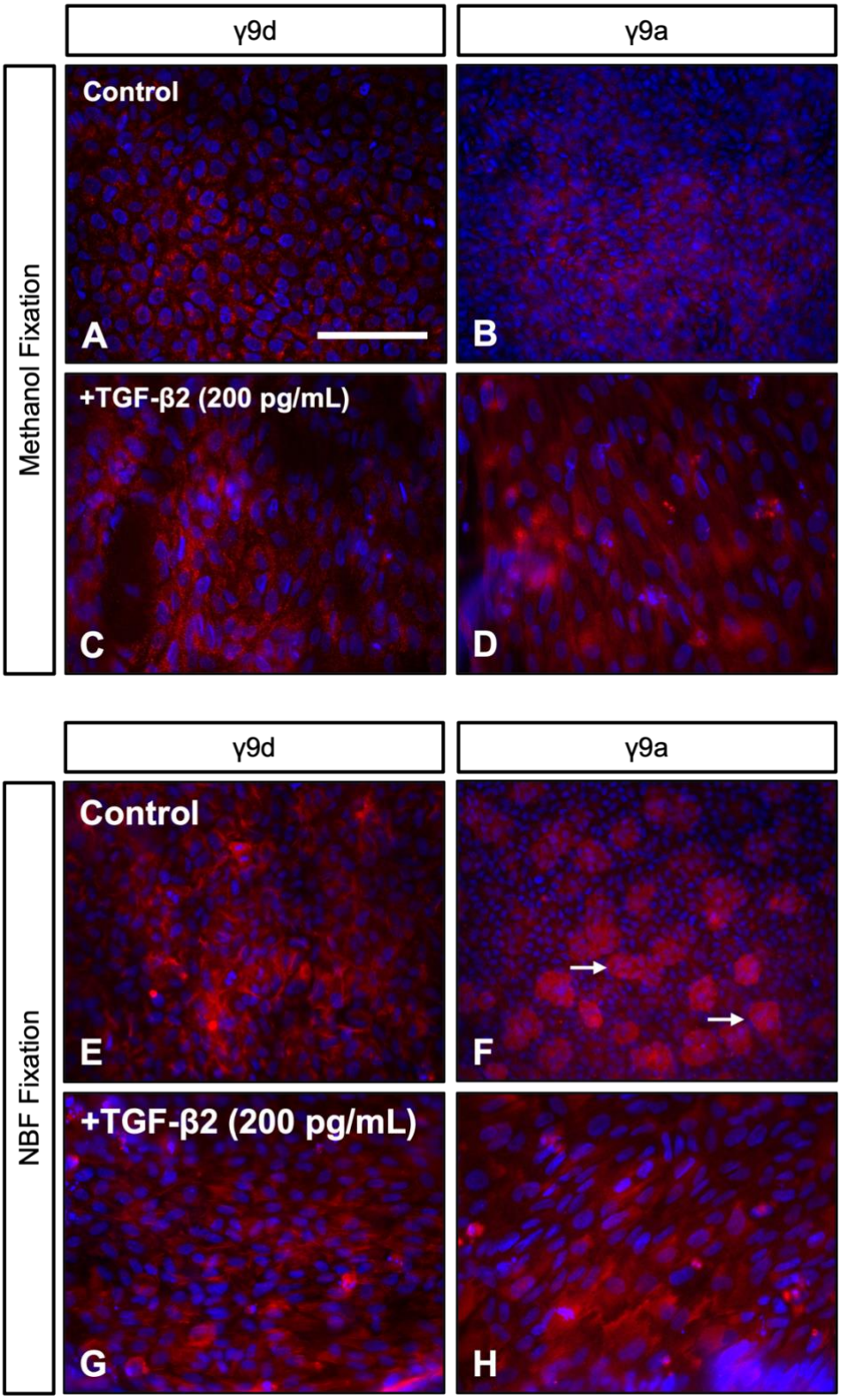

Figure 3.6. Fixative-dependent immunolabelling of Tropomyosin 3 during TGF-β2-induced lens EMT. Control (A, B, E, F) and TGF-β2 (200 pg/mL)-treated (C, D, E, H) rat LECs after 72 hours of culture, fixed in methanol (A–D) and 10% neutral buffered formalin (NBF, E–H). Explants were immunolabelled for Tpm3 using isoform-specific antibodies: γ9d (A, C, E, G) and γ9a (B, D, F, H) and counterstained with Hoechst (blue). Cytoplasmic patches of Tpm isoform bundles in LECs (white arrows). Scale bar: 100 μm.

3.3.2.4 Tropomyosin 4

Immunoreactivity of Tpm4.2 (δ9d) was similar in control explants fixed with either methanol (Figure 3.7 A) or NBF (Figure 3.7 B), with punctate localisation in actin filaments more apparent with NBF fixation. Treatment with TGF-β2 did not appear to change the Tpm4.2 punctate localisation in methanol fixed explants (Figure 3.7 C); however, there appeared to be fewer, more dispersed cells that reflects the transdifferentiation of LECs into myofibroblastic cells. Despite this, TGF-β2-stimulated LECs fixed with NBF showed high labelling intensity for Tpm4.2 with a robust localisation of δ9d in stress fibres (Figure 3.7 D).

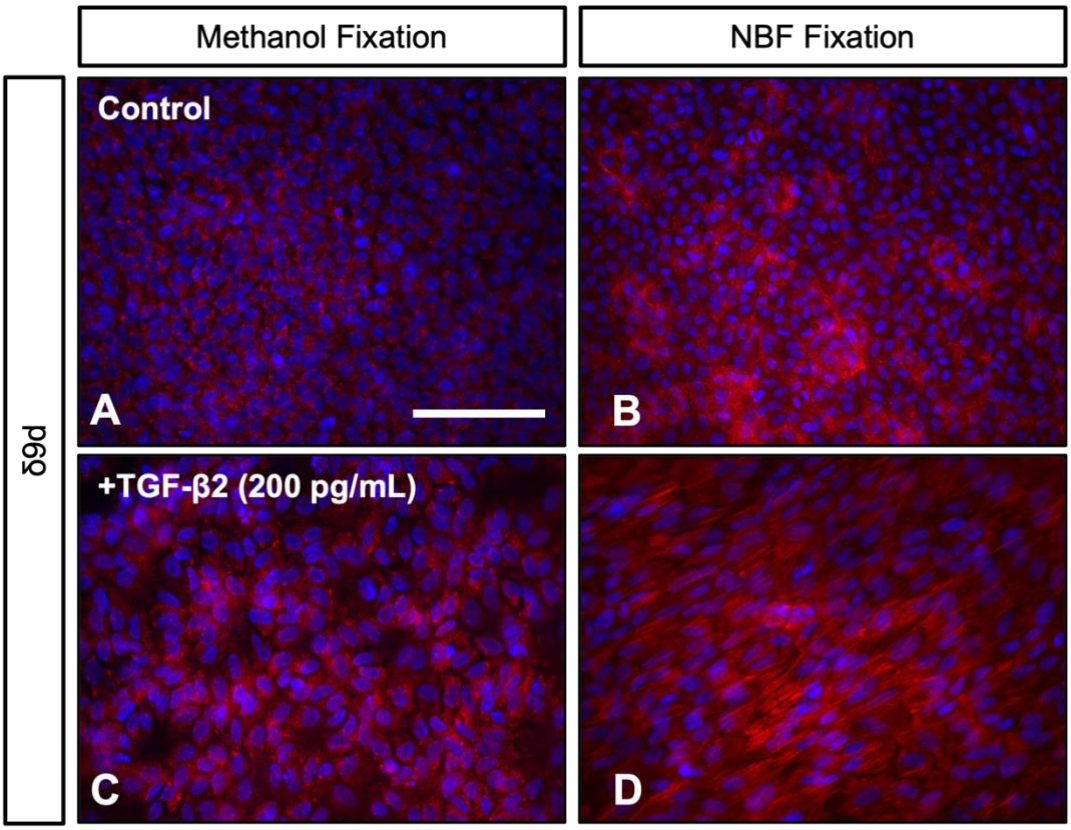

Figure 3.7. Fixative-dependent immunolabelling of Tropomyosin 4 during TGF-β2-induced lens EMT. Control (A, B) and TGF-β2 (200 pg/mL)-treated (C, D) P21 LECs after 72 hours of culture, fixed in 100% methanol (A, C) and 10% neutral buffered formalin (NBF, B, D). Merged representative images of Tpm4.2, using a Tpm4.2-specific antibody (δ9d, red) and nuclear visualisation with Hoechst (blue). Scale bar: 100 μm.

3.3.3 Tropomyosin is elevated during rat lens TGF-β2-induced EMT in an isoform-specific manner

Since we established that TGF-β2 can induce an EMT response in rat LEC explants, we wanted to compare Tpm isoforms levels in control explants, and how these may differ in cells of lens explants exposed to TGF-β2.

Tropomyosin 1. Rat LEC lysates probed with α9d, immunolabelled for two low molecular weight (LMW) proteins at 36 kDa (Tpm1.6/1.7) and 38 kDa (Tpm2.1) that coded for *Tpm1* and *Tpm2* proteins, with non-treated explants demonstrating minimal reactivity for Tpm1.6/1.7 and Tpm2.1 (Figure 3.8 A). Due to α9d detecting multiple bands, we conducted densitometry to calculate the total sum of the intensity of α9d (total α9d), Tpm1.6/1.7 alone, and Tpm2.1 alone, relative to loading control β-actin (Figure 3.8 B). Total α9d reactivity was elevated in TGF-β2-treated explants compared to control explants (p = 0.0796). In isolation, LMW protein Tpm1.6/1.7 reactivity was significantly elevated in the presence of TGF-β2 (p = 0.0394, Figure 3.8 B). In comparison, although elevated in the presence of TGF-β2, when compared to control explants, the slight elevation in Tpm2.1 protein levels was not statistically significant (p = 0.2163). CGβ6 recognised Tpm1.6 and Tpm1.7 in control and TGF-β2-treated lysates (Figure 3.8 C), as one large band, since both isoforms have close molecular weights of 34 and 36 kDa, respectively (Schevzov et al., 2011). CGβ6 immunoreactivity was relatively weak, with heightened background, when compared to the Tpm1.4, Tpm1.6–1.9, and Tpm2.1 targeted antibody, α9d (Figure 3.8 A). CGβ6 also detected a higher molecular weight (HMW) band at 38 kDa in control and TGF-β2-treated lysates. Although CGβ6 is reactive for Tpm1.8 and Tpm1.9 in mice and human tissue samples (Schevzov et al., 2011), these isoforms were not detected in rat LEC explant lysates. An increase in Tpm1.6/1.7 in the presence of TGF-β2, when compared to control explants, was not significant (p = 0.7787, Figure 3.8 D). α2a is selective for Tpm1.4 and presents as one band (40 kDa) in both control and TGF-β2-treated rat LEC lysates (Figure 3.8 E). Addition of TGF-β2 appeared to slightly reduce Tpm1.4 levels compared to control explant lysates, but this was not significant (p = 0.8942, Figure 3.8 F)

Tropomyosin 2. Rat LEC lysates immunolabelled with CG1, detected one band at 38 kDa, indicative of Tpm2.1 (Figure 3.8 G). There was no notable or significant difference between CG1 reactivity in control and TGF-β2-treated LEC lysates (p = 0.2494, Figure 3.8 H).

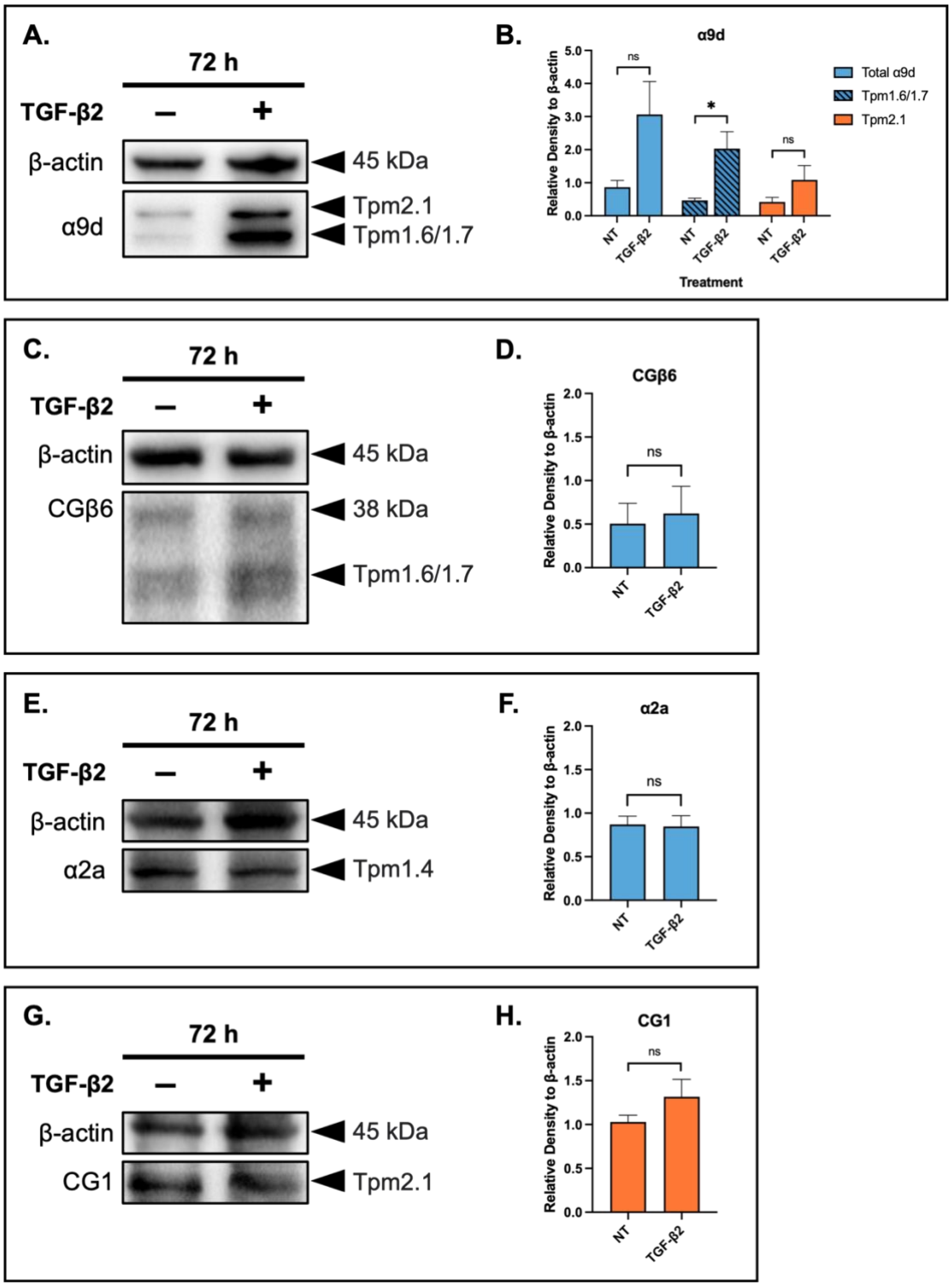

Figure 3.8. Tpm1 and Tpm2 are potential markers for EMT in TGF-β2 treated rat LEC explants. Representative western blots of protein isolated from non-treated (NT) or TGF-β2-treated rat LEC explant lysates at 72 hours of culture. Tropomyosin antibodies detecting isoforms coded by *TPM1* (blue) and *TPM2* (orange) genes. Rat LEC lysates probed for α9d (A, B), CGβ6 (C, D), α2a (E, F), and CG1 (G, H). Densitometry performed on probed Tpm antibodies relative to loading control β-actin (B, D, F, H). Equal loading (10 µg) of rat LEC protein samples ran using the same conditions and transferred onto separate PVDF membranes. Unpaired, parametric two-tailed t-test with $P < 0.05$ considered statistically significant (ns = not significant, $*P < 0.0332$).

Tropomyosin 3. Unlike α9d levels, regardless of the presence of TGF-β2 in rat LEC lysates, reactivity for Tpm3.1/3.2 using γ9d appeared uniform in both control and TGF-β2-treated explants (Figure 3.9 A–B), with no difference between treatments (p = 0.7980). Immunolabelling with γ9d produced one band at 30 kDa (Figure 3.9 A). γ9a was probed for Tpm3.3, Tpm3.5, and Tpm3.8/3.9 in control and TGF-β2 treated LEC lysates (Figure 3.9 C–D). Although these isoforms come in at 30 kDa, we did notice two greater bands at 34 and 36 kDa (Figure 3.9 C). These bands may be cross reacting to muscle Tpms with exon 9a known to have a higher molecular weight (Schevzov et al., 2011). For densitometry, we calculated the intensity of γ9a at 30 kDa relative to β-actin (Figure 3.9 D). Between control and TGF-β2, there was no significant difference in γ9a reactivity (p = 0.9704).

Tropomyosin 4. Immunolabelling with δ9d presented moderate protein levels of Tpm4.2 in rat control and TGF-β2-treated LEC lysates at 30 kDa (Figure 3.9 E). Despite a slight increase in δ9d reactivity in TGF-β2-treated lysates, this increase was not significant in comparison to control lysates (p = 0.6997, Figure 3.9 F). No cross reactivity for other Tpm isoforms was noted in lysates immunolabelled with δ9d.

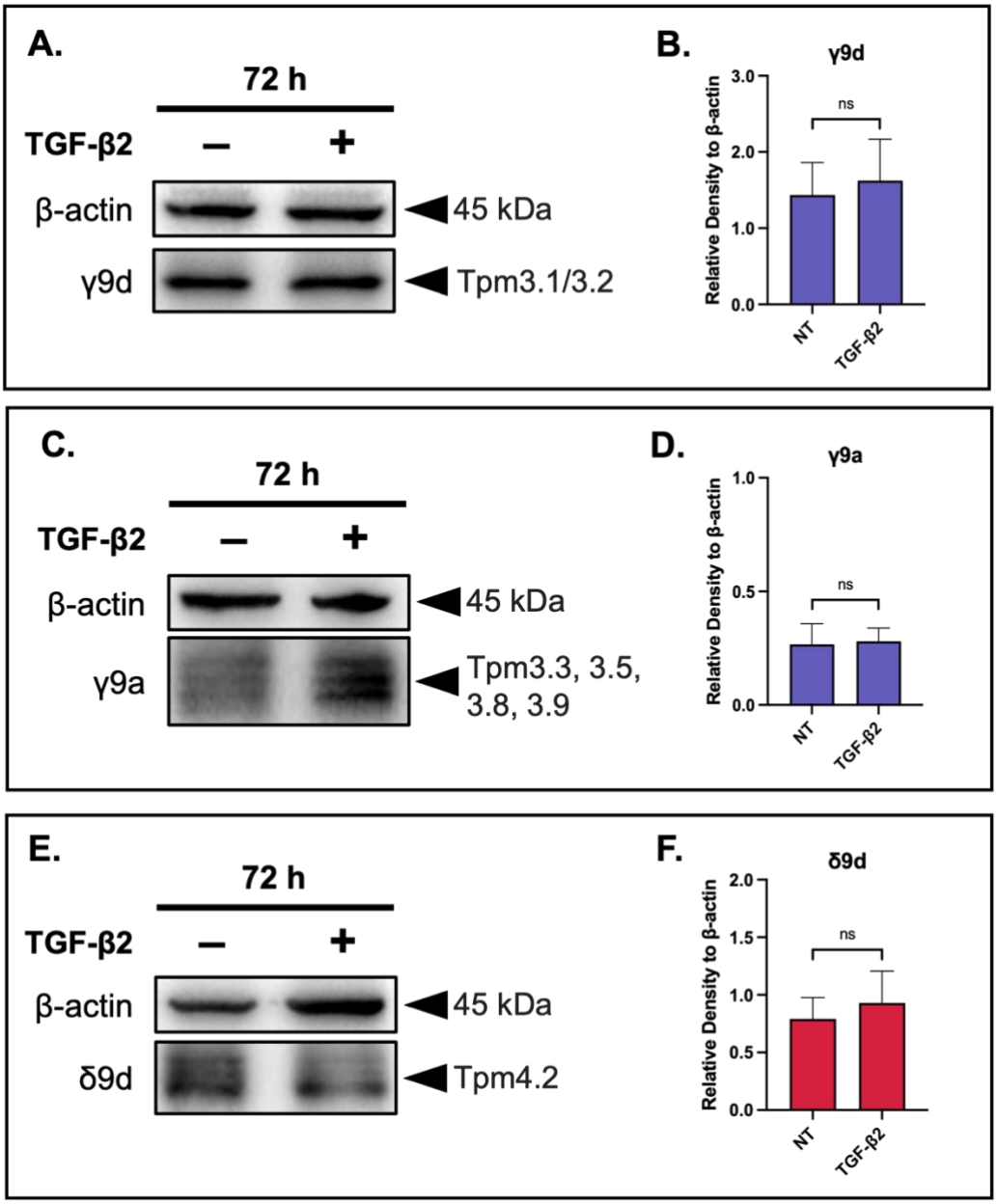

Figure 3.9. Tpm3 and Tpm4 are present but not essential for TGF-β2-induced EMT. Representative western blots of rat lens epithelial explant lysates in the absence (non-treated, NT) or presence of TGF-β2 (200 pg/mL) at 72 hours**.** Tropomyosin antibodies detecting isoforms coded by *TPM3* (purple) and *TPM4* (red) genes. Rat LEC lysates probed for γ9d (A, B), γ9a (C, D), and δ9d (E, F). β-actin used as a loading control to perform densitometric analysis (B, D, F). Equal loading (10 µg) of rat LEC protein samples ran using the same conditions and transferred onto separate PVDF membranes. Unpaired, parametric two-tailed t-test with $P < 0.05$ considered statistically significant (ns = not significant).

3.3.4 Tropomyosin expression in overexpressed TGF-β1-transgenic mice in vivo

We demonstrated that Tpm isoforms play specific roles in the mediation of cell regulation/dysregulation within the rodent lens. In this section, we further characterised its role during cataract development using a TGF-β1 TG *in vivo* mouse model. Throughout postnatal growth, these TG mice form a fibrotic plaque in the anterior pole of the lens (ASC).

3.3.4.1 Tropomyosin 1

At early stages of postnatal maturation of the eye lens in WT mice (P7–P14), low immunoreactivity for α9d was observed (Figure 3.10 A–B). Tpm1.4, Tpm1.6–1.9, and Tpm2.1 immunolabelling increased by P21 in α9d probed WT sections, compared to P7 and P14 WT sections, particularly in the lens epithelia cytoplasm and capsule, as well as adjacently, packed fibre cells (Figure 3.10 C). Compared to early stages of lens growth of WT mice, α9d probing exhibited moderate immunoreactivity and lens epithelia localisation in TG mice at P7 (Figure 3.10 D). At P14, there was no label for α9d in the forming ASC plaques; however, α9d localised to the underlying lens fibres (Figure 3.10 E). Intensity of α9d increased in ASC plaques of P21 TG sections, with localisation of α9d also evident in corneal keratinocytes (Figure 3.10 F). We noted minor regions of increased α9d in ASC plaques suggestive of some differential localisation in this heterogenous cell population. Unlike α9d, CGβ6 did not detect Tpm1.6–1.9 in either postnatal WT lens epithelia (Figure 3.10 G–I) or developing ASC plaques in TG mice (Figure 3.10 J–L). Some background labelling for CGβ6 was noted at P14 in WT mice lenses in fibre regions adjacent to the lens epithelium (Figure 3.10 H).

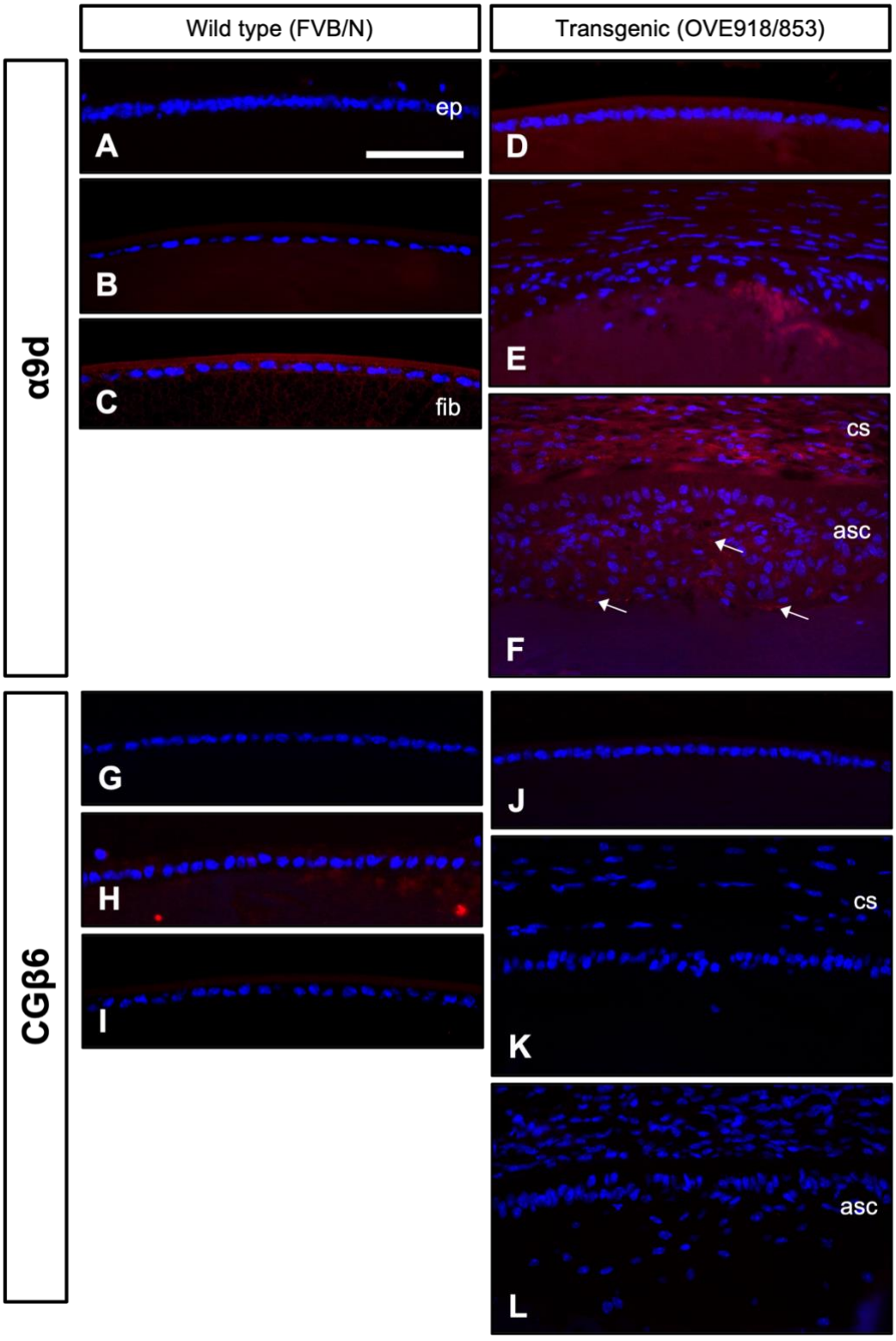

Figure 3.10. Tpm1 immunofluorescent localisation in postnatal wild type and TGF-β1 overexpressed transgenic mice. Paraffin sections from wild type (FVB/N) and transgenic overexpressed TGF-β1 mice (OVE918/853) eyes from several postnatal stages; P7 (A, D, G, J), P14 (B, E, H, K), and P21 (C, F, I, L). Representative stages of normal and aberrant lens growth (± 2 days). Tpm1.4, 1.6–1.9, and 2.1 probed using α9d (red), and Tpm1.6–1.9 probed using CGβ6, with Hoechst nuclear staining (blue). Speckled regions of differential localisation for α9d in ASC plaques (white arrows). Lens epithelium (ep), anterior subcapsular plaque (asc), cornea stroma keratinocytes (cs), lens fibres (fib). Images captured at 40X magnification. Scale bar: 50 µm.

α2a was used to detect Tpm1.4 in WT (Figure 3.11 A–C) and TG (Figure 3.11 D–F) postnatal mice eye lenses. Immunoreactivity for Tpm1.4 remained strong and was mostly localised to the cytoplasm of WT mice lens epithelial cells from P7–P21 (Figure 3.11 A–C). α2a also immunolabelled the adjacent fibre cells within the anterior lens compartment at these postnatal stages, as well as the corneal stroma. At P14 in WT mice lens (Figure 3.11 B), α2a was strongly detected in the anterior chamber. α2a immunolabelled in ASC plaques at P7 (Figure 3.11 D), P14 (Figure 3.11 E), and P21 (Figure 3.11 F) in TG mice, both myofibroblastic and fibre-like cells, as well as the neighbouring adjacent cornea stroma. At stages >P14, α2a labelled the fibre mass opposed to the ASC plaques. Reactivity levels for α2a appeared similar to that observed in WT lenses, suggesting that Tpm1.4 is present in both normal and mutant mice lenses.

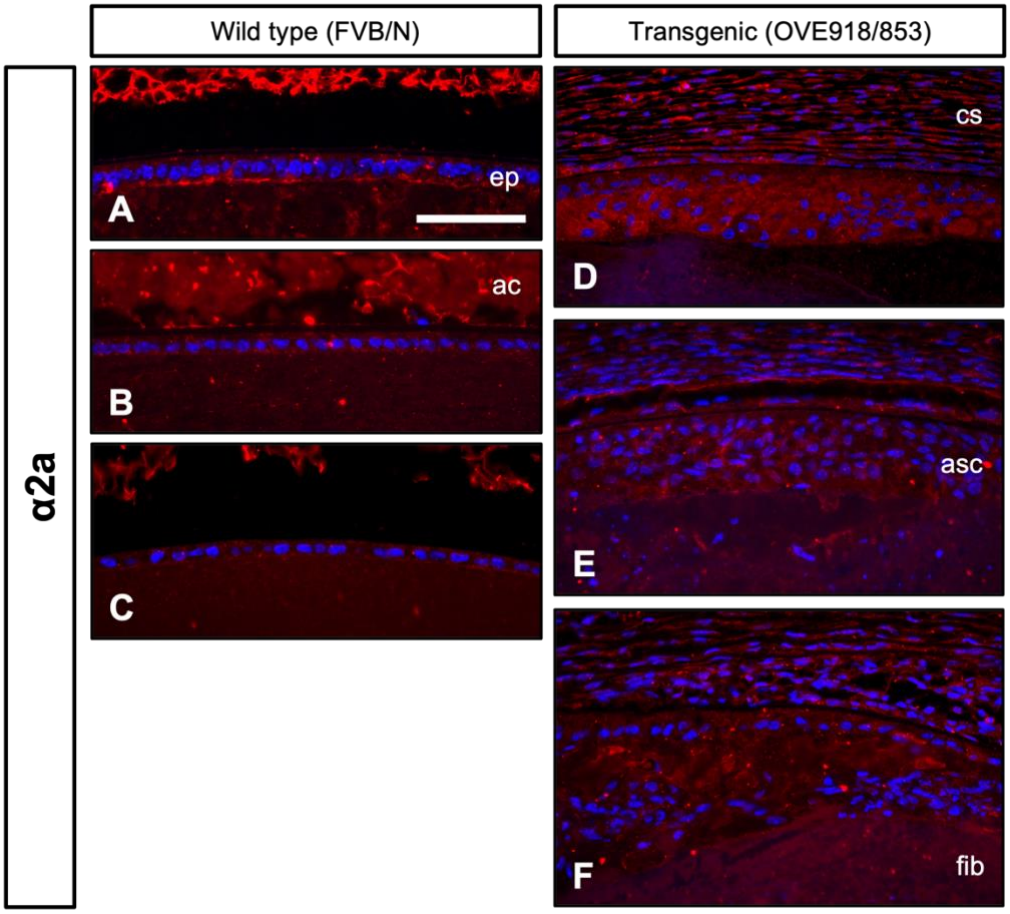

Figure 3.11. Immunofluorescent labelling of Tpm1.4 in postnatal sections from wild type and TGF-β1 overexpressed transgenic mice. Paraffin sections from wild type (FVB/N) and transgenic overexpressed TGF-β1 mice (OVE918/853) eyes from several postnatal stages; P7 (A, D), P14 (B, E), and P21 (C, F). Representative stages of normal and aberrant lens growth (± 2 days). Tpm1.4 probed using α2a (red) with Hoechst nuclear staining (blue). Anterior chamber (ac), lens epithelium (ep), anterior subcapsular plaque (asc), anterior chamber (ac), cornea stroma (cs), lens fibres (fib). Images captured at 40X magnification. Scale bar: 50 µm.

3.3.4.2 Tropomyosin 2

Tpm2.1 was probed using CG1 but could not be detected in WT lenses from P7 to P21 (Figure 3.12 A–C). CG1 was not detected in P7 TG mice lenses (Figure 3.12 D). Weak labelling for Tpm2.1 was observed in TG ASC plaques at P14 and P21, that was overwhelmed by intense CG1-immunoreactivity in the lens fibres below the plaque (Figure 3.12 E–F).

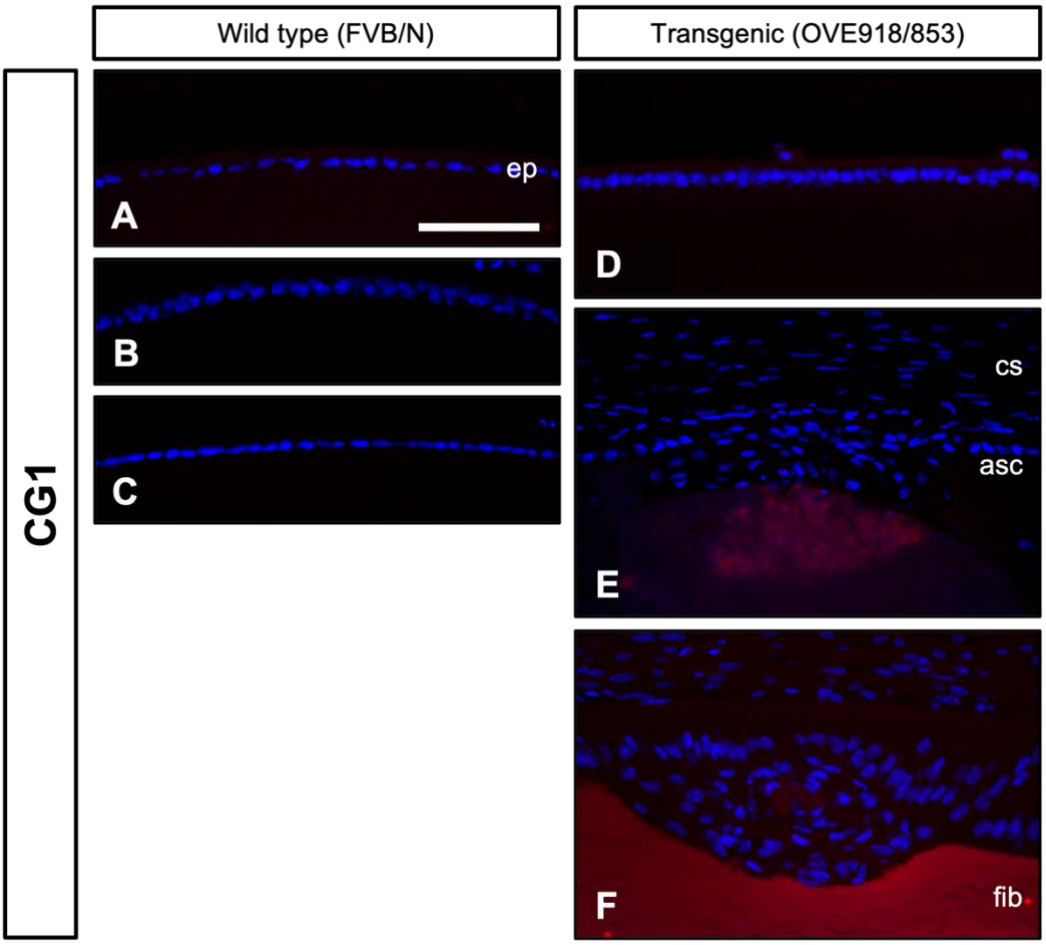

Figure 3.12. Immunofluorescent labelling of Tpm2.1 in postnatal sections from wild type and TGF-β1 overexpressed transgenic mice. Paraffin sections from wild type (FVB/N) and transgenic overexpressed TGF-β1 mice (OVE918/853) eyes from several postnatal stages; P7 (A, D), P14 (B, E), and P21 (C, F). Representative stages of normal and aberrant lens growth (± 2 days). Tpm2.1 probed using CG1 (red) and nuclear stained with Hoechst (blue). Lens epithelium (ep), anterior subcapsular plaque (asc), cornea stroma (cs), lens fibres (fib). Images captured at 40X magnification. Scale bar: 50 µm.

3.3.4.3 Tropomyosin 3

γ9d localisation of Tpm3.1/3.2 in WT mice is found mostly in the basal region of lens epithelial cells between P7–P14 (Figure 3.13 A–B). Some reactivity for Tpm3.1/3.2 was observed in lens fibres at P7 and P14. At P21, localisation of Tpm3.1/3.2 was solely in the cytosol of lens epithelial cells when probed with γ9d (Figure 3.13 C). Tpm3.1/3.2 presented a weak cytoplasmic localisation at P7 in TG mice when probed with γ9d, with some background basement membrane reactivity (Figure 3.13 D). γ9d only localised in the ASC plaques of P14 and P21 TG mice lens, with no localisation found in the underlying fibres (Figure 3.13 E–F). γ9a detected Tpm3.3, 3.5, 3.8/3.9 in the cytoplasm of lens epithelial cells from WT mice lenses across several postnatal stages (Figure 3.13 G–I). γ9a also reacted strongly in the lens fibres below the apical tips of epithelial cells, particularly at P7 and P14, with the label reducing by P21. In TG mice lenses, cell multilayering in the centre of the epithelium was observed as early as P7 (Figure 3.13 J). γ9a localised strongly to the lens epithelial cell cytoplasm and corneal stroma, with minimal labelling in the lens fibres in P7 TG eyes. The intensity and localisation of γ9a remained consistent across P14 and P21 stages (Figure 3.13 K–L), despite the growth of the ASC plaque in TG mice.

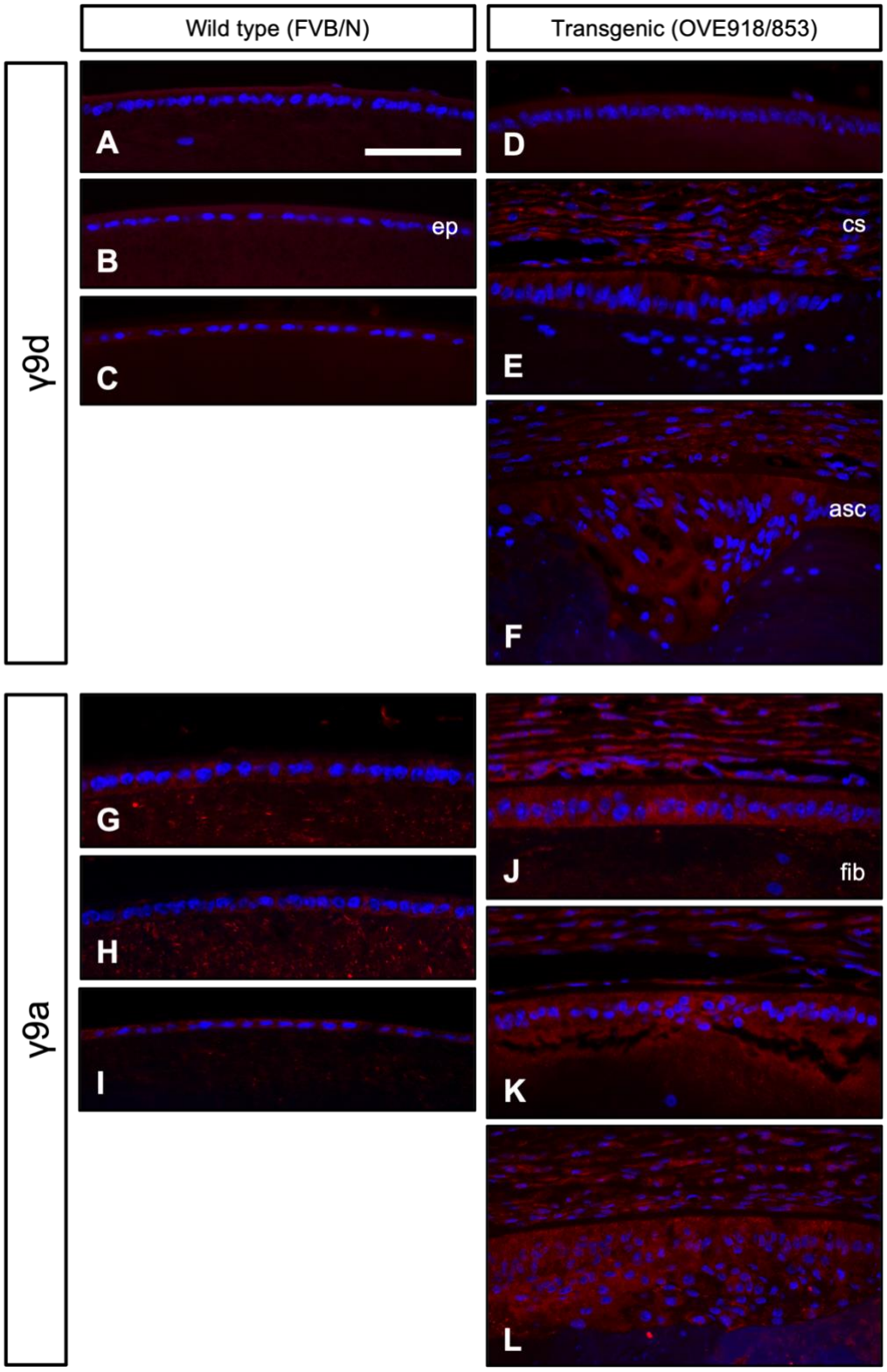

Figure 3.13. Immunofluorescent localisation of Tpm3 derived isoforms in postnatal sections from wild type and transgenic mice. Paraffin sections from wild type (FVB/N) and transgenic overexpressed TGF-β1 mice (OVE918/853) eyes from several postnatal stages; P7 (A, D, G, J), P14 (B, E, H, K), and P21 (C, F, I, L). Representative stages of normal and aberrant lens growth (± 2 days). Tpm3.1/3.2 probed using γ9d (red), and Tpm3.3, 3.5, 3.8/3.9 probed using γ9a (red), with Hoechst nuclear staining (blue). Lens epithelium (ep), anterior subcapsular plaque (asc), cornea stroma (cs), lens fibres (fib). Images captured at 40X magnification. Scale bar: 50 µm.

3.3.4.4 Tropomyosin 4

Tpm4.2 localised primarily in the cytoplasm of normal lens epithelial cells throughout postnatal maturation across all stages, P7 (Figure 3.14 A), P14 (Figure 3.14 B), and P21 (Figure 3.14 C), when WT ocular tissue was probed with δ9d. At P7, Tpm4.2 labelled strongly in the lens epithelium (Figure 3.14 A) and in the lens fibres below the apical regions of these cells. Localisation in the lens epithelium and adjacent lens fibres remained constant at P14 (Figure 3.14 B), although the label became more diffuse at P21 (Figure 3.14 C). Tpm4.2 in early stages of ASC development localised to the cytoplasm of lens epithelial cells and was reactive in the adjacent lens fibres and the anterior chamber (Figure 3.14 D). Throughout ASC development, the anterior chamber was reduced resulting in the cornea becoming closely associated with the anterior lens capsule (Figure 3.14 E). Tpm4.2 immunolabelling was detected in dispersed keratinocytes of the corneal stroma. δ9d was also reactive in the cytoplasm of transdifferentiating multilayered lens cells. This labelling with δ9d was maintained across postnatal maturation with Tpm4.2 detected in the maturing ASC plaque and cornea stroma of P21 TG mice (Figure 3.14 F).

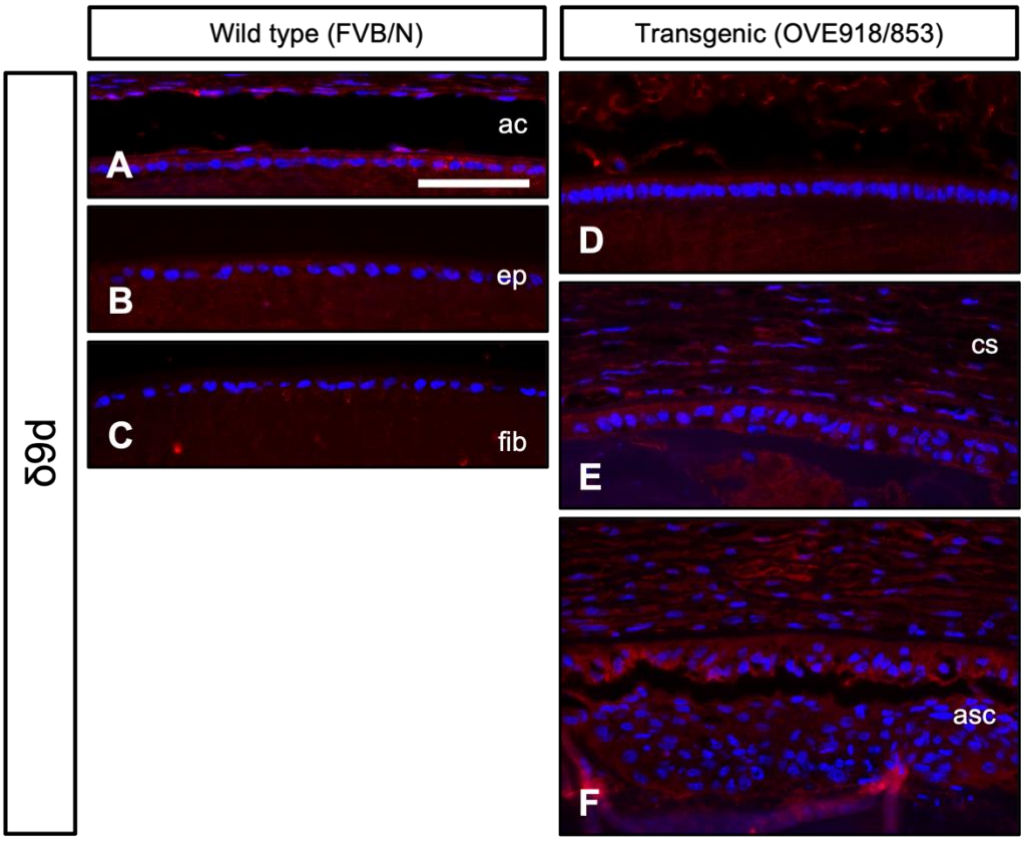

Figure 3.14. Tpm4.2 is present in wild type and TGF-β1 overexpressed mice lenses across postnatal maturation. Paraffin sections of eyes from wild type (FVB/N) and transgenic overexpressed TGF-β1 mice (OVE918/853) from several postnatal stages (± 2 days); P7 (A, D), P14 (B, E), and P21 (C, F). F) A horizontal tear was noted within the ASC plaque possibly due to technical issues during microtomy. Tpm4.2 probed using δ9d (red) and nuclear stained with Hoechst (blue). Anterior chamber (ac), lens epithelium (ep), lens fibres (fib), anterior subcapsular plaque (asc), cornea stroma (cs). Images captured at 40X magnification. Scale bar: 50 μm.

3.3.5 Total Tpm protein expression of WT vs. 918 mice

Based on differences in localisation and expression of Tpm throughout postnatal maturation of WT and overexpressing TGF-β1 mice (Figures 3.10–3.14), we compared total protein expression for specific Tpm isoforms. Wholemount LEC explant tissue was acquired after culling of P20–P25-day-old mice. We selected Tpm antibodies based on their increase, decrease, or consistent reactivity in both WT and TG P7–P21 mice eye sections.

We observed high background in α9d probed membranes and, as a result, we could not distinguish clear bands at 34 and 36 kDa to denote Tpm1.6 and Tpm1.7, as well as Tpm2.1 (38 kDa, Figure 3.15 A). Due to heightened background, we could not confirm a visible increase or decrease in WT or TG samples probed for α9d. Since there was minimal reactivity or background reactivity for Tpm1.6/1.7 in previous assays when probed for CGβ6, we choose not to test CGβ6 in WT or TG lens epithelia samples. α2a detected weak bands in both WT and TG mice lens epithelia samples, with the localisation of Tpm1.4 at 40 kDa (Figure 3.15 B). Two bands, at around 28 and 30 kDa, were also detected that may correlate to other *Tpm1* derived isoforms, such as Tpm1.2 or skeletal muscle Tpm (Tmskα1-1), and Tpm1.3 or smooth muscle Tpm (Tm6, Tmsmα-1), since the antibody is specific to the exon 2a from the *Tpm1* gene (Schevzov et al., 2005, 2011). The TG samples exhibited stronger reactivity for the two bands compared to WT lens epithelia samples. Similar to α2a, CG1 detected three bands in WT and TG tissue (Figure 3.15 C). Compared to WT, there was a slight increase in intensity of these bands in TG samples. CG1 localised at 38 kDa (Tpm2.1), but also cross-reacted with Tpm4.2 at 30 kDa. We also noted a slightly HMW band above Tpm2.1 that may potentially be skeletal Tpm (βTm). γ9d probed for Tpm3.1/3.2 (30 kDa) that appeared constant across both WT and TG samples; however, β-actin levels were lower in WT samples than TG lens epithelia samples in this instance (Figure 3.15 D). δ9d detected faint bands for Tpm4.2 (30 kDa) in both WT and TG tissue (Figure 3.15 E). δ9d also detected a slightly higher molecular weight at approximately 38 kDa, that could potentially be cross reacting with Tpm2.1, as seen in CG1 probed membranes (Figure 3.15 C).

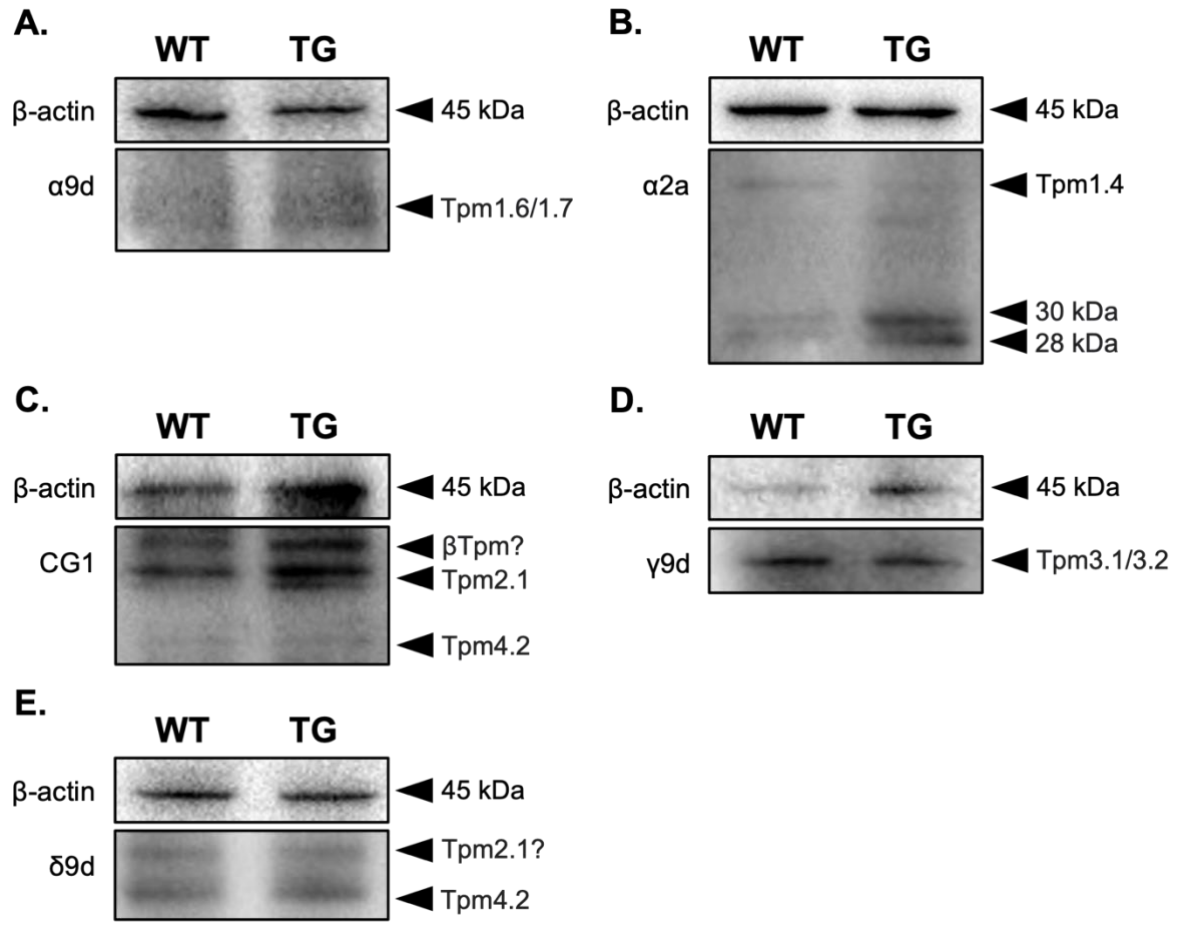

Figure 3.15. Expression of Tpm in P20-25-day-old wholemount lens epithelia tissue from wild type and transgenic mice. Representative western blots of 10 μg of loaded protein acquired from WT and TG (918) mouse wholemount lens epithelia with no culture period. Individual PVDF membrane blots probed with (A) α9d, (B) α2a, (C) CG1, (D), γ9d, and (E) δ9d. β-actin used as a loading control.

3.3.6 Tropomyosin is a potential marker for fibre differentiation in rat LEC explants

We have demonstrated in previous experiments that specific Tpm isoforms are associated with phenotypic changes involved in TGF-β-induced lens EMT. Since the ASC in our TG mice display a heterogenous cell population; myofibroblasts and aberrant fibre-like cells, we wanted to evaluate whether some of the Tpm isoforms associated with normal lens fibre cell differentiation were evident in fibrotic cataractogenesis. To do this, we induced a fibre-differentiation response in rat LEC explants using a relatively high dose of FGF-2 (200 ng/mL) and monitored cells over 5 days of culture (Figure 3.16 A–C). Cells within these explants underwent a marked elongation response noticeable between 3 to 5 days of culture (Figure 3.16 B–C). No phenotypic change was noted at day 1 of culture in explants (Figure 3.16 A). FGF-2 treated explants were fixed at day 5 and immunolabelled for Tpm isoforms (Figure 3.16 D–J). Actin populations of Tpm1.4, Tpm1.6–1.9, and Tpm2.1 were observed in explants treated with FGF-2 (Figure 3.16 D). Minimal, if any, labelling for CGβ6 or α2a was observed in FGF-2 induced lens explants (Figure 3.16 E–F). Lens cells treated with FGF-2 exhibited background immunolocalisation of Tpm2.1 (Figure 3.16 G). γ9d detected cytoplasmic localisation of Tpm3.1/3.2 in cells of FGF-2-treated lens explants (Figure 3.16 H). γ9a presented weaker immunoreactivity for Tpm3 compared to γ9d, with no definitive actin localisation (Figure 3.16 I). Tpm4.2 localised in the cytoplasm of FGF-2 treated LECs (Figure 3.16 J) and strong immunoreactivity for δ9d was similar to levels observed in cells probed with α9d. We confirmed FGF-2-induced immunoreactivity of Tpm using western blotting (Figure 3.17 A–G). Tpm1.6/1.7 and Tpm2.1 was detected in FGF-2 treated lens epithelial explants (Figure 3.17 A); however, as seen with immunofluorescence labelling (Figure 3.16 E), there was no Tpm1.6–1.9 detection in FGF-2-induced explants with CGβ6 (Figure 3.17 B). Weak intensity of Tpm1.4 was observed as a faint band (40 kDa, Figure 3.17 C). Tpm2.1 was present in FGF-2 treated explant lysates (Figure 3.17 D), as well as Tpm3.1/3.2 at 30 kDa (Figure 3.17 E). Reactivity for other isoforms coded by the *Tpm*3 gene, such as Tpm3.3, Tpm3.5, and Tpm3.8/3.9, were also present in FGF-2 treated lens epithelial explants (Figure 3.17 F), with γ9a detecting bands at two molecular weights around 30 and 34 kDa. Tpm4.2 was also detected as a faint band in FGF-2 treated explants (Figure 3.17 G).

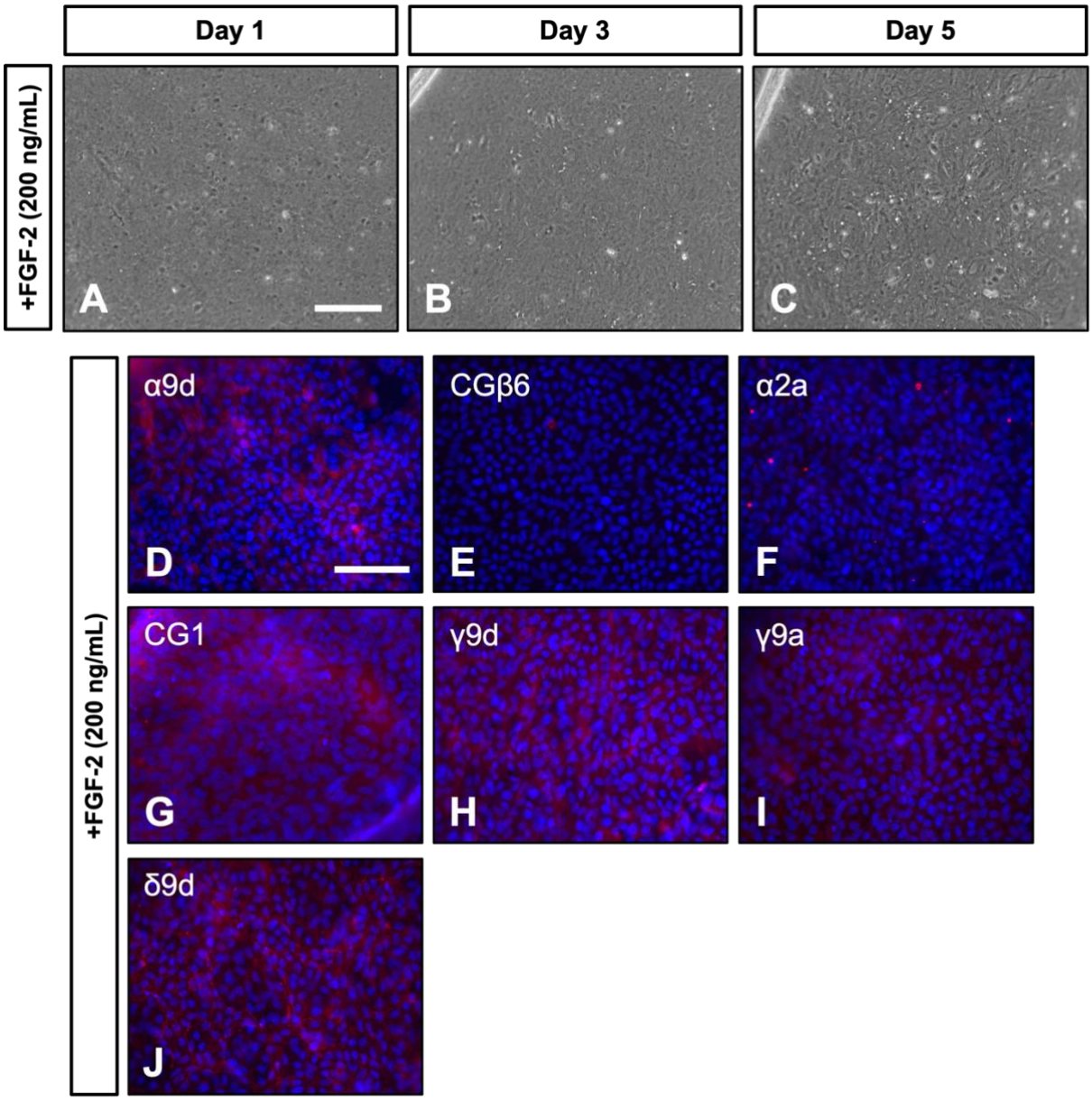

Figure 3.16. FGF-2 induces Tpm activity during fibre differentiation in rat LEC explants. Representative phase contrast images of rat P21 LEC explants treated with high dose of FGF-2 (200 ng/mL) to induce a fibre-like differentiation response across 5 days of culture (A–C). Explants treated with FGF-2 were fixed in 10% NBF and immunolabelled for Tpm-specific isoforms at day 5. Antibodies specific for Tpm including α9d (D), CGβ6 (E), α2a (F), CG1 (G), γ9d (H), γ9a (I), and δ9d (J). Scale bar: 200 µm (A–C), 100 µm (D–M).

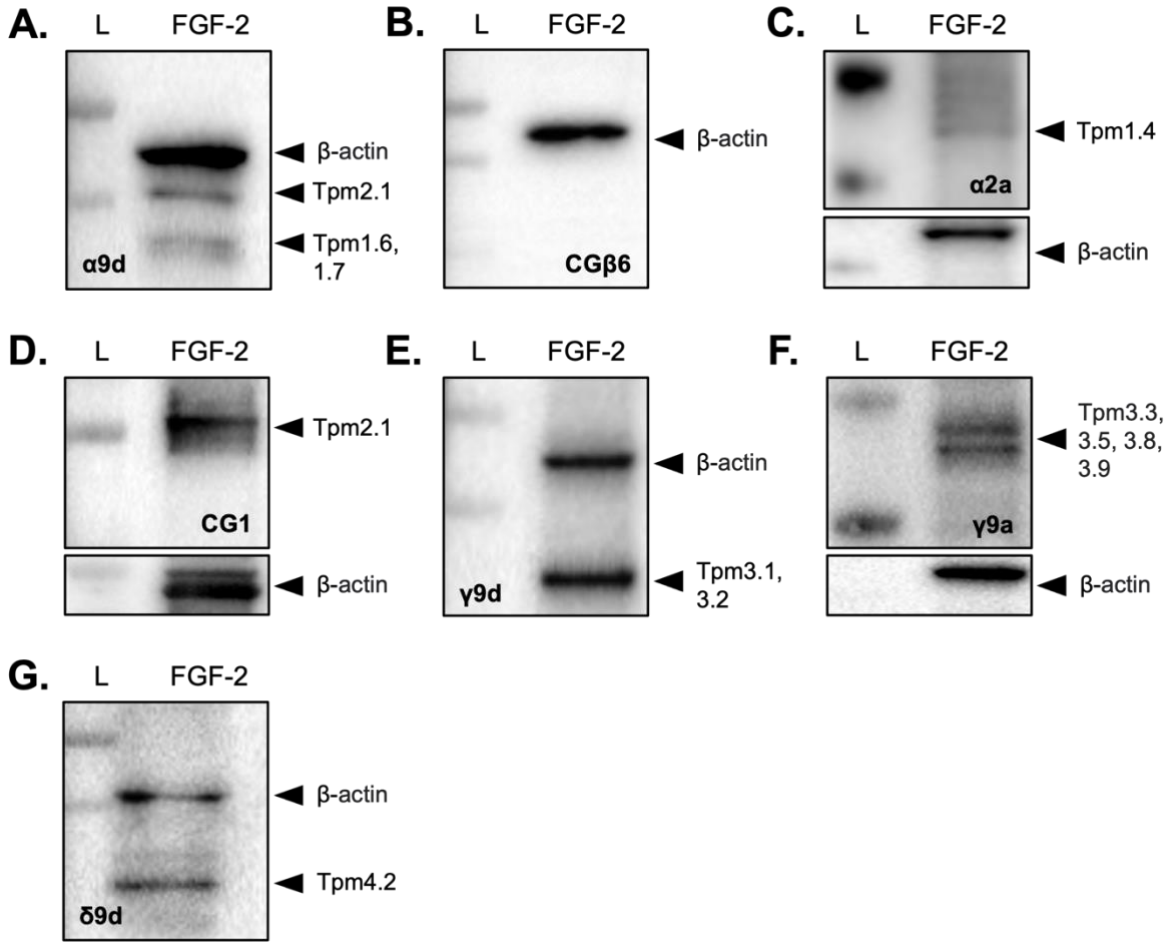

Figure 3.17. Expression of Tpm in FGF-2-induced rat LEC explants. Western blots of Tpm isoforms coded by four genes in cellular protein isolated from rat LEC explants. Equal loading of 10 μg of from explants treated with high dose of FGF-2 (200 ng/mL) to induce a fibre-like differentiation response after 5 days of culture. Individual PVDF membrane blots probed with (A) α9d, (B) CGβ6, (C) α2a, (D) CG1, (E) γ9d, (F) γ9a, and (G) δ9d antibodies. Loading control (β-actin) and protein standard ladder (L). Western blots representative of three independent experiments (n=3).

3.4 DISCUSSION

In this chapter, we reconfirmed that Tpm isoforms coded by all 4 *Tpm* genes are present within the postnatal rodent lens. As previously suggested, expression and localisation of Tpm is isoform-specific and these isoforms differentially contribute to various lens cell processes, including normal lens cytoskeletal stability, EMT, and fibre differentiation. In addition, the localisation of specific Tpm isoforms appeared to be dependent on the fixative used in rat LEC explants. We showed that Tpm is expressed in postnatal rat LECs at P10 and P21. In some instances, we showed that Tpm levels either remained constant or were elevated in the presence of growth factors, namely, TGF-β2 and FGF-2, suggesting an isoform-specific role for Tpm in different lens cellular processes: EMT and fibre differentiation. A summary of the findings from this chapter are presented below (Figure 3.18).

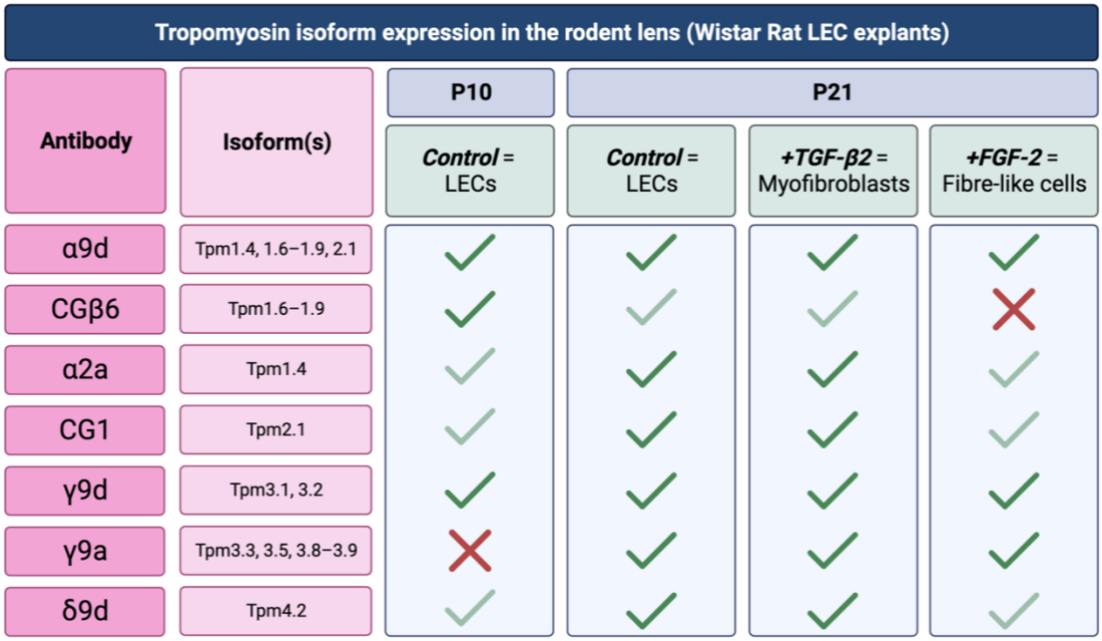

Figure 3.18. Summary of Tropomyosin isoform expression in postnatal Wistar Rat LEC explants. Summary of data acquired from Figures 3.2, 3.4–9, 3.16–17. Tropomyosin (Tpm) isoforms encoded by all 4 genes (*Tpm1–Tpm4*) were probed using the following antibodies (pink); α9d, CGβ6, α2a, CG1, γ9d, γ9a, and δ9d. Expression of Tpm in control (non-treated) P10 rat LEC explants at 24 hours of culture, as well as P21 rat LEC explants in control, TGF-β2 (200 pg/mL), and FGF-2 (200 ng/mL) induced conditions between 3-5 days of culture. Myofibroblastic and fibre-like cell phenotypes induced by TGF-β2 and FGF-2, respectively. Presence (green tick) or absence (red cross) of Tpm isoforms. A faint tick or cross indicates that the antibody probed for the respective isoform was present/absent in only one immunolabelling assay (immunofluorescence or western blot analysis).

3.4.1 Identification of Tpm isoforms during TGF-β2-induced lens EMT

Earlier studies investigating Tpms found that distribution of cytoskeletal Tpm can alter and reorganise depending on their functional demand, particularly during cell transitional processes

(Warren et al., 1985). In the past two decades, cytoskeletal stress fibre associated isoforms have shown to be present and stimulated by TGF-β in previous carcinoma and fibroblast models (Bakin et al., 2004; Varga et al., 2005; Prunotto et al., 2015), as well as in lens fibrosis (Kubo et al., 2013, 2018; Cheng et al., 2018; Shibata et al., 2018; Parreno et al., 2020; T. Shibata et al., 2021). Using immunolabelling, of all the tested Tpm antibodies, Tpm1.4, Tpm1.6–1.9, and Tpm2.1 isoforms showed an increase in the presence of TGF-β2 in P21 rat LEC explants when probed with α9d.

3.4.1.1 High molecular weight Tpms: Tpm1 and Tpm2

We confirmed that cytoskeletal Tpm proteins are present within the cytoplasm of postnatal rat lens epithelia. This is consistent with Tpm gene exon splicing variants that have previously been reviewed (Manstein et al., 2020) and were shown to be cytoplasmic in non-muscle cells (Schevzov et al., 2011). *Tpm1*-derived isoforms, Tpm1.4 and Tpm1.6–1.9, were examined in rat LECs at several postnatal stages. Based on the gene dataset, we expected to observe moderate levels of *Tpm1*-derived isoforms in our rat LEC explants particularly at stages >P20. While we could not detect Tpm1.6–1.9 using the CGβ6 antibody for immunofluorescence, when using α9d we demonstrated that Tpm1.4, Tpm1.6–1.9, and Tpm2.1 are, in fact, localised in normal LECs (Figure 3.18). This localisation was fixative-dependent, as we could only detect α9d in LEC explants fixed with 10% NBF and not methanol fixation. The actin filament stress fibre localisation of Tpm1.6–1.9 and Tpm2.1 in LECs is supported by the fact that these isoforms reportedly play functional roles in stress fibre stability and formation of cellular focal adhesions (Tojkander et al., 2011; Brayford et al., 2016; Meiring et al., 2018; Manstein et al., 2020). Tpm1.4 was also highly localised in control LECs, independent of the type of fixative, although its labelling pattern differed from cytoskeletal (methanol) to patchy cytoplasmic labelling (NBF).

In the presence of TGF-β2, α9d displayed strong reactivity with actin filament and stress fibre association in bundled regions of cells. Total protein levels of Tpm1.6/1.7 and Tpm2.1 were significantly upregulated in the presence of TGF-β2 at 72 hours when compared to control explants. We showed pockets of α2a-reactivity in TGF-β2-induced explants in myofibroblastic cells that differed to controls that presented cytoplasmic localisation of Tpm1.4; however, there were no significant changes between control and TGF-β2-treated explants when total protein levels for Tpm1.4 were quantified. A study by Bakin et al. (2004) demonstrated a role for *Tpm1*-derived isoforms during TGF-β induced transdifferentiation and motility in SiHa cervical

carcinoma cells and NMuMG epithelial cells, as well as downstream TGF-β signalling pathways that promoted Tpm activity. In this model, targeted inhibition of Smad-independent signalling in TGF-β1-treated SiHa cells, using a p38 MAPK targeted compound (SB202190), did not impact or significantly upregulate Tpm1.4 levels compared to cells only exposed to TGF-β1 (Bakin et al., 2004). From this study, as well as what we have observed, it appears that Tpm1.4 is not a primary marker required for TGF-β induced cell transformation.

As α9d cross reacts with *Tpm2*-derived isoform Tpm2.1, we assessed the levels of Tpm2.1 using a Tpm2.1 specific antibody, CG1. Tpm2.1 demonstrated low levels in control LECs from P10 and P21 rat explants when probed with CG1. A study by Kubo et al. (2013) found strong immunoreactivity for Tpm1.6/1.7 and Tpm2.1 (Tpm1α/Tpm2β) particularly in the cytoplasm of lens epithelial and fibre cells from hereditary SCR samples, rats with nuclear/perinuclear cataract. This localisation of these isoforms was translated in human lens cells; however, the localisation was limited to only epithelial cells (Kubo et al., 2013). Tpm2.1 was slightly elevated when exposed to TGF-β2, although this increase was not statistically significant. The findings in the current study of elevated Tpm1.6/1.7 and Tpm2.1 levels is supported by earlier studies (Prunotto et al., 2015), that investigated the role of stress fibre Tpms in TGF-β1-induced human subcutaneous fibroblasts. This study reported upregulation of Tpm1.6 and Tpm1.7 in fibroblasts, that corresponded with an increase in stress-fibre assembly of α-SMA across a 6-day culture period, with significant increase after only a 24-hour exposure to TGF-β1 (10 ng/mL^{-1}) (Prunotto et al., 2015). It was concluded that α-SMA may be dependent on Tpm1.6/1.7 bioavailability for actin filament association with stress fibres in TGF-β-induced conditions (Prunotto et al., 2015).

More recent studies have shown the presence and upregulation of Tpm1.7, Tpm2.1, Tpm3.1, and Tpm4.2 in imLECs treated with TGF-β2 (5 ng/mL) (Parreno et al., 2020), promoting Tpm1.6, Tpm1.7, and Tpm2.1 as potential markers for TGF-β-induced EMT leading to lens fibrosis. Other models have shown the importance of Tpm isoforms derived from *Tpm1* and *Tpm2* genes, particularly their requirement for TGF-β-induced stress fibre formation in epithelial cells (Varga et al., 2005) and human lung fibroblasts (Bradbury et al., 2021). The weak immunolabelling of Tpm1.6/1.7 using CGβ6 suggests a possible issue with our choice of fixatives and/or blocking agents. The same primary antibody has been tested and used in several other models for immunofluorescent assays, including human immortal fibroblasts and mouse embryonic fibroblasts (Schevzov et al., 2011), and human subcutaneous fibroblasts (Prunotto et al., 2015), so an alternative fixative such as 4% paraformaldehyde may deliver a different

outcome. It should be noted that all the Tpm-specific antibodies are IgG's, with the exception of CGβ6 that is a supernatant of an IgM hybridoma. While we applied an IgM-specific secondary antibody for both immunofluorescence and western blotting analysis, further trouble shooting is warranted.

3.4.1.2 Low molecular weight Tpms: Tpm3 and Tpm4

Tpm3.1/3.2 and Tpm4.2 both presented a punctate localisation in control LECs, when fixed in methanol and immunolabelled with γ9d or δ9d. This localisation could be labelling zonula adherens actomyosin structures in epithelial cells, as previously shown in colon carcinoma (Caco-2) epithelial cell lines (Caldwell et al., 2014). That study showed adjacent localisation of Tpm3.1/3.2 and E-cadherin, a zonula adherens protein, suggesting that Tpm3.1/3.2 could function as a cytoskeletal regulator for junctional regions in epithelial cells (Caldwell et al., 2014). Another study using U2OS cell lines confirmed the junctional cytoskeletal role of Tpm3.1/3.2, and Tpm2.1, as both isoforms localised to contractile stress fibres adjacent to regions of focal adhesions (Tojkander et al., 2011). In the presence of TGF-β2, we expected to see an upregulation in Tpm3.1/3.2 and Tpm4.2 levels and activity given their increase in TGF-β2-induced imLECs and native lens epithelia (Parreno et al., 2020) as well as other fibrosis and carcinoma models (Lees et al., 2013; Tao et al., 2014; Chen et al., 2021; Wang et al., 2022). Interestingly, neither of these genes are regulated by TGF-β in a mouse NMuMG cell line model (Bakin et al., 2004), or human lung fibroblasts after 24–48 hours of culture (Bradbury et al., 2021). The Bradbury et al. (2021) study used the same antibody clone as our study (γ9d), confirming the validity and reproducibility of this result in a different tissue/model. Explants probed with γ9a, specific for Tpm3.3, Tpm3.5, and Tpm3.8/3.9, showed an elevation in explants treated with TGF-β2, although it was not statistically significant. Interestingly, altered localisation of these Tpm isoforms was dependant on both fixative and/or treatment; control LECs exhibited cytoplasmic bundled regions of γ9a whereas treatment of cells with TGF-β2 promoted stress fibre localisation in myofibroblastic cells. This localisation aligns with the current literature suggesting that specific actin populations are spatially segregated depending on their functional needs (Bakin et al., 2004; Vrhovski et al., 2005; Tojkander et al., 2011; Kee et al., 2015; Meiring et al., 2018, 2019).

A study by Tojkander et al. (2011) showed that bundles of Tpm isoforms are required for stress fibre recruitment and stabilisation during contractile activity in human osteosarcoma cell lines, that localise in specific stress fibre regions due to their anatomical orientation (Small et

al., 1998; Hotulainen and Lappalainen, 2006; Dugina et al., 2009). High molecular weight (HMW) Tpms have been shown to be involved in cell stability during EMT, rather than cell migration and invasiveness, as seen in metastatic cells, that commonly utilise low molecular weight (LMW) Tpms (Varga et al., 2005; Zheng et al., 2008; Safina et al., 2009). This is believed to be due to the lack of HMW Tpms localising at focal adhesion contact points in transitioning cells (Tanaka et al., 1993; Zheng et al., 2008; Meiring et al., 2018, 2019; Manstein et al., 2020). LMW Tpms, such as Tpm3.1/3.2, may be more detrimental to dynamic cell types, and are more versatile in highly motile, proliferative, and invasive conditions, as suggested and reviewed for carcinoma and chemotherapeutic models (Stehn et al., 2006, 2013; Tao et al., 2014; Humayun-Zakaria et al., 2019). Based on this, while present in our model, Tpm3.1/3.2 may not be essential for promoting the myofibroblastic cell phenotype induced by TGF-β, as these cells in our explants are not evidently motile.

As seen with Tpm3.1/3.2 immunolabelling, Tpm4.2 showed an increase in immunoreactivity in TGF-β2-treated explants. In methanol-fixed explants, Tpm4.2 was found in the cytoplasm of control LECs, and this localisation did not change when explants were exposed to TGF-β2. Despite this, localisation for Tpm4.2 changed from cytoplasmic in control LECs to stress-fibre labelling in TGF-β2-induced myofibroblasts, further suggesting that Tpm isoform expression is fixative dependent in LECs. Tpm4.2 is another of the LMW Tpm isoforms (e.g., Tpm1.8, Tpm1.12, Tpm3.1) that has been classified as promoting fast actin dynamics (Zheng et al., 2008; Janco et al., 2016; Gateva et al., 2017; Matyushenko et al., 2020; Logvinov et al., 2023), due to weakened connection with other Tpm molecules. In non-muscle cells, this weaker binding is beneficial during conditions of rapid and high motility, as well as reorganisation of actin filaments, enabling these cells the ability to transform (Marchenko et al., 2021).

3.4.2 Identification of Tpm isoforms during FGF-2-induced fibre differentiation

We also observed specific Tpm-isoform labelling during lens fibre-like differentiation. By inducing a fibre differentiation response in our *in vitro* LEC explant model, using FGF-2 (Wang et al., 2010, 2017), we showed that Tpm isoforms; Tpm1.6/1.7, Tpm2.1, Tpm3.1/3.2, Tpm3.3, Tpm3.5, Tpm3.8/3.9, and Tpm4.2, are involved in lens fibre cell elongation and differentiation.

The cytoskeleton is an important structure for the reorganisation of cells during differentiation, particularly in the lens (Fischer et al., 2000; C. Cheng et al., 2017; Cheng et al., 2018), and therefore requires Tpm to accommodate for shifts in cell phenotype. During primary

embryonic chick lens morphogenesis, a study by (Fischer et al., 2000) showed that HMW Tpm isoforms (34–36 kDa isoforms) are required for the reorganisation of the cytoskeleton during early lens differentiation. A shift in requirement from HMW to LMW Tpm isoforms (28–30 kDa) occurs during later stages of lens cell differentiation into lentoids, with the latter being present throughout the differentiation stages from epithelial (undifferentiated) to lentoid (early and late) cell phenotypes (Fischer et al., 2000; Schevzov and O'Neill, 2008). A study by Kubo et al. (2017) looked at Tpm1/2 expression in mice (MLECs) and human (HLECs) lens epithelia cells in FGF-2 induced conditions. In MLECs, both Tpm1 and Tpm2 expression was reduced with FGF-2 (10 ng/mL) exposure between 2–4 days of culture (Kubo et al., 2017). Interestingly, results from this study also showed that a reduction in Tpm1 expression was linked to an increase in dosage of FGF-2 (0–10 ng/mL) (Kubo et al., 2017), suggesting that Tpm1 might be required for lens epithelial cell proliferation (low FGF-2 stimulation) and not fibre differentiation (high FGF-2 stimulation). From our study, we showed that Tpm isoforms expressed in the presence of a high FGF-2 differentiating dose were mostly LMW Tpm isoforms (30 kDa); Tpm3.1/3.2, Tpm3.3, Tpm3.5, Tpm3.8/3.9, and Tpm4.2, with the exception of HMW Tpm1.6/1.7 and Tpm2.1 (34–38 kDa). From this, we see that further research on isoform-specific roles for Tpms during fibre differentiation based on their sizing and dynamics, as well as FGF dose-dependent mechanisms in the lens, is warranted.

Of all the antibodies specific for *Tpm1*-derived isoforms we tested, α9d reacted strongly in both immunofluorescent and total protein level assays in explants treated with FGF-2 after 5 days. CGβ6 did not react in FGF-2-induced conditions, and weak reactivity for Tpm1.4 was noted in explants probed with α2a. Reactivity for Tpm1.6–1.9 (using α9d) in FGF-2-induced explants suggests a potential role for these specific *Tpm1*-derived isoforms in lens fibre differentiation, particularly in the remodelling of the cytoskeleton when cells are differentiating from epithelial to elongate fibre cells. This factor has been reported in another lens mouse model deficient for *Tpm1* (T. Shibata et al., 2021). T. Shibata et al. (2021) showed that *Tpm1* is required for postnatal lens growth and differentiation, as well as fibre cell rigidity and formation, in both pre- and postnatal *Tpm1*-CKO mice lenses. Other studies have shown that Tpm2.1 is influential in the elongation of actin filaments isolated from rabbit skeletal muscle (Janco et al., 2016), that is required during cell transformation processes including fibre differentiation. Tpm2.1 labelling in the present study exhibited background reactivity in our immunofluorescent assays, while protein levels in westerns for this isoform were strong in LEC explants treated with FGF-

2. Based on these two assays, it appears that Tpm2.1 may be involved in FGF-2-induced fibre differentiation, due to its elevated expression.

Antibodies probing for specific *Tpm3* and *Tpm4* gene derived isoforms, Tpm3.1/3.2 (γ9d), Tpm3.3, Tpm3.5, Tpm3.8/3.9 (γ9a), and Tpm4.2 (δ9d), also showed strong immunolabelling in lens cells exposed to FGF-2. The reactivity for *Tpm3*-derived isoforms in FGF-2-induced conditions aligns with the current literature; with Tpm3.5 shown to play a role specifically in lens fibre cell stabilisation and biomechanics (Cheng et al., 2018). While we did not quantify the expression of Tpm-specific isoforms in FGF-2 induced explants, other lens studies have investigated mRNA expression of Tpms in the presence and/or absence of TGF-β in imLECs and native lens cells (Parreno et al., 2020). In addition, a study by Parreno et al. (2020) did not investigate the role of Tpm in lens fibre cell differentiation, although they did examine cytoskeletal isoform expression in native/unstimulated lens fibres. An earlier study from the same laboratory also examined the presence of Tpm isoforms, Tpm3.1 and Tpm3.5, in fibre cells from Tpm3.1/3.2 KO mice (Cheng et al., 2018). Future studies could confirm the role of several Tpm isoforms in FGF-2-induced lens fibre differentiation; particularly Tpm1.6/1.7, Tpm2.1, Tpm3.1/3.2, Tpm3.3, 3.5, 3.8/3.9, and Tpm4.2. RT-PCR could be performed using the current model to determine whether genes for specific Tpm splice variant isoforms are upregulated in different growth factor conditions, such as TGF-β2 and FGF-2, when compared to non-treated LEC explants. In addition, lens epithelial samples could be examined at different stages of culture since TGF-β2-induced upregulation of EMT markers and associated morphological changes occurs between 48–72 hours (Kubo et al., 2017; Wojciechowski et al., 2017; Shu et al., 2019b, 2021), whereas FGF-2-induced fibre-like differentiation is slightly delayed and phenotype changes are more visible between 3–5 days of culture in lens epithelia explants (McAvoy and Chamberlain, 1989; Lovicu and McAvoy, 2001; Flokis and Lovicu, 2023). LEC explants could be exposed to a low proliferating dose of FGF-2 to investigate whether Tpm isoforms are required for differential cell regulation in the lens. This experimental concept may be beneficial since Tpm has also been shown to influence Ras/MAPK signalling activation, and consequently cell proliferative processes (Bakin et al., 2004; Safina et al., 2009; Coombes et al., 2015; Schevzov et al., 2015).

3.4.3 Overexpression of TGF-β1 promotes Tpm isoform-specific reactivity in ASC

To our knowledge, this study is the first to test the differential expression of Tpm isoforms throughout postnatal lens maturation in both WT (normal) and TG mice overexpressing TGF-

β1 that present congenital fibrotic ASC. Our laboratory has previously characterised the formation of ASC in this model, and resultantly noted the heterogenous cell population that arises throughout its postnatal maturation (Lovicu et al., 2004). Since these ASC plaques express differential localisation of the EMT marker α-SMA (Lovicu et al., 2004), and fibre cell markers such as β-crystallin and MIP (Lovicu et al., 2005), it was deduced that ASC, like fibrotic and pearl-like PCO, has two distinct cell phenotypes: aberrant fibre-like cells and myofibroblastic cells. Given that we observed differential Tpm expression in the rat LEC explant model when exposed to either TGF-β2 or FGF-2, and the wider literature has shown differential distribution and abundance of particular Tpm isoforms (Gunning et al., 2008, 2015; Pathan-Chhatbar et al., 2018), we hypothesised that Tpm may also display a differential localisation in ASC plaques when compared to normal lens epithelia of WT mice. We selected several Tpm antibodies that were specific for one or more Tpm isoforms derived from all 4 genes and examined total protein levels in both WT and TG mice wholemount lens epithelia. Given that all the provided antibodies were anti-mouse and the tissue acquired was of mouse origin, we experienced a lot of background immunoreactivity in our western blots. We managed to isolate protein at several molecular weights in both WT and TG lens tissue, that was similar to that observed in our rat LEC *in vitro* model (untreated *vs.* TGF-β2-treated cells).

Elevation of Tpm1.4, Tpm1.6–1.9, and Tpm2.1 labelling was observed between WT and TG tissues; however, localisation of total protein using α9d proved difficult due to high background. Future experiments are needed to quantify this qualitative increase in TG ASC sections (using α9d), to confirm whether these isoforms are differentially regulated during cataractogenesis. Based on the gene expression transcript data, *Tpm2* was the least expressed Tpm gene across P4–P60 postnatal stages. This was reflected in our WT and TG tissues, as eye sections from both lines did not localise for Tpm2.1 throughout several postnatal stages when probed with CG1. Despite this, Tpm2.1 was present in the lens fibres of TG mice between P14–P21. Moreover, we were able to identify Tpm2.1 in WT and TG wholemount lens epithelia samples using western blotting, that appeared to be elevated in the TG mice tissue compared to WT mice. In other lens cataract models, upregulation of Tpm2, as well as Tpm1.6/1.7, was in direct correlation with α-SMA elevated mRNA levels in lens epithelial cells of mice (Shibata et al., 2018) and rat (Kubo et al., 2013) PCO models, up to several weeks following extra capsular lens extraction (ECLE). A later study by Kubo et al. (2017) confirmed the upregulated expression of Tpm1 in mice LECs was dependent on the TGF-β isoform administered, with significant upregulation in TGF-β2 treated cells compared to TGF-β1. Differential expression

patterns of Tpm isoforms were also observed in HLECs cotreated with FGF-2 (10 ng/mL) and TGF-β2 (10 ng/mL) from this study (Kubo et al., 2017). Tpm2 more so than Tpm1 was also significantly downregulated in cotreated HLECs, compared to TGF-β2 only HLECs (Kubo et al., 2017). This result was translated in MLECs that showed a downregulation of Tpm1 correlated with a decrease in α-SMA expression in FGF-2/TGF-β2 treated cells (Kubo et al., 2017). From this result Kubo et al. (2017) proposed FGF-2 is modulating TGF-β induced Tpm stress fibre formation and consequently EMT, in this system. Despite this, cotreatment of FGF-2 and TGF-β2 increased cell migration in MLECs (Kubo et al., 2017), further confirming the role of other Tpm derived isoforms, possibly LMW isoforms (Tpm3 and Tpm4), in high dynamic movement and cell motility. Given the results from the wider literature, it appears that HMW Tpm1 and Tpm2 are required during cataractogenesis and differentiation (Kubo et al., 2017, 2018; Shibata et al., 2018), and wound healing responses (Shin et al., 2017), despite not being able to sufficiently immunolocalise for Tpm2.1 in the current *in vivo* model. The CG1 antibody may be sensitive to specific fixation and/or paraffin embedding protocols. Future experiments could implement another Tpm2.1 probing antibody, such as TM311, that is specific for Tpm1.4, Tpm1.6/1.7, and Tpm2.1 (Dugina et al., 2009; Schevzov et al., 2011; Tojkander et al., 2011; Prunotto et al., 2015; Kubo et al., 2017), similar to α9d.

Throughout lens postnatal growth, probing with γ9d showed Tpm3.1/3.2 localising in the basal and apical cytoplasmic regions of WT and TG lens epithelia. This localisation of Tpm3.1 was observed at the basal F-actin regions of mice native lens epithelia (Parreno et al., 2020), implying an initial demand for Tpm3.1 during organisation mechanisms in lens maturation before cell transformative processes are required. Previous literature has suggested that cell surface proteins, such as heparan sulfate proteoglycans (HSPGs) can regulate ECM adhesion of actin proteins during cytoskeletal modelling that is dependent on growth factor or cytokine ligand binding (Martinho et al., 1996; Samson et al., 2013). Since HSPGs have been shown to colocalise at regions of actin filament assembly in human skin fibroblasts (Martinho et al., 1996), this may be a potential factor impacting changes in Tpm3.1/3.2, as well as other cytoskeletal Tpms, distribution and localisation that was observed in WT and TG postnatal lens growth. For example, our laboratory has shown spatiotemporal immunolocalisation of various HSPGs during embryonic mice lens development as well as in postnatal Wistar rat lenses (Wishart and Lovicu, 2021, 2023). In the current study, we observed apical region immunolocalisation of α2a in lens epithelial cells of WT mice at P7, similar to P10 rat lens sections immunolabelled with HSPG core protein Glypican-6 (Wishart and Lovicu, 2021). In

addition, we observed γ9a diffuse immunolocalisation in LECs throughout postnatal stages in WT mice lenses, that was also similar to Glypican (1 and 4) immunolabelling patterns viewed in P10 rat lenses (Wishart and Lovicu, 2021).

Overall, all *Tpm3* derived isoforms presented similar localisation throughout P7–P21 ASC plaque development in TG mice, with the exception of Tpm3.3, Tpm3.5, Tpm3.8/3.9 expressing fibre cell immunoreactivity beneath the ASC plaques. We believe that these isoforms may be required for normal fibre cell function, stability, and differentiation, as reactivity and protein levels were strong in rat LECs induced by FGF-2.

Based on the gene dataset, we expected Tpm4.2 to exhibit the highest expression increase throughout postnatal WT tissue growth. In a study examining the concentration and patterns of Tpm expression in neurons from rat cerebellum, at P10–P14 postnatal stages Tpm4 was elevated, with a gradual decrease in expression throughout development (Had et al., 1994). Distribution of Tpm4.2 remained the same throughout postnatal maturation of WT and TG mice eyes, regardless of the TG mutant line, and localised in the cytoplasm for both WT lens epithelial cells and those transdifferentiating in response to overexpressed TGF-β1. Despite high background reactivity, total protein for Tpm4.2 also appeared constant in both WT and TG samples, with some cross reactivity for Tpm2.1 when probed with δ9d, that has previously been reported (Schevzov et al., 2011).

Given the qualitative difference between Tpm isoform expression between WT and TG lens, further investigation into differential distribution and abundance of Tpm, particularly cell-type specific roles for Tpm in either EMT and/or fibre differentiation, is required.

3.5 CONCLUSION

Tropomyosin isoforms encoded by all 4 mammalian genes are present and expressed in the postnatal rat and mice lens. We showed a multifaceted role for cytoskeletal Tpm isoforms, particularly stress-fibre associated Tpm1.6/1.7, Tpm2.1, Tpm3.1/3.2, and Tpm4.2, in EMT and/or fibre differentiation, that is dependent on Tpm isoform bundles. Future work with the current model is required to further elucidate the function and Tpm isoform-specific contributions required during various cell regulatory and deregulatory events in the lens. Further testing is required to determine the specific role of these important stress-fibre associated Tpms, Tpm1.6/1.7, Tpm2.1, Tpm3.1/3.2, and Tpm4.2, in the rodent lens during EMT.

CHAPTER 4: CHARACTERISATION OF TROPOMYOSIN ACTIVITY IN TGF-β INDUCED LENS EMT

4.1 PREFACE

In this chapter, we characterised a role for specific Tpm isoforms in rodent LECs during TGF-β-induced EMT. This data presented involves collaborative work with members of the laboratory of Professor Peter Gunning from the School of Biomedical Sciences at The University of New South Wales, Sydney, Australia. All contributions are stated below:

***Mary Flokis*[1]**

- Designed and executed experiments as described
- Writing and assembling manuscript

Jeff Hook[2]

- Provided technical assistance pertaining to Figures 4.4 A and 4.4 B

Edna C. Hardeman[2]

- Provided Tpm-specific antibodies
- Provided WT and Tpm deficient KO mice
- Provided anti-tropomyosin compounds for experimental usage

Peter W. Gunning[2]

- Provided Tpm-specific antibodies
- Provided WT and Tpm deficient KO mice
- Provided anti-tropomyosin compounds for experimental usage

Frank J. Lovicu[1,3]

- Aided experimental design and editing of the manuscript

Affiliations:
[1]*Molecular and Cellular Biomedicine, School of Medical Sciences, Faculty of Medicine and Health, The University of Sydney, NSW, Australia*
[2]*School of Biomedical Sciences, University of NSW, Sydney, NSW, Australia*
[3]*Save Sight Institute, The University of Sydney, NSW, Australia*

4.2 INTRODUCTION

Tropomyosin (Tpm) is a regulatory actin filament protein responsible for cell integrity and stabilisation, contractility/dynamics, and stress fibre formation. Novel splice variants of the Tpm genes code for tissue specific Tpm isoforms that have specialist roles in actin filament assembly. Recent studies have identified six cytoskeletal isoforms commonly associated with stress fibres, including Tpm1.6 and Tpm1.7, Tpm2.1, Tpm3.1 and Tpm3.2, as well as Tpm4.2 (Tojkander et al., 2011; Janco et al., 2016; Gateva et al., 2017; Stefen et al., 2018; Parreno et al., 2020; T. Shibata et al., 2021). During fibrosis, activation of TGF-β leads to EMT that is reported to involve Tpm during stress fibre formation in transdifferentiated myofibroblasts (Bakin et al., 2004; Malmström et al., 2004; Kubo et al., 2018; Bradbury et al., 2021). A role for some of these stress-fibre associated cytoskeletal Tpm isoforms; Tpm1.6/1.7, Tpm2.1, and Tpm3.1, has been shown in lens fibrosis resulting in cataract (Kubo et al., 2010, 2013; Shibata et al., 2018; Parreno et al., 2020; T. Shibata et al., 2021). Despite reported roles for Tpm isoforms in TGF-β-induced EMT, particularly Tpm3.1, discrepancies regarding their expression and localisation in the lens led us to further characterise their role in the lens EMT process.

In this section, we prepared LEC explants from postnatal wild type (WT), Tp7 (Tpm3.1/3.2 KO), and Tp16 (Tpm4.2 KO) mutant mice (all on C57BL/6J background), as well as postnatal Wistar rats. Despite showing earlier in the previous section that there is no significant upregulation of Tpm3.1/3.2 or Tpm4.2 during lens EMT (see Chapter 3: Sections 3.6–3.7 and 3.9), we utilised two Tpm-mutant lines of mice deficient for each respective isoform to further validate any role for them in lens EMT. Selective inhibitors targeting Tpm3.1/3.2 were also administered to lens epithelial explants treated with TGF-β2. In doing so, we planned to determine whether complete inhibition/deletion of Tpm3.1/3.2 and/or Tpm4.2 would impact TGF-β-induced EMT in rodent lens cells.

4.3 MATERIALS AND METHODS

4.3.1 Wild type and Tropomyosin-deficient mice

P20–P25-day-old weanling C57BL/6J wild type (WT), Tp7, and Tp16 mutant mice were provided by Professor's Peter Gunning and Edna Hardeman from The University of New South Wales, Australia. Mice were bred and housed at Australian BioResources (ABR, NSW, Australia) in accordance with the Animal Ethics and Research Integrity Committee (Project #2021/2018; The University of Sydney, Australia). Tpm-deficient KO lines were maintained on a C57BL/6J background, as previously described (Fath et al., 2010; Kee et al., 2015). The Tp7 line targets is deficient in the 9d exon from the *Tpm3* gene, that codes for Tpm isoforms Tpm 3.1, 3.2, and 3.13 (Kee et al., 2015; Cheng et al., 2018). The Tp16 line is deficient in the only Tpm4 isoform to be expressed in mice, Tpm4.2 (Pleines et al., 2017), coded by the *Tpm4* gene.

4.3.2 Wistar rat LEC explants and Assessment of Cell Morphology

Preparation of P21 (±1 day) Wistar rat lens epithelial explants, tissue culture, and assessment of changes in cell morphology have previously been described (see Chapter 2: Sections 2.1–2.3, 2.7).

4.3.3 Preparation of Anti-Tropomyosin Compounds

Anti-tropomyosin compounds (ATMs) were provided by Professor's Peter Gunning and Edna Hardeman, from The University of New South Wales, Australia. Two selective inhibitors, TR100 (422.61 g/mol) and ATM-3507 (612.54 g/mol), target Tpm3.1/3.2 at its C-terminus (Bonello et al., 2016; Janco et al., 2016; Ghosh et al., 2019). Each inhibitor was prepared and stored in fresh 100% dimethyl sulfoxide (DMSO) at a stock concentration of 50 mM. Once in solution, both ATM-3507 and TR100 compounds were further diluted with DMSO into 10 mM and 0.1 mM working stocks. Aliquots were stored at 4°C in the dark. In preparation for treatment, working aliquots (10 µl/0.1 mM) were thawed at room temperature, and diluted in fresh culture medium (M199, *v/v*, 1:10).

4.3.4 Treatment of LECs with TGF-β2 and ATMs

To induce an EMT response, rat and mouse (WT, Tp7, Tp16) lens epithelial explants were treated with TGF-β2 at a concentration of 200 pg/mL. Explants cultured in the absence of TGF-β2 were labelled as controls (non-treated). To determine whether Tpm3.1/3.2 and/or Tpm4.2

are required for TGF-β-induced EMT in the rodent lens, ATM3507 (0.5–2 µM) and/or TR100 (1–2 µM) were administered in the presence or absence of TGF-β2. For TR100, a dose < 5 µM was selected given any dose > 5 µM was reported to promote cell detachment in imLECs from P10 mice (Parreno et al., 2020).

4.3.5 Immunofluorescence of LEC explants

LEC explant fixation (10% NBF), permeabilisation (PBS/BSA/Tween-20), and blocking with normal goat serum (NGS) have been previously described (see Chapter 2: Section 2.10). In this section, the following primary antibodies were applied to assess for epithelial and stress-fibre associated markers; α-SMA (mouse, A2547, Sigma-Aldrich) and β-catenin (rabbit, ab6302, abcam). Additional markers immunolabelling for Tpm1.4, Tpm1.6–1.9, and Tpm2.1 (mouse, α9d, donated), Tpm3.1/3.2 (mouse, γ9d, donated), and Tpm4.2 (rabbit, δ9d, donated), were also applied. All primary antibodies were diluted 1:150–1:200 in NGS as described previously (see Chapter 2). The removal of excess primary antibody and the addition of secondary anti-rabbit (ab150077, abcam) and anti-mouse (ab150116, abcam) Alexa Fluor conjugated antibodies were applied and placed in the dark for a 2-hour incubation period. Nuclear Hoechst staining and consequent washes in PBS/BSA, followed by mounting of explants using PBS/glycerol-coated coverslips, has previously been described (see Chapter 2: Section 2.10).

4.3.6 SDS-Page and Western blotting

4.3.6.1 Non-lens tissue collection and sample preparation

A small biopsy of brain, kidney, and spleen tissue from WT and Tpm-deficient (Tp7, Tp16) mice was acquired and processed by Dr. Jeff Hook from the University of New South Wales, Australia (UNSW). Tissue was placed in Eppendorf tubes and placed on ice with cold RIPA lysis buffer added to each. A plastic pestle was used to homogenise the sample several times prior to ultrasonication. Organ tissue sample lysates were denatured in Laemmli sample buffer and PBS prior to heating for 5 minutes at 95ºC.

4.3.6.2 Lens tissue collection and sample preparation

At respective timepoints, all lens tissue was rinsed with cold PBS on ice to remove M199. WT and Tpm-deficient lens fibre cells were collected and pooled into individual Eppendorf tubes. For each fibre mass sample (1 x lens), 50 µl of RIPA lysis buffer was added for protein homogenisation and extraction. Collected lens epithelial cell explants were spun down briefly

before homogenising in cold RIPA lysis buffer (25–30 µl). All lens protein was extracted and centrifuged at 4ºC for 30 minutes (13,200 x g). Sample lysates were then separated from their respective tissue pellets and stored at -80ºC.

4.3.6.3 SDS-PAGE electrophoresis

WT and Tpm-deficient lens tissue lysates were prepared in Laemmli buffer with 5% β-merc (1:1) and denatured at 100ºC for 8 minutes. All samples were then briefly centrifuged. For whole organ tissue lysates (brain, kidney, spleen), 10–15 µg of total protein was loaded onto a 12.5% SDS-PAGE and carried out by Dr. Jeff Cook.

For both lens fibre and epithelial cell explant protein samples (from Wistar rat and WT, Tp7, and Tp16 mice), 10 µg was loaded onto an SDS-PAGE (12–12.5% Acrylamide gel) for 30 minutes (at 70 V) for protein stacking, then 100 V for 1.5 hours. Samples were then transferred onto a PVDF membrane for 1 hour at 4ºC (at 100 V).

For whole tissue lysates, membranes were blocked in 2.5% foetal bovine serum (FBS, *w/v*) in TBS for 1 hour at room temperature. Primary antibodies, γ9d (mouse, 1:1000), δ9d (rabbit, 1:2000–4000), and loading control α-Tubulin (rabbit, 1:2000), were diluted in 2.5% FBS in TBS.

For rat LEC and WT, Tp7, and Tp16 lens fibre and LEC sample lysates, membranes were blocked in 2.5% BSA (*w/v*) in TBS-Tween-20 (TBST) for 1 hour. Primary antibodies, β-catenin (rabbit, 1:1000), α-SMA (mouse, 1:2000), α9d (mouse, 1:1000), γ9d (mouse, 1:1000), δ9d (rabbit, 1:1000), and loading controls GAPDH (mouse, 1:5000) and β-actin (rabbit, 1:5000), were diluted in 2.5% BSA/TBST.

All membranes were incubated overnight in the respective primary antibodies. Primary antibodies were removed, and membranes were washed 3 x 5 min in TBST. Respective anti-mouse (7076, Cell Signal Tech.) and anti-rabbit (7074, Cell Signal Tech.) HRP secondary antibodies were applied for 2 hours. All membranes were washed (3 x 10 min) in TBST followed by 1–2 minutes of submersion in a chemiluminescent substrate (WBKLS0500, Merck Millipore). Proteins of interest were visualised using ChemiDoc Imaging, and densitometry was conducted using previously described methods (see Chapter 2: Section 2.11.4).

4.3.7 Statistical analysis

For western blots, examining changes in epithelial and EMT-associated marker levels in the presence/absence of TGF-β2 and/or ATM inhibitor compounds, were compared to loading

control GAPDH levels. Respective data was analysed using one-way ANOVA, with Tukey's multiple comparisons test. For this experimental series, a total of three independent experimental replicates were conducted (n=3).

For western blots examining changes in Tpm marker expression in the presence/absence of TGF-β2 and/or ATM inhibitor compounds, proteins of interest were compared relative to loading control β-actin. An average of 10–12 LEC explants were collected per treatment group, per mice line, across three independent replicates. Respective data was analysed using an unpaired, parametric two-tailed t-test. All graphed data was represented as the standard error of the mean (± SEM) and probability values with $p < 0.05$ considered statistically significant.

4.4 RESULTS

4.4.1 Tpm3.1/3.2 and/or Tpm4.2 are not required for TGF-β2 induced EMT

4.4.1.1 Phase contrast microscopy

In non-treated (control) lens explants of WT mice cells had no phenotypical change over the 5 days of culture (Figure 4.1 A–C), as seen with epithelial cells of control rat lens explants (see Chapter 3: Figure 3.1). Treatment of cells with TGF-β2 did not lead to any obvious morphological changes at day 1 of culture (Figure 4.1 D). By day 3 of culture, transdifferentiation of cells from an epithelial to myofibroblastic phenotype was evident, with increased cell elongation and capsular wrinkling evident (Figure 4.1 E). These cells were undergoing an obvious EMT by day 5 (Figure 4.1 F), with increased intercellular spacing and exposure of the underlying modulated capsule following marked cell loss. The EMT response in WT mice LEC explants was slightly prolonged in comparison to TGF-β2-induced rat LEC explants. Myofibroblastic cells in TGF-β2-treated rat lens explants underwent an EMT response with almost complete cell loss after 5 days (see Figure 4.12 C), whereas newly transitioned lens myofibroblastic cells of WT mice explants were still maintained by day 5 (Figure 4.1 F).

Cells of control (non-treated) Tp7 and Tp16 mice lens epithelial explants retained their epithelial phenotype (Figure 4.1 G–I, M–O), as also seen in control WT mouse lens explants (Figure 4.1 A–C), over 5 days of culture. By day 5, the epithelial cells remained tightly packed on the lens capsule (Figure 4.1 I, O). Cells of lens explants from Tp7 mice treated with TGF-β2 experienced a gradual induction of EMT. At day 1 of culture there were no evident morphological changes (Figure 4.1 J), similar to TGF-β2-treated cells of Tp16 mice lens explants at this same timepoint (Figure 4.1 P). TGF-β2-treated epithelial cells from Tp7 lens explants partially retained their epithelial phenotype at day 1, with intercellular spaces becoming more apparent (Figure 4.1 J). Throughout the culture period, capsular folds and cellular blebbing were notable alongside the formation of elongating transdifferentiated cells in TGF-β2-treated Tp7 lens explants (Figure 4.1 K), as well as increased regions of exposed lens capsule (Figure 4.1 L). Treatment with TGF-β2 in Tp16 lens explants led to increased capsular wrinkling and epithelial cell modulation between day 1 and 3 (Figure 4.1 P–Q), with elongate myofibroblastic cells more prominent at day 5 of culture (Figure 4.1 R).

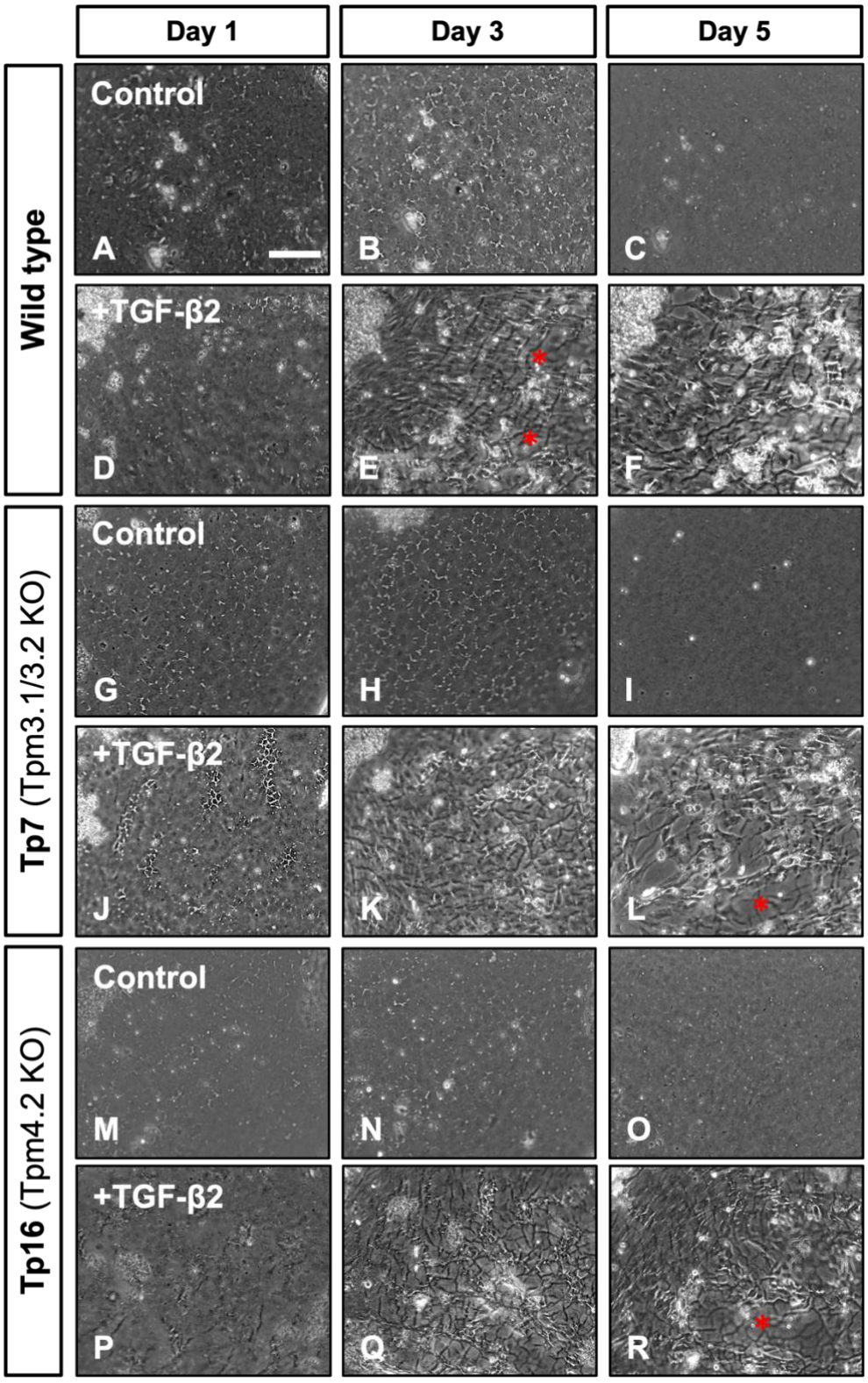

Figure 4.1. Knockout of Tropomyosin 3.1/3.2 and/or Tpm4.2 does not prevent TGF-β2 induced LEC EMT. Control (non-treated) lens epithelial explants monitored across 5 days of culture from wildtype (WT, A–C), Tp7 (Tpm3.1/3.2 KO, G–I), and Tp16 (Tpm4.2 KO, M–O) mice. No differences between control explants from all three lines was noted across culture. Addition of TGF-β2 (200 pg/mL) induced an EMT response in WT explants (D–F), more prominent from day 3 onwards, with myofibroblastic transdifferentiation occurring and newly acquired contractile properties in these cells caused capsular wrinkling (asterisks). An EMT response was also noted in TGF-β2-treated Tp7 (J–L) and Tp16 (P–R) mice lens epithelial explants. Scale bar: 200 µm.

4.4.1.2 Immunofluorescence

Based on morphological differences seen in mice lens epithelial explants during EMT induction (see Figure 4.1), we characterised these phenotypic changes using specific markers for lens epithelial cell membrane (β-catenin) and mesenchymal/myofibroblastic (α-SMA) cells. At 72 hours, cells in control lens explants of WT mice retained membrane-associated localisation of β-catenin (Figure 4.2 A) that was more diffuse and dispersed intracellularly after treatment with TGF-β2 (Figure 4.2 B). The relatively low basal reactivity for α-SMA seen in control lens explants from WT mice (Figure 4.2 A), was markedly increased in TGF-β2-treated lens explants (Figure 4.2 B), with strong localisation in stress fibres of cells. As seen in untreated lens epithelial explants of WT mice, control lens explants of Tp7 mice also exhibited localisation of β-catenin to cell membranes (Figure 4.2 C), with weak cytosolic localisation of α-SMA. Lens epithelial cells of Tp7 explants treated with TGF-β2 demonstrated a weaker and more diffuse label for β-catenin (Figure 4.2 D). As seen in TGF-β2-treated lens explants of WT mice, α-SMA reactivity appeared elevated in TGF-β2-treated lens cells of Tp7 mice (Figure 4.2 D). The epithelial cells of untreated lens explants from Tp16 mice showed strong levels for both β-catenin and α-SMA (Figure 4.2 E). Membrane localisation of β-catenin was more distinct; however, β-catenin was both reduced (levels) and more disperse in cells of TGF-β2-treated lens epithelial explants of Tp16 mice (Figure 4.2 F). Lens explants derived from Tp16 mice had stress fibre localisation of α-SMA in elongating myofibroblastic cells when treated with TGF-β2 (Figure 4.2 F).

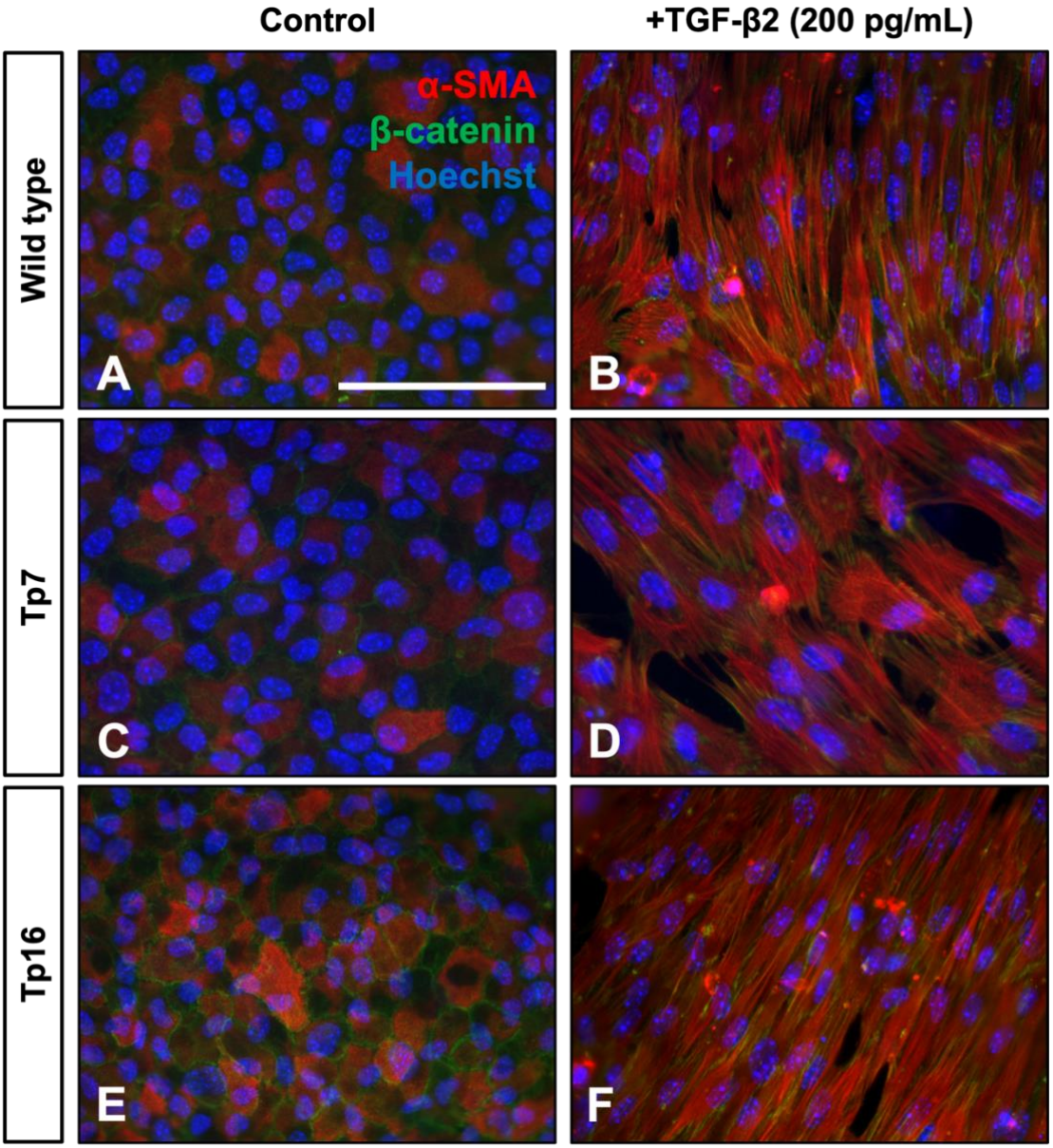

Figure 4.2. Immunofluorescent labelling of EMT and epithelial markers in LEC explants of WT and Tpm-deficient mice. Lens epithelial cell explants of WT, Tp7, and Tp16 mice were immunolabelled for epithelial (β-catenin, green) and EMT (α-SMA, red) markers and nuclear stained with Hoechst dye (blue) at 72 hours of culture. Control (non-treated) lens epithelial explants from WT (A), Tp7 (C), and Tp16 (E) mice. Stress fibre localisation of α-SMA across all mice lens epithelial explants treated with TGF-β2 (200 pg/mL) (B, D, F), with low levels for β-catenin. Scale bar: 100 µm.

4.4.1.3 Western blotting

We assessed for EMT marker protein changes between control (non-treated) and TGF-β2-treated lens explants of WT, Tp7, and Tp16 mice (Figure 4.3 A–C). Control explant lysates from all lines showed low levels of α-SMA at 72 hours (Figure 4.3 A–B). TGF-β2 treatment increased α-SMA protein expression in lens epithelial lysates, compared to non-treated lens epithelial lysates derived from WT mice, that was not significant (p = 0.0648). In lens explants of Tpm3.1/3.2 KO (Tp7) mice, α-SMA was increased in TGF-β2-treated epithelial cell lysates relative to low levels in non-treated lens epithelial cell lysates; however, this increase was not significant (p = 0.0637). Lens cells from Tp16 mice treated with TGF-β2 significantly increased α-SMA protein levels in comparison to non-treated lens cell lysates derived from Tp16 mice (p = 0.0470).

β-catenin protein levels remained strong in non-treated LEC lysates derived from WT, Tp7, and Tp16 mice (Figure 4.3 A, C). Addition of TGF-β2 to LECs significantly decreased β-catenin levels compared to control lens cell lysates derived from WT mice (p = 0.0359, Figure 4.3 C). A similar trend of decreased β-catenin levels was observed in Tpm4.2 KO (Tp16) mice LEC explants treated with TGF-β2 (p = 0.0150). In lens explants derived from Tp7 mice, there was no statistically significant difference between levels of β-catenin expression in control and TGF-β2-treated LEC lysates (p = 0.1920).

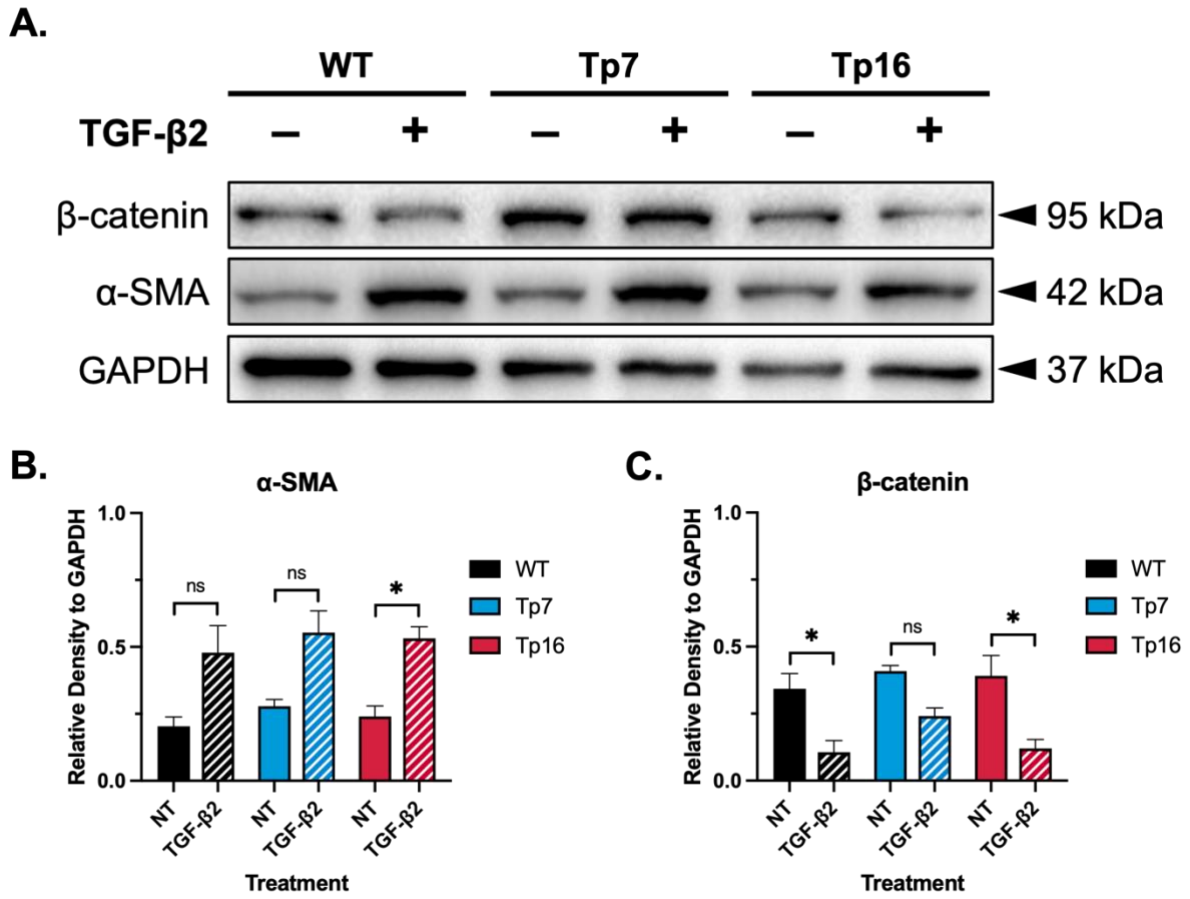

Figure 4.3. TGF-β2-induced EMT marker expression at 72 hours of culture in WT and Tpm-deficient mice. Representative western blots of mouse (WT, Tp7, Tp16) LEC explant lysates in the absence (non-treated, NT) or presence of TGF-β2 (200 pg/mL) at 72 hours of culture. Protein expression for epithelial (β-catenin) and EMT-associated (α-SMA) markers. Using densitometry, protein levels were quantified relative to loading control, GAPDH (B, C). One-way analysis of variance (ANOVA) with post-hoc Tukey's multiple comparisons test with the mean ± SEM (ns = not significant, * $P < 0.05$).

4.4.2 Confirmation of Tpm protein deficiency in Tpm KO mice

4.4.2.1 Wild type and Tpm-deficient whole organ tissue

We used western blotting to confirm the absence of Tpm3.1/3.2 and Tpm4.2 in tissues from each respective mutant mouse line. Lysates from several WT mice tissue biopsies (brain, kidney, spleen) were used as positive controls (Figure 4.4 A). γ9d probed strongly (at approximately 30 kDa) for Tpm3.1/3.2 in all whole organ tissue derived from WT mice. Tp7 mice tissue (brain, kidney, spleen) showed no reactivity for Tpm3.1/3.2, confirming the loss of Tpm3.1/3.2 in these mice (Figure 4.4 A). Lysates from WT and Tp16 kidney tissue were immunolabelled for Tpm4.2 (δ9d), with Tpm4.2 was only detected (30 kDa) in WT kidney tissue (Figure 4.4 B).

4.4.2.2 Wild type and Tpm-deficient lens tissue

We looked for the presence of Tpm3.1/3.2 and Tpm4.2 in lens fibres (LF) of WT, Tp7, and Tp16 mice (Figure 4.4 C–D). LF lysates derived from WT, Tp7, and Tp16 mice reacted to γ9d; however, at a different molecular weight (Figure 4.4 C). LF lysates derived from WT, Tp7, and Tp16 mice immunolabelled for Tpm4.2 and detected a band between 20–25 kDa (Figure 4.4 D). The 20–25 kDa weight range is not the molecular weight of either Tpm3.1/3.2 (30 kDa) or Tpm4.2 (30 kDa). The bands detected at 20–25 kDa are likely cross reacting with the abundant crystallin chaperone proteins, such as β-crystallin, found in lens fibre cells. We detected several bands for β-crystallin proteins between 20–25 kDa in WT lens fibres (Figure 4.4 E).

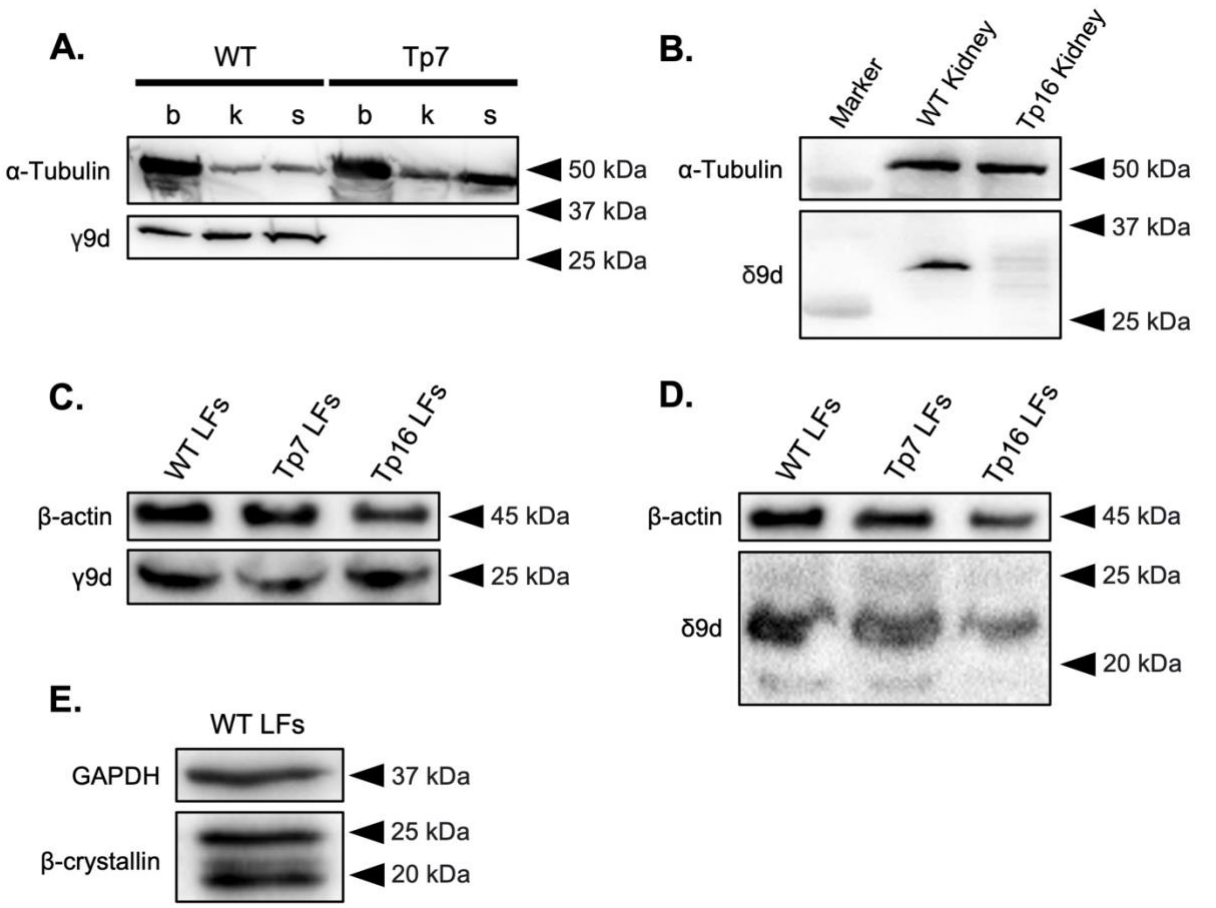

Figure 4.4. Western blot analysis of Tpm protein deficiency in organ tissues derived from postnatal WT, Tp7, and Tp16 mice. A) WT and Tp7 tissue lysates from brain (b), kidney (k), and spleen (s) are examined using a Tpm3.1/3.2-specific antibody (γ9d). γ9d recognises Tpm3.1/3.2 in WT tissue only. B) A separate blot with WT and Tp16 mouse kidney lysates. δ9d recognises Tpm4.2 in WT tissue only. α-Tubulin was used as a protein loading control (A, B). Marker refers to protein standard ladder. C) A separate blot loaded with 10 µg of protein from WT, Tp7, and Tp16 mouse lens fibre lysates (LFs) probed for γ9d. γ9d reacting to chaperone proteins found abundantly in lens fibres, crystallins, at 25 kDa. D) A separate blot with the same lysates and running conditions probed for δ9d. δ9d also reacting to crystallins at 20-25kDa. WT LFs probed for chaperone protein β-crystallin (E). β-actin and GAPDH used as loading controls (C–E).

4.4.3 Tpm3.1/3.2 and Tpm4.2 are confirmed KO in lens epithelial cell explants using immunofluorescence

We examined levels of Tpm3.1/3.2 and Tpm4.2 in lens epithelial explants of WT, Tp7, and Tp16 mice using Tpm-isoform-specific antibodies; γ9d (Tpm3.1/3.2) and δ9d (Tpm4.2). Control lens epithelial explants of WT mice at 3 days of culture displayed actin filament and cytoplasmic localisation of Tpm3.1/3.2 (Figure 4.5 A) and Tpm4.2 (Figure 4.5 G). Tpm3.1/3.2 localised in cytoskeletal components of stretched-out myofibroblastic cells in TGF-β2 (200 pg/mL)-treated explants derived from WT mice (Figure 4.5 D). When probed with δ9d, TGF-β2-treated lens epithelial explants of WT mice showed strong Tpm4.2 levels in the stress fibres of myofibroblastic cells (Figure 4.5 J). In Tpm3.1/3.2 deficient mice, there was minimal background labelling for Tpm3.1/3.2 in non-treated lens explants (Figure 4.5 B). There was some actin filament localisation of Tpm3.1/3.2 in TGF-β2-treated lens epithelial explants derived from Tp7 mice, potentially due to some cross reactivity with Tpm1.4, Tpm1.6–1.9, and Tpm2.1 (Figure 4.5 E), that has previously been reported (Schevzov et al., 2011). Actin filament and stress fibre localisation of Tpm4.2 in TGF-β2-treated lens epithelial cell explants derived from Tp7 mice (Figure 4.5 K) was strong in comparison to the low levels for Tpm4.2 in non-treated lens cells (Figure 4.5 H). Cytoplasmic localisation for Tpm3.1/3.2 was found in control lens epithelial explants of Tp16 mice (Figure 4.5 C). In TGF-β2-induced lens explants derived from Tp16 mice, strong stress fibre localisation of Tpm3.1/3.2 was noted in myofibroblastic cells (Figure 4.5 F). Lens cells were not reactive for Tpm4.2 in both non-treated and TGF-β2-treated explants from Tpm4.2-deficient mice (Figure 4.5 I, L).

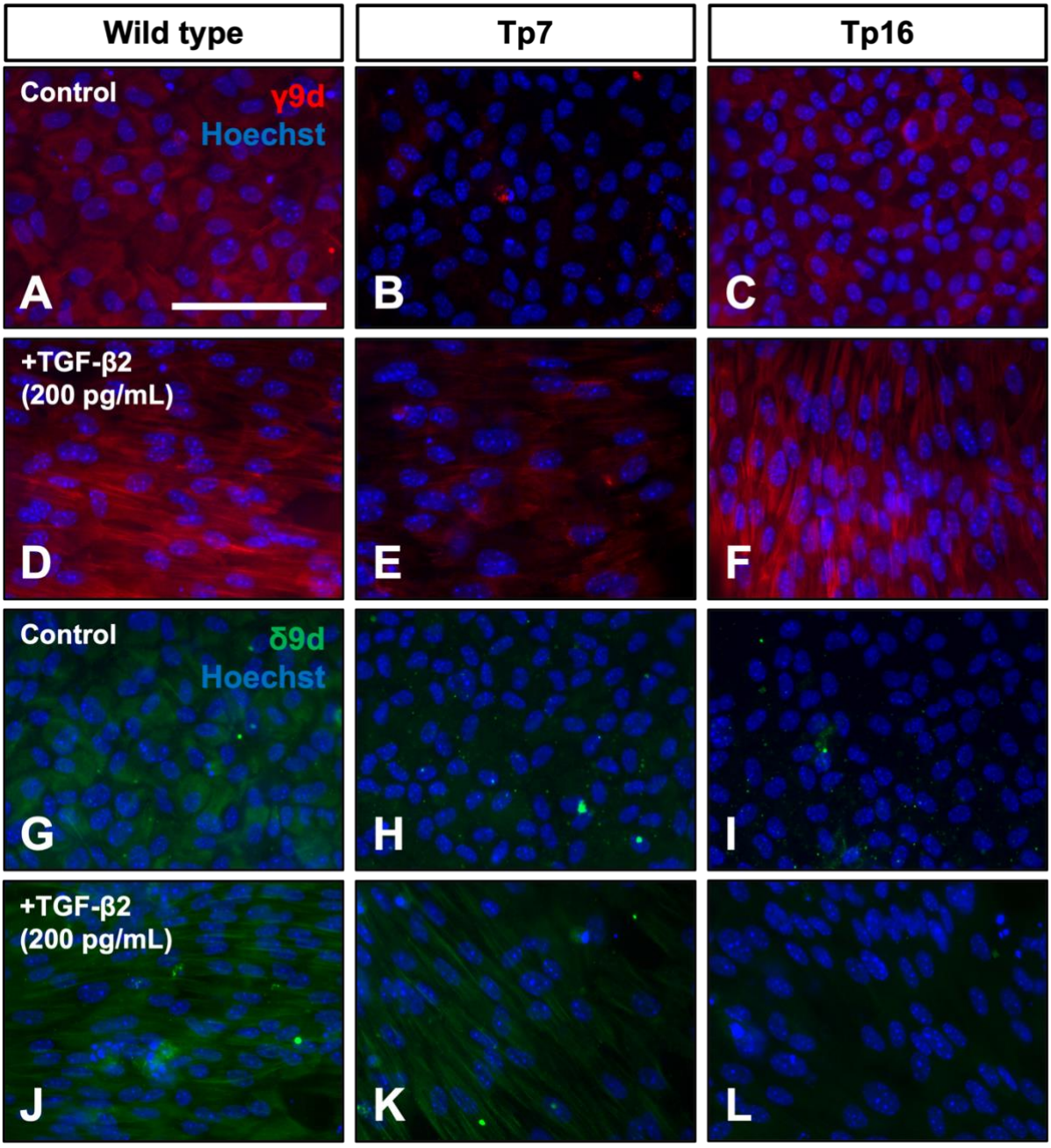

Figure 4.5. Immunofluorescent labelling of Tpm markers in wild type, Tp7, and Tp16 mice. Lens epithelial explants from WT (C57BL/6J), Tp7 (Tpm3.1/3.2 deficient), and Tp16 (Tpm4.2 deficient) mice were fixed at day 3 of culture and immunolabelled for Tpm-specific antibodies; γ9d (Tpm3.1/3.2, red), δ9d (Tpm4.2, green), and counterstained with Hoechst (blue). Control (non-treated; A–C, G–I) and TGF-β2 (200 pg/mL)-treated (D–F, J–L) lens explants. Treatment with TGF-β2 induced stress fibre localisation of γ9d in lens cells derived from WT (D) and Tp16 explants (F), as well as δ9d in WT (J) and Tp7 treated lens epithelial cell explants (K). Scale bar: 100 µm.

4.4.4 Elimination of Tpm3.1/3.2 and/or Tpm4.2 does not cause Tpm1 isoform compensation in Tpm KO mice

Based on the increased protein levels of Tpm1.6/1.7 and Tpm2.1 in rat LEC explants when exposed to TGF-β2 (see Chapter 3 Figures 3.4 and 3.8), we looked at its potential as a marker for EMT in lens explants derived from WT, Tp7, and Tp16 mice. Lens epithelial cells derived from WT mice demonstrated low levels and cytoplasmic localisation of Tpm1.4, Tpm1.6–1.9, and Tpm2.1 (α9d) in control lens cells after 72 hours (Figure 4.6 A). An increase in Tpm1.4, Tpm1.6–1.9, and Tpm2.1 levels was noted in lens explants from WT mice treated with TGF-β2, as well as α9d localising in stress fibres of myofibroblastic cells (Figure 4.6 B). Untreated lens explants of Tp7 (Figure 4.6 C) and Tp16 (Figure 4.6 E) mice showed similar cytoplasmic localisation for Tpm1.4, Tpm1.6–1.9, and Tpm2.1 as seen in control lens epithelial explants of WT mice. Addition of TGF-β2 to lens explants derived from Tp7 mice increased actin filament and stress fibre localisation of α9d in cells undergoing EMT (Figure 4.6 D), with these cells presenting an enlarged myofibroblastic phenotype. TGF-β2-treated lens explants from Tp16 mice showed strong levels and actin stress fibre localisation for Tpm1.4, Tpm1.6–1.9, and Tpm2.1 (Figure 4.6 F); however, in contrary to lens explants exposed to TGF-β2 derived from Tp7 mice, a more elongated myofibroblastic phenotype was noted.

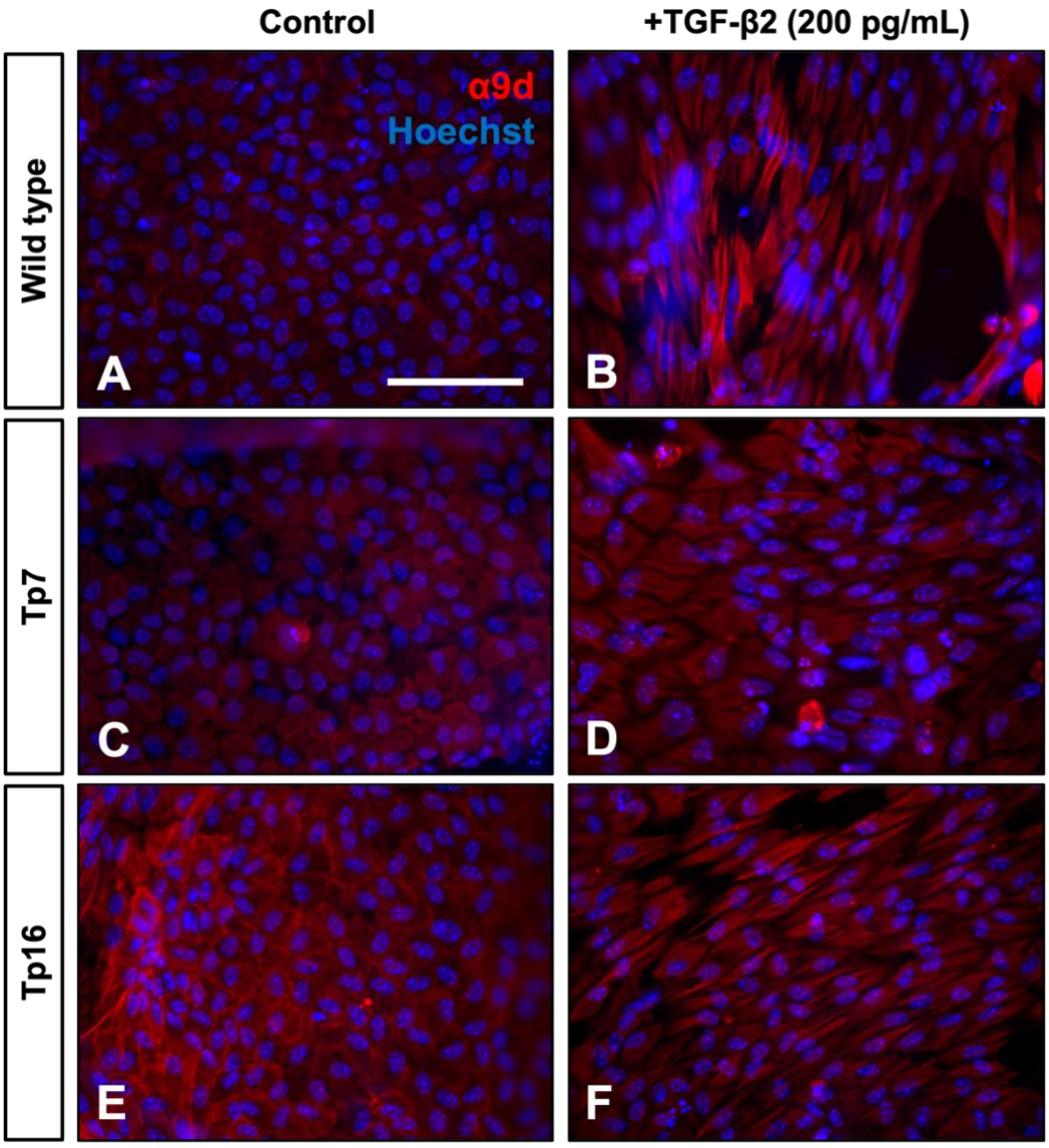

Figure 4.6. Immunofluorescent labelling of for Tpm1.4, Tpm1.6–1.9, and Tpm2.1 in WT and Tpm-deficient LEC mice explants. LEC explants from WT (A, B), Tp7 (C, D), and Tp16 (E, F) mice were immunolabelled for Tpm1.4, 1.6–1.9, and 2.1 using α9d (red) and nuclear stained with Hoechst dye (blue) at 72 hours of culture. Control (non-treated) (A, C, E) and TGF-β2 (200 pg/mL)-treated (B, D, F) lens explants. Strong actin filament localisation of α9d in TGF-β2-induced explants across all mice lines. Scale bar: 100 µm.

Since α9d is reactive for multiple isoforms (Schevzov et al., 2011), we wanted to distinguish which isoforms are required for EMT in the absence of Tpm3.1/3.2 or Tpm4.2. In mice (WT, Tp7, Tp16) lens explant lysates, α9d detected two bands at approximately 34–36 kDa (Tpm1.6/.17) and 38 kDa (Tpm2.1, Figure 4.7). We assessed all bands localising for α9d (total α9d), as well as Tpm2.1 only, and Tpm1.6/1.7 only. LEC explants from WT mice demonstrated elevated Tpm2.1 with TGF-β2 treatment when compared to control explants ($p = 0.0647$) (Table 4.1, Figure 4.7 A–B). This increase was also observed in lens explants from WT mice probed for Tpm1.6/1.7, although it was not statistically significant (control *vs.* TGF-β2: $p = 0.3523$). The combined protein level changes for Tpm1.6/1.7 and Tpm2.1 (total α9d) between control and TGF-β2-treated lens explants from WT mice was statistically significant ($p = 0.0052$).

Table 4.1. Summary of α9d protein levels in WT, Tp7, and Tp16 mice LEC explants.

Mouse line	Treatment groups	*P* value[1]		
		Tpm1.6/1.7	Tpm2.1	Total α9d
WT	NT *vs.* TGF-β2	0.3523	0.0647	0.0052*
Tp7	NT *vs.* TGF-β2	0.0459*	0.1852	0.0715
Tp16	NT *vs.* TGF-β2	0.2769	0.2222	0.1258

[1]Two-tailed, unpaired parametric t-test
*Statistically significant difference between treatment groups ($P < 0.0332$)
Abbreviations: Non-treated LEC explants (NT), tropomyosin (Tpm), wild type mice (WT), Tpm3.1/3.2 KO mice (Tp7), Tpm4.2 KO mice (Tp16). Refer to Figure 4.7 A–F.

TGF-β2-treated LECs demonstrated strong Tpm2.1 protein levels, when compared to control epithelial cells, from Tp7 mice lens explants ($p = 0.1852$, Figure 4.7 C–D). A statistically significant increase was observed in TGF-β2-induced lens epithelial explants of Tp7 mice for Tpm1.6/1.7, compared to control lens explants ($p = 0.0459$). No statistically significant difference was observed between the total sum of α9d protein levels in control and TGF-β2-induced lens epithelial explants from Tp7 mice ($p = 0.0715$). No significant difference was observed between lens epithelial cells in non-treated and TGF-β2-treated explants from Tp16 mice, when probed for Tpm1.6/1.7 ($p = 0.2769$) (see Table 4.1 and Figure 4.7 E–F). A slight increase in Tpm2.1 protein levels was noted in TGF-β2-treated lens explants, when compared to control explants, from Tp16 mice ($p = 0.2222$). The total sum of α9d protein levels in control and TGF-β2-treated lens explants derived from Tp16 mice exhibited no significant difference ($p = 0.1258$).

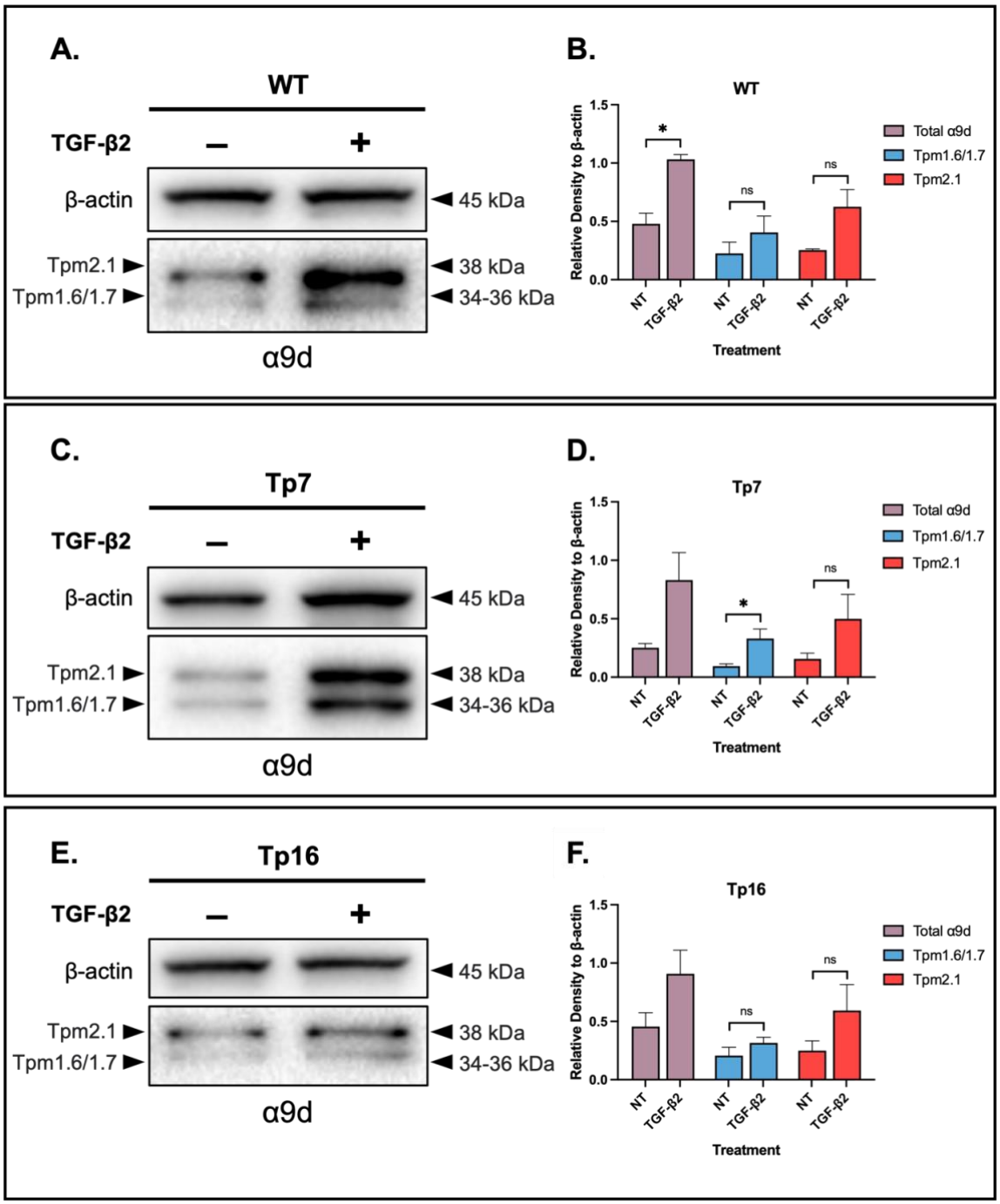

Figure 4.7. TGF-β2-induced Tpm1.6/1.7 and Tpm2.1 protein expression at 72 hours of culture in WT and Tpm-deficient mouse lens epithelial explants. Western blots of mouse LEC lysates in the absence (non-treated, NT) or presence of TGF-β2 (200 pg/mL) at 72 hours of culture. α9d probed for Tpm1.6/1.7 (34–36 kDa) and Tpm2.1 (38 kDa) in WT (A, B), Tp7 (C, D), and Tp16 (E, F) mice LEC lysates. Levels of Tpm1.6/1.7 and Tpm2.1 were elevated in TGF-β2 treated LEC explant lysates from all mice lines. α9d relative to loading control, β-actin. Unpaired, parametric two-tailed t-test with $P < 0.05$ considered statistically significant (ns = not significant, * $P < 0.0332$).

4.4.5 Inhibition of Tpm3.1/3.2 does not prevent TGF-β2-induced EMT in wildtype or Tpm4.2-deficient mice

4.4.5.1 Pharmacological inhibition of Tpm3.1/3.2 in WT mice

Tpm3.1/3.2 has previously been pharmacologically targeted using anti-tropomyosin compounds (ATMs), in imLECs and whole lenses, that impacted the formation of basal stress fibres during EMT (Parreno et al., 2020). Using our LEC explant model, we tested two different Tpm3.1/3.2 targeted inhibitors (TR100 and ATM-3507) on WT mice lens explants and monitored cells across 5 days to observe for morphological changes (Figure 4.8). The addition of ATM compounds, TR100 (2 μM) and ATM-3507 (0.5 μM) alone, did not cause any changes to the characteristic lens epithelial cell phenotype, with these cells from WT mice explants remaining tightly packed and cobblestone-like over the culture period (Figure 4.8 A–F). 1-hour pre-treatment with either TR100 or ATM-3507 did not cause significant changes in LEC morphology at day 1 of culture in TGF-β2-induced lens explants from WT mice (Figure 4.8 G, J). At day 3, both TR100/TGF-β2 (Figure 4.8 H) and ATM-3507/TGF-β2 (Figure 4.8 K) treated lens explants of WT mice underwent an EMT response, with refractile bodies and cell debris indicative of cell apoptosis, as well as the onset of lens capsule modulation as wrinkling. By day 5, most lens cells were lost in both treatment groups, with the few remaining cells exhibiting a myofibroblastic phenotype among regions of the exposed capsule of WT mice lens explants (Figure 4.8 I, L).

Immunofluorescent labelling in TR100-treated lens explants from WT mice at day 3 showed strong levels and distinct cell membrane localisation of β-catenin (Figure 4.8 M). Minimal cytoplasmic localisation for α-SMA was noted in these lens epithelial cells derived from WT mice treated with TR100. In WT mice lens explants, TR100- and TGF-β2-treated lens epithelial cells showed a more dispersed β-catenin membrane localisation, with α-SMA localised in actin stress fibres of myofibroblastic cells (Figure 4.8 N). Cytoplasmic localisation of α-SMA and membrane localisation of β-catenin was observed in WT lens explants exposed only to ATM-3507 (Figure 4.8 O), although β-catenin intensity was not as strong as lens explants exposed to TR100 alone. ATM-3507 and TGF-β2-treated lens explants from WT mice exhibited increased levels and actin stress fibre localisation of α-SMA, with significantly reduced β-catenin levels and localisation, that was more dispersed in the few remaining cells (Figure 4.8 P).

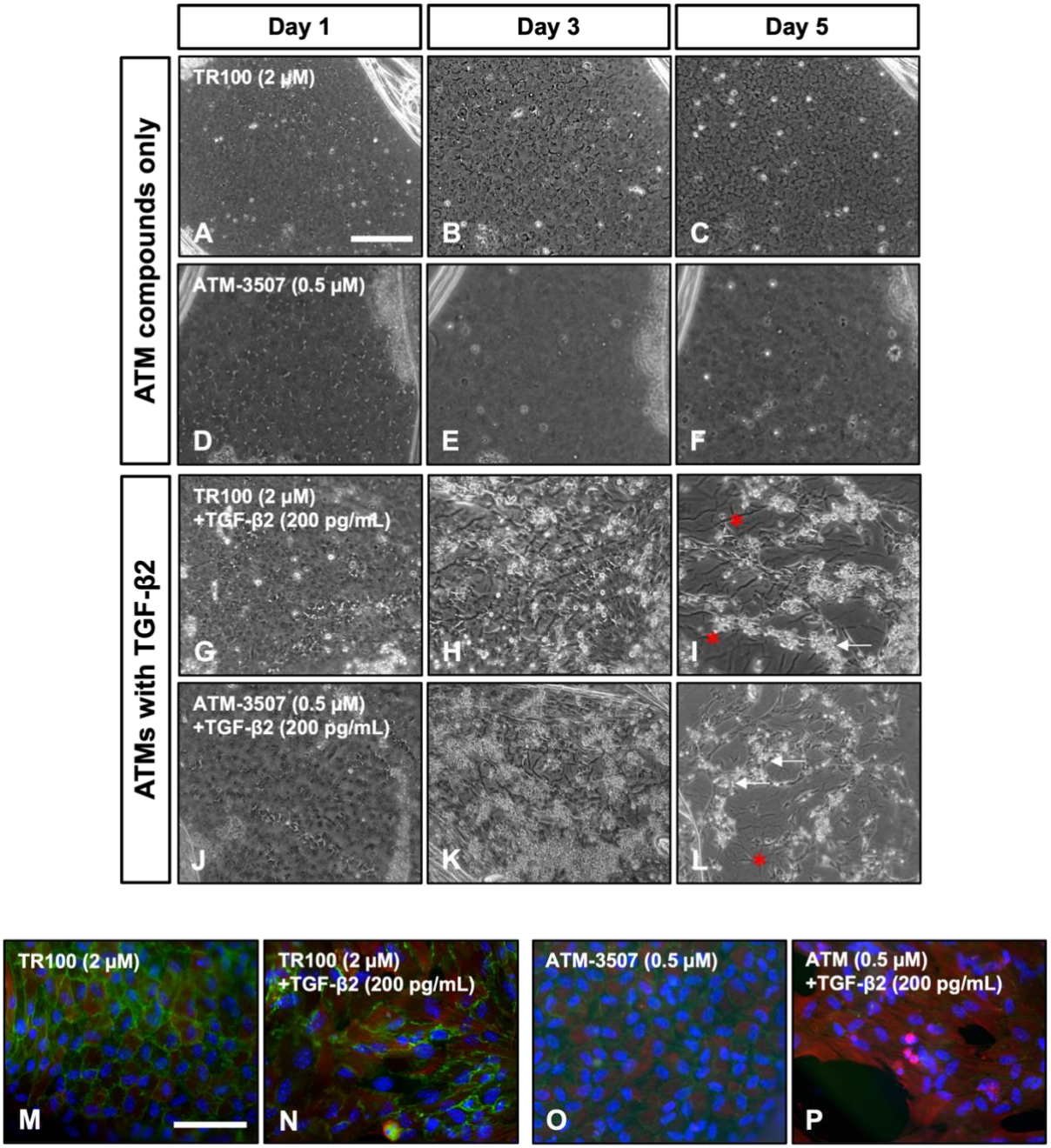

Figure 4.8. Inhibition of Tpm3.1/3.2 does not block TGF-β2 induced EMT in WT LEC explants. Selective anti-tropomyosin compounds (ATMs) targeting Tpm3.1/3.2, TR100 (2 μM) and ATM-3507 (0.5 μM). No morphological changes observed in WT LEC explants treated with either TR100 (A–C) or ATM-3507 (D–F) only across culture. EMT induction was observed in WT lens epithelia explants treated with TGF-β2 (200 pg/mL) and TR100 (G–I) or ATM-3507 (J–L). Myofibroblastic transdifferentiation noticeable in ATM/TGF-β2 treated explants, with capsular wrinkling (red asterisks) and refractile bodies indicative of cell apoptosis (white arrows). Representative immunofluorescent labelling for α-SMA (red), β-catenin (green), and nuclear stained with Hoechst (blue) in WT lens epithelia explants fixed at day 3 (M–P). ATMs administered without TGF-β2 (A–F, M, O), or 1-hour pre-TGF-β2 treatment (D-L, N, P). Scale bar: 200μm (A–L), 100 μm (M–P).

4.4.5.2 Pharmacological inhibition of Tpm3.1/3.2 in Tp16 mice lens epithelial explants

Explants derived from Tp16 (Tpm4.2 KO) mice were exposed to TR100 and ATM-3507 in the presence or absence of TGF-β2 and monitored across 5 days (Figure 4.9). 1-hour pre-treatment with either TR100 (2 μM) or ATM-3507 (0.5 μM) did not impact LEC morphology across the culture period, with a normal monolayer of epithelial cells maintained in these explants (Figure 4.9 A–F). Pre-treatment with TR100 in TGF-β2 exposed lens explants from Tp16 mice did not prevent EMT induction (Figure 4.9 G–I). Epithelial cell transdifferentiation into elongated myofibroblastic cells, particularly at peripheral regions of the explant, was evident at day 3 in TR100/TGF-β2-treated lens epithelial explants from Tp16 mice (Figure 4.9 H) and was maintained up to 5 days (Figure 4.9 I). The presence of myofibroblastic cells led to folds and capsular wrinkling within the central region of these lens explants (Figure 4.9 H–I). Tp16 mice lens explants exposed to ATM-3507 prior TGF-β2 treatment also showed capsular wrinkling, cell blebbing, and refractile bodies, as well as exposed regions of the underlying capsule at day 3 of culture (Figure 4.9 K). By day 5, the transdifferentiated lens cells from treated Tp16 mice still remained on the lens explant, with more areas of exposed modulated lens capsule (Figure 4.9 L). No morphological changes were noted at day 1 of culture for TR100/TGF-β2 and/or ATM-3507/TGF-β-treated lens explants of Tp16 mice (Figure 4.9 G, J). Tpm4.2 KO mice lens explants exposed to TR100 or ATM-3507 only, demonstrated low expression and cytoplasmic localisation for α-SMA after 5 days (Figure 4.9 M, O). In comparison, an increase in α-SMA levels in lens cells from TR100/TGF-β2-treated explants from Tp16 mice was noted (Figure 4.9 N), localising in the stress fibres of elongating myofibroblastic cells. ATM-3507 was unable to prevent TGF-β2-induced EMT in lens explants derived from Tp16 mice, evident by patches of empty spaces between α-SMA-reactive myofibroblastic cells, indicative of cell loss and migration (Figure 4.9 P).

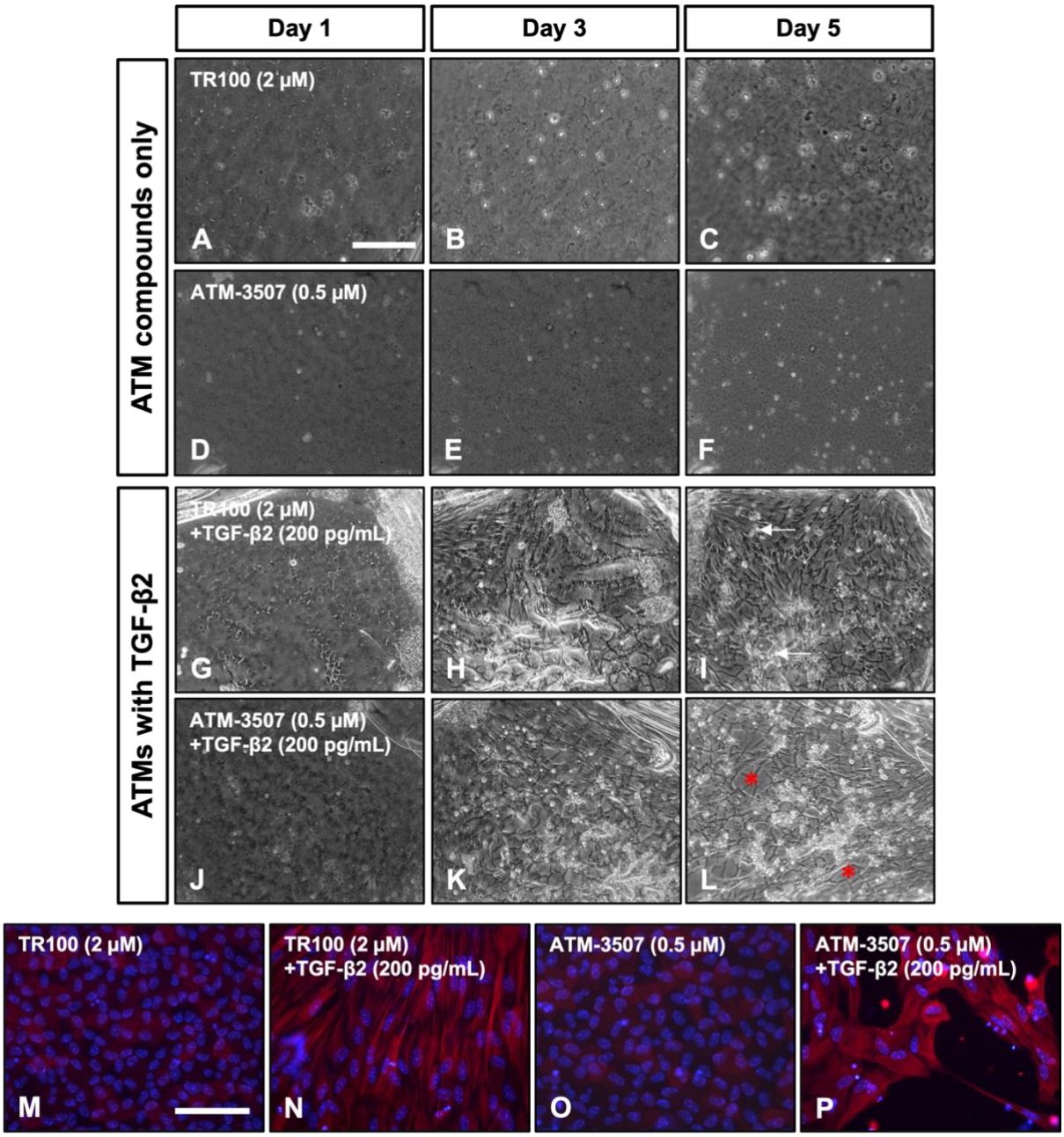

Figure 4.9. Inhibition of Tpm3.1/3.2 does not block TGF-β2 induced EMT in Tp16 LEC explants. Selective ATMs targeting Tpm3.1/3.2 did not alter lens epithelial cell morphology in LEC explants from Tp16 mice treated with either TR100 (A–C) or ATM-3507 (D–F) alone across 5 days of culture. EMT induction was observed in lens explants pre-treated with TR100 (G–I) or ATM-3507 (J–L) prior to TGF-β2 (200 pg/mL). Myofibroblastic transdifferentiation noticeable in ATMs/TGF-β2-treated explants, with capsular wrinkling (red asterisks) and refractile bodies indicative of cell apoptosis (white arrows). Capsule folds and modulation observed in TR100/TGF-β2 treated explants at day 3 (H). Immunofluorescent labelling of α-SMA (red) and nuclear staining with Hoechst (blue) in lens explants fixed at day 5 (M–P). ATMs administered without TGF-β2 (A–F, M, O), or 1-hour pre-TGF-β2 treatment (G–L, N, P). Scale bar: 200µm (A–L), 100 µm (M–P).

4.4.5.3 Inhibition of Tpm3.1/3.2 does not reduce EMT protein levels in WT or Tpm4.2-deficient TGF-β2-stimulated mice lens epithelial explants

To confirm that pharmacological inhibition of Tpm3.1/3.2 in WT and Tpm4.2 KO mice does not inhibit TGF-β2-induced lens EMT, we examined protein levels of β-catenin and α-SMA in the presence/absence of TR100 and/or TGF-β2 (Figure 4.10). At 72 hours, α-SMA was significantly elevated in TR100/TGF-β2 lens epithelial explants from WT mice, when compared to TR100 alone lens explant lysates (p = 0.0031, Figure 4.10 A–B). There was no difference between β-catenin protein levels in TR100/TGF-β2-treated lens explant lysates, when compared to levels in TR100-treated explants from WT mice (p = 0.5561, Figure 4.10 A, C). In Tp16 mice lens explants, inhibition of Tpm3.1/3.2 did not reduce α-SMA levels (Figure 4.10 A); however, the addition of TGF-β2 following TR100 exposure in lens explants increased α-SMA protein levels, although this increase was not significant (p = 0.1517, Figure 4.10 B). No difference in β-catenin protein levels was noted in TR100 *vs.* TR100/TGF-β2-treated lens

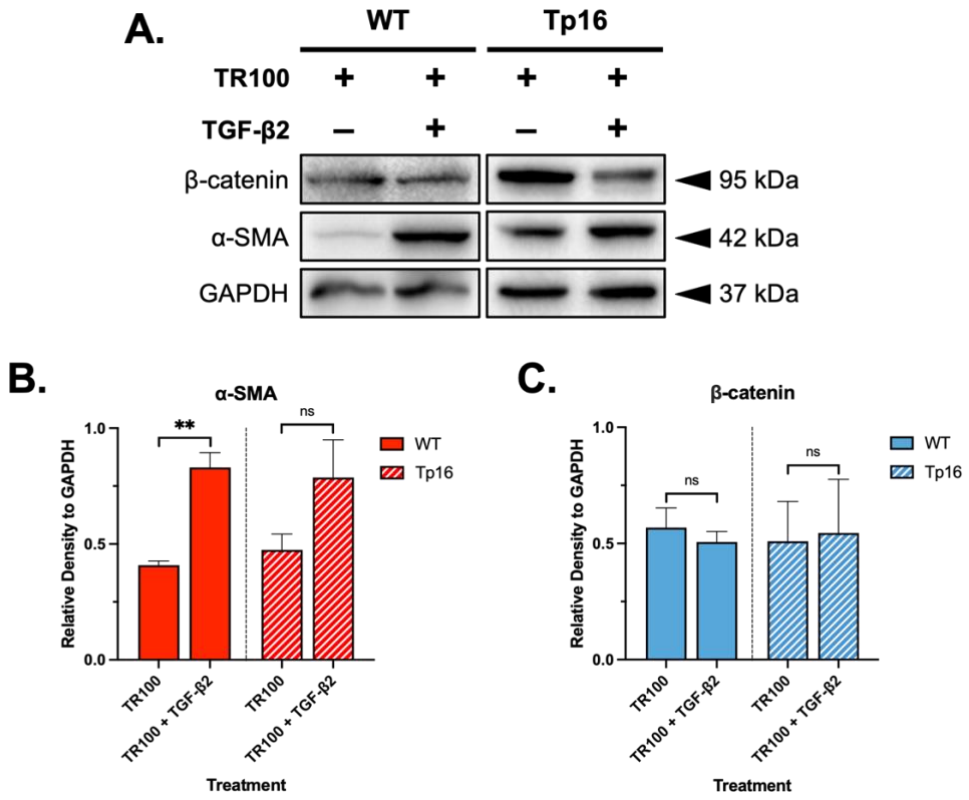

Figure 4.10. Inhibition of Tpm3.1/3.2 does not mediate EMT marker expression in TGF-β2-induced WT and/or Tp16 mice LEC explants. Separate and representative western blots of WT and Tp16 mice LEC lysates at 72 hours of culture (A). Protein expression for β-catenin and α-SMA markers in lens explants exposed to TR100 (2 μM) alone, or to TR100 1-hour prior to TGF-β2 (200 pg/mL) treatment. Densitometry for α-SMA and β-catenin quantified relative to GAPDH (B, C). Unpaired, parametric two-tailed t-test with $P < 0.05$ considered statistically significant (ns = not significant, ** $P < 0.0021$).

explants from Tp16 mice (p = 0.9078). TR100 did not block TGF-β2-induced EMT marker changes in WT or Tp16 mice.

4.4.5.4 Inhibition of Tpm3.1/3.2 does not lead to Tpm1 isoform compensation in lens epithelial cell explants

In lens explants from WT and Tp16 mice only treated with TR100 (2 μM), Tpm1.4, Tpm1.6–1.9, and Tpm2.1 (α9d) labelled actin filaments within the cytoplasm of these LECs (Figure 4.11 A, C). TR100/TGF-β2-treated lens explants of WT mice demonstrated a slight increase in α9d, with actin filament localisation in myofibroblastic cells (Figure 4.11 B). TR100/TGF-β2-treated lens explants from Tp16 mice exhibited α9d stress-fibre localisation in highly organised elongating, transdifferentiated cells (Figure 4.11 D). Using western blotting, we probed for Tpm1.6/1.7 and Tpm2.1 in WT and Tp16 LEC explants exposed to either TR100 alone, or TR100 and TGF-β2 treatment. Inhibition of Tpm3.1/3.2 using TR100 did not impact Tpm1.6/1.7 or Tpm2.1 protein levels in lens explants treated with TGF-β2 from WT mice (Figure 4.11 E). In fact, Tpm1.6/1.7 was significantly elevated in TR100/TGF-β2 lens explants, compared to WT mice lens explants exposed to only TR100 (p = 0.0095, Figure 4.11 E–F). Tpm2.1 was also significantly increased in TR100/TGF-β2 LEC explant lysates in comparison to TR100 only lysates from WT mice (p = 0.0235). The total α9d in LEC explants of WT mice showed no statistically significant difference when comparing cells treated with only TR100 and those treated with TR100/TGF-β2 (p = 0.0848). In lens lysates from Tp16 mice, no difference was observed for Tpm1.6/1.7 or Tpm2.1 protein levels with either TR100 alone or TR100/TGF-β2-treated LEC explants (Tpm1.6/1.7: TR100 *vs.* TR100/TGF-β2, p = 0.1524; Tpm2.1: TR100 *vs.* TR100/TGF-β2, p = 0.8802) (Figure 4.11 E, G).

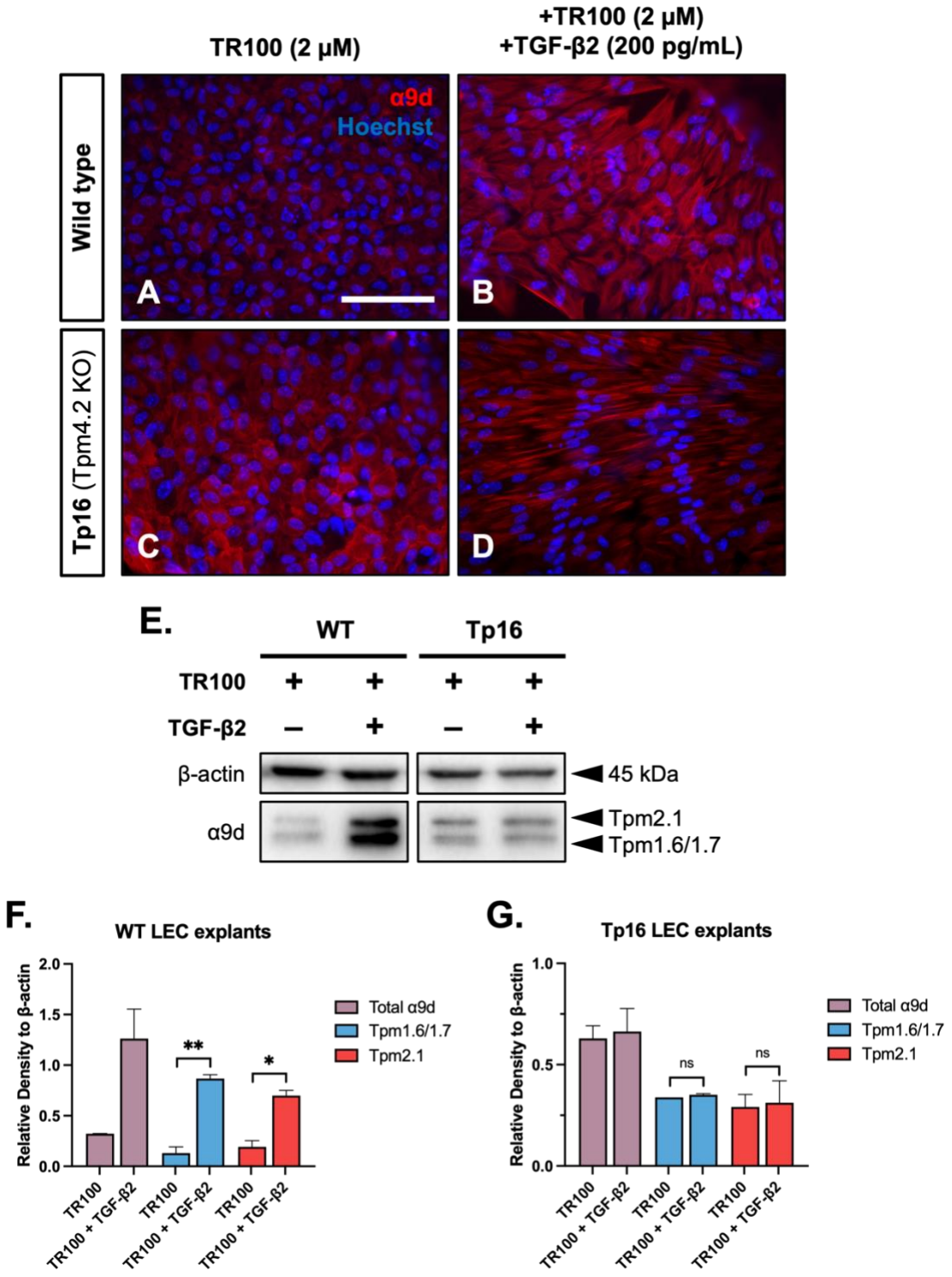

Figure 4.11. Inhibition of Tpm3.1/3.2 does not cause Tpm1 compensation in TGF-β2-induced WT and Tpm4.2 KO mice LEC explants. Representative immunolabelling for α9d (red) in wild type (WT; A, B) and Tpm4.2 KO (Tp16; C, D) mice lens explants and nuclear stained with Hoechst (blue) at 72 hours of culture. Explants exposed to 1-hour pre-treatment of TR100 (2 µM) in the presence or absence of TGF-β2 (200 pg/mL). Scale bar: 100 µm. Representative western blots from WT and Tp16 LEC explants at 72 hours probed for α9d (E). Membranes probed for α9d labelled for two bands, Tpm2.1 and Tpm1.6/1.7. Total sum of α9d intensity, Tpm2.1 band alone, and Tpm1.6/1.7 band alone was quantified using densitometry relative to β-actin (F, G). Unpaired, parametric two-tailed t-test with $P < 0.05$ considered statistically significant (ns = not significant, * $P < 0.0332$, ** $P < 0.0021$).

4.4.6 Inhibition of Tpm3.1/3.2 partially inhibits TGF-β2-induced EMT in the rat LEC explant model

We previously pharmacologically inhibited Tpm3.1/3.2 in WT and Tp16 mice LEC explants (see Figures 4.8–4.11) and demonstrated that Tpm3.1/3.2 and/or Tpm4.2 are not required for TGF-β2-induced lens EMT. In this section, we investigated whether this result was consistent with the rat LEC explant model.

4.4.6.1 ATM-5307 and/or TR100 impact on TGF-β2-induced rat lens EMT

TGF-β2 induces the transdifferentiation of epithelial cells into myofibroblastic cells through an EMT (Figure 4.12 A–C), with eventual loss of cells via apoptosis evident by day 5 of culture. The addition of Tpm3.1/3.2 inhibitor compound ATM-3507 (1 μM) alone (Figure 4.12 D–F) or TR100 alone (Figure 4.12 G–I) to rat lens explant cultures did not alter the LEC epithelial phenotype, with an abundant number of tightly packed cells evident by day 5. Rat lens explants exposed to ATM-3507 1-hour prior to TGF-β2 did not alter LEC morphology by day 1 of culture (Figure 4.12 J). An EMT response was noted at day 3 in TGF-β2-induced rat lens explants, with elongating cells and cellular blebbing/refractile bodies, indicative of apoptosis (Figure 4.12 K). A rapid loss in cells and capsule modulation as wrinkling was observed at day 5 in ATM-3507/TGF-β2-treated rat LEC explants (Figure 4.12 L). Similar to ATM-3507/TGF-β2-treated rat lens explants at day 1, TR100/TGF-β2-treated lens explants did not display any noticeable morphological change in LECs (Figure 4.12 M). After 3 days culture, a loss of the uniform epithelial cell structure was noted, with evidence of capsular wrinkling in TR100/TGF-β2-treated rat lens explants (Figure 4.12 N). By day 5, lens cells in TR100/TGF-β2-treated rat explants underwent a pronounced EMT response, with patches of cells across the explant, with evident cell loss and wrinkling in the surrounding exposed bare capsule regions (Figure 4.12 O). Immunofluorescence at day 3 of culture revealed strong membrane localisation for β-catenin in LECs of rat lens explants exposed only to ATM-3507 and TR100 (Figure 4.13 A, C), as well as low to no labelling for α-SMA. Addition of TGF-β2 in rat lens explants pre-treated with ATM-3507 had strong immunoreactivity for α-SMA as well as β-catenin (Figure 4.13 B). Lens cells of rat explants exposed to TR100 and subsequently TGF-β2 demonstrated reduced levels of α-SMA cytoplasmic localisation, as well as maintained strong β-catenin membrane localisation (Figure 4.13 D), compared to TGF-β2-treated lens explants.

For western blotting, given it has previously been shown to impact α-SMA localisation and F-actin stress fibre assembly in imLECs at doses < 5 μM (Parreno et al., 2020), we chose to

focus on TR100 pre-treatment of explants. At 72 hours of culture, non-treated and TR100-treated rat lens explants presented comparable, relatively low α-SMA protein levels ($p = 0.1801$, Figure 4.13 E–F). Treatment with TGF-β2 significantly elevated α-SMA protein levels in comparison to control ($p = 0.0238$) and TR100-treated rat lens explants ($p = 0.0014$). Pre-treatment with TR100 before TGF-β2 exposure significantly reduced α-SMA protein levels in comparison to TGF-β2-treated rat lens epithelial explants ($p = 0.0164$, Figure 4.13 E–F). TGF-β2-treated explants also demonstrated a significant decrease in β-catenin protein levels compared to control rat LEC explants ($p = 0.0044$). Rat LEC explants treated with both TR100 and TGF-β2 reduced β-catenin intensity compared to control rat lens explants ($p = 0.0242$).

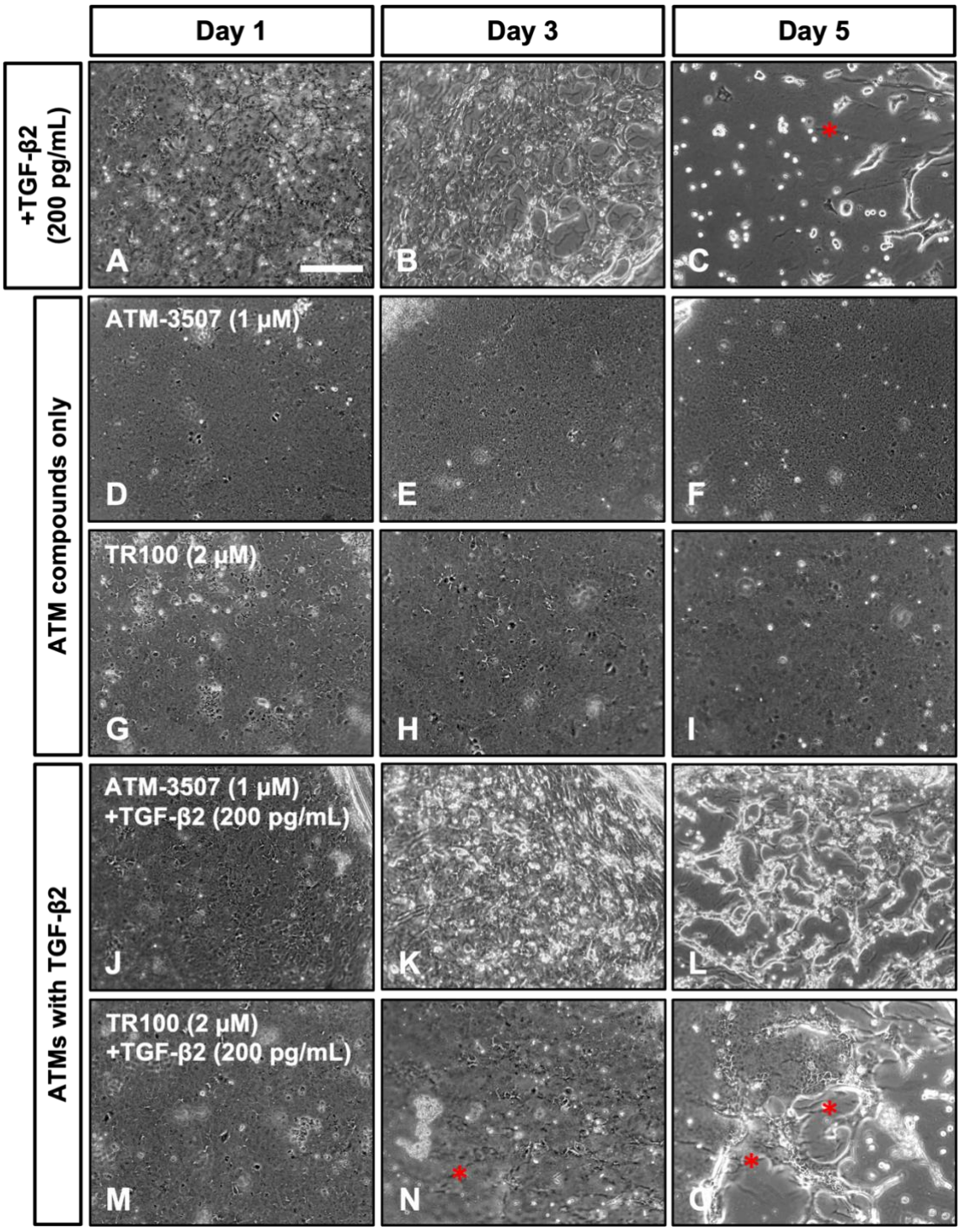

Figure 4.12. Pharmacologically targeting Tpm3.1/3.2 partially inhibits TGF-β2-induced EMT in rat LEC explants. Phase contrast images depicting rat LEC explants exposed to TGF-β2 (200 pg/mL) underwent EMT, with cell loss evident by day 5 (A–C). No morphological changes observed in explants exposed to Tpm3.1/3.2 specific inhibitors; ATM-3507 only (D–F) or TR100 only (G–I). Explants exposed to ATM-3507 1-hour prior to TGF-β2 did not inhibit EMT, with transdifferentiation from epithelial to myofibroblastic cells at day 3 (K), and rapid cell loss and apoptosis by day 5 (L).TR100 pre-treated TGF-β2-induced explants retained lens cells by day 3, although capsular wrinkling was evident (N, red asterisks). A partial EMT response was seen at day 5, with exposed capsule regions, wrinkling, and some patches of cells remaining (O). Day 1 of culture for ATMs/TGF-β2-induced explants did not show any morphological changes to the LEC phenotype (J, M). Scale: 200 μm.

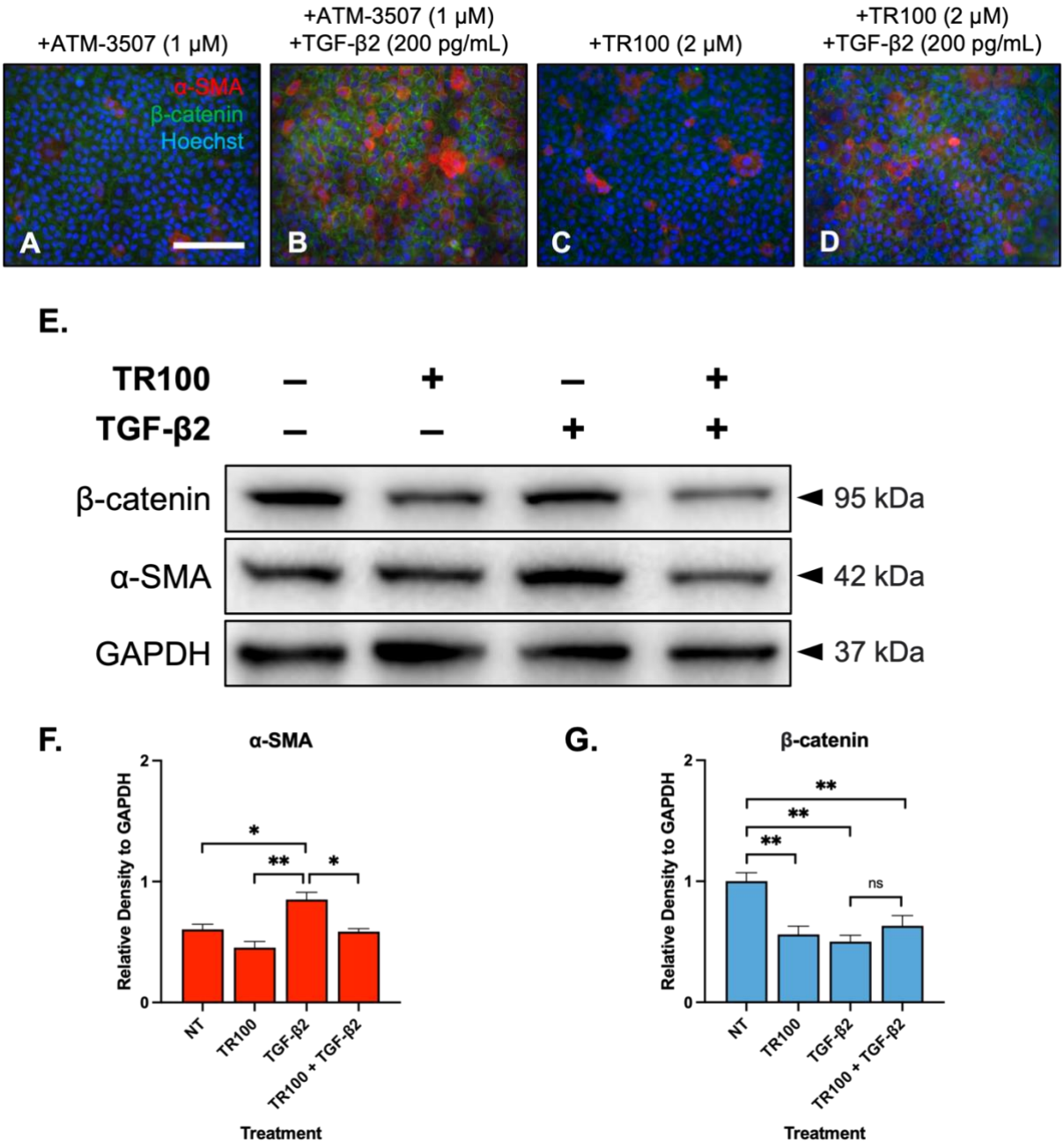

Figure 4.13. Pharmacologically targeting Tpm3.1/3.2 reduces α-SMA stress fibre association and protein expression in TGF-β2-induced rat LEC explants. At 72 hours of culture, ATM-3507 (1 μM) only (A), ATM-3507/TGF-β2 (200 pg/mL) (B), TR100 (2 μM) only (C), and TR100/TGF-β2 treated rat lens epithelial explants (D), were immunolabelled for α-SMA (red) and β-catenin (green), with nuclear visualisation using Hoechst dye (blue). Explants exposed to ATMs were pretreated for 1-hour prior to addition of TGF-β2. Western blot of rat lens epithelial explants from several treatment groups; control (non-treated, NT), TR100 (2 μM) only, TGF-β2 (200 pg/mL), and TR100/TGF-β2 (E), probed for α-SMA and β-catenin at 72 hours (E). Protein expression for α-SMA (F) and β-catenin (G) was compared relative to loading control GAPDH. One-way analysis of variance (ANOVA) with post-hoc Tukey's multiple comparisons test with the mean ± SEM (ns = not significant, * $P < 0.0332$, ** $P < 0.0021$).

4.5 DISCUSSION

In the present study, we focused on six cytoskeletal stress-fibre associated isoforms, Tpm1.6, Tpm1.7, Tpm2.1, Tpm3.1, Tpm3.2, and Tpm4.2, given that they are expressed in cells undergoing motility, morphogenesis, and transformation (Bakin et al., 2004; Kubo et al., 2013, 2017; Gunning et al., 2015; Shibata et al., 2018; Jansen and Goode, 2019; T. Shibata et al., 2021). This study specifically aimed to further characterise the stress-fibre associated Tpm isoforms in the lens and establish their role in TGF-β2-induced EMT, leading to lens pathology.

4.5.1 Tpm3.1/3.2 is expressed in WT and Tpm4.2 deficient mice lens tissue

In the current literature, there is some discrepancy regarding Tpm3.1 expression in the eye lens. The current study confirmed the absence of Tpm3.1/3.2 in Tp7 mice, as well as Tpm4.2 in Tp16 mice, using immunolabelling with Tpm isoform-specific antibodies. A study by Cheng et al. (2018) also showed deficiency of Tpm3.1 from brain and whole lens samples of the same Tpm3/Δexon9d$^{-/-}$ mouse line. Despite this, using a polyclonal antibody designed to target Tpm3.1, they found no Tpm3.1 in the positive control, WT (Tpm3/Δexon9d$^{+/+}$), or Tpm3/Δexon9d$^{-/-}$ 6-week-old whole lens protein samples (Cheng et al., 2018). More recent studies by Parreno et al. (2020) using an anti-Tpm5 monoclonal antibody; an antibody from the same clone used in the present study (γ9d; clone 2G10.2), they concluded that Tpm3.1 is indeed expressed only in imLECs, both in non-treated and TGF-β2-treated (5 ng/mL) LECs, as well as the native lens epithelium, but it was not detected in lens fibre cells. The use of imLECs in these studies, in contrast to our LEC explants, provides its own limitations in modelling lens EMT, since we can readily observe cell-cell and basement membrane adhesion, as well as lens capsule modulation (wrinkling) resulting from transdifferentiated myofibroblasts, as seen *in situ*. Despite the disparity between studies and models, we also confirmed that both Tpm3.1/3.2 and Tpm4.2 are present in the LECs of Wistar rats and WT mice. Immunolabelling for Tpm4.2 demonstrated no localisation in LEC explants (control and/or TGF-β2-treated) from Tpm4.2-deficient mice, since this antibody is specific for this *Tpm4* gene derived isoform. When we isolated the lens fibre cell masses (LFs) of WT, Tp7, and Tp16 mice to examine for Tpm3.1/3.2 and Tpm4.2, protein levels were found at the 20–25 kDa region using SDS-PAGE. Since this is not the expected Tpm isoform molecular weights of > 30 kDa, we believe we detected crystallin chaperone proteins that are highly abundant in lens fibres (Mousa and Trevithick, 1979), known to recruit Tpm for LFC structural integrity (Woo and Fowler, 1994). A recent study by Giannone et al. (2023) using single cell RNA-Seq from P2 WT (C57BL/6) mice lenses found β- and γ-

crystallin gene expression was elevated in a LEC cluster of "late differentiation" genes, a cluster of genes commonly upregulated during fibre cell differentiation (Peek et al., 1992). By probing for β-crystallin in WT LFs, we confirmed that we were, in fact, detecting crystallins at 20–25 kDa. Therefore, for future studies, a higher selective mechanism of Tpm protein extraction from our lens fibre samples is required.

4.5.2 The absence of Tpm3.1/3.2 and/or Tpm4.2 does not impair TGF-β2-induced lens EMT

Previous studies have reported a block to TGF-β-induced lens EMT using whole lenses of Tpm3.1/3.2 KO mice, proposing that Tpm3.1/3.2 are required for lens EMT (Parreno et al., 2020). To validate this result, we considered to cross our transgenic line overexpressing TGF-β1 in the lens, with the Tpm3.1/3.2 KO mice. Ahead of this we used lens epithelial explants isolated from both Tpm3.1/3.2-deficient and Tpm4.2-deficient mice and exposed them to TGF-β1 to confirm the earlier studies. What we discovered is that in contradiction to what has previously been shown in TGF-β2-treated imLECs (Parreno et al., 2020), TGF-β2 was able to induce EMT in LEC explants deficient for either Tpm3.1/3.2 or Tpm4.2. Moreover, LEC explants of Tp16 mice underwent a more prominent TGF-β2-induced EMT response compared to that of LEC explants of Tp7 mice, suggestive that the absence of Tpm3.1/3.2 may indeed impact EMT to some degree, at least more so than the loss of Tpm4.2. We set out to confirm whether Tpm3.1/3.2 or Tpm4.2 deficiency impacted α-SMA recruitment and stress fibre localisation during TGF-β-induced EMT. In the current study, immunolabelling assays revealed cytoplasmic localisation and low protein levels of α-SMA in untreated LEC explants across all three mice lines (Figure 4.14). After 72 hours of TGF-β2 treatment, LEC explants from WT and Tpm-deficient mice demonstrated recruitment of α-SMA into stress fibres of myofibroblastic cells. This elevation has been confirmed in other lens models showing α-SMA as a hallmark feature of TGF-β-induced EMT (Lovicu et al., 2004; Boswell et al., 2017; Jiang et al., 2018).

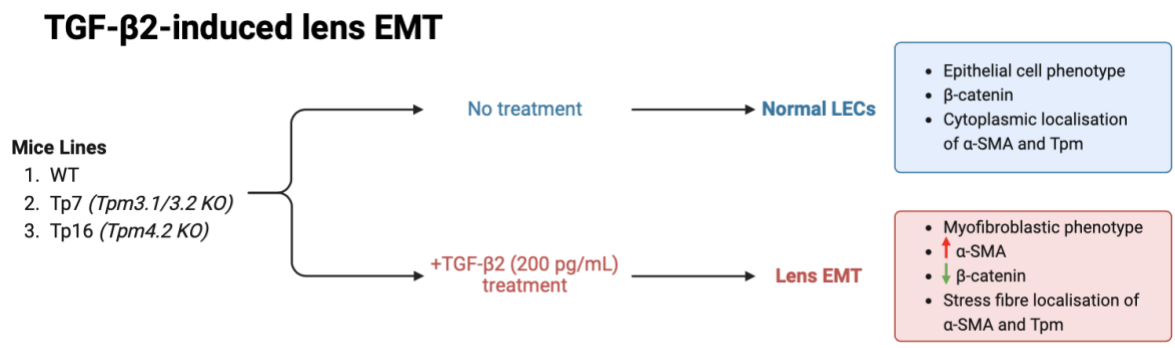

Figure 4.14. Summary of TGF-β2-induced lens EMT. Wild type (WT), Tp7 (Tpm3.1/3.2 KO), and Tp16 (Tpm4.2 KO) mice lens epithelial cell (LEC) explants treated with TGF-β2 (200 pg/mL) undergo an EMT response, regardless of Tpm deficiency. Addition of TGF-β2 induced cell phenotype changes, a reduction in β-catenin levels, as well as accumulation of α-SMA and Tpm into stress fibres of newly transitioned myofibroblastic cells. Non-treated LEC explants from all mice lines maintained the normal lens epithelial cell phenotype and cell-cell adhesion markers. Schematic diagram created using *Biorender.com*.

The current study showed that despite the absence of either Tpm3.1/3.2 or Tpm4.2, TGF-β2 treatment can still alter the spatial distribution and not the levels of β-catenin in lens cells, when comparing untreated *vs*. TGF-β2-treated lens epithelial explants isolated from all mice lines, particularly Tpm3.1/3.2 KO mice. Future studies could implement other junctional markers, such as E-cadherin or ZO-1, to confirm whether a deficiency for Tpm3.1/3.2 or Tpm4.2 mediates the structural integrity of cell-cell adherens junctional proteins, as previously reported (Caldwell et al., 2014; Jeong et al., 2014; Meiring et al., 2018).

Previous studies have demonstrated that *Tpm3* and *Tpm4* genes are not regulated by TGF-β; however, *Tpm1* and *Tpm2* are (Tada et al., 1997, 2000; Bakin et al., 2004; Zheng et al., 2008; Shibata et al., 2018; Bradbury et al., 2021). In human lung fibroblasts, no significant upregulation in Tpm3.1 expression was noted in the presence/absence of TGF-β1 (2 ng/mL) across a 48-hour culture period; however, TGF-β1 can induce and upregulate Tpm1.6/1.7 and Tpm2.1 expression, compared to non-treated fibroblasts, with significant upregulation noted at 48 hours (Bradbury et al., 2021), as previously noted in other carcinoma models (Bakin et al., 2004). Although these models vary from the current LEC explant model, as well as whole native lens or imLEC models (Parreno et al., 2020), it can be suggested that given Tpm3.1 is present in LECs for both non-treated and TGF-β-treated conditions, it is not required for EMT initiation during fibrotic or wound healing responses and may simply be a ubiquitous protein for the lens.

Although we could not establish a direct role for Tpm4.2 in our lens EMT model, other fibrosis models have investigated Tpm4 with regards to its modulation of the EMT-associated phenotype, particularly during tumour development, examining cell invasiveness, proliferation,

motility, and migration. A study by Zhao et al. (2019) showed that Tpm4 is required for cell motility biomechanics and cytoskeletal organisation during lung cancer. Using CRISPR/CAS9 Tpm4 knockout lung cancer cell lines, this study showed a reduction in cell migration as well as mesenchymal associated transcription factors (*ZEB1*, *Snail*), with disrupted organisation of actin filaments (Zhao et al., 2019). In the same study, overexpression of Tpm4 in lung cell lines increased cell invasiveness and cytoskeleton reorganisation (Zhao et al., 2019). From these studies, it can be proposed that Tpm4 may be required specifically in some cell types for phenotypic changes resulting from actin remodelling, during fibrosis and carcinoma development. A recent study also assessed scRNA-Seq and transcriptome expression analysis from publicly accessible datasets of glioma patients correlating *Tpm4* with elevated EMT biomarkers, such as vimentin, N-cadherin, and TWIST1 (Wang et al., 2022). A study by Curthoys et al. (2014) showed that overexpression of Tpm4.2 in undifferentiated rat B35 neuroblastoma cells promoted formation of filopodia and increased neurite branching. In addition, fascin, an actin-binding protein that is often recruited to sites forming filopodia and/or lamellipodia (Small et al., 1998; Cohan et al., 2001; Tanaka et al., 2019) was shown to be elevated when Tpm4.2 was overexpressed (Curthoys et al., 2014; Stefen et al., 2018). Given the findings from this study, in the absence of Tpm4.2, there may not be any formation of actin protrusions, such as filopodia and lamellipodia. Future assays could confirm this role for Tpm4.2 in cytoskeletal reorganisation during EMT by examining for other actin filament proteins or peptides, such as F-actin and phalloidin. Wound healing or scratch assays could also be used in Tpm4.2 KO mice lens epithelial explants to further explore its role in cell motility and migration during stress and/or injury responses. Therefore, there are still some discrepancies regarding Tpm4.2 activity in EMT, particularly the subtypes of EMT; Type 2 (wound healing/fibrosis) and Type 3 (carcinoma and metastasis) (Kalluri and Weinberg, 2009; Yang et al., 2020), demonstrating that this marker has tissue-specific roles that will need to be further characterised in lens fibrosis.

4.5.3 Loss of Tpm3.1/3.2 or Tpm4.2 does not lead to Tpm1 isoform compensation

Since Tpm3.1/3.2- and Tpm4.2-deficient mice lens explants underwent an EMT in response to TGF-β2, we investigated whether alternative Tpm-isoforms were being recruited and/or compensating during this process. We looked at Tpm3.1/3.2 in LECs derived from lens explants of WT, Tp7, and Tp16 mice in the presence/absence of TGF-β2. We showed that Tpm4.2-deficient mice lens explants in the presence of TGF-β2 demonstrated the same elevated

labelling of Tpm3.1/3.2 as seen in lens explants acquired from WT mice. We did observe low levels for Tpm3.1/3.2 in TGF-β2-treated LEC explants from Tp7 mice that may be due to previously reported cross reactivity of γ9d for Tpm1.6–1.9 and Tpm2.1 (Schevzov et al., 2011). Localisation of Tpm4.2 was consistent across control and TGF-β2-treated lens explants of WT and Tp7 mice. To support this, a study by Cheng et al. (2018) confirmed the expression of Tpm1.7–1.9 and Tpm4.2 in lenses from Tpm3/Δexon9d$^{-/-}$ mice. Protein levels for either isoform were not upregulated or compensated under Tpm3.1/3.2-deficent conditions. Previous studies have suggested a potential compensation mechanism for alternative Tpms in the event of an inhibited or targeted Tpm isoform (Cheng et al., 2018), such as Tpm1.9 upregulation in red blood cells (RBCs) of Tpm3.1 KO mice; the only two isoforms that comprise the membrane skeleton of RBCs (Fowler and Bennett, 1984; Sui et al., 2017). Given this dual dependency for both Tpm1.9 and Tpm3.1, the absence of Tpm3.1 caused compensation by Tpm1.9 to regulate Tpm levels in RBCs (Sui et al., 2017).

In our EMT model, Tpm1.4, Tpm1.6–1.9, and Tpm2.1 immunolabelling (see Table 4.1) demonstrated no significant changes in control LECs derived from Tp7 and Tp16 mice lens explants, compared to control WT LECs, with all lens cells exhibiting cytoplasmic localisation for α9d. Elevation of Tpm1.6/1.7 and Tpm2.1, as well as stress-fibre α9d localisation, was constant across all lines when lens explants were treated with TGF-β2.

Due to the sensitivity of acquiring LEC explants, it could be argued by some that the current model is inducing stress in these lens cells, leading to aberrant expression and function of Tpm isoforms. Compared to other lens cell models, such as imLECs (Parreno et al., 2020) and whole native lenses (Cheng et al., 2018) that examined Tpm isoform expression, our model appears to be slightly different. Although we remove the lens epithelia from their homeostatic environment, we allow the LECs to settle, recover, and acclimate to these new conditions for 24 hours before any treatment with growth factors/cytokines. Our model can also be regarded as more physiologically relevant given our primary lens cells remain attached to their native basement membrane, the lens capsule. Moreover, our cells respond to a much lower and more physiological dose of exogenous TGF-β2 (200 pg/mL), and we have previously shown that EMT can also be induced at even lower doses to this (50 pg/mL) (Shin et al., 2012; Shu and Lovicu, 2019; Flokis and Lovicu, 2023) compared to the Parreno et al. (2020) study (5 ng/mL), that is still higher than the *in situ* amounts of TGF-β2 in aqueous humour of cataractous patients (~2,000 pg/mL) (Yamamoto et al., 2005; Yan et al., 2022).

To confirm whether there is any Tpm isoform compensation in either Tpm3.1/3.2- or Tpm4.2-deficient conditions, as well as TGF-β2-induced conditions, future studies could utilise transcriptomics to observe for any differences in Tpm isoform expression during EMT in these mutant mice. It would be more effective to conduct transcriptome data analysis rather than RT-PCR due to the amount of splice variants from all four Tpm mammalian genes (> 40) (Pittenger et al., 1994; Cooley and Bergtrom, 2001). We do not believe that any compensatory mechanism was occurring in the Tpm-deficient mice LEC models. However, additional screening for gene splice variants in these KO tissues may be required, as proposed by Cheng et al. (2018), to assess potential compensatory mechanisms for Tpm isoforms. It is clear from this study that there is no individual Tpm isoform required for TGF-β-induced lens EMT; with more of a collaborative effort from several Tpm isoforms to carry out differential cell remodelling mechanisms.

4.5.4 Pharmacological inhibition of Tpm3.1/3.2 in lens epithelial explants differentially mediates TGF-β2-induced lens EMT

We used two anti-tropomyosin compounds (ATMs), ATM-3507 and TR100, shown previously to target Tpm3.1/3.2 (Stehn et al., 2013; Bonello et al., 2016; Parreno et al., 2020) to pharmacologically inhibit Tpm3.1/3.2 in TGF-β2-induced LEC explants of rat, WT mice, and Tpm4.2-deficient mice. We tested both inhibitors at doses < 5 μM, given doses >3–5 μM exhibited cytotoxic and/or cell detachment effects on cells in other models, including neuroblastoma, melanocytes, melanoma cell lines (Stehn et al., 2013), and imLECs (Parreno et al., 2020). Given that disruption/deletion of specific cytoskeletal Tpm isoforms alters actin filament formation (Tojkander et al., 2011; Manstein et al., 2020), we expected the pharmacological targeting of Tpm3.1/3.2 to impact EMT induction in LEC explants isolated from Tp16 mice. In lens epithelial explants of WT and Tp16 mice, TR100 or ATM-3507 treatment alone did not alter the normal LEC cobblestone-like morphology or associated marker expression across a 5-day culture period; however, lens explants of WT and Tp16 mice pre-treated with ATMs before TGF-β2 exposure, underwent a characteristic EMT response, with dispersed β-catenin localisation and acquisition of stress-fibre marker α-SMA, increased capsular wrinkling, cell transdifferentiation, and eventual cell apoptosis.

By treating Tpm4.2-deficient (Tp16) mice lens cells with ATMs selective for Tpm3.1/3.2, we essentially established a double knockdown of this protein activity, to examine their combined role in TGF-β2-induced lens EMT. ATM/TGF-β2 treated LEC explants of Tp16 mice

prevented complete cell death, as transdifferentiated myofibroblastic cells were maintained over 5 days of culture, compared to the almost complete loss of cells in lens explants derived from WT mice exposed to the same treatment. The loss of Tpm3.1/3.2 and Tpm4.2 in LEC explants of Tp16 mice could potentially be decreasing cell motility mechanisms commonly associated with LMW Tpms in invasive carcinoma and metastatic tumour progression (Miyado et al., 1996; Hook et al., 2004; Zheng et al., 2008; Stehn et al., 2013; Schevzov et al., 2015; Yu et al., 2017; Chen et al., 2021). In some carcinoma models, it was reported that Tpm3.1/3.2 or Tpm4.2 deficiency promoted cell apoptosis, and associated genes including *tgfb1* (Luo et al., 2021; Zhang et al., 2022), as well as cell migratory Rac1-signalling (Jeong et al., 2014). For example, silencing *Tpm3* model (siTpm3) in hepatocellular carcinoma cells (HCCs) reduced cell migration and invasive properties, promoting E-cadherin expression while reducing EMT markers, including Snai1, vimentin, and fibronectin (Choi et al., 2010). Another study with high-grade glioma cells showed that knockdown of *Tpm3* also decreased *Snai1* expression, cell invasiveness, migration, and wound healing responses (Tao et al., 2014). Given that the loss or suppression of *Tpm3* in these models is not resulting in the death of these carcinoma cells, as for our model, there are likely alternative Tpm isoforms, as well as other molecules, that are present and are preventing or retarding apoptosis.

Targeted inhibition of Tpm3.1/3.2 differentially regulated *Tpm1* and *Tpm2* derived isoform levels and localisation in LEC explants of WT and Tp16 mice. A study by Parreno et al. (2020) showed a reduction in α-SMA at 2 days of culture in TR100/TGF-β2-treated imLECs and WT mice lenses; however, in our mouse model, TGF-β2-treated lens explants of WT and Tp16 mice did not have reduced α-SMA protein levels in the presence of TR100. In addition, we observed significant elevation of Tpm1.6/1.7 and Tpm2.1 protein levels in TR100/TGF-β2-treated lens explants of WT mice, compared to TR100 only treated lens explants of WT mice. Based on our morphological assays, we did not see an inhibition of EMT and, as a result, inhibition of Tpm3.1/3.2 did not block EMT marker expression in WT mice. Despite this, TR100/TGF-β2-treated lens explants of Tpm4.2-deficient mice showed no significant changes in protein levels for Tpm1.6/1.7 and Tpm2.1, in comparison to TR100 only lens explant lysates of Tp16 mice. Given the previously reported elevation of Tpm1.6/1.7 and Tpm2.1 during induced lens EMT (Kubo et al., 2013, 2017, 2018), as well as what we have reported in this study (see Chapter 3 and Chapter 4: Figures 4.6–4.7), we did not expect *Tpm1* and *Tpm2* to be elevated in absence of Tpm3.1/3.2 activity since lens cells from Tp16 mice are not differentiating or undergoing TGF-β2-induced EMT. We cannot explain why there was an observed difference between WT

and Tp16 mice in Tpm1.6/1.7 and Tpm2.1 protein levels when Tpm3.1/3.2 was pharmacologically inhibited.

We tested the effectiveness of ATMs on rat LEC explants, in particular the responsiveness of cells exposed to TGF-β2. All cells in explants exposed to either ATM compound, in conjunction with TGF-β2, underwent an EMT. Despite both inhibitors not being able to completely block EMT, the EMT response we observed slightly varied between Tpm3.1/3.2 inhibitor compounds. For example, ATM-3507/TGF-β2-treated lens explants demonstrated clear morphological changes at day 3, with cell transdifferentiation and apoptosis more prominent by day 5. In contrast, cells in rat lens explants exposed to TR100 and TGF-β2 retained their epithelial phenotype until day 3, with regions of lens epithelia still present by day 5. Despite this, most of these treated explants underwent some EMT, with cell loss and capsular wrinkling around patches of compact, cobblestone-like epithelial lens cells. This EMT was supported by cytoplasmic α-SMA localisation, and a significant reduction in α-SMA protein levels in TR100/TGF-β2 rat lens explants compared to TGF-β2-treated rat lens explants. This suggests that TR100 may be preventing α-SMA recruitment into actin stress fibres when LECs are treated with TGF-β2.

Overall, the ATM compounds do not demonstrate a clear and consistent block of the morphologic effects of EMT in both rat and mouse lens explant models; however, they may be influencing the expression of EMT markers and other related cytoskeletal proteins. Given that our study only tested a small range of Tpm isoforms, further testing is needed to confirm that there is no compensation by other Tpm isoforms, particularly Tpm1 and Tpm2, in Tpm3.1/3.2- or Tpm4.2-deficient conditions. Our data suggests that there may be potential differences in rodent model sensitivity in response to the specific molecular components of both ATM compounds. Based on the reported linear shape of ATM-3507 and biomechanical functions during Tpm3.1/3.2 actin co-polymerisation (Currier et al., 2017; Janco et al., 2019), this compound may have a higher binding affinity and specificity to Tpm3.1/3.2 compared to TR100. It can be concluded that based on cell phenotype, both mice (WT, Tp16) and rat LEC explant models demonstrated that inhibition of Tpm3.1/3.2 did not impede the TGF-β induction of lens EMT, consistent with our Tp7 data.

4.5.5 Tpm1.6/1.7 and Tpm2.1: Potential markers for TGF-β induced lens EMT

Based on the current study, and the results from the previous chapter, Tpm1.6/1.7 and Tpm2.1 appear to play a role in the induction of EMT in TGF-β2 treated LEC explants. Future studies

using both mouse and rat LEC explant models could look at inhibitor compounds specifically targeting the activity and levels of Tpm1.6/1.7 and/or Tpm2.1. *Tpm1* and *Tpm2* derived isoforms have already been studied for their role in wound healing responses, particularly in lens following injury and cataractogenesis (Kubo et al., 2013, 2017, 2018; Shibata et al., 2018).

Tpm1.6/1.7 and Tpm2.1 have been linked to facilitating contractile properties in migratory/transitioning cells in the lens during EMT (Kubo et al., 2013, 2017, 2018) and in other systems such as human lung fibroblasts (Bradbury et al., 2021). In their absence, this transition from epithelial-myofibroblastic cells can be impeded (Hardeman et al., 2019). In a human lung fibroblast model, significant upregulation of Tpm1.6/1.7 and Tpm2.1 was noted after 48 hours of TGF-β1 treatment (2 ng/mL) compared to control fibroblasts (Bradbury et al., 2021). Induction of oxidative stress using H_2O_2 (250 μM) in human umbilical vein endothelial cells (HUVECs) promoted Tpm1 phosphorylation and F-actin stress-fibre localisation (Houle et al., 2003), further confirming the involvement of Tpm1 in stress-induced conditions. A study by Prunotto et al. (2015) demonstrated a significant reduction in α-SMA levels and stress fibre incorporation, in TGF-β1 treated human subcutaneous fibroblasts deficient for Tpm1.6/1.7. Interestingly, fibroblasts deficient for Tpm2.1 showed minimal requirement for this Tpm for α-SMA stress fibre assembly when stimulated by TGF-β1 (Prunotto et al., 2015), highlighting the specific dependency of α-SMA on Tpm1.6/1.7 for TGF-β-induced contractile stress-fibre assembly. Silencing of Tpm4.2 in untransformed breast epithelial cells (MCF10A) increased E-cadherin and β-catenin protein levels and their cell-cell adhesion localisation (Jeong et al., 2014). In addition, MCF10As silenced for Tpm4 and Tpm4.2 (using siRNA) did not alter Tpm1 or Tpm2 expression (Jeong et al., 2014), demonstrating no direct relation of Tpm4.2 levels on the expression of *Tpm1* and/or *Tpm2*.

Apart from being potential markers for TGF-β-induced fibrosis, particularly myofibroblastic formation during lens EMT, *Tpm1* and *Tpm2* derived isoforms have also been used as potential biomarkers in diagnosing and categorising the subtypes of cancer-associated fibroblasts (CAFs); myofibroblastic (high α-SMA expression) and inflammatory (low α-SMA expression), in tumour microenvironments (Zare et al., 2018; Elyada et al., 2019; Humayun-Zakaria et al., 2019; Takenawa et al., 2023). A study by Elyada et al. (2019) showed upregulation of *TPM1* specifically in myofibroblastic CAFs of contractile human pancreatic ductal adenocarcinoma (PDAC), in association with elevated *Smad2*, *ACTA2* (α-SMA), and *TGF-β1* genes. In addition, *Tpm1* has been classified as a tumour suppressor based on its role in reducing cell motility by stabilising actin stress fibres in tumour cells as previously reviewed

(Humayun-Zakaria et al., 2019; Geng et al., 2021; Meng et al., 2023). HMW Tpms (*Tpm1* and *Tpm2*) have not been shown to be involved in cell invasiveness or malignancy and are less expressed in carcinoma models (*in vitro* and *in vivo*) than LMW Tpms (*Tpm3* and *Tpm4*) (Franzén et al., 1996). For example, in human oral squamous carcinoma cells (OSCCs), depletion of *Tpm1* increased cell growth, proliferation, migration, and wound healing responses (Takenawa et al., 2023). In tissue acquired from squamous cell carcinoma of oesophageal cancer (SCCE) patients, Tpm1.6/1.7 levels were reported to be decreased, with higher levels in adjacent normal oesophageal tissue (Zare et al., 2018). A decrease in *Tpm1* mRNA correlated with poorly differentiated tumours of SCCE patient tissue (Zare et al., 2018). From these studies, it appears that the role of *Tpm1*-derived isoforms in carcinoma, may be dependent on the stage of cancer progression, and tumour types (benign or malignant), as well as the heterogenous cell phenotypes that exist within and around the tumour microenvironment. Given the reported role and upregulation of *Tpm1* specifically during fibrosis and in carcinoma (myofibroblastic CAFs) models, to better assess its role in lens fibrosis and determine whether *Tpm1*-derived isoforms are essential for ASC development, our future studies plan to cross mice overexpressing TGF-β1 with a lens with a *Tpm1* deficient line. T. Shibata et al. (2021) showed that a deficiency for *Tpm1* in lens resulted in age-related opacification and disruption to normal lens fibre differentiation. We would expect to see an earlier amelioration or prevention of ASC in our transgenic lines if *Tpm1* was directly involved.

HMW cytoskeletal Tpms have been linked to activation of Smad-dependent and Smad-independent TGF-β signalling during stress fibre formation (Shields et al., 2002; Bakin et al., 2004; Varga et al., 2005; Zheng et al., 2008; Safina et al., 2009). A study by Safina et al. (2009) using a mouse mammary epithelial (NMuMG) cell line transfected with oncogenic RASV12 showed that Ras-signalling is involved in mitigating TGF-β induced cytoskeletal reorganisation, stress fibre assembly, and the expression of Tpm1. These NMuMG-RASV12 cells had elevated ERK phosphorylation and Raf expression while reducing Tpm1 protein levels after 24 hours of TGF-β1 treatment; however, inhibition of p-ERK using U0126 upregulated Tpm1 in these same cells (Safina et al., 2009). Given the results from this study, it appears that Ras-Raf-ERK signalling is associated with morphological and cytoskeletal Tpm1 changes in TGF-β-induced conditions. A study by Shields et al. (2002) confirmed that downstream MAPK signalling cascades are required for *Tm1* (Tpm2.1), *Tm2* (Tpm1.6), and *Tm3* (Tpm1.7) expression associated with cell transformations in rat intestinal epithelial (RIE-1) cells. Pharmacological targeting of p38 MAPK using SB203580 in Raf-1 (a Ras effector protein) and

K-Ras4B-transfected RIE-1 cells reduced Tm1, Tm2, and Tm3 expression, suggesting Ras acts as a mediator of both p38 MAPK and Raf-MAPK induced Tpm expression (Shields et al., 2002). However, this SB203580 inhibitor compound has shown to have putative off target effects (Lali et al., 2000; Menon et al., 2015). Future studies in the current model could conduct proteomics in Tpm-deficient mice or pharmacologically targeted Tpm isoform models, to elucidate the role of TGF-β dependent and independent signalling on Tpm actin filament association and cell transformations during lens EMT.

4.6 CONCLUSION

Tpm isoforms are present in the normal lens and are upregulated in the presence of TGF-β2 in an isoform-specific manner. The absence of Tpm3.1/3.2 or Tpm4.2 did not prevent TGF-β2-induced EMT in lens epithelial explants. In Tp16 (Tpm4.2 deficient) lens epithelial explants, EMT still occurred when Tpm3.1/3.2 was also pharmacologically targeted. Therefore, while Tpm3.1/3.2 and/or Tpm4.2 are both present in lens epithelial cells, they do not appear to be required for TGF-β2-induced lens EMT. Given the significant upregulation of *Tpm1*-derived isoforms during TGF-β2-induced lens EMT, future studies targeting Tpm1.6/1.7 may prove more effective at regulating lens EMT. This current study highlights the need to better characterise the specific role of different stress-fibre associated Tpm isoforms in regulating lens fibrosis or cataractogenesis.

CHAPTER 5: FGF-2 DIFFERENTIALLY REGULATES LENS EPITHELIAL CELL BEHAVIOUR DURING TGF-β-INDUCED EMT

5.1 PREFACE

It is well established that TGF-β is a key inducer of lens EMT. Recent studies have shown TGF-β-induced EMT, leading to cataract, can be modulated by other growth factors and their receptors found within the ocular media surrounding the lens, particularly FGF (Cerra et al., 2003; Mansfield et al., 2004) and EGFR (Shu et al., 2019b; Shu and Lovicu, 2019). Secondary cataract, or PCO, is classified into two sub-types based on key phenotypical cell changes: fibrotic PCO and pearl-like PCO, as previously reviewed (Apple et al., 1992; Wormstone et al., 2020). Fibrotic PCO pertains to central cells of the anterior epithelium that are retained at cataract surgery that migrate to the posterior capsule undergoing an EMT into myofibroblastic cells, as a result of TGF-β stimulation (Apple et al., 1992; Wormstone et al., 2020). Pearl PCO results from peripheral cells undergoing a fibre differentiation response, that is believed to be the result of stimulation by regulatory growth factors, such as FGF (Meacock et al., 2000; Mansfield et al., 2004), that eventually forms either Soemmerring's ring or Elschnig's pearls (D'Antin et al., 2022). The present study aimed to characterise the responsiveness of rat lens epithelial cells in the presence of both FGF-2 and TGF-β2 using an *in vitro* lens epithelial cell explant model, to further understand their relevance to the aetiology of PCO.

This study was published in *Cells* in March 2023 (see Appendix). Included here in this chapter is the manuscript containing additional supplementary data not previously published. Author contributions are stated below:

Mary Flokis

- Designed and executed experiments as described
- Writing and assembling manuscript

Frank J. Lovicu

- Aided with concept and experimental design
- Assisted with editing and manuscript formatting

Reference: Flokis, M., Lovicu, F.J., 2023. FGF-2 Differentially Regulates Lens Epithelial Cell Behaviour during TGF-β-Induced EMT. Cells 12, 827. https://doi.org/10.3390/cells12060827

Title: FGF-2 differentially regulates lens epithelial cell behaviour during TGF-β-induced EMT

5.2 ABSTRACT

Fibroblast growth factor (FGF) and transforming growth factor-beta (TGF-β) can regulate and/or dysregulate lens epithelial cell (LEC) behaviour, including proliferation, fibre differentiation, and epithelial–mesenchymal transition (EMT). Earlier studies have investigated the crosstalk between FGF and TGF-β in dictating lens cell fate, that appears to be dose dependent. Here, we tested the hypothesis that a fibre-differentiating dose of FGF differentially regulates the behaviour of lens epithelial cells undergoing TGF-β-induced EMT. Postnatal 21-day-old rat lens epithelial explants were treated with a fibre-differentiating dose of FGF-2 (200 ng/mL) and/or TGF-β2 (50 pg/mL) over a 7-day culture period. We compared central LECs (CLECs) and peripheral LECs (PLECs) using immunolabelling for changes in markers for EMT (α-SMA), lens fibre differentiation (β-crystallin), epithelial cell adhesion (β-catenin), and the cytoskeleton (alpha-tropomyosin), as well as Smad2/3- and MAPK/ERK1/2-signalling. Lens epithelial explants cotreated with FGF-2 and TGF-β2 exhibited a differential response, with CLECs undergoing EMT while PLECs favoured more of a lens fibre differentiation response, compared to the TGF-β-only-treated explants where all cells in the explants underwent EMT. The CLECs cotreated with FGF and TGF-β immunolabelled for α-SMA, with minimal β-crystallin, whereas the PLECs demonstrated strong β-crystallin reactivity and little α-SMA. Interestingly, compared to the TGF-β-only-treated explants, α-SMA was significantly decreased in the CLECs cotreated with FGF/TGF-β. Smad-dependent and independent signalling was increased in the FGF-2/TGF-β2 co-treated CLECs, that had a heightened number of cells with nuclear localisation of Smad2/3 compared to the PLECs, that in contrast had more pronounced ERK1/2-signalling over Smad2/3 activation. The current study has confirmed that FGF-2 is influential in differentially regulating the behaviour of LECs during TGF-β-induced EMT, leading to a heterogenous cell population, typical of that observed in the development of post-surgical, posterior capsular opacification (PCO). This highlights the cooperative relationship between FGF and TGF-β leading to lens pathology, providing a different perspective when considering preventative measures for controlling PCO.

5.3 INTRODUCTION

The ocular lens is a transparent, avascular tissue responsible for transmitting light onto the retina. It contains two cell types: cuboidal epithelial cells and adjacent elongate fibre cells, both comprised of specialized molecular (e.g., crystallins) and cytoskeletal (e.g., intermediate filaments) properties to facilitate vision (Lovicu and McAvoy, 2005). Ocular growth factors, such as fibroblast growth factor (FGF) and transforming growth factor-beta (TGF-β), are key regulators of different cellular processes in the lens, including epithelial cell proliferation (Lovicu and McAvoy, 2001; Iyengar et al., 2007, 2009), fibre differentiation (Chamberlain and McAvoy, 1989, 1997; de Iongh et al., 1996; Lovicu and McAvoy, 2005; Zhao et al., 2008; West-Mays et al., 2009; Wang et al., 2017), and epithelial-mesenchymal transition (EMT) that leads to lens pathology (Wormstone et al., 2002, 2006; Cerra et al., 2003; Mansfield et al., 2004; de Iongh et al., 2005; Boswell et al., 2017; Kubo et al., 2017). *In situ*, FGF is thought to be required for regulating normal lens cell processes in a spatially dependent manner, as previously reviewed (Lovicu and McAvoy, 2005).

TGF-β can regulate and/or concurrently dysregulate normal lens homeostasis, cell growth, and survival, by altering lens epithelial cell (LEC) morphology (de Iongh et al., 2005; Xu et al., 2009; Lovicu et al., 2020). The dysregulation of lens epithelial cell architecture induced by TGF-β is characterised by EMT, a phenomenon that has been widely reviewed (Kalluri and Neilson, 2003; Martinez and de Iongh, 2010; Nieto et al., 2016), with normal cuboidal LECs transitioning to become aberrant migratory, contractile myofibroblastic cells. These myofibroblastic cells can aggregate to form a fibrotic plaque leading to cataracts (Marcantonio et al., 2003; Lovicu et al., 2004; Jiang et al., 2018). To date, cataracts, that have been extensively reviewed and studied, are still considered the most common form of blindness worldwide (Liu et al., 2017; Abdulhussein and Hussein, 2022), with the only form of treatment being surgical intervention. Despite the effectiveness of surgery, posterior capsular opacification (PCO), known also as a secondary cataract, may result post-surgery, requiring further intervention (Pandey et al., 2004; Karahan et al., 2014; Vasavada and Praveen, 2014). PCO results from the aberrant behaviour of LECs left after surgery, with these cells either undergoing EMT to form a posterior subcapsular plaque (fibrotic PCO) (Lovicu et al., 2004, 2015; Wormstone et al., 2006; Jiang et al., 2018), or differentiating into aberrant fibre cells leading to Elschnig's pearls and Soemmerring's ring (regenerative, pearl PCO) (D'Antin et al., 2022), as previously reviewed (Wormstone and Eldred, 2016; Wormstone et al., 2020). While these two different spatially distinct epithelial PCO pathologies are well characterised (Aslam et al., 2003; Lu et

al., 2019), the underlying molecular mechanisms regarding their formation are poorly understood.

Numerous models have established TGF-β-induced lens EMT responses in humans (Kubo et al., 2017), embryonic chicks (Boswell et al., 2010, 2017), and murine cell lines and explant models (Mansfield et al., 2004; Lovicu et al., 2015; Boswell et al., 2017; Jiang et al., 2018; Shu et al., 2019b). In dissociated embryonic chick lens epithelial cells treated with TGF-β, we see a heterogenous response, with some cells undergoing fibre differentiation, while others undergo EMT (Musil, 2012; Boswell et al., 2017). In *in vitro* studies using mammalian lens epithelia, exogenous treatment of LECs with TGF-β results in a homogenous EMT response (Liu et al., 1994; Lovicu et al., 2002; de Iongh et al., 2005; Shu et al., 2017). In situ, however, anterior subcapsular cataracts (ASCs) develop in transgenic mice in response to elevated activity of ocular TGF-β (Srinivasan et al., 1998); the subcapsular plaques are comprised a heterogenous population of aberrant lens fibre cells and myofibroblastic cells, similar to those seen in human cataracts (Lovicu et al., 2004). The *in situ* transgenic mouse model ideally replicates the human clinical pathology of fibrotic cataracts, that is attributed to the endogenous ocular milieu of different growth factors and cytokines, that do not act in isolation, unlike what we have *in vitro*. Since two disparate lens epithelial phenotypes contribute to ASC and PCO, it is important to better understand how they are derived, and the putative interplay of the different ocular factors involved.

While FGF is well established in regulating lens epithelial cell proliferation and fibre differentiation, it has also previously been shown to influence TGF-β-induced EMT and aberrant cell behaviour, promoting wound healing, repair, and fibrogenesis (Liu et al., 1994; Cerra et al., 2003; West-Mays et al., 2009; Koike et al., 2020). For example, different relatively low doses of FGF-2 (2.5–20 ng/mL) can exacerbate TGF-β2 (0.5–3 ng/mL)-induced lens opacification in intact rat lenses, with the higher dose combinations exhibiting the most pronounced response, resulting in dense cellular plaques and elevated deposition of ECM (Cerra et al., 2003). In contrast, other studies have shown that FGF can counteract and antagonise EMT in rodent LECs (Mansfield et al., 2004; Kubo et al., 2017). Rat lens epithelial cell explants cotreated with a relatively low dose of TGF-β2 (50 pg/mL) and a lower dose of FGF-2 (10 ng/mL) still formed spindle-like cells typical of EMT; however, with minimal cell loss compared to explants treated with TGF-β2 alone (Mansfield et al., 2004). This increased cell survival was unique to FGF as other regulatory ocular growth factors (e.g., EGF, IGF, HGF,

or PDGF) could not block the hallmark features of TGF-β-induced EMT, including lens capsular wrinkling, apoptosis, and cell loss (Maruno et al., 2002; Mansfield et al., 2004).

The influence of FGF regulating TGF-β-induced EMT may be attributed to the putative crosstalk between various downstream intracellular signalling pathways; the TGF-β-canonical Smad2/3-dependent proteins, and non-canonical mitogen-activated protein kinases (MAPK), such as extracellular signal-regulated kinase (ERK1/2) (Boswell et al., 2010; Shirakihara et al., 2011; Strand et al., 2014; Kubo et al., 2017; Wojciechowski et al., 2017). Studies using mouse LEC lines (MLECs) showed that cotreatment of cells with FGF-2 (10 ng/mL) and TGF-β2 (10 ng/mL) resulted in elongated fibroblastic-like cells and enhanced cell migratory mechanisms, with elevated ERK1/2-signalling (Kubo et al., 2017). Interestingly, in human lens epithelial cells (HLECs) from this same study, cotreated with the same doses of FGF-2/TGF-β2, they report on the antagonistic behaviour of FGF-2 with a reduction in cytoskeletal markers involved in stress fibre formation (Kubo et al., 2017). It is clear from these studies that there is no consistency in cell responsiveness to both FGF/TGF-β across different species.

In the current study, we characterised the influence that FGF has on TGF-β-induced cell behaviour in rat lens explants to best model the conditions needed to promote a heterogenous cell population typical of fibrotic cataracts as seen in situ. We demonstrate that a high fibre-differentiating dose of FGF is protective of TGF-β-induced EMT in peripheral lens epithelia; however, this is not evident in central lens epithelia induced by TGF-β. This emulates the spatial phenotypic response of lens cells seen in human PCO and may serve as a model to better understand the mechanisms leading to this post-surgical pathology.

5.4 MATERIALS AND METHODS

5.4.1 Animals and Tissue Culture

All procedures conducted abided by the Australian Code for animal care and usage for scientific purposes and the Association for Research in Vision and Ophthalmology (ARVO) Statement for the Use of Animals for Ophthalmic and Vision biomedical research (USA). The experiments were approved by the Animal Ethics Committee of The University of Sydney, NSW, Australia (AEC# 2021/1913). Wistar rats (*rattus norvegicus*) at 21-days of age (P21 ± 1 day) were humanely euthanized with CO_2 followed by cervical dislocation.

5.4.2 Lens Epithelial Explants

All collected primary rat ocular tissues were kept in medium 199 with Earle's Salts (M199) (11825015, Gibco™, Thermo Fisher Scientific, Sydney, NSW, Australia) in 35 mm Nunc™ culture dishes (NUN150460, Thermo Fisher Scientific). The media was supplemented with 2.5 µg/mL Amphotericin B (15290-018, Gibco™, Thermo Fisher Scientific), 0.1% bovine serum albumin (BSA) (9048-46-8, Sigma-Aldrich Corp., St. Louis, MO, USA), 0.1 µg/mL L-glutamine (200 mM) (25030081, Gibco™, Life Technologies, Carlsbad, CA, USA), and penicillin (100 IU/mL)/streptomycin (100 µg/mL) (15140-122, Gibco™, Life Technologies). The collected eyes were placed under a dissecting microscope to remove the lenses. The posterior capsule of the lens was torn using fine forceps and the remaining intact anterior capsule containing a sheet of lens epithelial cells (LECs) was pinned to the base of the culture dish using the gentle pressure of the forceps, as previously described (West-Mays et al., 2009). Explants were maintained in a humidified incubator (37 °C, 5% CO_2).

Different doses of recombinant human TGF-β2 (302-B2-002, R&D systems, Minneapolis, MN, USA) were used to induce EMT in the lens explants, as previously described (Shu et al., 2019b). A lower dose of TGF-β2 (50 pg/mL) gave a more regulated EMT response over 7 days, while a higher dose (200 pg/mL) was used to induce a more rapid EMT response in the lens explants over this same time period. To determine the impact of FGF-2 on TGF-β2-induced lens EMT, we cotreated TGF-β2-treated LECs with either a low proliferating dose of recombinant human FGF-2 (5 ng/mL: 233-FB, R&D systems) or a high fibre-differentiating dose of FGF-2 (200 ng/mL) (Wang et al., 2010, 2017). Control explants had no growth factors added to the media.

5.4.3 Assessment of Cell Morphology and Immunofluorescence

Cultured LEC explants were monitored and photographed daily over 7 days using phase contrast microscopy (Leica FireCam imaging, Leica Microsystems, Version 1.5, 2007). To examine the extent of how transdifferentiated cells modulated the underlying lens capsule, some treated explants were rinsed with filtered Milli-Q H_2O to debride all cells from the explant to completely expose the underlying lens capsule. Phase contrast images were captured before and after rinsing.

Following the different growth factor treatments, at set time points, the explants were fixed in 10% neutral buffered formalin (NBF; HT501320-9.5L, Sigma-Aldrich Corp) for 10 min, followed by 3 × 5 min rinses in phosphate-buffered saline (PBS) supplemented with BSA

(0.1%, *v*/*w*; PBS/BSA). The cells were permeabilised using PBS/BSA supplemented with Tween-20 (0.05%, *v*/*v*; 3 × 5 min), followed by subsequent rinses in PBS/BSA (2 × 5 min). The explants were then incubated at room temperature for 30 min with 3% normal goat serum (NGS diluted in PBS/BSA, *w*/*v*), before adding the primary antibodies; anti-mouse α-SMA (A2547, Sigma-Aldrich Corp.), anti-alpha tropomyosin (Tpm; α9d; provided by Prof. Gunning, University of New South Wales, Sydney, NSW, Australia), anti-rabbit β-catenin (ab6302, Abcam, Fremont, CA, USA), anti-β-crystallin, and anti-total-Smad2/3 (t-Smad2/3: 8685, Cell Signaling Tech., Danvers, MA, USA), all diluted 1:100 in NGS/PBS/BSA. The explants were incubated overnight at 4°C, followed by rinsing in PBS/BSA (3 × 5 min). The respective secondary antibodies were then applied for a 2-hour incubation at room temperature: goat anti-rabbit IgG Alexa-Fluor® 488 (ab150077, Abcam), and goat anti-mouse Alexa-Fluor® 594 (ab150116, Abcam), all diluted 1:1000 in PBS/BSA. Three 5 min rinses in PBS/BSA were followed before a 5 min application of 3 μg/mL bisbenzimide (H33342 trihydrochloride, Hoechst counterstain, B2261, Sigma-Aldrich) diluted in PBS/BSA. The explants were rinsed again before mounting with 10% glycerol in PBS and imaged using epifluorescence microscopy (Leica DMLB 100S with DFC-450C camera, Leica Application Suite, Version 4.8, 2021).

5.4.4 SDS-Page and Western Blotting

Cultured lens epithelial explants at set time points were rinsed in cold PBS. The central and peripheral regions of the explants were isolated using a scalpel blade to delineate each region. A central square of tissue, no more than a third of the explant diameter (central LECs, CLECs), and the remaining surrounding peripheral LECs (PLECs) were isolated separately. CLEC, PLEC, and total LEC (wholemount explant) protein was harvested, pooled into allocated Eppendorf tubes, and lysed with cold radioimmunoprecipitation assay (RIPA) lysis buffer containing 150 mM NaCl, 0.5% sodium deoxycholate, 0.1% Sodium dodecyl sulphate (SDS), 1 mM sodium orthovanadate, 1 mM NaF, 50 mM Tris-HCl (pH 7.5), 0.1% Triton X-100, phosphatase (PhosSTOP™), and protease (cOmplete™) EASYpacks inhibitor tablets (04906837001 and 05892970001; Roche Applied Science, Basel, Switzerland). LECs were homogenised and centrifuged for 10 min at 4 °C (14,400× *g*) for lysate/supernatant separation. Quantification of the total lens protein of each supernatant sample was conducted using a Pierce™ Micro bicinchoninic acid (BCA) protein assay reagent kit (23235; Thermo Fisher Scientific).

LEC protein sample lysates were prepared using 5% 2-mercaptoethanol (M6250, Sigma-Aldrich) combined with 2× Laemmli sample buffer at a 1:1 (*v/v*) ratio (1610737, Bio-Rad Laboratories, NSW, Australia). For electrophoresis, 10 µg of protein lysates were loaded onto 12% SDS-PAGE gels for 20 min at 70 V followed by 2 hours at 120 V. LEC protein was then transferred onto an immobilon®-PSQ polyvinylidene fluoride (PVDF) membrane (ISEQ00010, Merck Millipore, Rahway, NJ, USA) for 1 hour at 100 V. PVDF membranes were incubated in 2.5% BSA blocking buffer diluted in tris-buffered saline with 0.1% Tween-20 (TBST) and incubated for 1 hour with agitation at room temperature. Primary antibodies were added to the membranes and left overnight to incubate (at 4°C): anti-mouse α-SMA, anti-GAPDH (G8795, Sigma-Aldrich Corp.), anti-tropomyosin alpha, and anti-β-crystallin, t-Smad2/3, phospho-Smad2/3 (p-Smad2/3, 8828, Cell Signalling Tech., Danvers, MA, USA), phospho-ERK1/2 (p-ERK1/2, 9101, Cell Signalling Tech.), and total-ERK1/2 (t-ERK1/2, 9102, Cell Signalling Tech.), all diluted in blocking buffer/TBST at 1:1000, apart from α-SMA and GAPDH (1:2000). Following overnight incubation, the membranes were rinsed in TBST (3 × 5 min) and incubated with the appropriate horseradish peroxidase (HRP)-conjugated secondary antibodies for 2 hours at room temperature: HRP-conjugated goat anti-rabbit IgG (7074, Cell Signalling Tech.) and horse anti-mouse IgG (7076, Cell Signalling Tech.), diluted in TBST at 1:5000. The membranes were rinsed in TBST (3 × 10 min) followed by the application of an immobilon chemiluminescent HRP substrate for 3–5 min (WBKLS0500, Merck Millipore). Protein chemiluminescent signals were imaged using Bio-Rad ChemiDoc™ MP imaging.

Following immunolabelling, PVDF membranes were stripped for 10 min in stripping buffer (10% SDS, 0.5 M Tris HCl pH 6.8, Milli-Q H_2O, and 0.8% 2-mercaptoethanol) with gentle agitation. The membranes were then washed in TBST (3 × 5 min) and re-blocked in blocking buffer/TBST for 1 hour. Following blocking, the membranes were probed for loading control GAPDH (1:2000, 1 hour) and incubated with an HRP-conjugated horse anti-mouse secondary antibody for 1 hour prior to chemiluminescent signalling analysis. Protein densitometry was carried out using Bio-Rad ImageLab software (Version 6.1.0, 2019).

5.4.5 Statistical Analysis

For each experimental analysis, three independent experiments were carried out. For every experiment, a minimum of three individual replicates ($n = 3$) per treatment group (different treatment of explants) were used. For Western blotting, each group contained up to eight explants to isolate central and peripheral lens cells that were randomly obtained from different

P21 rats. For measuring changes in protein expression, we used densitometry to calculate the selected protein intensity relative to the loading control (GAPDH). To calculate protein levels of Tpm, the sum of the intensity of the two resultant bands (34–36, 38 kDa) representing α9d, and was compared relative to GAPDH levels.

For Western blot experiments examining differences in Smad-dependent (Smad2/3) and Smad-independent (MAPK/ERK1/2) activity, phosphorylated protein expression was calculated using the following ratio: relative phosphorylated density per total protein. Prior to the use of one-way analysis of variance (ANOVA), several assumptions were tested and confirmed; we assumed equal standard deviation (SD) and residuals appeared normally distributed. Based on these confirmed assumptions, we compared the differences among the means of all treatment groups using one-way ANOVA, followed by Tukey's multiple comparisons post-hoc test. All data acquired were plotted appropriately using GraphPad Prism software version 9.0 (GraphPad Software Inc., San Diego, CA, USA).

To quantify the spatial differences in t-Smad2/3 immunoreactivity, six separate images of central and peripheral regions were captured per explant across three randomised explants per treatment group, over three individual experiments. Nuclear and cytoplasmic localisation of t-Smad2/3 was manually counted using ImageJ's Cell Counter plugin. The mean percentage of t-Smad2/3 nuclear and cytoplasmic fluorescence was calculated and statistically analysed using GraphPad Prism.

Tabled data were represented as the standard error of the mean (± SEM) and probability values, where $p < 0.05$ was considered statistically significant.

5.5 RESULTS

5.5.1 Induction and rate of progression of TGF-β2-induced lens EMT is dose dependent

It is well established and well documented (Shu et al., 2017; Wojciechowski et al., 2017; Taiyab et al., 2019) that the addition of exogenous TGF-β2 to LEC rodent explants can induce an EMT response *in vitro*. For the current study, we initially used two different doses of TGF-β2 to control the rate of EMT induction; a low (50 pg/mL) and high (200 pg/mL) dose that induced an EMT across 5–7 days of culture (Figure 5.1). A lower dose of TGF-β2 extends the lens epithelial cell culture period to 7 days. Throughout the culture period, cells in all control (non-treated with TGF-β2) explants remained and retained their normal epithelial phenotype across the entire explant; a uniform monolayer of and cobblestone-like, typical of that observed *in situ* (Figure 5.1 A). A lower dose of TGF-β2 (50 pg/mL) administered to LECs 24 hours after explant acquisition, had no significant impact on the epithelial cell phenotype by day 1 of culture (Figure 5.1 B). By day 3, cell blebbing (white refractile bodies) and cell debris associated with apoptosis was evident, with some exposed bare patches of capsule appearing between cells, indicating the initiation of epithelial cell transdifferentiation and modulation of the lens capsule (Figure 5.1 D). The progression of EMT with a low dose of TGF-β2-treated was more prominent by day 5, with increased exposure of the underlying lens capsule (Figure 5.1 F). Newly transdifferentiated myofibroblastic cells caused capsular wrinkling (Figure 5.1 F). By day 7, increased cell death, left minimal cells on the capsule, signifying the end point of the EMT process in this model (Figure 5.1 H). LECs exposed to a higher dose of TGF-β2 (200 pg/mL) experienced a greater rate of EMT with the process concluding after 5 days of culture. Transdifferentiation and loss of cell uniformity was evident by day 1 of culture (Figure 5.1 C) and at day 3, LECs administered with this higher dose of TGF-β2 demonstrated more regions of bare capsule with little to no cells (Figure 5.1 E). Clusters of myofibroblastic cells were visible, with prominent wrinkling of the lens capsule. Unlike LECs treated with a low dose of TGF-β2, complete cell loss and exposure of the bare lens capsule was evident earlier, by day 5 when applying the higher dose TGF-β2 to LECs (Figure 5.1 G).

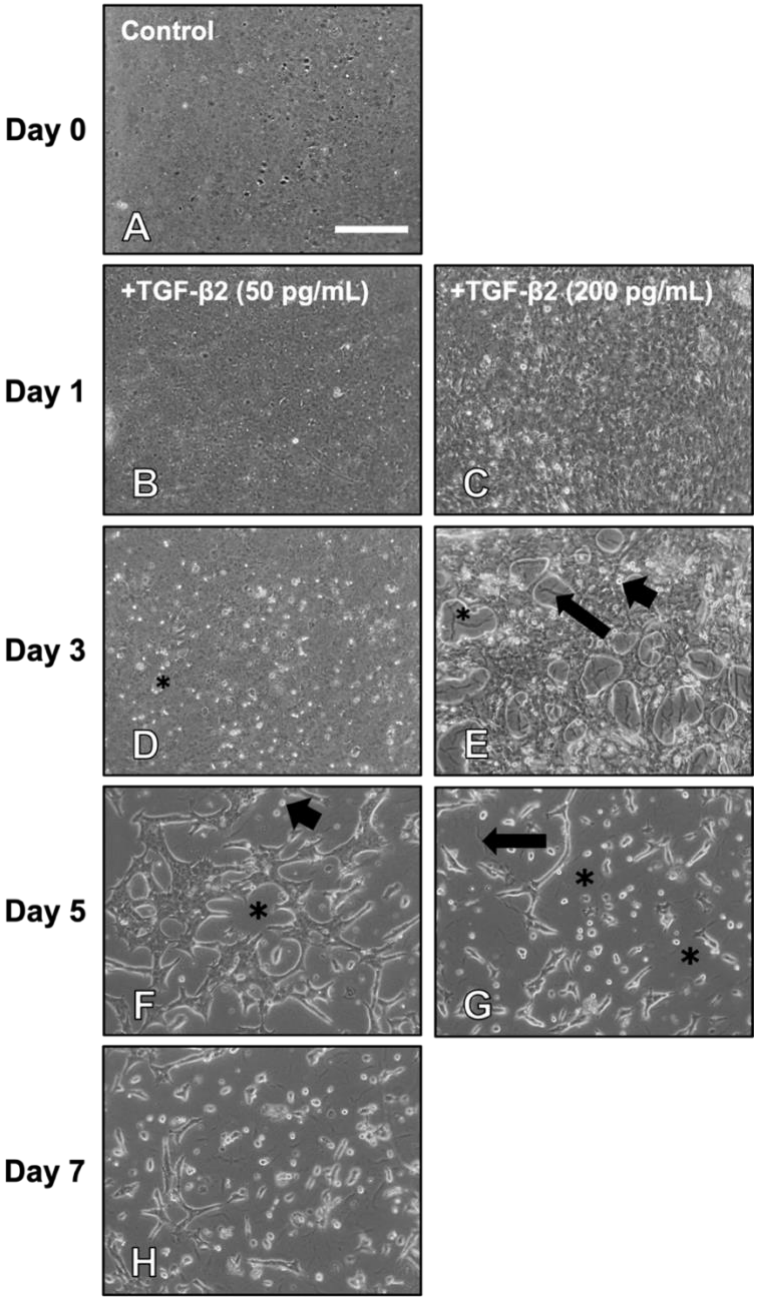

Figure 5.1. TGF-β2-induced lens EMT. Non-treated (Control) explants imaged at 24 hours of culture, Day 0 (A), maintained a tightly packed monolayer of epithelial cells across 7 days. Low dose TGF-β2 (50 pg/mL) treated explants exhibited no significant morphological changes at day 1 (B) and 3 (D). A prolonged EMT with progressive cell loss is evident through refractile bodies indicating cell blebbing (arrowheads) between days 3-5 (F), and exposure of the underlying lens capsule (asterisks) due to transdifferentiated cell migration and/or cell loss by day 7. contractile myofibroblastic cells caused capsular winkling (arrows). A higher dose of TGF-β2 (200 pg/mL) led to a more expeditious induction of EMT, occurring between day 1 and 3 (C, E), with complete cell loss by day 5 of culture (G). Scale bar: 200 µm.

5.5.2 FGF-2 promotes dose-dependent modulation of TGF-β2-induced EMT

Since we established that rate of TGF-β2-induced EMT is dose-dependent (Figure 5.1), we then examined the efficacy of different doses of FGF-2 in modulating the effect of TGF-β2 on LECs induced to undergo EMT. Using phase contrast microscopy, control LECs without FGF-2 or TGF-β2 treatment (Figure 5.2 A–B), as well as explants treated with only a low proliferating dose of FGF-2 (5 ng/mL) (Figure 5.2 C, G, K, O), demonstrated no significant morphological changes and retained their epithelial phenotype over a 5-day culture period.

With different dose combinations of FGF-2 and TGF-β2, most cells in the explants underwent a uniform EMT response over 3-5 days (Figure 5.2 D–F, H–J, L–N, P–R). A lower dose of FGF-2 was not sufficient to prevent EMT induction in central regions of explants exposed to both a low dose (Figure 5.2 D) and a high dose of TGF-β2 (Figure 5.2 E). This response was exacerbated over 5 days of culture, with prevalent capsular modulation and cell loss (Figure 5.2 L–M). Despite this, peripheral regions of explants from these same treatment groups underwent a prolonged EMT response (Figure 5.2 H–I), with exposure to the underlying lens capsule more evident at 5 days, with fewer cells transdifferentiating into myofibroblasts (Figure 5.2 P–Q).

Explants cotreated with a higher dose of both FGF-2 (200 ng/mL) and TGF-β2 (200 pg/mL) increased the rate of EMT induction, with central regions demonstrating heightened capsular wrinkling and more exposed areas of the underlying capsule by day 3 (Figure 5.2 F) and day 5 (Figure 5.2 N). Peripheral cells in these cotreated explants demonstrated prominent myofibroblastic cells (Figure 5.2 J, arrows), that were lost by day 5, leading the explant at the periphery to contract and shrivel (Figure 5.2 R).

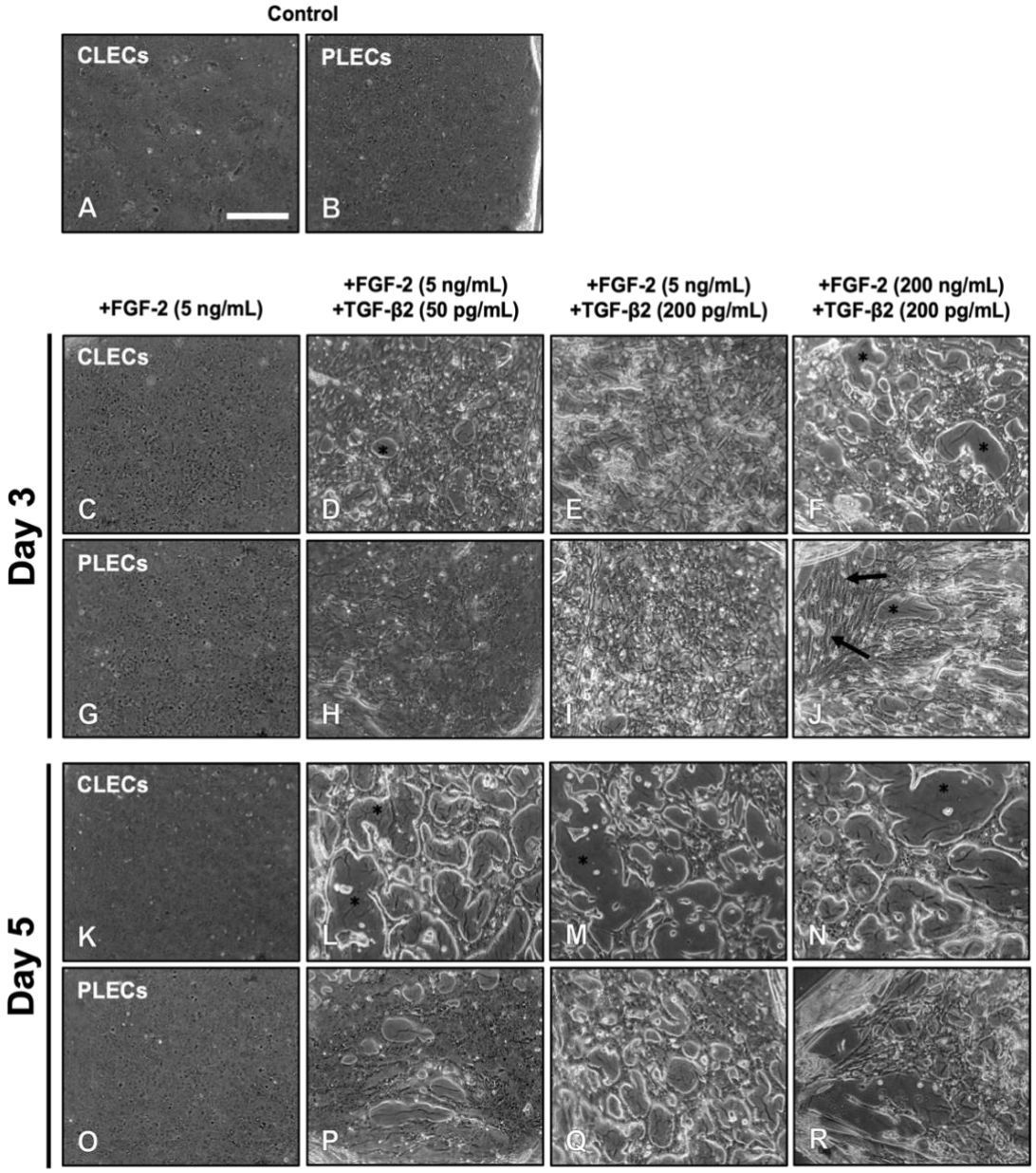

Figure 5.2. FGF-2 promotes dose-dependent modulation of TGF-β2-induced EMT. Representative images of LEC explants of control (non-treated) explants at day 3 of culture with epithelial cells remaining present in central (CLECs, A) and peripheral regions (PLECs, B). LEC explants treated with a low proliferating dose of FGF-2 (5 ng/mL) at 3 days (C, G) and 5 days of culture (K, O). A low dose FGF-2 and low dose of TGF-β2 (50 pg/mL) underwent an EMT response in central (D, L) and peripheral regions (H, P), with some epithelial cells remaining after 5 days in the explant periphery (P). Modulation/wrinkling of the exposed underlying lens capsule (asterisks). A low dose of FGF-2 and high dose of TGF-β2 (200 pg/mL) led to an EMT response in both CLECs (E, M) and PLECs (I, Q). A high dose of FGF-2 (200 ng/mL) and TGF-β2 (200 pg/mL) also led to an EMT response in both CLECs and PLECs (F, J, N), with prominent myofibroblastic cells (J, arrows) and increased capsule modulation. By day 5, high doses of FGF-2 and TGF-β2 caused the explant to shrivel in the explant peripheral regions (R). Scale bar: 200 μm. Figures C–J previously published in (Flokis and Lovicu, 2023).

5.5.3 FGF-2 promotes a spatially dependent TGF-β2-induced EMT response in lens epithelial explants

Despite a uniform EMT response in most dose combinations of FGF-2 and TGF-β2 (Table 5.1, Figure 5.2), we found that cells in explants cotreated with a relatively high dose of FGF-2 (200 ng/mL) and the lower dose of TGF-β2 (50 pg/mL), a differential response between CLECs and PLECs was observed (Figure 5.3).

Table 5.1. Regional, dose-dependent effects of FGF-2 and TGF-β2 on LEC explants.

Treatment	Concentration		Regional Cell Response in Explant	
	FGF-2 (ng/mL)	TGF-β2 (pg/mL)	FGF-2 (ng/mL)	TGF-β2 (pg/mL)
f/t	5	50	EMT	EMT
f/T	5	200	EMT	EMT
F/t	200	50	EMT	*Fibre Differentiation*
F/T	200	200	EMT	EMT

Low dose FGF-2 (f); low dose TGF-β2 (t); high dose FGF-2 (F); high dose TGF-β2 (T). Table previously published in (Flokis and Lovicu, 2023).

The cells in the lens epithelial explants treated with the high a fibre-differentiating dose of FGF-2 elongated over 5 days (Figure 5.3 B, F, J, N), compared to the control LEC explants (no growth factor treatment; Figure 5.3 A, E, I, M). This FGF-induced fibre differentiation response was more pronounced in PLECs compared to CLECs. LECs in explants treated with a low dose of TGF-β2 (Figure 5.3 C, G) displayed prominent EMT by day 5 (Figure 5.3 K, O), with the LECs losing their uniform packing and adhesion as they transdifferentiated into myofibroblastic cells. TGF-β2 treatment also led to increased cellular blebbing (refractile bodies) and apoptotic cell loss, evident by areas of bare lens capsule that displayed prominent signs of capsular modification in the form of wrinkling throughout the explant (Figure 5.3 K, O).

When the explants were cotreated with TGF-β2 and FGF-2, CLECs underwent similar morphological transformations at day 3 (Figure 5.3 D) and day 5 (Figure 5.3 L) to that seen with TGF-β2-treatment alone (Figure 5.3 C, K). In contrast, PLECs in the explants cotreated with FGF-2/TGF-β2 showed no evidence of EMT at day 3 (Figure 5.3 H), instead demonstrating morphological changes more consistent with that observed in the explants treated with FGF-2 alone (Figure 5.3 F, N). PLECs in cotreated explants maintained this change in the LEC phenotype across 5 days, with parallel elongating cells forming and abutting to epithelial cells (Figure 5.3 P).

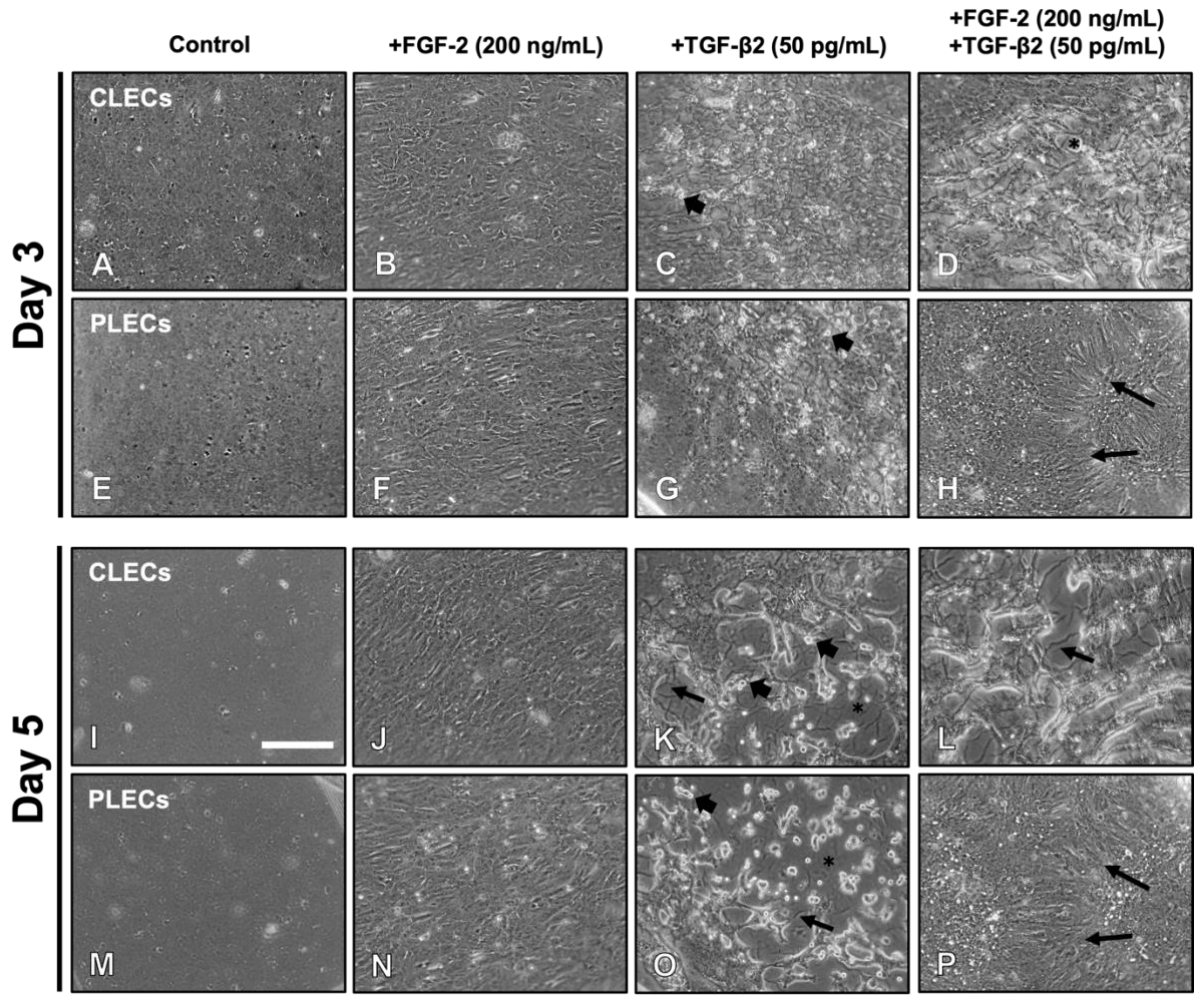

Figure 5.3. FGF-2 promotes a spatially dependent TGF-β2-induced EMT response in lens epithelial explants. Control LECs maintained a cobblestone-like epithelial phenotype after 3 days (A, E) and 5 days (I, M). FGF-2-induced cell elongation typical of lens fibre differentiation (B, F, J, N). TGF-β2 induced EMT, highlighted by elongated myofibroblastic cells, with prominent cell blebbing/refractile bodies (C, G, arrowheads) and loss of cells exposing the lens capsule (asterisk) with capsular wrinkling (arrows) after 5 days (K, O). FGF-2 and TGF-β2 cotreated explants led to EMT of CLECs (D, L) but a fibre differentiation response in PLECs (H) that was maintained across culture (P, arrows). Scale bar: 200 μm. Data previously published in (Flokis and Lovicu, 2023).

Loss of all cells after 3 days revealed the underlying lens capsule, with no apparent capsular modulation (no folds or wrinkles) in either control (Figure 5.4 A, D) or FGF-2 treated (Figure 5.4 B, E) explants. In the TGF-β2-treated explants, increased capsular modulation was apparent with wrinkling and folds in the central explant regions (Figure 5.4 C) and in the peripheral regions (Figure 5.4 F). Consistent with the differential cell response in the central and peripheral regions of the F/t-cotreated explants (Figure 5.4 G, G1, G3), the explants exhibited capsular modulation only in the central explant region (Figure 5.4 G2), with no capsular wrinkling observed in the peripheral region (Figure 5.4 G4).

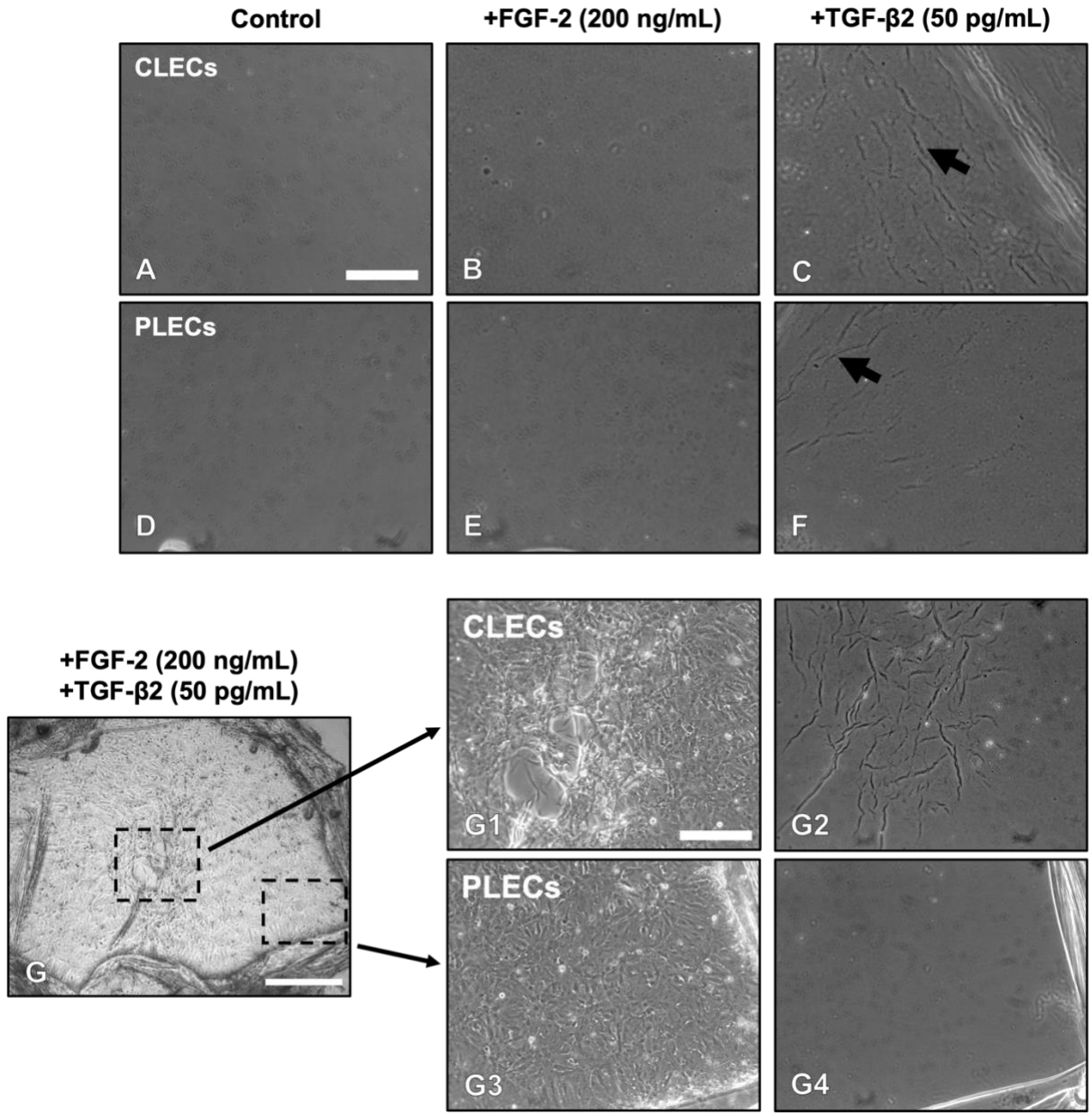

Figure 5.4. Lens capsule modulation during TGF-β2-induced EMT. Seventy-two hours post treatment, the explants were rinsed consecutively in filtered Milli-Q H_2O to remove all lens epithelial cells and view the underlying lens capsule. No capsular wrinkling was evident in control (A, D) and/or FGF-2 treated (B, E) explants. Capsular modulation was evident in TGF-β2 treated explants in both central (C) and peripheral (F) cell regions with increased wrinkling (arrowheads). In the F/t cotreated explants (G, G1, G3), after cell removal (G2, G4), capsular wrinkling was only apparent in regions that were previously populated with CLECs (G2), with no wrinkling visible in regions that were previously populated with PLECs (G4). Scale bar: 200 µm (A–F, G1–G4), 400 µm (G). Data previously published in (Flokis and Lovicu, 2023).

We observed that with ongoing culture (up to 7 days), regardless of the explant region or treatment, all of the cells exposed to TGF-β2 (200 pg/mL) are lost by 7 days (Figure 5.5 A); however, in the cotreated explants (F/t), with continual supplementation of the media with FGF-2 (200 ng/mL) after day 3 of culture, this promoted cell survival, whereby we continue to

observe many myofibroblastic cells in the central region of the explants (Figure 5.5 B) and, similarly, relatively normal lens cells at the periphery of the explants are also maintained (Figure 5.5 C).

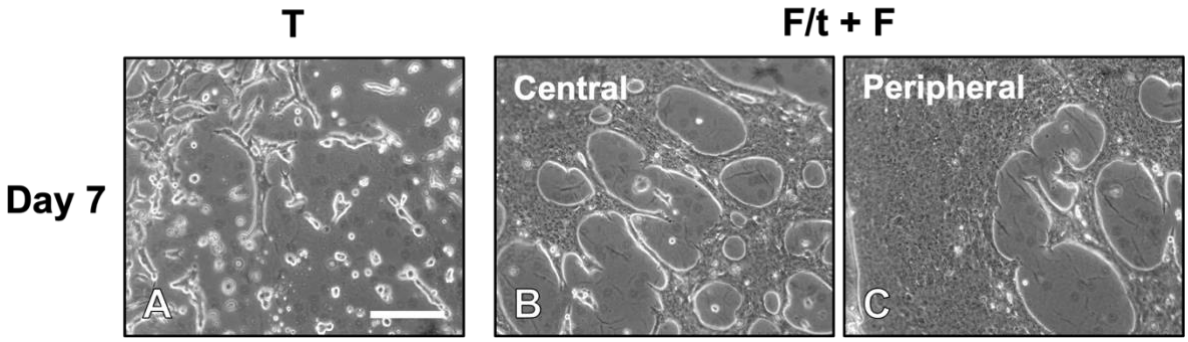

Figure 5.5. Re-supplementation of FGF-2 promotes cell survival. A) Representative image of a wholemount explant treated with a high dose of TGF-β2 (200 pg/mL, T), undergoing an EMT response and cell death by day 7 of culture. Re-supplementation with FGF-2 in explants cotreated with a high dose of FGF-2 (200 ng/mL, F) and low dose of TGF-β2 (50 pg/mL, t) after 3 days of culture, promotes cell survival in both central (B) and peripheral (C) lens cells after 7 days. Scale bar: 200 µm. Data previously published as a Supplementary Figure in (Flokis and Lovicu, 2023).

5.5.4 FGF-2 promotes spatial differences in labelling for EMT and fibre differentiation markers in TGF-β2-treated LECs

5.5.4.1 Immunofluorescent Labelling

We used immunofluorescence to characterise the different cell types in explants treated with TGF-β2 and/or FGF-2 over 3 days, labelling for lens fibre differentiation markers, β-crystallin, and alpha-tropomyosin (α9d), as well as the EMT marker, α-SMA. Isotype controls for all primary antibodies tested show little to no specific labelling (Figure 5.6).

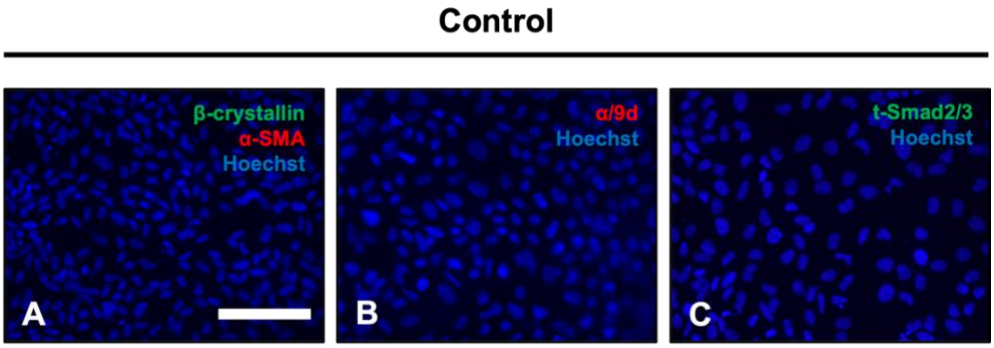

Figure 5.6. Isotype controls for immunofluorescence labelling. Representative immunofluorescent imaging of isotype controls in control (non-treated) rat LEC explants at 3 days of culture. A) Explants without primary antibodies for β-crystallin (green) and α-SMA (red), B) α9d (red), and C) t-Smad2/3 (green) with nuclear dye Hoechst (blue). Anti-mouse Alexa Fluor 594 and anti-rabbit Alexa Fluor 488 secondary antibodies used diluted in PBS/BSA (1:1000). Scale bar: 100 µm.

Control LECs throughout the explant exhibited no reactivity for β-crystallin and/or α-SMA after 3–5 days of culture (Figures 5.7 A and 5.8 A, E), labelling only for α9d at 3 days (Figure 5.7 B). FGF-2-treated LECs exhibited strong reactivity for β-crystallin throughout the explant (Figure 5.7 C, I), with stronger labelling in PLECs (Figure 5.7 I). Treatment with FGF-2 did not promote α-SMA reactivity in any cultured lens epithelia across 5 days (Figures 5.7 C, I and 5.8 B, F). FGF-2-treated CLECs presented diffuse α9d-reactivity (Figure 5.7 F), while PLECs had a more defined reactivity for α9d, highlighting actin filaments in the elongating, differentiating fibre cells (Figure 5.7 L). LECs treated with only TGF-β2 displayed clear evidence of an EMT response, with strong reactivity for α-SMA, with no β-crystallin observed throughout the explant (Figure 5.7 D, J), and was sustained across 5 days (Figure 5.8 C, G). TGF-β2-treated CLECs had a highly specific localisation of α9d to actin stress fibres (Figure 5.7 G), which were also very prominent in PLECs (Figure 5.7 M).

Unlike cells treated with only FGF-2 or only TGF-β2, that had a relatively uniform label for the different markers across the entire explant, in the FGF-2/TGF-β2 cotreated explants, we observed distinct spatial differences in the labelling of the markers, consistent with our earlier morphological observations. The CLECs in the TGF-β2/FGF-2-treated explants predominantly labelled for α-SMA with little to no β-crystallin reactivity at day 3 (Figure 5.7 E) or day 5 (Figure 5.8 D), similar to the explants treated with only TGF-β2 (Figures 5.7 D, J and 5.8 C, G). In contrast, the PLECs in these same cotreated explants displayed the inverse label, with strong reactivity primarily for β-crystallin in elongated cells, with few neighbouring smaller cells immunolabelling for α-SMA (Figure 5.7 K). This differential β-crystallin and α-SMA reactivity in the cotreated explants was sustained up to 5 days of culture (Figure 5.8 D, H). Stronger labelling for α9d was also observed throughout the cotreated explants (Figure 5.7 H, N), highlighting the marked elongation of peripheral fibre-like cells (Figure 5.7 K, N), as well as central myofibroblastic cells (Figure 5.7 E, H).

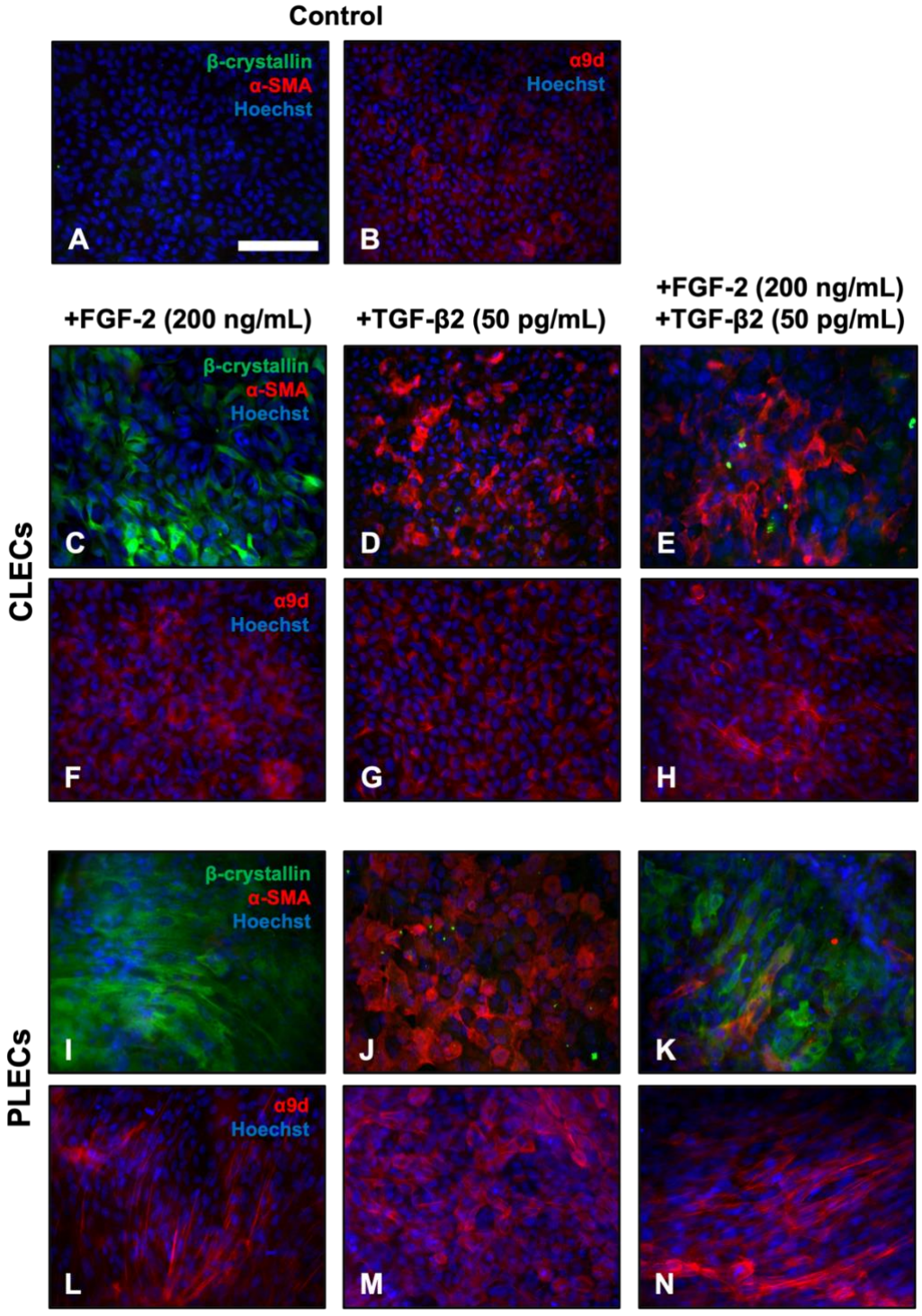

Figure 5.7. FGF-2 modulates EMT and fibre differentiation markers in TGF-β2-treated LECs. Immunolabelling of β-crystallin (green), α-SMA (red), and alpha-tropomyosin (α9d; red), counterstained with Hoechst nuclear stain (blue), in CLECs (C–H) and PLECs (I–N) following 3 days of culture with no growth factors (control; A, B), FGF-2 (200 ng/mL; C, F, I, L), and TGF-β2 (50 pg/mL; D, G, J, M), or cotreated with FGF-2 and TGF-β2 (E, H, K, N). Images are representative of three independent experiments. Scale bar: 100 μm. Data previously published in (Flokis and Lovicu, 2023).

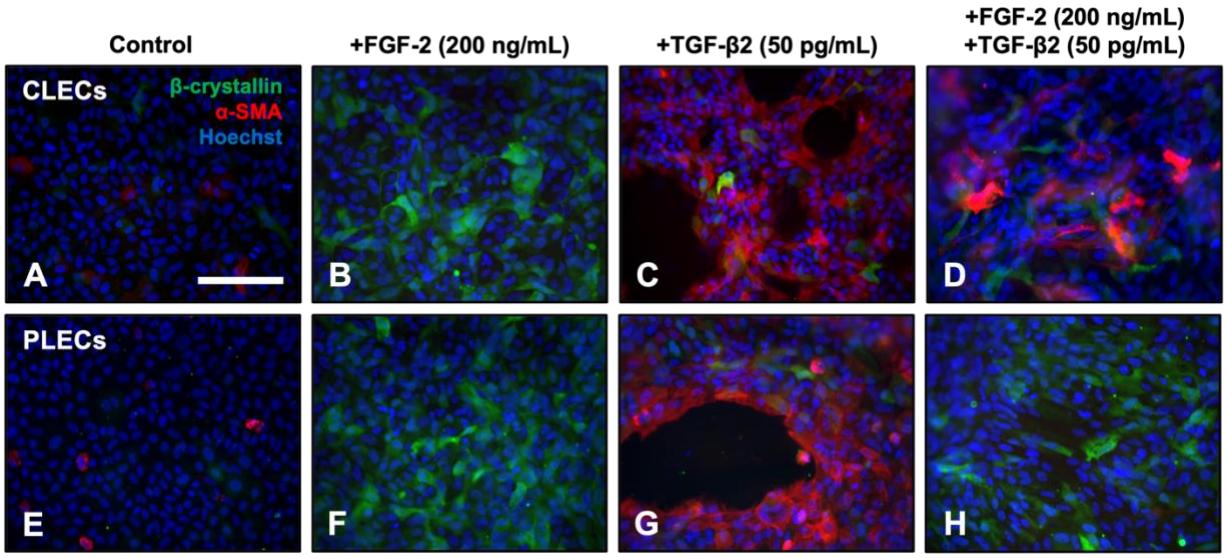

Figure 5.8. FGF-2 modulates EMT and fibre differentiation markers in TGF-β2-treated LECs. Representative immunolabelling for β-crystallin (green), and α-SMA (red), counter-stained with Hoechst nuclear dye (blue), in CLECs (A–D) and PLECs (E–H) following 5 days of culture with no growth factors (Control; A, E), FGF-2 (200 ng/mL; B, F), TGF-β2 (50 pg/mL; C, G), or cotreated with FGF-2/TGF-β2 (D, H). Scale bar: 100 μm. Data previously published as a Supplementary Figure in (Flokis and Lovicu, 2023).

5.5.5 A high dose of FGF-2 exacerbates EMT and fibre differentiation markers in TGF-β2-treated LEC explants

Although most explants cotreated with F/T underwent a complete EMT response (see Figure 5.2), some outlier explants demonstrated an exacerbated EMT and fibre differentiation response across 5 days of culture (Figure 5.9), similar to that observed in F/t-treated explants (see Figures 5.3–5.4, 5.7–5.8). At 3 days, central regions of outlier explants cotreated with high dose FGF-2 (200 ng/mL) and high dose TGF-β2 (200 pg/mL) showed archetypal EMT induction with aberrant capsular folds (Figure 5.9 A), that progressively became more prominent by day 5 of culture (Figure 5.9 B).

When immunolabelled at day 5, CLECs in F/T cotreated explants exhibited strong reactivity for α-SMA, with minor reactivity for β-crystallin, indicative of an EMT induction (Figure 5.9 C). Interestingly, PLECs from the same F/T cotreated explants demonstrated highly specialised elongated fibre-like cells that appeared multilayered (Figure 5.9 D). These fibre-like cells induced by a high dose of FGF-2 were sustained across 5 days (Figure 5.9 E) and immunolabelled strongly for β-crystallin (Figure 5.9 F).

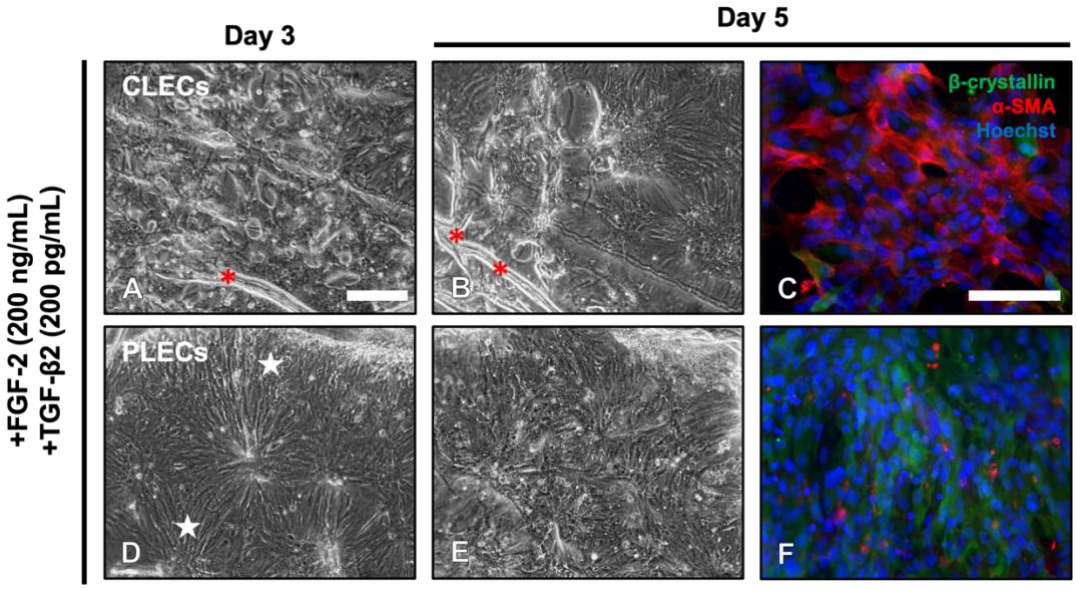

Figure 5.9. FGF-2 can exacerbate EMT and fibre differentiation marker expression in TGF-β2-treated LECs. Explants cotreated with a high dose of FGF-2 (200 ng/mL) and a high dose of TGF-β2 (200 pg/mL) across 5 days of culture. Central cells demonstrated a heightened EMT response at day 3 (A) and day 5 (B) of culture, with aberrant folds within the central region of the explant (red asterisks). The presence of FGF-2 and TGF-β2 in PLECs promoted a fibre differentiation response (D, white stars) that was maintained across 5 days (E). Cotreated explants were fixed at day 5 of culture and immunolabelled for β-crystallin (green), α-SMA (red), and counterstained with Hoechst nuclear dye (blue). Representative images of a central (C) and peripheral (F) region of a cotreated explant. Scale bar: 100 µm (A–F).

5.5.6 Protein expression in CLEC vs. PLEC lysates

We quantified protein changes in the treated explants using Western blotting. CLECs had a significant increase in α-SMA when treated with TGF-β2, compared to the relatively lower levels in the control (NT) and FGF-2-treated explants ($p < 0.0001$, Figure 5.10 A, C). FGF-2 treatment did not impact α-SMA levels in the CLECs compared to the control cells ($p = 0.3429$). In the FGF-2/TGF-β2 cotreated explants, there was a significant reduction in α-SMA levels in the CLECs relative to the TGF-β2 alone CLECs ($p < 0.0001$). In fact, these CLECs in the cotreated explants displayed no significant difference in levels of α-SMA compared to the CLECs of the control ($p > 0.9999$) or FGF-2 alone ($p = 0.3249$) explants. In the PLECs of the FGF-2/TGF-β2 cotreated explants, consistent with the reduced EMT response, there were reduced α-SMA levels when compared to the CLECs, comparable to the lower α-SMA levels seen in the PLECs of the control ($p = 0.7371$), FGF-2 ($p > 0.9999$)-, and TGF-β2-treated explants ($p = 0.0053$) (Figure 5.10 B, D). The PLECs in the explants treated with FGF-2 alone did not have increased α-SMA levels when compared to the control cells ($p = 7366$); however,

the PLECs in the explants treated with TGF-β2 alone had significantly increased α-SMA levels, compared to the control ($p = 0.0203$) and the FGF-2-treated ($p = 0.0053$) explants.

α9d levels were significantly elevated only in the CLECs and PLECs of the TGF-β2-treated explants, when compared to the corresponding cells of all other treatment groups (Figure 5.10 A–D). For the CLECs, levels of α9d in the control explants were reduced in both the FGF-2 ($p = 0.0924$)- and FGF-2/TGF-β2-treated explants ($p = 0.0959$) and were significantly reduced when compared to the elevated α9d levels found in the CLECs of the TGF-β2-treated explants (control *vs.* TGF-β2, $p = 0.0034$; FGF-2 *vs.* TGF-β2, $p = 0.0002$) (Figure 5.10 C). In the PLECs, there was no obvious difference in the levels of α9d across all of the treatment groups (Figure 5.10 B), except for elevated levels in the PLECs of the TGF-β2-treated explants as mentioned (control *vs.* TGF-β2, $p = 0.0103$; FGF-2 *vs.* TGF-β2, $p = 0.0039$; TGF-β2 *vs.* FGF-2/TGF-β2, $p = 0.0249$) (Figure 5.10 D).

When compared to the control cells, there was no significant difference in the levels of β-crystallin in the CLECs of the explants treated with FGF-2 ($p = 0.8742$) (Figure 5.10 A, C). Treatment with TGF-β2 did not significantly increase levels of β-crystallin in the CLECs compared to the control ($p = 0.5844$), FGF-2 ($p = 0.2260$), or the cotreated explants ($p = 0.1459$). We did observe a significant decrease in β-crystallin in the CLECs of the cotreated explants, relative to the control ($p = 0.0160$) and FGF-2 ($p = 0.0044$)-treated explants (Figure 5.10 A, C). Treatment of the explants with FGF-2 significantly increased β-crystallin levels in the PLECs when compared to the PLECs of the control ($p = 0.0374$) and the TGF-β2-treated explants ($p = 0.0003$, Figure 5.10 B, D). The PLECs in the explants treated with TGF-β2 alone had reduced β-crystallin levels when compared to the control PLECs ($p = 0.0222$). The PLECs of the explants cotreated with FGF-2/TGF-β2 had slightly elevated β-crystallin levels in comparison to the PLECs of the control ($p = 0.6396$) or the TGF-β2-treated ($p = 0.0056$) explants (Figure 5.10 B, D).

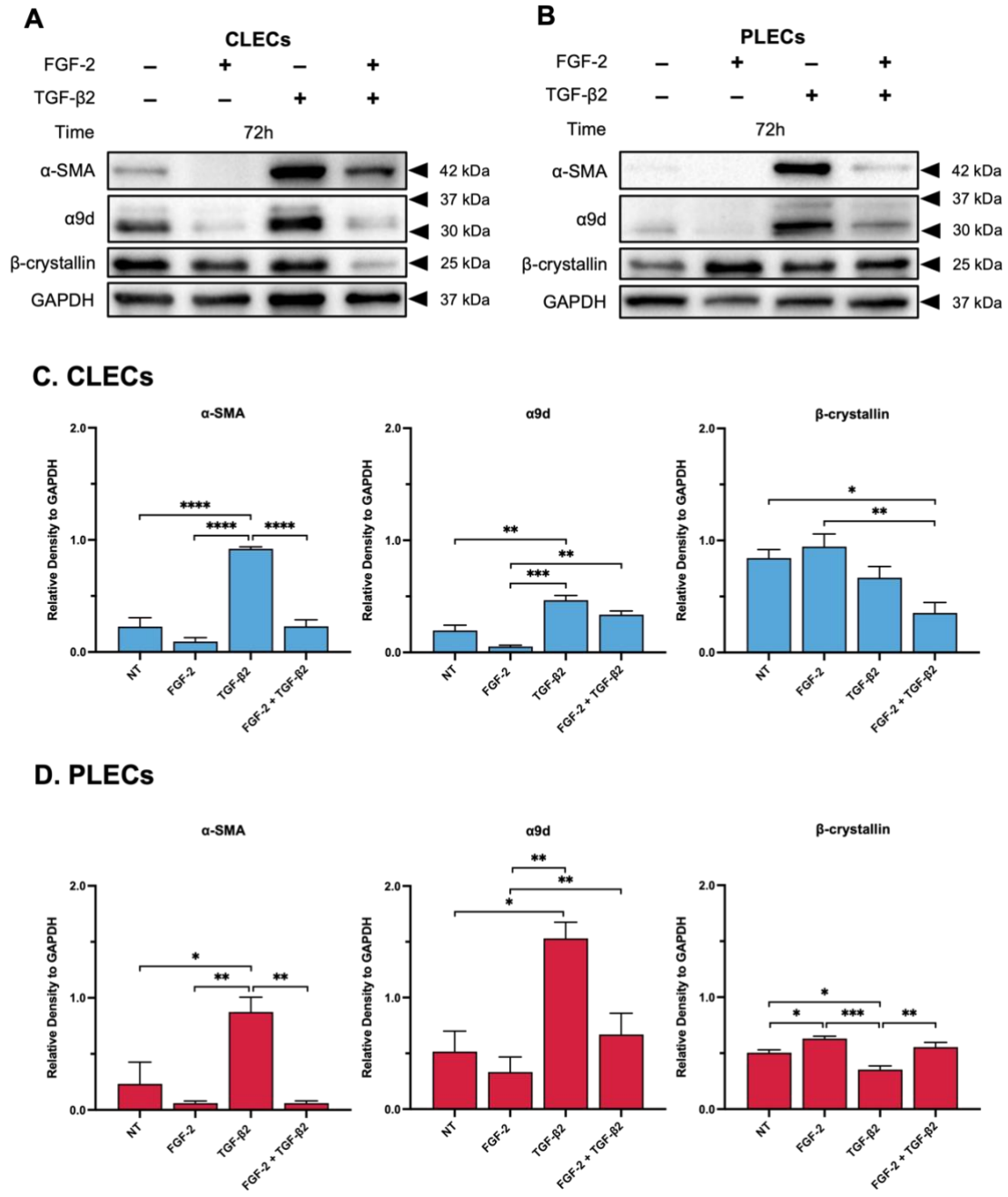

Figure 5.10. FGF-2 modulates levels of different protein markers in TGF-β2-treated LECs. Representative Western blot for alpha-tropomyosin (α9d), α-SMA, and β-crystallin in the control (non-treated, NT), FGF-2, TGF-β2, and FGF-2/TGF-β2 cotreated CLECs (A, C) and PLECs (B, D). Protein levels were normalised relative to GAPDH levels (C, D). One-way ANOVA with the mean ± SEM and post-hoc Tukey's multiple comparisons test (* $p < 0.0332$, ** $p < 0.0021$, *** $p < 0.002$, **** $p < 0.001$). Data previously published in (Flokis and Lovicu, 2023).

5.5.7 Protein changes in wholemount LEC lysates

To further explore the differential impact of FGF-2 on cells treated with TGF-β2, we examined for changes in proteins at 72 hours in wholemount explants known as markers for epithelial or mesenchymal cells, and for fibre differentiation. We previously compared protein expression changes in CLEC *vs.* PLEC lysates and showed a significant difference between fibre differentiation and EMT/cytoskeletal marker expression (Figure 5.10).

In whole explant cultures, treatment with FGF-2 did not impact α-SMA levels compared to levels of α-SMA in control (non-treated) wholemount explants ($p = 0.8739$, Figure 5.11 A–B). There was a clear upregulation of α-SMA only in TGF-β2-treated wholemount LECs when compared to control and FGF-2-treated explants (control *vs.* TGF-β2, $p = 0.0076$; FGF-2 *vs.* TGF-β2, $p = 0.0030$). Cotreatment with FGF-2 and TGF-β2 significantly reduced α-SMA intensity at 72 hours, in comparison to treatment with only TGF-β2 ($p = 0.0153$).

TGF-β2 significantly elevated alpha-tropomyosin (α9d) levels in comparison to control ($p = 0.0094$), FGF-2-alone ($p = 0.0371$), and FGF-2/TGF-β2-treated ($p = 0.0317$) wholemount LEC explants (Figure 5.11 A, C). FGF-2 treatment did not influence α9d levels compared to control ($p = 0.7432$) and cotreated FGF-2/TGF-β2 explants ($p = 0.9995$).

Lower molecular weight and fibre differentiation marker, β-crystallin, was elevated in FGF-2-treated wholemount LEC explants when compared to TGF-β2-treated LECs ($p = 0.0145$), and control explants ($p = 0.3325$, Figure 5.11 A, D). Treatment with TGF-β2 decreased β-crystallin levels when compared to control explants ($p = 0.1799$). The presence of both FGF-2 and TGF-β2 in wholemount explants significantly increased β-crystallin intensity in comparison to TGF-β2-alone LEC explants ($p = 0.0486$). Reduction in β-crystallin reactivity in FGF-2/TGF-β2-treated explants, compared to FGF-2 alone, was not significant ($p = 0.8135$).

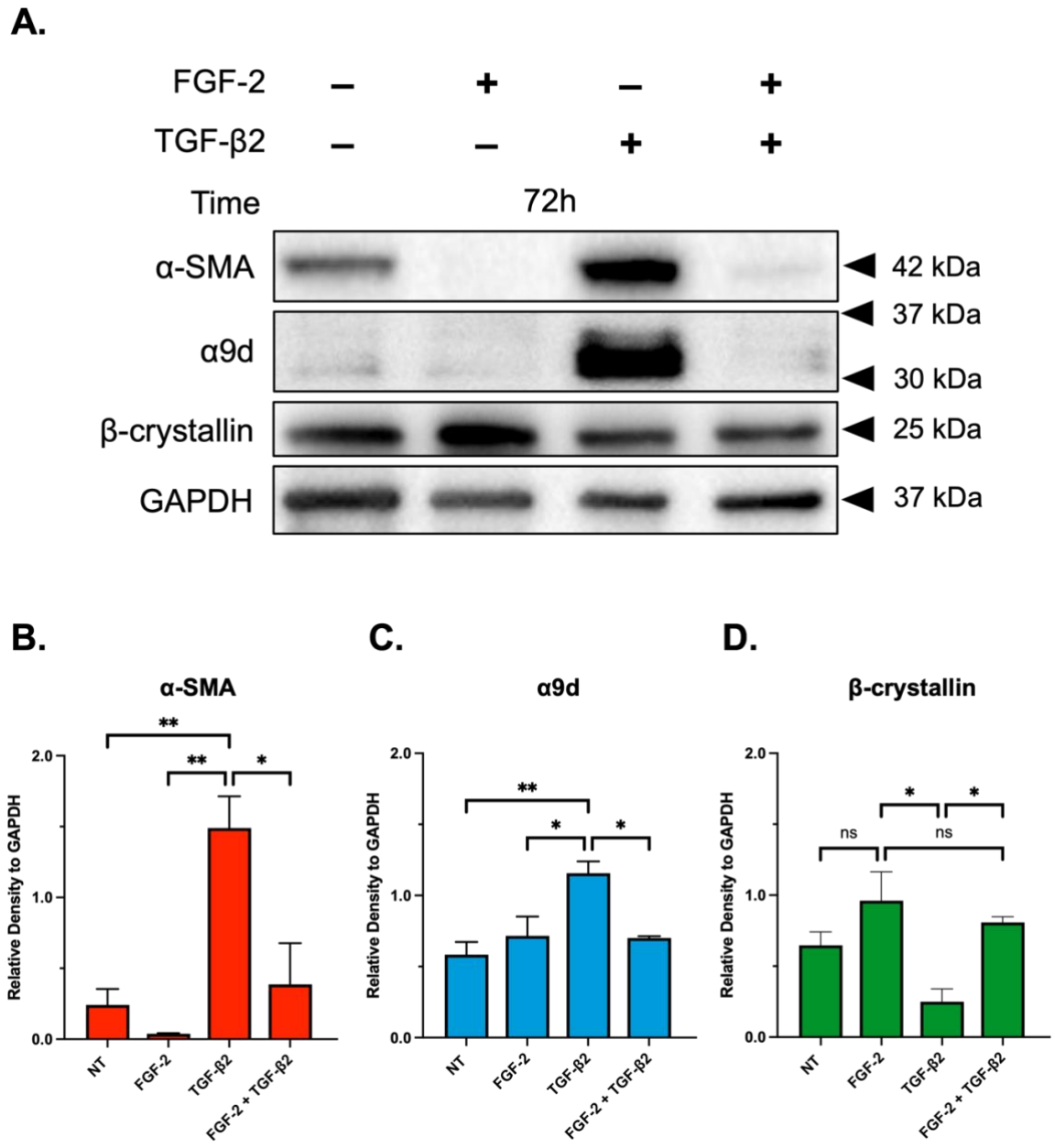

Figure 5.11. FGF-2 regulates TGF-β2-induced EMT marker expression in wholemount explants. Representative Western blot for alpha-tropomyosin (α9d), α-SMA, and β-crystallin in wholemount LEC explant lysates from three independent experiments. α-SMA (B), α9d (C), and β-crystallin (D) protein levels were normalised relative to loading control GAPDH. One-way ANOVA with the mean ± SEM and post-hoc Tukey's multiple comparisons test (* $p < 0.0332$, ** $p < 0.0021$).

5.5.8 Impact of FGF-2 on TGF-β2-Mediated Intracellular Signalling

5.5.8.1 Nuclear Translocation of Smad2/3

Given that FGF-2 can differentially regulate TGF-β2-mediated LEC behaviour, we tested its impact on TGF-β2 mediated Smad2/3-signalling. Active TGF-β2-signalling is evident with the nuclear translocation of phosphorylated Smad2/3 (Figures 5.12 and 5.13). We first examined LEC explants fixed 15 minutes after growth factor treatment and immunolabelled for t-Smad2/3 (Figure 5.12). Control and FGF-2-treated explants, in both central and peripheral explant regions, did not have any Smad2/3 within the nucleus, only in the cytoplasm (Figure 5.12 A–B, E–F). Cotreatment with FGF-2 and TGF-β2 also demonstrated no nuclear localisation at 15 minutes in CLECs (Figure 5.12 D) or PLECs (Figure 5.12 H). Treatment with TGF-β2 alone promoted Smad2/3-signalling activation with nuclear localisation in CLECs (Figure 5.12 C) and partial nuclear localisation in PLECs (Figure 5.12 G).

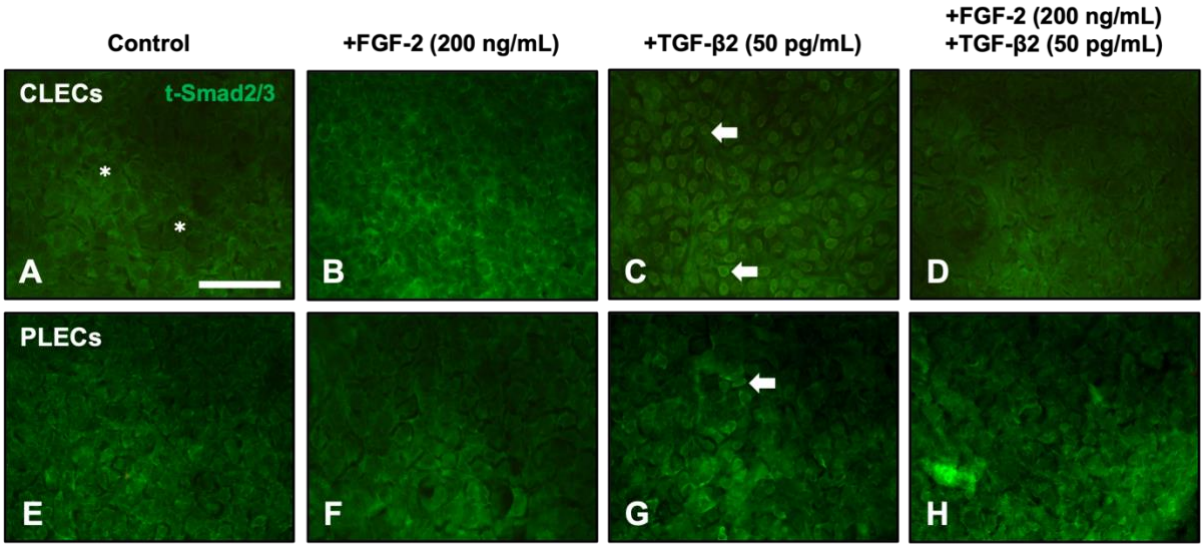

Figure 5.12. TGFβ-2-induced nuclear translocation of total Smad2/3 following 15 minutes of culture. Representative immunolabelling of total-Smad2/3 (t-Smad2/3, green) following 15 minutes of culture in P21 lens epithelial cell explants. Central (A–D) and peripheral (E–H) regions of explants with no growth factor treatment (Control; A, E), or FGF-2 alone (200 ng/mL; B, F), TGF-β2 alone (50 pg/mL; C, G), or co-treatment with FGF-2 and TGF-β2 (D, H). Cytosol (asterisks) and nuclear (arrowheads) localisation. Scale bar: 50 μm.

After 2 hours of culture, we saw visible regional differences between treatment groups regarding the localisation of Smad2/3 and quantified this using manual cell counting. Cells were counted based on the nuclear localisation of t-Smad2/3, and the mean percentage of t-Smad2/3 nuclear *vs.* cytoplasmic fluorescence was calculated (Table 5.2). In both the control (Figure 5.13 A, E) and the FGF-2 (Figure 5.13 B, F)-treated explants, we do not see any Smad2/3

nuclear localisation: 0.45–2.81% nuclear labelling (see Table 5.2 and Figure 5.13 I, J). In contrast, distinct nuclear localisation of Smad2/3 was evident throughout the TGF-β2-treated explants (Figure 5.13 C, G): 86.44–88.8% nuclear labelling. In the lens epithelial explants cotreated with FGF-2/TGF-β2, we observed prominent nuclear translocation of Smad2/3 in the CLECs (Figure 5.13 D, I): 44.87% nuclear labelling; however, in the PLECs the Smad2/3-labelling was primarily cytosolic with significantly reduced nuclear labelling: 19.85% (see Table 5.2 and Figure 5.13 H, J).

Table 5.2. Nuclear vs. cytoplasmic localisation of t-Smad2/3 in CLECs and PLECs.

Treatment	CLECs		PLECs	
	Nuclear	**Cytoplasmic**	**Nuclear**	**Cytoplasmic**
Control	0.35 ± 0.351	99.65 ± 0.351	2.91 ± 0.833	97.09 ± 0.833
FGF-2 (200 ng/mL)	1.70 ± 0.988	98.30 ± 0.988	2.55 ± 1.047	97.45 ± 1.047
TGF-β2 (50 pg/mL)	88.80 ± 4.217	11.20 ± 4.217	86.40 ± 5.444	13.60 ± 5.444
FGF-2 (200 ng/mL) + TGF-β2 (50 pg/mL)	44.87 ± 14.058	55.13 ± 14.058	19.85 ± 9.090	80.15 ± 9.090

The values are the mean percentage of fluorescence of t-Smad2/3 reactivity (%) ±SEM. *Abbreviations*: Central lens epithelial cells (CLECs); control (non-treated explants); peripheral lens epithelial cells (PLECs). Refer to Figure 5.13. Table previously published in (Flokis and Lovicu, 2023).

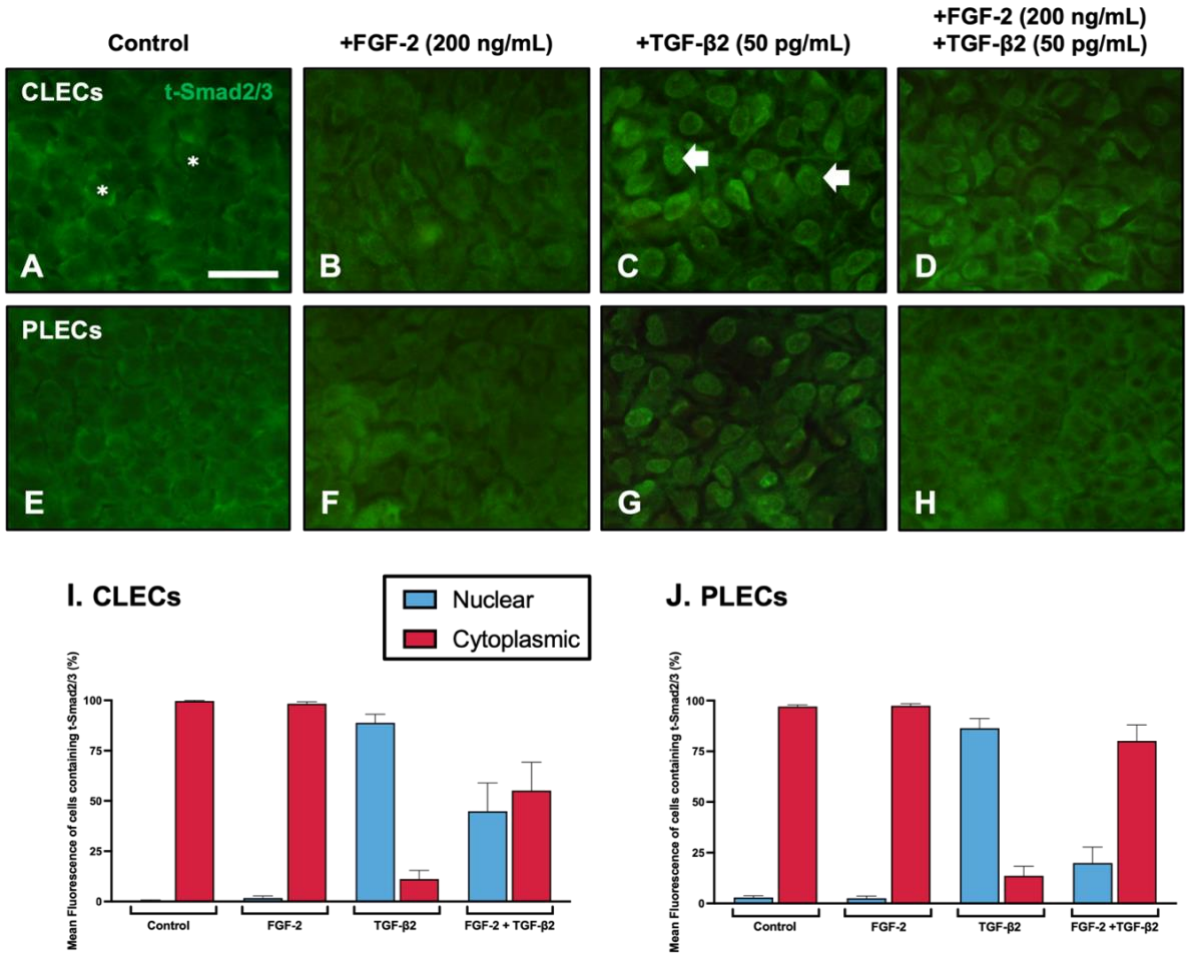

Figure 5.13. FGF-2 modulates TGFβ-2-induced Smad2/3 nuclear translocation. Immunolabelling of total Smad2/3 (t-Smad2/3, green) in LEC explants following two hours of culture (A–H). CLECs (A–D) and PLECs (E–H) in explants treated with no growth factors (control; A, E), FGF-2 (200 ng/mL; B, F), TGF-β2 (50 pg/mL; C, G), or cotreated with FGF-2/TGF-β2 (D, H). Examples of cytosolic (asterisks) and nuclear (arrowheads) localisation. Mean percentage (±SEM) fluorescence of cells with nuclear (blue) and cytoplasmic (red) t-Smad2/3 localisation in CLECs (I) and PLECs (J). Scale bar: 50 μm. Data previously published in (Flokis and Lovicu, 2023).

5.5.8.2 Smad2/3-Signalling

<u>*CLEC vs PLEC lysates.*</u> Treatment of the explants with FGF-2 did not impact p-Smad2/3 levels in CLECs when compared to similar levels in the control CLECs ($p = 0.9768$, Figure 5.14 A–B) or the PLECs ($p = 0.9310$, Figure 5.14 D–E) after 6 h of culture. Consistent with our immunofluorescent nuclear localisation of Smad2/3 (Figure 5.13), TGF-β2 significantly elevated p-Smad2/3 levels in the CLECs compared to the CLECs of the control explants ($p = 0.0061$) and the FGF-2-treated explants ($p = 0.0101$, Figure 5.14 A–B). In the CLECs of the explants cotreated with FGF/TGF-β2, there was no significant difference in p-Smad2/3 levels

when compared to the CLECs of the TGF-β2 (p = 0.5944) and the FGF-2-treated explants (p = 0.0585); however, p-Smad2/3 levels significantly increased in the cotreated CLECs compared to the control explants (p= 0.0334, Figure 5.14 A–B). In the PLECs, the TGF-β2 treated explants exhibited elevated p-Smad2/3 levels in comparison to the control (p = 0.0178), FGF-2 alone (p = 0.0403), and cotreated PLEC explants (p = 0.6496) (Figure 5.14 D, E). Compared to the control- and FGF-2-treated PLEC explants, cotreatment with FGF-2/TGF-β2 increased p-Smad2/3 levels (p = 0.0933 for the control, p = 0.2122 for FGF-2, Figure 5.14 D–E).

Wholemount LEC explant lysates. Control and FGF-2 treated wholemount LEC explants exhibited minimal activation of Smad2/3 at 6 hours of culture (p = 0.8267, Figure 5.15 A–B). Addition of TGF-β2 to wholemount explants elevated Smad2/3 levels compared to control (p = 0.1990) and FGF-2-treated (p = 0.5558) explants. Cotreatment with FGF-2 and TGF-β2 slightly reduced Smad2/3 reactivity compared wholemount explants treated with only TGF-β2 (p = 0.6192).

5.5.8.3 MAPK/ERK1/2-Signalling

CLEC vs PLEC lysates. Levels of phosphorylated ERK1/2 (p-ERK1/2) remained constant in the CLECs of the control and FGF-2-treated (p= 0.7703, Figure 5.14 A, C) explants after 6 hours but were elevated in the PLECs of the FGF-2-treated explants, compared to the control PLECs (p = 0.0140, Figure 5.14 D, F). TGF-β2 treatment of the explants slightly increased p-ERK1/2 activity in the CLECs compared to the levels in the CLECs of the control (p = 0.0227) and FGF-2 treated explants (p = 0.0880, Figure 5.14 A, C). In contrast, the PLECs of the TGF-β2-treated explants had decreased p-ERK1/2 levels compared to the PLECs of the control (p = 0.6711) and FGF-2-treated explants (p = 0.0033, Figure 5.14 D, F). CLECs in the explants cotreated with FGF-2/TGF-β2 had reduced p-ERK1/2 levels in comparison to the CLECs in the TGF-β2-treated (p = 0.0174), FGF-2-treated (p = 0.6641), and control explants (p = 0.9972) (Figure 5.14 A, C). Interestingly, the PLECs of the cotreated explants demonstrated a significant increase in their p-ERK1/2 levels in contrast to the low levels in the PLECs of the control (p = 0.0195) and TGF-β2-treated explants (p = 0.0242) (Figure 5.14 D, F).

Wholemount LEC explant lysates. Treatment with FGF-2 increased ERK1/2 activity in wholemount LEC explants at 6 hours of culture (Figure 5.15 A, C), compared to low levels of ERK1/2 activity in control explants (p = 0.1209). Explants exposed to TGF-β2 demonstrated low ERK1/2 levels when compared to FGF-2-treated explants (p = 0.2019). Cotreatment with FGF-2 and TGF-β2 appeared to elevate phosphorylation of ERK1/2, compared to control and

TGF-β2-only treated explants, although this difference was not statistically significant (p = 0.6201 for the control, p = 0.8205 for TGF-β2).

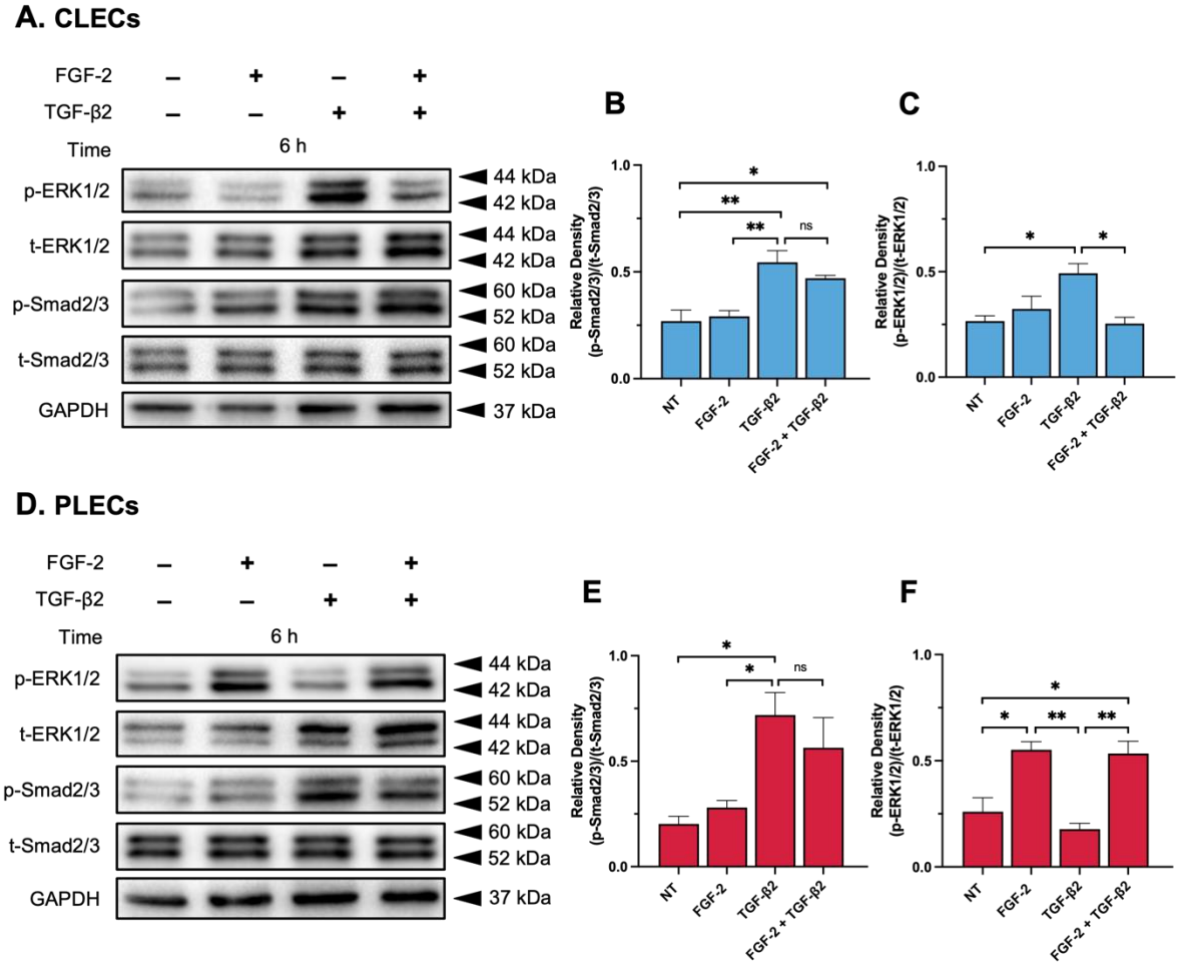

Figure 5.14. FGF-2 modulates TGF-β2-signalling. Representative Western blots demonstrating protein levels of phosphorylated and total Smads (p-Smad2/3 and t-Smad2/3) and MAPK/ERK1/2 (p-ERK1/2 and t-ERK1/2) in the control (non-treated, NT), FGF-2, TGF-β2, and FGF-2/TGF-β2 cotreated CLECs (A–C) and PLECs (D–F). The protein densitometry analysis shows changes in the levels of relative phosphorylation of Smad2/3 (B, E) and ERK1/2 (C, F). One-way ANOVA with the mean ± SEM and post-hoc Tukey's multiple comparisons test (ns = not significant, * P < 0.0332, ** P < 0.0021). Data previously published in (Flokis and Lovicu, 2023).

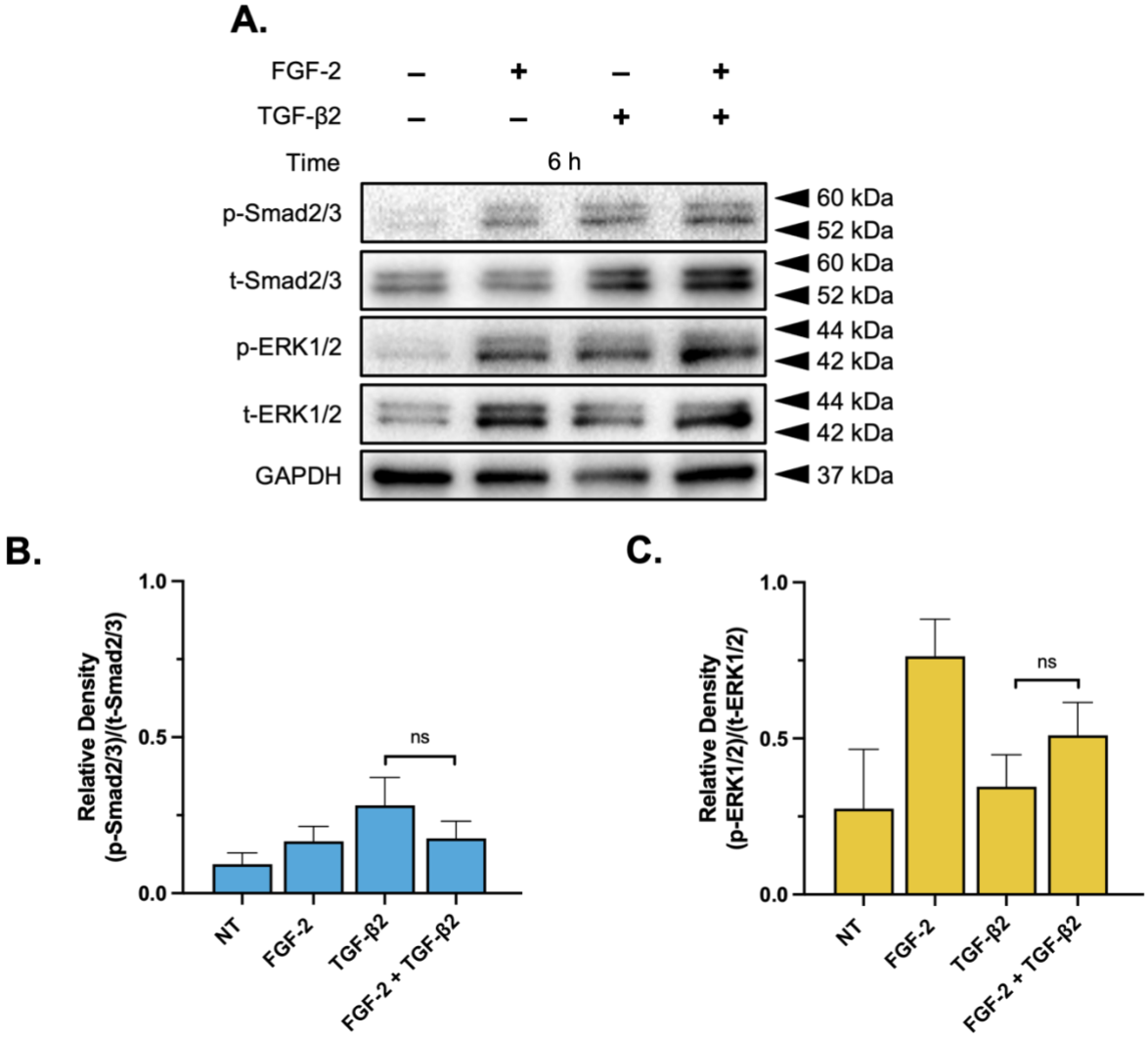

Figure 5.15. FGF-2 modulates TGF-β2-signalling in wholemount LEC explant lysates. Representative Western blots demonstrating protein levels of phosphorylated and total Smad2/3 signalling (p-Smad2/3, t-Smad2/3) and MAPK/ERK1/2 (p-ERK1/2, t-ERK1/2) proteins in wholemount LEC explants at 6 hours of culture (A). Protein levels of Smad2/3 and ERK1/2 were observed in control (non-treated, NT), FGF-2, TGF-β2, and FGF-2/TGF-β2 cotreated wholemount LEC explants. Both MAPK/ERK1/2 and Smad2/3 signalling proteins were compared relative to loading control GAPDH. Protein densitometry analysis shows changes in the levels of relative phosphorylation of Smad2/3 (B) and ERK1/2 (C). One-way ANOVA with the mean ± SEM and post-hoc Tukey's multiple comparisons test (ns = not significant).

5.6 DISCUSSION

The contents of this chapter established and characterised the impact of FGF-2 on the behaviour of LECs induced to undergo EMT in response to TGF-β. A lens fibre differentiating dose of FGF-2 was able to block low dose TGF-β2-induced lens EMT in only the peripheral LECs in explants (equivalent to the germinative region of the intact lens) and not in the central (more anterior) lens epithelia. As seen in previous wholemount rat lens epithelial cell explant models, we have demonstrated that CLECs and PLECs exposed to TGF-β2 alone undergo an EMT response, with no evidence of lens fibre differentiation (Liu et al., 1994; de Iongh et al., 2001b; Lovicu et al., 2004); however, in combination with FGF-2, FGF-2 potentiates this TGF-β2-induced activity, with elevation of canonical Smad2/3 signalling activity, as well as EMT-associated markers, more so in the CLECs.

For our lens epithelial explant model, we used relatively low doses of TGF-β2 (50 and 200 pg/mL) to induce an EMT response across a short culture period (Wojciechowski et al., 2017; Shu and Lovicu, 2019). This dose is physiologically representative of concentrations of TGF-β2 in its mature (approx. 100 pg/mL) and total (>3000 pg/mL) forms observed *in situ* (Kokawa et al., 1996). In addition, it is comparable to active forms of TGF-β2 (approx. 100–400 pg/mL) found in cataractous patients (Cousins et al., 1991; Kokawa et al., 1996; Ochiai and Ochiai, 2002; Yamamoto et al., 2005; Agarwal et al., 2015), during stress and inflammation in aqueous and vitreous humours (Connor et al., 1989; Jampel et al., 1990; Yamamoto et al., 2005; Boswell et al., 2010; Gao et al., 2022). Our use of a lower TGF-β2 dose contrasts to other studies that have used much higher doses (0.5–1.5 ng/mL) to elicit an EMT response in rodent lens cells (Cerra et al., 2003; Boswell et al., 2017; Kubo et al., 2017), which could potentially lead to off-target growth factor signalling activity. Exogenous addition of FGF-2 at a high dose encourages all lens epithelial cells (both CLECs and PLECs) to undergo a change in cell morphology typical of fibre differentiation (de Iongh et al., 1997; Lovicu and McAvoy, 2001; Iyengar et al., 2007; Dawes et al., 2014). In explants cotreated with TGF-β2 and FGF-2, FGF-2 appeared to protect PLECs from TGF-β-induced EMT by promoting a fibre differentiation response. We showed that the PLECs in these FGF-2/TGF-β2 cotreated explants had prominent elongated fibres, reminiscent of many earlier studies from our laboratory (Liu et al., 1994; Dawes et al., 2014). An elevated dose of TGF-β2, was able to prevent any fibre differentiation in the PLECs, leading to an enhanced EMT response in both central and peripheral cells. In addition, we demonstrated that the PLECs in the cotreated explants did not exhibit contractile properties as evidenced by the lack of capsular wrinkling in this region, unlike the region of the CLECs undergoing EMT.

The inhibition of lens epithelial cell contraction by FGF despite the presence of TGF-β has been shown in other fibrotic models to be dose dependent, such as in bovine LECs cultured in collagen I gel (Kurosaka et al., 1995) and valvular interstitial cells (VICs) modelling valvular fibrosis (Cushing et al., 2008), which is also correlated with reduced α-SMA expression.

We not only report how TGF-β can impact FGF-induced lens cell responsiveness but how FGF in turn influences TGF-β-induced responses in LECs, the main focus of our study. When we examined for changes in cytoskeletal and stress-fibre associated proteins, the CLECs in TGF-β/FGF-cotreated lens explants exhibited predominant α-SMA localisation and little to no β-crystallin, suggesting that these cells cannot resist the EMT process, despite the presence of a high differentiating dose of FGF-2. The co-influence of FGF-2 and TGF-β on fibre differentiation, epithelial, and EMT-associated marker expression has previously been reported in other models, including human lung epithelial cells and rat alveolar epithelial-like cells (Ramos et al., 2010), as well as E10 chick lens epithelial cells (Boswell et al., 2017) and lenses of postnatal mice (Wang et al., 2017). Despite the CLECs in the TGF-β/FGF-cotreated explants undergoing a prominent EMT response, we noted reduced α-SMA and α9d levels, compared to the TGF-β-alone-treated explants, suggesting that FGF-2 may be potentially compromising Tpm activity (a recruiter for actin assembly) and attenuating α-SMA stress fibre association. It has been previously shown that FGF may influence Tpm activity and expression, as well as cell biomechanics, in the presence of TGF-β (Kubo et al., 2017). For example, when murine LECs (MLECs) are cotreated with FGF-2/TGF-β2, the loss of Tpm1 corresponded with decreased α-SMA reactivity (Kubo et al., 2017). This same study also confirmed FGF-2 modulation of Tpm in HLECs, when cotreated with TGF-β2, with a significant reduction in both Tpm1 and Tpm2 levels (Kubo et al., 2017). We localised Tpm (α9d) in LECs undergoing different phenotypic changes in fibre differentiation, but more compellingly in cells undergoing EMT, where it was associated with the α-SMA-reactive stress fibres of myofibroblasts. This may be attributed to the fact that the α9d antibody we used specifically targets several isoform splice variant products of the αTm gene (*TPM1*), including Tpm1.4, Tpm1.6–1.9, and Tpm2.1, with some cross-reactivity also for Tpm3.1 (Schevzov et al., 2011). Tpm1.6, Tpm2.1, and Tpm3.1 have all previously been characterised as being stress-fibre associated and are suggested to play a role in TGF-β induced EMT (Gateva et al., 2017; Cheng et al., 2018; Parreno et al., 2020). FGF has shown a role in propagating stress-induced EMT in conjunction with TGF-β in other pathologies, such as wound healing in mice skin keratinocytes (Koike et al., 2020), and in the tumour stromal cell microenvironment of prostate fibroblasts (Strand et al., 2014). Consistent

with our findings, Koike et al. (2020) found that FGF-2 could not solely induce EMT in mice keratinocytes; however, in keratinocytes cotreated with FGF-2 and TGF-β1, there was a significant upregulation of cell migratory/motility and EMT-associated genes (e.g., *VIM* and *SNAI2*), similar to keratinocytes with only TGF-β1 stimulation. In a non-transformed mouse mammary gland epithelial cell line (NMuMG), TGF-β modulated FGF receptor activation, increased FGF-2 cell sensitivity, and promoted an EMT response through activation of ERK1/2 signalling (Shirakihara et al., 2011), highlighting the synergistic signalling role of these two growth factors.

To determine how FGF-2 was modulating and antagonising TGF-β2-induced EMT in PLECs of cotreated LEC explants, we explored changes in their signalling activity, namely changes to Smad2/3 and ERK1/2. In cotreated lens epithelial explants, we saw stronger signalling for the respective pathways in different regions; CLECs undergoing EMT had more pronounced p-Smad2/3 activity, while PLECs undergoing fibre differentiation had more pronounced p-ERK1/2-signalling. FGF is a well-known regulator of ERK1/2 within the lens, with its marked phosphorylation evident in lens cells within minutes post treatment (Le and Musil, 2001; Lovicu and McAvoy, 2001; Iyengar et al., 2007; Wang et al., 2008). While ERK1/2 has been shown to be required for lens epithelial cell proliferation, it is also very important for lens fibre differentiation (Le and Musil, 2001; Lovicu and McAvoy, 2001; Wang et al., 2008; Shin et al., 2015; Susanto et al., 2019). This differs from TGF-β2-induced EMT, where we found that while ERK is also involved in this EMT process, blocking ERK1/2 does not completely block TGF-β2-mediated EMT progression in lens epithelia (Wojciechowski et al., 2017; Shu et al., 2019b; Shu and Lovicu, 2019). In fact, canonical Smad2/3-signalling is most evident in EMT, as shown here in our cotreated CLECs, and in many earlier studies examining TGF-β2-induced lens EMT (Saika et al., 2002, 2004; Wormstone et al., 2006; Boswell et al., 2010, 2017; Shu and Lovicu, 2019).

While we and others have shown FGF-2 is not able to promote Smad2/3-signalling in LECs (Wang et al., 2017), FGF-2 was shown to impede nuclear localisation of Smad2/3 in PLECs in explants cotreated with TGF-β2; however, in CLECs of these same explants, FGF-2 appeared to have less of an impact on TGF-β2-induced Smad2/3-activity. How FGF-2 directly blocks Smad2/3 activity in PLECs is not clear but given the strong ERK1/2 activation in these cells, this may favour lens fibre differentiation and cell survival, as we see here and has been shown by others (Stolen et al., 1997; Iyengar et al., 2007, 2009; Wang et al., 2008). Conversely, FGF-mediated ERK1/2 signalling can correlate with the upregulation of TGF-β activity, as seen in

other fibrosis models (Strutz et al., 2001; Shirakihara et al., 2011; Kubo et al., 2017, 2018; Akatsu et al., 2019), as well as the current study where TGF-β-induced CLECs are associated with elevated ERK1/2-signalling. Similar to the current study, in valvular interstitial cells (VICs) modelling valvular fibrosis, it was shown that inhibition of this fibrosis was dependent on FGF-2-mediated MAPK signalling when cotreated with TGF-β1 (Cushing et al., 2008). This study demonstrated that FGF (10 ng/mL) prevented Smad3 nuclear localisation in VICs cotreated with TGF-β1 (5 ng/mL), and at higher doses (100 ng/mL), it was able to perturb TGF-β1-mediated α-SMA expression (Cushing et al., 2008), highlighting the ability of FGF to modulate canonical TGF-β signalling activity and downstream gene expression.

While we did observe a predominant fibre differentiation response in the PLECs of cotreated explants, this was not totally independent of TGF-β activity. Compared to explants treated with FGF-2 alone, we saw an increased level of β-crystallin in PLECs cotreated with TGF-β. This is supported by early studies that showed a requirement for TGF-β receptor-signalling in lens fibre differentiation (de Iongh et al., 2001b), where the loss of TGF-β receptor-signalling using a dominant negative form of its receptor overexpressed in lens, led to fibre cell death, in a region where we would expect to see elevated β-crystallin *in situ* (de Iongh et al., 2001b). This is consistent with other studies using lens explants, that showed FGF-induced lens fibre differentiation was associated with elevated TGF-β receptor reactivity (de Iongh et al., 2001b, 2001a). Interestingly, aberrant elevation of β-crystallin synthesis in response to TGF-β has previously been seen in other ocular pathologies, including high myopia (Zhu et al., 2021). This was reportedly due to the build-up of aberrant lens fibre cells and was proposed to be via TGF-β-induced Smad2/3 signalling (Zhu et al., 2021).

Although not completely understood, crosstalk between FGF and TGF-β signalling has proven influential in mediating various fibrotic disorders and carcinoma progression. For example, a study implementing mouse tumour-associated endothelial cells (TECs) demonstrated how FGF can promote a differential cell response by reducing TGF-β-induced contractile and myofibroblastic properties, while concurrently promoting cell proliferation and motility (Akatsu et al., 2019). A similar finding was observed in primary human dermal fibroblasts (HDFs), whereby FGF-2 with TGF-β1 cotreatment, both positively and negatively regulated fibroblast transition into cancer associated fibroblasts (CAFs) (Bordignon et al., 2019). This same study also showed how this FGF-2/TGF-β1 treatment of HDFs can downregulate common CAF-activated and EMT-associated markers (e.g., *ACTA2*, *ITGA11*, and

COL1A1) as well as upregulate cell motility and morphogenetic genes (e.g., *HGF*, and *BMP2*) (Bordignon et al., 2019).

Additional fibroblast models have conveyed a role for TGF-β in regulating FGF expression and activity through Smad2/3- and MAPK-signalling (Yang et al., 2008; Strand et al., 2014). In a study by Strand et al. (2014), mouse prostate gland fibroblasts treated with TGF-β1 and MAPK inhibitors, ERK1/2 (UO126) and p38 (SB203580), significantly reduced FGF-2 mRNA expression when compared to control fibroblasts (no inhibitor administration). A study by Ramos et al. (2010) reported that FGF-1 was able to antagonise and revert TGF-β1-induced EMT in human and rat lung epithelial cells. Despite this, the inhibition of FGF-1-mediated MAPK-signalling in these same cells was not sufficient to revert TGF-β1-induced EMT (Ramos et al., 2010), further signifying the importance of FGF/TGF-β modulated signalling during EMT development.

It has been documented that Smad3 is potentially more essential for TGF-β induced EMT and associated gene transduction, than Smad2 (Datto et al., 1999; Banh et al., 2006; Strand et al., 2014). The current study showed that despite weaker reactivity for the Smad2/3 complex in FGF/TGF-β treated PLECs, both CLECs and PLECs in cotreated explants favoured stronger lower molecular weight immunolabelling for Smad3, suggesting FGF mediation of Smad3 activity; however, we cannot rule out that the antibody used may have a higher affinity for p-Smad3 than p-Smad2. Future studies may benefit in confirming the specific role of Smad3 in TGF-β induced lens EMT, by accurately quantifying differences in Smad2 *vs.* Smad3 phosphorylation, as previously suggested after lens injury (Saika et al., 2002, 2004; Banh et al., 2006).

We showed that FGF can modulate Smad2/3 activity in wholemount explants when cotreated with TGF-β2. The high FGF insult in these F/t cotreated explants, resulting in the activation of MAPKs, may potentially cause the regulation and/or disruption at the Smad2 and Smad3 phosphorylation linker region, as previously seen in carcinoma models (Kamaraju and Roberts, 2005; Hough et al., 2012) and reviewed (Matsuzaki, 2012; Kamato et al., 2020). Using the current model, future studies could assess the interaction of other MAPKs, such as p38 MAPK, known to be activated in the presence of either TGF-β or FGF (Dawes et al., 2009; Boswell et al., 2010).

Research into the mechanisms surrounding differential types of PCO involving lens fibre cell types is ongoing and is believed to be due to FGF/TGF-β interactions during EMT induction (Cerra et al., 2003; Mansfield et al., 2004; Symonds et al., 2006; Boswell et al., 2010, 2017;

Kubo et al., 2018). As FGF is a major factor influencing normal lens fibre differentiation, it is important to understand what promotes aberrant fibre differentiation during pearl PCO development at the lens equator (Lovicu et al., 1995, 2004; Wormstone and Eldred, 2016; Boswell et al., 2017). *In situ*, for ASC and for post-operative PCO, the more anterior lens epithelial cells are likely exposed to a high insult of TGF-β, and relatively low levels of FGF normally found in the aqueous humour. At the lens equator, however, epithelial cells in the posterior chamber are regularly exposed to elevated levels of FGF, and regardless of any increased TGF-β levels, the cells here likely undergo aberrant fibre differentiation, leading to pearl PCO. This may result from the heightened sensitivity to FGF of these peripheral LECs, namely due to their elevated levels of high-affinity FGF receptor tyrosine kinase (RTK) receptors, compared to the central lens epithelia (Lovicu and McAvoy, 1992; de Iongh et al., 1996, 1997; Kondo et al., 2014). *In situ*, during lens fibrosis, we do not see EMT resulting in cell death, likely due to survival growth factors present within the ocular media. Given the findings from the current study, we propose that FGF is a putative survival factor *in situ*, maintaining fibre cells at the lens equator and the myofibroblastic phenotype leading to fibrotic PCO. Further studies investigating differences/changes in levels of FGF and TGF-β receptors, between central and peripheral lens cells in cotreated explants, may be a key factor in determining lens cell fates *in situ*. We also cannot rule out that changes in expression of RTK antagonists, such as Sprouty and Spreds (Shin et al., 2015; Zhao et al., 2018; Susanto et al., 2019), including those more specific for FGF, such as Sef (Newitt et al., 2010), in these active regions of the lens may be protective of peripheral LECs from any aberrant TGF-β insult of which they have previously been reported to block (Shin et al., 2015).

Despite a high dose FGF-2 differentially modulating TGF-β2 induced EMT, we note some F/t-cotreated explants with an exacerbated EMT and fibre differentiation response in central and peripheral regions. In addition, marker levels in these regions with strong expression of α-SMA in CLECs, and PLECs favouring β-crystallin, conveyed a similar response to F/t-treated explants. When assessing total LECs from wholemount F/t-treated explants, we also saw a significant decrease in EMT/cytoskeletal marker expression and a preferential upregulation of β-crystallin. This change in cell phenotype had previously been reported in P10 rat explants cotreated with TGF-β1 (20 ng/mL) and FGF-2 (40 ng/mL) (Liu et al., 1994).

By isolating the whole lens epithelial explant with its higher abundance of FGF receptors in peripheral lens epithelia, an overall FGF-2 driven mechanism is potentially favoured and, as a result, promoting more FGF-mediated MAPK/ERK1/2 than Smad2/3 signalling, to prevent

widespread TGF-β-induced EMT. This reinforces the nature of the differential dose-dependent activity of FGF-2 in this model, acting both as a promoter and modulator of TGF-β-induced EMT, as shown previously in lens (Cerra et al., 2003; Mansfield et al., 2004; Kubo et al., 2017, 2018) and other systems (Shirakihara et al., 2011; Kurimoto et al., 2016; Bordignon et al., 2019).

5.7 CONCLUSION

A fine balance between levels of FGF-2 and TGF-β2 can promote differential responses in lens epithelial cells. More specifically, this responsiveness is spatially regulated, with the anterior central lens epithelia more sensitive to EMT induction, whilst peripheral cells primarily undergo fibre differentiation in the presence of high levels of FGF, avoiding apoptotic cell death associated with EMT. This induced heterogeneous population of cells in lens epithelial explants may provide an alternative model better suited to the study of the cellular processes at play *in situ*, leading to the formation of ASC, and more importantly both fibrotic and pearl forms of PCO.

CHAPTER 6: THE ROLE OF p38α MAPK IN TGF-β INDUCED LENS EMT

6.1 PREFACE

This chapter involves some technical support by members of the Lens Research Laboratory at The University of Sydney, Australia. All contributions are stated below:

Mary Flokis

- Designed and executed and analysed experiments as described
- Writing and assembling manuscript

Zi Lin Wang

- Provided technical assistance pertaining to Figures 6.2 and 6.3

Youhaoran (Ellen) Wu

- Provided technical assistance pertaining to Figure 6.10

Frank J. Lovicu

- Consulted on experimental design and editing this chapter

6.2 INTRODUCTION

In previous chapters, we have shown that treatment of LECs with TGF-β leads to EMT in both mouse and rat LEC explants. As TGF-β activation is implicated in the development of ASC and PCO, it is crucial to further understand the mechanisms of canonical (Smad-dependent) and non-canonical (Smad-independent) TGF-β signalling, and how these pathways contribute. p38 is a stress-induced MAP kinase protein activated by various internal and external environmental factors, including UV radiation, oxidative stress, as well as growth factors/cytokines, such as TGF-β (New and Han, 1998; Cuadrado and Nebreda, 2010; Bai et al., 2015; Han et al., 2020; Canovas and Nebreda, 2021). The p38 MAPK family is comprised of four isoforms: p38α, p38β, p38γ, and p38δ (Cuenda and Rousseau, 2007; Cuadrado and Nebreda, 2010; Han et al., 2020), that have differential expression in both normal and aberrant tissue types, particularly p38α and p38β, found in myofibroblasts during stress-induced fibrosis and tumourigenesis (Stambe et al., 2004; Sebe et al., 2008; Xu et al., 2018).

p38 has been shown to be activated and even upregulated with TGF-β in various models (Hanafusa et al., 1999; Liao et al., 2001; Chen et al., 2013; Boswell et al., 2017; Hou et al., 2021). Activation of the p38 MAPK pathway has been linked to altered cell cytoskeletal organisation leading to changes in cell morphology and migration (Huot et al., 1998; Hedges et al., 1999; Bakin et al., 2002, 2004; Sebe et al., 2008; Dvashi et al., 2015). In the lens, TGF-β has been shown to stimulate p38 activation in human LE cells (Dawes et al., 2009), as well as in embryonic chick lens cells lines (DCDMLs) during epithelial to myofibroblast transition (Boswell et al., 2017). Based on previous studies, targeting this p38 pathway using different inhibitor compounds, such as SB203580, SB220025, and SB239068, has proven it to be a potential mechanism for modulating TGF-β-induced EMT, as well as cell proliferation, migration, and apoptosis in various systems (Zhou and Menko, 2004; Meyer-ter-Vehn et al., 2006; Menon et al., 2015; Ling et al., 2016; Boswell et al., 2017; X. Han et al., 2018). In recent years, there has been reports pertaining to the specificity of the inhibitor compounds targeting p38α, as they have been shown to target both p38α and p38β (Kumar et al., 1999; Laping et al., 2002; Menon et al., 2015), as well as other unrelated off target pathways (Birkenkamp et al., 2000; Lali et al., 2000; McGuire et al., 2013).

In this study, we revisited the role of p38α during lens EMT in rat lens explants, using a reportedly more selective p38α MAPK inhibitor. For this, we employed Skepinone-L, first conducting dose optimisation studies to determine its efficacy on TGF-β-induced lens EMT, examining its impact on epithelial, cytoskeletal, and EMT-associated marker protein changes.

By targeting p38α before and after TGF-β2 exposure, we assessed when p38 was active in lens EMT. By characterising and targeting non-canonical downstream TGF-β signalling proteins in the rodent lens, this may lead to a better understanding of the development of lens fibrosis and the effectiveness of potential therapeutic agents to reduce and/or prevent early onset of secondary cataract.

6.3 MATERIALS AND METHODS

6.3.1 Rodent tissue collection and primary cell culture

Ocular tissue was acquired from Wistar rats at the postnatal age of 21 days old (± 1 day). All animal ethics, welfare, and housing protocols have been previously described (see Chapter 2: Section 2.1). The LEC explant system (anterior lens capsule) using P21 rat lenses were isolated and pinned to the base of 35mm Nunc tissue culture dishes, as previously described (see Chapter 2). LEC explants were maintained in freshly supplemented M199 and incubated at 37°C, 5% CO_2, until treatment.

6.3.2 Preparation of p38α MAPK inhibitor compound

Skepinone-L (506174, Merck; MW = 425.42 g/mol), a selective p38α MAPK inhibitor (Koeberle et al., 2012; Borst et al., 2013) was diluted in 235 µl of tissue culture grade DMSO to achieve a stock concentration of 50 mM. This stock was then vortexed until Skepinone-L was incorporated into solution and aliquoted. For concentrations of 1 mM Skepinone-L, this stock was diluted 1:50 with DMSO. Working stocks of 0.1 mM Skepinone-L/DMSO were also prepared and stored at 4°C.

6.3.3 Treatment with TGF-β2 and Skepinone-L

LEC explants were treated with TGF-β2 (200 pg/mL) to induce an EMT response over 5 days of culture. For dose optimisation studies, explants were exposed to Skepinone-L for 1 hour at increasing concentrations (0.5 µM, 1 µM, 2 µM, and 5 µM) prior to TGF-β2 treatment (Figure 6.1 A). To determine the inhibitory efficacy of p38α on the progression of TGF-β-induced lens EMT, Skepinone-L was added to cells at 15 minutes prior to TGF-β2 (Figure 6.1 A), at the same time as TGF-β2 (Figure 6.1 B), as well as post TGF-β2 treatment after 15 minutes or 2 hours (Figure 6.1 C). Explants with no growth factor treatment, or Skepinone-L alone, were classed as controls.

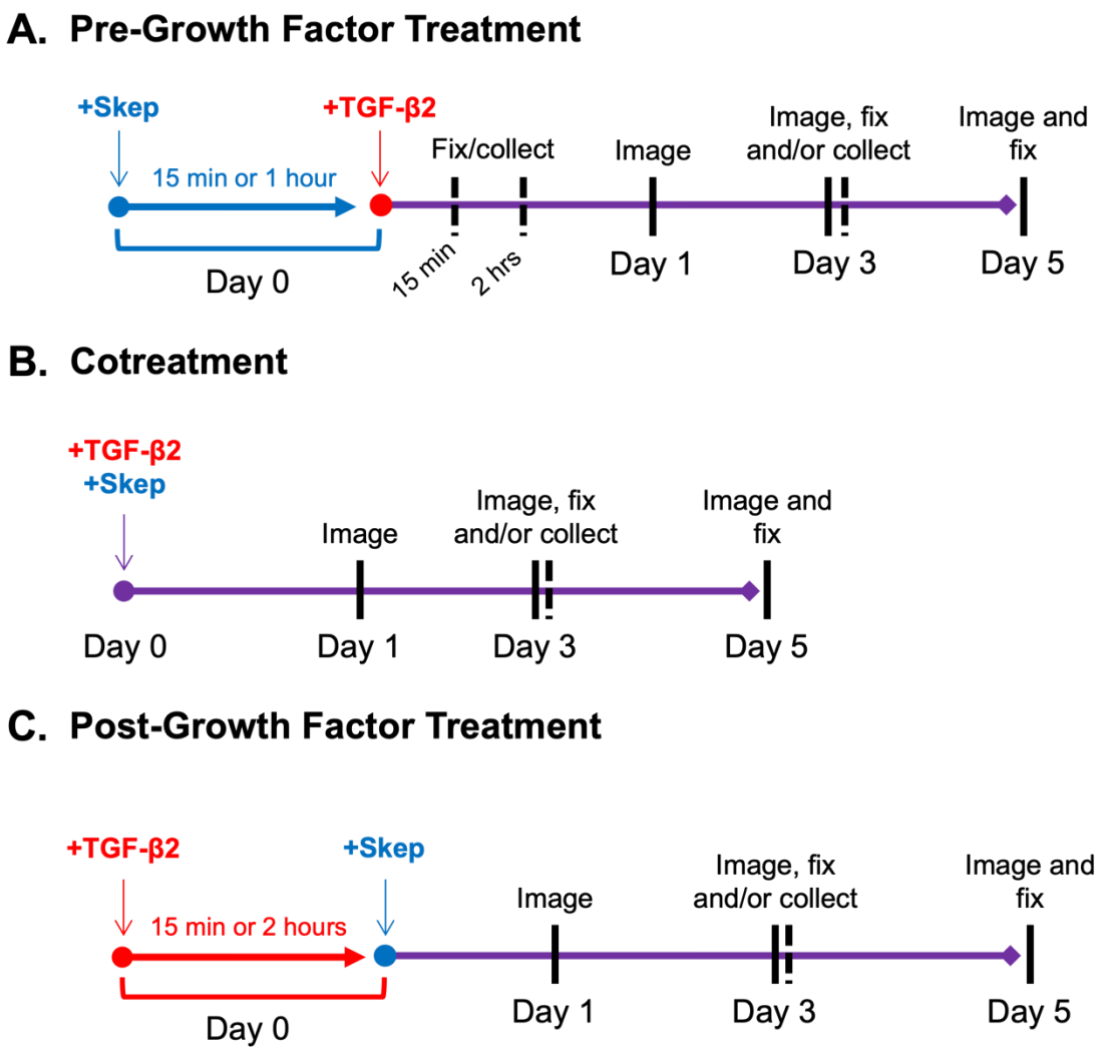

Figure 6.1. Schematic timelines illustrating treatment with p38 MAPK inhibitor, Skepinone-L, in conjunction with TGF-β2. LEC explants were exposed to Skepinone-L (blue) A) 15 minutes or 1-hour before TGF-β2 addition (red), B) combined with TGF-β2 treatment, or C) 15 minutes or 2 hours after TGF-β2 treatment. Explants were fixed or collected for immunofluorescence and/or western blotting at 15 minutes, 2 hours, or 72 hours (dashed lines). Assessment and imaging of changes in LEC morphology was conducted across 5 days of culture (solid lines).

6.3.4 Phase contrast microscopy

Assessment for changes in LEC morphology were conducted using phase contrast microscopy. For all experiments, including inhibitor dose optimisation and pre-, co-, and post-growth factor treatment studies, LEC explants were monitored daily over 5-days. Images were taken at day 1 (24 hours post treatment), day 3, and day 5, unless stated otherwise (Figure 6.1). Phase contrast images were captured as previously discussed (see Chapter 2: Section 2.7).

6.3.5 Immunofluorescence with LEC explants

At respective timepoints, explants were fixed in 10% NBF (10 min) and then rinsed in PBS/BSA (0.1%, *w/v*) for 3 x 5 minutes followed by permeabilisation in 0.05% Tween-20 detergent diluted in PBS/BSA (3 x 5 min). Tween-20 was cleared with 3 x 5 min in PBS/BSA washes before adding normal goat serum (3% NGS) as a blocking buffer, for 30 minutes at room temperature. For observing differences in epithelial, cytoskeletal, and EMT-associated marker expression and localisation, LEC explants were probed for α-SMA (mouse, A2547: Sigma Aldrich), β-catenin (rabbit, ab6302: Abcam), and α9d (mouse, donated by Prof. Peter Gunning from UNSW, Australia), all diluted 1:150–1:200 in NGS/PBS/BSA. For experiments investigating TGF-β2 Smad-dependent and independent signalling activity in LEC explants, the following primary antibodies were applied: t-Smad2/3 (rabbit, 8685: Cell Signaling Tech.) and total p38 (p38, rabbit, 8690: Cell Signaling Tech.). These downstream signalling proteins were diluted in NGS/PBS/BSA (1:100–1:200) and remained for overnight incubation (4ºC). Explants were rinsed in PBS/BSA (3 x 5 min) before applying the appropriate Alexa Fluor conjugated secondary antibody, anti-mouse (ab150116: Abcam) and anti-rabbit (ab150077: Abcam), for 2 hours. Explants were then washed in PBS/BSA followed by a 5-minute wash in Hoechst dye (6 mg/mL) for cell nuclei visualisation. Tissue was again rinsed (3 x 5 min PBS/BSA washes) and mounted using 10% PBS in glycerol, in preparation for epifluorescent microscopy.

6.3.6 Western blotting analysis

Following treatment, rat LEC explant tissue was prepared as previously described methods (see Chapter 2: Sections 2.11.1–2.11.3). 10 µg of total protein was loaded onto a 12% acrylamide SDS-PAGE gel at 70 V for 50 minutes then 110 V for 2 hours. Protein samples were then transferred onto a PVDF membrane for 1 hour at 100 V. Membranes were incubated in 2.5% BSA in TBST for 1 hour at room temperature. Primary antibodies were added to respective membranes, α-SMA (mouse), β-catenin (rabbit), α9d (mouse), p38 MAPK (rabbit), p-p38 (rabbit, 4511, Cell Signaling Tech.), GAPDH (mouse, G8795, Sigma-Aldrich), β-actin (rabbit, 4970, Cell Signaling Tech.), for overnight incubation (4ºC). All primary antibodies were diluted in BSA/TBST at 1:1000–1:2000. Membranes were washed in TBST (3 x 5 min) then probed with respective HRP-conjugated secondary antibodies; anti-mouse (7076, Cell Signaling Tech.) and anti-rabbit (7074, Cell Signaling Tech.), diluted 1:5000 in TBST for 2 hours at room temperature. Secondary antibodies were removed by rinsing membranes in TBST (3 x 10 min).

Membranes were incubated for 30 seconds in an HRP-conjugated chemiluminescent substrate (1:1; WBKLS0500, Merck Millipore) for protein visualisation using ChemiDoc imaging and ImageLab software analysis (version 6.1.0 build 7, Bio-Rad Laboratories Inc.). Densitometry was conducted by assessing the raw intensity values of each protein band for quantification.

6.3.7 Statistical Analysis

For all morphological and immunofluorescent assays, a minimum of 4 explants were fixed per treatment group, per experiment, for a total of three independent experimental replicates (n=3). For western blot analysis, a minimum of 6 x LEC explants comprised one sample, for each treatment group, across three independent experimental replicates. For epithelial and EMT-associated marker protein levels, densitometry was conducted and the proteins of interest, β-catenin and α-SMA, were compared relative to the total intensity of the loading control, GAPDH. Western blots examining differences in Tpm1.6/1.7 and Tpm2.1 protein levels when probed for α9d, in the presence or absence of Skepinone-L and/or TGF-β2, were calculated using densitometry relative to the loading control β-actin. All data was graphed using GraphPad Prism (Version 10) and represented as one-way analysis of variance (ANOVA), by comparing the mean of each column (treatment group) with each other column (treatment groups). A post-hoc Tukey's multiple comparisons test was also conducted to confirm statistical significance. Values represented as the standard error of the mean (± SEM) with $p < 0.05$ considered statistically significant.

6.4 RESULTS

6.4.1 Skepinone-L inhibits TGF-β-induced EMT in rat LEC explants

6.4.1.1 Cell Morphology

We first tested Skepinone-L and optimised the ideal dose to potentially inhibit TGF-β-induced lens EMT (Figure 6.2). We exposed rat LEC explants to Skepinone-L (1 μM) and monitored for changes across 5 days of culture (Figure 6.2 A–C). Skepinone-L alone did not induce any morphological changes and maintained the lens epithelial cell phenotype across the culture period. As shown in previous chapters (see Chapters 3–5), addition of TGF-β2 (200 pg/mL) induced an EMT response in LEC explants as early as day 3 of culture (Figure 6.1 E), with capsular modulation and cells undergoing a transdifferentiation response into myofibroblastic cells (Figure 6.2 F). No major changes were observed at day 1 (Figure 6.2 D). Pre-treatment with 0.5 μM and 1 μM of Skepinone-L maintained the lens epithelial cell phenotype, with tightly-packed cells present and this was sustained across 5 days despite the addition of TGF-β2 (Figure 6.2 G–L). Slightly enlarged cells were noted in Skepinone-L (1 μM) pre-TGF-β2 treated LEC explants at day 1 of culture (Figure 6.2 J) that were more settled and packed by day 3 and 5 (Figure 6.2 K–L). At day 5, the Skepinone-L (1 μM)/TGF-β2 treated explants appeared to have more refractile bodies (Figure 6.2 L). TGF-β2 induced changes to lens epithelial cell morphology at day 1 (Figure 6.2 M) in explants pre-treated with 2 μM Skepinone-l demonstrated slightly enlarged cells; however, these cells settled by day 3 (Figure 6.2 N) with some refractile bodies indicative of impending cell death. By day 5, pockets of lens cells were maintained in regions across the explant with some areas of exposed bare lens capsule, although there was no evidence of capsular wrinkling (Figure 6.2 O). Skepinone-L doses > 5 μM induced capsular wrinkling and modulation, as well as cell loss due to cell transdifferentiation across 3–5 days of culture (Figure 6.2 Q–R). No morphological changes were noted at day 1 in these treated explants (Figure 6.2 P). Therefore, a dose > 5 μM of Skepinone-L was insufficient to inhibit TGF-β2-induced lens EMT.

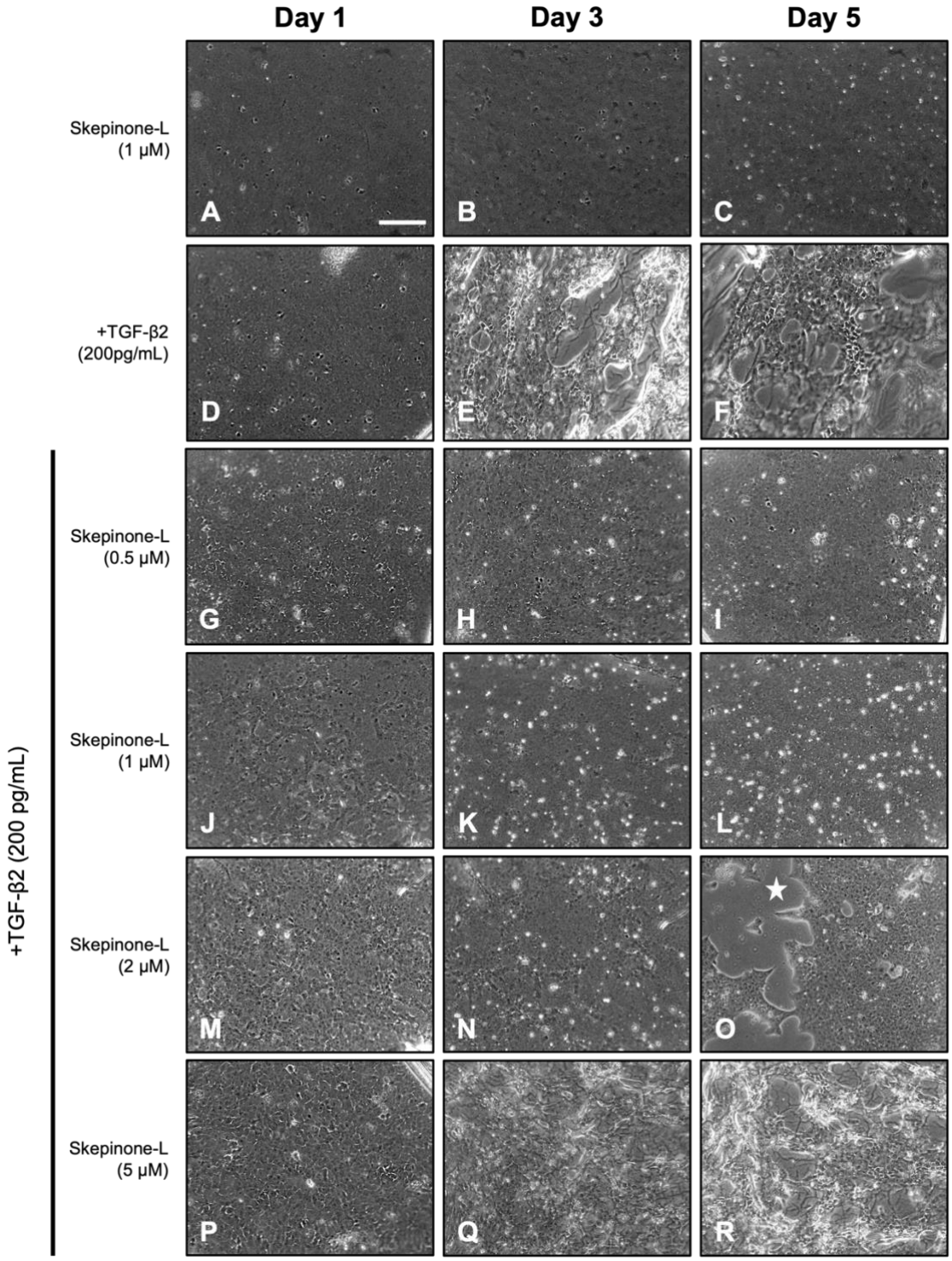

Figure 6.2. Optimisation of p38 MAPK inhibitor Skepinone-L in rat LEC explants. Phase contrast images of LEC explants across 5 days of culture (A–R). p38 MAPK inhibitor Skepinone-L (1 µM) only explants sustained LECs across 5 days (A–C), causing no morphological changes. Explants exposed to 1-hour pre-treatment with Skepinone-L before the addition of TGF-β2 (200 pg/mL). Skepinone-L doses ranged from 0.5–5 µM. TGF-β2-treated explants administered Skepinone-L <5 µM maintained the epithelial cell phenotype, including Skepinone-L 0.5 µM (G–I), 1 µM (J–L), and 2 µM (M–O). Skepinone-L 2 µM/TGF-β2 treated explants retained lens cells and exposed regions of lens capsule (O, star) with no capsular wrinkling. Explants pretreated with 5 µM Skepinone-L underwent TGF-β2-induced EMT (P–R). Scale bar: 200 µm.

6.4.1.2 EMT marker immunolocalisation in TGF-β2-induced LECs

In control LEC explants, widespread epithelial cell junctional localisation of β-catenin was noted at 72 hours (Figure 6.3 A). A similar response was observed in explants exposed to Skepinone-L (1 μM) only (Figure 6.3 C), and both control and Skepinone-L-treated explants expressed minimal intensity and cytoplasmic localisation of α-SMA (Figure 6.3 B, D). Lens epithelial cell explants treated with TGF-β2 had reduced β-catenin levels and a dispersed membrane localisation (Figure 6.3 E). TGF-β2 treated explants had increased α-SMA labelling and actin stress fibre localisation (Figure 6.3 F), reflective of LECs transitioning into more myofibroblastic cells. LEC explants exposed to Skepinone-L doses between 0.5–2 μM, administered prior to the addition of TGF-β2, demonstrated similar membrane localisation for β-catenin as unstimulated (control) LEC explants (Figure 6.3 G, I, K); however, TGF-β2-induced actin stress fibre localisation of α-SMA in Skepinone-L (0.5 μM) pre-treated explants, compared to the more cytoplasmic localisation in Skepinone-L pre-treated explants at 1 μM (Figure 6.3 J) and 2 μM (Figure 6.3 L). Explants treated with Skepinone-L (5 μM) and TGF-β2 did not exhibit the normal lens epithelial cell phenotype (Figure 6.2), with elongated cell nuclei, a dispersed β-catenin immunolabel, and bare patches of lens capsule, indicative of migration or cell loss (Figure 6.3 M). Cells from this treatment group demonstrated strong stress fibre localisation of α-SMA (Figure 6.3 N).

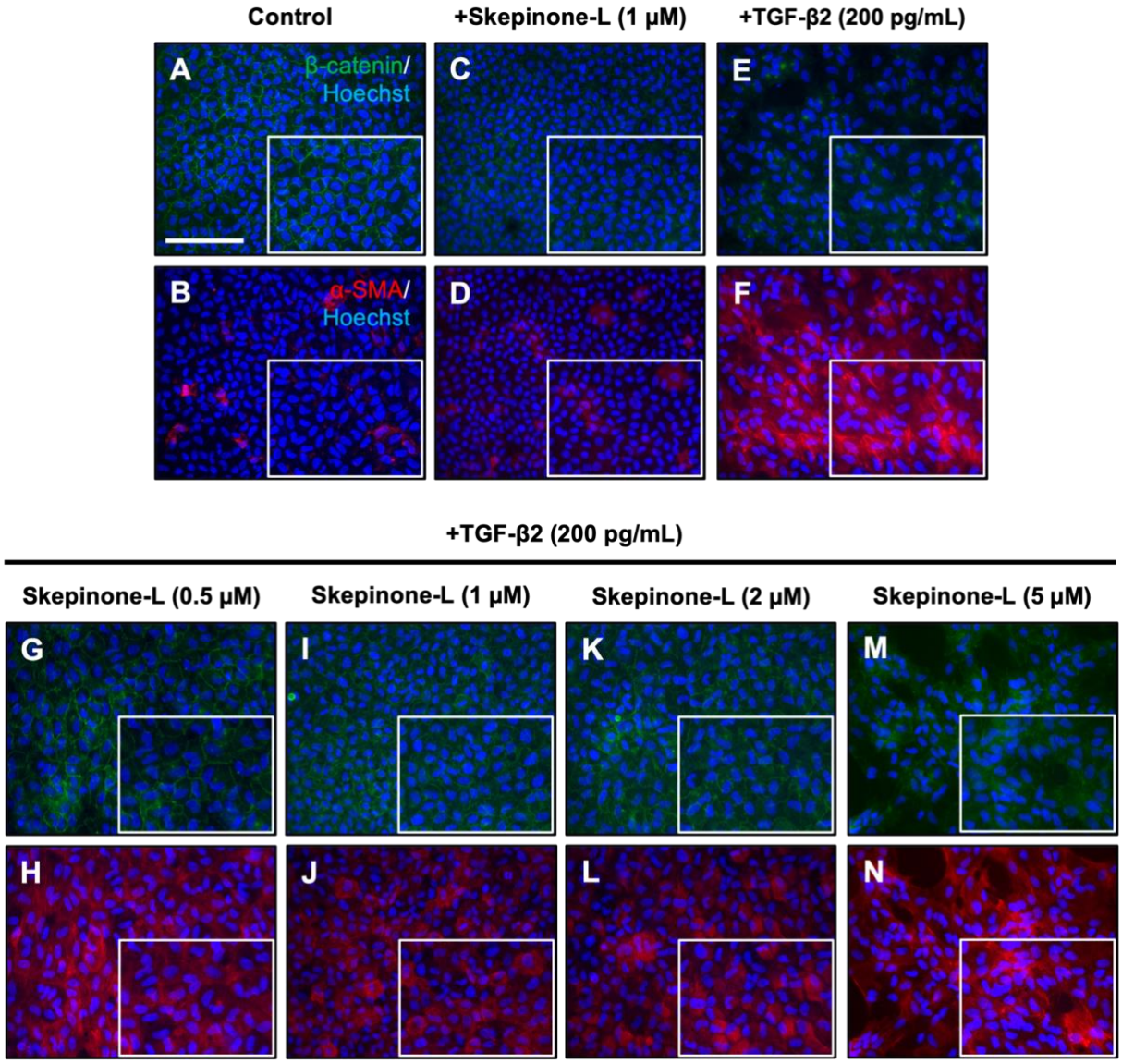

Figure 6.3. Dose response immunofluorescence of Skepinone-L in LEC explants probing for epithelial and EMT markers at 72 hours. Explants immunolabelling for α-SMA (red) and β-catenin (green) with Hoechst nuclear stain (blue). Control (non-treated, A, B), Skepinone-L only (1 μM, C, D), TGF-β2 only (200 pg/mL, E, F) treated explants. LEC explants exposed for 1 hour with Skepinone-L in an increasing range of concentrations, including 0.5 μM (G, H), 1 μM (I, J), 2 μM (K, L), and 5 μM (M, N), followed by TGF-β2 treatment. Zoomed-in inset (white squares). Scale bar: 100 μm.

Western blotting was used to observe any differences in EMT marker total protein levels with an increasing concentration of Skepinone-L added with TGF-β2 after 72 hours (Figure 6.4 A–C). Despite the differences in spatial immunolocalisation of β-catenin between treatment groups (Figure 6.3), there was no statistically significant difference observed for β-catenin protein levels across all treatment groups (p = 0.4473, Figure 6.4 C). A summary of the statistical analysis between all treatment groups is stated in Table 6.1.

Table 6.1. Summary of β-catenin protein levels in rat LEC explants.

Treatment group comparisons	*P* value[1]
NT *vs.* Skepinone-L (1 μM)	0.9960
NT *vs.* TGF-β2 (200 pg/mL)	0.9604
NT *vs.* Skepinone-L (0.5 μM) + TGF-β2	>0.9999
NT *vs.* Skepinone-L (1 μM) + TGF-β2	0.8694
NT *vs.* Skepinone-L (2 μM) + TGF-β2	0.9997
NT *vs.* Skepinone-L (5 μM) + TGF-β2	>0.9999
Skepinone-L (1 μM) *vs.* TGF-β2	0.7232
Skepinone-L (1 μM) *vs*. Skepinone-L (0.5 μM) + TGF-β2	0.9961
Skepinone-L (1 μM) *vs*. Skepinone-L (1 μM) + TGF-β2	0.9959
Skepinone-L (1 μM) *vs*. Skepinone-L (2 μM) + TGF-β2	0.9529
Skepinone-L (1 μM) *vs*. Skepinone-L (5 μM) + TGF-β2	>0.9999
TGF-β2 *vs.* Skepinone-L (0.5 μM) + TGF-β2	0.9597
TGF-β2 *vs.* Skepinone-L (1 μM) + TGF-β2	0.3333
TGF-β2 *vs.* Skepinone-L (2 μM) + TGF-β2	0.9971
TGF-β2 *vs.* Skepinone-L (5 μM) + TGF-β2	0.8668
Skepinone-L (0.5 μM) + TGF-β2 *vs.* Skepinone-L (1 μM) + TGF-β2	0.8708
Skepinone-L (0.5 μM) + TGF-β2 *vs.* Skepinone-L (2 μM) + TGF-β2	0.9997
Skepinone-L (0.5 μM) + TGF-β2 *vs.* Skepinone-L (5 μM) + TGF-β2	>0.9999
Skepinone-L (1 μM) + TGF-β2 *vs.* Skepinone-L (2 μM) + TGF-β2	0.6631
Skepinone-L (1 μM) + TGF-β2 *vs.* Skepinone-L (5 μM) + TGF-β2	0.9655
Skepinone-L 21 μM) + TGF-β2 *vs.* Skepinone-L (5 μM) + TGF-β2	0.9918

[1] One-way ANOVA with Tukey's multiple comparisons test

*Statistically significant difference between treatment groups ($P < 0.05$)

Abbreviations: Non-treated LEC explants (NT). Refer to Figure 6.4 C.

Control (non-treated) and Skepinone-L (1 μM) only treated LEC samples showed no differences in levels of α-SMA (p = 0.9982, Figure 6.4 A–B). Addition of TGF-β2 significantly increased α-SMA protein levels relative to control and Skepinone-L only treated LEC lysates ($p < 0.0001$). Pre-treatment of Skepinone-L at increasing doses (0.5–5 μM), in the presence of TGF-β2, also significantly increased α-SMA protein expression in comparison to control LEC explants (NT *vs.* Skepinone-L (0.5 μM) + TGF-β2; p = 0.0016, NT *vs.* Skepinone-L (1 μM) +

TGF-β2; $p = 0.0008$, NT *vs.* Skepinone-L (2 μM) + TGF-β2; $p = 0.0026$, NT *vs.* Skepinone-L (5 μM) + TGF-β2; $p = 0.0461$); however, there was no significant decrease in α-SMA protein levels noted in TGF-β2 exposed LEC explants pre-treated with Skepinone-L at doses 0.5 μM, 1 μM, and 2 μM, when compared to explants only treated with TGF-β2 ($p > 0.2499$). A significant reduction in α-SMA protein levels was noted in lens explants exposed to Skepinone-L (5 μM) before TGF-β2, compared to TGF-β2 only treated explants ($p = 0.0141$).

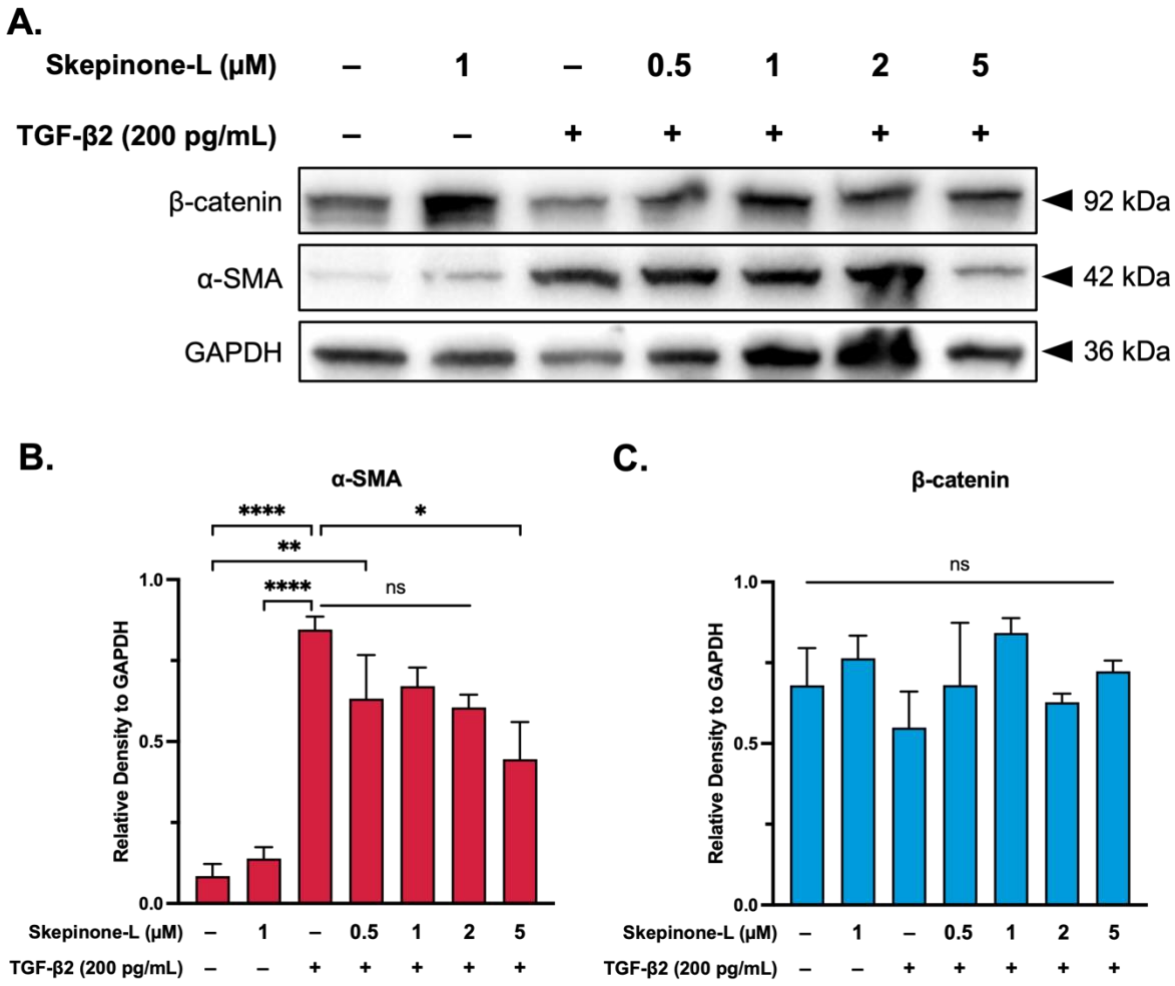

Figure 6.4. Dose optimisation of Skepinone-L in the presence or absence of TGF-β2 at 72 hours. Representative western blot of rat LEC explant lysates from control (non-treated, NT), Skepinone only (1 μM), or pre-treated with Skepinone-L at varying doses (0.5–5 μM) 1-hour prior to TGF-β2 exposure (A). EMT (α-SMA) and epithelial (β-catenin) markers were probed, and densitometry was calculated relative to loading control GAPDH (B, C). Statistical analysis conducted using one-way analysis of variance (ANOVA) with post-hoc Tukey's multiple comparisons test. Error bars represent standard error of the mean (±SEM). ns = not significant, *$P < 0.0332$, **$P < 0.0021$, ****$P < 0.001$.

When we reduced our pre-treatment time of Skepinone-L to 15 minutes, we saw similar morphological and immunolabelling trends in Skepinone-L/TGF-β2-treated LEC explants. Explants exposed to Skepinone-L (1 μM) 15 minutes before addition of exogenous TGF-β2 showed no morphological changes were observed across 5 days of culture, with LECs still present and tightly packed (Figure 6.5 A–C). We did observe minor capsular wrinkling that was maintained across culture. At day 3 of culture, Skepinone-L/TGF-β2-treated explants were fixed and immunolabelled for β-catenin and α-SMA (Figure 6.5 D–E). β-catenin localised in the cell membranes of these lens epithelial cells (Figure 6.5 D). In these same cells, α-SMA localised in the cytoplasm of some LECs (Figure 6.5 E). At 72 hours, we collected lens explant samples for western blotting in the presence or absence of TGF-β2, and/or with 15-minute pre-treatment of Skepinone-L (Figure 6.5 F–G). There was no significant difference between α-SMA protein levels in control or Skepinone-L only LEC explants ($p > 0.9999$, Figure 6.5 G). Addition of TGF-β2 elevated α-SMA expression compared to non-treated and Skepinone-L only LEC explants ($p < 0.0001$). 15-minute Skepinone-L pre-treatment in TGF-β2-treated explants increased α-SMA total protein levels in comparison to low levels in control and Skepinone-L only explants ($p = 0.0005$). A reduction in α-SMA in pre-treated Skepinone-L/TGF-β2 lens explants, compared to TGF-β2-treated lens explants, was not statistically significant ($p = 0.1841$). Despite changes to β-catenin spatial distribution observed in our dose optimisation immunofluorescent assays (see Figure 6.3), we did not observe any significant β-catenin protein level changes across all treatment groups. For representative western blots of β-catenin protein levels in TGF-β2-treated LEC lysates pre-treated with Skepinone-L (1 μM) at 72 hours of culture, see Supplementary Figure 6.1 and Supplementary Table 6.1.

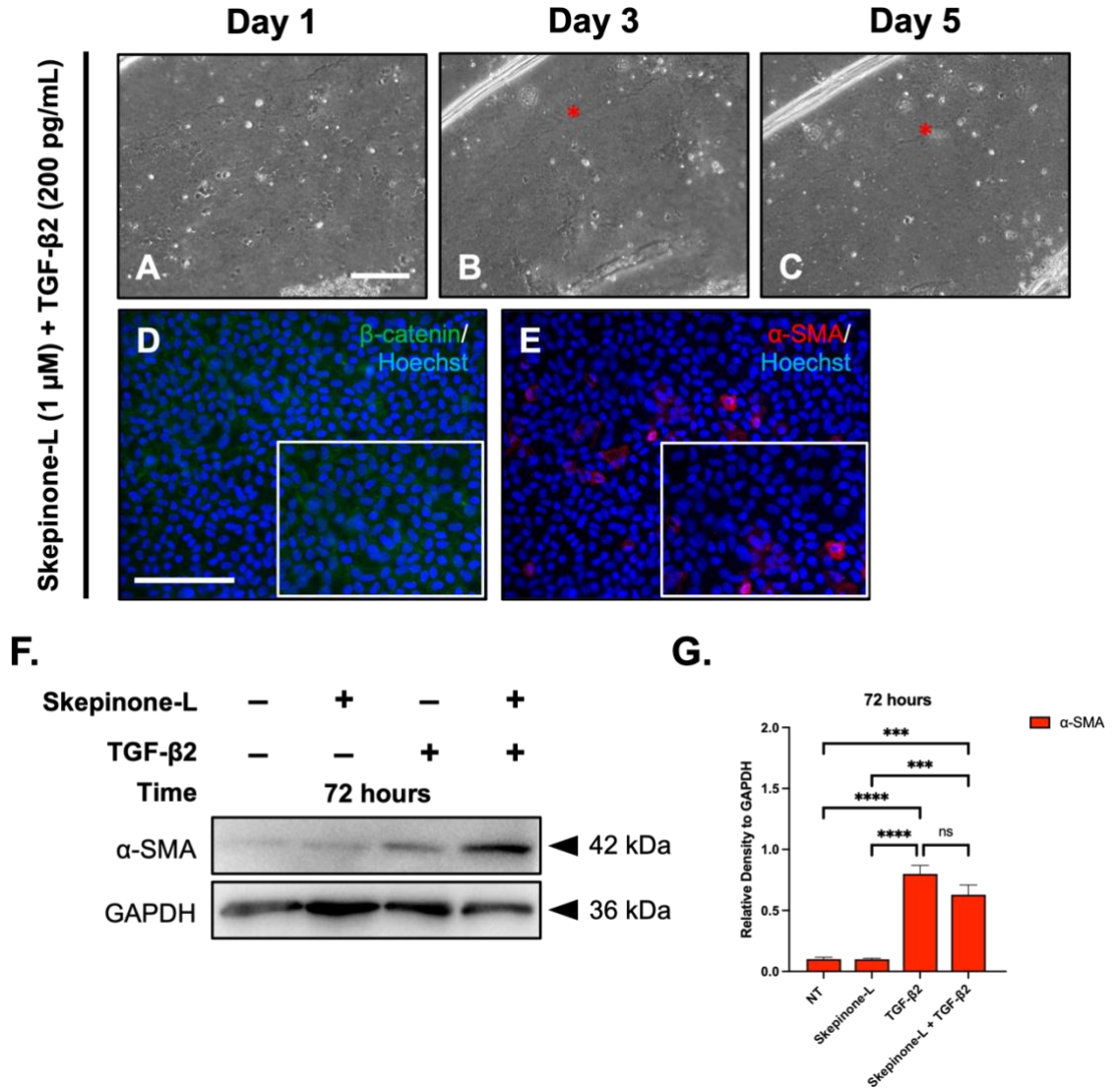

Figure 6.5. 15 minutes pre-treatment with Skepinone-L inhibits EMT in TGF-β2-treated lens explants. Phase contrast imaging of rat explants across 5 days of culture pre-treated with Skepinone-L (1 µM) 15 minutes prior to TGF-β2 (200 pg/mL) treatment (A–C). 15-minute pretreatment saw no significant changes to the tightly packed epithelial phenotype across 5 days except for some capsule wrinkling (asterisks) and refractile bodies. Immunolabelling for α-SMA (red) and β-catenin (green) with Hoechst nuclear dye (blue) at day 3. Pre-treatment of Skepinone-L at 15 minutes before addition of TGF-β2 (D–E). Scale bar: 200 µm (A–C), 100 µm (D–E). Zoomed-in inset (white squares). Western blot of non-treated (NT), Skepinone-L only, TGF-β2 only, and 15-minute pre-treated Skepinone-L/TGF-β2 explants collected at 72 hours (F). Densitometry of α-SMA conducted relative to GAPDH (G). Statistical analysis performed using one-way ANOVA and post-hoc Tukey's multiple comparisons test (ns = not significant, *** $P < 0.002$, **** $P < 0.001$).

6.4.1.3 Skepinone-L regulates Tpm1 and Tpm2 derived isoforms in TGF-β2-induced LECs

Pre-treatment with Skepinone-L at a concentration between 0.5–1 μM prevented TGF-β2-induced lens EMT, particularly phenotypical changes to LECs (Figures 6.2–6.3). For ongoing studies, 1 μM for Skepinone-L treatment was selected. In previous chapters, we identified that Tpm1.6/1.7 and Tpm2.1 are markers for TGF-β2-induced lens EMT. At 72 hours of culture, lens explants were fixed and immunolabelled using α9d (Figure 6.6 A–D), specific for several Tpm isoforms, including Tpm1.4, Tpm1.6–1.9, and Tpm2.1 (Schevzov et al., 2011). Given the broad specificity of α9d for six isoforms, that are known to form isoform bundles at actin structural sites (Glass et al., 2015; Pathan-Chhatbar et al., 2018), we were unable to distinguish each of these Tpm isoforms using immunofluorescence. Therefore, we will refer to Tpm1.4, Tpm1.6–1.9, and Tpm2.1 detection as α9d in our assays (see Table 6.2). In control (non-treated) explants, we detected low basal levels of α9d in cytoplasmic actin filaments of LECs (Figure 6.6 A). This intracellular cytoplasmic localisation pattern was observed in LEC explants exposed to Skepinone-L (1 μM) only (Figure 6.6 B). TGF-β2-induced lens explants exhibited elevated intensity for α9d, particularly in actin stress fibres of transdifferentiating myofibroblastic cells (Figure 6.6 C). We also noted that TGF-β2-treated explants had fewer cells compared to non-treated and Skepinone-L only LEC explants. 1-hour pre-treatment of Skepinone-L in TGF-β2 treated explants exhibited α9d localising predominantly in cytoplasmic actin fibres surrounding cell nuclei (Figure 6.6 D), similar to control and Skepinone-L alone explants.

Table 6.2. Immunolocalisation of α9d in rat LEC explants

Treatment	Intracellular localisation of α9d		Intensity of α9d	Comments
	Cytoplasmic (actin filaments)	Stress fibre actin filaments		
Control	X	-	Low	Localisation in actin filaments of LEC cytoplasm
Skepinone-L (1 μM)	X	-	Low	Localisation similar to control LECs
TGF-β2 (200 pg/mL)	-	X	High	Localisation in stress fibres of myofibroblastic cells
Skepinone-L (1 μM) + TGF-β2 (200 pg/mL)	X	-	Moderate	Heightened reactivity for α9d in regions of actin bundles

Immunofluorescent labelling of α9d detects Tpm1.4, Tpm1.6–1.9, and Tpm2.1
"X" indicates region of α9d immunolocalisation
Abbreviations: lens epithelial cells (LECs)
Refer to Figures 6.6 A–D.

As shown in previous chapters, using western blotting, we were able to detect total Tpm1.6/1.7 and Tpm2.1 levels (using α9d), as well as the individual levels of Tpm1.6/1.7 and Tpm2.1 (Figure 6.6 E–F). Skepinone-L only treated explants did not significantly increase Tpm1.6/1.7 or Tpm2.1 protein levels, similar to the low basal levels in control LEC explants (see Table 6.2, $p > 0.8000$). A significant increase in Tpm1.6/1.7 protein levels was noted in TGF-β2-treated lens explants in comparison to non-treated and Skepinone-L alone treated explants (Table 6.3 and Figure 6.6 F). This trend was also observed in Tpm2.1 increased protein levels, specifically in TGF-β2-treated explants, in comparison to non-treated and Skepinone-L treated lens explants (Table 6.3). Total α9d (combined Tpm1.6/1.7 and Tpm2.1) protein levels were significantly increased in TGF-β2-treated explants compared to control explants ($p = 0.0068$), as well as Skepinone-L only explants ($p = 0.0038$). Pre-treatment with Skepinone-L in TGF-β2-treated explants significantly reduced Tpm2.1 protein levels compared to TGF-β2-treated explants ($p = 0.0261$). A decrease in total α9d levels as well as Tpm1.6/1.7 levels in Skepinone-L/TGF-β2-treated explants, when compared to lens explants treated only with TGF-β2, was not significant (Table 6.3).

Table 6.3. Summary of α9d protein levels in rat LEC explants.

Tpm isoform(s)	Treatment group comparisons[1]					
	NT *vs.* Skep	NT *vs.* TGF-β2	NT *vs.* Skep + TGF-β2	Skep *vs.* TGF-β2	Skep *vs.* Skep + TGF-β2	TGF-β2 *vs.* Skep + TGF-β2
Tpm1.6/1.7	>0.9999	0.0134*	0.6184	0.0129*	0.6058	0.1125
Tpm2.1	>0.8979	0.0122*	0.9713	0.0037*	0.6806	0.0261*
Total α9d	0.9852	0.0068*	0.6044	0.0038*	0.4130	0.0612

[1]One-way ANOVA with Tukey's multiple comparisons test
*Statistically significant difference between treatment groups ($P < 0.05$)
Abbreviations: Non-treated LEC explants (NT), Skepinone-L (Skep), tropomyosin (Tpm). Refer to Figure 6.6 E–F.

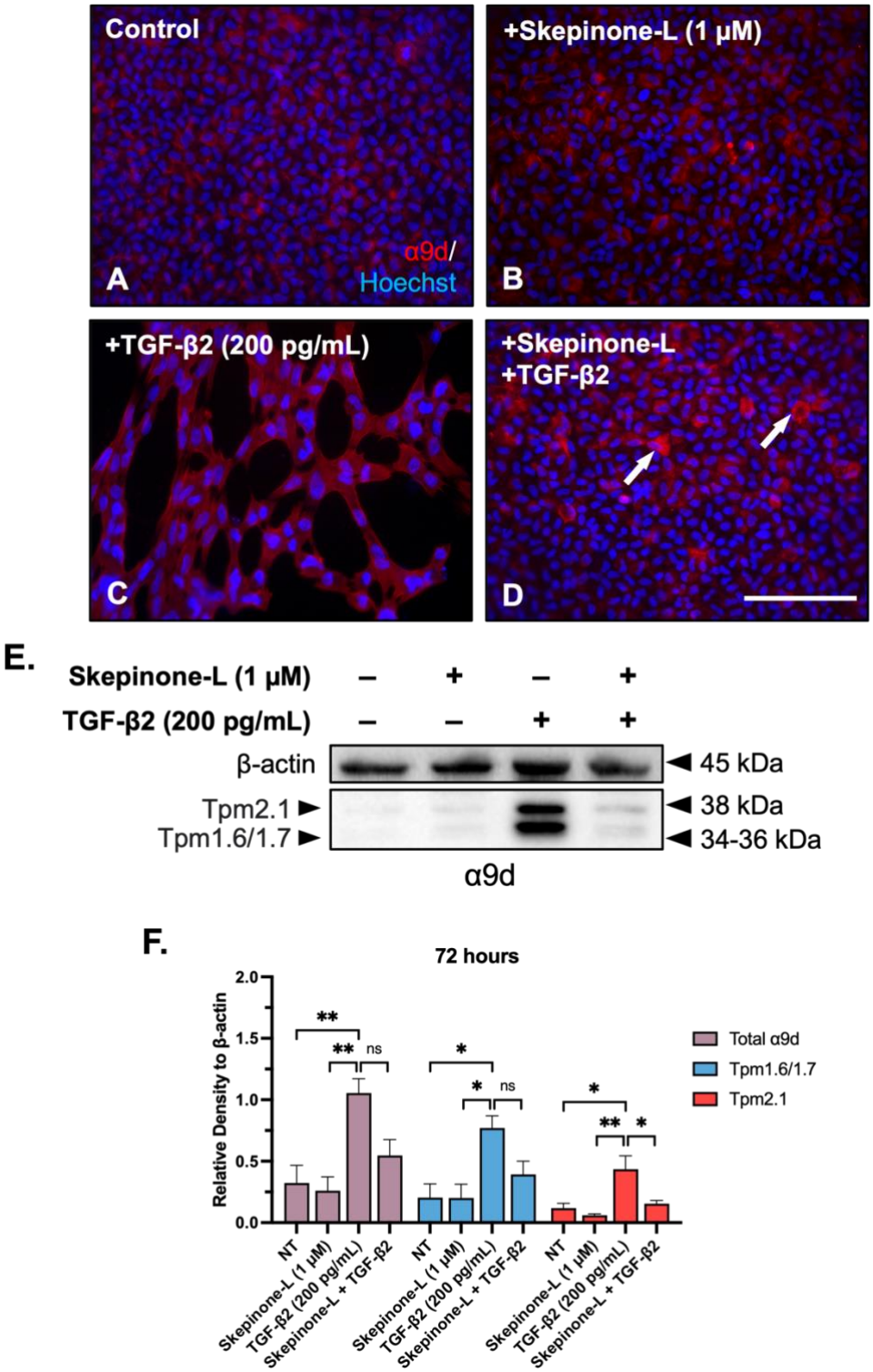

Figure 6.6. Inhibition of p38 reduces Tropomyosin activity during TGF-β2 induced EMT. Immunofluorescence of alpha tropomyosin (α9d; red), specific for Tpm1.4, 1.6–1.9, and 2.1, in rat LEC explants at 72 hours with nuclear counterstain Hoechst (blue). Control (non-treated, A), Skepinone-L (1 μM, B), TGF-β2 (200 pg/mL, C), and TGF-β2-induced explants exposed to 1-hour pre-treatment with Skepinone-L (D). Bundles of Tpm isoforms (white arrows). Scale bar: 100 μm (A–D). Western blot of α9d probed in rat LEC explant samples in the presence or absence of Skepinone-L and/or TGF-β2 (E). Tpm1.6/1.7, Tpm2.1, and total α9d (sum of Tpm1.6/1.7 and Tpm2.1) protein levels calculated using densitometry relative to β-actin (E, F). Statistical analysis conducted using one-way ANOVA with post-hoc Tukey's multiple comparisons test (ns = not significant, *$P < 0.0332$, **$P < 0.0021$). Graphed data represented as standard error of the mean (± SEM).

6.4.2 Pre-treatment with Skepinone-L does not impact TGF-β canonical Smad signalling

We examined the inhibition of p38 MAPK activity 1-hour prior to TGF-β2 treatment, and its potential link to other TGF-β signalling molecules, notably total Smad2/3 (t-Smad2/3). At 15 minutes of culture, t-Smad2/3 localised within the cytoplasm of control (non-treated) LECs (Figure 6.7 A), as well as LECs exposed to Skepinone-L (1 µM) (Figure 6.7 B). This cytoplasmic localisation of t-Smad2/3 was sustained across 2 hours in both control and Skepinone-L-treated LECs (Figure 6.7 E–F). Treatment with TGF-β2 (200 pg/mL) induced nuclear localisation of t-Smad2/3 as early as 15 minutes of culture (Figure 6.7 C), with some cytoplasmic reactivity, that was maintained at 2 hours post growth factor treatment (Figure 6.7 G). Pre-treated Skepinone-L/TGF-β2-treated explants exhibited t-Smad2/3 nuclear localisation at both 15 minutes (Figure 6.7 D) and 2 hours of culture (Figure 6.7 H).

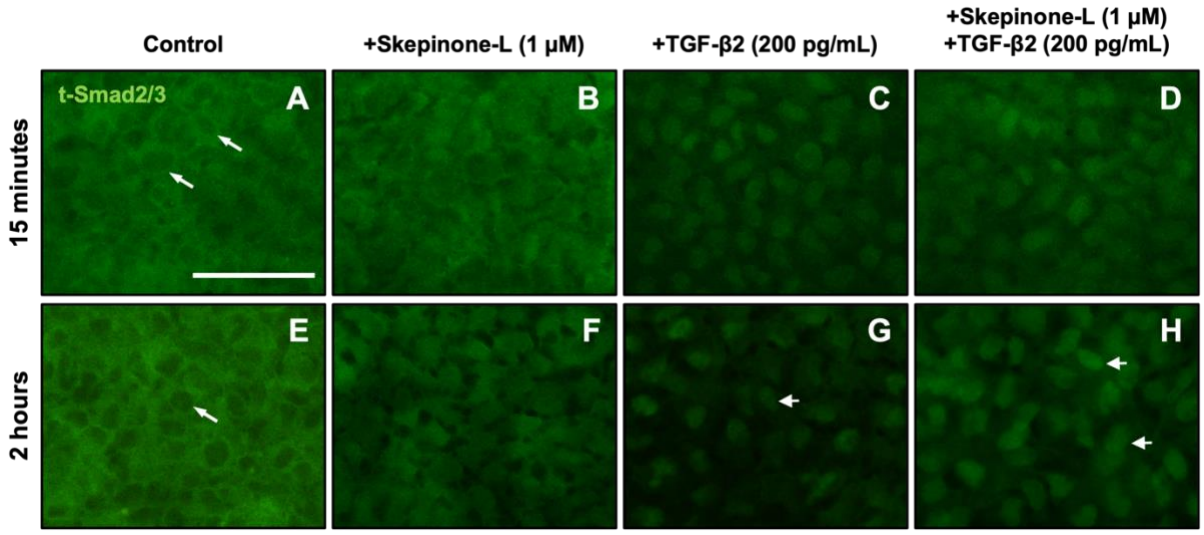

Figure 6.7. Pre-inhibition of p38 MAPK does not inhibit activation of TGF-β canonical signalling. Representative immunofluorescence of total-Smad2/3 (t-Smad2/3) localisation in P21 LEC explants fixed after 15 minutes (A–D) and 2 hours (E–H) of culture. Immunofluorescence of t-Smad2/3 (green) in control (non-treated; A, E), Skepinone-L alone (1 µM; B, F), TGF-β2 (200 pg/mL) alone (C, G), and Skepinone-L/TGF-β2 treated explants (D, H). Skepinone-L administered 1-hour prior to the addition of TGF-β2 (D, H). Nuclear (large arrowheads) and cytoplasmic (arrows) localisation of t-Smad2/3. Scale bar: 50 µm.

6.4.3 Cotreatment with Skepinone-L prevents TGF-β2-induced lens EMT

At day 1 and day 3 culture, LECs in Skepinone-L/TGF-β2 cotreated explants were maintained and lens cells remained tightly adhered to each other (Figure 6.8 A–B). At day 5, LECs remained although we observed areas of prominent intercellular space, as well as some small, exposed capsule patches (Figure 6.8 C). Cocultured Skepinone-L/TGF-β2 lens explants demonstrated strong β-catenin cell membrane localisation at day 3 (Figure 6.8 D), with a noticeable decrease in α-SMA intensity that was found only in small cytoplasmic patches (Figure 6.8 E). As seen with pre-treatment with Skepinone-L in TGF-β2-treated LEC explants (see Supplementary Figure 6.1), β-catenin levels did not significantly change between treatment groups (see Supplementary Figure 6.2 and Supplementary Table 6.2). Addition of TGF-β2 to LEC explants significantly increased α-SMA protein levels when compared to low basal levels in control (p = 0.0010) and Skepinone-L only treated explants (p = 0.0018, Figure 6.8 F). Despite low immunofluorescent intensity for α-SMA (Figure 6.8 E), cotreatment with Skepinone-L and TGF-β2 significantly increased α-SMA total protein levels compared to low levels in control (p = 0.0030) and Skepinone-L only (p = 0.0061) explants (Figure 6.8 G). However, this increase in α-SMA protein levels was not as strong as TGF-β2 only treated explants (p = 0.7345). We observed low levels of Tpm1.6/1.7 and Tpm2.1 in non-treated and Skepinone-L only treated LEC explants when probed for α9d at 72 hours of culture (Figure 6.8 H). As seen previously (see Figure 6.6 E–F), TGF-β2 elevated the Tpm1.6/1.7 and Tpm2.1 protein levels in comparison to non-treated and Skepinone-L only treated LEC explants. Cotreatment with Skepinone-L and TGF-β2 reduced Tpm1.6/1.7 and Tpm2.1, when compared to TGF-β2-treated LEC explants (Figure 6.8 H), as seen previously in LEC explants treated with Skepinone-L prior to TGF-β2 (see Figure 6.6 E–F).

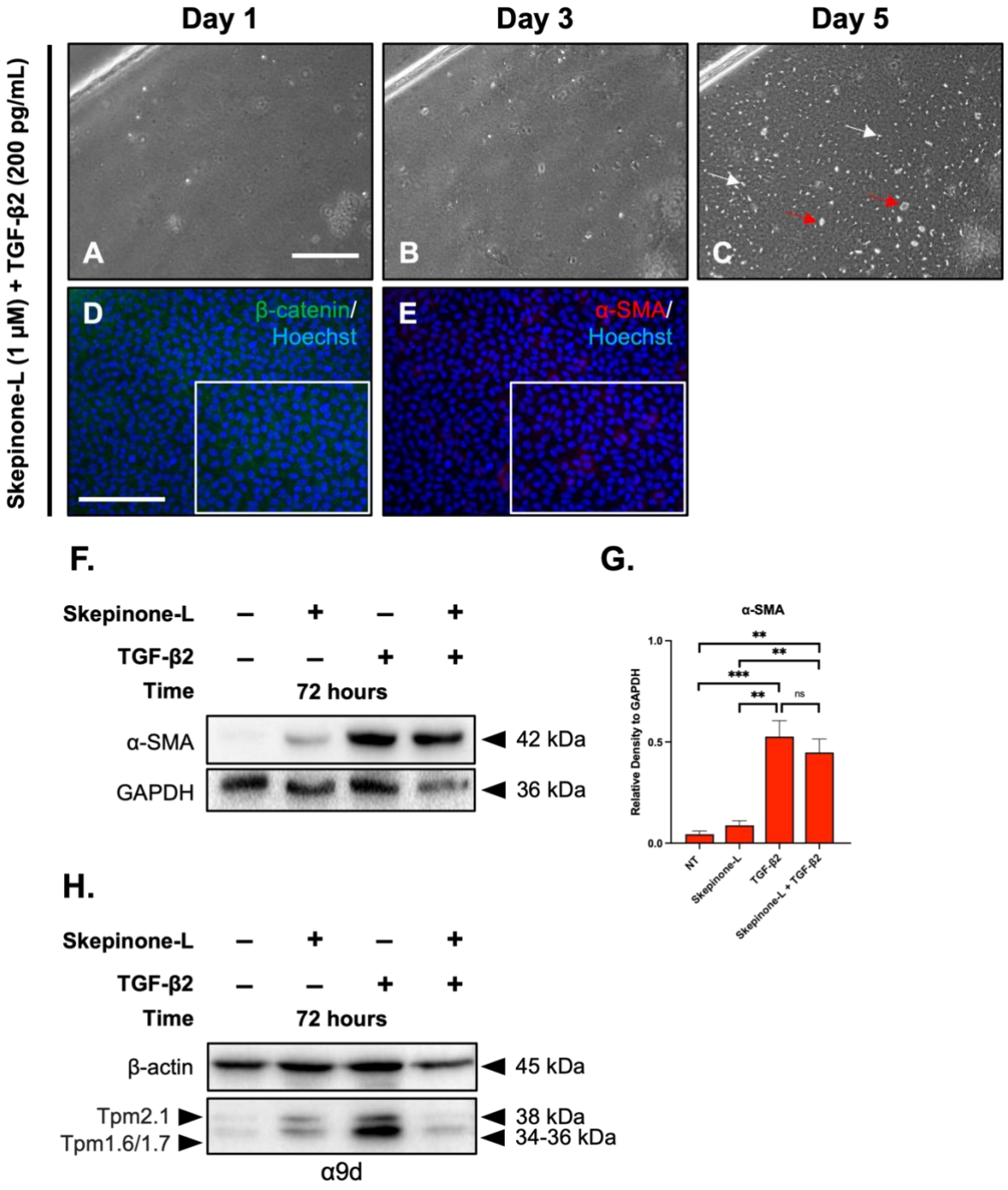

Figure 6.8. Cotreatment with Skepinone-L and TGF-β2 in rat LEC explants. Phase contrast imaging of rat explants across 5 days of culture cotreated with Skepinone-L (1 µM) and TGF-β2 (200 pg/mL) (A–C). Small areas of exposed anterior capsule (red arrows) and prominent intercellular space (white arrows) noted at day 5. Explants immunolabelling for β-catenin (green, D) and α-SMA (red, E) with Hoechst nuclear stain (blue) at day 3. Zoomed-in inset (white squares). Scale bar: 200 µm (A–C), 100 µm (D–E). Representative western blot of α-SMA protein levels in non-treated (NT), Skepinone-L only, TGF-β2 only, or cotreated Skepinone-L/TGF-β2 LEC lysates at 72 hours (F). Density of α-SMA relative to loading control GAPDH (G). Graphed data representative of post-hoc Tukey's comparisons test and one-way ANOVA (ns = not significant, $^{**}P < 0.0021$, $^{***}P < 0.002$). H) A separate western blot with the same treatment groups as Figure F. LEC explant lysates probed for Tpm1.6/1.7 (34–36 kDa) and Tpm2.1 (38 kDa) using α9d, with β-actin as a protein loading control. Western blot representative of three independent experimental replicates (n=3).

6.4.4 Skepinone-L inhibits p38 activation in TGF-β2-treated LECs

To confirm the effectiveness of Skepinone-L in blocking TGF-β2-induced EMT, as observed previously (see Figures 6.2, 6.5–6.6, and 6.8), we looked at p38 localisation in LECs using immunolabelling. At 15 minutes of culture, non-treated explants presented cytoplasmic localisation of total p38 (p38) in LEC explants (Figure 6.9 A). Low levels of p38 were noted in Skepinone-L (1 μM)-treated LECs compared to non-treated LEC explants (Figure 6.9 B). In TGF-β2 stimulated explants, p38 levels were heightened in the nucleus of LECs (Figure 6.9 C). We observed transient localisation of p38 in explants 1-hour pre-treated with Skepinone-L before TGF-β2, compared to cotreated Skepinone-L/TGF-β2 LEC explants. Skepinone-L/TGF-β2 pre-treated explants exhibited both nuclear and cytoplasmic localisation of p38 (Figure 6.9 D), similar to that observed in non-stimulated explants. p38 was noticeably reduced and cytoplasmic in Skepinone-L/TGF-β2 cotreated LEC explants (Figure 6.9 E).

Given the inhibitory properties of Skepinone-L taking effect as early as 15 minutes of pre-treatment and cotreatment in our morphological studies, we collected samples for western blotting. In non-treated LEC explants, we noted basal levels of p-p38 with one band weighing between 40–43 kDa (Figure 6.10). The addition of Skepinone-L (1 μM) to LECs reduced basal levels of activated p38, as only a faint band could be probed in these samples. After 15 minutes of TGF-β2 treatment, p38 is activated with a strong p-p38 band noticeable in these samples compared to low levels in control and Skepinone-L lens explant samples (Figure 6.10). 1-hour pre-treatment with Skepinone-L in TGF-β2-treated LEC explants blocked p38 phosphorylation after 15 minutes, and this was also consistent in explant samples cotreated with Skepinone-L and TGF-β2. Blocking p-p38 did not impact total p38 levels.

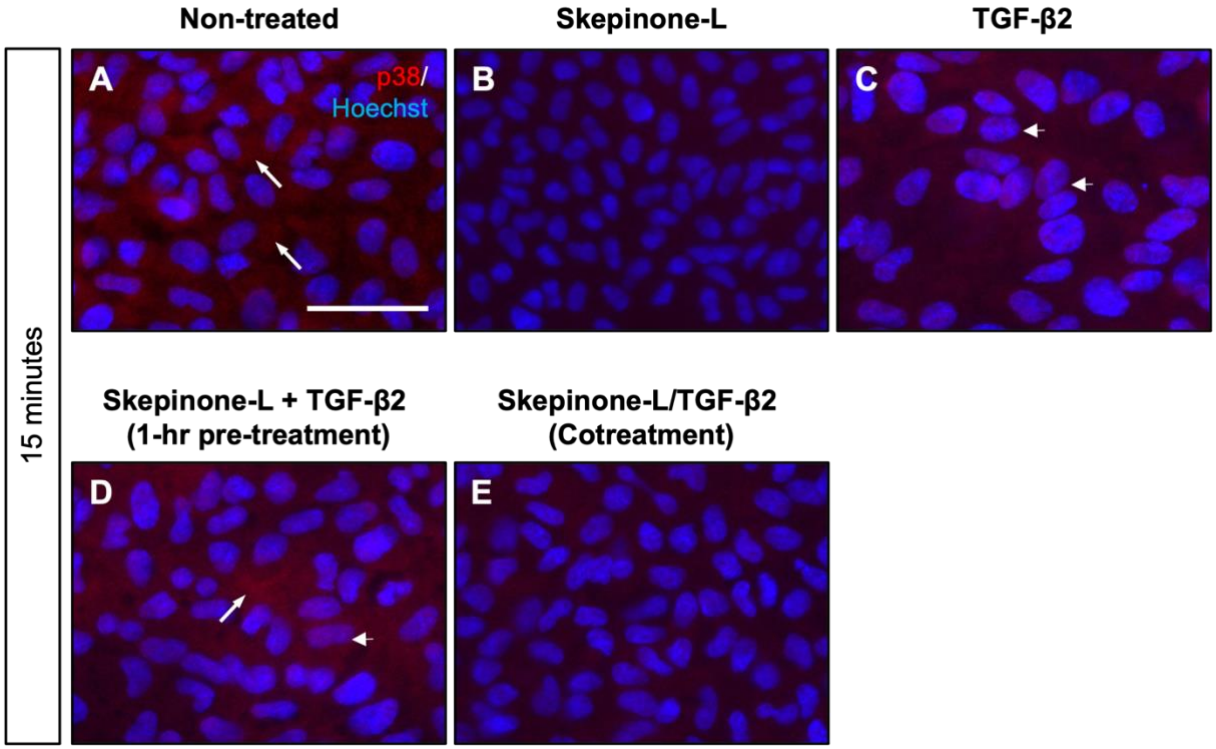

Figure 6.9. Total p38 immunolocalisation in Skepinone-L and TGF-β-treated LEC explants. Representative immunofluorescence of total-p38 MAPK (p38) localisation in P21 LEC explants fixed after 15 minutes of culture. Immunofluorescence of p38 (red) with a nuclear dye (Hoechst, blue) in control (non-treated; A), Skepinone-L alone (1 µM; B), TGF-β2 (200 pg/mL) alone (C), explants exposed to Skepinone-L 1-hour before TGF-β2 (D), and explants cotreated with Skepinone-L and TGF-β2 (E). Nuclear (large arrowheads) and cytoplasmic (long arrows) localisation of p38. Scale bar: 50 µm.

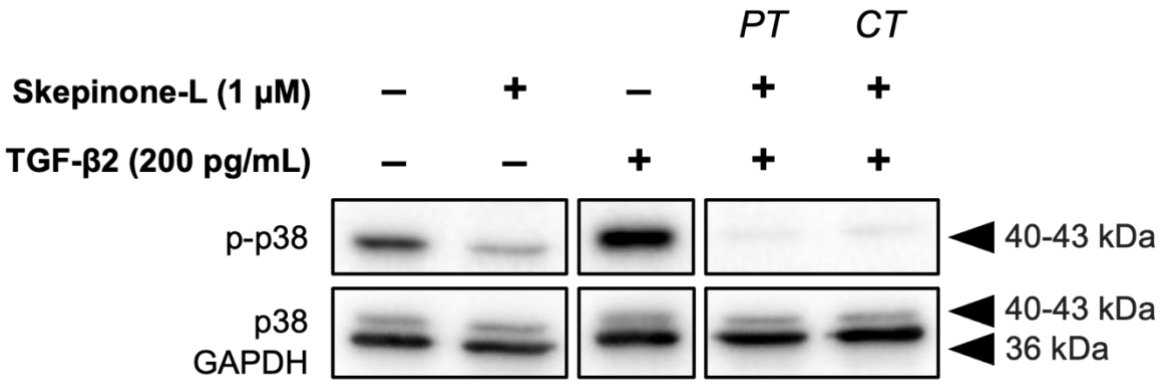

Figure 6.10. Effectiveness of Skepinone-L in inhibiting TGF-β2-induced p38 activity. Representative western blots of total p38 (p38) and phosphorylated p38 (p-p38) protein levels in rat LEC explants following 15 minutes of culture. Treatment groups: control (non-treated), Skepinone-L (1 µM) only, TGF-β2 (200 pg/mL) only, 1-hour pre-treatment with Skepinone-L in TGF-β2-treated explants (PT), and cotreated Skepinone-L/TGF-β2 explants (CT). p-p38 and p38 protein levels were relative to loading control GAPDH.

6.4.5 Post-treatment with Skepinone-L does not prevent TGF-β2-induced lens EMT

We altered the time we treated cells with Skepinone-L to determine when p38 activity is required for lens EMT by adding it after TGF-β application; we treated LEC explants with TGF-β2 for 15 minutes or 2 hours before introducing Skepinone-L. Both 15 minutes and 2 hours of Skepinone-L post-treatment in TGF-β2 exposed lens explants induced no morphological changes at day 1 (Figure 6.11 A, D) and day 3 (Figure 6.11 B, E) of culture. Cells in both explant treatment groups remained cobblestone-like, compact, and maintained, with some refractile bodies observed at day 3. At day 5, loss of cells was noted in explants exposed to Skepinone-L 15 minutes after TGF-β2, with minimal, if any, capsular wrinkling (Figure 6.11 C). Some patches of lens cells remained while areas of the underlying capsule were visible, suggesting EMT was prolonged but not completely blocked. However, EMT was not inhibited when LEC explants were exposed to Skepinone-L 2 hours after TGF-β2 treatment with prominent capsular wrinkling at day 5 (Figure 6.11 F). In these lens explants, exposed lens capsule regions were also observed, characteristic of a morphological EMT response. Explants were fixed at day 5 of culture to observe any molecular marker changes in localisation when Skepinone-L is introduced 15 minutes and 2 hours after TGF-β2. Explants exposed to Skepinone-L 15 minutes post-growth factor treatment showed strong immunoreactivity for β-catenin and localisation remained cell membranous (Figure 6.11 G). These explants also had a large population of cells still present. α-SMA intensity was reduced and limited to regions of cells, with cytoplasmic localisation and some minor stress fibre reactivity (Figure 6.11 H). A reduction in the number of cells was noted in explants exposed to Skepinone-L 2 hours after TGF-β2 as a result of an EMT induction (Figure 6.11 I–J). Localisation for β-catenin was diffuse and reduced in comparison to explants exposed to TGF-β2 only for 15 minutes before Skepinone-L. Despite this, α-SMA immunoreactivity was increased in these cells, with more areas of stress fibre localisation (Figure 6.11 J).

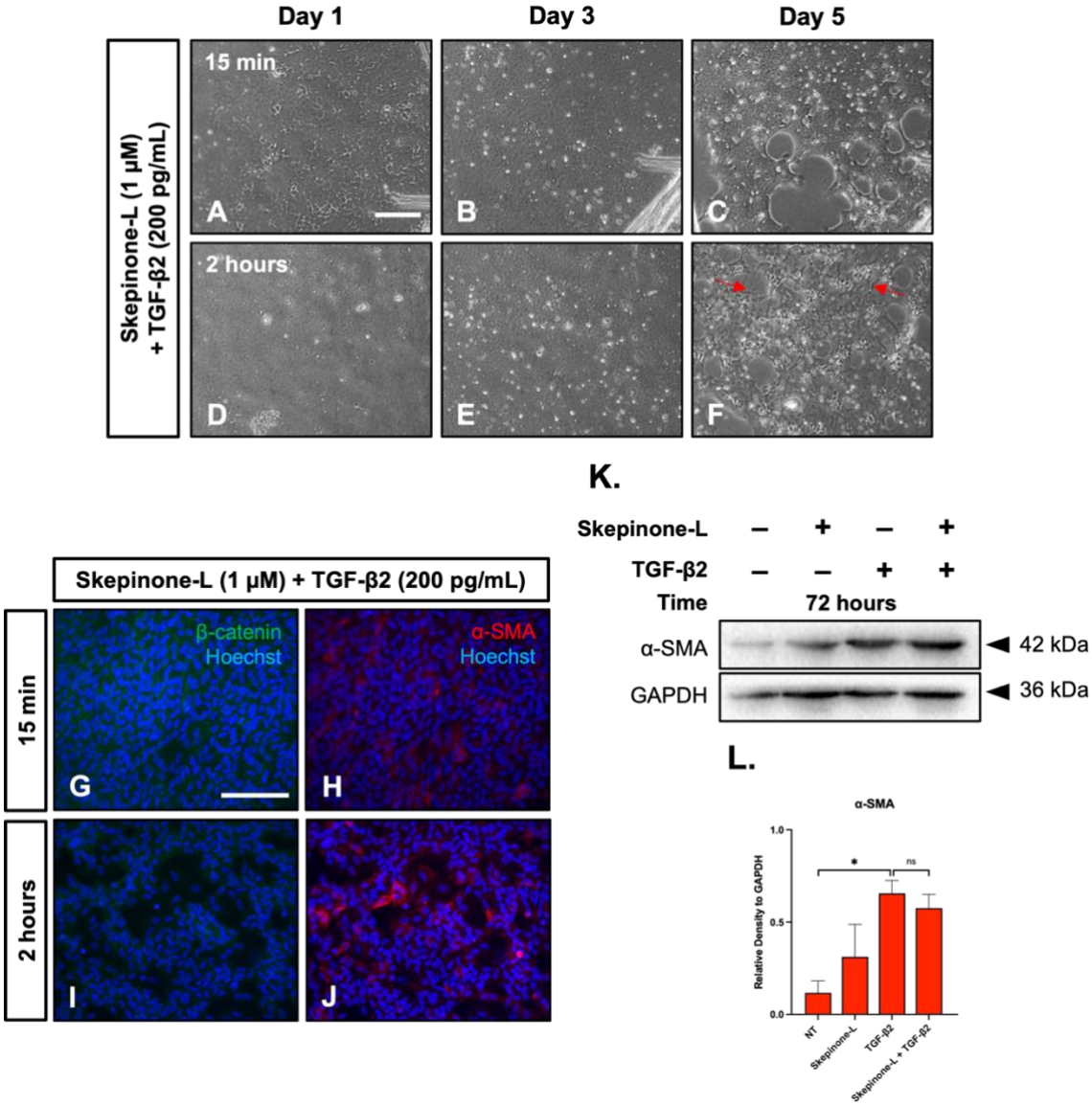

Figure 6.11. Addition of Skepinone-L post TGF-β2-treatment impacts EMT induction in rat LEC explants. Phase contrast images of LEC explants across 5 days of culture exposed to Skepinone-L (1 µM) and TGF-β2 (200 pg/mL). Explants exposed to Skepinone-L at 15 minutes (A–C) and 2 hours (D–F) post TGF-β2 treatment. Capsular wrinkling observed with 2 hours of Skepinone-L post TGF-β2 treatment (red arrows). Immunofluorescent labelling of β-catenin (green, G, I) and α-SMA (red, H, J), with Hoechst nuclear counterstain (blue) in rat LEC explants at 5 days of culture. Post TGF-β2 treated explants exposed to Skepinone-L for 15 minutes (G, H), 2 hours (I, J). Scale bar: 200 µm (A–F), 100 µm (G–J). Representative western blots of α-SMA protein levels in non-treated (NT), Skepinone-L only, TGF-β2 only, and Skepinone-L treated explants 2 hours after TGF-β2 addition (K). Protein density relative to loading control GAPDH (L). Graphed data shows post-hoc Tukey's comparisons test and one-way ANOVA with ±SEM (ns = not significant, $*P < 0.0332$).

Since we noted morphological changes only at day 5 of culture, particularly in the 2-hour post-treatment group (Figure 6.11 F), we looked at whether there were any molecular differences at 72 hours between protein levels in explants with no treatment, Skepinone-L only,

TGF-β2 only, or Skepinone-L 2 hours following TGF-β2 exposure (Figure 6.11 K–L). Representative western blots for β-catenin protein levels at 72 hours of culture in this section are not shown given there were no significant differences observed among treatment groups (see Supplementary Figure 6.3 and Supplementary Table 6.3), as viewed in previous blots from other treatment conditions (both pre- and cotreatment). As seen in previous western blots (see Figures 6.4–6.5 and 6.8), non-treated and Skepinone-L treated LEC explants showed low protein levels for α-SMA and no significant difference between treatment groups ($p = 0.5895$). As expected, TGF-β2 significantly increased α-SMA immunoreactivity compared to control explants ($p = 0.0296$), but not Skepinone-L only explants ($p = 0.1819$, Figure 6.11 L). 2-hour post-treatment with Skepinone-L in TGF-β2-treated explants increased α-SMA intensity in comparison to Skepinone-L only ($p = 0.3620$) and control explants ($p = 0.0625$). No significant difference was noted between α-SMA protein expression in TGF-β2 alone and Skepinone-L/TGF-β2 treated explants ($p = 0.9486$). As we did not expect to see a significant change to α-SMA levels in our Skepinone-L/TGF-β2 LEC explants, compared to TGF-β2 only samples ($p = 0.9486$), we examined another EMT-associated marker, Tpm, when probed for α9d (Figure 6.12). Unlike pre- and coculture with Skepinone-L and TGF-β2, that showed a reduction in Tpm1.6/1.7 and Tpm2.1 levels (see Figures 6.6 and 6.8), post-treatment with Skepinone-L did not block TGF-β2-induced lens EMT associated Tpm1.6/1.7 and Tpm2.1 levels that remained relatively high and on par with TGF-β2-alone treated LEC explants (Figure 6.12).

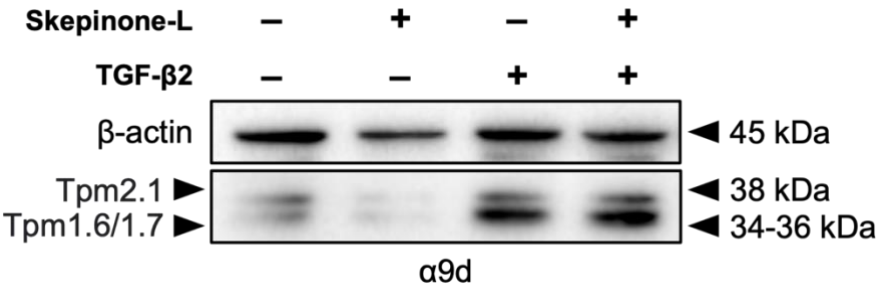

Figure 6.12. Tpm1 and Tpm2 in lens explants exposed to Skepinone-L 2 hours post TGF-β2-treatment. Western blot of non-treated, Skepinone-L (1 μM) only, TGF-β2 (200 pg/mL) only, and LEC explants exposed to Skepinone-L 2 hours after TGF-β2 treatment. LEC explant lysates probed for Tpm1.6/1.7 (34–36 kDa) and Tpm2.1 (38 kDa) using α9d. β-actin used as a protein loading control. Representative blot of three independent replicates (n=3).

6.5 DISCUSSION

To the best of our knowledge, this is the first study to test the p38α MAPK targeted inhibitor Skepinone-L using the eye lens, and in the LEC explant model. Due to its recent discovery and limited usage to date in other fibrotic models, we first optimised working concentrations that would not result in any cytotoxicity of cells. As p38 MAPK is reported to be stimulated by stress-induced conditions, as well as cytokines/growth factors (New and Han, 1998; Cuadrado and Nebreda, 2010; Lee et al., 2020), we used rat LEC explants to examine the role of p38 in TGF-β2 induced EMT.

Previous studies in the lens (Zhou and Menko, 2004; Wang et al., 2009; Bai et al., 2015; Boswell et al., 2017), as well as in other fibrotic and cancer models (Düzgün et al., 2017; X. Han et al., 2018; Hao et al., 2021) have used SB203580, an inhibitor proposed to specifically target p38α MAPK. In fact, SB203580 has been shown to impact not only p38α and p38β (Menon et al., 2015; Boswell et al., 2017), but also trigger off target inhibition of other downstream molecules and transcription factors, including TGF-β-induced Smad3 (Laping et al., 2002), CREB, HSP27, NF-κB, TNF-α, and IL-6 (Birkenkamp et al., 2000; Wang et al., 2009; Shi et al., 2015; Sreekanth et al., 2016), as previously reviewed (Clark et al., 2007; Munoz, 2017). This inhibitor has also shown to target p38 activity as well as some associated substrates such as MAPKAP K2 (Kumar et al., 1999; Kumphune et al., 2010; Sreekanth et al., 2016; X. Han et al., 2018). SB203580 at doses >10 μM can also negatively regulate other signalling pathways, such as p-Akt (McGuire et al., 2013), p-ERK1/2, p-JNK1/2 (Birkenkamp et al., 2000), and p-PKB (Lali et al., 2000). Given this, the current study focused on an alternative p38 inhibitor, Skepinone-L, with a known high potency and specificity for targeting p38α at doses < 2 μM (Koeberle et al., 2012; Borst et al., 2013). We found that pre-treatment of lens cells with doses of Skepinone-L < 2 μM in TGF-β2-treated lens epithelial explants effectively prevented EMT processes.

6.5.1 Tropomyosin and p38 MAPK

We have shown Tpm1.6/1.7 and Tpm2.1 to be upregulated in TGF-β-induced lens EMT (see Chapters 3–5). Since TGF-β2-treated LECs pre-treated with Skepinone-L did not demonstrate capsular wrinkling at doses < 2 μM, we hypothesised that p38 may be impacting on the cell cytoskeleton to regulate the contractile properties of cells during EMT. We examined HMW Tpms, such as Tpm1.4, Tpm1.6–1.9, and Tpm2.1, expression and localisation in LEC explants exposed to Skepinone-L pre-growth factor treatment, since Tpm has previously been linked to

recruiting α-SMA during stress fibre formation (Kubo et al., 2013; Prunotto et al., 2015; Parreno et al., 2020). We saw that inhibition of p38 in TGF-β2-treated explants resulted in cytoplasmic labelling of Tpm1.4, Tpm1.6–1.9, and Tpm2.1, as well as α-SMA. The resultant Skepinone-L/TGF-β2-treated lens cells were not myofibroblastic and therefore did not display the contractile features or reorganisation of actin stress fibre filaments, as well as α-SMA decoration of stress fibres. We observed a reduction in Tpm1.6/1.7 and Tpm2.1 protein levels when explants were exposed to Skepinone-L pre-TGF-β2 treatment and coculture, as well as Skepinone-L only treated explants; however, Skepinone-L exposure post TGF-β2 treatment in LECs did not inhibit Tpm1.6/1.7 and Tpm2.1 protein levels, consistent with what was observed in our morphological assays, given that EMT was prolonged but not completely inhibited in LEC explants. From this we propose that p38 may be instrumental in regulating HMW Tpms during TGF-β-induced cell contractility and the EMT-associated phenotype, leading to capsular wrinkling in the current LEC explant model. A study by Bakin et al. (2004) demonstrated that p38 inhibition with a p38α/p38β specific compound, SB202190 (10 μM), in combination with TGF-β1 (2 ng/mL), blocked 30–45% expression of total induction of the studied Tpm isoforms. In particular, the study showed that SB202190 1-hour pre-treatment reduced Tpm1.6/1.7 protein levels in mouse NMuMG epithelial cells as early as 1 hour of culture with TGF-β1 but did not significantly impact mRNA levels (Bakin et al., 2004). This study, as well as studies by others, proposed that p38 MAPK and Smad2/3/4-signalling propagated by TGF-β is required for Tpm expression, particularly HMW isoforms, and regulating cytoskeletal activity (Bakin et al., 2004; Varga et al., 2005; Zheng et al., 2008; Safina et al., 2009). As stated in Chapters 3 and 4, HMW Tpm isoforms such as Tpm1.6/1.7 and Tpm2.1 have been shown to be influential in cytoskeletal reorganisation and stress fibre formation during EMT (Bakin et al., 2004; Varga et al., 2005; Zheng et al., 2008; Safina et al., 2009), whereas LMW isoforms (e.g., Tpm3.1 and Tpm4.2) are required for high invasiveness, migration, and proliferation during cancer metastasis (Choi et al., 2010; Tao et al., 2014; Yu et al., 2017; Zhao et al., 2019; Li et al., 2021). Therefore, further studies using our lens explant model is warranted to examine the role of p38 in differential Tpm activation and localisation of HMW and LMW Tpm isoforms.

p38 MAPK signalling is involved in regulating cell apoptosis in TGF-β-induced mouse mammary epithelial cells (NMuMGs) (Yu et al., 2002) and oxidative stress-induced HLECs (Bai et al., 2015), as well as other models such as mice dermal studies (pemphigus foliaceus) (Lee et al., 2009) and ischemic heart injury (Ma et al., 1999). Other studies have also shown a mechanism for p38 signalling in regulating actin reorganisation during apoptosis-

related cellular blebbing in umbilical endothelial cells (HUVECs) (Huot et al., 1998). In our TGF-β2-treated LEC explants, when p38 was inhibited within 2 hours, we did not observe many refractile bodies or cell blebbing commonly associated with apoptosis during EMT. This was not the case for LEC explants exposed to Skepinone-L post TGF-β2 treatment, that showed signs of cell apoptosis and remodelling through early blebbing, and cell loss leading to exposed areas of bare lens capsule.

Studies have shown that Tpm1 and Tpm2 derived isoforms are involved in regulating cell apoptosis and anoikis (a sub-category of apoptosis) in breast cancer cell lines (Bharadwaj et al., 2005), endothelial HUVECs (Zhang et al., 2002), and rat B35 neuroepithelial cells (Desouza-Armstrong et al., 2017). Anoikis is most likely the programmed cell death we see in our model given that it is associated with the loss of cell-cell and basement membrane/ECM (e.g., the lens capsule) contact, as previously reviewed (Cao et al., 2016). We demonstrated that pre- and cotreatment with Skepinone-L inhibited cell apoptosis in TGF-β2-treated LEC explants, that also correlated with a decrease in Tpm1.6/1.7 and Tpm2.1 protein levels. Therefore, inhibition of p38 activation in the current model could potentially be influencing HMW Tpm formation and cytoskeletal reorganisation, as well as apoptosis, in TGF-β2-treated LECs.

6.5.2 p38 MAPK is required for cell phenotypic changes during TGF-β-induced lens EMT

Pre- and cotreatment with Skepinone-L blocked the myofibroblastic phenotype associated with TGF-β-induced lens EMT independent of TGF-β-induced Smad2/3-signalling, as highlighted by the continued ability of cells to accumulate α-SMA. Our study has shown that p38α may be required for myofibroblastic transdifferentiation including cell contractility during lens EMT. In TGF-β stimulated explants pre-treated and cotreated with Skepinone-L, lens cells retained cobblestone-like epithelia as well as no evidence of myofibroblastic cells. In addition, when exposed lens capsule areas were noted with Skepinone-L (2 μM)/TGF-β2-treatment, they did not show any capsular wrinkling, suggesting that these cells were not contractile and able to modify the underlying ECM. Given that pre-treatment with Skepinone-L did not affect Smad2/3-signalling, targeting p38 activity was sufficient to block the phenotypic cell changes associated with EMT, with TGF-β-activated Smad2/3-signalling continuing to promote α-SMA stress-fibre accumulation in LECs. As shown in previous chapters (Chapters 3–5), and previously reported, α-SMA localised to stress fibres of TGF-β2-induced myofibroblasts that is a factor commonly associated with cell contractility (Hinz et al., 2001). Interestingly, fibrotic

and mesenchymal cell models (Stambe et al., 2004; Molkentin et al., 2017) have confirmed that α-SMA-positive cells, particularly when localising to stress fibres, is related to p38 activation in myofibroblastic differentiation. To further characterise the role of p38α in lens EMT, future studies could examine other molecular markers upregulated during EMT and ECM deposition, such as collagen I and III, as well as fibronectin, filensin, N-cadherin, MMPs, and vimentin (Lovicu et al., 2002; Dobaczewski et al., 2010; Ramos et al., 2010; Korol et al., 2014).

p38 inhibition can reduce cell remodelling in diseased and fibrotic tissues (Kompa et al., 2008; Kolosova et al., 2011; Molkentin et al., 2017; Bageghni et al., 2018). A model for pulmonary idiopathic fibrosis has also shown a role for p38 during ECM gene expression, cell transformation, and stress fibre formation under TGF-β1-induced conditions (Kolosova et al., 2011). For example, inhibition of p38 activity using SB203580 1-hour before TGF-β1 treatment, decreased ECM markers (fibronectin and collagen I) in human airway epithelial cell (1HAEo^{-}) lines, and the monolayer of 1HAEo^{-} cells did not undergo any morphological transformations in cells (Kolosova et al., 2011), further suggesting a mechanism for p38 in mediating cell transformation during TGF-β-induced EMT.

In human glioma cells, TGF-β-transfection in combination with p38 inhibition reduced cell migration and invasiveness (Ling et al., 2016). Although inhibition of p38 elevated E-cadherin expression, while reducing N-cadherin expression in TGF-β-transfected cells was proposed to be linked to p38 phosphorylation during EMT, this study used SB203580 that had off target effects that also impacted cell remodelling MMPs (Ling et al., 2016). Based on this study, a more highly selective compound targeting p38 is needed to discount inhibition of off-target molecules during EMT. Silencing p38α (using shRNA) in human melanoma cells significantly decreased motility, cell migration, and proliferation, as well as EMT markers including vimentin and Twist (Wen et al., 2019). This study also silenced p38β in melanoma cells, demonstrating no effect on EMT marker expression, and cell motility, when compared to control and p38α-silenced cells (Wen et al., 2019). It could be hypothesised that p38α is more essential for EMT in this system than p38β. To support this, a reduction in fibroblast-to-myofibroblast cell differentiation was observed in mouse embryonic fibroblasts (MEFs) deficient of p38α (Molkentin et al., 2017), further confirming a dependency for p38α regulation in EMT-associated cell remodelling.

Another reported p38α targeting compound, VX-745, has been shown to inhibit pro-inflammatory cytokine release in lipopolysaccharide (LPS)-induced THP-1 monocytes (Singh et al., 2018). Another model showed that this same inhibitor did not block or target Smad2

phosphorylation in TGF-β stimulated mouse embryonic fibroblasts (MEFs) (Sapkota, 2013). From these studies, VX-745 appears to selectively inhibit p38α. Other studies from our laboratory have shown VX-745 to be as effective as Skepinone-L (Wu, Flokis, and Lovicu, unpublished data). Given its high specificity for p38α, our current model should also consider characterising the effectiveness of VX-745 in inhibiting TGF-β induced p38α activity to further validate our work with Skepinone-L.

6.5.3 Early onset of Smad2/3 and p38 MAPK signalling during TGF-β-induced EMT

In the current lens model, TGF-β-induced EMT is dependent on both Smad-dependent and Smad-independent downstream signalling molecules. In cardiac fibroblasts from Smad3 deficient mouse, treatment with TGF-β1 reduced but did not completely inhibit α-SMA and phalloidin labelling, as well as α-SMA cytoskeletal stress fibre assembly (Dobaczewski et al., 2010) In the present study, pre-treatment with Skepinone-L resulted in an uncoupling of TGF-β-induced EMT, with only the myofibroblastic cell phenotype blocked and its associated Tpm1.6/1.7 and Tpm2.1 protein levels, but not the accumulation of α-SMA. Based on our findings, as well as previous fibrotic studies (Sebe et al., 2008; Dobaczewski et al., 2010; Kolosova et al., 2011; Boswell et al., 2017; Molkentin et al., 2017), α-SMA stress fibre assembly does not solely depend on TGF-β-induced Smad2/3 signalling, and may likely require other downstream signalling cascades, like p38, to regulate epithelial-myofibroblastic transdifferentiation in lens cells.

We showed that p38α inhibition within 1-hour pre-TGF-β2 treatment blocked lens EMT, suggesting that p38 is an early mediator of lens EMT. This was confirmed when LEC explants were exposed to Skepinone-L 15 minutes and 2 hours post-TGF-β2 treatment that prolonged, but did not completely block, an EMT. By testing different timepoints of Skepinone-L application, we may be able to find an approximate window or timeframe where p38 is active/ phosphorylated. Future studies could implement these additional timepoints to identify the exact profile of p38 activity in TGF-β2-treated LECs. Given the differences in cell types and environmental factors in other models, it has made finding a definitive activation pattern inconclusive.

A model for EMT development in pulmonary fibrosis (1HAEo$^-$ cells) showed that p38 was activated as early as 30 minutes in response to TGF-β1 (Kolosova et al., 2011). A study by Sebe et al. (2008) showed that TGF-β1 (5 ng/mL) stimulated a biphasic activation response for p-Smad2 and p-p38β signalling across 96 hours of culture in renal tubular (LLCPK1/AT1) cells.

TGF-β1-treated LLCPK1/AT1 cells activated p38β in two peaks, the first at 1 hour and later at 48 hours, with p38β activity relatively quiescent between 2–24 hours compared to the activation of p-Smad2 and p-Smad3 (Sebe et al., 2008). This study could not detect p38α or p38γ, but only observe p38β and p38δ labelling in LLCPK1/AT1 cells (Sebe et al., 2008). Other studies have shown that this biphasic response also occurs early in TGF-β1 (2 ng/mL)-treated human tenon fibroblasts (HTFs); first phase (< 2 hours) and second phase (> 12 hours) of TGF-β1 treatment, the latter phase aligning with the initiation of α-SMA expression (Meyer-ter-Vehn et al., 2006). In our study, we observed the activation of phosphorylated p38α in TGF-β2-treated LECs after 15 minutes of culture, and Skepinone-L was able to inhibit this activation with 1-hour pre- or co-treatment with TGF-β2. The Meyer-ter-Vehn et al. (2006) study showed that targeted inhibition of p38 by pre-treating HTFs with SB203580 (10 μM) in TGF-β1-treated conditions mediated, but did not completely block, α-SMA actin association or cell contractility. Although Meyer-ter-Vehn et al. (2006) showed p38 inhibition in TGF-β-induced conditions, a p38α/β inhibitor, and not a p38α selective inhibitor, was used. Future studies in LEC explants using pre-, co-, and post-treatments with SB203580 may validate the specificity and efficacy of Skepinone-L for p38α inhibition. Moreover, different (both earlier and later) timepoints of Skepinone-L application could be tested to establish any peaks, or phasic patterns of p38α activation in TGF-β2-induced LEC explants.

6.5.4 p38 MAPK signalling mechanisms in the eye lens

Following TGF-β stimulation, as reported in human LE cells (Dawes et al., 2009), it is of interest to determine whether p38 is downstream of other ocular growth factors/cytokines, and their associated receptor signalling. Studies by Boswell et al. (2010, 2017) demonstrated relatively early (within 1.5 hours) phosphorylation of p38 in embryonic chick lens epithelial cells (DCDMLs) after FGF and/or TGF-β stimulation. In a postnatal mice lens model, activation of p38 correlated with a deficiency for αA-crystallin in both lens epithelial and fibre cell extracts from $\alpha A^{-/-}$ mice, that is a lens fibre cell protective and structural protein required for maintaining overall lens transparency (Menko and Andley, 2010). This study corroborated this result in human LE cells transfected with cataract-inducing mutant αA-crystallin R116C (Litt et al., 1998), with elevated p-p38 compared to WT αA-crystallin transfected human LE cells, conveying a role for p38 in regulating stress-induced mechanisms in lens cells during cataractogenesis (Menko and Andley, 2010).

In the lens, our laboratory has previously shown that when ERK1/2 signalling is inhibited in TGF-β-induced rat LEC explants, EMT is partly blocked, with cell death persisting, suggestive of other downstream signalling cascades, such as p38, required to regulate apoptosis (Wojciechowski et al., 2017). A more recent study from our laboratory showed that blocking EGFR resulted in a reduction in p-ERK1/2 and the complete inhibition of EMT in TGF-β2-treated LEC explants (Shu and Lovicu, 2019). This disparity in blocking EMT in lens by blocking EGFR-signalling or ERK1/2-signalling implies another EGFR-mediated pathway may also be involved. It has previously been suggested that there may be a potential link between EGFR activation and p38 activation during cell migration of immortalised mouse colonic epithelial cells (Frey et al., 2004, 2006), for intracellular trafficking (Vergarajauregui et al., 2006), as well as normal and aberrant lung epithelial cell proliferation (Ventura et al., 2007). Given this correlation, and the reported role of p38 during TGF-β-induced cell apoptosis (Liao et al., 2001; Yu et al., 2002), it could be hypothesised that p38 may be downstream of EGFR specifically during TGF-β-induced lens EMT. Further studies are needed to investigate whether any increase in p38 activity coincides with EGFR signalling activation in TGF-β2-treated LECs given p38 inhibition, like EGFR inhibition, is effective at preventing EMT.

6.5.5 Transient immunolocalisation of p38

Across the wider literature, there appears to be no general consensus as to the intracellular localisation of active p38. For example, in 293T kidney cells, p38α is localised to the nucleus once cells are exposed to UV damage, in comparison to cytoplasmic localisation in unstimulated 293T cells (Wood et al., 2009). In contrast, a study by Stambe et al. (2004) showed p38α-labelled nuclei and cytoplasmic immunolocalisation in normal kidney tubules from Sprague-Dawley rats, with phosphorylated p38 found in some tubule cell nuclei. Interestingly, total p38α and p-p38 nuclear-labelling was increased in myofibroblasts in tubules 1-week after surgical intervention (Stambe et al., 2004). Given the Wood et al. (2009) study was a pro-inflammatory stress model and the surgical insult model by Stambe et al. (2004) was non-inflammatory, this suggests that environmental, tissue-specific factors, and differential cell functions may determine the intracellular localisation of p38 after its activation.

We found total p38 in unstimulated LECs and found with inhibition of p38α using Skepinone-L reduced these levels. A study by Saika et al. (2005) also showed basal levels of p38α and cytoplasmic localisation in retinal pigment cells (ARPE-19s) at < 30 minutes of culture; however, TGF-β2 stimulation presented a transient localisation of activated p38 in cell

nuclei between 6–12 hours, reverting to the cytoplasm after 24 hours. Although we observed transient localisation for p38α, both cytoplasmic and nuclear, the nuclear localisation of p-p38α may or may not dictate its activity in LECs. Previous studies have shown that p38 can be activated in both the cell cytoplasm and nucleus based on culture conditions (Ben-Levy et al., 1998; Greenberg et al., 2002; Wood et al., 2009; Gong et al., 2010; Maik-Rachline et al., 2020), suggesting a tissue-specific role for p38 activation. The reduction in p38 intensity and cytoplasmic localisation in cotreated Skepinone-L/TGF-β2-treated explants, when compared to 1-hour Skepinone-L pre-treated TGF-β2-stimulated LEC explants, suggests that p38 must be phosphorylated within 15 minutes given that we are blocking a portion of this p38 activity. To elucidate, we may have potentially missed the precise timepoint at which p38α is phosphorylated by TGF-β. Therefore, it would be beneficial for future studies to examine the localisation of p-p38 in LECs in unstimulated, and growth factor stimulated conditions, to confirm at what timepoint p38 is activated and where p-p38 is intracellularly during its activation.

Since p38 has previously been reported to be involved in TGF-β-induced EMT (Yu et al., 2002; Kolosova et al., 2011; Boswell et al., 2017; Liu et al., 2020; Sugiyama et al., 2021), future studies could localise for p38 and phosphorylated p38 in ASC. Using our TG mice overexpressing TGF-β1 we observed isoform-specific Tpm expression throughout postnatal growth in Chapter 3. By using our TG mice model, we could test whether p38 accompanies the formation of myofibroblastic cells in ASC plaques, and if it is required for other cell processes such as proliferation, cell survival, and fibre differentiation. Lens epithelia could be acquired from both WT and TG mice to compare levels of p-p38 and p38 throughout ASC formation, given that previous studies have shown activation of p38 in embryonic chick (Zhou and Menko, 2004) and postnatal cataract mice and human LEC models (Menko and Andley, 2010).

6.6 CONCLUSION

p38/MAPK signalling is required for TGF-β-induced lens EMT, particularly in the transdifferentiation of epithelial to myofibroblastic cells. Inhibition of p38α using Skepinone-L (< 2 μM) can effectively reduce EMT-associated phenotypic changes in lens. Early inhibition of p38α does not impact the phosphorylation of Smad2/3, confirming p38 MAPK as a Smad-independent TGF-β-induced pathway during EMT. p38 MAPK can regulate cytoskeletal *Tpm1* and *Tpm2* gene derived isoforms that may influence α-SMA recruitment but not levels during

stress fibre assembly. Targeting early onset p38α MAPK activity may be a potential therapeutic in preventing TGF-β-induced EMT, leading to lens fibrosis.

6.7 SUPPLEMENTARY FIGURES

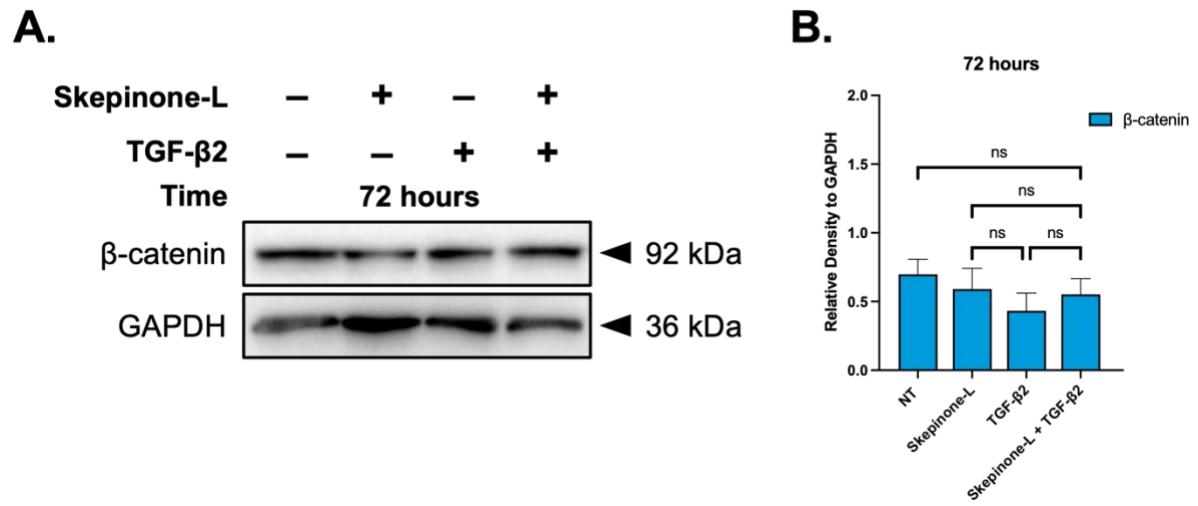

Supplementary Figure 6.1. Pre-treatment with Skepinone-L does not impact epithelial marker induction in TGF-β2-treated lens explants. Representative western blots of β-catenin protein levels in non-treated (NT), Skepinone-L (1 µM) only, TGF-β2 (200 pg/mL) only, and 15-minute pre-treated Skepinone-L/TGF-β2 explants collected at 72 hours (A). Densitometry of β-catenin conducted relative to GAPDH (B). Statistical analysis performed using one-way ANOVA and post-hoc Tukey's multiple comparisons test (ns = not significant).

Supplementary Table 6.1. Summary of β-catenin protein levels in rat LEC explants exposed to Skepinone-L 15 minutes prior to TGF-β2.

Treatment group comparisons	***P* value**[1]
NT *vs.* Skepinone-L (1 µM)	0.9289
NT *vs.* TGF-β2 (200 pg/mL)	0.4882
NT *vs.* Skepinone-L (1 µM) + TGF-β2	0.8449
Skepinone-L (1 µM) *vs.* TGF-β2	0.8136
Skepinone-L (1 µM) *vs*. Skepinone-L (1 µM) + TGF-β2	0.9961
TGF-β2 *vs.* Skepinone-L (1 µM) + TGF-β2	0.9066

[1]One-way ANOVA with Tukey's multiple comparisons test
*Statistically significant difference between treatment groups ($P < 0.05$)
Abbreviations: Non-treated LEC explants (NT), Skepinone-L. Refer to Supplementary Figure 6.1 B.

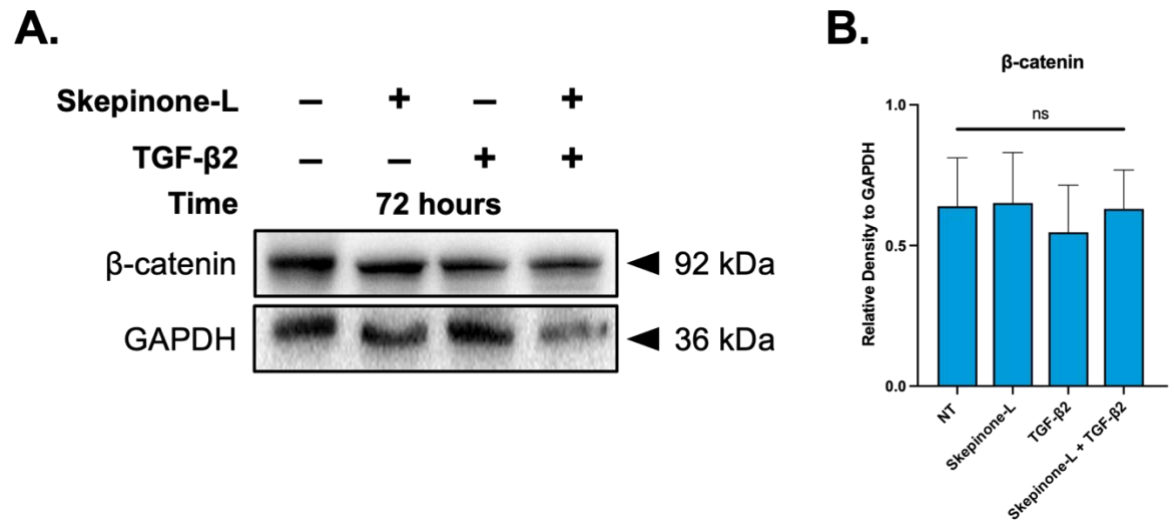

Supplementary Figure 6.2. Cotreatment with Skepinone-L and TGF-β2 in rat LEC explants. Representative western blots of β-catenin protein levels in non-treated (NT), Skepinone-L (1 μM) only, TGF-β2 (200 pg/mL) only, and cotreated Skepinone-L/TGF-β2 LEC lysates at 72 hours (A). Densitometry of β-catenin conducted relative to GAPDH (B). Graphed data representative of post-hoc Tukey's comparisons test and one-way ANOVA (ns = not significant).

Supplementary Table 6.2. Summary of β-catenin protein levels in rat LEC explants exposed to Skepinone-L with TGF-β2.

Treatment group comparisons	***P* value**[1]
NT *vs.* Skepinone-L (1 μM)	>0.9999
NT *vs.* TGF-β2 (200 pg/mL)	0.9772
NT *vs.* Skepinone-L (1 μM) + TGF-β2	>0.9999
Skepinone-L (1 μM) *vs.* TGF-β2	0.9683
Skepinone-L (1 μM) *vs*. Skepinone-L (1 μM) + TGF-β2	0.9997
TGF-β2 *vs.* Skepinone-L (1 μM) + TGF-β2	0.9833

[1]One-way ANOVA with Tukey's multiple comparisons test
*Statistically significant difference between treatment groups ($P < 0.05$)
Abbreviations: Non-treated LEC explants (NT), Skepinone-L. Refer to Supplementary Figure 6.2 B.

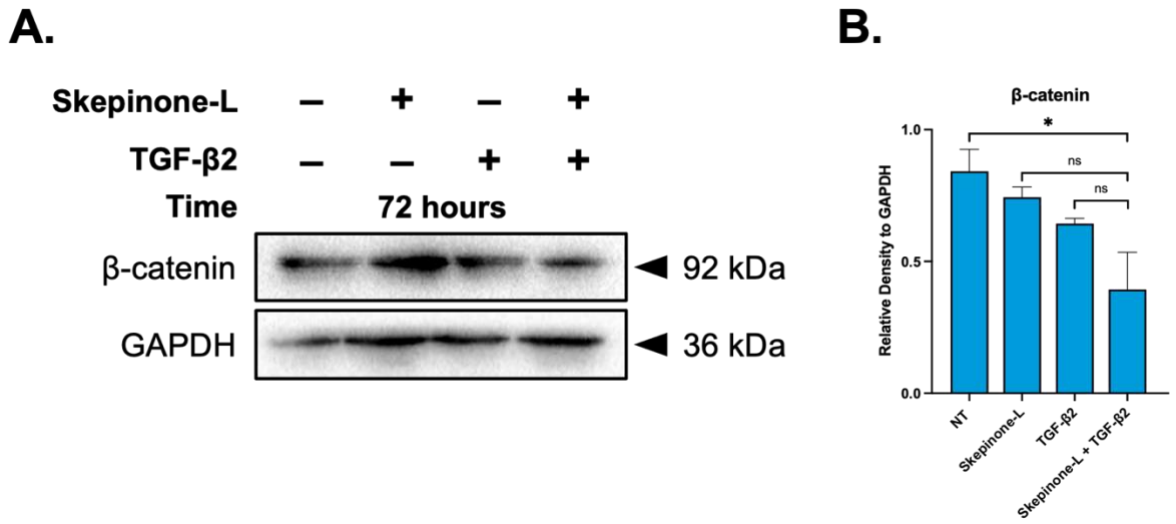

Supplementary Figure 6.3. Addition of Skepinone-L post TGF-β2-treatment impacts epithelial marker induction in rat LEC explants. Representative western blots of β-catenin protein levels in non-treated (NT), Skepinone-L (1 μM) only, TGF-β2 (200 pg/mL) only, and Skepinone-L treated explants 2 hours after TGF-β2 addition (A). Protein density relative to loading control GAPDH (B). Graphed data shows post-hoc Tukey's comparisons test and one-way ANOVA with ±SEM (ns = not significant, **P* < 0.0332).

Supplementary Table 6.3. Summary of β-catenin protein levels in rat LEC explants exposed to Skepinone-L 2 hours after TGF-β2 treatment.

Treatment group comparisons	***P* value**[1]
NT *vs.* Skepinone-L (1 μM)	0.8439
NT *vs.* TGF-β2 (200 pg/mL)	0.4026
NT *vs.* Skepinone-L (1 μM) + TGF-β2	0.0236
Skepinone-L (1 μM) *vs.* TGF-β2	0.8352
Skepinone-L (1 μM) *vs*. Skepinone-L (1 μM) + TGF-β2	0.0741
TGF-β2 *vs.* Skepinone-L (1 μM) + TGF-β2	0.2362

[1]One-way ANOVA with Tukey's multiple comparisons test
*Statistically significant difference between treatment groups ($P < 0.05$)
Abbreviations: Non-treated LEC explants (NT), Skepinone-L. Refer to Supplementary Figure 6.3 B.

CHAPTER 7: GENERAL DISCUSSION

We have focused on the role and interactions between different growth factors, associated downstream signalling molecules, as well as cell cytoskeletal protein tropomyosin (Tpm), in either regulating and/or dysregulating lens epithelial cell behaviour associated with EMT. The findings from this body of work have reaffirmed the importance of growth factor modulation during lens EMT leading to fibrotic cataract.

TGF-β induces EMT in various fibrotic disorders, in the lens this can lead to cataractogenesis (Lovicu et al., 2002; Wormstone et al., 2002; de Iongh et al., 2005; Boswell et al., 2017; Kubo et al., 2018). When lens epithelial explants are treated with TGF-β2, the cells transdifferentiate into myofibroblastic cells that will eventually undergo apoptosis (Liu et al., 1994; Maruno et al., 2002); *in situ*, during ASC or PCO development, the mesenchymal-like/myofibroblastic cells that form can be maintained (Saika et al., 2002; Lovicu et al., 2004) likely owing to the presence of endogenous ocular factors. The use of the mutant mouse model overexpressing TGF-β1 leading to ASC postnatally provides a unique *in vivo* model replicating the human condition (Lovicu et al., 2004), presenting a heterogenous population of myofibroblastic and/or fibre-like cells in these plaques reactive for α-SMA, β-crystallin, and MIP (Lovicu et al., 2005). As previously suggested by Lovicu et al. (2004, 2005) and de Iongh et al. (2005), the ocular media provides other soluble factors that are influencing EMT during cataractogenesis that we have explored here.

TGF-β-mediated EMT induces early p38 activation that modulates Tpm and leads to morphological changes and apoptosis. FGF-2 can differentially regulate this EMT response by promoting other MAPKs (ERK1/2) to preferentially drive fibre differentiation associated more with pearl-like PCO, compared to Smad2/3-driven fibrotic PCO. We have shown that the interplay of Smads (canonical) and non-canonical TGF-β signalling is involved in regulating lens pathology (Figure 7.1).

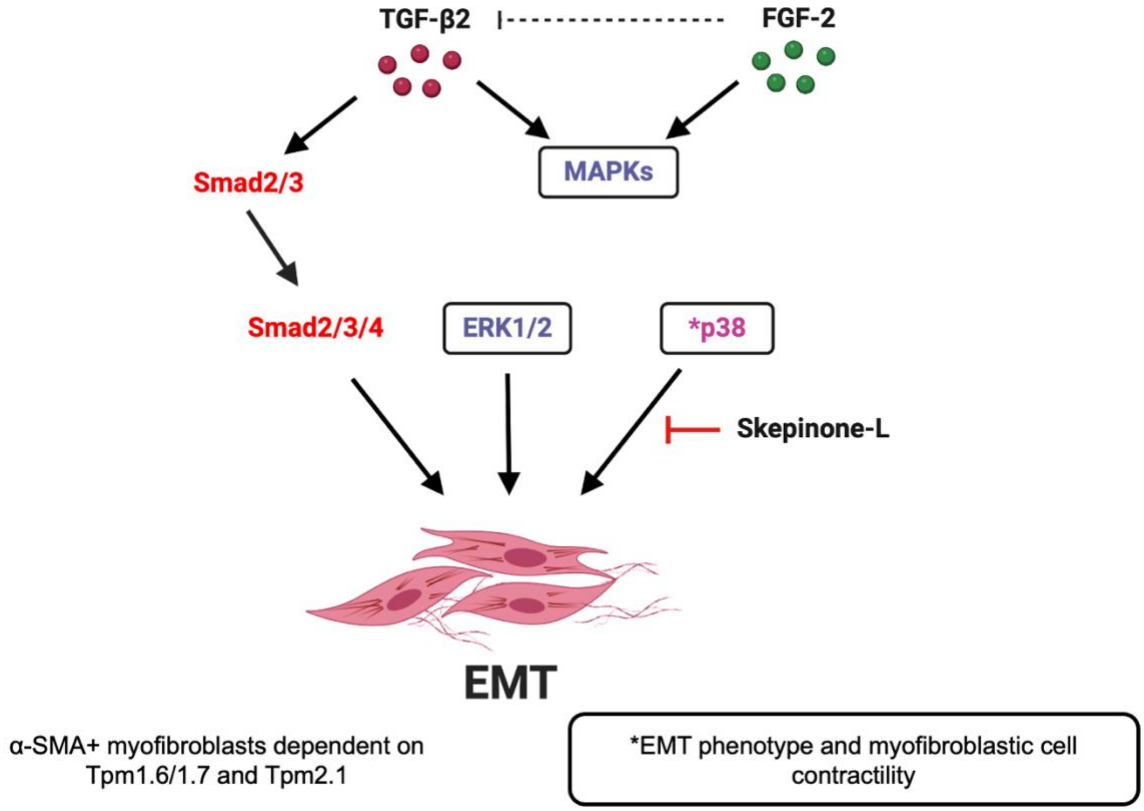

Figure 7.1. FGF-2 and TGF-β2 downstream signalling, as well as cytoskeletal proteins, in the induction of lens EMT and promotion of the contractile α-SMA+ myofibroblast phenotype. FGF-2 counteracts (dotted line) TGF-β2-induced rat lens EMT in a dose- and spatially dependent manner. Activation of Smad-dependent (Smad2/3, red) and Smad-independent (MAPKs, purple) signalling results in an EMT. TGF-β2-induced downstream Smad2/3/4 signalling and/or MAPK (boxed, ERK1/2, p38) signalling is associated with the myofibroblastic phenotype and consequently α-SMA positive lens cells. α-SMA stress fibre association in transitioned myofibroblasts is dependent on cytoskeletal actin filament proteins Tpm1.6/1.7 and Tpm2.1. Targeting downstream p38 MAPK using pharmacological compound Skepinone-L (red line) prevented the formation of EMT-associated myofibroblastic, contractile cells (*) but did not alter α-SMA protein accumulation in TGF-β2-treated LECs. Illustration created using *Biorender.com*.

7.1 TROPOMYOSIN: MARKERS FOR LENS FIBROSIS

Tropomyosin (Tpm) are required for the regulation of the cell actin cytoskeleton and its stabilisation in muscle and non-muscle cell types, as previously reviewed (Gunning et al., 2008). We investigated the role of Tpms in the postnatal rodent lens, during different cellular processes. In doing so, we validated that Tpm is differentially required for normal lens cell maintenance, fibre differentiation, and EMT, in both normal and mutant rodent lenses. We found isoform-specific Tpm expression in the postnatal rodent lens that was dependent on treatments and fixative protocols, with differential localisation and immunolabelling of Tpms

observed in unstimulated and growth factor stimulated (TGF-β2 or FGF-2) LEC explants. By treating LECs with TGF-β2 or FGF-2, we were able to model *in vitro* the cell phenotypes that are generated during fibrotic cataract; myofibroblasts and fibre-like cells (Lovicu et al., 2002, 2004), to discern a role for Tpm during LEC transformation processes.

We demonstrated that various Tpm isoforms are localised in LECs (see Figure 7.2). Using western blotting (SDS-PAGE), LEC explants stimulated by TGF-β2 either, i) elevated protein levels for Tpm1.6/1.7, Tpm2.1, Tpm3.1/3.2, and Tpm4.2, or ii) did not change protein levels for Tpm1.4, Tpm3.3, Tpm3.5, and Tpm3.8/3.9, compared to non-treated LECs (Figure 7.2). TGF-β is a known inducer of Tpm during cell remodelling and cytoskeletal stabilisation in various fibrotic and carcinoma models (Bakin et al., 2004; Varga et al., 2005; Zheng et al., 2008; Safina et al., 2009; Prunotto et al., 2015; Kubo et al., 2018). We confirmed the role of specific isoforms, particularly Tpm1.6/1.7 and Tpm2.1, that are reportedly dependent on TGF-β for upregulation in human and rodent lens fibrosis models (Kubo et al., 2013, 2017; Shibata et al., 2018; Parreno et al., 2020). The significant increase in Tpm1.6/1.7 levels in the presence of TGF-β2 demonstrates that these isoforms are indeed good markers for lens EMT in our LEC explant system. Future studies specifically targeting Tpm1.6 using the current model will be beneficial, since studies have shown that in the absence of this isoform, α-SMA cannot be

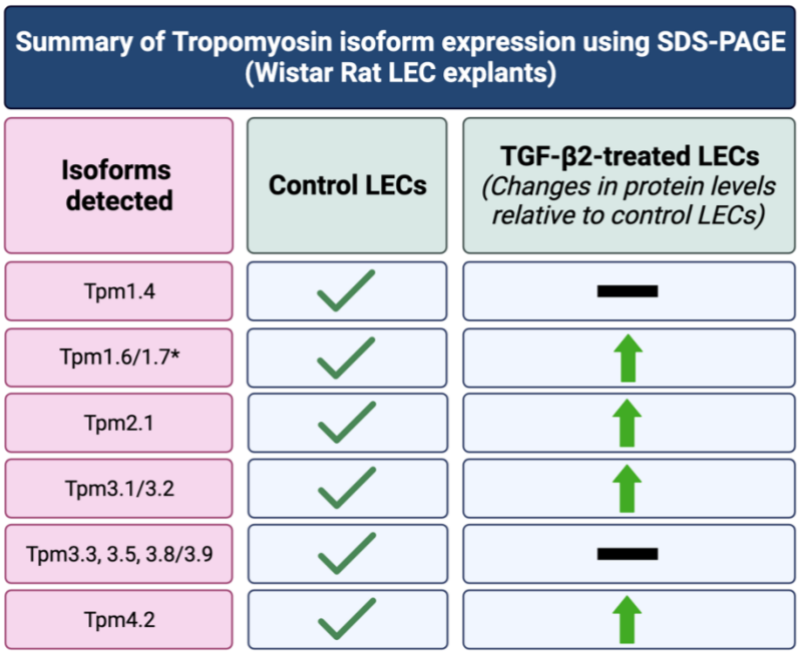

Figure 7.2. Summary of changes in Tpm protein levels using SDS-PAGE. A summary of the data acquired in Chapter 3: Figures 3.8–3.9. Green tick indicates presence of Tpm isoforms in unstimulated (control) lens epithelial cell (LEC) explants. Increased (green arrow) or constant/no change (black line) protein levels of Tpm isoforms in TGF-β2-treated LECs when compared to control LECs. *Statistically significant difference between control and TGF-β2-treated LECs.

recruited for actin filament assembly in contractile cells (Prunotto et al., 2015; Hardeman et al., 2019).

F-actin filamentous networks are essential for normal cell stabilisation and, in instances of cell transformation, for reassembly of cytoskeletal arrangements (Fischer et al., 2000; Lee et al., 2000; Ecken et al., 2015). In the lens, rearrangement of F-actin filaments occurs during lens cellular morphological alterations, including cell growth, migration, and the elongation of lens fibre cells during differentiation (Mousa and Trevithick, 1979; Ramaekers et al., 1981; Fischer et al., 2000; Rao and Maddala, 2006). Among its role in F-actin cytoskeletal stress fibre reorganisation during EMT (Fischer et al., 2000; Bakin et al., 2004; Parreno et al., 2020; Inguito et al., 2022), Tpm is also involved in morphological changes during lens fibre differentiation (Fischer et al., 2000; T. Shibata et al., 2021). Tpm isoforms decorate actin filaments in lens fibres, and are expressed in native lens fibres isolated from 6–10-week-old C57BL6/J WT mice (Cheng et al., 2018; Parreno et al., 2020), in particular Tpm1.13, Tpm3.5, and Tpm4.2. In addition, Tpm has been shown to be recruited and consequently colocalised to F-actin in undifferentiating and differentiating embryonic chick lens epithelial cells (Fischer et al., 2000). In our LEC explants, a high fibre differentiating dose of FGF-2 elevated levels of Tpm1.6–1.9, Tpm2.1, Tpm3.1–3.3, Tpm3.5, Tpm3.8/3.9, and Tpm4.2. This finding is consistent with the expression of Tpm3.5 and Tpm4.2 in isolated lens fibres from WT mice in previous studies (Cheng et al., 2018; Parreno et al., 2020), and we identified several additional isoforms that could be considered new markers for lens fibre cell differentiation.

The use of mutant mice overexpressing TGF-β1 in the eye allowed us to examine the role of Tpm during postnatal cataractogenesis *in situ*. We found various Tpm isoforms to be localised in the lens epithelium of WT mice (as per our rat LEC explants), as well as in ASC plaques of TG mice, from P7–P21; however, we could not discern their specific immunolocalisation or their role in the different cell types of the ASC plaques. Despite this, we were able to detect several cytoskeletal stress-fibre associated Tpm isoforms, such as Tpm1.6/1.7, Tpm2.1, Tpm3.1/3.2, and Tpm4.2. Further transcriptomic analysis of these cells for different Tpms, to investigate for any significant differences between unstimulated, and growth factor stimulated LECs, can be compared to whole lens epithelia from ASC samples from TG mice lens. This will lead to a better understanding of the requirement for specific Tpm isoforms during normal postnatal lens growth and lens pathology.

We set out to better understand the role of Tpm3.1 using the LEC explant system, given that previous studies have shown that F-actin stress fibre assembly and formation was limited in

native lenses of Tpm3.1 KO mice, and pharmacological inhibition of Tpm3.1 in conjunction to TGF-β treatment reduced EMT development in imLECs (Parreno et al., 2020). One objective was to cross the Tpm3.1/3.2 KO line with our TGF-β1 overexpressing mutant mice, to determine whether the loss of Tpm3.1/3.2 will impact ASC formation; however, when we first tested lens explants from these Tpm3.1/3.2 or Tpm4.2 mutants, EMT induction still occurred when LEC were treated with TGF-β2.

We confirmed a protein deficiency of Tpm3.1/3.2 and Tpm4.2 in Tp7 and Tp16 mice, respectively, by probing for Tpm3.1/3.2 and Tpm4.2 in different organ tissues (e.g., brain, kidney, lens). While we observed low molecular weight proteins (< 25 kDa) in LF samples of WT and Tpm KO mice, we proposed these were chaperone crystallin proteins, previously shown to recruit Tpm isoforms for structural maintenance of lens fibre cells (Woo and Fowler, 1994). However, it is worth considering other Tpm isoforms that are likely present in the lens fibres acquired from WT and Tpm3.1/3.2 and Tpm4.2 KO mice. This is a limitation of the present study that may need to be addressed as a future avenue of research, by using other assays to detect antibody specificity for Tpm isoforms.

Tpm3.1/3.2 or Tpm4.2 do not appear to be necessary for α-SMA, as we showed α-SMA to continue to be recruited into the stress fibres of myofibroblastic cells in both Tp7 and Tp16 LEC explants treated with TGF-β. α-SMA is likely more reliant on other Tpm isoforms specifically coded by the *Tpm1* and *Tpm2* genes, as shown in human subcutaneous fibroblast cell models (Prunotto et al., 2015). Our findings from these Tpm protein deficient mouse models confirm a previously identified function for TGF-β in regulating *Tpm1* and *Tpm2*, and not *Tpm3* and/or *Tpm4* derived isoforms (Bakin et al., 2004; Zheng et al., 2008; Prunotto et al., 2015). We showed this phenomenon in TGF-β2-treated LECs with an upregulation of Tpm1.6/1.7 and Tpm2.1 protein levels compared to unstimulated LECs (Figure 7.2). It would be beneficial for future studies to test the potential of other inhibitor compounds and genetic modification tools to selectively target EMT-associated Tpm isoforms, including silencing RNA and CRISPR, in the LEC explant system.

Consistent with our mutant mouse findings, targeting Tpm3.1/3.2 using pharmacological compounds such as ATMs (TR100 and ATM-3507) was not successful in preventing TGF-β-induced EMT in LEC explants, even in the absence of Tpm4.2. Pharmacological inhibition of Tpm3.1/3.2 appeared to reduce EMT marker levels (α-SMA) in TGF-β2-treated rat LECs but did not inhibit α-SMA levels in TGF-β2-treated LECs of WT mice, and we cannot explain this inconsistency other than that there may be varying sensitivity of the different cells for ATMs.

Although Tpm3.1/3.2 and Tpm4.2 are required during stress fibre formation (Gateva et al., 2017; Manstein et al., 2020), in their absence stress fibres can still form in TGF-β-induced myofibroblasts in rodent lens explants, suggesting that other stress-fibre associated isoforms are sufficient. While Tpm3.1/3.2 and Tpm4.2 are present during LEC cytoskeletal reorganisation, we cannot exactly specify what their role is, based on our findings.

Inhibition of Tpm3.1/3.2 did not appear to cause compensation of *Tpm1* derived isoforms in LECs of WT or Tpm4.2 KO mice. Since TR100/TGF-β2-treated LECs of both WT and Tp16 mice are still undergoing an EMT response, we did not expect to see Tpm1.6/1.7 and/or Tpm2.1 to be significantly reduced in these lens cells, given that these isoforms are reported to normally be upregulated during EMT (Kubo et al., 2013; Prunotto et al., 2015; S. Shibata et al., 2021). While we have shown and stated the limitations of using Tpm3.1/3.2 and Tpm4.2 KO mice lines in the current study, a different conditional Tpm KO line is required to further understand the role of Tpm isoforms during lens fibrosis. As mentioned, Tpm1.6 may be an ideal candidate for playing a significant role in lens EMT given its elevated expression in other cataractous models (Kubo et al., 2013, 2017; Shibata et al., 2018; Parreno et al., 2020). For future studies, we plan to target *Tpm1* derived isoforms using lens conditional Tpm1.6/1.7 KO mice and repeating the *in vitro* LEC explant experiments conducted in this study. Crossing Tpm1.6 CKO mice with our TG mice overexpressing TGF-β1 may lead to a better understanding of the direct role of Tpm1 *in situ* during cataractogenesis.

Based on results acquired in Chapter 3, Tpm1.6/1.7, Tpm2.1, Tpm3.1/3.2, Tpm3.3, Tpm3.5, Tpm3.8/3.9, and Tpm4.2 were all elevated in FGF-induced fibre differentiation in rat LEC explants. A study by Cheng et al. (2018) confirmed that Tpm3.5 is required in lens fibre cell membranes as F-actin stabilising proteins, reporting that its expression and membranous localisation was reduced in Tpm3/Δexon9d$^{-/-}$ mice compared to WT mice lenses. Another study by T. Shibata et al. (2021) using a conditional *Tpm1* KO lens model showed fibre differentiation was dysregulated with apical focal points of cells adjacent to the lens epithelium not fusing during postnatal growth. Despite this, lenses from these mice lines still formed (T. Shibata et al., 2021). Since we observed that a high fibre differentiating dose of FGF-2 stimulated Tpm1.6–1.9, Tpm2.1, Tpm3.1–3.3, Tpm3.5, Tpm3.8/3.9, and Tpm4.2 accumulation in rat LEC explants, an experiment using LEC explants from Tp7 and Tp16 mice could potentially investigate whether the inhibition or deficiency for either Tpm3.1/3.2 or Tpm4.2 impacts lens fibre differentiation. Our primary observations discount the involvement of these Tpm isoforms in fibre differentiation considering that the lenses that we acquired from these KO mice and

used for our LEC explants were relatively normal. Therefore, this proposed experimental concept may not be required, since other non-muscle Tpm isoforms are still required for lens fibre differentiation and stability for cell biomechanics, reprogramming, stiffness, and polarity (Woo and Fowler, 1994; Fischer et al., 2000; Nowak et al., 2009; Kubo et al., 2010; C. Cheng et al., 2017; Kubo et al., 2017; Cheng et al., 2018).

Future studies are required to further understand the role of Tpms in lens fibrosis, given that cytoskeletal Tpms have previously been shown to regulate genes required for cell biomechanics, signalling, and morphogenesis, in a differential manner in neuroblastoma cells (Stefen et al., 2018). Overall, our study has provided several key Tpm isoforms that could be used to further characterise the differential cell types that develop during ASC and PCO.

7.2 THE INTERPLAY BETWEEN FGF-2 AND TGF-β2 DURING LENS FIBROSIS

A dose-dependent gradient of FGF is required within the ocular media to tightly regulate lens cell proliferation and fibre differentiation, to facilitate normal lens growth and maintenance of its polarity for its overall function and transparency (Chamberlain and McAvoy, 1989, 1997; McAvoy and Chamberlain, 1989; Klok et al., 1998; Lovicu and McAvoy, 2001; West-Mays et al., 2009). During lens fibrosis, stimulation of FGF from the posterior and vitreous humour most likely contributes to regenerative or pearl-like PCO (Nishi et al., 1996; Cerra et al., 2003).

Various models to date have demonstrated that FGF, and its associated receptors, can regulate and/or mediate TGF-β-induced EMT (Mansfield et al., 2004; Yang et al., 2008; Ramos et al., 2010; Shirakihara et al., 2011; Kurimoto et al., 2016; Kubo et al., 2017, 2018; Bordignon et al., 2019; Koike et al., 2020; Flokis and Lovicu, 2023). Modelling the interplay between FGF and TGF-β is not a new concept, as this FGF/TGF-β combination has been of interest in understanding lens cell fibrosis in mouse, rat, and human models (Cerra et al., 2003; Mansfield et al., 2004; Kubo et al., 2017, 2018; S. Shibata et al., 2021). During PCO, FGF can modulate its progression and reduce EMT-associated marker expression, while promoting collagen deposition and LEC mitosis, events dependent on different concentrations of TGF-β (Nishi et al., 1996; Meacock et al., 2000; Kubo et al., 2017; Flokis and Lovicu, 2023). Given the reported increase in FGF-2 concentrations following surgical intervention in mammalian lens models (Namiki, 1994; Wallentin et al., 1998; Wormstone et al., 2001), the Cerra et al. (2003) study used a higher dose of FGF-2/TGF-β2 to treat whole lens cultures to study the formation of ASC. In this study, FGF-2 was shown to exacerbate TGF-β-induced EMT particularly cataractous

modifications in rat lenses (Cerra et al., 2003), while other studies have shown it to antagonise TGF-β-induced EMT marker expression in mouse and human LECs (Kubo et al., 2017).

In our LEC explant system, we demonstrated a dose dependent regulatory mechanism between FGF-2 and TGF-β2 in dictating lens cell fates. At the right dose concentrations, a high differentiating dose of FGF-2 (200 ng/mL) combined with a low dose of TGF-β2 (50 pg/mL), widespread EMT induction in lens epithelial cells was prevented. Central explant regions (CLECs), experienced preferential EMT induction, whereas lens cells in peripheral regions (PLECs) underwent a fibre-like differentiation response under the same conditions. This differential response in cells is more indicative of what may be happening *in situ* during PCO, with both fibrotic (EMT-related) or pearl-like/regenerative (lens fibre cell differentiation) presented (Figure 7.3) (Wormstone and Eldred, 2016; Koch et al., 2019; Wormstone et al., 2020).

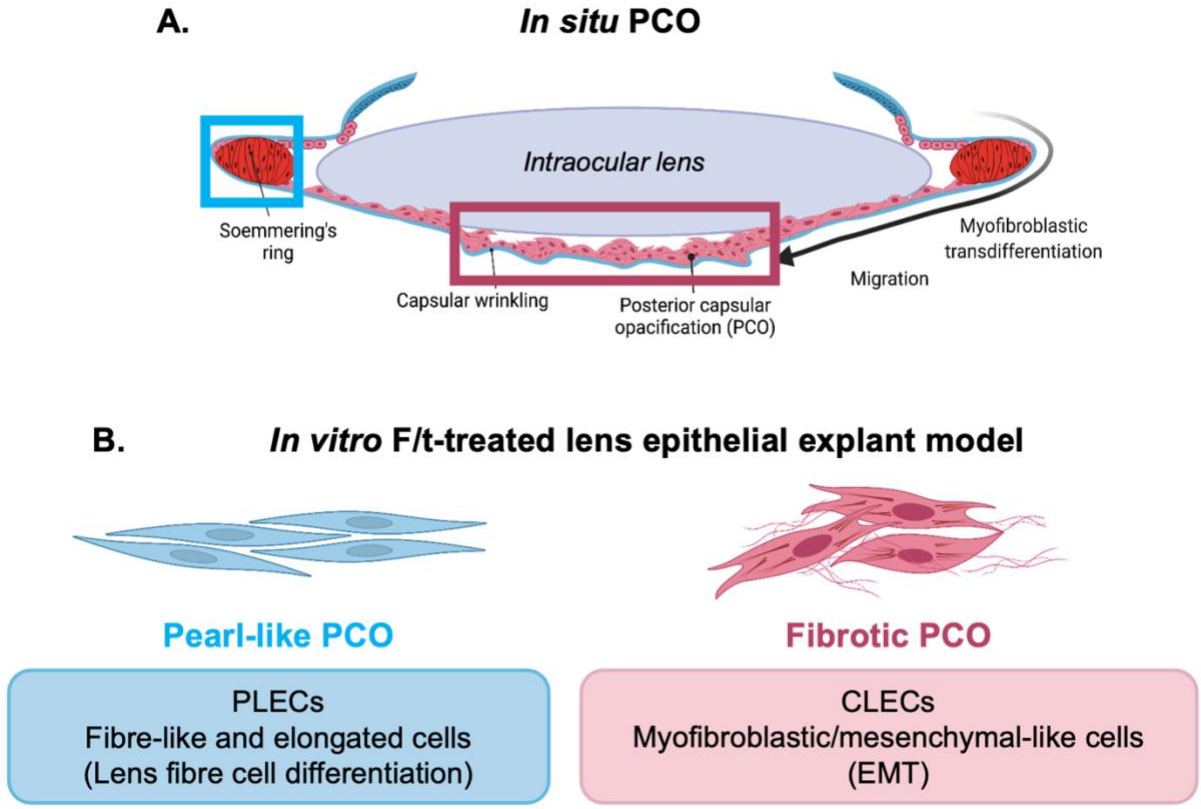

Figure 7.3. In situ vs. in vitro models for PCO development. A) *In situ*, following cataract surgery, posterior capsule opacification (PCO) develops and is characterised as either fibrotic via myofibroblastic transdifferentiation (EMT, pink box) or regenerative/pearl-like via lens fibre cell differentiation (blue box). B) *In vitro*, our LEC explants treated with a high differentiating dose of FGF-2 and low dose of TGF-β2 (F/t) underwent a differential cell response. Central lens epithelial cells (CLECs) preferentially underwent an EMT response, similar to fibrotic PCO, and peripheral cells (PLECs) preferred a fibre-like differentiation response (pearl-like PCO). F: High FGF-2 dose, l: low TGF-β2 dose. Diagrams created using *Biorender.com*.

Given FGF-2 has been shown to be a much stronger inducer of ERK1/2 activation in PLECs compared to TGF-β2, we propose that PLECs present a higher ratio of ERK1/2-to-Smad2/3 signalling compared to CLECs driving them to differentiate into fibre-like cells. FGF-2-induced ERK1/2 signalling, as well as PI3K/Akt signalling, has been linked to lens fibre elongation (ERK1/2-signalling) and associated fibre cell marker expression of β- and γ-crystallin proteins (PI3K/Akt-signalling) (Lovicu and McAvoy, 2001; Wang et al., 2008, 2010). The results from our study showed that a differentiating dose of FGF-2 is required for the accumulation of β-crystallin across 5 days of culture, particularly in the elongating fibre-like cells (PLECs) of cotreated F/t LEC explants.

The differential cell fates of CLEC and PLECs is reflective of the differences shown between pearl-like and fibrotic PCO *in situ*, as previously suggested (Wormstone et al., 2020). For example, future studies isolating the central cells of F/t cotreated LEC explants may reveal a repression of fibre differentiation genes while concurrently activating mesenchymal/EMT-associated genes, and vice versa for peripheral cells, as depicted in the current study's immunolabelling at the protein level. This study was limited to protein analysis. It is becoming clearer that the lens epithelium is a heterogenous population, as shown recently in single cell RNA-Seq transcriptomic studies (Giannone et al., 2023). For future studies, it would be beneficial and more informative to implement gene analysis assays, to effectively determine specific molecular markers at the mRNA level, characteristic of these F/t cotreated LECs. This future research venture could be clinically significant in terms of further understanding the mechanisms of how lens cells operate during regenerative and fibrotic PCO, that, in turn, may lead to developing potential therapies for treatment and/or prevention.

Given our findings from Chapters 3 and 4, this dual cell type F/t treated LEC explant model could be used to compare the various cytoskeletal functions of Tpm during lens fibre-like differentiation and EMT by observing differential labelling of Tpms. In the current study, we only characterised several Tpm isoforms coded by *Tpm1* and *Tpm2* genes in the F/t-treated LEC explant model, as they have previously been used as markers for EMT in other fibrotic systems (Prunotto et al., 2015; Desouza-Armstrong et al., 2017; Shin et al., 2017; Zare et al., 2018; Bradbury et al., 2021), as well as the lens (see Section 7.1) (Kubo et al., 2017, 2018; Shibata et al., 2018; Parreno et al., 2020; S. Shibata et al., 2021). A study by Kubo et al. (2017) showed that FGF-2 could not independently stimulate Tpm1 and Tpm2 expression in MLECs treated with <10 ng/mL of FGF-2. This study also showed that FGF-2 antagonised TGF-β upregulation of Tpm isoforms, in cotreated MLECs and HLECs, that appeared dependent on the doses of

either growth factor administered (Kubo et al., 2017). We observed a similar response in our study as Tpm1.6/Tpm1.7 and Tpm2.1 localised in the cell cytoskeletons of both fibre-like (PLECs) and myofibroblastic cells (CLECs) of F/t cotreated lens explants, suggesting a role for these isoforms during both lens fibre differentiation and EMT.

7.3 p38 MAPK: AN EARLY MEDIATOR OF TGF-β-INDUCED EMT?

During TGF-β-induced LEC EMT, the endpoint of this pathological response *in vitro* is typically cell death; however, transitioned cells during wound healing responses in ASC or PCO are still maintained *in situ* (Wormstone et al., 2001; Lovicu et al., 2004). Therefore, it is important to understand the mechanisms that are causing and/or regulating cell death in our LEC explant model. TGF-β stimulated EMT during fibrosis relies on the activation of canonical (Smad-dependent) and non-canonical (Smad-independent) signalling for the functionality and reassembly of the cell cytoskeleton, and its associated components (Bakin et al., 2004; Meyer-ter-Vehn et al., 2006). In particular, TGF-β non-canonical downstream stress-induced protein p38 MAPK is involved in apoptosis, with p38α being the most abundant and well-studied across various systems (Porras et al., 2004; Oh et al., 2014).

We reassessed the role of p38α and set out to evaluate the effectiveness of p38α-specific inhibitor, Skepinone-L, during lens EMT. Skepinone-L has a reportedly high selectivity for p38α (Koeberle et al., 2012; Borst et al., 2013; F. Cheng et al., 2017), that can effectively inhibit TGF-β2-induced EMT, as well as cell apoptosis, in our pre- and cotreated LEC explants at doses < 2 μM, with all cells remaining viable. We found that these LEC explants showed little phenotypic changes, with no evidence of capsular modulation, suggesting a potential mechanism for p38 in regulating cell contractility and cytoskeletal reorganisation during lens EMT (Figure 7.1). Inhibition of p38α did not impact t-Smad2/3 activation, and specifically prevented p38 activation (phosphorylation) after 15 minutes in TGF-β2-treated LECs, further validating the efficacy of Skepinone-L as an inhibitor for p38α.

The activation of p38 has been linked to cell blebbing and apoptosis in numerous models (Huot et al., 1998; Ma et al., 1999; Houle et al., 2003; Lee et al., 2009). For example, an *in vivo* neonatal mouse skin model injected with a pemphigus foliaceus (PF) IgG, known to cause blistering in the upper epidermis, showed that inhibition of the initial peak of p38 phosphorylation prevented cell apoptosis and resultant blistering (Lee et al., 2009). This study also showed that inhibition of p38 after the second wave of p38 activation (> 4 hours) was

unable to block cell apoptosis (Lee et al., 2009), suggesting early mediation of p38 during cell apoptotic responses.

Previous studies in ocular tissues, including human corneal cells (Shu et al., 2019a), human LE cells (Jiang et al., 2006; Bai et al., 2015), and chick LEC lines (Zhou and Menko, 2004; Boswell et al., 2017), have used inhibitor compounds to target p38 MAPK activity during lens EMT and cataractogenesis. In human LE cells stimulated with H_2O_2 to induce oxidative stress, inhibition of p38 using SB203580 reduced cell apoptosis within 6 hours of treatment (Bai et al., 2015), but was not effective between 12–24 hours following H_2O_2 treatment. This finding provides evidence for p38 MAPK signalling activation during cell apoptosis, that could be applied to our TGF-β-induced lens EMT model. However, the inhibitor used in this study, SB203580, has been shown to inhibit both p38α and p38β (Lali et al., 2000; Laping et al., 2002; McGuire et al., 2013; Sreekanth et al., 2016), as well as impacting other signalling proteins (Liverton et al., 1999; Godl et al., 2003; O'Keefe et al., 2007; Xu et al., 2013). In addition, given that p38 has been shown to be activated in the presence of other growth factors or stimulants, such as EGF, in other tissues and systems (Rice et al., 2002; Frey et al., 2004, 2006; Jiang et al., 2006), it would be interesting to look at whether p38 is directly or indirectly regulated by other growth factors besides TGF-β in the ocular media.

Cytoskeletal reorganisation is an essential stage during cell apoptosis, as previously reviewed (Pawlak and Helfman, 2001). From our study, we have shown that p38α inhibition reduced Tpm1.6/1.7 and Tpm2.1 protein levels in TGF-β2-treated LEC explants, reconfirming these Tpm isoforms as ideal markers for lens EMT, as previously mentioned (see Section 7.1 and Figure 7.2). In addition, p38α preferentially regulates the morphological phenotype of myofibroblastic cells during TGF-β2-induced EMT. Tpms are required for F-actin assembly in the formation of actin filaments, and by inhibiting these cytoskeletal arrangements, stress fibre formation in myofibroblasts is disrupted in our explant model, as previously reported in other systems (Ljungdahl et al., 1998; Shields et al., 2002; Bakin et al., 2004; Tojkander et al., 2011). We showed a reduction in α-SMA protein levels in pre- and cotreated Skepinone-L/TGF-β2 explants; however, α-SMA still accumulated in these LECs. α-SMA is reportedly reliant on Tpm1.6 and Tpm1.7 for stress fibre assembly of TGF-β-induced myofibroblastic cells (Prunotto et al., 2015). Inhibition of p38α/β in TGF-β1 treated human tenon fibroblasts (Meyer-ter-Vehn et al., 2006) and renal tubular LLCPK1/AT1 cells (Sebe et al., 2008) reduced α-SMA protein levels and actin stress-fibre localisation, demonstrating a role for p38 in regulating α-SMA

stress fibre assembly; however, both the Meyer-ter-Ven et al. (2006) and Sebe et al. (2008) studies used SB203580 that is not as specific for p38α (Davies et al., 2000; Godl et al., 2003).

Given the promising effectiveness of Skepinone-L in inhibiting p38 MAPK in TGF-β2 treated rat LECs, potential *in vivo* experiments could be established to examine the interrelation between stress-induced proteins and cytoskeletal organisation, and their role in the α-SMA+ phenotype in transdifferentiated LECs. The current *in vitro* studies using LEC explants of Tpm3.1/3.2 and Tpm4.2 KO mice did not provide a clear characterisation of the role of *Tpm3* and *Tpm4* derived isoforms in lens EMT. Therefore, before approaching future *in vivo* work, the usage of other Tpm-deficient models, such as Tpm1.6 CKO or Tpm2.1 KO mice, may be more suited and warranted given the upregulation of these Tpm isoforms during TGF-β-induced lens EMT (Kubo et al., 2013, 2017; Shibata et al., 2018). Therefore, future research targeting p38α as well as Tpm1.6/1.7 may provide key stages of cytoskeletal reorganisation and cell apoptosis during TGF-β-induced lens EMT.

When LEC explants were exposed to Skepinone-L post-TGF-β2 treatment after 2 hours, it prolonged but did not inhibit EMT morphological and/or associated marker expression. Given that we were able to block TGF-β-induced EMT within 1 hour when LECs explants were pre-exposed to Skepinone-L, we believe p38 is activated early during this process. Although we showed p38 activation at 15 minutes, we could not discern the exact localisation of p38 in our LECs as it appeared to be transient. Studies have shown that p38 when activated is found in either the nucleus and/or the cytoplasm (Stambe et al., 2004; Saika et al., 2005; Wood et al., 2009), or both (Ben-Levy et al., 1998; Greenberg et al., 2002; Maik-Rachline et al., 2020), depending on the culture, tissue or cell type, and experimental conditions. For future studies, more selective timepoints are needed to discern the time and intracellular location of p38 activation, given that p38 reportedly has a biphasic activation response (Sebe et al., 2008; Lee et al., 2009; Shu et al., 2019a).

7.4 CLINICAL SIGNIFICANCE

To date, the only present solution for cataract removal is surgical intervention. Although there are invasive and non-invasive measures that can be applied as a form of treatment, but not prevention, such as eyedrops containing anti-inflammatory NSAIDs (Hoffman et al., 2016; Shihan et al., 2019), “drop-less” cataract surgery using slow-release drug administration to reduce post-surgical inflammation (Walters et al., 2015; Liegner et al., 2017; Bardoloi et al., 2020), or Nd-YAG (Karahan et al., 2014; Shihan et al., 2019; Joshi and Rasal, 2023), there is

still no immediate cure for this ocular disease. In addition, the main limitation for existing treatments is that patients cannot receive eyedrop treatment without first acquiring a lens pathology. Therefore, there is a necessity to find alternative treatments.

The current study provides insight into how cytokines and growth factors, TGF-β and FGF, respectively, are vital components during the stimulation of lens EMT leading to fibrosis. By examining growth factor interactions and their respective downstream signalling pathways *in vitro*, this study contributes to the wider understanding of the mechanisms occurring during EMT *in situ*. Given the complexity and cocktail of growth factors found within the ocular media, it is difficult to target one molecule or pathway in the hopes of completely inhibiting lens EMT leading to ASC and/or PCO, as certain pharmacological compounds have been shown to present unwanted off-target effects. The usage of Skepinone-L as a selective p38 MAPK inhibitor in this study has shown promise in inhibiting the morphological and cytoskeletal components (i.e. Tpm) commonly associated with transdifferentiating cells during TGF-β-induced EMT. Although Skepinone-L, as well as Tpm isoform inhibitors, may not be the complete solution for targeting lens EMT, it is a small key to unlocking a wider area of research leading towards a comprehensive understanding of the early causation of ASC and PCO.

7.5 CONCLUDING REMARKS

Overall, this thesis has set out to provide more pieces to a larger puzzle. There ultimately needs to be a fine balance between growth factors and stimulants within the ocular media to efficiently regulate normal lens growth and maintenance. By modelling specific mechanisms surrounding growth factor regulation/dysregulation in the eye lens, and how lens cells experience morphological transformations, we hope this thesis can contribute to a greater understanding of the ocular environment during lens pathology. Given that cataract is one of the leading causes of blindness globally, there is a necessity to find effective, alternative treatments to prevent primary fibrotic cataract (ASC) as well as the onset of secondary lens fibrosis (PCO). If we can further classify effective markers and cellular events that help us understand or best model lens EMT, we can then search for potential therapeutic agents to suppress or prolong cataract.

REFERENCES

Abdulhussein, D., Hussein, M.A., 2022. WHO Vision 2020: Have We Done It? Ophthalmic Epidemiol 1–9. https://doi.org/10.1080/09286586.2022.2127784

Agarwal, P., Daher, A.M., Agarwal, R., 2015. Aqueous humor TGF-β2 levels in patients with open-angle glaucoma: A meta-analysis. Mol Vis 21, 612–20.

Akatsu, Y., Takahashi, N., Yoshimatsu, Y., Kimuro, S., Muramatsu, T., Katsura, A., Maishi, N., Suzuki, H.I., Inazawa, J., Hida, K., Miyazono, K., Watabe, T., 2019. Fibroblast growth factor signals regulate transforming growth factor-β-induced endothelial-to-myofibroblast transition of tumor endothelial cells via Elk1. Mol Oncol 13, 1706–1724. https://doi.org/10.1002/1878-0261.12504

Apple, D.J., Solomon, K.D., Tetz, M.R., Assia, E.I., Holland, E.Y., Legler, U.F.C., Tsai, J.C., Castaneda, V.E., Hoggatt, J.P., Kostick, A.M.P., 1992. Posterior capsule opacification. Surv Ophthalmol 37, 73–116. https://doi.org/10.1016/0039-6257(92)90073-3

Arnold, D.R., Moshayedi, P., Schoen, T.J., Jones, B.E., Chader, G.J., Waldbillig, R.J., 1993. Distribution of IGF-I and -II, IGF Binding Proteins (IGFBPs) and IGFBP mRNA in Ocular Fluids and Tissues: Potential Sites of Synthesis of IGFBPs in Aqueous and Vitreous. Exp Eye Res 56, 555–565. https://doi.org/10.1006/exer.1993.1069

Aslam, T.M., Aspinall, P., Dhillon, B., 2003. Posterior capsule morphology determinants of visual function. Graefe's Archive Clin Exp Ophthalmol 241, 208–212. https://doi.org/10.1007/s00417-003-0626-8

Aykul, S., Martinez-Hackert, E., 2016. Transforming Growth Factor-β Family Ligands Can Function as Antagonists by Competing for Type II Receptor Binding*. J Biol Chem 291, 10792–10804. https://doi.org/10.1074/jbc.m115.713487

Bach, C.T.T., Creed, S., Zhong, J., Mahmassani, M., Schevzov, G., Stehn, J., Cowell, L.N., Naumanen, P., Lappalainen, P., Gunning, P.W., O'Neill, G.M., 2009. Tropomyosin Isoform Expression Regulates the Transition of Adhesions To Determine Cell Speed and Direction ▿ †. Mol Cell Biol 29, 1506–1514. https://doi.org/10.1128/mcb.00857-08

Bageghni, S.A., Hemmings, K.E., Zava, N., Denton, C.P., Porter, K.E., Ainscough, J.F.X., Drinkhill, M.J., Turner, N.A., 2018. Cardiac fibroblast-specific p38α MAP kinase promotes cardiac hypertrophy via a putative paracrine interleukin-6 signaling mechanism. FASEB J. 32, 4941–4954. https://doi.org/10.1096/fj.201701455rr

Bai, J., Zheng, Y., Dong, L., Cai, X., Wang, G., Liu, P., 2015. Inhibition of p38 mitogen-activated protein kinase phosphorylation decreases H2O2-induced apoptosis in human lens epithelial cells. Graefe's Arch. Clin. Exp. Ophthalmol. 253, 1933–1940. https://doi.org/10.1007/s00417-015-3090-3

Bailey, K., 1946. Tropomyosin: a New Asymmetric Protein Component of Muscle. Nature 157, 368–369. https://doi.org/10.1038/157368b0

Bakin, A.V., Rinehart, C., Tomlinson, A.K., Arteaga, C.L., 2002. p38 mitogen-activated protein kinase is required for TGFβ-mediated fibroblastic transdifferentiation and cell migration. J. Cell Sci. 115, 3193–3206. https://doi.org/10.1242/jcs.115.15.3193

Bakin, A.V., Safina, A., Rinehart, C., Daroqui, C., Darbary, H., Helfman, D.M., 2004. A Critical Role of Tropomyosins in TGF-β Regulation of the Actin Cytoskeleton and Cell Motility in Epithelial Cells. Mol Biol Cell 15, 4682–4694. https://doi.org/10.1091/mbc.e04-04-0353

Banh, A., Deschamps, P.A., Gauldie, J., Overbeek, P.A., Sivak, J.G., West-Mays, J.A., 2006. Lens-Specific Expression of TGF-β Induces Anterior Subcapsular Cataract Formation in the Absence of Smad3. Investigative Opthalmology Vis Sci 47, 3450. https://doi.org/10.1167/iovs.05-1208

Bao, X., Song, H., Chen, Z., Tang, X., 2012. Wnt3a promotes epithelial-mesenchymal transition, migration, and proliferation of lens epithelial cells. Mol Vis 18, 1983–90.

Bardoloi, N., Sarkar, S., Pilania, A., Das, H., 2020. Efficacy and safety of dropless cataract surgery. Indian J. Ophthalmol. 68, 1081–1085. https://doi.org/10.4103/ijo.ijo_1186_19

Basta, M.D., Paulson, H., Walker, J.L., 2021. The local wound environment is a key determinant of the outcome of TGFβ signaling on the fibrotic response of CD44+ leader cells in an ex vivo post-cataract-surgery model. Exp. Eye Res. 213, 108829. https://doi.org/10.1016/j.exer.2021.108829

Batlle, E., Sancho, E., Francí, C., Domínguez, D., Monfar, M., Baulida, J., Herreros, A.G. de, 2000. The transcription factor Snail is a repressor of E-cadherin gene expression in epithelial tumour cells. Nat Cell Biol 2, 84–89. https://doi.org/10.1038/35000034

Batur, M., Gül, A., Seven, E., Can, E., Yaşar, T., 2016. Posterior Capsular Opacification in Preschool- and School-Age Patients after Pediatric Cataract Surgery without Posterior Capsulotomy. Turkish J Ophthalmol 46, 205–208. https://doi.org/10.4274/tjo.24650

Ben-Levy, R., Hooper, S., Wilson, R., Paterson, H.F., Marshall, C.J., 1998. Nuclear export of the stress-activated protein kinase p38 mediated by its substrate MAPKAP kinase-2. Curr. Biol. 8, 1049–1057. https://doi.org/10.1016/s0960-9822(98)70442-7

Bharadwaj, S., Thanawala, R., Bon, G., Falcioni, R., Prasad, G.L., 2005. Resensitization of breast cancer cells to anoikis by Tropomyosin-1: role of Rho kinase-dependent cytoskeleton and adhesion. Oncogene 24, 8291–8303. https://doi.org/10.1038/sj.onc.1208993

Bhattacharya, B., Prasad, G.L., Valverius, E.M., Salomon, D.S., Cooper, H.L., 1990. Tropomyosins of human mammary epithelial cells: consistent defects of expression in mammary carcinoma cell lines. Cancer Res 50, 2105–12.

Bicer, S., Reiser, P.J., 2013. Complex tropomyosin and troponin T isoform expression patterns in orbital and global fibers of adult dog and rat extraocular muscles. J Muscle Res Cell M 34, 211–231. https://doi.org/10.1007/s10974-013-9346-9

Bierie, B., Moses, H.L., 2009. Transforming growth factor beta (TGF-beta) and inflammation in cancer. Cytokine Growth F R 21, 49–59. https://doi.org/10.1016/j.cytogfr.2009.11.008

Birkenkamp, K.U., Tuyt, L.M.L., Lummen, C., Wierenga, A.T.J., Kruijer, W., Vellenga, E., 2000. The p38 MAP kinase inhibitor SB203580 enhances nuclear factor-kappa B transcriptional activity by a non-specific effect upon the ERK pathway. Br. J. Pharmacol. 131, 99–107. https://doi.org/10.1038/sj.bjp.0703534

Bollenbecker, S., Barnes, J.W., Krick, S., 2023. Fibroblast Growth Factor Signaling in Development and Disease. Int. J. Mol. Sci. 24, 9734. https://doi.org/10.3390/ijms24119734

Bolós, V., Peinado, H., Pérez-Moreno, M.A., Fraga, M.F., Esteller, M., Cano, A., 2002. The transcription factor Slug represses E-cadherin expression and induces epithelial to mesenchymal transitions: a comparison with Snail and E47 repressors. J Cell Sci 116, 499–511. https://doi.org/10.1242/jcs.00224

Bonello, T.T., Janco, M., Hook, J., Byun, A., Appaduray, M., Dedova, I., Hitchcock-DeGregori, S., Hardeman, E.C., Stehn, J.R., Böcking, T., Gunning, P.W., 2016. A small molecule inhibitor of tropomyosin dissociates actin binding from tropomyosin-directed regulation of actin dynamics. Sci Rep-uk 6, 19816. https://doi.org/10.1038/srep19816

Bordignon, P., Bottoni, G., Xu, X., Popescu, A.S., Truan, Z., Guenova, E., Kofler, L., Jafari, P., Ostano, P., Röcken, M., Neel, V., Dotto, G.P., 2019. Dualism of FGF and TGF-β Signaling in Heterogeneous Cancer-Associated Fibroblast Activation with ETV1 as a Critical Determinant. Cell Reports 28, 2358-2372.e6. https://doi.org/10.1016/j.celrep.2019.07.092

Borst, O., Walker, B., Münzer, P., Russo, A., Schmid, E., Faggio, C., Bigalke, B., Laufer, S., Gawaz, M., Lang, F., 2013. Skepinone-L, a Novel Potent and Highly Selective Inhibitor of p38 MAP Kinase, Effectively Impairs Platelet Activation and Thrombus Formation. Cell. Physiol. Biochem. 31, 914–924. https://doi.org/10.1159/000350110

Boswell, B.A., Korol, A., West-Mays, J.A., Musil, L.S., 2017. Dual function of TGFβ in lens epithelial cell fate: implications for secondary cataract. Mol Biol Cell 28, 907–921. https://doi.org/10.1091/mbc.e16-12-0865

Boswell, B.A., VanSlyke, J.K., Musil, L.S., 2010. Regulation of Lens Gap Junctions by Transforming Growth Factor Beta. Mol Biol Cell 21, 1686–1697. https://doi.org/10.1091/mbc.e10-01-0055

Boyer, B., Vallés, A.M., Edme, N., 2000. Induction and regulation of epithelial–mesenchymal transitions. Biochem Pharmacol 60, 1091–1099. https://doi.org/10.1016/s0006-2952(00)00427-5

Bradbury, P., Nader, C.P., Cidem, A., Rutting, S., Sylvester, D., He, P., Rezcallah, M.C., O'Neill, G.M., Ammit, A.J., 2021. Tropomyosin 2.1 collaborates with fibronectin to promote TGF-β1-induced contraction of human lung fibroblasts. Respir Res 22, 129. https://doi.org/10.1186/s12931-021-01730-y

Brayford, S., Bryce, N.S., Schevzov, G., Haynes, E.M., Bear, J.E., Hardeman, E.C., Gunning, P.W., 2016. Tropomyosin Promotes Lamellipodial Persistence by Collaborating with Arp2/3 at the Leading Edge. Curr. Biol. 26, 1312–1318. https://doi.org/10.1016/j.cub.2016.03.028

Brayford, S., Schevzov, G., Vos, J., Gunning, P., 2015. The Cytoskeleton in Health and Disease 373–391. https://doi.org/10.1007/978-1-4939-2904-7_16

Buehl, W., Menapace, R., Sacu, S., Kriechbaum, K., Koeppl, C., Wirtitsch, M., Georgopoulos, M., Findl, O., 2004. Effect of a silicone intraocular lens with a sharp posterior optic edge on posterior capsule opacification. J Cataract Refract Surg 30, 1661–1667. https://doi.org/10.1016/j.jcrs.2004.02.051

Burren, C.P., Berka, J.L., Edmondson, S.R., Werther, G.A., Batch, J.A., 1996. Localization of mRNAs for insulin-like growth factor-I (IGF-I), IGF-I receptor, and IGF binding proteins in rat eye. Invest Ophth Vis Sci 37, 1459–68.

Caldwell, B.J., Lucas, C., Kee, A.J., Gaus, K., Gunning, P.W., Hardeman, E.C., Yap, A.S., Gomez, G.A., 2014. Tropomyosin isoforms support actomyosin biogenesis to generate contractile tension at the epithelial zonula adherens. Cytoskeleton 71, 663–676. https://doi.org/10.1002/cm.21202

Canovas, B., Nebreda, A.R., 2021. Diversity and versatility of p38 kinase signalling in health and disease. Nat. Rev. Mol. Cell Biol. 22, 346–366. https://doi.org/10.1038/s41580-020-00322-w

Cao, Z., Livas, T., Kyprianou, N., 2016. Anoikis and EMT: Lethal "Liaisons" during Cancer Progression. Crit. Rev. Oncog. 21, 155–168. https://doi.org/10.1615/critrevoncog.2016016955

Cerra, A., Mansfield, K.J., Chamberlain, C.G., 2003. Exacerbation of TGF-beta-induced cataract by FGF-2 in cultured rat lenses. Mol Vis 9, 689–700.

Cevenini, A., Orrù, S., Mancini, A., Alfieri, A., Buono, P., Imperlini, E., 2018. Molecular Signatures of the Insulin-like Growth Factor 1-mediated Epithelial-Mesenchymal Transition in Breast, Lung and Gastric Cancers. Int J Mol Sci 19, 2411. https://doi.org/10.3390/ijms19082411

Chamberlain, C.G., McAvoy, J.W., 1997. Fibre differentiation and polarity in the mammalian lens: a key role for FGF. Prog Retin Eye Res 16, 443–478. https://doi.org/10.1016/s1350-9462(96)00034-1

Chamberlain, C.G., McAvoy, J.W., 1989. Induction of Lens Fibre Differentiation by Acidic and Basic Fibroblast Growth Factor (FGF). Growth Factors 1, 125–134. https://doi.org/10.3109/08977198909029122

Chen, H., Zhou, X., Shi, Y., Yang, J., 2013. Roles of p38 MAPK and JNK in TGF-β1-induced Human Alveolar Epithelial to Mesenchymal Transition. Arch. Méd. Res. 44, 93–98. https://doi.org/10.1016/j.arcmed.2013.01.004

Chen, S., Shen, Z., Gao, L., Yu, S., Zhang, P., Han, Z., Kang, M., 2021. TPM3 mediates epithelial-mesenchymal transition in esophageal cancer via MMP2/MMP9. Ann. Transl. Med. 9, 1338–1338. https://doi.org/10.21037/atm-21-4043

Chen, X., Ye, S., Xiao, W., Wang, W., Luo, L., Liu, Y., 2014. ERK1/2 pathway mediates epithelial-mesenchymal transition by cross-interacting with TGFβ/Smad and Jagged/Notch signaling pathways in lens epithelial cells. Int. J. Mol. Med. 33, 1664–1670. https://doi.org/10.3892/ijmm.2014.1723

Chen, X.-F., Zhang, H.-J., Wang, H.-B., Zhu, J., Zhou, W.-Y., Zhang, H., Zhao, M.-C., Su, J.-M., Gao, W., Zhang, L., Fei, K., Zhang, H.-T., Wang, H.-Y., 2012. Transforming growth factor-β1 induces epithelial-to-mesenchymal transition in human lung cancer cells via PI3K/Akt and MEK/Erk1/2 signaling pathways. Mol. Biol. Rep. 39, 3549–3556. https://doi.org/10.1007/s11033-011-1128-0

Cheng, C., Nowak, R.B., Amadeo, M.B., Biswas, S.K., Lo, W.-K., Fowler, V.M., 2018. Tropomyosin 3.5 protects the F-actin networks required for tissue biomechanical properties. J Cell Sci 131, jcs222042. https://doi.org/10.1242/jcs.222042

Cheng, C., Nowak, R.B., Fowler, V.M., 2017. The lens actin filament cytoskeleton: Diverse structures for complex functions. Exp Eye Res 156, 58–71. https://doi.org/10.1016/j.exer.2016.03.005

Cheng, F., Twardowski, L., Fehr, S., Aner, C., Schaeffeler, E., Joos, T., Knorpp, T., Dorweiler, B., Laufer, S., Schwab, M., Torzewski, M., 2017. Selective p38α MAP kinase/MAPK14 inhibition in enzymatically modified LDL-stimulated human monocytes: implications for atherosclerosis. FASEB J. 31, 674–686. https://doi.org/10.1096/fj.201600669r

Cho, H.J., Baek, K.E., Saika, S., Jeong, M.-J., Yoo, J., 2006. Snail is required for transforming growth factor-beta-induced epithelial-mesenchymal transition by activating PI3 kinase/Akt signal pathway. Biochem. Biophys. Res. Commun. 353, 337–43. https://doi.org/10.1016/j.bbrc.2006.12.035

Choi, H.-S., Yim, S.-H., Xu, H.-D., Jung, S.-H., Shin, S.-H., Hu, H.-J., Jung, C.-K., Choi, J.Y., Chung, Y.-J., 2010. Tropomyosin3 overexpression and a potential link to epithelial-mesenchymal transition in human hepatocellular carcinoma. BMC Cancer 10, 122. https://doi.org/10.1186/1471-2407-10-122

Choi, J., Park, S.Y., Joo, C.-K., 2004. Hepatocyte Growth Factor Induces Proliferation of Lens Epithelial Cells through Activation of ERK1/2 and JNK/SAPK. Invest Ophth Vis Sci 45, 2696–2704. https://doi.org/10.1167/iovs.03-1371

Chong, C.C.W., Stump, R.J.W., Lovicu, F.J., McAvoy, J.W., 2009. TGFβ promotes Wnt expression during cataract development. Exp Eye Res 88, 307–313. https://doi.org/10.1016/j.exer.2008.07.018

Chua, C.C., Rahimi, N., Forsten-Williams, K., Nugent, M.A., 2004. Heparan Sulfate Proteoglycans Function as Receptors for Fibroblast Growth Factor-2 Activation of Extracellular Signal–Regulated Kinases 1 and 2. Circ. Res. 94, 316–323. https://doi.org/10.1161/01.res.0000112965.70691.ac

Chylack, L.T., Cheng, H.-M., 1978. Sugar metabolism in the crystalline lens. Surv Ophthalmol 23, 26–34. https://doi.org/10.1016/0039-6257(78)90195-9

Clark, J.E., Sarafraz, N., Marber, M.S., 2007. Potential of p38-MAPK inhibitors in the treatment of ischaemic heart disease. Pharmacol. Ther. 116, 192–206. https://doi.org/10.1016/j.pharmthera.2007.06.013

Cohan, C.S., Welnhofer, E.A., Zhao, L., Matsumura, F., Yamashiro, S., 2001. Role of the actin bundling protein fascin in growth cone morphogenesis: Localization in filopodia and lamellipodia. Cell Motil. Cytoskelet. 48, 109–120. https://doi.org/10.1002/1097-0169(200102)48:2<;109::aid-cm1002>3.0.co;2-g

Connor, T.B., Roberts, A.B., Sporn, M.B., Danielpour, D., Dart, L.L., Michels, R.G., Bustros, S. de, Enger, C., Kato, H., Lansing, M., 1989. Correlation of fibrosis and transforming growth factor-beta type 2 levels in the eye. J Clin Invest 83, 1661–1666. https://doi.org/10.1172/jci114065

Cooley, B.C., Bergtrom, G., 2001. Multiple Combinations of Alternatively Spliced Exons in Rat Tropomyosin-α Gene mRNA: Evidence for 20 New Isoforms in Adult Tissues and Cultured Cells. Arch. Biochem. Biophys. 390, 71–77. https://doi.org/10.1006/abbi.2001.2347

Coombes, J.D., Schevzov, G., Kan, C.-Y., Petti, C., Maritz, M.F., Whittaker, S., Mackenzie, K.L., Gunning, P.W., 2015. Ras Transformation Overrides a Proliferation Defect Induced by Tpm3.1 Knockout. Cell. Mol. Biol. Lett. 20, 626–646. https://doi.org/10.1515/cmble-2015-0037

Cousins, S.W., McCabe, M.M., Danielpour, D., Streilein, J.W., 1991. Identification of transforming growth factor-beta as an immunosuppressive factor in aqueous humor. Invest Ophth Vis Sci 32, 2201–11.

Creed, S.J., Desouza, M., Bamburg, J.R., Gunning, P., Stehn, J., 2011. Tropomyosin isoform 3 promotes the formation of filopodia by regulating the recruitment of actin-binding proteins to actin filaments. Exp. Cell Res. 317, 249–261. https://doi.org/10.1016/j.yexcr.2010.10.019

Cuadrado, A., Nebreda, A.R., 2010. Mechanisms and functions of p38 MAPK signalling. Biochem. J. 429, 403–417. https://doi.org/10.1042/bj20100323

Cuenda, A., Rousseau, S., 2007. p38 MAP-Kinases pathway regulation, function and role in human diseases. Biochim. Biophys. Acta (BBA) - Mol. Cell Res. 1773, 1358–1375. https://doi.org/10.1016/j.bbamcr.2007.03.010

Cui, X., Lin, Q., Huang, P., Liang, Y., 2020. Antiepithelial-Mesenchymal Transition of Herbal Active Substance in Tumor Cells via Different Signaling. Oxid Med Cell Longev 2020, 9253745. https://doi.org/10.1155/2020/9253745

Currier, M.A., Stehn, J.R., Swain, A., Chen, D., Hook, J., Eiffe, E., Heaton, A., Brown, D., Nartker, B.A., Eaves, D.W., Kloss, N., Treutlein, H., Zeng, J., Alieva, I.B., Dugina, V.B., Hardeman, E.C., Gunning, P.W., Cripe, T.P., 2017. Identification of Cancer-Targeted

Tropomyosin Inhibitors and Their Synergy with Microtubule Drugs. Mol. Cancer Ther. 16, 1555–1565. https://doi.org/10.1158/1535-7163.mct-16-0873

Curthoys, N.M., Freittag, H., Connor, A., Desouza, M., Brettle, M., Poljak, A., Hall, A., Hardeman, E., Schevzov, G., Gunning, P.W., Fath, T., 2014. Tropomyosins induce neuritogenesis and determine neurite branching patterns in B35 neuroblastoma cells. Mol. Cell. Neurosci. 58, 11–21. https://doi.org/10.1016/j.mcn.2013.10.011

Cushing, M.C., Mariner, P.D., Liao, J., Sims, E.A., Anseth, K.S., 2008. Fibroblast growth factor represses Smad-mediated myofibroblast activation in aortic valvular interstitial cells. Faseb J 22, 1769–1777. https://doi.org/10.1096/fj.07-087627

Dailey, L., Ambrosetti, D., Mansukhani, A., Basilico, C., 2005. Mechanisms underlying differential responses to FGF signaling. Cytokine Growth Factor Rev. 16, 233–247. https://doi.org/10.1016/j.cytogfr.2005.01.007

D'Antin, J.C., Tresserra, F., Barraquer, R.I., Michael, R., 2022. Soemmerring's Rings Developed around IOLs, in Human Donor Eyes, Can Present Internal Transparent Areas. Int J Mol Sci 23, 13294. https://doi.org/10.3390/ijms232113294

Das, S.J., Lovicu, F.J., Collinson, E.J., 2016. Nox4 Plays a Role in TGF-β-Dependent Lens Epithelial to Mesenchymal Transition. Invest Ophth Vis Sci 57, 3665–73. https://doi.org/10.1167/iovs.16-19114

Datta, A., Deng, S., Gopal, V., Yap, K.C.-H., Halim, C.E., Lye, M.L., Ong, M.S., Tan, T.Z., Sethi, G., Hooi, S.C., Kumar, A.P., Yap, C.T., 2021. Cytoskeletal Dynamics in Epithelial-Mesenchymal Transition: Insights into Therapeutic Targets for Cancer Metastasis. Cancers 13, 1882. https://doi.org/10.3390/cancers13081882

Datto, M.B., Frederick, J.P., Pan, L., Borton, A.J., Zhuang, Y., Wang, X.-F., 1999. Targeted Disruption of Smad3 Reveals an Essential Role in Transforming Growth Factor β-Mediated Signal Transduction. Mol Cell Biol 19, 2495–2504. https://doi.org/10.1128/mcb.19.4.2495

Davies, S.P., Reddy, H., Caivano, M., Cohen, P., 2000. Specificity and mechanism of action of some commonly used protein kinase inhibitors. Biochem. J. 351, 95. https://doi.org/10.1042/0264-6021:3510095

Dawes, L.J., Sleeman, M.A., Anderson, I.K., Reddan, J.R., Wormstone, I.M., 2009. TGFβ/Smad4-Dependent and -Independent Regulation of Human Lens Epithelial Cells. Invest Ophth Vis Sci 50, 5318–5327. https://doi.org/10.1167/iovs.08-3223

Dawes, L.J., Sugiyama, Y., Lovicu, F.J., Harris, C.G., Shelley, E.J., McAvoy, J.W., 2014. Interactions between lens epithelial and fiber cells reveal an intrinsic self-assembly mechanism. Dev Biol 385, 291–303. https://doi.org/10.1016/j.ydbio.2013.10.030

Dawes, L.J., Sugiyama, Y., Tanedo, A.S., Lovicu, F.J., McAvoy, J.W., 2013. Wnt-Frizzled Signaling Is Part of an FGF-Induced Cascade that Promotes Lens Fiber Differentiation. Investig. Opthalmology Vis. Sci. 54, 1582. https://doi.org/10.1167/iovs.12-11357

de Iongh, R.U., Gordon-Thomson, C., Chamberlain, C.G., Hales, A.M., McAvoy, J.W., 2001a. TGFβ Receptor Expression in Lens: Implications for Differentiation and Cataractogenesis. Exp Eye Res 72, 649–659. https://doi.org/10.1006/exer.2001.1001

de Iongh, R.U., Lovicu, F.J., Chamberlain, C.G., McAvoy, J.W., 1997. Differential expression of fibroblast growth factor receptors during rat lens morphogenesis and growth. Invest Ophth Vis Sci 38, 1688–99.

de Iongh, R.U., Lovicu, F.J., Hanneken, A., Baird, A., McAvoy, J.W., 1996. FGF receptor-1 (flg) expression is correlated with fibre differentiation during rat lens morphogenesis and growth. Dev. Dyn. 206, 412–426. https://doi.org/10.1002/(sici)1097-0177(199608)206:4<;412::aid-aja7>3.0.co;2-l

de Iongh, R.U., Lovicu, F.J., Overbeek, P.A., Schneider, M.D., Joya, J., Hardeman, E.D., McAvoy, J.W., 2001b. Requirement for TGFbeta receptor signaling during terminal lens fiber differentiation. Dev Camb Engl 128, 3995–4010.

de Iongh, R.U., Wederell, E., Lovicu, F.J., McAvoy, J.W., 2005. Transforming Growth Factor-β-Induced Epithelial-Mesenchymal Transition in the Lens: A Model for Cataract Formation. Cells Tissues Organs 179, 43–55. https://doi.org/10.1159/000084508

Derynck, R., Zhang, Y.E., 2003. Smad-dependent and Smad-independent pathways in TGF-β family signalling. Nature 425, 577–584. https://doi.org/10.1038/nature02006

Desouza, M., Gunning, P.W., Stehn, J.R., 2012. The actin cytoskeleton as a sensor and mediator of apoptosis. Bioarchitecture 2, 75–87. https://doi.org/10.4161/bioa.20975

Desouza-Armstrong, M., Gunning, P.W., Stehn, J.R., 2017. Tumor suppressor tropomyosin Tpm2.1 regulates sensitivity to apoptosis beyond anoikis characterized by changes in the levels of intrinsic apoptosis proteins. Cytoskeleton 74, 233–248. https://doi.org/10.1002/cm.21367

Dobaczewski, M., Bujak, M., Li, N., Gonzalez-Quesada, C., Mendoza, L.H., Wang, X.-F., Frangogiannis, N.G., 2010. Smad3 Signaling Critically Regulates Fibroblast Phenotype and Function in Healing Myocardial Infarction. Circ. Res. 107, 418–428. https://doi.org/10.1161/circresaha.109.216101

Doi, S., Zou, Y., Togao, O., Pastor, J.V., John, G.B., Wang, L., Shiizaki, K., Gotschall, R., Schiavi, S., Yorioka, N., Takahashi, M., Boothman, D.A., Kuro-o, M., 2011. Klotho Inhibits Transforming Growth Factor-β1 (TGF-β1) Signaling and Suppresses Renal Fibrosis and Cancer Metastasis in Mice*. J. Biol. Chem. 286, 8655–8665. https://doi.org/10.1074/jbc.m110.174037

Duffy, J.P., Harrington, E.M., Salituro, F.G., Cochran, J.E., Green, J., Gao, H., Bemis, G.W., Evindar, G., Galullo, V.P., Ford, P.J., Germann, U.A., Wilson, K.P., Bellon, S.F., Chen, G., Taslimi, P., Jones, P., Huang, C., Pazhanisamy, S., Wang, Y.-M., Murcko, M.A., Su, M.S.S., 2011. The Discovery of VX-745: A Novel and Selective p38α Kinase Inhibitor. ACS Med. Chem. Lett. 2, 758–763. https://doi.org/10.1021/ml2001455

Dugina, V., Zwaenepoel, I., Gabbiani, G., Clément, S., Chaponnier, C., 2009. β- and γ-cytoplasmic actins display distinct distribution and functional diversity. J. Cell Sci. 122, 2980–2988. https://doi.org/10.1242/jcs.041970

Düzgün, Ş.A., Yerlikaya, A., Zeren, S., Bayhan, Z., Okur, E., Boyacı, İ., 2017. Differential effects of p38 MAP kinase inhibitors SB203580 and SB202190 on growth and migration of human MDA-MB-231 cancer cell line. Cytotechnology 69, 711–724. https://doi.org/10.1007/s10616-017-0079-2

Dvashi, Z., Goldberg, M., Adir, O., Shapira, M., Pollack, A., 2015. TGF-β1 Induced Transdifferentiation of RPE Cells is Mediated by TAK1. PLoS ONE 10, e0122229. https://doi.org/10.1371/journal.pone.0122229

Ecken, J. von der, Müller, M., Lehman, W., Manstein, D.J., Penczek, P.A., Raunser, S., 2015. Structure of the F-actin–tropomyosin complex. Nature 519, 114–117. https://doi.org/10.1038/nature14033

Eldred, J.A., Dawes, L.J., Wormstone, I.M., 2011. The lens as a model for fibrotic disease. Philos. Trans. R. Soc. B: Biol. Sci. 366, 1301–1319. https://doi.org/10.1098/rstb.2010.0341

Ellis, M.F., 2001. Sharp-edged intraocular lens design as a cause of permanent glare. J. Cataract Refract. Surg. 27, 1061–1064. https://doi.org/10.1016/s0886-3350(00)00856-7

Elyada, E., Bolisetty, M., Laise, P., Flynn, W.F., Courtois, E.T., Burkhart, R.A., Teinor, J.A., Belleau, P., Biffi, G., Lucito, M.S., Sivajothi, S., Armstrong, T.D., Engle, D.D., Yu, K.H., Hao, Y., Wolfgang, C.L., Park, Y., Preall, J., Jaffee, E.M., Califano, A., Robson, P., Tuveson, D.A., 2019. Cross-Species Single-Cell Analysis of Pancreatic Ductal Adenocarcinoma Reveals Antigen-Presenting Cancer-Associated Fibroblasts. Cancer Discov. 9, 1102–1123. https://doi.org/10.1158/2159-8290.cd-19-0094

Farooq, M., Khan, A.W., Kim, M.S., Choi, S., 2021. The Role of Fibroblast Growth Factor (FGF) Signaling in Tissue Repair and Regeneration. Cells 10, 3242. https://doi.org/10.3390/cells10113242

Fath, T., Chan, Y.-K.A., Vrhovski, B., Clarke, H., Curthoys, N., Hook, J., Lemckert, F., Schevzov, G., Tam, P., Watson, C.M., Khoo, P.-L., Gunning, P., 2010. New aspects of tropomyosin-regulated neuritogenesis revealed by the deletion of Tm5NM1 and 2. Eur J Cell Biol 89, 489–498. https://doi.org/10.1016/j.ejcb.2009.11.028

Fatma, N., Kubo, E., Sharma, P., Beier, D.R., Singh, D.P., 2005. Impaired homeostasis and phenotypic abnormalities in Prdx6−/−mice lens epithelial cells by reactive oxygen species: increased expression and activation of TGFβ. Cell Death Differ 12, 734–750. https://doi.org/10.1038/sj.cdd.4401597

Findl, O., Buehl, W., Bauer, P., Sycha, T., 2010. Interventions for preventing posterior capsule opacification. Cochrane Database Syst. Rev. 2010, CD003738. https://doi.org/10.1002/14651858.cd003738.pub3

Fischer, R.S., Lee, A., Fowler, V.M., 2000. Tropomodulin and tropomyosin mediate lens cell actin cytoskeleton reorganization in vitro. Investig. Ophthalmol. Vis. Sci. 41, 166–74.

Flokis, M., Lovicu, F.J., 2023. FGF-2 Differentially Regulates Lens Epithelial Cell Behaviour during TGF-β-Induced EMT. Cells 12, 827. https://doi.org/10.3390/cells12060827

Forsten-Williams, K., Chu, C.L., Fannon, M., Buczek-Thomas, J.A., Nugent, M.A., 2008. Control of Growth Factor Networks by Heparan Sulfate Proteoglycans. Ann. Biomed. Eng. 36, 2134–2148. https://doi.org/10.1007/s10439-008-9575-z

Fowler, V.M., Bennett, V., 1984. Erythrocyte membrane tropomyosin. Purification and properties. J. Biol. Chem. 259, 5978–5989. https://doi.org/10.1016/s0021-9258(18)91110-5

Franzén, B., Linder, S., Uryu, K., Alaiya, A., Hirano, T., Kato, H., Auer, G., 1996. Expression of tropomyosin isoforms in benign and malignant human breast lesions. Brit J Cancer 73, 909–913. https://doi.org/10.1038/bjc.1996.162

Frey, M.R., Dise, R.S., Edelblum, K.L., Polk, D.B., 2006. p38 kinase regulates epidermal growth factor receptor downregulation and cellular migration. EMBO J. 25, 5683–5692. https://doi.org/10.1038/sj.emboj.7601457

Frey, M.R., Golovin, A., Polk, D.B., 2004. Epidermal Growth Factor-stimulated Intestinal Epithelial Cell Migration Requires Src Family Kinase-dependent p38 MAPK Signaling*. J. Biol. Chem. 279, 44513–44521. https://doi.org/10.1074/jbc.m406253200

Fuhrmann, S., 2008. Wnt signaling in eye organogenesis. Organogenesis 4, 60–67. https://doi.org/10.4161/org.4.2.5850

Fujimura, N., 2016. WNT/β-Catenin Signaling in Vertebrate Eye Development. Frontiers Cell Dev Biology 4, 138. https://doi.org/10.3389/fcell.2016.00138

Gao, C., Lin, X., Fan, F., Liu, X., Wan, H., Yuan, T., Zhao, X., Luo, Y., 2022. Status of higher TGF-β1 and TGF-β2 levels in the aqueous humour of patients with diabetes and cataracts. Bmc Ophthalmol 22, 156. https://doi.org/10.1186/s12886-022-02317-x

Garcia, C.M., Yu, K., Zhao, H., Ashery-Padan, R., Ornitz, D.M., Robinson, M.L., Beebe, D.C., 2005. Signaling through FGF receptor-2 is required for lens cell survival and for withdrawal from the cell cycle during lens fiber cell differentiation. Dev Dynam 233, 516–527. https://doi.org/10.1002/dvdy.20356

Garner, M.H., Spector, A., 1980. Selective oxidation of cysteine and methionine in normal and senile cataractous lenses. Proc National Acad Sci 77, 1274–1277. https://doi.org/10.1073/pnas.77.3.1274

Gateva, G., Kremneva, E., Reindl, T., Kotila, T., Kogan, K., Gressin, L., Gunning, P.W., Manstein, D.J., Michelot, A., Lappalainen, P., 2017. Tropomyosin Isoforms Specify Functionally Distinct Actin Filament Populations In Vitro. Curr Biol 27, 705–713. https://doi.org/10.1016/j.cub.2017.01.018

Geeves, M.A., Hitchcock-DeGregori, S.E., Gunning, P.W., 2015. A systematic nomenclature for mammalian tropomyosin isoforms. J Muscle Res Cell M 36, 147–153. https://doi.org/10.1007/s10974-014-9389-6

Geng, X., Chen, H., Zhao, L., Hu, J., Yang, W., Li, G., Cheng, C., Zhao, Z., Zhang, T., Li, L., Sun, B., 2021. Cancer-Associated Fibroblast (CAF) Heterogeneity and Targeting Therapy of CAFs in Pancreatic Cancer. Front. Cell Dev. Biol. 9, 655152. https://doi.org/10.3389/fcell.2021.655152

Ghorbaninejad, M., Abdollahpour-Alitappeh, M., Shahrokh, S., Fayazzadeh, S., Asadzadeh-Aghdaei, H., Meyfour, A., 2023. TGF-β receptor I inhibitor may restrict the induction of EMT in inflamed intestinal epithelial cells. Exp. Biol. Med. 248, 665–676. https://doi.org/10.1177/15353702231151959

Ghosh, A., Janco, M., Böcking, T., Gunning, P.W., Lehman, W., Rynkiewicz, M.J., 2019. Structure of the Tpm3.1 N-Terminus: A New Target for Anti-Cancer Treatment. Biophys J 116, 253a–254a. https://doi.org/10.1016/j.bpj.2018.11.1382

Giannone, A.A., Sellitto, C., Rosati, B., McKinnon, D., White, T.W., 2023. Single-Cell RNA Sequencing Analysis of the Early Postnatal Mouse Lens Epithelium. Investig. Ophthalmol. Vis. Sci. 64, 37. https://doi.org/10.1167/iovs.64.13.37

Gimbel, H.V., Neuhann, T., 1991. Continuous Curvilinear Capsulorhexis. J Cataract Refract Surg 17, 110–111. https://doi.org/10.1016/s0886-3350(13)81001-2

Glass, J.J., Phillips, P.A., Gunning, P.W., Stehn, J.R., 2015. Hypoxia alters the recruitment of tropomyosins into the actin stress fibres of neuroblastoma cells. BMC Cancer 15, 712. https://doi.org/10.1186/s12885-015-1741-8

Godl, K., Wissing, J., Kurtenbach, A., Habenberger, P., Blencke, S., Gutbrod, H., Salassidis, K., Stein-Gerlach, M., Missio, A., Cotten, M., Daub, H., 2003. An efficient proteomics method to identify the cellular targets of protein kinase inhibitors. Proc. Natl. Acad. Sci. 100, 15434–15439. https://doi.org/10.1073/pnas.2535024100

Gong, X., Ming, X., Deng, P., Jiang, Y., 2010. Mechanisms regulating the nuclear translocation of p38 MAP kinase. J. Cell. Biochem. 110, 1420–1429. https://doi.org/10.1002/jcb.22675

Gordon-Thomson, C., Iongh, R.U. de, Hales, A.M., Chamberlain, C.G., McAvoy, J.W., 1998. Differential cataractogenic potency of TGF-beta1, -beta2, and -beta3 and their expression in the postnatal rat eye. Invest Ophth Vis Sci 39, 1399–409.

Greenberg, A.K., Basu, S., Hu, J., Yie, T., Tchou-Wong, K.M., Rom, W.N., Lee, T.C., 2002. Selective p38 Activation in Human Non–Small Cell Lung Cancer. Am. J. Respir. Cell Mol. Biol. 26, 558–564. https://doi.org/10.1165/ajrcmb.26.5.4689

Gunning, P., O'neill, G., Hardeman, E., 2008. Tropomyosin-Based Regulation of the Actin Cytoskeleton in Time and Space. Physiol Rev 88, 1–35. https://doi.org/10.1152/physrev.00001.2007

Gunning, P., Weinberger, R., Jeffrey, P., Hardeman, E., 1998. ISOFORM SORTING AND THE CREATION OF INTRACELLULAR COMPARTMENTS. Annu Rev Cell Dev Bi 14, 339–372. https://doi.org/10.1146/annurev.cellbio.14.1.339

Gunning, P.W., Hardeman, E.C., Lappalainen, P., Mulvihill, D.P., 2015. Tropomyosin – master regulator of actin filament function in the cytoskeleton. J Cell Sci 128, 2965–2974. https://doi.org/10.1242/jcs.172502

Gunning, P.W., Schevzov, G., Kee, A.J., Hardeman, E.C., 2005. Tropomyosin isoforms: divining rods for actin cytoskeleton function. Trends Cell Biol 15, 333–341. https://doi.org/10.1016/j.tcb.2005.04.007

Guo, R., Meng, Q., Guo, H., Xiao, L., Yang, X., Cui, Y., Huang, Y., 2016. TGF-β2 induces epithelial-mesenchymal transition in cultured human lens epithelial cells through activation of the PI3K/Akt/mTOR signaling pathway. Mol. Med. Rep. 13, 1105–1110. https://doi.org/10.3892/mmr.2015.4645

Had, L., Faivre-Sarrailh, C., Legrand, C., Méry, J., Brugidou, J., Rabié, A., 1994. Tropomyosin isoforms in rat neurons: the different developmental profiles and distributions of TM-4 and TMBr-3 are consistent with different functions. J. Cell Sci. 107, 2961–2973. https://doi.org/10.1242/jcs.107.10.2961

Hales, A.M., Chamberlain, C.G., McAvoy, J.W., 1995. Cataract induction in lenses cultured with transforming growth factor-beta. Invest Ophth Vis Sci 36, 1709–13.

Han, J., Lee, J.-D., Bibbs, L., Ulevitch, R.J., 1994. A MAP Kinase Targeted by Endotoxin and Hyperosmolarity in Mammalian Cells. Science 265, 808–811. https://doi.org/10.1126/science.7914033

Han, J., Wu, J., Silke, J., 2020. An overview of mammalian p38 mitogen-activated protein kinases, central regulators of cell stress and receptor signaling. F1000Research 9, F1000 Faculty Rev-653. https://doi.org/10.12688/f1000research.22092.1

Han, X., Chen, H., Zhou, J., Steed, H., Postovit, L.-M., Fu, Y., 2018. Pharmacological Inhibition of p38 MAPK by SB203580 Increases Resistance to Carboplatin in A2780cp Cells and Promotes Growth in Primary Ovarian Cancer Cells. Int. J. Mol. Sci. 19, 2184. https://doi.org/10.3390/ijms19082184

Han, Z., Wang, Fang, Wang, Fu-Lei, Liu, Q., Zhou, J., 2018. Regulation of transforming growth factor β-mediated epithelial-mesenchymal transition of lens epithelial cells by c-Src kinase under high glucose conditions. Exp Ther Med 16, 1520–1528. https://doi.org/10.3892/etm.2018.6348

Hanafusa, H., Ninomiya-Tsuji, J., Masuyama, N., Nishita, M., Fujisawa, J., Shibuya, H., Matsumoto, K., Nishida, E., 1999. Involvement of the p38 Mitogen-activated Protein Kinase Pathway in Transforming Growth Factor-β-induced Gene Expression*. J. Biol. Chem. 274, 27161–27167. https://doi.org/10.1074/jbc.274.38.27161

Hao, B., Sun, R., Guo, X., Zhang, L., Cui, J., Zhou, Y., Hong, W., Zhang, Y., He, J., Liu, X., Li, B., Ran, P., Chen, J., 2021. NOX4-Derived ROS Promotes Collagen I Deposition in Bronchial Smooth Muscle Cells by Activating Noncanonical p38MAPK/Akt-Mediated TGF-β Signaling. Oxidative Med. Cell. Longev. 2021, 6668971. https://doi.org/10.1155/2021/6668971

Hardeman, E.C., Bryce, N.S., Gunning, P.W., 2019. Impact of the actin cytoskeleton on cell development and function mediated via tropomyosin isoforms. Semin Cell Dev Biol 102, 122–131. https://doi.org/10.1016/j.semcdb.2019.10.004

Hay, E.D., 1968. Organization and fine structure of epithelium and mesenchyme in the developing chick embryo, in: Fleischmajer, R., Billingham, R.E. (Eds.), Epithelial-mesenchymal Interactions: 18th Hahnemann Symposium. Williams and Wilkins Co., Baltimore, pp. 31–55.

Hedges, J.C., Dechert, M.A., Yamboliev, I.A., Martin, J.L., Hickey, E., Weber, L.A., Gerthoffer, W.T., 1999. A Role for p38MAPK/HSP27 Pathway in Smooth Muscle Cell Migration*. J. Biol. Chem. 274, 24211–24219. https://doi.org/10.1074/jbc.274.34.24211

Heldin, C.-H., Moustakas, A., 2016. Signaling Receptors for TGF-β Family Members. Cold Spring Harb. Perspect. Biol. 8, a022053. https://doi.org/10.1101/cshperspect.a022053

Hinz, B., Celetta, G., Tomasek, J.J., Gabbiani, G., Chaponnier, C., 2001. Alpha-Smooth Muscle Actin Expression Upregulates Fibroblast Contractile Activity. Mol. Biol. Cell 12, 2730–2741. https://doi.org/10.1091/mbc.12.9.2730

Hoffman, R.S., Braga-Mele, R., Donaldson, K., Emerick, G., Henderson, B., Kahook, M., Mamalis, N., Miller, K.M., Realini, T., Shorstein, N.H., Stiverson, R.K., Wirostko, B., Society, A.C.C.C. and the A.G., 2016. Cataract surgery and nonsteroidal antiinflammatory drugs. J. Cataract Refract. Surg. 42, 1368–1379. https://doi.org/10.1016/j.jcrs.2016.06.006

Hohmann, T., Dehghani, F., 2019. The Cytoskeleton—A Complex Interacting Meshwork. Cells 8, 362. https://doi.org/10.3390/cells8040362

Hook, J., Lemckert, F., Qin, H., Schevzov, G., Gunning, P., 2004. Gamma Tropomyosin Gene Products Are Required for Embryonic Development. Mol Cell Biol 24, 2318–2323. https://doi.org/10.1128/mcb.24.6.2318-2323.2004

Hook, J., Lemckert, F., Schevzov, G., Fath, T., Gunning, P., 2011. Functional identity of the Gamma Tropomyosin gene. Bioarchitecture 1, 49–59. https://doi.org/10.4161/bioa.1.1.15172

Hotulainen, P., Lappalainen, P., 2006. Stress fibers are generated by two distinct actin assembly mechanisms in motile cells. J. Cell Biol. 173, 383–394. https://doi.org/10.1083/jcb.200511093

Hou, M., Bao, X., Luo, F., Chen, X., Liu, L., Wu, M., 2018. HMGA2 Modulates the TGFβ/Smad, TGFβ/ERK and Notch Signaling Pathways in human Lens Epithelial-Mesenchymal Transition. Curr Mol Med 18. https://doi.org/10.2174/1566524018666180705104844

Hou, T.-Y., Wu, S.-B., Kau, H.-C., Tsai, C.-C., 2021. JNK and p38 Inhibitors Prevent Transforming Growth Factor-β1-Induced Myofibroblast Transdifferentiation in Human Graves' Orbital Fibroblasts. Int J Mol Sci 22, 2952. https://doi.org/10.3390/ijms22062952

Hough, C., Radu, M., Doré, J.J.E., 2012. TGF-Beta Induced Erk Phosphorylation of Smad Linker Region Regulates Smad Signaling. Plos One 7, e42513. https://doi.org/10.1371/journal.pone.0042513

Houle, F., Rousseau, S., Morrice, N., Luc, M., Mongrain, S., Turner, C.E., Tanaka, S., Moreau, P., Huot, J., 2003. Extracellular Signal-regulated Kinase Mediates Phosphorylation of Tropomyosin-1 to Promote Cytoskeleton Remodeling in Response to Oxidative Stress: Impact on Membrane Blebbing. Mol. Biol. Cell 14, 1418–1432. https://doi.org/10.1091/mbc.e02-04-0235

Hu, J., Sella, R., Afshari, N.A., 2018. Dysphotopsia: a multifaceted optic phenomenon. Curr Opin Ophthalmol 29, 61–68. https://doi.org/10.1097/icu.0000000000000447

Humayun-Zakaria, N., Arnold, R., Goel, A., Ward, D., Savill, S., Bryan, R.T., 2019. Tropomyosins: Potential Biomarkers for Urothelial Bladder Cancer. Int J Mol Sci 20, 1102. https://doi.org/10.3390/ijms20051102

Huot, J., Houle, F., Rousseau, S., Deschesnes, R.G., Shah, G.M., Landry, J., 1998. SAPK2/p38-dependent F-Actin Reorganization Regulates Early Membrane Blebbing during Stress-induced Apoptosis. J. Cell Biol. 143, 1361–1373. https://doi.org/10.1083/jcb.143.5.1361

Huxley, H.E., 1960. Muscle Cells. The Cell: Biochemistry, Physiology, Morphology 365–481.

Ibaraki, N., Lin, L.R., Reddy, V.N., 1995. Effects of growth factors on proliferation and differentiation in human lens epithelial cells in early subculture. Invest Ophth Vis Sci 36, 2304–12.

Inatani, M., Tanihara, H., Katsuta, H., Honjo, M., Kido, N., Honda, Y., 2001. Transforming growth factor-β2 levels in aqueous humor of glaucomatous eyes. Graefe's Archive Clin Exp Ophthalmol 239, 109–113. https://doi.org/10.1007/s004170000241

Inguito, K.L., Schofield, M.M., Faghri, A.D., Bloom, E.T., Heino, M., West, V.C., Ebron, K.M.M., Elliott, D.M., Parreno, J., 2022. Stress deprivation of tendon explants or Tpm3.1 inhibition in tendon cells reduces F-actin to promote a tendinosis-like phenotype. Mol. Biol. Cell 33, ar141. https://doi.org/10.1091/mbc.e22-02-0067

Iyengar, L., Patkunanathan, B., Lynch, O.T., McAvoy, J.W., Rasko, J.E.J., Lovicu, F.J., 2006. Aqueous humour- and growth factor-induced lens cell proliferation is dependent on MAPK/ERK1/2 and Akt/PI3-K signalling. Exp. Eye Res. 83, 667–678. https://doi.org/10.1016/j.exer.2006.03.008

Iyengar, L., Patkunanathan, B., Mcavoy, J.W., Lovicu, F.J., 2009. Growth factors involved in aqueous humour-induced lens cell proliferation. Growth Factors 27, 50–62. https://doi.org/10.1080/08977190802610916

Iyengar, L., Wang, Q., Rasko, J.E.J., McAvoy, J.W., Lovicu, F.J., 2007. Duration of ERK1/2 phosphorylation induced by FGF or ocular media determines lens cell fate. Differentiation 75, 662–668. https://doi.org/10.1111/j.1432-0436.2007.00167.x

Izdebska, M., Zielińska, W., Grzanka, D., Gagat, M., 2018. The Role of Actin Dynamics and Actin-Binding Proteins Expression in Epithelial-to-Mesenchymal Transition and Its Association with Cancer Progression and Evaluation of Possible Therapeutic Targets. Biomed Res Int 2018, 1–13. https://doi.org/10.1155/2018/4578373

Jalilian, I., Heu, C., Cheng, H., Freittag, H., Desouza, M., Stehn, J.R., Bryce, N.S., Whan, R.M., Hardeman, E.C., Fath, T., Schevzov, G., Gunning, P.W., 2015. Cell Elasticity Is Regulated by the Tropomyosin Isoform Composition of the Actin Cytoskeleton. PLoS ONE 10, e0126214. https://doi.org/10.1371/journal.pone.0126214

Jampel, H.D., Roche, N., Stark, W.J., Roberts, A.B., 1990. Transforming growth factor-β in human aqueous humor. Curr Eye Res 9, 963–969. https://doi.org/10.3109/02713689009069932

Janco, M., Bonello, T.T., Byun, A., Costre, A.C.F., Lebhar, H., Dedova, I., Gunning, P.W., Böcking, T., 2016. The impact of tropomyosins on actin filament assembly is isoform specific. Bioarchitecture 6, 1–15. https://doi.org/10.1080/19490992.2016.1201619

Janco, M., Rynkiewicz, M.J., Li, L., Hook, J., Eiffe, E., Ghosh, A., Böcking, T., Lehman, W.J., Hardeman, E.C., Gunning, P.W., 2019. Molecular integration of the anti-tropomyosin compound ATM-3507 into the coiled coil overlap region of the cancer-associated Tpm3.1. Sci. Rep. 9, 11262. https://doi.org/10.1038/s41598-019-47592-9

Jansen, S., Goode, B.L., 2019. Tropomyosin isoforms differentially tune actin filament length and disassembly. Mol. Biol. Cell 30, 671–679. https://doi.org/10.1091/mbc.e18-12-0815

Jeong, S., Lim, S., Schevzov, G., Gunning, P.W., Helfman, D.M., 2014. Loss of Tpm4.1 leads to disruption of cell-cell adhesions and invasive behavior in breast epithelial cells via increased Rac1 signaling. Oncotarget 5, 33544–33559. https://doi.org/10.18632/oncotarget.16825

Jiang, F., Qin, Y., Yang, Y., Li, Z., Cui, B., Ju, R., Wu, M., 2023. BMP-4 and BMP-7 Inhibit EMT in a Model of Anterior Subcapsular Cataract in Part by Regulating the Notch Signaling Pathway. Investig. Ophthalmol. Vis. Sci. 64, 12. https://doi.org/10.1167/iovs.64.4.12

Jiang, J., Shihan, M.H., Wang, Y., Duncan, M.K., 2018. Lens Epithelial Cells Initiate an Inflammatory Response Following Cataract Surgery. Investigative Opthalmology Vis Sci 59, 4986. https://doi.org/10.1167/iovs.18-25067

Jiang, Q., Zhou, C., Bi, Z., Wan, Y., 2006. EGF-Induced Cell Migration Is Mediated by ERK and PI3K/AKT Pathways in Cultured Human Lens Epithelial Cells. J. Ocul. Pharmacol. Ther. 22, 93–102. https://doi.org/10.1089/jop.2006.22.93

Jolly, M.K., Boareto, M., Huang, B., Jia, D., Lu, M., Ben-Jacob, E., Onuchic, J.N., Levine, H., 2015. Implications of the Hybrid Epithelial/Mesenchymal Phenotype in Metastasis. Frontiers Oncol 5, 155. https://doi.org/10.3389/fonc.2015.00155

Joshi, R.S., Rasal, A.V., 2023. Posterior capsular opacification and Nd:YAG capsulotomy rates in patients implanted with square-edged and non-square-edged intraocular lenses in manual

small-incision cataract surgery: A randomized controlled study. Indian J. Ophthalmol. 71, 3219–3223. https://doi.org/10.4103/ijo.ijo_359_23

Kakrana, A., Yang, A., Anand, D., Djordjevic, D., Ramachandruni, D., Singh, A., Huang, H., Ho, J.W.K., Lachke, S.A., 2018. iSyTE 2.0: a database for expression-based gene discovery in the eye. Nucleic Acids Res 46, D875–D885. https://doi.org/10.1093/nar/gkx837

Kalluri, R., Neilson, E.G., 2003. Epithelial-mesenchymal transition and its implications for fibrosis. J Clin Invest 112, 1776–1784. https://doi.org/10.1172/jci20530

Kalluri, R., Weinberg, R.A., 2009. The basics of epithelial-mesenchymal transition. J. Clin. Investig. 119, 1420–1428. https://doi.org/10.1172/jci39104

Kamaraju, A.K., Roberts, A.B., 2005. Role of Rho/ROCK and p38 MAP Kinase Pathways in Transforming Growth Factor-β-mediated Smad-dependent Growth Inhibition of Human Breast Carcinoma Cells in Vivo *. J Biol Chem 280, 1024–1036. https://doi.org/10.1074/jbc.m403960200

Kamato, D., Do, B.H., Osman, N., Ross, B.P., Mohamed, R., Xu, S., Little, P.J., 2020. Smad linker region phosphorylation is a signalling pathway in its own right and not only a modulator of canonical TGF-β signalling. Cell Mol Life Sci 77, 243–251. https://doi.org/10.1007/s00018-019-03266-3

Karahan, E., Er, D., Kaynak, S., 2014. An Overview of Nd:YAG Laser Capsulotomy. Medical Hypothesis Discov Innovation Ophthalmol 3, 45–50.

Kee, A.J., Yang, L., Lucas, C.A., Greenberg, M.J., Martel, N., Leong, G.M., Hughes, W.E., Cooney, G.J., James, D.E., Ostap, E.M., Han, W., Gunning, P.W., Hardeman, E.C., 2015. An Actin Filament Population Defined by the Tropomyosin Tpm3.1 Regulates Glucose Uptake. Traffic 16, 691–711. https://doi.org/10.1111/tra.12282

Khairallah, M., Kahloun, R., Bourne, R., Limburg, H., Flaxman, S.R., Jonas, J.B., Keeffe, J., Leasher, J., Naidoo, K., Pesudovs, K., Price, H., White, R.A., Wong, T.Y., Resnikoff, S., Taylor, H.R., Study, V.L.E.G. of the G.B. of D., 2015. Number of People Blind or Visually Impaired by Cataract Worldwide and in World Regions, 1990 to 2010. Investigative Opthalmology Vis Sci 56, 6762. https://doi.org/10.1167/iovs.15-17201

Khokhar, S., Pillay, G., Dhull, C., Agarwal, E., Mahabir, M., Aggarwal, P., 2017. Pediatric cataract. Indian J Ophthalmol 65, 1340. https://doi.org/10.4103/ijo.ijo_1023_17

Kingsley, D.M., 1994. The TGF-beta superfamily: new members, new receptors, and new genetic tests of function in different organisms. Genes Dev. 8, 133–146. https://doi.org/10.1101/gad.8.2.133

Kirby, D.B., 1927. The Cultivation Of Lens Epithelium In Vitro. J Exp Medicine 45, 1009–1016. https://doi.org/10.1084/jem.45.6.1009

Kleiman, N.J., 2012. Radiation cataract. Ann Icrp 41, 80–97. https://doi.org/10.1016/j.icrp.2012.06.018

Klok, E.J., Lubsen, N.H., Chamberlain, C.G., McAvoy, J.W., 1998. Induction and Maintenance of Differentiation of Rat Lens Epithelium by FGF-2, Insulin and IGF-1. Exp. Eye Res. 67, 425–431. https://doi.org/10.1006/exer.1998.0534

Koch, C.R., D'Antin, J.C., Tresserra, F., Barraquer, R.I., Michael, R., 2019. Histological comparison of in vitro and in vivo development of peripheral posterior capsule opacification in human donor tissue. Exp. Eye Res. 188, 107807. https://doi.org/10.1016/j.exer.2019.107807

Koeberle, S.C., Romir, J., Fischer, S., Koeberle, A., Schattel, V., Albrecht, W., Grütter, C., Werz, O., Rauh, D., Stehle, T., Laufer, S.A., 2012. Skepinone-L is a selective p38 mitogen-activated protein kinase inhibitor. Nat. Chem. Biol. 8, 141–143. https://doi.org/10.1038/nchembio.761

Koike, Y., Yozaki, M., Utani, A., Murota, H., 2020. Fibroblast growth factor 2 accelerates the epithelial–mesenchymal transition in keratinocytes during wound healing process. Sci Rep-uk 10, 18545. https://doi.org/10.1038/s41598-020-75584-7

Kokawa, N., Sotozono, C., Nishida, K., Kinoshita, S., 1996. High total TGF-β2 levels in normal human tears. Curr Eye Res 15, 341–343. https://doi.org/10.3109/02713689609007630

Kolosova, I., Nethery, D., Kern, J.A., 2011. Role of Smad2/3 and p38 MAP kinase in TGF-β1-induced epithelial–mesenchymal transition of pulmonary epithelial cells. J. Cell. Physiol. 226, 1248–1254. https://doi.org/10.1002/jcp.22448

Kompa, A.R., See, F., Lewis, D.A., Adrahtas, A., Cantwell, D.M., Wang, B.H., Krum, H., 2008. Long-Term but Not Short-Term p38 Mitogen-Activated Protein Kinase Inhibition Improves Cardiac Function and Reduces Cardiac Remodeling Post-Myocardial Infarction. J. Pharmacol. Exp. Ther. 325, 741–750. https://doi.org/10.1124/jpet.107.133546

Kondo, T., Ishiga-Hashimoto, N., Nagai, H., Takeshita, A., Mino, M., Morioka, H., Kusakabe, K.T., Okada, T., 2014. Expression of transforming growth factor β and fibroblast growth factor 2 in the lens epithelium of Morioka cataract mice. Congenit Anom 54, 104–109. https://doi.org/10.1111/cga.12042

Konopińska, J., Młynarczyk, M., Dmuchowska, D.A., Obuchowska, I., 2021. Posterior Capsule Opacification: A Review of Experimental Studies. J Clin Medicine 10, 2847. https://doi.org/10.3390/jcm10132847

Konturek, P.Ch., Konturek, S.J., Brzozowski, T., Ernst, H., 1995. Epidermal growth factor and transforming growth factor-α: role in protection and healing of gastric mucosal lesions. Eur J Gastroen Hepat 7, 933–938. https://doi.org/10.1097/00042737-199510000-00005

Kopantzev, E.P., Kopantseva, M.R., Grankina, E.V., Mikaelyan, A., Egorov, V.I., Sverdlov, E.D., 2019. Activation of IGF/IGF-IR signaling pathway fails to induce epithelial-mesenchymal transition in pancreatic cancer cells. Pancreatol Official J Int Assoc Pancreatol Iap Et Al 19, 390–396. https://doi.org/10.1016/j.pan.2019.01.010

Korol, A., Pino, G., Dwivedi, D., Robertson, J.V., Deschamps, P.A., West-Mays, J.A., 2014. Matrix Metalloproteinase-9–Null Mice Are Resistant to TGF-β–Induced Anterior

Subcapsular Cataract Formation. Am. J. Pathol. 184, 2001–2012. https://doi.org/10.1016/j.ajpath.2014.03.013

Korol, A., Taiyab, A., West-Mays, J.A., 2016. RhoA/ROCK Signaling Regulates TGFβ-Induced Epithelial-Mesenchymal Transition of Lens Epithelial Cells through MRTF-A. Mol. Med. 22, 713–723. https://doi.org/10.2119/molmed.2016.00041

Kubo, E., Hasanova, N., Fatma, N., Sasaki, H., Singh, D.P., 2013. Elevated tropomyosin expression is associated with epithelial–mesenchymal transition of lens epithelial cells. J Cell Mol Med 17, 212–221. https://doi.org/10.1111/j.1582-4934.2012.01654.x

Kubo, E., Hasanova, N., Tanaka, Y., Fatma, N., Takamura, Y., Singh, D.P., Akagi, Y., 2010. Protein expression profiling of lens epithelial cells from Prdx6-depleted mice and their vulnerability to UV radiation exposure. Am J Physiol-cell Ph 298, C342–C354. https://doi.org/10.1152/ajpcell.00336.2009

Kubo, E., Shibata, S., Shibata, T., Kiyokawa, E., Sasaki, H., Singh, D.P., 2017. FGF2 antagonizes aberrant TGFβ regulation of tropomyosin: role for posterior capsule opacity. J Cell Mol Med 21, 916–928. https://doi.org/10.1111/jcmm.13030

Kubo, E., Shibata, T., Singh, D.P., Sasaki, H., 2018. Roles of TGF β and FGF Signals in the Lens: Tropomyosin Regulation for Posterior Capsule Opacity. Int J Mol Sci 19, 3093. https://doi.org/10.3390/ijms19103093

Kumar, S., Jiang, M.S., Adams, J.L., Lee, J.C., 1999. Pyridinylimidazole Compound SB 203580 Inhibits the Activity but Not the Activation of p38 Mitogen-Activated Protein Kinase. Biochem. Biophys. Res. Commun. 263, 825–831. https://doi.org/10.1006/bbrc.1999.1454

Kumphune, S., Bassi, R., Jacquet, S., Sicard, P., Clark, J.E., Verma, S., Avkiran, M., O'Keefe, S.J., Marber, M.S., 2010. A Chemical Genetic Approach Reveals That p38α MAPK Activation by Diphosphorylation Aggravates Myocardial Infarction and Is Prevented by the Direct Binding of SB203580*. J. Biol. Chem. 285, 2968–2975. https://doi.org/10.1074/jbc.m109.079228

Kurimoto, R., Iwasawa, S., Ebata, T., Ishiwata, T., Sekine, I., Tada, Y., Tatsumi, K., Koide, S., Iwama, A., Takiguchi, Y., 2016. Drug resistance originating from a TGF-β/FGF-2-driven epithelial-to-mesenchymal transition and its reversion in human lung adenocarcinoma cell lines harboring an EGFR mutation. Int J Oncol 48, 1825–1836. https://doi.org/10.3892/ijo.2016.3419

Kurosaka, D., Kato, K., Nagamoto, T., Negishi, K., 1995. Growth factors influence contractility and alpha-smooth muscle actin expression in bovine lens epithelial cells. Invest Ophth Vis Sci 36, 1701–8.

Lachke, S.A., Ho, J.W.K., Kryukov, G.V., O'Connell, D.J., Aboukhalil, A., Bulyk, M.L., Park, P.J., Maas, R.L., 2012. iSyTE: Integrated Systems Tool for Eye Gene Discovery. Investigative Opthalmology Vis Sci 53, 1617. https://doi.org/10.1167/iovs.11-8839

LaJevic, M.D., Suleiman, S., Cohen, R.L., Chambers, D.A., 2011. Activation of p38 mitogen-activated protein kinase by norepinephrine in T-lineage cells. Immunology 132, 197–208. https://doi.org/10.1111/j.1365-2567.2010.03354.x

Lali, F.V., Hunt, A.E., Turner, S.J., Foxwell, B.M.J., 2000. The Pyridinyl Imidazole Inhibitor SB203580 Blocks Phosphoinositide-dependent Protein Kinase Activity, Protein Kinase B Phosphorylation, and Retinoblastoma Hyperphosphorylation in Interleukin-2-stimulated T Cells Independently of p38 Mitogen-activated Protein Kinase*. J. Biol. Chem. 275, 7395–7402. https://doi.org/10.1074/jbc.275.10.7395

Lamouille, S., Xu, J., Derynck, R., 2014. Molecular mechanisms of epithelial-mesenchymal transition. Nat Rev Mol Cell Biology 15, 178–96. https://doi.org/10.1038/nrm3758

Laping, N.J., Grygielko, E., Mathur, A., Butter, S., Bomberger, J., Tweed, C., Martin, W., Fornwald, J., Lehr, R., Harling, J., Gaster, L., Callahan, J.F., Olson, B.A., 2002. Inhibition of Transforming Growth Factor (TGF)-β1–Induced Extracellular Matrix with a Novel Inhibitor of the TGF-β Type I Receptor Kinase Activity: SB-431542. Mol. Pharmacol. 62, 58–64. https://doi.org/10.1124/mol.62.1.58

Lax, I., Wong, A., Lamothe, B., Lee, A., Frost, A., Hawes, J., Schlessinger, J., 2002. The Docking Protein FRS2α Controls a MAP Kinase-Mediated Negative Feedback Mechanism for Signaling by FGF Receptors. Mol. Cell 10, 709–719. https://doi.org/10.1016/s1097-2765(02)00689-5

Le, A.-C.N., Musil, L.S., 2001. FGF Signaling in Chick Lens Development. Dev Biol 233, 394–411. https://doi.org/10.1006/dbio.2001.0194

Lechner, C., Zahalka, M.A., Giot, J.F., Møller, N.P., Ullrich, A., 1996. ERK6, a mitogen-activated protein kinase involved in C2C12 myoblast differentiation. Proc. Natl. Acad. Sci. 93, 4355–4359. https://doi.org/10.1073/pnas.93.9.4355

Lee, A., Fischer, R.S., Fowler, V.M., 2000. Stabilization and remodeling of the membrane skeleton during lens fiber cell differentiation and maturation. Dev. Dyn. 217, 257–270. https://doi.org/10.1002/(sici)1097-0177(200003)217:3<;257::aid-dvdy4>3.0.co;2-5

Lee, H.E., Berkowitz, P., Jolly, P.S., Diaz, L.A., Chua, M.P., Rubenstein, D.S., 2009. Biphasic Activation of p38MAPK Suggests That Apoptosis Is a Downstream Event in Pemphigus Acantholysis*. J. Biol. Chem. 284, 12524–12532. https://doi.org/10.1074/jbc.m808204200

Lee, J.C., Laydon, J.T., McDonnell, P.C., Gallagher, T.F., Kumar, S., Green, D., McNulty, D., Blumenthal, M.J., Keys, J.R., vatter, S.W.L., Strickler, J.E., McLaughlin, M.M., Siemens, I.R., Fisher, S.M., Livi, G.P., White, J.R., Adams, J.L., Young, P.R., 1994. A protein kinase involved in the regulation of inflammatory cytokine biosynthesis. Nature 372, 739–746. https://doi.org/10.1038/372739a0

Lee, S., Rauch, J., Kolch, W., 2020. Targeting MAPK Signaling in Cancer: Mechanisms of Drug Resistance and Sensitivity. Int. J. Mol. Sci. 21, 1102. https://doi.org/10.3390/ijms21031102

Lees, J.G., Ching, Y.W., Adams, D.H., Bach, C.T.T., Samuel, M.S., Kee, A.J., Hardeman, E.C., Gunning, P., Cowin, A.J., O'Neill, G.M., 2013. Tropomyosin Regulates Cell Migration during Skin Wound Healing. J Invest Dermatol 133, 1330–1339. https://doi.org/10.1038/jid.2012.489

Leggett, S.E., Hruska, A.M., Guo, M., Wong, I.Y., 2021. The epithelial-mesenchymal transition and the cytoskeleton in bioengineered systems. Cell Commun. Signal. 19, 32. https://doi.org/10.1186/s12964-021-00713-2

Leivonen, S.-K., Lazaridis, K., Decock, J., Chantry, A., Edwards, D.R., Kähäri, V.-M., 2013. TGF-β-Elicited Induction of Tissue Inhibitor of Metalloproteinases (TIMP)-3 Expression in Fibroblasts Involves Complex Interplay between Smad3, p38α, and ERK1/2. PLoS ONE 8, e57474. https://doi.org/10.1371/journal.pone.0057474

Li, J., Tang, X., Chen, X., 2011. Comparative effects of TGF-β2/Smad2 and TGF-β2/Smad3 signaling pathways on proliferation, migration, and extracellular matrix production in a human lens cell line. Exp Eye Res 92, 173–179. https://doi.org/10.1016/j.exer.2011.01.009

Li, L., Ye, T., Zhang, Q., Li, X., Ma, L., Yan, J., 2021. The expression and clinical significance of TPM4 in hepatocellular carcinoma. Int. J. Méd. Sci. 18, 169–175. https://doi.org/10.7150/ijms.49906

Li, M., Li, C., Liu, Y., Xing, Y., Hu, L., Borok, Z., Kwong, K.Y.-C., Minoo, P., 2008. Mesodermal Deletion of Transforming Growth Factor-β Receptor II Disrupts Lung Epithelial Morphogenesis Cross-talk between TGF-β and Sonic Hedgehog Pathways*. J. Biol. Chem. 283, 36257–36264. https://doi.org/10.1074/jbc.m806786200

Li, Y., Ding, Y., 2016. Pediatric Lens Diseases 1–9. https://doi.org/10.1007/978-981-10-2627-0_1

Liao, J.H., Chen, J.S., Chai, M.Q., Zhao, S., Song, J.G., 2001. The involvement of p38 MAPK in transforming growth factor β1-induced apoptosis in murine hepatocytes. Cell Res. 11, 89–94. https://doi.org/10.1038/sj.cr.7290072

Liegner, J., Grzybowski, A., Galloway, M., Lindstrom, R., 2017. Dropless Cataract Surgery: An Overview. Curr Pharm Design 23, 558–564. https://doi.org/10.2174/1381612822666161129150628

Ling, G., Ji, Q., Ye, W., Ma, D., Wang, Y., 2016. Epithelial-mesenchymal transition regulated by p38/MAPK signaling pathways participates in vasculogenic mimicry formation in SHG44 cells transfected with TGF-β cDNA loaded lentivirus in vitro and in vivo. Int. J. Oncol. 49, 2387–2398. https://doi.org/10.3892/ijo.2016.3724

Litt, M., Kramer, P., LaMorticella, D.M., Murphey, W., Lovrien, E.W., Weleber, R.G., 1998. Autosomal Dominant Congenital Cataract Associated with a Missense Mutation in the Human Alpha Crystallin Gene CRYAA. Hum. Mol. Genet. 7, 471–474. https://doi.org/10.1093/hmg/7.3.471

Liu, G., Zhao, X., Zhou, J., Cheng, X., Ye, Z., Ji, Z., 2018. Long non-coding RNA MEG3 suppresses the development of bladder urothelial carcinoma by regulating miR-96 and TPM1. Cancer Biol Ther 19, 1039–1056. https://doi.org/10.1080/15384047.2018.1480279

Liu, H., Mao, Y., Xia, B., Long, C., Kuang, X., Huang, H., Ning, J., Ma, X., Zhang, H., Wang, R., Tang, H., Du, H., Yan, J., Zhang, Q., Zhang, X., Shen, H., 2020. Curcumin Inhibits Proliferation and Epithelial-Mesenchymal Transition in Lens Epithelial Cells through Multiple Pathways. BioMed Res. Int. 2020, 6061894. https://doi.org/10.1155/2020/6061894

Liu, J., Hales, A.M., Chamberlain, C.G., McAvoy, J.W., 1994. Induction of cataract-like changes in rat lens epithelial explants by transforming growth factor beta. Invest Ophth Vis Sci 35, 388–401.

Liu, Q., Mao, H., Nie, J., Chen, W., Yang, Q., Dong, X., Yu, X., 2008. Transforming growth factor {beta}1 induces epithelial-mesenchymal transition by activating the JNK-Smad3 pathway in rat peritoneal mesothelial cells. Perit. Dial. Int. : J. Int. Soc. Perit. Dial. 28 Suppl 3, S88-95.

Liu, Y.-C., Wilkins, M., Kim, T., Malyugin, B., Mehta, J.S., 2017. Cataracts. Lancet Lond Engl 390, 600–612. https://doi.org/10.1016/s0140-6736(17)30544-5

Liverton, N.J., Butcher, J.W., Claiborne, C.F., Claremon, D.A., Libby, B.E., Nguyen, K.T., Pitzenberger, S.M., Selnick, H.G., Smith, G.R., Tebben, A., Vacca, J.P., Varga, S.L., Agarwal, L., Dancheck, K., Forsyth, A.J., Fletcher, D.S., Frantz, B., Hanlon, W.A., Harper, C.F., Hofsess, S.J., Kostura, M., Lin, J., Luell, S., O'Neill, E.A., Orevillo, C.J., Pang, M., Parsons, J., Rolando, A., Sahly, Y., Visco, D.M., O'Keefe, S.J., 1999. Design and Synthesis of Potent, Selective, and Orally Bioavailable Tetrasubstituted Imidazole Inhibitors of p38 Mitogen-Activated Protein Kinase. J. Med. Chem. 42, 2180–2190. https://doi.org/10.1021/jm9805236

Ljungdahl, S., Linder, S., Franzén, B., Binétruy, B., Auer, G., Shoshan, M.C., 1998. Down-regulation of tropomyosin-2 expression in c-Jun-transformed rat fibroblasts involves induction of a MEK1-dependent autocrine loop. Cell growth Differ. : Mol. Biol. J. Am. Assoc. Cancer Res. 9, 565–73.

Logvinov, A.S., Nefedova, V.V., Yampolskaya, D.S., Kleymenov, S.Y., Levitsky, D.I., Matyushenko, A.M., 2023. Structural and Functional Properties of Tropomyosin Isoforms Tpm4.1 and Tpm2.1. Biochem. (Mosc.) 88, 801–809. https://doi.org/10.1134/s0006297923060081

Lovicu, F.J., Ang, S., Chorazyczewska, M., McAvoy, J.W., 2005. Deregulation of Lens Epithelial Cell Proliferation and Differentiation during the Development of TGFβ-Induced Anterior Subcapsular Cataract. Dev. Neurosci. 26, 446–455. https://doi.org/10.1159/000082286

Lovicu, F.J., Chamberlain, C.G., McAvoy, J.W., 1995. Differential effects of aqueous and vitreous on fiber differentiation and extracellular matrix accumulation in lens epithelial explants. Invest Ophth Vis Sci 36, 1459–69.

Lovicu, F.J., Flokis, M., Wojciechowski, M., Mao, B., Shu, D., 2020. Understanding Fibrotic Cataract: Regulation of TGFβ-Mediated Pathways Leading to Lens Epithelial to Mesenchymal Transition (EMT). J Jpn Soc Cataract Res 32, 23–32. https://doi.org/10.14938/cataract.12-004

Lovicu, F.J., McAvoy, J.W., 2005. Growth factor regulation of lens development. Dev Biol 280, 1–14. https://doi.org/10.1016/j.ydbio.2005.01.020

Lovicu, F.J., McAvoy, J.W., 2001. FGF-induced lens cell proliferation and differentiation is dependent on MAPK (ERK1/2) signalling. Development 128, 5075–5084. https://doi.org/10.1242/dev.128.24.5075

Lovicu, F.J., McAvoy, J.W., 1992. The age of rats affects the response of lens epithelial explants to fibroblast growth factor. An ultrastructural analysis. Invest Ophth Vis Sci 33, 2269–78.

Lovicu, F.J., McAvoy, J.W., Iongh, R.U. de, 2011. Understanding the role of growth factors in embryonic development: insights from the lens. Philosophical Transactions Royal Soc Lond Ser B Biological Sci 366, 1204–18. https://doi.org/10.1098/rstb.2010.0339

Lovicu, F.J., Schulz, M.W., Hales, A.M., Vincent, L.N., Overbeek, P.A., Chamberlain, C.G., McAvoy, J.W., 2002. TGFβ induces morphological and molecular changes similar to human anterior subcapsular cataract. Brit J Ophthalmol 86, 220. https://doi.org/10.1136/bjo.86.2.220

Lovicu, F.J., Shin, E.H., McAvoy, J.W., 2015. Fibrosis in the lens. Sprouty regulation of TGFβ-signaling prevents lens EMT leading to cataract. Exp Eye Res 142, 92–101. https://doi.org/10.1016/j.exer.2015.02.004

Lovicu, F.J., Steven, P., Saika, S., McAvoy, J.W., 2004. Aberrant Lens Fiber Differentiation in Anterior Subcapsular Cataract Formation: A Process Dependent on Reduced Levels of Pax6. Invest Ophth Vis Sci 45, 1946–1953. https://doi.org/10.1167/iovs.03-1206

Lu, C., Yu, S., Song, H., Zhao, Y., Xie, S., Tang, X., Yuan, X., 2019. Posterior capsular opacification comparison between morphology and objective visual function. Bmc Ophthalmol 19, 40. https://doi.org/10.1186/s12886-019-1051-z

Luo, Y., Yu, P., Zhao, J., Guo, Q., Fan, B., Diao, Y., Jin, Y., Wu, J., Zhang, C., 2021. Inhibitory Effect of Crocin Against Gastric Carcinoma via Regulating TPM4 Gene. OncoTargets Ther. 14, 111–122. https://doi.org/10.2147/ott.s254167

Ma, X.L., Kumar, S., Gao, F., Louden, C.S., Lopez, B.L., Christopher, T.A., Wang, C., Lee, J.C., Feuerstein, G.Z., Yue, T.-L., 1999. Inhibition of p38 Mitogen-Activated Protein Kinase Decreases Cardiomyocyte Apoptosis and Improves Cardiac Function After Myocardial Ischemia and Reperfusion. Circulation 99, 1685–1691. https://doi.org/10.1161/01.cir.99.13.1685

Maddala, R., Reddy, V.N., Epstein, D.L., Rao, V., 2003. Growth factor induced activation of Rho and Rac GTPases and actin cytoskeletal reorganization in human lens epithelial cells. Mol. Vis. 9, 329–36.

Mahadev, K., Raval, G., Bharadwaj, S., Willingham, M.C., Lange, E.M., Vonderhaar, B., Salomon, D., Prasad, G.L., 2002. Suppression of the Transformed Phenotype of Breast Cancer by Tropomyosin-1. Exp. Cell Res. 279, 40–51. https://doi.org/10.1006/excr.2002.5583

Maik-Rachline, G., Lifshits, L., Seger, R., 2020. Nuclear P38: Roles in Physiological and Pathological Processes and Regulation of Nuclear Translocation. Int. J. Mol. Sci. 21, 6102. https://doi.org/10.3390/ijms21176102

Makrides, N., Wang, Q., Tao, C., Schwartz, S., Zhang, X., 2022. Jack of all trades, master of each: the diversity of fibroblast growth factor signalling in eye development. Open Biol 12, 210265. https://doi.org/10.1098/rsob.210265

Malmström, J., Lindberg, H., Lindberg, C., Bratt, C., Wieslander, E., Delander, E.-L., Särnstrand, B., Burns, J.S., Mose-Larsen, P., Fey, S., Marko-Varga, G., 2004. Transforming Growth Factor-β1 Specifically Induce Proteins Involved in the Myofibroblast Contractile Apparatus*. Mol. Cell. Proteom. 3, 466–477. https://doi.org/10.1074/mcp.m300108-mcp200

Mansfield, K.J., Cerra, A., Chamberlain, C.G., 2004. FGF-2 counteracts loss of TGFbeta affected cells from rat lens explants: implications for PCO (after cataract). Mol Vis 10, 521–32.

Manstein, D.J., Meiring, J.C.M., Hardeman, E.C., Gunning, P.W., 2020. Actin–tropomyosin distribution in non-muscle cells. J Muscle Res Cell M 41, 11–22. https://doi.org/10.1007/s10974-019-09514-0

Marcantonio, J.M., Syam, P.P., Liu, C.S.C., Duncan, G., 2003. Epithelial transdifferentiation and cataract in the human lens. Exp Eye Res 77, 339–346. https://doi.org/10.1016/s0014-4835(03)00125-8

Marchenko, M., Nefedova, V., Artemova, N., Kleymenov, S., Levitsky, D., Matyushenko, A., 2021. Structural and Functional Peculiarities of Cytoplasmic Tropomyosin Isoforms, the Products of TPM1 and TPM4 Genes. Int. J. Mol. Sci. 22, 5141. https://doi.org/10.3390/ijms22105141

Marston, S., 2015. Important announcement: a rational nomenclature for tropomyosin variants. J Muscle Res Cell M 36, 145–145. https://doi.org/10.1007/s10974-014-9393-x

Marston, S., Gautel, M., 2013. Introducing a special edition of the Journal of Muscle Research and Cell Motility on tropomyosin: form and function. J Muscle Res Cell M 34, 151–153. https://doi.org/10.1007/s10974-013-9361-x

Marston, S.B., Copeland, O., Messer, A.E., MacNamara, E., Nowak, K., Zampronio, C.G., Ward, D.G., 2013. Tropomyosin isoform expression and phosphorylation in the human heart in health and disease. J Muscle Res Cell M 34, 189–197. https://doi.org/10.1007/s10974-013-9347-8

Martinez, G., de Iongh, R.U., 2010. The lens epithelium in ocular health and disease. Int J Biochem Cell Biology 42, 1945–1963. https://doi.org/10.1016/j.biocel.2010.09.012

Martinho, R.G., Castel, S., Ureña, J., Fernández-Borja, M., Makiya, R., Olivecrona, G., Reina, M., Alonso, A., Vilaró, S., 1996. Ligand binding to heparan sulfate proteoglycans induces their aggregation and distribution along actin cytoskeleton. Mol. Biol. Cell 7, 1771–1788. https://doi.org/10.1091/mbc.7.11.1771

Maruno, K.A., Lovicu, F.J., Chamberlain, C.G., WMcAvoy, J., 2002. Apoptosis is a feature of TGFß-induced cataract. Clin Exp Optom 85, 76–82. https://doi.org/10.1111/j.1444-0938.2002.tb03012.x

Massagué, J., 2000. How cells read TGF-β signals. Nat Rev Mol Cell Bio 1, 169–178. https://doi.org/10.1038/35043051

Massagué, J., 1990. The Transforming Growth Factor-beta Family. Annu Rev Cell Biol 6, 597–641. https://doi.org/10.1146/annurev.cb.06.110190.003121

Massagué, J., Cheifetz, S., Ignotz, R.A., Boyd, F.T., 1987. Multiple type-β transforming growth factors and their receptors. J Cell Physiol 133, 43–47. https://doi.org/10.1002/jcp.1041330409

Massagué, J., Seoane, J., Wotton, D., 2005. Smad transcription factors. Gene Dev 19, 2783–2810. https://doi.org/10.1101/gad.1350705

Masszi, A., Ciano, C.D., Sirokmány, G., Arthur, W.T., Rotstein, O.D., Wang, J., McCulloch, C.A.G., Rosivall, L., Mucsi, I., Kapus, A., 2003. Central role for Rho in TGF-β1-induced α-smooth muscle actin expression during epithelial-mesenchymal transition. Am. J. Physiol.-Ren. Physiol. 284, F911–F924. https://doi.org/10.1152/ajprenal.00183.2002

Matsuzaki, K., 2012. Smad phosphoisoform signals in acute and chronic liver injury: similarities and differences between epithelial and mesenchymal cells. Cell Tissue Res. 347, 225–243. https://doi.org/10.1007/s00441-011-1178-6

Mattila, P.K., Lappalainen, P., 2008. Filopodia: molecular architecture and cellular functions. Nat. Rev. Mol. Cell Biol. 9, 446–454. https://doi.org/10.1038/nrm2406

Matyushenko, A.M., Shchepkin, D.V., Kopylova, G.V., Bershitsky, S.Y., Levitsky, D.I., 2020. Unique functional properties of slow skeletal muscle tropomyosin. Biochimie 174, 1–8. https://doi.org/10.1016/j.biochi.2020.03.013

McAvoy, J.W., 1978. Cell division, cell elongation and the co-ordination of crystallin gene expression during lens morphogenesis in the rat. Development 45, 271–281. https://doi.org/10.1242/dev.45.1.271

McAvoy, J.W., Chamberlain, C.G., 1990. Growth factors in the eye. Prog Growth Factor Res 2, 29–43. https://doi.org/10.1016/0955-2235(90)90008-8

McAvoy, J.W., Chamberlain, C.G., 1989. Fibroblast growth factor (FGF) induces different responses in lens epithelial cells depending on its concentration. Development 107, 221–228. https://doi.org/10.1242/dev.107.2.221

McAvoy, J.W., Chamberlain, C.G., Longh, R.U. de, Hales, A.M., Lovicu, F.J., 1999. Lens development. Eye 13, 425–437. https://doi.org/10.1038/eye.1999.117

McAvoy, J.W., Chamberlain, C.G., Schulz, M., Lovicu, F.J., 1992. The role of fibroblast growth factor in lens growth and diffrentiation. Exp Eye Res 55, 221. https://doi.org/10.1016/0014-4835(92)90989-6

McGuire, V.A., Gray, A., Monk, C.E., Santos, S.G., Lee, K., Aubareda, A., Crowe, J., Ronkina, N., Schwermann, J., Batty, I.H., Leslie, N.R., Dean, J.L.E., O'Keefe, S.J., Boothby, M., Gaestel, M., Arthur, J.S.C., 2013. Cross Talk between the Akt and p38α Pathways in Macrophages Downstream of Toll-Like Receptor Signaling. Mol. Cell. Biol. 33, 4152–4165. https://doi.org/10.1128/mcb.01691-12

Meacock, W.R., Spalton, D.J., Stanford, M.R., 2000. Role of cytokines in the pathogenesis of posterior capsule opacification. Brit J Ophthalmol 84, 332. https://doi.org/10.1136/bjo.84.3.332

Meiring, J.C.M., Bryce, N.S., Cagigas, M.L., Benda, A., Whan, R.M., Ariotti, N., Parton, R.G., Stear, J.H., Hardeman, E.C., Gunning, P.W., 2019. Colocation of Tpm3.1 and myosin IIa heads defines a discrete subdomain in stress fibres. J Cell Sci 132, jcs228916. https://doi.org/10.1242/jcs.228916

Meiring, J.C.M., Bryce, N.S., Wang, Y., Taft, M.H., Manstein, D.J., Lau, S.L., Stear, J., Hardeman, E.C., Gunning, P.W., 2018. Co-polymers of Actin and Tropomyosin Account for a Major Fraction of the Human Actin Cytoskeleton. Curr Biol 28, 2331-2337.e5. https://doi.org/10.1016/j.cub.2018.05.053

Meng, F., Li, J., Yang, X., Yuan, X., Tang, X., 2018. Role of Smad3 signaling in the epithelial-mesenchymal transition of the lens epithelium following injury. Int. J. Mol. Med. 42, 851–860. https://doi.org/10.3892/ijmm.2018.3662

Meng, X., Nikolic-Paterson, D.J., Lan, H.Y., 2016. TGF-β: the master regulator of fibrosis. Nat Rev Nephrol 12, 325–338. https://doi.org/10.1038/nrneph.2016.48

Meng, Y., Huang, K., Shi, M., Huo, Y., Han, L., Liu, B., Li, Y., 2023. Research Advances in the Role of the Tropomyosin Family in Cancer. Int. J. Mol. Sci. 24, 13295. https://doi.org/10.3390/ijms241713295

Menko, A.S., Andley, U.P., 2010. αA-Crystallin associates with α6 integrin receptor complexes and regulates cellular signaling. Exp. Eye Res. 91, 640–651. https://doi.org/10.1016/j.exer.2010.08.006

Menon, M.B., Dhamija, S., Kotlyarov, A., Gaestel, M., 2015. The problem of pyridinyl imidazole class inhibitors of MAPK14/p38α and MAPK11/p38β in autophagy research. Autophagy 11, 1425–1427. https://doi.org/10.1080/15548627.2015.1059562

Meyer-ter-Vehn, T., Gebhardt, S., Sebald, W., Buttmann, M., Grehn, F., Schlunck, G., Knaus, P., 2006. p38 Inhibitors Prevent TGF-β–Induced Myofibroblast Transdifferentiation in Human Tenon Fibroblasts. Invest Ophth Vis Sci 47, 1500–1509. https://doi.org/10.1167/iovs.05-0361

Michael, R., Bron, A.J., 2011. The ageing lens and cataract: a model of normal and pathological ageing. Philosophical Transactions Royal Soc Lond Ser B Biological Sci 366, 1278–92. https://doi.org/10.1098/rstb.2010.0300

Miettinen, P.J., Ebner, R., Lopez, A.R., Derynck, R., 1994. TGF-beta induced transdifferentiation of mammary epithelial cells to mesenchymal cells: involvement of type I receptors. J Cell Biology 127, 2021–2036. https://doi.org/10.1083/jcb.127.6.2021

Miller, D.A., Pelton, R.W., Derynck, R., Moses, H.L., 1990. Transforming Growth Factor-β: A Family of Growth Regulatory Peptides. Ann Ny Acad Sci 593, 208–217. https://doi.org/10.1111/j.1749-6632.1990.tb16113.x

Miyado, K., Kimura, M., Taniguchi, S., 1996. Decreased Expression of a Single Tropomyosin Isoform, TM5/TM30nm, Results in Reduction in Motility of Highly Metastatic B16-F10 Mouse Melanoma Cells. Biochem. Biophys. Res. Commun. 225, 427–435. https://doi.org/10.1006/bbrc.1996.1190

Molkentin, J.D., Bugg, D., Ghearing, N., Dorn, L.E., Kim, P., Sargent, M.A., Gunaje, J., Otsu, K., Davis, J., 2017. Fibroblast-Specific Genetic Manipulation of p38 Mitogen-Activated Protein Kinase In Vivo Reveals Its Central Regulatory Role in Fibrosis. Circulation 136, 549–561. https://doi.org/10.1161/circulationaha.116.026238

Morris, H.T., Machesky, L.M., 2015. Actin cytoskeletal control during epithelial to mesenchymal transition: focus on the pancreas and intestinal tract. Br. J. Cancer 112, 613–620. https://doi.org/10.1038/bjc.2014.658

Morrison, C.D., Parvani, J.G., Schiemann, W.P., 2013. The relevance of the TGF-β Paradox to EMT-MET programs. Cancer Lett 341, 30–40. https://doi.org/10.1016/j.canlet.2013.02.048

Mousa, G.Y., Trevithick, J.R., 1979. Actin in the lens: Changes in actin during differentiation of lens epithelial cells in vivo. Exp. Eye Res. 29, 71–81. https://doi.org/10.1016/0014-4835(79)90167-2

Moustakas, A., Heldin, C.-H., 2005. Non-Smad TGF-β signals. J Cell Sci 118, 3573–3584. https://doi.org/10.1242/jcs.02554

Munoz, L., 2017. Non-kinase targets of protein kinase inhibitors. Nat. Rev. Drug Discov. 16, 424–440. https://doi.org/10.1038/nrd.2016.266

Musil, L.S., 2012. Primary Cultures of Embryonic Chick Lens Cells as a Model System to Study Lens Gap Junctions and Fiber Cell Differentiation. J Membr Biology 245, 357–368. https://doi.org/10.1007/s00232-012-9458-y

Nakanishi, A., Wada, Y., Kitagishi, Y., Matsuda, S., 2014. Link between PI3K/AKT/PTEN Pathway and NOX Protein in Diseases. Aging Dis 5, 203. https://doi.org/10.14336/ad.2014.0500203

Nalluri, S.M., O'Connor, J.W., Gomez, E.W., 2015. Cytoskeletal signaling in TGFβ-induced epithelial–mesenchymal transition. Cytoskeleton 72, 557–569. https://doi.org/10.1002/cm.21263

Namiki, M., 1994. [Quantification of basic fibroblast growth factor (bFGF) and transforming growth factor (TGF alpha) in rabbit aqueous humor after intraocular lens implantation]. Nippon Ganka Gakkai zasshi 98, 334–9.

Nebreda, A.R., Porras, A., 2000. p38 MAP kinases: beyond the stress response. Trends Biochem. Sci. 25, 257–260. https://doi.org/10.1016/s0968-0004(00)01595-4

New, L., Han, J., 1998. The p38 MAP Kinase Pathway and Its Biological Function. Trends Cardiovasc. Med. 8, 220–228. https://doi.org/10.1016/s1050-1738(98)00012-7

Newitt, P., Boros, J., Madakashira, B.P., Robinson, M.L., Reneker, L.W., McAvoy, J.W., Lovicu, F.J., 2010. Sef is a negative regulator of fiber cell differentiation in the ocular lens. Differentiation 80, 53–67. https://doi.org/10.1016/j.diff.2010.05.005

Nieto, M.A., Huang, R.Y.-J., Jackson, R.A., Thiery, J.P., 2016. EMT: 2016. Cell 166, 21–45. https://doi.org/10.1016/j.cell.2016.06.028

Nieto, M.A., Sargent, M.G., Wilkinson, D.G., Cooke, J., 1994. Control of Cell Behavior During Vertebrate Development by Slug , a Zinc Finger Gene. Science 264, 835–839. https://doi.org/10.1126/science.7513443

Nishi, O., Nishi, K., Fujiwara, T., Shirasawa, E., Ohmoto, Y., 1996. Effects of the cytokines on the proliferation of and collagen synthesis by human cataract lens epithelial cells. Br. J. Ophthalmol. 80, 63. https://doi.org/10.1136/bjo.80.1.63

Nowak, R.B., Fischer, R.S., Zoltoski, R.K., Kuszak, J.R., Fowler, V.M., 2009. Tropomodulin1 is required for membrane skeleton organization and hexagonal geometry of fiber cells in the mouse lens. J. Cell Biol. 186, 915–928. https://doi.org/10.1083/jcb.200905065

Ochi, H., Ogino, H., Kageyama, Y., Yasuda, K., 2003. The Stability of the Lens-specific Maf Protein is Regulated by Fibroblast Growth Factor (FGF)/ERK Signaling in Lens Fiber Differentiation*. J. Biol. Chem. 278, 537–544. https://doi.org/10.1074/jbc.m208380200

Ochiai, Y., Ochiai, H., 2002. Higher Concentration of Transforming Growth Factor-β in Aqueous Humor of Glaucomatous Eyes and Diabetic Eyes. Jpn J Ophthalmol 46, 249–253. https://doi.org/10.1016/s0021-5155(01)00523-8

Oh, C.C., Nguy, M.Q., Schwenke, D.C., Migrino, R.Q., Thornburg, K., Reaven, P., 2014. p38α mitogen-activated kinase mediates cardiomyocyte apoptosis induced by palmitate. Biochem. Biophys. Res. Commun. 450, 628–633. https://doi.org/10.1016/j.bbrc.2014.06.023

Okada, T.S., Eguchi, G., Takeichi, M., 1971. The expression of differentiation by chicken lens epithelium in in vitro cell culture*. Dev Growth Differ 13, 323–336. https://doi.org/10.1111/j.1440-169x.1971.00323.x

O'Keefe, S.J., Mudgett, J.S., Cupo, S., Parsons, J.N., Chartrain, N.A., Fitzgerald, C., Chen, S.-L., Lowitz, K., Rasa, C., Visco, D., Luell, S., Carballo-Jane, E., Owens, K., Zaller, D.M., 2007. Chemical Genetics Define the Roles of p38α and p38β in Acute and Chronic Inflammation. J. Biol. Chem. 282, 34663–34671. https://doi.org/10.1074/jbc.m704236200

Olivey, H.E., Barnett, J.V., Ridley, B.D., 2003. Expression of the type III TGFβ receptor during chick organogenesis. Anat. Rec. Part A: Discov. Mol., Cell., Evol. Biol. 272A, 383–387. https://doi.org/10.1002/ar.a.10049

Ooshima, A., Park, J., Kim, S., 2019. Phosphorylation status at Smad3 linker region modulates transforming growth factor-β-induced epithelial-mesenchymal transition and cancer progression. Cancer Sci 110, 481–488. https://doi.org/10.1111/cas.13922

Ornitz, D.M., Itoh, N., 2015. The Fibroblast Growth Factor signaling pathway. Wiley Interdiscip. Rev.: Dev. Biol. 4, 215–266. https://doi.org/10.1002/wdev.176

Ornitz, D.M., Xu, J., Colvin, J.S., McEwen, D.G., MacArthur, C.A., Coulier, F., Gao, G., Goldfarb, M., 1996. Receptor Specificity of the Fibroblast Growth Factor Family*. J. Biol. Chem. 271, 15292–15297. https://doi.org/10.1074/jbc.271.25.15292

Pandey, S.K., Apple, D.J., Werner, L., Maloof, A.J., Milverton, E.J., 2004. Posterior capsule opacification: a review of the aetiopathogenesis, experimental and clinical studies and factors for prevention. Indian J Ophthalmol 52, 99–112.

Parreno, J., Amadeo, M.B., Kwon, E.H., Fowler, V.M., 2020. Tropomyosin 3.1 Association With Actin Stress Fibers is Required for Lens Epithelial to Mesenchymal Transition. Invest Ophth Vis Sci 61, 2. https://doi.org/10.1167/iovs.61.6.2

Pathan-Chhatbar, S., Taft, M.H., Reindl, T., Hundt, N., Latham, S.L., Manstein, D.J., 2018. Three mammalian tropomyosin isoforms have different regulatory effects on nonmuscle myosin-2B and filamentous β-actin in vitro. J. Biological Chem. 293, 863–875. https://doi.org/10.1074/jbc.m117.806521

Pawlak, G., Helfman, D.M., 2001. Cytoskeletal changes in cell transformation and tumorigenesis. Curr. Opin. Genet. Dev. 11, 41–47. https://doi.org/10.1016/s0959-437x(00)00154-4

Peek, R., McAvoy, J.W., Lubsen, N.H., Schoenmakers, J.G.G., 1992. Rise and fall of crystallin gene messenger levels during fibroblast growth factor induced terminal differentiation of lens cells. Dev. Biol. 152, 152–160. https://doi.org/10.1016/0012-1606(92)90165-d

Peng, Y., Yu, D., Gregorich, Z., Chen, X., Beyer, A.M., Gutterman, D.D., Ge, Y., 2013. In-depth proteomic analysis of human tropomyosin by top-down mass spectrometry. J Muscle Res Cell M 34, 199–210. https://doi.org/10.1007/s10974-013-9352-y

Perry, S.V., 2001. Vertebrate tropomyosin: distribution, properties and function. J Muscle Res Cell Motil 22, 5–49. https://doi.org/10.1023/a:1010303732441

Philpott, G.W., Coulombre, A.J., 1965. Lens development. Exp Cell Res 38, 635–644. https://doi.org/10.1016/0014-4827(65)90387-3

Pittenger, M.F., Kazzaz, J.A., Helfman, D.M., 1994. Functional properties of non-muscle tropomyosin isoforms. Curr Opin Cell Biol 6, 96–104. https://doi.org/10.1016/0955-0674(94)90122-8

Pleines, I., Woods, J., Chappaz, S., Kew, V., Foad, N., Ballester-Beltrán, J., Aurbach, K., Lincetto, C., Lane, R.M., Schevzov, G., Alexander, W.S., Hilton, D.J., Astle, W.J., Downes, K., Nurden, P., Westbury, S.K., Mumford, A.D., Obaji, S.G., Collins, P.W., BioResource, N., Delerue, F., Ittner, L.M., Bryce, N.S., Holliday, M., Lucas, C.A., Hardeman, E.C., Ouwehand, W.H., Gunning, P.W., Turro, E., Tijssen, M.R., Kile, B.T., 2017. Mutations in tropomyosin 4 underlie a rare form of human macrothrombocytopenia. J Clin Investigation 127, 814–829. https://doi.org/10.1172/jci86154

Porras, A., Zuluaga, S., Black, E., Valladares, A., Alvarez, A.M., Ambrosino, C., Benito, M., Nebreda, A.R., 2004. p38α Mitogen-activated Protein Kinase Sensitizes Cells to Apoptosis Induced by Different Stimuli. Mol. Biol. Cell 15, 922–933. https://doi.org/10.1091/mbc.e03-08-0592

Powers, C.J., McLeskey, S.W., Wellstein, A., 2000. Fibroblast growth factors, their receptors and signaling. Endocr.-Relat. Cancer 7, 165–197. https://doi.org/10.1677/erc.0.0070165

Prunotto, M., Bruschi, M., Gunning, P., Gabbiani, G., Weibel, F., Ghiggeri, G.M., Petretto, A., Scaloni, A., Bonello, T., Schevzov, G., Alieva, I., Bochaton-Piallat, M., Candiano, G., Dugina, V., Chaponnier, C., 2015. Stable incorporation of α-smooth muscle actin into stress fibers is dependent on specific tropomyosin isoforms. Cytoskeleton 72, 257–267. https://doi.org/10.1002/cm.21230

Pua, L.J.W., Mai, C.-W., Chung, F.F.-L., Khoo, A.S.-B., Leong, C.-O., Lim, W.-M., Hii, L.-W., 2022. Functional Roles of JNK and p38 MAPK Signaling in Nasopharyngeal Carcinoma. Int. J. Mol. Sci. 23, 1108. https://doi.org/10.3390/ijms23031108

Pusnik, A., Petrovski, G., Lumi, X., 2022. Dysphotopsias or Unwanted Visual Phenomena after Cataract Surgery. Life 13, 53. https://doi.org/10.3390/life13010053

Raghavan, C.T., Smuda, M., Smith, A.J.O., Howell, S., Smith, D.G., Singh, A., Gupta, P., Glomb, M.A., Wormstone, I.M., Nagaraj, R.H., 2016. AGEs in human lens capsule promote the TGFβ2-mediated EMT of lens epithelial cells: implications for age-associated fibrosis. Aging Cell 15, 465–476. https://doi.org/10.1111/acel.12450

Ramaekers, F.C.S., Boomkens, T.R., Bloemendal, H., 1981. Cytoskeletal and contractile structures in bovine lens cell differentiation. Exp. Cell Res. 135, 454–461. https://doi.org/10.1016/0014-4827(81)90190-7

Ramos, C., Becerril, C., Montaño, M., García-De-Alba, C., Ramírez, R., Checa, M., Pardo, A., Selman, M., 2010. FGF-1 reverts epithelial-mesenchymal transition induced by TGF-β1 through MAPK/ERK kinase pathway. Am J Physiol-lung C 299, L222–L231. https://doi.org/10.1152/ajplung.00070.2010

Ranganathan, P., Agrawal, A., Bhushan, R., Chavalmane, A.K., Kalathur, R.K.R., Takahashi, T., Kondaiah, P., 2007. Expression profiling of genes regulated by TGF-beta: Differential regulation in normal and tumour cells. Bmc Genomics 8, 98. https://doi.org/10.1186/1471-2164-8-98

Rao, P.V., Maddala, R., 2006. The role of the lens actin cytoskeleton in fiber cell elongation and differentiation. Semin Cell Dev Biol 17, 698–711. https://doi.org/10.1016/j.semcdb.2006.10.011

Rice, A.B., Ingram, J.L., Bonner, J.C., 2002. p38 Mitogen-Activated Protein Kinase Regulates Growth Factor–Induced Mitogenesis of Rat Pulmonary Myofibroblasts. Am. J. Respir. Cell Mol. Biol. 27, 759–765. https://doi.org/10.1165/rcmb.2002-0070oc

Rio-Tsonis, K.D., Jung, J.C., Chiu, I.-M., Tsonis, P.A., 1997. Conservation of fibroblast growth factor function in lens regeneration. Proc. Natl. Acad. Sci. 94, 13701–13706. https://doi.org/10.1073/pnas.94.25.13701

Risco, A., Cuenda, A., 2012. New Insights into the p38γ and p38δ MAPK Pathways. J. Signal Transduct. 2012, 520289. https://doi.org/10.1155/2012/520289

Robaszkiewicz, K., Ostrowska, Z., Marchlewicz, K., Moraczewska, J., 2016. Tropomyosin isoforms differentially modulate the regulation of actin filament polymerization and depolymerization by cofilins. Febs J 283, 723–737. https://doi.org/10.1111/febs.13626

Robertson, J.V., Nathu, Z., Najjar, A., Dwivedi, D., Gauldie, J., West-Mays, J.A., 2007. Adenoviral gene transfer of bioactive TGFbeta1 to the rodent eye as a novel model for anterior subcapsular cataract. Mol Vis 13, 457–69.

Robinson, M.L., 2006. An essential role for FGF receptor signaling in lens development. Semin. Cell Dev. Biol. 17, 726–740. https://doi.org/10.1016/j.semcdb.2006.10.002

Roelen, B.A.J., Lin, H.Y., Knežević, V., Freund, E., Mummery, C.L., 1994. Expression of TGF-βs and Their Receptors during Implantation and Organogenesis of the Mouse Embryo. Dev. Biol. 166, 716–728. https://doi.org/10.1006/dbio.1994.1350

Safina, A.F., Varga, A.E., Bianchi, A., Zheng, Q., Kunnev, D., Liang, P., Bakin, A., 2009. Ras alters epithelial-mesenchymal transition in response to TGF-β by reducing actin fibers and cell-matrix adhesion. Cell Cycle 8, 284–298. https://doi.org/10.4161/cc.8.2.7590

Saika, S., Kono-Saika, S., Ohnishi, Y., Sato, M., Muragaki, Y., Ooshima, A., Flanders, K.C., Yoo, J., Anzano, M., Liu, C.-Y., Kao, W.W. –Y., Roberts, A.B., 2004. Smad3 Signaling Is Required for Epithelial-Mesenchymal Transition of Lens Epithelium after Injury. Am J Pathology 164, 651–663. https://doi.org/10.1016/s0002-9440(10)63153-7

Saika, S., Miyamoto, T., Ishida, I., Shirai, K., Ohnishi, Y., Ooshima, A., McAvoy, J.W., 2002. TGFβ-Smad signalling in postoperative human lens epithelial cells. Brit J Ophthalmol 86, 1428. https://doi.org/10.1136/bjo.86.12.1428

Saika, S., Yamanaka, O., Ikeda, K., Kim-Mitsuyama, S., Flanders, K.C., Yoo, J., Roberts, A.B., Nishikawa-Ishida, I., Ohnishi, Y., Muragaki, Y., Ooshima, A., 2005. Inhibition of p38MAP kinase suppresses fibrotic reaction of retinal pigment epithelial cells. Lab. Investig. 85, 838–850. https://doi.org/10.1038/labinvest.3700294

Saito, A., Horie, M., Nagase, T., 2018. TGF-β Signaling in Lung Health and Disease. Int J Mol Sci 19, 2460. https://doi.org/10.3390/ijms19082460

Samson, S.C., Ferrer, T., Jou, C.J., Sachse, F.B., Shankaran, S.S., Shaw, R.M., Chi, N.C., Tristani-Firouzi, M., Yost, H.J., 2013. 3-OST-7 Regulates BMP-Dependent Cardiac Contraction. PLoS Biol. 11, e1001727. https://doi.org/10.1371/journal.pbio.1001727

Santibañez, J.F., 2006. JNK mediates TGF-β1-induced epithelial mesenchymal transdifferentiation of mouse transformed keratinocytes. FEBS Lett. 580, 5385–5391. https://doi.org/10.1016/j.febslet.2006.09.003

Sapkota, G.P., 2013. The TGFβ-induced phosphorylation and activation of p38 mitogen-activated protein kinase is mediated by MAP3K4 and MAP3K10 but not TAK1. Open Biol. 3, 130067. https://doi.org/10.1098/rsob.130067

Sarabipour, S., Hristova, K., 2016. Mechanism of FGF receptor dimerization and activation. Nat. Commun. 7, 10262. https://doi.org/10.1038/ncomms10262

Savill, S.A., Leitch, H.F., Harvey, J.N., Thomas, T.H., 2012. Functional structure of the promoter regions for the predominant low molecular weight isoforms of tropomyosin in human kidney cells. J. Cell. Biochem. 113, 3576–3586. https://doi.org/10.1002/jcb.24236

Schevzov, G., Kee, A.J., Wang, B., Sequeira, V.B., Hook, J., Coombes, J.D., Lucas, C.A., Stehn, J.R., Musgrove, E.A., Cretu, A., Assoian, R., Fath, T., Hanoch, T., Seger, R., Pleines, I., Kile, B.T., Hardeman, E.C., Gunning, P.W., 2015. Regulation of cell proliferation by ERK and signal-dependent nuclear translocation of ERK is dependent on Tm5NM1-containing actin filaments. Mol Biol Cell 26, 2475–2490. https://doi.org/10.1091/mbc.e14-10-1453

Schevzov, G., O'Neill, G., 2008. Tropomyosin. Adv. Exp. Med. Biol. 43–59. https://doi.org/10.1007/978-0-387-85766-4_4

Schevzov, G., Vrhovski, B., Bryce, N.S., Elmir, S., Qiu, M.R., O'Neill, G.M., Yang, N., Verrills, N.M., Kavallaris, M., Gunning, P.W., 2005. Tissue-specific Tropomyosin Isoform Composition. J Histochem Cytochem 53, 557–570. https://doi.org/10.1369/jhc.4a6505.2005

Schevzov, G., Whittaker, S.P., Fath, T., Lin, J.J.-C., Gunning, P.W., 2011. Tropomyosin isoforms and reagents. Bioarchitecture 1, 135–164. https://doi.org/10.4161/bioa.1.4.17897

Schlessinger, J., 2000. Cell Signaling by Receptor Tyrosine Kinases. Cell 103, 211–225. https://doi.org/10.1016/s0092-8674(00)00114-8

Schulz, M.W., Chamberlain, C.G., Iongh, R.U. de, McAvoy, J.W., 1993. Acidic and basic FGF in ocular media and lens: implications for lens polarity and growth patterns. Development 118, 117–126. https://doi.org/10.1242/dev.118.1.117

Schulz, M.W., Chamberlain, C.G., McAvoy, J.W., 1997. Binding of FGF-1 and FGF-2 to Heparan Sulphate Proteoglycans of the Mammalian Lens Capsule. Growth Factors 14, 1–13. https://doi.org/10.3109/08977199709021506

Sebe, A., Leivonen, S.-K., Fintha, A., Masszi, A., Rosivall, L., Kähäri, V.-M., Mucsi, I., 2008. Transforming growth factor-β-induced alpha-smooth muscle cell actin expression in renal proximal tubular cells is regulated by p38β mitogen-activated protein kinase, extracellular

signal-regulated protein kinase1,2 and the Smad signalling during epithelial–myofibroblast transdifferentiation. Nephrol. Dial. Transplant. 23, 1537–1545. https://doi.org/10.1093/ndt/gfm789

Segev, F., Mor, O., Segev, A., Belkin, M., Assia, E.I., 2005. Downregulation of gene expression in the ageing lens: a possible contributory factor in senile cataract. Eye 19, 80–85. https://doi.org/10.1038/sj.eye.6701423

Shi, Q., Cheng, L., Liu, Z., Hu, K., Ran, J., Ge, D., Fu, J., 2015. The p38 MAPK inhibitor SB203580 differentially modulates LPS-induced interleukin 6 expression in macrophages. Cent.-Eur. J. Immunol. 40, 276–282. https://doi.org/10.5114/ceji.2015.54586

Shibata, S., Shibata, N., Ohtsuka, S., Yoshitomi, Y., Kiyokawa, E., Yonekura, H., Singh, D.P., Sasaki, H., Kubo, E., 2021. Role of Decorin in Posterior Capsule Opacification and Eye Lens Development. Cells 10, 863. https://doi.org/10.3390/cells10040863

Shibata, T., Ikawa, M., Sakasai, R., Ishigaki, Y., Kiyokawa, E., Iwabuchi, K., Singh, D.P., Sasaki, H., Kubo, E., 2021. Lens–specific conditional knockout of tropomyosin 1 gene in mice causes abnormal fiber differentiation and lens opacity. Mech Ageing Dev 196, 111492. https://doi.org/10.1016/j.mad.2021.111492

Shibata, T., Shibata, S., Ishigaki, Y., Kiyokawa, E., Ikawa, M., Singh, D.P., Sasaki, H., Kubo, E., 2018. Tropomyosin 2 heterozygous knockout in mice using CRISPR-Cas9 system displays the inhibition of injury-induced epithelial-mesenchymal transition, and lens opacity. Mech Ageing Dev 171, 24–30. https://doi.org/10.1016/j.mad.2018.03.001

Shields, J.M., Mehta, H., Pruitt, K., Der, C.J., 2002. Opposing Roles of the Extracellular Signal-Regulated Kinase and p38 Mitogen-Activated Protein Kinase Cascades in Ras-Mediated Downregulation of Tropomyosin. Mol. Cell. Biol. 22, 2304–2317. https://doi.org/10.1128/mcb.22.7.2304-2317.2002

Shihan, M.H., Novo, S.G., Duncan, M.K., 2019. Cataract surgeon viewpoints on the need for novel preventative anti-inflammatory and anti-posterior capsular opacification therapies. Curr Med Res Opin 35, 1971–1981. https://doi.org/10.1080/03007995.2019.1647012

Shin, E.H., Zhao, G., Wang, Q., Lovicu, F.J., 2015. Sprouty gain of function disrupts lens cellular processes and growth by restricting RTK signaling. Dev Biol 406, 129–146. https://doi.org/10.1016/j.ydbio.2015.09.005

Shin, E.H.H., Basson, M.A., Robinson, M.L., McAvoy, J.W., Lovicu, F.J., 2012. Sprouty Is a Negative Regulator of Transforming Growth Factor β-Induced Epithelial-to-Mesenchymal Transition and Cataract. Mol. Med. 18, 861–873. https://doi.org/10.2119/molmed.2012.00111

Shin, H., Kim, D., Helfman, D.M., 2017. Tropomyosin isoform Tpm2.1 regulates collective and amoeboid cell migration and cell aggregation in breast epithelial cells. Oncotarget 8, 95192–95205. https://doi.org/10.18632/oncotarget.19182

Shirakihara, T., Horiguchi, K., Miyazawa, K., Ehata, S., Shibata, T., Morita, I., Miyazono, K., Saitoh, M., 2011. TGF-β regulates isoform switching of FGF receptors and epithelial–mesenchymal transition. Embo J 30, 783–795. https://doi.org/10.1038/emboj.2010.351

Shu, D.Y., Hutcheon, A.E.K., Zieske, J.D., Guo, X., 2019a. Epidermal Growth Factor Stimulates Transforming Growth Factor-Beta Receptor Type II Expression In Corneal Epithelial Cells. Sci. Rep. 9, 8079. https://doi.org/10.1038/s41598-019-42969-2

Shu, D.Y., Lovicu, F.J., 2019. Enhanced EGF receptor-signaling potentiates TGFβ-induced lens epithelial-mesenchymal transition. Exp Eye Res 185, 107693. https://doi.org/10.1016/j.exer.2019.107693

Shu, D.Y., Lovicu, F.J., 2017. Myofibroblast transdifferentiation: The dark force in ocular wound healing and fibrosis. Prog Retin Eye Res 60, 44–65. https://doi.org/10.1016/j.preteyeres.2017.08.001

Shu, D.Y., Ng, K., Wishart, T.F.L., Chui, J., Lundmark, M., Flokis, M., Lovicu, F.J., 2021. Contrasting roles for BMP-4 and ventromorphins (BMP agonists) in TGFβ-induced lens EMT. Exp Eye Res 206, 108546. https://doi.org/10.1016/j.exer.2021.108546

Shu, D.Y., Wojciechowski, M., Lovicu, F.J., 2019b. ERK1/2-mediated EGFR-signaling is required for TGFβ-induced lens epithelial-mesenchymal transition. Exp Eye Res 178, 108–121. https://doi.org/10.1016/j.exer.2018.09.021

Shu, D.Y., Wojciechowski, M.C., Lovicu, F.J., 2017. Bone Morphogenetic Protein-7 Suppresses TGFβ2-Induced Epithelial-Mesenchymal Transition in the Lens: Implications for Cataract Prevention. Invest Ophth Vis Sci 58, 781–796. https://doi.org/10.1167/iovs.16-20611

Singh, R., Diwan, M., Dastidar, S., Najmi, A., 2018. Differential effect of p38 and MK2 kinase inhibitors on the inflammatory and toxicity biomarkers in vitro. Hum. Exp. Toxicol. 37, 521–531. https://doi.org/10.1177/0960327117715901

Sisto, M., Lorusso, L., Ingravallo, G., Ribatti, D., Lisi, S., 2020. TGFβ1-Smad canonical and -Erk noncanonical pathways participate in interleukin-17-induced epithelial–mesenchymal transition in Sjögren's syndrome. Lab. Investig. 100, 824–836. https://doi.org/10.1038/s41374-020-0373-z

Small, J.V., Rottner, K., Kaverina, I., Anderson, K.I., 1998. Assembling an actin cytoskeleton for cell attachment and movement. Biochim. Biophys. Acta (BBA) - Mol. Cell Res. 1404, 271–281. https://doi.org/10.1016/s0167-4889(98)00080-9

Sørensen, V., Zhen, Y., Zakrzewska, M., Haugsten, E.M., Wälchli, S., Nilsen, T., Olsnes, S., Wiedlocha, A., 2008. Phosphorylation of Fibroblast Growth Factor (FGF) Receptor 1 at Ser777 by p38 Mitogen-Activated Protein Kinase Regulates Translocation of Exogenous FGF1 to the Cytosol and Nucleus. Mol. Cell. Biol. 28, 4129–4141. https://doi.org/10.1128/mcb.02117-07

Sporn, M.B., Newton, D.L., 1981. Inhibition of Tumor Induction and Development 71–100. https://doi.org/10.1007/978-1-4615-9218-1_3

Sporn, M.B., Todaro, G.J., 1980. Autocrine Secretion and Malignant Transformation of Cells. New Engl J Med 303, 878–880. https://doi.org/10.1056/nejm198010093031511

Sreekanth, G.P., Chuncharunee, A., Sirimontaporn, A., Panaampon, J., Noisakran, S., Yenchitsomanus, P., Limjindaporn, T., 2016. SB203580 Modulates p38 MAPK Signaling and Dengue Virus-Induced Liver Injury by Reducing MAPKAPK2, HSP27, and ATF2 Phosphorylation. PLoS ONE 11, e0149486. https://doi.org/10.1371/journal.pone.0149486

Srinivasan, Y., Lovicu, F.J., Overbeek, P.A., 1998. Lens-specific expression of transforming growth factor beta1 in transgenic mice causes anterior subcapsular cataracts. J Clin Invest 101, 625–634. https://doi.org/10.1172/jci1360

Stambe, C., Atkins, R.C., Tesch, G.H., Masaki, T., Schreiner, G.F., Nikolic-Paterson, D.J., 2004. The Role of p38α Mitogen-Activated Protein Kinase Activation in Renal Fibrosis. J. Am. Soc. Nephrol. 15, 370–379. https://doi.org/10.1097/01.asn.0000109669.23650.56

Stefen, H., Suchowerska, A.K., Chen, B.J., Brettle, M., Kuschelewski, J., Gunning, P.W., Janitz, M., Fath, T., 2018. Tropomyosin isoforms have specific effects on the transcriptome of undifferentiated and differentiated B35 neuroblastoma cells. Febs Open Bio 8, 570–583. https://doi.org/10.1002/2211-5463.12386

Stehn, J., Schevzov, G., O'Neill, G., Gunning, P., 2006. Specialisation of the Tropomyosin Composition of Actin Filaments Provides New Potential Targets for Chemotherapy. Curr Cancer Drug Tar 6, 245–256. https://doi.org/10.2174/156800906776842948

Stehn, J.R., Haass, N.K., Bonello, T., Desouza, M., Kottyan, G., Treutlein, H., Zeng, J., Nascimento, P.R.B.B., Sequeira, V.B., Butler, T.L., Allanson, M., Fath, T., Hill, T.A., McCluskey, A., Schevzov, G., Palmer, S.J., Hardeman, E.C., Winlaw, D., Reeve, V.E., Dixon, I., Weninger, W., Cripe, T.P., Gunning, P.W., 2013. A Novel Class of Anticancer Compounds Targets the Actin Cytoskeleton in Tumor Cells. Cancer Res. 73, 5169–5182. https://doi.org/10.1158/0008-5472.can-12-4501

Stolen, C.M., Jackson, M.W., Griep, A.E., 1997. Overexpression of FGF-2 modulates fiber cell differentiation and survival in the mouse lens. Dev Camb Engl 124, 4009–17. https://doi.org/10.1242/dev.124.20.4009

Strand, D.W., Liang, Y.-Y., Yang, F., Barron, D.A., Ressler, S.J., Schauer, I.G., Feng, X.-H., Rowley, D.R., 2014. TGF-β induction of FGF-2 expression in stromal cells requires integrated smad3 and MAPK pathways. Am J Clin Exp Urology 2, 239–48.

Strutz, F., Zeisberg, M., Renziehausen, A., Raschke, B., Becker, V., Kooten, C.V., Müller, G.A., 2001. TGF-β1 induces proliferation in human renal fibroblasts via induction of basic fibroblast growth factor (FGF-2). Kidney Int 59, 579–592. https://doi.org/10.1046/j.1523-1755.2001.059002579.x

Stump, R.J.W., Ang, S., Chen, Y., Bahr, T. von, Lovicu, F.J., Pinson, K., Iongh, R.U. de, Yamaguchi, T.P., Sassoon, D.A., McAvoy, J.W., 2003. A role for Wnt/β-catenin signaling in lens epithelial differentiation. Dev. Biol. 259, 48–61. https://doi.org/10.1016/s0012-1606(03)00179-9

Sugiyama, Y., Nakazawa, Y., Sakagami, T., Kawata, S., Nagai, N., Yamamoto, N., Funakoshi-Tago, M., Tamura, H., 2021. Capsaicin attenuates TGFβ2-induced epithelial-mesenchymal-transition in lens epithelial cells in vivo and in vitro. Exp Eye Res 213, 108840. https://doi.org/10.1016/j.exer.2021.108840

Sui, Z., Gokhin, D.S., Nowak, R.B., Guo, X., An, X., Fowler, V.M., 2017. Stabilization of F-actin by tropomyosin isoforms regulates the morphology and mechanical behavior of red blood cells. Mol. Biol. Cell 28, 2531–2542. https://doi.org/10.1091/mbc.e16-10-0699

Sumara, G., Formentini, I., Collins, S., Sumara, I., Windak, R., Bodenmiller, B., Ramracheya, R., Caille, D., Jiang, H., Platt, K.A., Meda, P., Aebersold, R., Rorsman, P., Ricci, R., 2009. Regulation of PKD by the MAPK p38δ in Insulin Secretion and Glucose Homeostasis. Cell 136, 235–248. https://doi.org/10.1016/j.cell.2008.11.018

Susanto, A., Zhao, G., Wazin, F., Feng, Y., Rasko, J.E.J., Bailey, C.G., Lovicu, F.J., 2019. Spred negatively regulates lens growth by modulating epithelial cell proliferation and fiber differentiation. Exp Eye Res 178, 160–175. https://doi.org/10.1016/j.exer.2018.09.019

Symonds, J.G., Lovicu, F.J., Chamberlain, C.G., 2006. Posterior capsule opacification-like changes in rat lens explants cultured with TGFβ and FGF: Effects of cell coverage and regional differences. Exp Eye Res 82, 693–699. https://doi.org/10.1016/j.exer.2005.09.008

Tada, A., Kato, H., Hasegawa, S., 2000. Antagonistic effect of EGF against TGF beta1 on transformed phenotype and tropomyosin expression of human lung carcinoma A549 cells. Oncol. Rep. 7, 1323–6. https://doi.org/10.3892/or.7.6.1323

Tada, A., Kato, H., Takenaga, K., Hasegawa, S., 1997. Transforming growth factor β1 increases the expressions of high molecular weight tropomyosin isoforms and vinculin and suppresses the transformed phenotypes in human lung carcinoma cells. Cancer Lett. 121, 31–37. https://doi.org/10.1016/s0304-3835(97)00319-4

Taiyab, A., Holms, J., West-Mays, J.A., 2019. β-Catenin/Smad3 Interaction Regulates Transforming Growth Factor-β-Induced Epithelial to Mesenchymal Transition in the Lens. Int J Mol Sci 20, 2078. https://doi.org/10.3390/ijms20092078

Taiyab, A., West-Mays, J., 2022. Lens Fibrosis: Understanding the Dynamics of Cell Adhesion Signaling in Lens Epithelial-Mesenchymal Transition. Front. Cell Dev. Biol. 10, 886053. https://doi.org/10.3389/fcell.2022.886053

Takenawa, T., Harada, K., Ferdous, T., Kawasaki, K., Kuramitsu, Y., Mishima, K., 2023. Silencing of Tropomyosin 1 suppresses the proliferation, invasion and metastasis of oral squamous cell carcinoma in vitro. J. Oral Maxillofac. Surg., Med., Pathol. 35, 282–287. https://doi.org/10.1016/j.ajoms.2022.10.004

Tan, Y., Rouse, J., Zhang, A., Cariati, S., Cohen, P., Comb, M.J., 1996. FGF and stress regulate CREB and ATF-1 via a pathway involving p38 MAP kinase and MAPKAP kinase-2. EMBO J. 15, 4629–4642. https://doi.org/10.1002/j.1460-2075.1996.tb00840.x

Tanaka, J., Watanabe, T., Nakamura, N., Sobue, K., 1993. Morphological and biochemical analyses of contractile proteins (actin, myosin, caldesmon and tropomyosin) in normal and transformed cells. J. Cell Sci. 104, 595–606. https://doi.org/10.1242/jcs.104.2.595

Tanaka, M., Fujii, Y., Hirano, K., Higaki, T., Nagasaki, A., Ishikawa, R., Okajima, T., Katoh, K., 2019. Fascin in lamellipodia contributes to cell elasticity by controlling the orientation of filamentous actin. Genes Cells 24, 202–213. https://doi.org/10.1111/gtc.12671

Tao, T., Shi, Y., Han, D., Luan, W., Qian, J., Zhang, J., Wang, Y., You, Y., (CGCG), C.G.C.G., 2014. TPM3, a strong prognosis predictor, is involved in malignant progression through MMP family members and EMT-like activators in gliomas. Tumor Biol. 35, 9053–9059. https://doi.org/10.1007/s13277-014-1974-1

Teven, C.M., Farina, E.M., Rivas, J., Reid, R.R., 2014. Fibroblast growth factor (FGF) signaling in development and skeletal diseases. Genes Dis. 1, 199–213. https://doi.org/10.1016/j.gendis.2014.09.005

Tojkander, S., Gateva, G., Schevzov, G., Hotulainen, P., Naumanen, P., Martin, C., Gunning, P.W., Lappalainen, P., 2011. A Molecular Pathway for Myosin II Recruitment to Stress Fibers. Curr Biol 21, 539–550. https://doi.org/10.1016/j.cub.2011.03.007

Tortorella, L.L., Lin, C.B., Pilch, P.F., 2003. ERK6 is expressed in a developmentally regulated manner in rodent skeletal muscle. Biochem. Biophys. Res. Commun. 306, 163–168. https://doi.org/10.1016/s0006-291x(03)00936-7

Trelstad, R.L., Hay, E.D., Revel, J.-P., 1967. Cell contact during early morphogenesis in the chick embryo. Dev Biol 16, 78–106. https://doi.org/10.1016/0012-1606(67)90018-8

Tsang, M., Dawid, I.B., 2004. Promotion and Attenuation of FGF Signaling Through the Ras-MAPK Pathway. Sci.'s STKE 2004, pe17. https://doi.org/10.1126/stke.2282004pe17

Turner, N., Grose, R., 2010. Fibroblast growth factor signalling: from development to cancer. Nat. Rev. Cancer 10, 116–129. https://doi.org/10.1038/nrc2780

Tzanakakis, G., Kavasi, R.-M., Voudouri, K., Berdiaki, A., Spyridaki, I., Tsatsakis, A., Nikitovic, D., 2017. Role of the extracellular matrix in cancer-associated epithelial to mesenchymal transition phenomenon: Extracellular Matrix and EMT. Dev Dynam 247, 368–381. https://doi.org/10.1002/dvdy.24557

Valcourt, U., Kowanetz, M., Niimi, H., Heldin, C.-H., Moustakas, A., 2005. TGF-β and the Smad Signaling Pathway Support Transcriptomic Reprogramming during Epithelial-Mesenchymal Cell Transition. Mol Biol Cell 16, 1987–2002. https://doi.org/10.1091/mbc.e04-08-0658

Varga, A.E., Stourman, N.V., Zheng, Q., Safina, A.F., Quan, L., Li, X., Sossey-Alaoui, K., Bakin, A.V., 2005. Silencing of the Tropomyosin-1 gene by DNA methylation alters tumor suppressor function of TGF-β. Oncogene 24, 5043–5052. https://doi.org/10.1038/sj.onc.1208688

Vasavada, A.R., Praveen, M.R., 2014. Posterior Capsule Opacification After Phacoemulsification: Annual Review. Asia-pacific J Ophthalmol Phila Pa 3, 235–40. https://doi.org/10.1097/apo.0000000000000080

Ventura, J.J., Tenbaum, S., Perdiguero, E., Huth, M., Guerra, C., Barbacid, M., Pasparakis, M., Nebreda, A.R., 2007. p38α MAP kinase is essential in lung stem and progenitor cell proliferation and differentiation. Nat. Genet. 39, 750–758. https://doi.org/10.1038/ng2037

Vergarajauregui, S., Miguel, A.S., Puertollano, R., 2006. Activation of p38 Mitogen-Activated Protein Kinase Promotes Epidermal Growth Factor Receptor Internalization. Traffic 7, 686–698. https://doi.org/10.1111/j.1600-0854.2006.00420.x

Vrhovski, B., McKay, K., Schevzov, G., Gunning, P.W., Weinberger, R.P., 2005. Smooth Muscle-specific α Tropomyosin Is a Marker of Fully Differentiated Smooth Muscle in Lung. J Histochem Cytochem 53, 875–883. https://doi.org/10.1369/jhc.4a6504.2005

Walker, J.L., Bleaken, B.M., Romisher, A.R., Alnwibit, A.A., Menko, A.S., 2018. In wound repair vimentin mediates the transition of mesenchymal leader cells to a myofibroblast phenotype. Mol. Biol. Cell 29, 1555–1570. https://doi.org/10.1091/mbc.e17-06-0364

Walker, J.L., Bleaken, B.M., Wolff, I.M., Menko, A.S., 2015. Establishment of a Clinically Relevant Ex Vivo Mock Cataract Surgery Model for Investigating Epithelial Wound Repair in a Native Microenvironment. J. Vis. Exp. https://doi.org/10.3791/52886-v

Walker, J.L., Wolff, I.M., Zhang, L., Menko, A.S., 2007. Activation of SRC kinases signals induction of posterior capsule opacification. Investig. Ophthalmol. Vis. Sci. 48, 2214–23. https://doi.org/10.1167/iovs.06-1059

Wallentin, N., Wickström, K., Lundberg, C., 1998. Effect of cataract surgery on aqueous TGF-beta and lens epithelial cell proliferation. Invest Ophth Vis Sci 39, 1410–8.

Walters, T., Endl, M., Elmer, T.R., Levenson, J., Majmudar, P., Masket, S., 2015. Sustained-release dexamethasone for the treatment of ocular inflammation and pain after cataract surgery. J. Cataract Refract. Surg. 41, 2049–2059. https://doi.org/10.1016/j.jcrs.2015.11.005

Walton, K.L., Johnson, K.E., Harrison, C.A., 2017. Targeting TGF-β Mediated SMAD Signaling for the Prevention of Fibrosis. Front Pharmacol 08, 461. https://doi.org/10.3389/fphar.2017.00461

Wang, D., Wang, E., Liu, K., Xia, C., Li, S., Gong, X., 2017. Roles of TGFβ and FGF signals during growth and differentiation of mouse lens epithelial cell in vitro. Sci Rep-uk 7, 7274. https://doi.org/10.1038/s41598-017-07619-5

Wang, J., Yang, Y., Du, B., 2022. Clinical Characterization and Prognostic Value of TPM4 and Its Correlation with Epithelial–Mesenchymal Transition in Glioma. Brain Sci. 12, 1120. https://doi.org/10.3390/brainsci12091120

Wang, L.-P., Chen, B.-X., Sun, Y., Chen, J.-P., Huang, S., Liu, Y.-Z., 2019. Celastrol inhibits migration, proliferation and transforming growth factor-β2-induced epithelial-mesenchymal

transition in lens epithelial cells. Int J Ophthalmol-chi 12, 1517–1523. https://doi.org/10.18240/ijo.2019.10.01

Wang, Q., McAvoy, J.W., Lovicu, F.J., 2010. Growth factor signaling in vitreous humor-induced lens fiber differentiation. Invest Ophth Vis Sci 51, 3599–610. https://doi.org/10.1167/iovs.09-4797

Wang, Q., Stump, R., McAvoy, J.W., Lovicu, F.J., 2008. MAPK/ERK1/2 and PI3-kinase signalling pathways are required for vitreous-induced lens fibre cell differentiation. Exp Eye Res 88, 293–306. https://doi.org/10.1016/j.exer.2008.08.023

Wang, X.S., Diener, K., Manthey, C.L., Wang, S., Rosenzweig, B., Bray, J., Delaney, J., Cole, C.N., Chan-Hui, P.-Y., Mantlo, N., Lichenstein, H.S., Zukowski, M., Yao, Z., 1997. Molecular Cloning and Characterization of a Novel p38 Mitogen-activated Protein Kinase*. J. Biol. Chem. 272, 23668–23674. https://doi.org/10.1074/jbc.272.38.23668

Wang, Z., Gao, R., Huang, Y., Tian, B., Zhou, Y., 2009. Effects of mitogen-activated protein kinase signal pathway on heat shock protein 27 expression in human lens epithelial cells exposed to sodium salicylate in vitro. J. Huazhong Univ. Sci. Technol. Méd. Sci. 29, 377–382. https://doi.org/10.1007/s11596-009-0323-x

Warren, R.H., Gordon, E., Azarnia, R., 1985. Tropomyosin in peripheral ruffles of cultured rat kidney cells. Eur. J. cell Biol. 38, 245–53.

Weber, G.F., Menko, A.S., 2006. Phosphatidylinositol 3-Kinase Is Necessary for Lens Fiber Cell Differentiation and Survival. Investig. Opthalmology Vis. Sci. 47, 4490. https://doi.org/10.1167/iovs.06-0401

Wen, S.-Y., Cheng, S.-Y., Ng, S.-C., Aneja, R., Chen, C.-J., Huang, C.-Y., Kuo, W.-W., 2019. Roles of p38α and p38β mitogen-activated protein kinase isoforms in human malignant melanoma A375 cells. Int. J. Mol. Med. 44, 2123–2132. https://doi.org/10.3892/ijmm.2019.4383

West-Mays, J.A., Pino, G., Lovicu, F.J., 2009. Development and use of the lens epithelial explant system to study lens differentiation and cataractogenesis. Prog Retin Eye Res 29, 135–43. https://doi.org/10.1016/j.preteyeres.2009.12.001

Wishart, T.F.L., Flokis, M., Shu, D.Y., Das, S.J., Lovicu, F.J., 2021. Hallmarks of lens aging and cataractogenesis. Exp Eye Res 210, 108709. https://doi.org/10.1016/j.exer.2021.108709

Wishart, T.F.L., Lovicu, F.J., 2023. Spatiotemporal Localisation of Heparan Sulphate Proteoglycans throughout Mouse Lens Morphogenesis. Cells 12, 1364. https://doi.org/10.3390/cells12101364

Wishart, T.F.L., Lovicu, F.J., 2021. An Atlas of Heparan Sulfate Proteoglycans in the Postnatal Rat Lens. Investig. Ophthalmol. Vis. Sci. 62, 5. https://doi.org/10.1167/iovs.62.14.5

Wojciechowski, M.C., Mahmutovic, L., Shu, D.Y., Lovicu, F.J., 2017. ERK1/2 signaling is required for the initiation but not progression of TGFβ-induced lens epithelial to

mesenchymal transition (EMT). Exp Eye Res 159, 98–113. https://doi.org/10.1016/j.exer.2017.03.012

Wojciechowski, M.C., Shu, D.Y., Lovicu, F.J., 2018. ERK1/2-Dependent Gene Expression Contributing to TGFβ-Induced Lens EMT. Curr Eye Res 43, 986–997. https://doi.org/10.1080/02713683.2018.1464193

Woo, M.K., Fowler, V.M., 1994. Identification and characterization of tropomodulin and tropomyosin in the adult rat lens. J. Cell Sci. 107, 1359–1367. https://doi.org/10.1242/jcs.107.5.1359

Wood, C.D., Thornton, T.M., Sabio, G., Davis, R.A., Rincon, M., 2009. Nuclear Localization of p38 MAPK in Response to DNA Damage. Int. J. Biol. Sci. 5, 428–437. https://doi.org/10.7150/ijbs.5.428

Wormstone, I.M., Anderson, I.K., Eldred, J.A., Dawes, L.J., Duncan, G., 2006. Short-term exposure to transforming growth factor β induces long-term fibrotic responses. Exp Eye Res 83, 1238–1245. https://doi.org/10.1016/j.exer.2006.06.013

Wormstone, I.M., Eldred, J.A., 2016. Experimental models for posterior capsule opacification research. Exp Eye Res 142, 2–12. https://doi.org/10.1016/j.exer.2015.04.021

Wormstone, I.M., Rio-Tsonis, K.D., McMahon, G., Tamiya, S., Davies, P.D., Marcantonio, J.M., Duncan, G., 2001. FGF: an autocrine regulator of human lens cell growth independent of added stimuli. Invest Ophth Vis Sci 42, 1305–11.

Wormstone, I.M., Tamiya, S., Anderson, I., Duncan, G., 2002. TGF-beta2-induced matrix modification and cell transdifferentiation in the human lens capsular bag. Invest Ophth Vis Sci 43, 2301–8.

Wormstone, I.M., Wang, L., Liu, C.S.C., 2008. Posterior capsule opacification. Exp Eye Res 88, 257–69. https://doi.org/10.1016/j.exer.2008.10.016

Wormstone, I.M., Wormstone, Y.M., Smith, A.J.O., Eldred, J.A., 2020. Posterior capsule opacification: What's in the bag? Prog Retin Eye Res 100905. https://doi.org/10.1016/j.preteyeres.2020.100905

Xiao, Y.Q., Malcolm, K., Worthen, G.S., Gardai, S., Schiemann, W.P., Fadok, V.A., Bratton, D.L., Henson, P.M., 2002. Cross-talk between ERK and p38 MAPK Mediates Selective Suppression of Pro-inflammatory Cytokines by Transforming Growth Factor-β*. J Biol Chem 277, 14884–14893. https://doi.org/10.1074/jbc.m111718200

Xie, L., Law, B.K., Chytil, A.M., Brown, K.A., Aakre, M.E., Moses, H.L., 2004. Activation of the Erk Pathway Is Required for TGF-β1-Induced EMT In Vitro. Neoplasia 6, 603–610. https://doi.org/10.1593/neo.04241

Xie, Y., Su, N., Yang, J., Tan, Q., Huang, S., Jin, M., Ni, Z., Zhang, B., Zhang, D., Luo, F., Chen, H., Sun, X., Feng, J.Q., Qi, H., Chen, L., 2020. FGF/FGFR signaling in health and disease. Signal Transduct. Target. Ther. 5, 181. https://doi.org/10.1038/s41392-020-00222-7

Xu, J., Lamouille, S., Derynck, R., 2009. TGF-beta-induced epithelial to mesenchymal transition. Cell Res 19, 156–72. https://doi.org/10.1038/cr.2009.5

Xu, M., Wang, S., Wang, Y., Wu, H., Frank, J.A., Zhang, Z., Luo, J., 2018. Role of p38γ MAPK in regulation of EMT and cancer stem cells. Biochim. Biophys. Acta (BBA) - Mol. Basis Dis. 1864, 3605–3617. https://doi.org/10.1016/j.bbadis.2018.08.024

Xu, Q., Tan, Y., Zhang, K., Li, Y., 2013. Crosstalk between p38 and Smad3 through TGF-β1 in JEG-3 choriocarcinoma cells. Int. J. Oncol. 43, 1187–1193. https://doi.org/10.3892/ijo.2013.2026

Yamamoto, N., Itonaga, K., Marunouchi, T., Majima, K., 2005. Concentration of Transforming Growth Factor β2 in Aqueous Humor. Ophthalmic Res 37, 29–33. https://doi.org/10.1159/000083019

Yan, W., Zhang, Y., Cao, J., Yan, H., 2022. TGF-β2 levels in the aqueous humor are elevated in the second eye of high myopia within two weeks after sequential cataract surgery. Sci. Rep. 12, 17974. https://doi.org/10.1038/s41598-022-22746-4

Yang, F., Strand, D.W., Rowley, D.R., 2008. Fibroblast growth factor-2 mediates transforming growth factor-β action in prostate cancer reactive stroma. Oncogene 27, 450–459. https://doi.org/10.1038/sj.onc.1210663

Yang, J., Antin, P., Berx, G., Blanpain, C., Brabletz, T., Bronner, M., Campbell, K., Cano, A., Casanova, J., Christofori, G., Dedhar, S., Derynck, R., Ford, H.L., Fuxe, J., Herreros, A.G. de, Goodall, G.J., Hadjantonakis, A.-K., Huang, R.J.Y., Kalcheim, C., Kalluri, R., Kang, Y., Khew-Goodall, Y., Levine, H., Liu, J., Longmore, G.D., Mani, S.A., Massagué, J., Mayor, R., McClay, D., Mostov, K.E., Newgreen, D.F., Nieto, M.A., Puisieux, A., Runyan, R., Savagner, P., Stanger, B., Stemmler, M.P., Takahashi, Y., Takeichi, M., Theveneau, E., Thiery, J.P., Thompson, E.W., Weinberg, R.A., Williams, E.D., Xing, J., Zhou, B.P., Sheng, G., (TEMTIA), E.I.A., 2020. Guidelines and definitions for research on epithelial-mesenchymal transition. Nat Rev Mol Cell Biology 21, 341–352. https://doi.org/10.1038/s41580-020-0237-9

Yu, L., Hébert, M.C., Zhang, Y.E., 2002. TGF-β receptor-activated p38 MAP kinase mediates Smad-independent TGF-β responses. EMBO J. 21, 3749–3759. https://doi.org/10.1093/emboj/cdf366

Yu, S.-B., Gao, Q., Lin, W.-W., Kang, M.-Q., 2017. Proteomic analysis indicates the importance of TPM3 in esophageal squamous cell carcinoma invasion and metastasis. Mol. Med. Rep. 15, 1236–1242. https://doi.org/10.3892/mmr.2017.6145

Yu, Y., Xiao, C.-H., Tan, L.-D., Wang, Q.-S., Li, X.-Q., Feng, Y.-M., 2014. Cancer-associated fibroblasts induce epithelial–mesenchymal transition of breast cancer cells through paracrine TGF-β signalling. Br. J. Cancer 110, 724–732. https://doi.org/10.1038/bjc.2013.768

Yun, Y.-R., Won, J.E., Jeon, E., Lee, S., Kang, W., Jo, H., Jang, J.-H., Shin, U.S., Kim, H.-W., 2010. Fibroblast Growth Factors: Biology, Function, and Application for Tissue Regeneration. J. Tissue Eng. 1, 218142. https://doi.org/10.4061/2010/218142

Zare, M., Hadi, F., Alivand, M.R., 2018. Considering the downregulation of Tpm1.6 and Tpm1.7 in squamous cell carcinoma of esophagus as a potent biomarker. Pers. Med. 15, 361–370. https://doi.org/10.2217/pme-2018-0015

Zeisberg, M., Neilson, E.G., 2009. Biomarkers for epithelial-mesenchymal transitions. J Clin Investigation 119, 1429–37. https://doi.org/10.1172/jci36183

Zhang, F., Zhang, Z., Lin, X., Beenken, A., Eliseenkova, A.V., Mohammadi, M., Linhardt, R.J., 2009. Compositional Analysis of Heparin/Heparan Sulfate Interacting with Fibroblast Growth Factor·Fibroblast Growth Factor Receptor Complexes. Biochemistry 48, 8379–8386. https://doi.org/10.1021/bi9006379

Zhang, J.-C., Doñate, F., Qi, X., Ziats, N.P., Juarez, J.C., Mazar, A.P., Pang, Y.-P., McCrae, K.R., 2002. The antiangiogenic activity of cleaved high molecular weight kininogen is mediated through binding to endothelial cell tropomyosin. Proc. Natl. Acad. Sci. 99, 12224–12229. https://doi.org/10.1073/pnas.192668299

Zhang, P., Zhang, W., Jiang, J., Shen, Z., Chen, S., Yu, S., Kang, M., 2022. MiR-107 inhibits the malignant biological behavior of esophageal squamous cell carcinoma by targeting TPM3. J. Gastrointest. Oncol. 0, 0–0. https://doi.org/10.21037/jgo-22-575

Zhang, Q., Yu, N., Lee, C., 2014. Mysteries of TGF-β Paradox in Benign and Malignant Cells. Frontiers Oncol 4, 94. https://doi.org/10.3389/fonc.2014.00094

Zhang, Y., Li, J., Partovian, C., Sellke, F.W., Simons, M., 2003. Syndecan-4 modulates basic fibroblast growth factor 2 signaling in vivo. Am. J. Physiol.-Hear. Circ. Physiol. 284, H2078–H2082. https://doi.org/10.1152/ajpheart.00942.2001

Zhang, Y.E., 2009. Non-Smad pathways in TGF-beta signaling. Cell Res 19, 128–39. https://doi.org/10.1038/cr.2008.328

Zhao, G., Bailey, C.G., Feng, Y., Rasko, J., Lovicu, F.J., 2018. Negative regulation of lens fiber cell differentiation by RTK antagonists Spry and Spred. Exp Eye Res 170, 148–159. https://doi.org/10.1016/j.exer.2018.02.025

Zhao, G., Pan, A.Y., Feng, Y., Rasko, J.E.J., Bailey, C.G., Lovicu, F.J., 2022. Sprouty and Spred temporally regulate ERK1/2-signaling to suppress TGFβ-induced lens EMT. Exp. Eye Res. 219, 109070. https://doi.org/10.1016/j.exer.2022.109070

Zhao, H., Yang, T., Madakashira, B.P., Thiels, C.A., Bechtle, C.A., Garcia, C.M., Zhang, H., Yu, K., Ornitz, D.M., Beebe, D.C., Robinson, M.L., 2008. Fibroblast growth factor receptor signaling is essential for lens fiber cell differentiation. Dev Biol 318, 276–288. https://doi.org/10.1016/j.ydbio.2008.03.028

Zhao, X., Jiang, M., Wang, Z., 2019. TPM4 promotes cell migration by modulating F-actin formation in lung cancer. OncoTargets Ther. 12, 4055–4063. https://doi.org/10.2147/ott.s198542

Zheng, Q., Safina, A., Bakin, A.V., 2008. Role of high-molecular weight tropomyosins in TGF-β-mediated control of cell motility. Int. J. Cancer 122, 78–90. https://doi.org/10.1002/ijc.23025

Zhou, J., Menko, A.S., 2004. Coordinate Signaling by Src and p38 Kinases in the Induction of Cortical Cataracts. Invest Ophth Vis Sci 45, 2314–2323. https://doi.org/10.1167/iovs.03-1210

Zhu, X., Du, Y., Li, D., Xu, J., Wu, Q., He, W., Zhang, Keke, Zhu, J., Guo, L., Qi, M., Liu, A., Qi, J., Wang, G., Meng, J., Yang, Z., Zhang, Kang, Lu, Y., 2021. Aberrant TGF-β1 signaling activation by MAF underlies pathological lens growth in high myopia. Nat Commun 12, 2102. https://doi.org/10.1038/s41467-021-22041-2

Zi, Z., Chapnick, D.A., Liu, X., 2012. Dynamics of TGF-β/Smad signaling. Febs Lett 586, 1921–1928. https://doi.org/10.1016/j.febslet.2012.03.063

APPENDIX

PEER-REVIEWED JOURNAL ARTICLE

Chapter 5 contains a peer-reviewed journal article published previously in *Cells* (March 2023). All author contributions have been stated previously (see Chapter 5: Section 5.1). The original peer-reviewed manuscript has been provided on the following page.

Reference: Flokis, M., Lovicu, F.J., 2023. FGF-2 Differentially Regulates Lens Epithelial Cell Behaviour during TGF-β-Induced EMT. Cells 12, 827. https://doi.org/10.3390/cells12060827

cells

MDPI

Article

FGF-2 Differentially Regulates Lens Epithelial Cell Behaviour during TGF-β-Induced EMT

Mary Flokis [1] and Frank J. Lovicu [1,2,*]

[1] Molecular and Cellular Biomedicine, School of Medical Sciences, Faculty of Medicine and Health, The University of Sydney, Sydney, NSW 2006, Australia
[2] Save Sight Institute, The University of Sydney, Sydney, NSW 2006, Australia
* Correspondence: frank.lovicu@sydney.edu.au

Abstract: Fibroblast growth factor (FGF) and transforming growth factor-beta (TGF-β) can regulate and/or dysregulate lens epithelial cell (LEC) behaviour, including proliferation, fibre differentiation, and epithelial–mesenchymal transition (EMT). Earlier studies have investigated the crosstalk between FGF and TGF-β in dictating lens cell fate, that appears to be dose dependent. Here, we tested the hypothesis that a fibre-differentiating dose of FGF differentially regulates the behaviour of lens epithelial cells undergoing TGF-β-induced EMT. Postnatal 21-day-old rat lens epithelial explants were treated with a fibre-differentiating dose of FGF-2 (200 ng/mL) and/or TGF-β2 (50 pg/mL) over a 7-day culture period. We compared central LECs (CLECs) and peripheral LECs (PLECs) using immunolabelling for changes in markers for EMT (α-SMA), lens fibre differentiation (β-crystallin), epithelial cell adhesion (β-catenin), and the cytoskeleton (alpha-tropomyosin), as well as Smad2/3- and MAPK/ERK1/2-signalling. Lens epithelial explants cotreated with FGF-2 and TGF-β2 exhibited a differential response, with CLECs undergoing EMT while PLECs favoured more of a lens fibre differentiation response, compared to the TGF-β-only-treated explants where all cells in the explants underwent EMT. The CLECs cotreated with FGF and TGF-β immunolabelled for α-SMA, with minimal β-crystallin, whereas the PLECs demonstrated strong β-crystallin reactivity and little α-SMA. Interestingly, compared to the TGF-β-only-treated explants, α-SMA was significantly decreased in the CLECs cotreated with FGF/TGF-β. Smad-dependent and independent signalling was increased in the FGF-2/TGF-β2 co-treated CLECs, that had a heightened number of cells with nuclear localisation of Smad2/3 compared to the PLECs, that in contrast had more pronounced ERK1/2-signalling over Smad2/3 activation. The current study has confirmed that FGF-2 is influential in differentially regulating the behaviour of LECs during TGF-β-induced EMT, leading to a heterogenous cell population, typical of that observed in the development of post-surgical, posterior capsular opacification (PCO). This highlights the cooperative relationship between FGF and TGF-β leading to lens pathology, providing a different perspective when considering preventative measures for controlling PCO.

Keywords: transforming growth factor-beta (TGF-β); fibroblast growth factor (FGF); epithelial-mesenchymal transition (EMT); fibrosis; cataract; lens

Citation: Flokis, M.; Lovicu, F.J. FGF-2 Differentially Regulates Lens Epithelial Cell Behaviour during TGF-β-Induced EMT. *Cells* **2023**, *12*, 827. https://doi.org/10.3390/cells12060827

Academic Editor: Alexander V. Ljubimov

Received: 14 February 2023
Revised: 2 March 2023
Accepted: 6 March 2023
Published: 7 March 2023

1. Introduction

The ocular lens is a transparent, avascular tissue responsible for transmitting light onto the retina. It contains two cell types: cuboidal epithelial cells and adjacent elongate fibre cells, both comprised of specialized molecular (e.g., crystallins) and cytoskeletal (e.g., intermediate filaments) properties to facilitate vision [1]. Ocular growth factors, such as fibroblast growth factor (FGF) and transforming growth factor-beta (TGF-β), are key regulators of different cellular processes in the lens, including epithelial cell proliferation [2–4], fibre differentiation [1,5–10], and epithelial–mesenchymal transition (EMT) that lead to lens pathology [11–17]. In situ, FGF is thought to be required for regulating normal lens cell processes in a spatially dependent manner, as previously reviewed [1].

TGF-β can regulate and/or concurrently dysregulate normal lens homeostasis, cell growth, and survival, by altering lens epithelial cell (LEC) morphology [17–19]. The dysregulation of lens epithelial cell architecture induced by TGF-β is characterized by EMT, a phenomenon that has been widely reviewed [20–22], with normal cuboidal LECs transitioning to become aberrant migratory, contractile myofibroblastic cells. These myofibroblastic cells can aggregate to form a fibrotic plaque leading to cataracts [23–25]. To date, cataracts, that have been extensively reviewed and studied, are still considered the most common form of blindness worldwide [26–28], with the only form of treatment being surgical intervention. Despite the effectiveness of surgery, posterior capsular opacification (PCO), known also as a secondary cataract, may result post surgery, requiring further intervention [29–31]. PCO results from the aberrant behaviour of LECs left after surgery, with these cells either undergoing EMT to form a posterior subcapsular plaque (fibrotic PCO) [11,24,25,32], or differentiating into aberrant fibre cells leading to Elschnig's pearls and Soemmerring's ring (regenerative, pearl PCO) [33], as previously reviewed [34,35]. While these two different spatially distinct epithelial PCO pathologies are well characterised [36,37], the underlying molecular mechanisms regarding their formation are poorly understood.

Numerous models have established TGF-β-induced lens EMT responses in humans [14], embryonic chicks [13,38], and murine cell lines and explant models [13,15,25,32,39]. In dissociated embryonic chick lens epithelial cells treated with TGF-β, we see a heterogenous response, with some cells undergoing fibre differentiation, while others undergo EMT [13,40]. In in vitro studies using mammalian lens epithelia, exogenous treatment of LECs with TGF-β results in a homogenous EMT response [17,41–43]. In situ, however, anterior subcapsular cataracts (ASCs) develop in transgenic mice in response to elevated activity of ocular TGF-β [44]; the subcapsular plaques are comprised a heterogenous population of aberrant lens fibre cells and myofibroblastic cells, similar to those seen in human cataracts [24]. The in situ transgenic mouse model ideally replicates the human clinical pathology of fibrotic cataracts, that is attributed to the endogenous ocular milieu of different growth factors and cytokines, that do not act in isolation, unlike what we have in vitro. Since two disparate lens epithelial phenotypes contribute to ASC and PCO, it is important to better understand how they are derived, and the putative interplay of the different ocular factors involved.

While FGF is well established in regulating lens epithelial cell proliferation and fibre differentiation, it has also previously been shown to influence TGF-β-induced EMT and aberrant cell behaviour, promoting wound healing, repair, and fibrogenesis [5,16,41,45]. For example, different relatively low doses of FGF-2 (2.5–20 ng/mL) can exacerbate TGF-β2 (0.5–3 ng/mL)-induced lens opacification in intact rat lenses, with the higher dose combinations exhibiting the most pronounced response, resulting in dense cellular plaques and elevated deposition of ECM [16]. In contrast, other studies have shown that FGF can counteract and antagonise EMT in rodent LECs [14,15]. Rat lens epithelial cell explants cotreated with a relatively low dose of TGF-β2 (50 pg/mL) and a lower dose of FGF-2 (10 ng/mL) still formed spindle-like cells typical of EMT; however, with minimal cell loss compared to explants treated with TGF-β2 alone [15]. This increased cell survival was unique to FGF as other regulatory ocular growth factors (e.g., EGF, IGF, HGF, or PDGF) could not block the hallmark features of TGF-β-induced EMT, including lens capsular wrinkling, apoptosis, and cell loss [15,46].

The influence of FGF regulating TGF-β-induced EMT may be attributed to the putative crosstalk between various downstream intracellular signalling pathways; the TGF-β-canonical Smad2/3-dependent proteins, and non-canonical mitogen-activated protein kinases (MAPK), such as extracellular signal-regulated kinase (ERK1/2) [14,38,47–49]. Studies using mouse LEC lines (MLECs) showed that cotreatment of cells with FGF-2 (10 ng/mL) and TGF-β2 (10 ng/mL) resulted in elongated fibroblastic-like cells and enhanced cell migratory mechanisms, with elevated ERK1/2-signalling [14]. Interestingly, in human lens epithelial cells (HLECs) from this same study, cotreated with the same doses of FGF-2/TGF-β2, they report on the antagonistic behaviour of FGF-2 with a reduction in cy-

toskeletal markers involved in stress fibre formation [14]. It is clear from these studies that there is no consistency in cell responsiveness to both FGF/TGF-β across different species.

In the current study, we characterized the influence that FGF has on TGF-β-induced cell behaviour in rat lens explants to best model the conditions needed to promote a heterogenous cell population typical of fibrotic cataracts as seen in situ. We demonstrate that a high fibre-differentiating dose of FGF is protective of TGF-β-induced EMT in peripheral lens epithelia; however, this is not evident in central lens epithelia induced by TGF-β. This emulates the spatial phenotypic response of lens cells seen in human PCO and may serve as a model to better understand the mechanisms leading to this post-surgical pathology.

2. Materials and Methods

2.1. Animals and Tissue Culture

All procedures conducted abided by the Australian Code for animal care and usage for scientific purposes and the Association for Research in Vision and Ophthalmology (ARVO) Statement for the Use of Animals for Ophthalmic and Vision biomedical research (USA). The experiments were approved by the Animal Ethics Committee of The University of Sydney, NSW, Australia (AEC# 2021/1913). Wistar rats (*rattus norvegicus*) at 21-days of age (P21 $\pm$ 1 day) were humanely euthanized with CO_2 followed by cervical dislocation.

2.2. Lens Epithelial Explants

All collected primary rat ocular tissues were kept in medium 199 with Earle's Salts (M199) (11825015, Gibco^{TM}, Thermo Fisher Scientific, Sydney, NSW, Australia) in 35 mm Nunc™ culture dishes (NUN150460, Thermo Fisher Scientific). The media was supplemented with 2.5 µg/mL Amphotericin B (15290-018, Gibco^{TM}, Thermo Fisher Scientific), 0.1% bovine serum albumin (BSA) (9048-46-8, Sigma-Aldrich Corp., St. Louis, MO, USA), 0.1 µg/mL L-glutamine (200 mM) (25030081, Gibco^{TM}, Life Technologies, Carlsbad, CA, USA), and penicillin (100 IU/mL)/streptomycin (100 µg/mL) (15140-122, Gibco^{TM}, Life Technologies). The collected eyes were placed under a dissecting microscope to remove the lenses. The posterior capsule of the lens was torn using fine forceps and the remaining intact anterior capsule containing a sheet of lens epithelial cells (LECs) was pinned to the base of the culture dish using the gentle pressure of the forceps, as previously described [5]. Explants were maintained in a humidified incubator (37 °C, 5% CO_2).

Different doses of recombinant human TGF-β2 (302-B2-002, R&D systems, Minneapolis, MN, USA) were used to induce EMT in the lens explants, as previously described [39]. A lower dose of TGF-β2 (50 pg/mL) gave a more regulated EMT response over 7 days, while a higher dose (200 pg/mL) was used to induce a more rapid EMT response in the lens explants over this same time period. To determine the impact of FGF-2 on TGF-β2-induced lens EMT, we cotreated TGF-β2-treated LECs with either a low proliferating dose of recombinant human FGF-2 (5 ng/mL: 233-FB, R&D systems) or a high fibre-differentiating dose of FGF-2 (200 ng/mL) [10,50]. Control explants had no growth factors added to the media.

2.3. Assessment of Cell Morphology and Immunofluorescence

Cultured LEC explants were monitored and photographed daily over 7 days using phase contrast microscopy (Leica FireCam imaging, Leica Microsystems, Version 1.5, 2007). To examine the extent of how transdifferentiated cells modulated the underlying lens capsule, some treated explants were rinsed with filtered Milli-Q H_2O to debride all cells from the explant to completely expose the underlying lens capsule. Phase contrast images were captured before and after rinsing.

Following the different growth factor treatments, at set time points, the explants were fixed in 10% neutral buffered formalin (NBF; HT501320-9.5L, Sigma-Aldrich Corp) for 10 min, followed by 3 $\times$ 5 min rinses in phosphate-buffered saline (PBS) supplemented with BSA (0.1%, v/w; PBS/BSA). The cells were permeabilized using PBS/BSA supplemented with Tween-20 (0.05%, v/v; 3 $\times$ 5 min), followed by subsequent rinses in PBS/BSA (2 $\times$ 5 min). The explants were then incubated at room temperature for 30 min with 3%

normal goat serum (NGS diluted in PBS/BSA, *w*/*v*), before adding the primary antibodies; anti-mouse α-SMA (A2547, Sigma-Aldrich Corp.), anti-alpha tropomyosin (Tpm; α/9d; provided by Prof. Gunning, University of New South Wales, Sydney, NSW, Australia), anti-rabbit β-catenin (ab6302, Abcam, Fremont, CA, USA), anti-β-crystallin, and anti-total-Smad2/3 (t-Smad2/3: 8685, Cell Signaling Tech., Danvers, MA, USA), all diluted 1:100 in NGS/PBS/BSA. The explants were incubated overnight at 4 °C, followed by rinsing in PBS/BSA (3 × 5 min). The respective secondary antibodies were then applied for a 2 h incubation at room temperature: goat anti-rabbit IgG Alexa-Fluor® 488 (ab150077, Abcam), and goat anti-mouse Alexa-Fluor® 594 (ab150116, Abcam), all diluted 1:1000 in PBS/BSA. Three 5 min rinses in PBS/BSA were followed before a 5 min application of 3 µg/mL bis-benzimide (H33342 trihydrochloride, Hoechst counterstain, B2261, Sigma-Aldrich) diluted in PBS/BSA. The explants were rinsed again before mounting with 10% glycerol in PBS and imaged using epifluorescence microscopy (Leica DMLB 100S with DFC-450C camera, Leica Application Suite, Version 4.8, 2021).

2.4. SDS-Page and Western Blotting

Cultured lens epithelial explants at set time points were rinsed in cold PBS. The central and peripheral regions of the explants were isolated using a scalpel blade to delineate each region. A central square of tissue, no more than a third of the explant diameter (central LECs, CLECs), and the remaining surrounding peripheral LECs (PLECs) were isolated separately. CLEC and PLEC protein was harvested, pooled into allocated Eppendorf tubes, and lysed with cold radioimmunoprecipitation assay (RIPA) lysis buffer containing 150 mM NaCl, 0.5% sodium deoxycholate, 0.1% Sodium dodecyl sulphate (SDS), 1 mM sodium orthovanadate, 1 mM NaF, 50 mM Tris-HCl (pH 7.5), 0.1% Triton X-100, phosphatase (PhosSTOP™), and protease (cOmplete™) EASYpacks inhibitor tablets (04906837001 and 05892970001; Roche Applied Science, Basel, Switzerland). LECs were homogenized and centrifuged for 10 min at 4 °C (14,400× *g*) for lysate/supernatant separation. Quantification of the total lens protein of each supernatant sample was conducted using a Pierce™ Micro bicinchoninic acid (BCA) protein assay reagent kit (23235; Thermo Fisher Scientific).

LEC protein sample lysates were prepared using 5% 2-mercaptoethanol (M6250, Sigma-Aldrich) combined with 2× Laemmli sample buffer at a 1:1 (*v*/*v*) ratio (1610737, Bio-Rad Laboratories, NSW, Australia). For electrophoresis, 10 µg of protein lysates were loaded onto 12% SDS-PAGE gels for 20 min at 70 V followed by 2 h at 120 V. LEC protein was then transferred onto an immobilon®-PSQ polyvinylidene fluoride (PVDF) membrane (ISEQ00010, Merck Millipore, Rahway, NJ, USA) for 1 h at 100 V. PVDF membranes were incubated in 2.5% BSA blocking buffer diluted in tris-buffered saline with 0.1% Tween-20 (TBST) and incubated for 1 h with agitation at room temperature. Primary antibodies were added to the membranes and left overnight to incubate (at 4 °C): anti-mouse α-SMA, anti-GAPDH (G8795, Sigma-Aldrich Corp.), anti-tropomyosin alpha, and anti-β-crystallin, t-Smad2/3, phospho-Smad2/3 (p-Smad2/3, 8828, Cell Signalling Tech., Danvers, MA, USA), phospho-ERK1/2 (p-ERK1/2, 9101, Cell Signalling Tech.), and total-ERK1/2 (t-ERK1/2, 9102, Cell Signalling Tech.), all diluted in blocking buffer/TBST at 1:1000, apart from α-SMA and GAPDH (1:2000). Following overnight incubation, the membranes were rinsed in TBST (3 × 5 min) and incubated with the appropriate horseradish peroxidase (HRP)-conjugated secondary antibodies for 2 h at room temperature: HRP-conjugated goat anti-rabbit IgG (7074, Cell Signalling Tech.) and horse anti-mouse IgG (7076, Cell Signalling Tech.), diluted in TBST at 1:5000. The membranes were rinsed in TBST (3 × 10 min) followed by the application of an immobilon chemiluminescent HRP substrate for 3–5 min (WBKLS0500, Merck Millipore). Protein chemiluminescent signals were imaged using Bio-Rad ChemiDoc™ MP imaging.

Following immunolabeling, PVDF membranes were stripped for 10 min in stripping buffer (10% SDS, 0.5 M Tris HCl pH 6.8, Milli-Q H_2O, and 0.8% 2-mercaptoethanol) with gentle agitation. The membranes were then washed in TBST (3 × 5 min) and re-blocked in blocking buffer/TBST for 1 h. Following blocking, the membranes were probed for

loading control GAPDH (1:2000, 1 h) and incubated with an HRP-conjugated horse anti-mouse secondary antibody for 1 h prior to chemiluminescent signalling analysis. Protein densitometry was carried out using Bio-Rad ImageLab software (Version 6.1.0, 2019).

2.5. Statistical Analysis

For each experimental analysis, three independent experiments were carried out. For every experiment, a minimum of three individual replicates ($n = 3$) per treatment group (different treatment of explants) were used. For Western blotting, each group contained up to eight explants to isolate central and peripheral lens cells that were randomly obtained from different P21 rats. For measuring changes in protein expression, we used densitometry to calculate the selected protein intensity relative to the loading control (GAPDH).

For Western blot experiments examining differences in Smad-dependent (Smad2/3) and Smad-independent (MAPK/ERK1/2) activity, phosphorylated protein expression was calculated using the following ratio: relative phosphorylated density per total protein.

Prior to the use of one-way analysis of variance (ANOVA), several assumptions were tested and confirmed; we assumed equal standard deviation (SD) and residuals appeared normally distributed. Based on these confirmed assumptions, we compared the differences among the means of all treatment groups using one-way ANOVA, followed by Tukey's multiple comparisons post-hoc test. All data acquired were plotted appropriately using GraphPad Prism software version 9.0 (GraphPad Software Inc., San Diego, CA, USA).

To quantify the spatial differences in t-Smad2/3 immunoreactivity, six separate images of central and peripheral regions were captured per explant across three randomized explants per treatment group, over three individual experiments. Nuclear and cytoplasmic localisation of t-Smad2/3 was manually counted using ImageJ's Cell Counter plugin. The mean percentage of t-Smad2/3 nuclear and cytoplasmic fluorescence was calculated and statistically analysed using GraphPad Prism.

Tabled data were represented as the standard error of the mean (±SEM) and probability values, where $p < 0.05$ was considered statistically significant.

3. Results

3.1. FGF-2 Promotes a Spatially Dependent TGF-β2-Induced EMT Response in Lens Epithelial Explants

We examined the efficacy of different doses of FGF-2 in modulating the effect of TGF-β2 on lens epithelial cells induced to undergo EMT. Using phase contrast microscopy, control LECs without FGF-2 or TGF-β2 treatment (Figure 1A,E), as well as explants treated with only a low dose of FGF-2, demonstrated no significant morphological changes and retained their epithelial phenotype over the culture period. When the lens epithelial explants were treated with a low dose of TGF-β2 (50 pg/mL), this promoted an EMT response across the entire explant, similar to a higher dose (200 pg/mL) of TGF-β2, albeit at a slower rate, consistent with previous studies [42].

With different dose combinations of FGF-2 and TGF-β2, most cells in the explants underwent a uniform EMT response over 5 days, with the exception of cells in the explants cotreated with a relatively high dose of FGF-2 (200 ng/mL) and the lower dose of TGF-β2 (Figure 1), where we observed a differential response between CLECs and PLECs (Table 1, Supplementary Figure S1).

The cells in the lens epithelial explants treated with the high a fibre-differentiating dose of FGF-2 elongated over 5 days (Figure 1B,F), compared to the control LEC explants (no growth factor treatment; Figure 1A,E). This FGF-induced fibre differentiation response was more pronounced in PLECs compared to CLECs (Figure 1B,F). LECs in explants treated with a low dose of TGF-β2 (Figure 1C,G) displayed prominent EMT by day 5, with the LECs losing their uniform packing and adhesion as they transdifferentiated into myofibroblastic cells. TGF-β2 treatment also led to increased cellular blebbing (refractile bodies) and apoptotic cell loss, evident by areas of bare lens capsule that displayed prominent signs of capsular modification in the form of wrinkling throughout the explant. When the explants

were cotreated with TGF-β2 and FGF-2, CLECs underwent similar morphological transformations by day 5 (Figure 1D) to that seen with TGF-β2-treatment alone (Figure 1C,G). In contrast, PLECs in the explants cotreated with FGF-2/TGF-β2 showed no evidence of EMT (Figure 1H), instead demonstrating morphological changes more consistent with that observed in the explants treated with FGF-2 alone (Figure 1B,F).

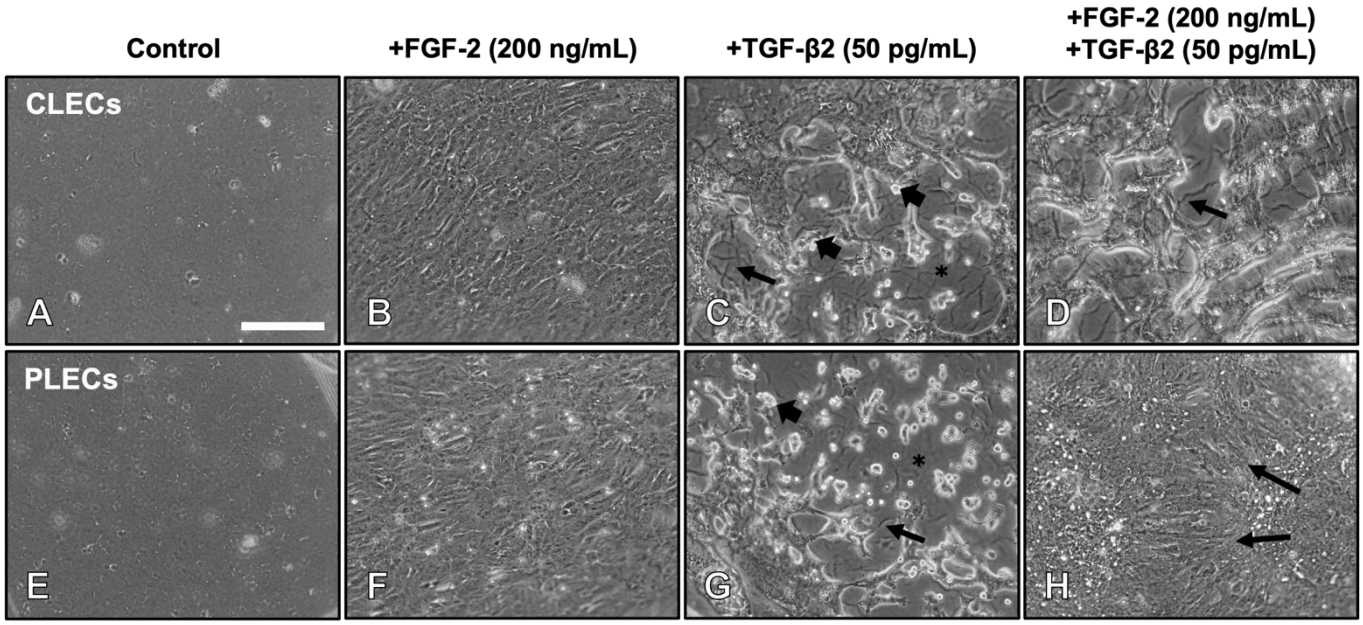

Figure 1. FGF-2 promotes a spatially dependent TGF-β2-induced EMT response in lens epithelial explants. Control LECs maintained a cobblestone-like epithelial phenotype after 5 days (**A**,**E**). FGF-2-induced cell elongation typical of lens fibre differentiation (**B**,**F**). TGF-β2 induced EMT, highlighted by elongated myofibroblastic cells, with prominent cell blebbing/refractile bodies ((**C**,**G**), arrowheads) and loss of cells exposing the lens capsule (asterisk) with capsular wrinkling (arrows). FGF-2 and TGF-β2 cotreated explants led to EMT of CLECs (**D**) but a fibre differentiation response in PLECs ((**H**), arrows). Scale bar: 200 μm.

Table 1. Regional, dose-dependent effects of FGF-2 and TGF-β2 on LEC explants.

Treatment	Concentration		Regional Cell Response in Explant	
	FGF-2 (ng/mL)	TGF-β2 (pg/mL)	FGF-2 (ng/mL)	TGF-β2 (pg/mL)
f/t	5	50	EMT	EMT
f/T	5	200	EMT	EMT
F/t	200	50	EMT	*Fibre Differentiation*
F/T	200	200	EMT	EMT

Low dose FGF-2 (f); low dose TGF-β2 (t); high dose FGF-2 (F); high dose TGF-β2 (T).

PLECs in cotreated explants exhibited changes in the LEC phenotype as early as day 3 (Supplementary Figure S2H). Debridement of all cells at this time revealed the underlying lens capsule with no apparent capsular modulation (no folds or wrinkles) in either control (Supplementary Figure S3A,D) or FGF-2 treated (Supplementary Figure S3B,E) explants. In the TGF-β2-treated explants, increased capsular modulation was apparent with wrinkling and folds in the central explant regions (Supplementary Figure S3C) and in the peripheral regions (Supplementary Figure S3F). Consistent with the differential cell response in the central and peripheral regions of the F/t-cotreated explants (Figure 2A,A1,A3), the explants exhibited capsular modulation only in the central explant region (Figure 2A2), with no capsular wrinkling observed in the peripheral region (Figure 2A4).

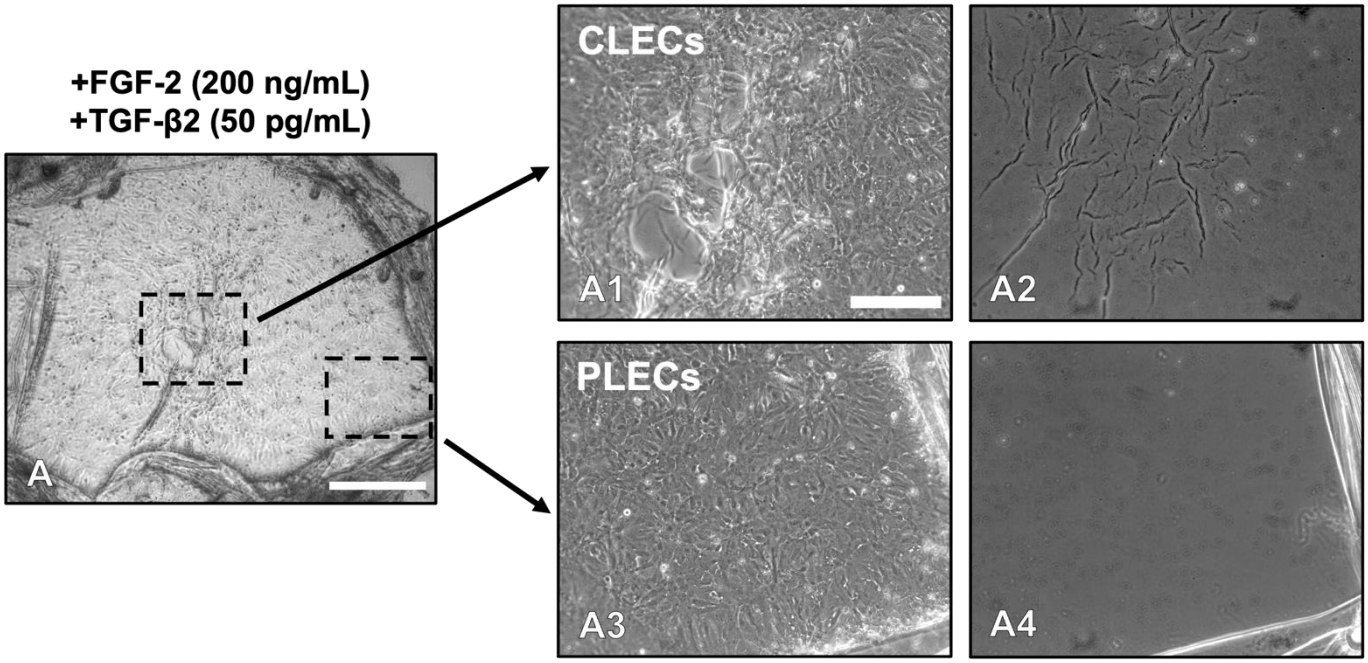

Figure 2. Lens capsule modulation during TGF-β2-induced EMT. Seventy-two h post treatment, the explants were rinsed consecutively in filtered Milli-Q H_2O to remove all lens epithelial cells and view the underlying lens capsule. In the F/t cotreated explants (**A**,**A1**,**A3**), after cell removal (**A2**,**A4**), capsular wrinkling was only apparent in regions that were previously populated with CLECs (**A2**), with no wrinkling visible in regions that were previously populated with PLECs (**A4**). Scale bar: 400 μm (**A**), 200 μm (**A1**–**A4**).

We observed that with ongoing culture (up to 7 days), regardless of the explant region or treatment, all of the cells exposed to TGF-β2 (200 pg/mL) are lost by 7 days (Supplementary Figure S4A); however, in the cotreated explants (F/t), with continual supplementation of the media with FGF-2 (200 ng/mL) after day 3 of culture, this promoted cell survival, whereby we continue to observe many myofibroblastic cells in the central region of the explants (Supplementary Figure S4B) and, similarly, relatively normal lens cells at the periphery of the explants are also maintained (Supplementary Figure S4C).

3.2. FGF-2 Promotes Spatial Differences in Labelling for EMT and Fibre Differentiation Markers in TGF-β2-Treated LECs

3.2.1. Immunofluorescent Labelling

We used immunofluorescence to characterise the different cell types in explants treated with TGF-β2 and/or FGF-2 over 3 days, labeling for lens fibre differentiation markers, β-crystallin, and alpha-tropomyosin (α/9d), as well as the EMT marker, α-SMA (Figure 3). Isotype controls for all of the antibodies show little to no specific labelling. Control LECs throughout the explant exhibited no reactivity for β-crystallin and/or α-SMA after 3 days of culture (Figure 3A), labelling only for α/9d (Figure 3B). FGF-2-treated LECs exhibited strong reactivity for β-crystallin throughout the explant (Figure 3C,I), with stronger labelling in PLECs (Figure 3I). Treatment with FGF-2 did not promote α-SMA reactivity in any cultured lens epithelia. FGF-2-treated CLECs presented diffuse α/9d-reactivity (Figure 3F), while PLECs had a more defined reactivity for α/9d, highlighting actin filaments in the elongating, differentiating fibre cells (Figure 3L). LECs treated with only TGF-β2 displayed clear evidence of an EMT response, with strong reactivity for α-SMA, with no β-crystallin observed throughout the explant (Figure 3D,J).

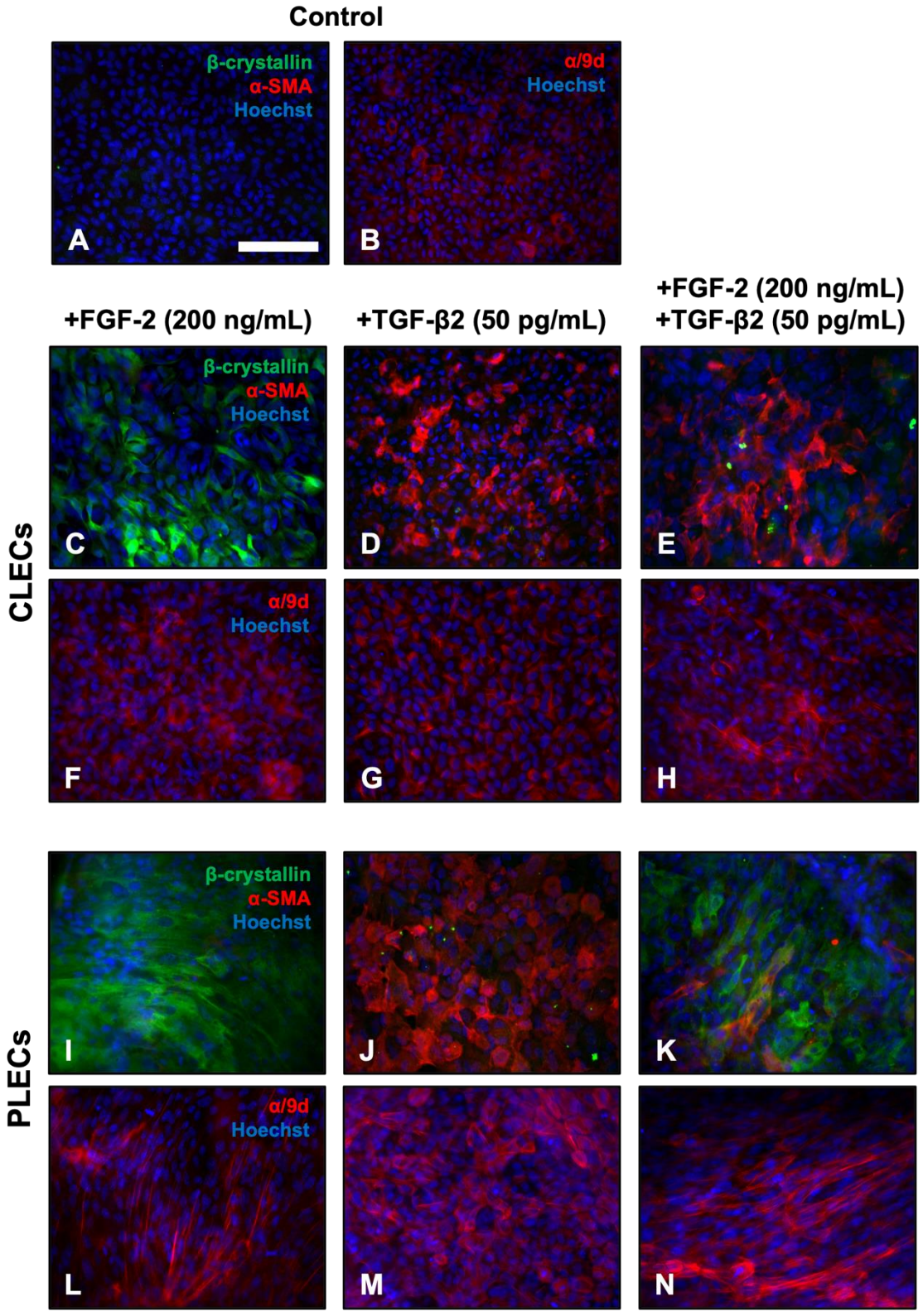

Figure 3. FGF-2 modulates EMT and fibre differentiation markers in TGF-b2-treated LECs. Immunolabeling of β-crystallin (green), α-SMA (red), and alpha-tropomyosin (α/9d; red), counterstained with Hoechst nuclear stain (blue), in CLECs (**C**–**H**) and PLECs (**I**–**N**) following 3 days of culture with no growth factors (Control, (**A**,**B**)), FGF-2 (200 ng/mL; (**C**,**F**,**I**,**L**)), and TGF-β2 (50 pg/mL; (**D**,**G**,**J**,**M**)), or cotreated with FGF-2 and TGF-β2 (**E**,**H**,**K**,**N**). Images are representative of three independent experiments. Scale bar: 100 µm.

TGF-β2-treated CLECs had a highly specific localisation of α/9d to actin stress fibres (Figure 3G), which were also very prominent in PLECs (Figure 3M). Unlike cells treated with only FGF-2 or only TGF-β2, that had a relatively uniform label for the different markers across the entire explant, in the FGF-2/TGF-β2 cotreated explants, we observed distinct spatial differences in the labelling of the markers, consistent with our earlier morphological observations. The CLECs in the TGF-β2/FGF-2-treated explants predominantly labelled for α-SMA with little to no β-crystallin reactivity at day 3 (Figure 3E), similar to the explants treated with only TGF-β2 (Figure 3D,J). In contrast, the PLECs in these same cotreated explants displayed the inverse label, with strong reactivity primarily for β-crystallin in elongated cells, with few neighboring smaller cells immunolabelling for α-SMA (Figure 3K). This differential β-crystallin and α-SMA reactivity in the cotreated explants was sustained up to 5 days of culture (Supplementary Figure S5). Stronger labelling for α/9d was also observed throughout the cotreated explants (Figure 3H,N), highlighting the marked elongation of peripheral fibre-like cells (Figure 3K,N), as well as central myofibroblastic cells (Figure 3E,H).

3.2.2. Western Blotting

Alpha-Smooth Muscle Actin. We quantified protein changes in the treated explants using Western blotting. CLECs had a significant increase in α-SMA when treated with TGF-β2, compared to the relatively lower levels in the control (NT) and FGF-2-treated explants ($p < 0.0001$) (Figure 4A,C). FGF-2 treatment did not impact α-SMA levels in the CLECs compared to the control cells ($p = 0.3429$). In the FGF-2/TGF-β2 cotreated explants, there was a significant reduction in α-SMA levels in the CLECs relative to the TGF-β2 alone CLECs ($p < 0.0001$). In fact, these CLECs in the cotreated explants displayed no significant difference in levels of α-SMA compared to the CLECs of the control ($p > 0.9999$) or FGF-2 alone ($p = 0.3249$) explants. In the PLECs of the FGF-2/TGF-β2 cotreated explants, consistent with the reduced EMT response, there were reduced α-SMA levels when compared to the CLECs, comparable to the lower α-SMA levels seen in the PLECs of the control ($p = 0.7371$), FGF-2 ($p > 0.9999$)-, and TGF-β2-treated explants ($p = 0.0053$) (Figure 4B,D). The PLECs in the explants treated with FGF-2 alone did not have increased α-SMA levels when compared to the control cells ($p = 7366$); however, the PLECs in the explants treated with TGF-β2 alone had significantly increased α-SMA levels, compared to the control ($p = 0.0203$) and the FGF-2-treated ($p = 0.0053$) explants.

β-crystallin. When compared to the control cells, there was no significant difference in the levels of β-crystallin in the CLECs of the explants treated with FGF-2 ($p = 0.8742$) (Figure 4A,C). Treatment with TGF-β2 did not significantly increase levels of β-crystallin in the CLECs compared to the control ($p = 0.5844$), FGF-2 ($p = 0.2260$) or the cotreated explants ($p = 0.1459$). We did observe a significant decrease in β-crystallin in the CLECs of the cotreated explants, relative to the control ($p = 0.0160$) and FGF-2 ($p = 0.0044$)-treated explants (Figure 4A,C). Treatment of the explants with FGF-2 significantly increased β-crystallin levels in the PLECs when compared to the PLECs of the control ($p = 0.0374$) and the TGF-β2-treated explants ($p = 0.0003$) (Figure 4B,D). The PLECs in the explants treated with TGF-β2 alone had reduced β-crystallin levels when compared to the control PLECs ($p = 0.0222$). The PLECs of the explants cotreated with FGF-2/TGF-β2 had slightly elevated β-crystallin levels in comparison to the PLECs of the control ($p = 0.6396$) or the TGF-β2-treated ($p = 0.0056$) explants (Figure 4B,D).

Alpha-Tropomyosin. α/9d levels were significantly elevated only in the CLECs and PLECs of the TGF-β2-treated explants, when compared to the corresponding cells of all other treatment groups (Figure 4A–D). For the CLECs, levels of α/9d in the control explants were reduced in both the FGF-2 ($p = 0.0924$)- and FGF-2/TGF-β2-treated explants ($p = 0.0959$) and were significantly reduced when compared to the elevated α/9d levels found in the CLECs of the TGF-β2-treated explants (control vs. TGF-β2, $p = 0.0034$; FGF-2 vs. TGF-β2, $p = 0.0002$) (Figure 4C). In the PLECs, there was no obvious difference in the levels of α/9d across all of the treatment groups (Figure 4B), except for elevated levels in

the PLECs of the TGF-β2-treated explants as mentioned (control vs. TGF-β2, $p = 0.0103$; FGF-2 vs. TGF-β2, $p = 0.0039$; TGF-β2 vs. FGF-2/TGF-β2, $p = 0.0249$) (Figure 4D).

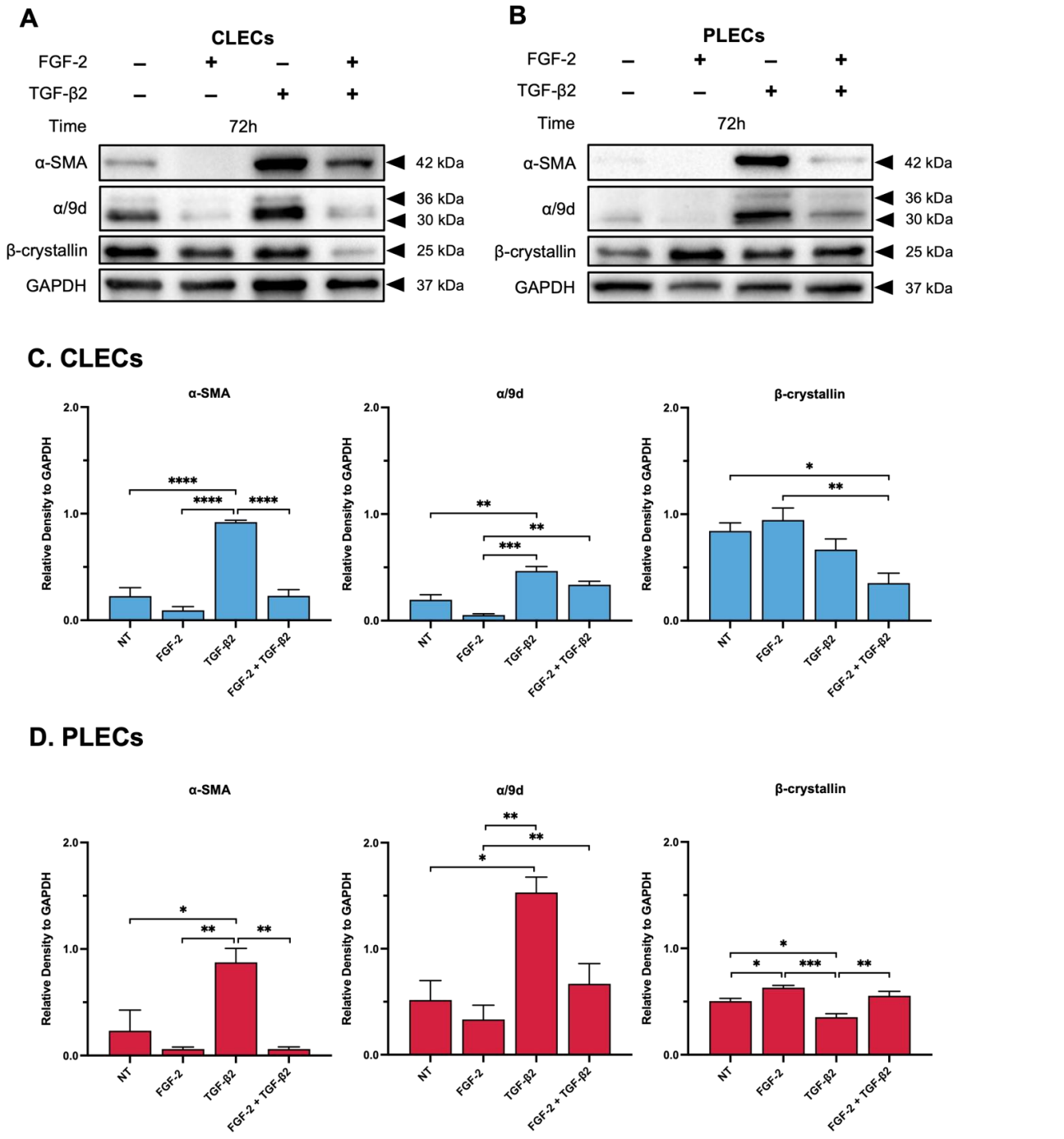

Figure 4. FGF-2 modulates levels of different protein markers in TGF-β2-treated LECs. Representative Western blot for alpha-tropomyosin (α/9d), α-SMA, and β-crystallin in the control (non-treated, NT), FGF-2, TGF-β2, and FGF-2/TGF-β2 cotreated CLECs (**A**,**C**) and PLECs (**B**,**D**). Protein levels were normalized relative to GAPDH levels (**C**,**D**). One-way ANOVA with the mean ± SEM and post-hoc Tukey's multiple comparisons test (* $p < 0.0332$, ** $p < 0.0021$, *** $p < 0.002$, **** $p < 0.001$).

3.3. Impact of FGF-2 on TGF-β2-Mediated Intracellular Signalling

3.3.1. Nuclear Translocation of Smad2/3

Given that FGF-2 can differentially regulate TGF-β2-mediated LEC behaviour, we tested its impact on TGF-β2 mediated Smad2/3-signalling. Active TGF-β2-signalling is evident with the nuclear translocation of phosphorylated Smad2/3 (Figure 5).

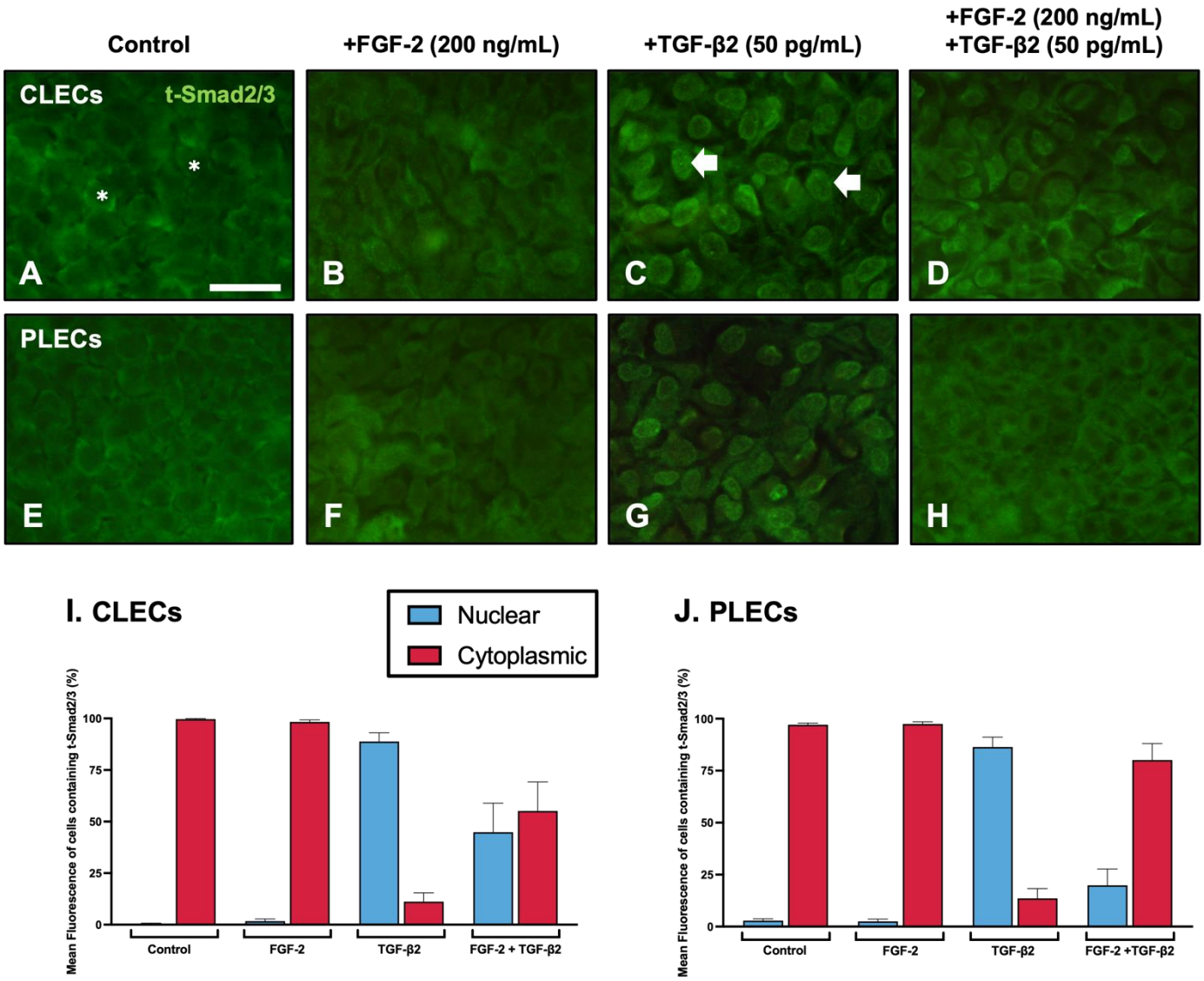

Figure 5. FGF-2 modulates TGFβ-2-induced Smad2/3 nuclear translocation. Immunolabelling of total Smad2/3 (t-Smad2/3, green) in LEC explants following two hours of culture (**A**–**H**). CLECs (**A**–**D**) and PLECs (**E**–**H**) in explants treated with no growth factors (control; (**A**,**E**)), FGF-2 (200 ng/mL; (**B**,**F**)), TGF-β2 (50 pg/mL; (**C**,**G**)), or cotreated with FGF-2/TGF-β2 (**D**,**H**). Examples of cytosolic (asterisks) and nuclear (arrowheads) localisation. Mean percentage (±SEM) fluorescence of cells with nuclear (blue) and cytoplasmic (red) t-Smad2/3 localisation in CLECs (**I**) and PLECs (**J**). Scale bar: 50 µm.

After 2 h of culture, in both the control (Figure 5A,E) and the FGF-2 (Figure 5B,F)-treated explants, we do not see any Smad2/3 nuclear localisation: 0.45–2.81% nuclear labelling (Table 2, Figure 5I,J). In contrast, distinct nuclear localisation of Smad2/3 was evident throughout the TGF-β2-treated explants (Figure 5C,G): 86.44–88.8% nuclear labelling. In the lens epithelial explants cotreated with FGF-2/TGF-β2, we observed prominent nuclear translocation of Smad2/3 in the CLECs (Figure 5D,I): 44.87% nuclear labelling;

however, in the PLECs the Smad2/3-labelling was primarily cytosolic with significantly reduced nuclear labelling: 19.85% (Table 2, Figure 5H,J).

Table 2. Nuclear vs. cytoplasmic localisation of t-Smad2/3 in CLECs and PLECs.

Localisation of t-Smad2/3 (Total Mean % of Fluorescence)				
Treatment	**CLECs**		**PLECs**	
	Nuclear	**Cytoplasmic**	**Nuclear**	**Cytoplasmic**
Control	0.35 ± 0.351	99.65 ± 0.351	2.91 ± 0.833	97.09 ± 0.833
FGF-2 (200 ng/mL)	1.70 ± 0.988	98.30 ± 0.988	2.55 ± 1.047	97.45 ± 1.047
TGF-β2 (50 pg/mL)	88.80 ± 4.217	11.20 ± 4.217	86.40 ± 5.444	13.60 ± 5.444
FGF-2 (200 ng/mL) + TGF-β2 (50 pg/mL)	44.87 ± 14.058	55.13 ± 14.058	19.85 ± 9.090	80.15 ± 9.090

The values are the mean percentage of fluorescence of t-Smad2/3 reactivity (%) ± SEM. *Abbreviations*: Central lens epithelial cells (CLECs); control (non-treated explants); peripheral lens epithelial cells (PLECs). Refer to Figure 5.

3.3.2. Smad2/3-Signalling

Treatment of the explants with FGF-2 did not impact p-Smad2/3 levels in CLECs when compared to similar levels in the control CLECs (p = 0.9768, Figure 6A,B) or the PLECs (p = 0.9310, Figure 6D,E) after 6 h of culture. Consistent with our immunofluorescent nuclear localisation of Smad2/3 (Figure 5), TGF-β2 significantly elevated p-Smad2/3 levels in the CLECs compared to the CLECs of the control explants (p = 0.0061) and the FGF-2-treated explants (p = 0.0101) (Figure 6A,B). In the CLECs of the explants cotreated with FGF/TGF-β2, there was no significant difference in p-Smad2/3 levels when compared to the CLECs of the TGF-β2 (p = 0.5944)- and the FGF-2-treated explants (p = 0.0585); however, p-Smad2/3 levels significantly increased in the cotreated CLECs compared to the control explants (p = 0.0334) (Figure 6A,B). In the PLECs, the TGF-β2 treated explants exhibited elevated p-Smad2/3 levels in comparison to the control (p = 0.0178), FGF-2 alone (p = 0.0403), and cotreated PLEC explants (p = 0.6496, Figure 5D,E) (Figure 6D,E). Compared to the control- and FGF-2-treated PLEC explants, cotreatment with FGF-2/TGF-β2 increased p-Smad2/3 levels (p = 0.0933 for the control, p = 0.2122 for FGF-2) (Figure 6D,E).

3.3.3. MAPK/ERK1/2-Signalling

Levels of phosphorylated ERK1/2 (p-ERK1/2) remained constant in the CLECs of the control and FGF-2-treated (p = 0.7703, Figure 6A,C) explants after 6 h but were elevated in the PLECs of the FGF-2-treated explants, compared to the control PLECs (p = 0.0140, Figure 6D,F). TGF-β2 treatment of the explants slightly increased p-ERK1/2 activity in the CLECs compared to the levels in the CLECs of the control (p = 0.0227) and FGF-2 treated explants (p = 0.0880) (Figure 6A,C). In contrast, the PLECs of the TGF-β2-treated explants had decreased p-ERK1/2 levels compared to the PLECs of the control (p = 0.6711) and FGF-2-treated explants (p = 0.0033) (Figure 6D,F). The CLECs in the explants cotreated with FGF-2/TGF-β2 had reduced p-ERK1/2 levels in comparison to the CLECs in the TGF-β2-treated (p = 0.0174), FGF-2-treated (p = 0.6641), and control explants (p = 0.9972) (Figure 6A,C). Interestingly, the PLECs of the cotreated explants demonstrated a significant increase in their p-ERK1/2 levels in contrast to the low levels in the PLECs of the control (p = 0.0195) and TGF- β2 treated explants (p = 0.0242) (Figure 6D,F).

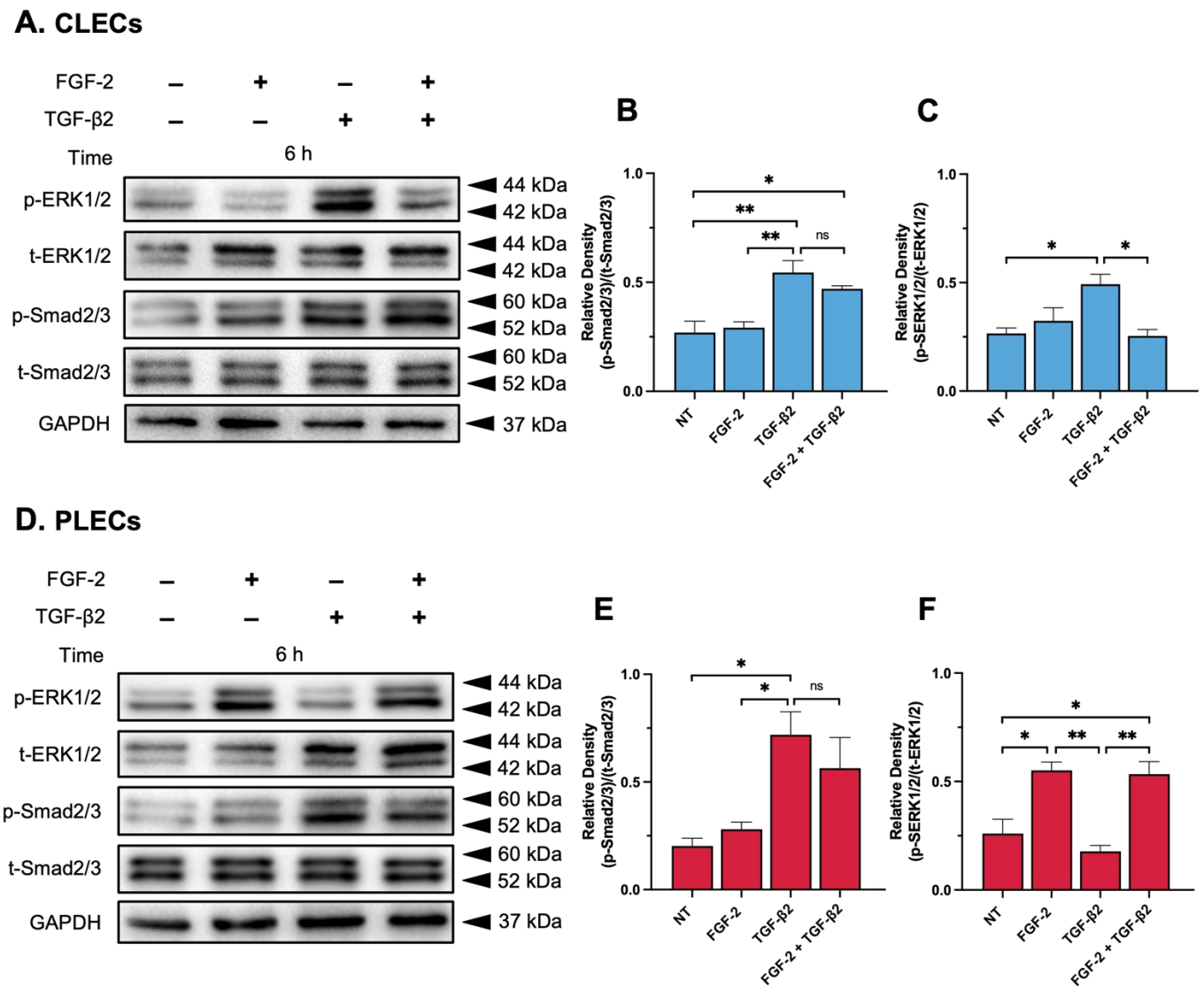

Figure 6. FGF-2 modulates TGF-β2-signalling. Representative Western blots demonstrating protein levels of phosphorylated and total Smads (p-Smad2/3 and t-Smad2/3) and MAPK/ERK1/2 (p-ERK1/2 and t-ERK1/2) in the control (non-treated, NT), FGF-2, TGF-β2, and FGF-2/TGF-β2 cotreated CLECs (**A**–**C**) and PLECs (**D**–**F**). The protein densitometry analysis shows changes in the levels of relative phosphorylation of Smad2/3 (**B**,**E**) and ERK1/2 (**C**,**F**). One-way ANOVA with the mean ± SEM and post-hoc Tukey's multiple comparisons test (ns = not significant, * $p < 0.0332$, ** $p < 0.0021$).

4. Discussion

The present study has demonstrated the impact of FGF-2 on the behaviour of lens epithelial cells induced to undergo EMT in response to TGF-β. A lens-fibre-differentiating dose of FGF-2 was able to block TGF-β2-induced lens EMT in only the peripheral LECs in explants (equivalent to the germinative region of the intact lens) and not in the central (more anterior) lens epithelia. As seen in previous wholemount rat lens epithelial cell explant models, we have demonstrated that CLECs and PLECs exposed to TGF-β2 alone undergo an EMT response, with no evidence of lens fibre differentiation [24,41,51]; however, in combination with FGF-2, FGF-2 potentiates this TGF-β2-induced activity, with elevation of canonical Smad2/3 signalling activity, as well as EMT-associated markers, more so in the CLECs.

For our lens epithelial explant model, we used relatively low doses of TGF-β2 (50 and 200 pg/mL) to induce an EMT response across a short culture period [48,52]. This dose is physiologically representative of concentrations of TGF-β2 in its mature (approx. 100 pg/mL) and total (>3000 pg/mL) forms observed in situ [53]. In addition, it is comparable to active forms of TGF-β2 (approx. 100–400 pg/mL) found in cataractous patients [53–57]. Our use of a lower TGF-β2 dose contrasts to other studies that have used much higher doses (0.5–1.5 ng/mL) to elicit an EMT response in rodent lens cells [13,14,16], which could potentially lead to off-target growth factor signalling activity. Exogenous addition of FGF-2 at a high dose encourages all lens epithelial cells (both CLECs and PLECs) to undergo a change in cell morphology typical of fibre differentiation [3,4,58,59]. In explants cotreated with TGF-β2 and FGF-2, FGF-2 appeared to protect PLECs from TGF-β-induced EMT by promoting a fibre differentiation response. We showed that the PLECs in these FGF-2/TGF-β2 cotreated explants had prominent elongated fibres, reminiscent of many earlier studies from our laboratory [59]. An elevated dose of TGF-β2, was able to prevent any fibre differentiation in the PLECs, leading to an enhanced EMT response in both central and peripheral cells. In addition, we demonstrated that the PLECs in the cotreated explants did not exhibit contractile properties as evidenced by the lack of capsular wrinkling in this region, unlike the region of the CLECs undergoing EMT. The inhibition of lens epithelial cell contraction by FGF despite the presence of TGF-β has been shown in other fibrotic models to be dose dependent, such as in bovine LECs cultured in collagen I gel [60] and valvular interstitial cells (VICs) modelling valvular fibrosis [61], which is also correlated with reduced α-SMA expression.

We not only report how TGF-β can impact FGF-induced lens cell responsiveness but how FGF in turn influences TGF-β-induced responses in LECs, the main focus of our study. When we examined for changes in cytoskeletal and stress-fibre associated proteins, the CLECs in TGF-β/FGF-cotreated lens explants exhibited predominant α-SMA localisation and little to no β-crystallin, suggesting that these cells cannot resist the EMT process, despite the presence of a high differentiating dose of FGF-2. The co-influence of FGF-2 and TGF-β on fibre differentiation, epithelial, and EMT-associated marker expression has previously been reported in other models, including human lung epithelial cells and rat alveolar epithelial-like cells [62], as well as E10 chick lens epithelial cells [13], and the lenses of postnatal mice [10]. Despite the CLECs in the TGF-β/FGF-cotreated explants undergoing a prominent EMT response, we noted reduced α-SMA and α/9d levels, compared to the TGF-β-alone-treated explants, suggesting that FGF-2 may be potentially compromising Tpm activity (a recruiter for actin assembly) and attenuating α-SMA stress fibre association. It has been previously shown that FGF may influence Tpm activity and expression, as well as cell biomechanics, in the presence of TGF-β [14]. For example, when murine LECs (MLECs) are cotreated with FGF-2/TGF-β2, the loss of Tpm1 corresponded with decreased α-SMA reactivity [14]. This same study also confirmed FGF-2 modulation of Tpm in HLECs, when cotreated with TGF-β2, with a significant reduction in both Tpm1 and Tpm2 levels [14]. We localized Tpm (α/9d) in LECs undergoing different phenotypic changes in fibre differentiation, but more compellingly in cells undergoing EMT, where it was associated with the α-SMA-reactive stress fibres of myofibroblasts. This may be attributed to the fact that the α/9d antibody we used specifically targets several isoform splice variant products of the αTm gene (TPM1), including Tpm1.4, Tpm1.6–1.9, and Tpm2.1, with some cross-reactivity also for Tpm3.1 [63]. Tpm1.6, Tpm2.1, and Tpm3.1 have all previously been characterized as being stress-fibre associated and are suggested to play a role in TGF-β induced EMT [64–66]. FGF has shown a role in propagating stress-induced EMT in conjunction with TGF-β in other pathologies, such as wound healing in mice skin keratinocytes [45] and in the tumor stromal cell microenvironment of prostate fibroblasts [47]. Consistent with our findings, Koike et al. (2020) [45] found that FGF-2 could not solely induce EMT in mice keratinocytes; however, in keratinocytes cotreated with FGF-2 and TGF-β1, there was a significant upregulation of cell migratory/motility and EMT-associated genes (e.g., *VIM* and *SNAI2*), similar to keratinocytes with only TGF-β1

stimulation. In a non-transformed mouse mammary gland epithelial cell line (NMuMG), TGF-β modulated FGF receptor activation, increased FGF-2 cell sensitivity, and promoted an EMT response through activation of ERK1/2 signalling [49], highlighting the synergistic signalling role of these two growth factors.

To determine how FGF-2 was modulating and antagonizing TGF-β2-induced EMT in PLECs of cotreated LEC explants, we explored changes in their signalling activity, namely changes to Smad2/3 and ERK1/2. In cotreated lens epithelial explants, we saw stronger signalling for the respective pathways in different regions; CLECs undergoing EMT had more pronounced p-Smad2/3 activity, while PLECs undergoing fiber differentiation had more pronounced p-ERK1/2-signalling. FGF is a well-known regulator of ERK1/2 within the lens, with its marked phosphorylation evident in lens cells within minutes post treatment [3,4,67,68]. While ERK1/2 has been shown to be required for lens epithelial cell proliferation, it is also very important for lens fiber differentiation [4,67–70]. This differs from TGF-β2-induced EMT, where we found that while ERK is also involved in this EMT process, blocking ERK1/2 does not completely block TGF-β2-mediated EMT progression in lens epithelia [39,48,52]. In fact, canonical Smad2/3-signalling is most evident in EMT, as shown here in our cotreated CLECs, and in many earlier studies examining TGF-β2-induced lens EMT [11,13,38,52,71,72].

While we and others have shown FGF-2 is not able to promote Smad2/3-signalling in LECs [10], FGF-2 was shown to impede nuclear localisation of Smad2/3 in PLECs in explants cotreated with TGF-β2; however, in CLECs of these same explants, FGF-2 appeared to have less of an impact on TGF-β2-induced Smad2/3-activity. How FGF-2 directly blocks Smad2/3 activity in PLECs is not clear but given the strong ERK1/2 activation in these cells, this may favour lens fibre differentiation and cell survival, as we see here and has been shown by others [2,3,67,73]. Conversely, FGF-mediated ERK1/2 signalling can correlate with the upregulation of TGF-β activity, as seen in other fibrosis models [14,49,74–76], as well as the current study where TGF-β-induced CLECs are associated with elevated ERK1/2-signalling. Similar to the current study, in valvular interstitial cells (VICs) modelling valvular fibrosis, it was shown that inhibition of this fibrosis was dependent on FGF-2-mediated MAPK signalling when cotreated with TGF-β1 [61]. This study demonstrated that FGF (10 ng/mL) prevented Smad3 nuclear localisation in VICs cotreated with TGF-β1 (5 ng/mL), and at higher doses (100 ng/mL), it was able to perturb TGF-β1-mediated α-SMA expression [61], highlighting the ability of FGF to modulate canonical TGF-β signalling activity and downstream gene expression.

Although not completely understood, crosstalk between FGF and TGF-β signalling has proven influential in mediating various fibrotic disorders and carcinoma progression. For example, a study implementing mouse tumor-associated endothelial cells (TECs) demonstrated how FGF can promote a differential cell response by reducing TGF-β-induced contractile and myofibroblastic properties, while concurrently promoting cell proliferation and motility [75]. A similar finding was observed in primary human dermal fibroblasts (HDFs), whereby FGF-2 with TGF-β1 cotreatment, both positively and negatively regulated fibroblast transition into cancer-associated fibroblasts (CAFs) [77]. This same study also showed how this FGF-2/TGF-β1 treatment of HDFs can downregulate common CAF-activated and EMT-associated markers (e.g., *ACTA2*, *ITGA11*, and *COL1A1*) as well as upregulating cell motility and morphogenetic genes (e.g., *HGF* and *BMP2*) [77].

Research into the mechanisms surrounding differential types of PCO involving lens fibre cell types is ongoing and it is believed to be due to FGF/TGF-β interactions during EMT induction [13,15,16,38,74,78]. As FGF is a major factor influencing normal lens fibre differentiation, it is important to understand what promotes aberrant fibre differentiation during pearl PCO development at the lens equator [13,24,35,79]. In situ, for ASC and for post-operative PCO, more anterior lens epithelial cells are likely exposed to a high insult of TGF-β, and relatively low levels of FGF are normally found in the aqueous humour. At the lens equator, however, epithelial cells in the posterior chamber are regularly exposed to elevated levels of FGF, and regardless of any increased TGF-β levels, the cells here likely

undergo aberrant fibre differentiation, leading to pearl PCO. This may result from the heightened sensitivity to FGF of these peripheral LECs, namely due to their elevated levels of high-affinity FGF receptor tyrosine kinase (RTK) receptors, compared to the central lens epithelia [6,58,80,81]. In situ, during lens fibrosis, we do not see EMT resulting in cell death, likely due to survival growth factors present within the ocular media. Given the findings from the current study, we propose that FGF is a putative survival factor in situ, maintaining fiber cells at the lens equator and the myofibroblastic phenotype leading to fibrotic PCO. Further studies investigating differences/changes in levels of FGF and TGF-β receptors, between central and peripheral lens cells in cotreated explants, may be a key factor in determining lens cell fates in situ. We also cannot rule out that changes in the expression of RTK antagonists, such as Sprouty and Spreds [69,70,82], including those more specific for FGF, such as Sef [83], in these active regions of the lens may be protective of peripheral LECs from any aberrant TGF-β insult of which they have previously been reported to block [69].

5. Conclusions

A fine balance between levels of FGF-2 and TGF-β2 can promote differential responses in lens epithelial cells. More specifically, this responsiveness is spatially regulated, with the anterior central lens epithelia more sensitive to EMT induction, whilst peripheral cells primarily undergo fibre differentiation in the presence of high levels of FGF, avoiding apoptotic cell death associated with EMT. This induced heterogeneous population of cells in lens epithelial explants may provide an alternative model better suited to the study of the cellular processes at play in situ, leading to the formation of ASC, and more importantly both fibrotic and pearl forms of PCO.

Supplementary Materials: The following supporting information can be downloaded at: https://www.mdpi.com/article/10.3390/cells12060827/s1, Figure S1: FGF dose-dependent modulation of TGF-β2-induced EMT; Figure S2: FGF-2 modulates LEC behaviour during TGF-β2-induced EMT; Figure S3: Lens capsule modulation; Figure S4: Re-supplementation of FGF-2 promotes cell survival; Figure S5: FGF-2 modulates EMT and fibre differentiation markers in TGF-β2-treated LECs.

Author Contributions: Conceptualization, F.J.L. and M.F.; methodology, M.F.; software, M.F.; validation, M.F. and F.J.L.; formal analysis, M.F.; investigation, M.F.; resources, M.F. and F.J.L.; data curation, M.F.; writing—original draft preparation, M.F.; writing—review and editing, F.J.L.; visualization, M.F. and F.J.L.; supervision, F.J.L.; project administration, F.J.L.; funding acquisition, F.J.L. All authors have read and agreed to the published version of the manuscript.

Funding: This research received no external funding.

Institutional Review Board Statement: All animal experimentation was approved by the Animal Ethics Committee of The University of Sydney, NSW, Australia (AEC# 2021/1913).

Informed Consent Statement: Not applicable.

Data Availability Statement: Not applicable.

Acknowledgments: We would like to thank Professor Peter Gunning from the University of New South Wales, Australia, for providing the anti-tropomyosin alpha-1 antibody (α/9d).

Conflicts of Interest: M.F. and F.J.L. declare no conflict of interest.

Abbreviations

ASC	Anterior subcapsular cataract
α-SMA	Alpha-smooth muscle actin
α/9d	Alpha tropomyosin 9d antibody
CLECs	Central lens epithelial cells
EMT	Epithelial–mesenchymal transition
ERK	Extracellular signal-regulated kinase
FGF	Fibroblast growth factor
LECs	Lens epithelial cells
MAPK	Mitogen-activated protein kinase
PLECs	Peripheral lens epithelial cells
PCO	Posterior capsular opacification
TGF-β	Transforming growth factor-beta
Tpm	Tropomyosin

References

1. Lovicu, F.J.; McAvoy, J.W. Growth factor regulation of lens development. *Dev. Biol.* **2005**, *280*, 1–14. [CrossRef]
2. Iyengar, L.; Patkunanathan, B.; Mcavoy, J.W.; Lovicu, F.J. Growth factors involved in aqueous humour-induced lens cell proliferation. *Growth Factors* **2009**, *27*, 50–62. [CrossRef]
3. Iyengar, L.; Wang, Q.; Rasko, J.E.J.; McAvoy, J.W.; Lovicu, F.J. Duration of ERK1/2 phosphorylation induced by FGF or ocular media determines lens cell fate. *Differentiation* **2007**, *75*, 662–668. [CrossRef]
4. Lovicu, F.J.; McAvoy, J.W. FGF-induced lens cell proliferation and differentiation is dependent on MAPK (ERK1/2) signalling. *Development* **2001**, *128*, 5075–5084. [CrossRef]
5. West-Mays, J.A.; Pino, G.; Lovicu, F.J. Development and use of the lens epithelial explant system to study lens differentiation and cataractogenesis. *Prog. Retin. Eye Res.* **2009**, *29*, 135–143. [CrossRef] [PubMed]
6. De Iongh, R.U.; Lovicu, F.J.; Hanneken, A.; Baird, A.; McAvoy, J.W. FGF receptor-1 (flg) expression is correlated with fibre differentiation during rat lens morphogenesis and growth. *Dev. Dyn.* **1996**, *206*, 412–426. [CrossRef]
7. Chamberlain, C.G.; McAvoy, J.W. Fibre differentiation and polarity in the mammalian lens: A key role for FGF. *Prog. Retin. Eye Res.* **1997**, *16*, 443–478. [CrossRef]
8. Zhao, H.; Yang, T.; Madakashira, B.P.; Thiels, C.A.; Bechtle, C.A.; Garcia, C.M.; Zhang, H.; Yu, K.; Ornitz, D.M.; Beebe, D.C.; et al. Fibroblast growth factor receptor signaling is essential for lens fiber cell differentiation. *Dev. Biol.* **2008**, *318*, 276–288. [CrossRef] [PubMed]
9. Chamberlain, C.G.; McAvoy, J.W. Induction of Lens Fibre Differentiation by Acidic and Basic Fibroblast Growth Factor (FGF). *Growth Factors* **1989**, *1*, 125–134. [CrossRef]
10. Wang, D.; Wang, E.; Liu, K.; Xia, C.-H.; Li, S.; Gong, X. Roles of TGFβ and FGF signals during growth and differentiation of mouse lens epithelial cell in vitro. *Sci. Rep.* **2017**, *7*, 7274. [CrossRef] [PubMed]
11. Wormstone, I.M.; Anderson, I.K.; Eldred, J.A.; Dawes, L.J.; Duncan, G. Short-term exposure to transforming growth factor β induces long-term fibrotic responses. *Exp. Eye Res.* **2006**, *83*, 1238–1245. [CrossRef]
12. Wormstone, I.M.; Tamiya, S.; Anderson, I.; Duncan, G. TGF-beta2-induced matrix modification and cell transdif-ferentiation in the human lens capsular bag. *Investig. Ophth. Vis. Sci.* **2002**, *43*, 2301–2308.
13. Boswell, B.A.; Korol, A.; West-Mays, J.A.; Musil, L.S. Dual function of TGFβ in lens epithelial cell fate: Implications for secondary cataract. *Mol. Biol. Cell* **2017**, *28*, 907–921. [CrossRef]
14. Kubo, E.; Shibata, S.; Shibata, T.; Kiyokawa, E.; Sasaki, H.; Singh, D.P. FGF2 antagonizes aberrant TGFβ regulation of tropomyosin: Role for posterior capsule opacity. *J. Cell. Mol. Med.* **2017**, *21*, 916–928. [CrossRef] [PubMed]
15. Mansfield, K.J.; Cerra, A.; Chamberlain, C.G. FGF-2 counteracts loss of TGFbeta affected cells from rat lens explants: Implications for PCO (after cataract). *Mol. Vis.* **2004**, *10*, 521–532.
16. Cerra, A.; Mansfield, K.J.; Chamberlain, C.G. Exacerbation of TGF-beta-induced cataract by FGF-2 in cultured rat lenses. *Mol. Vis.* **2003**, *9*, 689–700. [PubMed]
17. de Iongh, R.U.; Wederell, E.; Lovicu, F.J.; McAvoy, J.W. Transforming Growth Factor-β-Induced Epithelial-Mesenchymal Transition in the Lens: A Model for Cataract Formation. *Cells Tissues Organs* **2005**, *179*, 43–55. [CrossRef] [PubMed]
18. Lovicu, F.J.; Flokis, M.; Wojciechowski, M.; Mao, B.; Shu, D. Understanding Fibrotic Cataract: Regulation of TGFβ-Mediated Pathways Leading to Lens Epithelial to Mesenchymal Transition (EMT). *J. Jpn. Soc. Cataract. Res.* **2020**, *32*, 23–32.
19. Xu, J.; Lamouille, S.; Derynck, R. TGF-beta-induced epithelial to mesenchymal transition. *Cell Res.* **2009**, *19*, 156–172. [CrossRef]
20. Nieto, M.A.; Huang, R.Y.-J.; Jackson, R.A.; Thiery, J.P. EMT: 2016. *Cell* **2016**, *166*, 21–45. [CrossRef]
21. Kalluri, R.; Neilson, E.G. Epithelial-mesenchymal transition and its implications for fibrosis. *J. Clin. Investig.* **2003**, *112*, 1776–1784. [CrossRef] [PubMed]

22. Martinez, G.; de Iongh, R.U. The lens epithelium in ocular health and disease. *Int. J. Biochem. Cell Biol.* **2010**, *42*, 1945–1963. [CrossRef] [PubMed]
23. Marcantonio, J.M.; Syam, P.P.; Liu, C.S.C.; Duncan, G. Epithelial transdifferentiation and cataract in the human lens. *Exp. Eye Res.* **2003**, *77*, 339–346. [CrossRef] [PubMed]
24. Lovicu, F.J.; Steven, P.; Saika, S.; McAvoy, J.W. Aberrant Lens Fiber Differentiation in Anterior Subcapsular Cataract Formation: A Process Dependent on Reduced Levels of Pax6. *Investig. Ophthalmol. Vis. Sci.* **2004**, *45*, 1946–1953. [CrossRef]
25. Jiang, J.; Shihan, M.H.; Wang, Y.; Duncan, M.K. Lens Epithelial Cells Initiate an Inflammatory Response Following Cataract Surgery. *Investig. Ophthalmol. Vis. Sci.* **2018**, *59*, 4986–4997. [CrossRef]
26. Liu, Y.C.; Wilkins, M.; Kim, T.; Malyugin, B.; Mehta, J.S. Cataracts. *Lancet* **2017**, *390*, 600–612. [CrossRef]
27. Abdulhussein, D.; Hussein, M.A. WHO Vision 2020: Have We Done It? *Ophthalmic Epidemiol.* **2022**, 1–9. [CrossRef]
28. GBD Blindness and Vision Impairment Collaborators; Vision Loss Expert Group of the Global Burden of Disease Study. Trends in prevalence of blindness and distance and near vision impairment over 30 years: An analysis for the Global Burden of Disease Study. *Lancet Glob. Health* **2021**, *9*, e130–e143. [CrossRef]
29. Vasavada, A.R.; Praveen, M.R. Posterior Capsule Opacification After Phacoemulsification: Annual Review. *Asia-Pacific J. Ophthalmol.* **2014**, *3*, 235–240. [CrossRef]
30. Karahan, E.; Er, D.; Kaynak, S. An Overview of Nd:YAG Laser Capsulotomy. *Med. Hypothesis Discov. Innov. Ophthalmol.* **2014**, *3*, 45–50.
31. Pandey, S.K.; Apple, D.J.; Werner, L.; Maloof, A.J.; Milverton, E.J. Posterior capsule opacification: A review of the aetiopathogenesis, experimental and clinical studies and factors for prevention. *Indian J. Ophthalmol.* **2004**, *52*, 99–112.
32. Lovicu, F.J.; Shin, E.H.; McAvoy, J.W. Fibrosis in the lens. Sprouty regulation of TGFβ-signaling prevents lens EMT leading to cataract. *Exp. Eye Res.* **2015**, *142*, 92–101. [CrossRef]
33. D'Antin, J.C.; Tresserra, F.; Barraquer, R.I.; Michael, R. Soemmerring's Rings Developed around IOLs, in Human Donor Eyes, Can Present Internal Transparent Areas. *Int. J. Mol. Sci.* **2022**, *23*, 13294. [CrossRef]
34. Wormstone, I.M.; Wormstone, Y.M.; Smith, A.J.O.; Eldred, J.A. Posterior capsule opacification: What's in the bag? *Prog. Retin. Eye Res.* **2020**, *82*, 100905. [CrossRef]
35. Wormstone, I.M.; Eldred, J.A. Experimental models for posterior capsule opacification research. *Exp. Eye Res.* **2016**, *142*, 2–12. [CrossRef] [PubMed]
36. Lu, C.; Yu, S.; Song, H.; Zhao, Y.; Xie, S.; Tang, X.; Yuan, X. Posterior capsular opacification comparison between morphology and objective visual function. *BMC Ophthalmol.* **2019**, *19*, 40. [CrossRef] [PubMed]
37. Aslam, T.M.; Aspinall, P.; Dhillon, B. Posterior capsule morphology determinants of visual function. *Graefe's Arch. Clin. Exp. Ophthalmol.* **2003**, *241*, 208–212. [CrossRef]
38. Boswell, B.A.; VanSlyke, J.K.; Musil, L.S. Regulation of Lens Gap Junctions by Transforming Growth Factor Beta. *Mol. Biol. Cell* **2010**, *21*, 1686–1697. [CrossRef] [PubMed]
39. Shu, D.Y.; Wojciechowski, M.; Lovicu, F.J. ERK1/2-mediated EGFR-signaling is required for TGFβ-induced lens epithelial-mesenchymal transition. *Exp. Eye Res.* **2019**, *178*, 108–121. [CrossRef] [PubMed]
40. Musil, L.S. Primary Cultures of Embryonic Chick Lens Cells as a Model System to Study Lens Gap Junctions and Fiber Cell Differentiation. *J. Membr. Biol.* **2012**, *245*, 357–368. [CrossRef]
41. Liu, J.; Hales, A.M.; Chamberlain, C.G.; McAvoy, J.W. Induction of cataract-like changes in rat lens epithelial explants by transforming growth factor beta. *Investig. Ophthalmol. Vis. Sci.* **1994**, *35*, 388–401.
42. Shu, D.Y.; Wojciechowski, M.C.; Lovicu, F.J. Bone Morphogenetic Protein-7 Suppresses TGFβ2-Induced Epithelial-Mesenchymal Transition in the Lens: Implications for Cataract Prevention. *Investig. Ophthalmol. Vis. Sci.* **2017**, *58*, 781–796. [CrossRef]
43. Lovicu, F.J.; Schulz, M.W.; Hales, A.M.; Vincent, L.N.; Overbeek, P.A.; Chamberlain, C.G.; McAvoy, J.W. TGFβ induces morphological and molecular changes similar to human anterior subcapsular cataract. *Br. J. Ophthalmol.* **2002**, *86*, 220. [CrossRef] [PubMed]
44. Srinivasan, Y.; Lovicu, F.J.; A Overbeek, P. Lens-specific expression of transforming growth factor beta1 in transgenic mice causes anterior subcapsular cataracts. *J. Clin. Investig.* **1998**, *101*, 625–634. [CrossRef]
45. Koike, Y.; Yozaki, M.; Utani, A.; Murota, H. Fibroblast growth factor 2 accelerates the epithelial–mesenchymal transition in keratinocytes during wound healing process. *Sci. Rep.* **2020**, *10*, 1–13. [CrossRef] [PubMed]
46. Maruno, K.A.; Lovicu, F.J.; Chamberlain, C.G.; WMcAvoy, J. Apoptosis is a feature of TGFß-induced cataract. *Clin. Exp. Optom.* **2002**, *85*, 76–82. [CrossRef] [PubMed]
47. Strand, D.W.; Liang, Y.-Y.; Yang, F.; Barron, D.A.; Ressler, S.J.; Schauer, I.G.; Feng, X.-H.; Rowley, D.R. TGF-β in-duction of FGF-2 expression in stromal cells requires integrated smad3 and MAPK pathways. *Am. J. Clin. Exp. Urol.* **2014**, *2*, 239–248.
48. Wojciechowski, M.C.; Mahmutovic, L.; Shu, D.Y.; Lovicu, F.J. ERK1/2 signaling is required for the initiation but not progression of TGFβ-induced lens epithelial to mesenchymal transition (EMT). *Exp. Eye Res.* **2017**, *159*, 98–113. [CrossRef]
49. Shirakihara, T.; Horiguchi, K.; Miyazawa, K.; Ehata, S.; Shibata, T.; Morita, I.; Miyazono, K.; Saitoh, M. TGF-β regulates isoform switching of FGF receptors and epithelial-mesenchymal transition. *EMBO J.* **2011**, *30*, 783–795. [CrossRef] [PubMed]
50. Wang, Q.; McAvoy, J.W.; Lovicu, F.J. Growth Factor Signaling in Vitreous Humor–Induced Lens Fiber Differentiation. *Investig. Ophthalmol. Vis. Sci.* **2010**, *51*, 3599–3610. [CrossRef]

51. de Iongh, R.U.; Lovicu, F.J.; Overbeek, P.A.; Schneider, M.D.; Joya, J.; Hardeman, E.D.; McAvoy, J.W. Requirement for TGFbeta receptor signaling during terminal lens fiber differentiation. *Development* **2001**, *128*, 3995–4010. [CrossRef]
52. Shu, D.Y.; Lovicu, F.J. Enhanced EGF receptor-signaling potentiates TGFβ-induced lens epithelial-mesenchymal transition. *Exp. Eye Res.* **2019**, *185*, 107693. [CrossRef] [PubMed]
53. Kokawa, N.; Sotozono, C.; Nishida, K.; Kinoshita, S. High total TGF-β2 levels in normal human tears. *Curr. Eye Res.* **1996**, *15*, 341–343. [CrossRef] [PubMed]
54. Yamamoto, N.; Itonaga, K.; Marunouchi, T.; Majima, K. Concentration of Transforming Growth Factor β2 in Aqueous Humor. *Ophthalmic Res.* **2005**, *37*, 29–33. [CrossRef] [PubMed]
55. Ochiai, Y.; Ochiai, H. Higher Concentration of Transforming Growth Factor-β in Aqueous Humor of Glaucomatous Eyes and Diabetic Eyes. *Jpn. J. Ophthalmol.* **2002**, *46*, 249–253. [CrossRef] [PubMed]
56. Agarwal, P.; Daher, A.M.; Agarwal, R. Aqueous humor TGF-β2 levels in patients with open-angle glaucoma: A meta-analysis. *Mol. Vis.* **2015**, *21*, 612–620. [PubMed]
57. Cousins, S.W.; McCabe, M.M.; Danielpour, D.; Streilein, J.W. Identification of transforming growth factor-beta as an immunosuppressive factor in aqueous humor. *Investig. Ophthalmol. Vis. Sci.* **1991**, *32*, 2201–2211.
58. de Iongh, R.U.; Lovicu, F.J.; Chamberlain, C.G.; McAvoy, J.W. Differential expression of fibroblast growth factor receptors during rat lens morphogenesis and growth. *Investig. Ophthalmol. Vis. Sci.* **1997**, *38*, 1688–1699.
59. Dawes, L.J.; Sugiyama, Y.; Lovicu, F.J.; Harris, C.G.; Shelley, E.J.; McAvoy, J.W. Interactions between lens epithelial and fiber cells reveal an intrinsic self-assembly mechanism. *Dev. Biol.* **2014**, *385*, 291–303. [CrossRef]
60. Kurosaka, D.; Kato, K.; Nagamoto, T.; Negishi, K. Growth factors influence contractility and alpha-smooth muscle actin expression in bovine lens epithelial cells. *Investig. Ophthalmol. Vis. Sci.* **1995**, *36*, 1701–1708.
61. Cushing, M.C.; Mariner, P.D.; Liao, J.; Sims, E.A.; Anseth, K.S. Fibroblast growth factor represses Smad-mediated myofibroblast activation in aortic valvular interstitial cells. *FASEB J.* **2008**, *22*, 1769–1777. [CrossRef]
62. Ramos, C.; Becerril, C.; Montaño, M.; García-De-Alba, C.; Ramírez, R.; Checa, M.; Pardo, A.; Selman, M. FGF-1 reverts epithelial-mesenchymal transition induced by TGF-β1 through MAPK/ERK kinase pathway. *Am. J. Physiol. Cell. Mol. Physiol.* **2010**, *299*, L222–L231. [CrossRef] [PubMed]
63. Schevzov, G.; Whittaker, S.P.; Fath, T.; Lin, J.J.-C.; Gunning, P.W. Tropomyosin isoforms and reagents. *Bioarchitecture* **2011**, *1*, 135–164. [CrossRef] [PubMed]
64. Cheng, C.; Nowak, R.B.; Amadeo, M.B.; Biswas, S.K.; Lo, W.-K.; Fowler, V.M. Tropomyosin 3.5 protects the F-actin networks required for tissue biomechanical properties. *J. Cell Sci.* **2018**, *131*, jcs222042. [CrossRef] [PubMed]
65. Parreno, J.; Amadeo, M.B.; Kwon, E.H.; Fowler, V.M. Tropomyosin 3.1 association with actin stress fibers is required for lens epithelial to mesenchymal transition. *Investig. Ophthalmol. Vis. Sci.* **2020**, *61*, 2. [CrossRef] [PubMed]
66. Gateva, G.; Kremneva, E.; Reindl, T.; Kotila, T.; Kogan, K.; Gressin, L.; Gunning, P.W.; Manstein, D.J.; Michelot, A.; Lappalainen, P. Tropomyosin Isoforms Specify Functionally Distinct Actin Filament Populations In Vitro. *Curr. Biol.* **2017**, *27*, 705–713. [CrossRef]
67. Wang, Q.; Stump, R.; McAvoy, J.W.; Lovicu, F.J. MAPK/ERK1/2 and PI3-kinase signalling pathways are required for vitreous-induced lens fibre cell differentiation. *Exp. Eye Res.* **2008**, *88*, 293–306. [CrossRef] [PubMed]
68. Le, A.-C.N.; Musil, L.S. FGF Signaling in Chick Lens Development. *Dev. Biol.* **2001**, *233*, 394–411. [CrossRef]
69. Shin, E.H.; Zhao, G.; Wang, Q.; Lovicu, F.J. Sprouty gain of function disrupts lens cellular processes and growth by restricting RTK signaling. *Dev. Biol.* **2015**, *406*, 129–146. [CrossRef]
70. Susanto, A.; Zhao, G.; Wazin, F.; Feng, Y.; Rasko, J.E.; Bailey, C.G.; Lovicu, F.J. Spred negatively regulates lens growth by modulating epithelial cell proliferation and fiber differentiation. *Exp. Eye Res.* **2019**, *178*, 160–175. [CrossRef]
71. Saika, S.; Kono-Saika, S.; Ohnishi, Y.; Sato, M.; Muragaki, Y.; Ooshima, A.; Flanders, K.C.; Yoo, J.; Anzano, M.; Liu, C.-Y.; et al. Smad3 Signaling Is Required for Epithelial-Mesenchymal Transition of Lens Epithelium after Injury. *Am. J. Pathol.* **2004**, *164*, 651–663. [CrossRef]
72. Saika, S.; Miyamoto, T.; Ishida, I.; Shirai, K.; Ohnishi, Y.; Ooshima, A.; McAvoy, J.W. TGFbeta-Smad signalling in postoperative human lens epithelial cells. *Br. J. Ophthalmol.* **2002**, *86*, 1428–1433. [CrossRef] [PubMed]
73. Stolen, C.M.; Jackson, M.W.; Griep, A.E. Overexpression of FGF-2 modulates fiber cell differentiation and survival in the mouse lens. *Development* **1997**, *124*, 4009–4017. [CrossRef]
74. Kubo, E.; Shibata, T.; Singh, D.P.; Sasaki, H. Roles of TGF β and FGF Signals in the Lens: Tropomyosin Regulation for Posterior Capsule Opacity. *Int. J. Mol. Sci.* **2018**, *19*, 3093. [CrossRef] [PubMed]
75. Akatsu, Y.; Takahashi, N.; Yoshimatsu, Y.; Kimuro, S.; Muramatsu, T.; Katsura, A.; Maishi, N.; Suzuki, H.; Inazawa, J.; Hida, K.; et al. Fibroblast growth factor signals regulate transforming growth factor-β-induced endothelial-to-myofibroblast transition of tumor endothelial cells via Elk1. *Mol. Oncol.* **2019**, *13*, 1706–1724. [CrossRef] [PubMed]
76. Strutz, F.; Zeisberg, M.; Renziehausen, A.; Raschke, B.; Becker, V.; Kooten, C.V.; Müller, G.A. TGF-β1 induces proliferation in human renal fibroblasts via induction of basic fibroblast growth factor (FGF-2). *Kidney Int.* **2001**, *59*, 579–592. [CrossRef]
77. Bordignon, P.; Bottoni, G.; Xu, X.; Popescu, A.S.; Truan, Z.; Guenova, E.; Kofler, L.; Jafari, P.; Ostano, P.; Röcken, M.; et al. Dualism of FGF and TGF-β Signaling in Heterogeneous Cancer-Associated Fibroblast Activation with ETV1 as a Critical Determinant. *Cell Rep.* **2019**, *28*, 2358–2372.e6. [CrossRef]
78. Symonds, J.G.; Lovicu, F.J.; Chamberlain, C.G. Posterior capsule opacification-like changes in rat lens explants cultured with TGFβ and FGF: Effects of cell coverage and regional differences. *Exp. Eye Res.* **2006**, *82*, 693–699. [CrossRef]

79. Lovicu, F.J.; Chamberlain, C.G.; McAvoy, J.W. Differential effects of aqueous and vitreous on fiber differentiation and extracellular matrix accumulation in lens epithelial explants. *Investig. Ophthalmol. Vis. Sci.* **1995**, *36*, 1459–1469.
80. Kondo, T.; Ishiga-Hashimoto, N.; Nagai, H.; Takeshita, A.; Mino, M.; Morioka, H.; Kusakabe, K.T.; Okada, T. Expression of transforming growth factor β and fibroblast growth factor 2 in the lens epithelium of Morioka cataract mice. *Congenit. Anom.* **2014**, *54*, 104–109. [CrossRef]
81. Lovicu, F.J.; McAvoy, J.W. The age of rats affects the response of lens epithelial explants to fibroblast growth factor. An ultrastructural analysis. *Investig. Ophthalmol. Vis. Sci.* **1992**, *33*, 2269–2278.
82. Zhao, G.; Bailey, C.G.; Feng, Y.; Rasko, J.; Lovicu, F.J. Negative regulation of lens fiber cell differentiation by RTK antagonists Spry and Spred. *Exp. Eye Res.* **2018**, *170*, 148–159. [CrossRef] [PubMed]
83. Newitt, P.; Boros, J.; Madakashira, B.P.; Robinson, M.L.; Reneker, L.W.; McAvoy, J.W.; Lovicu, F.J. Sef is a negative regulator of fiber cell differentiation in the ocular lens. *Differentiation* **2010**, *80*, 53–67. [CrossRef] [PubMed]